



Academic Year 2010-2011

Ghent University – Faculty of Sciences  
Department of Biomedical Molecular Biology  
Molecular Cell Biology Unit  
VIB Department for Molecular Biomedical Research

---

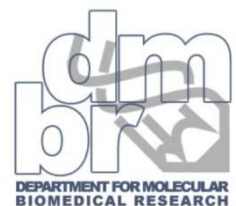
# Functional analysis of mice harboring a knockout or knockin of the alternatively spliced exon C of p120ctn

---

**Tim Pieters**

Thesis submitted in partial fulfilment of the requirements for the degree of  
DOCTOR IN SCIENCES: BIOTECHNOLOGY

Promoter: Prof. Dr. F. Van Roy  
Co-promoter: Dr. J. van Hengel



# **Functional analysis of mice harboring a knock-out or knock-in of the alternatively spliced exon C of p120ctn**

By Tim Pieters

Ghent University – Faculty of Sciences  
Department of Biomedical Molecular Biology  
Molecular Cell Biology Unit  
VIB Department for Molecular Biomedical Research  
Technologiepark 927  
B-9052 Gent-Zwijnaarde

## **Promoters**

Prof. Dr. Frans Van Roy<sup>1</sup>  
Dr. Jolanda Van Hengel<sup>1</sup>

## **Examination committee**

### **Chairman**

Prof. Dr. Johan Grooten<sup>1</sup>

### **Reading committee**

Prof. Dr. Jody Haigh<sup>1</sup>  
Prof. Dr. Patrick Derksen<sup>2</sup>  
Dr. Marc Stemmler<sup>3</sup>  
Dr. Anja Lambrechts<sup>4</sup>

### **Additional members**

Prof. Dr. Frans Van Roy<sup>1</sup>  
Prof. Dr. Kris Vleminckx<sup>1</sup>  
Dr. Jolanda Van Hengel<sup>1</sup>  
Dr. Tino Hochepped<sup>1</sup>

<sup>1</sup> Department of Biomedical Molecular Biology, Ghent University, Technologiepark 927, B-9052 Ghent, Belgium

<sup>2</sup> Department of Pathology, University Medical Center Utrecht, Heidelberglaan 100, 3584 CX Utrecht, The Netherlands

<sup>3</sup> Department of Molecular Embryology, Max-Planck Institute of Immunobiology, Stuebeweg 51, 79108 Freiburg, Germany

<sup>4</sup> Department of Biochemistry, Faculty of Medicine and Health Sciences, Ghent University, Albert Baertsoenkaai 3, B-9000 Ghent, Belgium

## Dankwoord

**E**r was eens heel lang geleden een jonge wetenschapper die op zoek was naar eeuwige roem, door een remedie te vinden tegen kanker, dit te publiceren in een top-journal en hiervoor misschien ook nog een Nobel-prijsje wou meepikken. Op een zonnige dag in augustus (2004) trok deze vorser, gewapend met een dosis ambitie en naïviteit, naar een vestiging in Zwijnaarde. Daar vervoegde hij enkele jonge enthousiastelingen van het 'U7 legioen' (Vanessa, Céline, Hanne, Michaël), die ten strijde trokken tegen Marc pollet en zijn leger van inconsistente uarrige afkorting(en) (IWT). De strijd was hevig. Slechts enkelen konden de schatkist van Marc beroven, en waren in staat 4 jaar lang alchemie te bedrijven. Het echte avontuur kon nu beginnen. Maar zoals in elke episch heldenepos kon de jonge vorser rekenen op een team van trouwe bondgenoten die hem op zijn quest vergezelden. Zij zorgden ervoor dat de jonge vorser ondanks de vele moeilijke hindernissen toch zijn avontuur heelhuids overleefde. Nu de jonge vorser al zijn belevenissen heeft neergepend, wil hij zijn metgezellen bedanken voor hun tomeloze inzet en heldenmoed.

Vooreerst wil ik Prof. Dr. Frans van Roy en Dr. Jolanda van Hengel bedanken om mij de kans te geven om als vorser op internationaal niveau te kunnen wedijveren. Jullie hebben de krijtlijnen van mijn project uitgetekend en lieten mij de wondere werelden van ontwikkelingsbiologie, stamcelonderzoek en neurobiologie ontdekken. Jullie hebben mij altijd onvoorwaardelijk gesteund tijdens de vele ups and downs in mijn tocht. Door nieuwe tools te introduceren en alternatieve paden te tonen, leiden jullie mij langsheen vele obstakels. Bedankt.

Daarnaast wil ik ook alle moedige strijders van de FvR-Unit (aka unit 7 of kortweg U7) bedanken. Karl, jij bent als ware een walking 'Maniatis'. Je weet raad op al mijn praktische vragen, van transducties tot het goed zetten van de klok op mijn PC. Daarenboven ben je mijn hofleverancier van pdf-kes en zal je fungeren als een vice-rik (niet te verwarren met viezerik) op mijn verdediging. Alvast bedankt voor alles. Vanessa, wij kwamen als enigen van U7 heelhuids (en met een dikke beurs dukaten) terug na een hevige strijd in Brussel tegen Marc Pollet en zijn discipels. Je hebt bewezen dat je die beurs waardig bent. Hoe kan ik u ooit bedanken voor de vele carpoolsessies waarin je mij na een lange dag op het labo naar huis bracht. Tijdens die ritten hadden we vele toffe babbels waarbij we onze

wetenschappelijke (en andere) frustraties konden uiten. Een dikke merci en ik kijk al uit naar uw doctoraatsverdediging. Irene, my neighbour. I want to thank you for the nice chats we had and I hope will be successful in generating and analyzing all your proto-cadherin X knockout mice. Keep on blotting. Huiyu, good luck in finishing up the 'Eye' work and I hope that your p120ctn article will be published soon. Ele, you are a sunshine in our lab due to your frank Italian attitude and your honest (LR?) reactions. Koen, ik was verheugd toen jij bij onze unit kwam om de mannelijke fractie te versterken. Ik heb genoten van onze vele hilarische conversaties en south park-humor. Echte Vente-praat. Geniet nog maar van mijn buro en misschien quizen we nog eens samen. Ook veel dank aan Katrien, Ellen en Mara voor hun technische en mentale ondersteuning. Dank aan allen.

Maar tijdens de strijd hebben we ook veel U7-mensen verloren. Waaronder mijn oude burens Steven G. en Joana. Ik wil ook Petra en Philippe bedanken voor de toffe babbels en de hulp bij het genotyperen van mijn vele muizen. Zerihun, it was a pleasure working with you and I enjoyed your relaxed 'Ethiopian' view on life. Uta, It was a pleasure to work and discuss with you. I hope you are doing well in Germany and best wishes to Gwen and Stefan. Tetyana, thanks for sharing your insight in mouse experiments and good luck with your article. Christophe, je was een toffee college, goede wetenschapper en een super surprise-act op mijn birthday party. Merci en groeten aan Raf en Riene. Hanne, Céline en Michaël, we waren samen gestart maar helaas was de schatkist van het IWT niet groot genoeg voor ons allemaal. Ik ben blij dat jullie allemaal goed terecht zijn gekomen en wens jullie nog veel geluk in het verdere leven.

Verder wil ik onze ideologische verwanten van U10 (Ellen, Nicolas en Griet) en U12 (Bram, Mara, Alexander) bedanken voor toffe babbels, informatieve kennisoverdracht, hilarische filmscenes en voor de leuke brainstorm in de Ardennen.

Ik wil ook alle andere mensen van het DMBR bedanken die bijgedragen hebben aan mijn onderzoek. Tino, bedankt voor alle technische ondersteuning. Zonder jou had ik nooit muisembryos kunnen flushen via het infundibulum en was ons ES-celderivatatie protocol nooit tot stand gekomen. Ook bedankt voor alle verkregen materieel, zoals flushnaalden, MEFs en Bl6 muizen. Samen met Steven V. en Petra vormden we ook het Maximuss test-team. Het was een toffe ervaring om als tester ons muisbeheer te vereenvoudigen en personaliseren. Ik wil ook alle mensen van de unit van Prof. Dr. Jody Haigh bedanken voor het gebruik van hun



binocular, om mij toe te laten in hun ES-cell room en voor de vele hulp die ik van hen kreeg bij mijn experimenten. Lieven, ik hoop dat jou ES cellijnen leiden tot succesvolle germline transmissie. Verder wil ik Eef, bob, Wies en Sam bedanken van de Microscopy Core voor de professionele begeleiding, nuttige adviezen, en voor al de hulp bij het opzetten van ‘time-lapse monitoring’ apparatuur en het maken van de bijhorende filmkes. Merci. Ook wens ik Paco en het voltallige BioIT-team (en Karl) te bedanken, voor de intensieve analyse van het mysterieuze geconserveerde blok rondom exon C. Jullie hebben alvast een tipje van de sluier kunnen oplichten. Als laatste wil ik uitdrukkelijk alle mensen bedanken die behoren tot de overige Core-faciliteiten: keuken (An en Tim), animalarium (Céline, merci voor alle tailsnips), TC (Ann en Wilma), ITers (Steven V, Didier), receptie en secretariaat. Dankzij jullie ondersteuning konden wij ons enkel op wetenschap focussen. Merci

Ik wil ook de niet-DMBRers bedanken waarmee we succesvol samenwerkten. Anja, bedankt voor alle hulp bij de neuronale culturen. Marc, Lenka, Ivan, Stefan and Daniel, I enjoyed the one-month training in Freiburg. I learned a lot in and outside the Max-Planck Institute. Thanks a lot for this nice experience. Tevens een word van dank voor de mensen van het bioimaging lab (Universiteit Antwerpen) voor de MRI analyse. I also thank all the members of jury that participated in my defense PhD.

Niet te vergeten: alle muizen die hebben meegewerkt aan deze thesis. Dank u wel. Speciaal voor hen deze toepasselijke quote van Viktor Hamburger. *"Our real teacher, has been and still is the embryo-who is, incidentally, the only teacher who is always right"*

Dan wil ik ook mijn familie, vrienden, studiegenoten, ploegmaten (volley) bedanken voor de steun en voor het voorzien van de broodnodige ontspanning buiten de muren van het labo. Het was niet altijd eenvoudig om uit te leggen waarmee ik bezig was, maar ik hoop dat ik tijdens de publieke verdediging het een en ander kan ophelderen.

Mama en papa, zonder jullie had dit doctoraat en deze doctor(andus) nooit bestaan. Ik wil jullie van harte bedanken om mij te verwekken, maar ook voor de goede zorg en liefde die ik van jullie heb mogen ontvangen nadat ik verwekt was. Samen met Annemieke maakte ik deel uit van jullie warme nest, waarin ik de kans heb kregen om te studeren (graduaat), verder te studeren (Industrieel ingenieur), te specialiseren (Master na Master aka GGS) en om

uiteindelijk te doctoreren. Bedankt voor alle steun, zorg, trots, ... Ik zal jullie hiervoor altijd dankbaar zijn.

Last but not least, Debora, mijn lieve zielsverwant, mijn schatje. Twee kindjes opvoeden en doctoreren was zeker geen eenvoudige combinatie. En de vele labbezoeken 's nachts of in het weekend maakten ons leven niet altijd gemakkelijk te organiseren. Maar jij was er altijd voor mij en met zo een liefdevolle trouwe partner aan mijn zijde zijn we deze periode goed doorgekomen. Ik hoop dat er nu wat meer tijd vrijkomt voor ons twee. Bedankt voor alle onvoorwaardelijke steun en liefde! Deze liefde heeft zich geuit in twee fantastische kinderen. Amalia, je bent een mooie slimme meid, een toegewijde grote zus en buiten spelen met jou is de beste ontspanning die er is. Thomas, onze lieve grote knuffelbeer, gezien jouw fascinatie voor knopjes, gsm's en computers ligt misschien nog een toekomst voor u in de bio-IT. Mijn drie schatten, ik hou zielsveel van jullie en draag dit eindwerk aan jullie op.

Tim

... en ze leefden nog lang en gelukkig.

## Overview of the thesis

This thesis contains the following parts: Introduction, Research aims, Results and Discussion, General Discussion and Perspectives, and Summary.

The *Introduction* is composed of two chapters. Chapter 1 is a comprehensive literature overview on p120ctn and its many isoforms. Chapter 2 deals with mouse development and transcription factor networks, which are important in both preimplantation embryos and stem cells. The latter chapter was included because a substantial portion of the work presented in this dissertation deals with analysis of early mouse embryos and with methods to derive embryonic stem (ES) cells from them.

Since our laboratory previously demonstrated the occurrence of different p120ctn isoforms, we were eager to find out more about their roles *in vivo*. Mice with forced expression of specific p120ctn isoforms were generated. This was the starting point of my research. More about the scope of my thesis is presented in *Research Aims*.

The *Results and Discussion* part is composed of five chapters. First, isoform-C specific p120ctn knockout (KO) and knockin (KI) mice and their respective phenotypes are presented in Chapter 3. Because homozygous isoform-C specific p120ctn KO and KI embryos exhibit early lethal phenotypes, I optimized two techniques for analyzing these early developmental defects. In Chapter 4, I describe a method to monitor preimplantation development *in vitro* via time lapse recordings. The establishment of a modified protocol to derive ES cells from early mouse embryos is presented in Chapter 5. The last two chapters deal with transgenic strategies that circumvent the early lethality of homozygous isoform-C specific p120ctn KO or KI embryos by crossing heterozygous isoform-C specific p120ctn KO or KI mice with, respectively, liver-specific total (all isoforms) p120ctn KO mice (Chapter 6) or with brain-specific total p120ctn KO mice (Chapter 7).

The thesis ends with a *General Discussion and Perspectives*, and a *Summary*.

## TABLE OF CONTENTS

---

Overview of the thesis

Table of contents

List of abbreviations

INTRODUCTION 1

Chapter 1. p120ctn in normal development and tumorigenesis 3

---

1. ABSTRACT.....	6
2. INTRODUCTION: AN HISTORICAL OVERVIEW OF P120CTN RESEARCH.....	7
3. P120CTN ISOFORMS AND ALTERNATIVE SPLICING.....	9
4. P120CTN GENE FAMILY.....	15
5. P120CTN AND E-CADHERIN REGULATION.....	17
5.1. p120ctn interacts with cadherins and modulates adherens junctions.....	17
5.2. p120ctn regulates cadherin turnover: evidence from genetic and knockdown studies.....	18
5.3. p120ctn and cadherin biogenesis, endocytosis and degradation.....	19
6. P120CTN AND RHO GTPASES.....	20
6.1 p120ctn and dendritic-like branching.....	20
6.2. p120ctn mediates RhoA inhibition and activation of both Rac1 and Cdc42.....	23
6.3. Interaction between p120ctn and RhoA.....	24
6.4. Mechanism of p120ctn-mediated RhoA inhibition.....	24
6.5. RhoGTPases and cadherin-based junctions.....	26
6.6. p120ctn subfamily members and RhoGTPases.....	26
7. P120CTN INTERACTS WITH TRANSCRIPTION FACTORS IN THE NUCLEUS.....	27
8. P120CTN AND PHOSPHORYLATION.....	29
8.1. Phosphorylation of the cadherin-catenin complex.....	29
8.2. Phosphorylation of p120ctn.....	33
8.3. p120ctn isoforms and phosphorylation.....	35
9. THE P120CTN FAMILY IN ANIMAL MODELS.....	36
9.1. Animal models for p120ctn.....	36
9.2. Animal models for p120ctn family members.....	38
10. P120CTN AND CANCER.....	38
10.1. Altered expression of p120ctn in tumors.....	38
10.2. p120ctn isoforms in EMT and cancer.....	39
10.3. Differential regulation of RhoGTPases by p120ctn in cancer.....	41
10.4. p120ctn isoforms: effects on proliferation and tumor growth.....	42
10.5. p120ctn isoforms: effects on motility and invasion.....	42
10.6. p120ctn and anchorage-independent growth (AIG).....	43
10.7. p120ctn in inflammation and cancer.....	44
11. ACKNOWLEDGEMENTS.....	44
12. REFERENCES.....	45

## Table of contents

### **Chapter 2. Mouse development 69**

---

INTRODUCTION .....	71
Mice as animal model system.....	71
Overview of mouse development.....	72
PREIMPLANTION DEVELOPMENT IN MOUSE.....	72
Fertilization and early cleavage cycles.....	72
Morula compaction and polarization.....	74
Blastocyst formation and the first cell type diversification: TE and ICM.....	76
Late blastocyst stage and establishment of epiblast and primitive endoderm lineages.....	78
TRANSCRIPTION FACTORS GOVERNING BLASTOCYST LINEAGE ALLOCATION ...	79
ICM-specific transcription factors.....	79
TE-specific transcription factors .....	84
PE-specific transcription factors.....	86
IMPLANTATION AND GASTRULATION.....	86
REFERENCES .....	91

### **RESEARCH AIMS 99**

### **RESULTS AND DISCUSSION 103**

### **Chapter 3. Expression of p120ctn during early mouse development 105**

---

ABSTRACT.....	108
INTRODUCTION .....	109
MATERIAL AND METHODS .....	110
Immunofluorescence .....	110
Confocal microscopy.....	110
Histology and immunohistochemistry.....	110
RT-PCR .....	111
Western blot analysis.....	111
RESULTS .....	112
p120ctn expression in wild-type preimplantation embryos.....	112
p120ctn expression in gastrulating embryos .....	115
Cadherin expression in gastrulating embryos.....	117
DISCUSSION .....	121
ACKNOWLEDGEMENTS.....	124
REFERENCES .....	124

## Chapter 4. p120ctn isoform C knockout and knockin mice rescue E-cadherin loss and embryonic lethality in p120ctn-deficient embryos 129

ABSTRACT.....	133
INTRODUCTION .....	134
MATERIAL AND METHODS .....	137
Immunofluorescence .....	137
Confocal microscopy .....	137
Histology and immunohistochemistry.....	137
Bioinformatic analyses .....	138
RT-PCR .....	138
Production and purification of a polyclonal antibody against p120ctn isoform C.....	139
Plasmid construction and cell culture.....	139
Western blot analysis.....	140
Generating p120ctn <sup>KOC/+</sup> and p120ctn <sup>KIC/+</sup> mice .....	140
Southern blot analysis.....	141
Generating p120ctn <sup>+/-</sup> , p120ctn <sup>KOC/-</sup> and p120ctn <sup>KIC/-</sup> mice.....	142
Generating p120ctn <sup>fl/fl</sup> ; Alb-Cre, p120ctn <sup>KOC/fl</sup> ; Alb-Cre and p120ctn <sup>KIC/fl</sup> ; Alb-Cre mice.....	142
Mouse breeding, embryo isolation and genotyping.....	142
ES cell isolation and culture .....	143
RhoA Activity assay.....	143
RESULTS .....	144
p120ctn exon C encoded amino acids inhibit nuclear translocation and dendritic-like branching <i>in vitro</i> .....	145
Homozygous p120ctn KOC and KIC embryos die very early in development .....	149
Homozygous p120ctn KOC and KIC embryos fail to implant .....	153
Evolutionarily conserved p120ctn exon C is expressed during early development.....	158
Blastocysts from homozygous p120ctn knockout mice fail to stabilize E-cadherin at the cell membrane .....	162
p120ctn <sup>KOC/-</sup> and p120ctn <sup>KIC/-</sup> mice are viable and can stabilize E-cadherin at the cell membrane of blastocysts .....	164
Generation and characterization of p120ctn <sup>KOC/-</sup> and p120ctn <sup>KIC/-</sup> ES cell lines.....	167
Both the p120ctn KOC and KIC allele can rescue defects seen in p120ctn-deficient livers. ..	170
DISCUSSION .....	173
Interplay between p120ctn and E-cadherin <i>in vivo</i> .....	173
p120ctn isoform C: essential for life, conserved in evolution.....	175
ACKNOWLEDGEMENTS .....	178
REFERENCES .....	179

## Table of contents

### **Chapter 5. Time lapse monitoring of *in vitro* preimplantation development 185**

---

MATERIAL AND METHODS .....	188
Mouse breeding .....	188
Time lapse microscopy .....	188
RESULTS AND DISCUSSION .....	189
Time lapse monitoring of <i>in vitro</i> preimplantation development .....	189
Optimizing time lapse monitoring of <i>in vitro</i> preimplantation development .....	194
Rock inhibition delays blastocyst formation .....	196
ACKNOWLEDGEMENTS .....	198
REFERENCES .....	198

### **Chapter 6. Efficient and user-friendly pluripotin-based derivation of mouse embryonic stem cells 201**

---

ABSTRACT .....	204
INTRODUCTION .....	205
MATERIAL AND METHODS .....	208
Mouse strains, breeding and genotyping .....	208
Classical ES cell derivation .....	208
Pluripotin-based ES cell isolation, ES cell culture, and embryoid body formation .....	209
Immunofluorescence .....	210
RESULTS .....	211
Classical derivation of ES cells for transgenic embryos in not efficient .....	211
Efficient pluripotin-based derivation of mouse ES cells .....	212
Characterization of newly established mouse ES cell lines .....	217
Attempt to generate homozygous p120ctn KOC, p120ctn KIC and p120ctn null ES cell lines .....	217
Generation and characterization of p120ctn <sup>KOC/-</sup> and p120ctn <sup>KIC/-</sup> ES cell lines .....	220
DISCUSSION .....	221
ACKNOWLEDGEMENTS .....	226
REFERENCES .....	226

**Chapter 7. Knockout and Knockin of exon C of p120ctn in brain 231**

ABSTRACT.....	234
INTRODUCTION .....	235
MATERIAL AND METHODS .....	237
Generating p120ctn <sup>fl/fl</sup> ; Nes-Cre, p120ctn <sup>KOC/fl</sup> ; Nes-Cre and p120ctn <sup>KIC/fl</sup> ; Nes-Cre mice .....	237
Nissl staining, immunostaining and immunohistochemistry .....	237
Hippocampal cultures .....	238
RT-PCR and Q-PCR.....	239
Transfection of hippocampal cultures .....	239
Western blot analysis.....	240
RhoGTPase Activity assay .....	240
RESULTS AND DISCUSSION .....	241
p120ctn exon C is highly expressed in mouse brain .....	241
Brain-specific p120ctn knockout mice are viable .....	241
Sustained N-cadherin levels in p120ctn-deficient brains .....	246
Increased RhoA activity in p120ctn-deficient brains .....	247
NestinCre transgenic females and males show premature recombination .....	248
Revised mating strategy to obtain p120ctn <sup>KOC/fl</sup> ; Nes-Cre and p120ctn <sup>KIC/fl</sup> ; Nes-Cre mice ...	254
p120ctn <sup>KOC/fl</sup> ; Nes-Cre hippocampi display discrete medial abnormalities .....	256
Microcephaly in p120ctn <sup>KIC/fl</sup> ; Nes-Cre mice.....	262
p120ctn expression in hippocampal neurons.....	263
Fasciculation in p120ctn <sup>KIC/fl</sup> ; Nes-Cre hippocampal neurons .....	265
Transfection of transgenic hippocampal cultures.....	268
Immunohistochemistry with pAbexC on brain sections.....	270
CONCLUSION.....	272
ACKNOWLEDGEMENTS .....	272
REFERENCES .....	273

**GENERAL DISCUSSION AND FUTURE PERSPECTIVES 277****SUMMARY 289****SAMENVATTING 295****Curriculum vitae 301**



### List of abbreviations

2i: two small-molecule inhibitors  
3i: three small-molecule inhibitors  
AA: amino acid  
Ab: abembryonic pole  
AIG: anchorage-independent growth  
aPKC: atypical protein kinase C  
ARM: Armadillo repeat  
ARVCF: Armadillo repeat gene deleted in Velo-Cardio-Facial syndrome  
BMP: bone morphogenic protein  
CA: constitutively active  
CBD: beta-catenin binding domain  
CK1 $\alpha$ : casein kinase 1 $\alpha$   
DA: Dark Agouti  
DIV: days *in vitro*  
DMEM: Dulbecco's minimal essential medium  
DN: dominant negative  
dpc: day post coitum  
DSH: dishevelled  
EC: extracellular cadherin repeat  
EGFR: epidermal growth factor receptor  
Em: embryonic pole  
EMT: epithelial-to-mesenchymal transition  
Eomes: Eomesodermin  
epiSC: epiblast stem cell  
ERK: extracellular signal-related kinase  
ES: embryonic stem  
ESRP: epithelial splicing regulatory proteins  
FBS: fetal bovine serum  
FGF: fibroblast growth factor  
GAP: GTPase activating protein  
GAP1: Ras GTPase-Activating Protein 1  
GDI: guanine nucleotide dissociation inhibitor  
GDP: guanine diphosphate  
GEF: Guanine exchange factors  
GFP: green fluorescent protein  
Grb2: growth factor receptor-bound protein 2  
GSK-3: glycogen synthase kinase-3  
GTP: guanine triphosphate  
H&E: hematoxylin and eosin  
HGF: hepatocyte growth factor  
ICM: inner cell mass  
ILC: invasive lobular carcinoma  
iPS: induced pluripotent stem  
JAK: Janus kinase  
JMD: juxtamembrane domain  
KBS: Kaiso binding sites

## List of Abbreviations

KD: knockdown  
KIC: knockin of the alternatively spliced exon C of p12octn  
Klf4: kruppel-like factor 4  
KO: knockout  
KOC: knockout of the alternatively spliced exon C of p12octn  
LEF: lymphoid enhancer factor  
LIF: leukemia inhibitory factor  
LPA: lysophosphatidic acid  
M: methionine  
MAPK: mitogen-activated protein kinase  
MDCK: Madin-Darby Canine Kidney  
MEF: mouse embryonic fibroblast  
MEK: MAPK/ERK kinase  
MRI: magnetic resonance imaging  
NCAM: cell adhesion molecule  
NCOR: nuclear co-repressor  
NES: nuclear export signal  
NGF: nerve growth factor  
NLS: nuclear localization signal  
NOD: non-obese diabetic  
NPRAP: neural plakophilin-related Armadillo protein  
NSCLC: non-small cell lung cancer cells  
OR: olfactory receptor  
pAbexC: rabbit polyclonal antibody against amino acids encoded by exon C of p12octn  
PAR: partition-defective  
PD: phosphorylation domain  
PDGFR: platelet-derived growth factor receptor  
PE: primitive endoderm  
PI<sub>3</sub>K: phosphatidylinositol 3-kinase  
POZ: poxvirus and zinc finger  
PSD-95: post synaptic density protein 95  
PTP: protein tyrosine phosphatases  
RBD: RhoA-binding domain  
Roaz: Rat O/E-1-associated zinc finger  
ROCK: Rho-associated coiled kinase  
RTK: receptor tyrosine kinases  
RT-PCR: reverse transcriptase polymerase chain reaction  
SD: Sprague-Dawley  
SH2: Src homology 2 domain  
SHP-1: SH2 domain-containing protein tyrosine phosphatase 1  
SR: serum replacement  
STAT: signal transducer and activator of transcription.  
TCF: T-cell factor  
TE: trophectoderm  
TG: trophoblast giant  
TS: trophectoderm stem cells  
XEN: extraembryonic endoderm cells  
ZO: zonula occludens

# Introduction

---

# Chapter 1

---

## p120CTN IN NORMAL DEVELOPMENT AND TUMORIGENESIS

Text presented in this chapter forms the basis for two review articles in *Frontiers in Bioscience*:

Tim Pieters, Jolanda van Hengel, Frans van Roy

p120ctn family members in development and disease

submitted to *Frontiers in Bioscience* (invited review: special issue on “E-cadherin function in development and cancer”)

Tim Pieters, Frans van Roy, Jolanda van Hengel

p120 catenin: function follows isoform

submitted to *Frontiers in Bioscience* (invited review: special issue on “Cell Cell Adhesion and Communications in Development and Tumorigenesis”)

## **p120ctn in normal development and tumorigenesis**

# p120ctn in normal development and tumorigenesis

Tim Pieters<sup>1,2</sup>, Jolanda van Hengel<sup>1,2</sup>, Frans van Roy<sup>1,2</sup>

<sup>1</sup> Department for Molecular Biomedical Research, VIB, B-9052 Ghent, Belgium

<sup>2</sup> Department of Molecular Biology, Ghent University, Technologiepark 927, B-9052 Ghent, Belgium

## TABLE OF CONTENTS

1. Abstract.....	6
2. Introduction: An historical overview of p120ctn research.....	6
3. p120ctn isoforms and alternative splicing.....	9
4. p120ctn gene family.....	15
5. p120ctn and E-cadherin regulation.....	17
5.1. p120ctn interacts with cadherins and modulates adherens junctions.....	17
5.2. p120ctn regulates cadherin turnover: evidence from genetic and knockdown studies.....	18
5.3. p120ctn and cadherin biogenesis, endocytosis and degradation.....	19
6. p120ctn and RhoGTPases.....	20
6.1. p120ctn and dendritic-like branching.....	20
6.2. p120ctn mediates RhoA inhibition and activation of both Rac1 and Cdc42.....	23
6.3. Interaction between p120ctn and RhoA.....	24
6.4. Mechanism of p120ctn-mediated RhoA inhibition.....	24
6.5. RhoGTPases and cadherin-based junctions.....	26
6.6. p120ctn subfamily members and rhoGTPases.....	26
7. p120ctn interacts with transcription factors in the nucleus.....	27
8. p120ctn and phosphorylation.....	29
8.1. Phosphorylation of the cadherin-catenin complex.....	29
8.2. Phosphorylation of p120ctn.....	33
8.3. p120ctn isoforms and phosphorylation.....	35
9. The p120ctn family in animal models.....	36
9.1. Animal models for p120ctn.....	36
9.2. Animal models for p120ctn family members.....	38
10. p120ctn and cancer.....	38
10.1. Altered expression of p120ctn in tumors.....	38
10.2. p120ctn isoforms in emt and cancer.....	39
10.3. Differential regulation of rhoGTPases by p120ctn in cancer.....	41
10.4. p120ctn isoforms: effects on proliferation and tumor growth.....	42
10.5. p120ctn isoforms: effects on motility and invasion.....	42
10.6. p120ctn and anchorage-independent growth (AIG).....	43
10.7. p120ctn in inflammation and cancer.....	44
11. Acknowledgements.....	44
12. References.....	45

### 1. ABSTRACT

p120 catenin (p120ctn) belongs to the Armadillo family and is a component of the cadherin-catenin complex. It fulfils pleiotropic functions according to its subcellular localization: modulating the turnover rate of membrane-bound cadherins, regulating the activation of small RhoGTPases in the cytoplasm, and modulating nuclear transcription. Over the last two decades, knowledge of p120ctn obtained from in vitro experiments was confirmed and extended by different animal models. It became clear that, at least in frog and mammals, p120ctn is essential for normal development and homeostasis. p120ctn was originally identified as a Src substrate that can be phosphorylated at different tyrosine, serine and threonine residues, and can dock various kinases and phosphatases. Thereby, p120ctn regulates the phosphorylation status and the junctional stability of the cadherin-catenin complex. Multiple p120ctn isoforms have been identified. These isoforms result from alternative splicing, which allows the translation of p120ctn isoforms from four start codons and enables the inclusion of four alternatively used exons. In this review, we will discuss the effects of different p120ctn isoforms on cadherin turnover, RhoGTPase activity, Kaiso-binding, and phosphorylation. p120ctn is frequently downregulated and/or mislocalized in various human tumors, and the functional implications of p120ctn isoforms in various aspects of tumorigenesis will be reviewed. Finally, we will elaborate on the other members of the p120ctn subfamily, ARVCF, p0071 and delta-catenin, which are also affected by alternative splicing and are involved in the same processes as p120ctn.

## 2. INTRODUCTION: AN HISTORICAL OVERVIEW OF p120<sup>CTN</sup> RESEARCH

In this introductory part we look back upon the history of p120<sup>ctn</sup> and highlight several landmarks, such as the identification of p120<sup>ctn</sup>, the cloning of mouse and human p120<sup>ctn</sup> genes, and the major breakthroughs in understanding the functions of p120<sup>ctn</sup> (Fig. 1).

The founder of the p120<sup>ctn</sup> family was identified in 1989 as a most efficient substrate for the oncogenic Src tyrosine kinase A 120-kDa protein (hence the name p120<sup>ctn</sup>) was detected by phospho-tyrosine specific antibodies in cells expressing pp60<sup>527F</sup>, an oncogenic c-Src mutant, but it was not detected in cells expressing a non-membrane-associated pp60<sup>2A/527F</sup> double mutant (1). That study elegantly shows that the phosphorylation status of p120<sup>ctn</sup> correlates well with transformation. Src-mediated tyrosine phosphorylation of p120<sup>ctn</sup> and other constituents of adherens junctions was found to modulate or to perturb cadherin-based adhesion (Section 8) (2). The mouse p120<sup>ctn</sup> cDNA was cloned in a labor-intensive manner in 1992 and the predicted protein was found to encode armadillo repeats like those of beta-catenin (3). And like in the case of beta-catenin, the armadillo domain of p120<sup>ctn</sup> was found to interact with E-cadherin, a component of the adherens junction (4). The encoding mouse gene *Ctnnd1* was localized on chromosome 2, whereas the human gene *CTNND1* was localized on chromosome 11q11 (259, 260) More recently, the relationship between p120<sup>ctn</sup> and E-cadherin was further elucidated by generating p120<sup>ctn</sup>-uncoupled E-cadherin mutants, as well as by knockdown and knockout studies (Section 5). Using a very reliable pp120 monoclonal antibody, which recognizes an epitope in the C-terminal part of p120<sup>ctn</sup>, four main different protein isoforms could be distinguished, differing from each other by the extension of their N-termini (4). Detailed analysis of human p120<sup>ctn</sup> transcripts revealed that an even larger diversity (48 predictable isoforms) of the p120<sup>ctn</sup> protein occurred due to alternative splicing (Section 3) (5). Long isoforms have extended N-termini. Interestingly, these different p120<sup>ctn</sup> isoforms were expressed heterogeneously in normal cell lines and in tumor cell lines (6, 7). Further investigation on p120<sup>ctn</sup> isoforms showed that they are differentially expressed under several conditions pointing at specific roles in development and disease, in particular cancer (Section 10). Along with the identification of p120<sup>ctn</sup> isoforms came the identification of p120<sup>ctn</sup> family members, such ARVCF (Armadillo repeat gene deleted in Velo-Cardio-Facial syndrome), p0071 and *delta*-catenin/NPRAP/neurojungin (neural plakophilin-related Armadillo protein), and the more distantly related plakophilins 1-3 (Section 4) (reviewed in 8, 9).

Besides binding to membrane-bound cadherins, p120<sup>ctn</sup> can also perform functions in the cytoplasm and in the nucleus by interacting with RhoGTPases and Kaiso, respectively (Fig. 2). The first hint about the role of cytoplasmatic p120<sup>ctn</sup> came from overexpression studies. Strong overexpression of p120<sup>ctn</sup> saturated the cadherin-binding sites, and the excess p120<sup>ctn</sup> translocated to the cytoplasm, where it induced extensions that were neurite-like (10). Additional research revealed that p120<sup>ctn</sup> elicits a dendritic-like branching phenotype by modulating RhoGTPase activity (11-13), and this was confirmed by genetic and RNAi-mediated ablation of p120<sup>ctn</sup> (Section 6). Because p120<sup>ctn</sup> interacts physically with the transcription factor Kaiso (14), a nuclear function for p120<sup>ctn</sup> was envisioned. Indeed, p120<sup>ctn</sup> can tether away Kaiso from the nucleus, preventing its transcriptional repression (Section 7).



# p120ctn in normal development and tumorigenesis

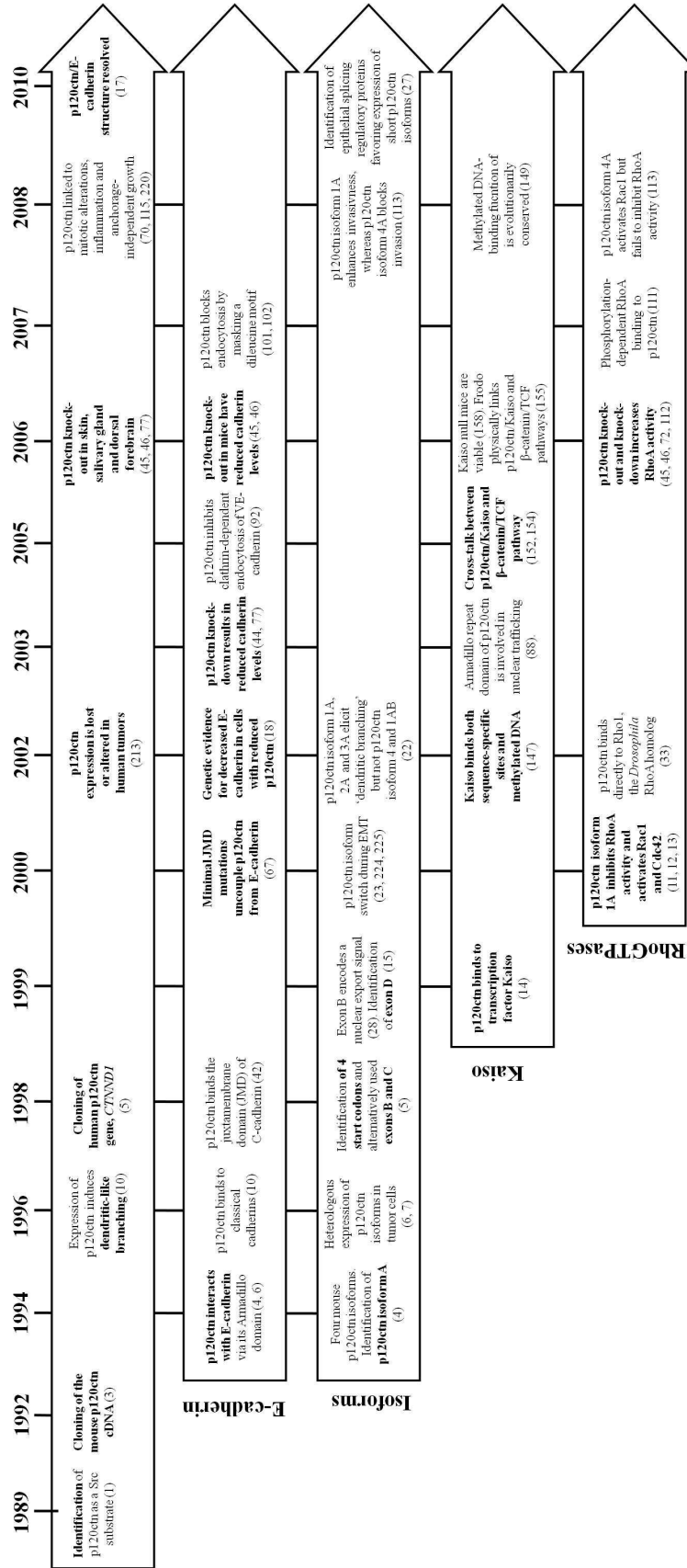


Figure 1. Time line depicting hallmarks of p120ctn research.

During the last decade, all those research leads were further pursued to gain some mechanistic insight into p120ctn biology. These investigations, which also included experiments on different animal models, overall showed that p120ctn is indispensable for normal vertebrate development (Section 9).

During its short history, it became clear that p120ctn is not translated as a single protein and that multiple p120ctn protein isoforms exist. Although p120ctn isoforms were discovered early, their regulation and significance in p120ctn biology remains largely unresolved. In this article we will review current knowledge of p120ctn by focusing on p120ctn isoforms, how they are expressed, and how they influence the several functions of p120ctn.

### 3. P120CTN ISOFORMS AND ALTERNATIVE SPLICING

In 1998, the human p120ctn gene (*CTNND1*), situated on chromosome 11q11, was cloned, and inter- and intra-exonic splicing events generated multiple p120ctn mRNA variants encoding different isoforms (5). Forty-eight putative p120ctn isoforms were generated by employing four different translation initiation sites (M1-4) combined with four alternatively spliced exons (A to D; Fig. 3) (5, 15). p120ctn 1ABC is the longest isoform with 968 amino acid residues (AA), contains all the alternatively spliced internal exons, and is translated from the first start codon to produce a protein with the longest N-terminal domain (Fig. 3). p120ctn isoform 3 has a shortened N-terminal domain as it lacks 100 AA containing a coiled-coil domain, whereas p120ctn isoform 4 lacks almost the entire N-terminal domain in front of the armadillo repeat domain, including the phosphorylation domain (PD) containing most phosphorylation sites of p120ctn. The central armadillo repeat domain has nine armadillo repeats (not ten as was previously proposed), with each repeat consisting of three helices (16, 17). This armadillo repeat domain is not much affected by alternative splicing. Only the six AA encoded by the alternatively spliced exon C are situated in the insert loop between armadillo repeat ARM5 and ARM6, but this will probably not cause conformational changes in the overall structure of the armadillo repeat domain (16, 17). In retrospect the four p120ctn isoforms identified by Reynolds et al. (4) were the long p120ctn isoforms 1N and 1A and short p120ctn isoforms 3N and 3A, with additional internal AA being encoded by the alternatively spliced exon A.

p120ctn is ubiquitously expressed during development and in adult organisms, except for several non-adherent hematopoietic cell lines and loosely organized SW48 colon carcinoma cells, which exhibit very weak p120ctn expression (7, 18). p120ctn isoform 1 (120 kDa or long isoform) and p120ctn isoform 3 (100 kDa or short isoform) display tissue-specific and cell-specific expression patterns (Table 1). Long p120ctn isoform 1 is predominantly expressed in highly motile cells, such as fibroblasts (e.g. NIH3T3 cells) and macrophages (4, 7, 19). In normal tissues, long p120ctn isoforms are predominantly expressed in the central and peripheral nervous systems, heart, spleen, testis, ovary and endothelial cells (15, 20, 21). In contrast, p120ctn isoform 3 is abundant in epithelial cell lines (4, 7, 19) and epithelial structures of the skin and the gastro-intestinal lining, which have a rapid turnover, as well as in kidney, liver, pancreas, mammary gland and prostate (5, 15, 20, 21). These cells and tissues show bias for expression of

## p120ctn in normal development and tumorigenesis

certain p120ctn isoforms, but most cells and tissues express both long and short isoforms. Even different cell types within the same organ can express different p120ctn isoforms. For example, the skin is composed of keratinocytes and melanocytes. Primary keratinocytes express mainly short p120ctn isoforms in a honey-comb pattern, whereas melanocytes, which have a dendritic-like morphology, express mainly long p120ctn isoforms (22). Since long p120ctn isoforms are expressed in endothelial cells, which are present in all organs to provide oxygen, tissue preparations from any organ might be contaminated with these isoforms. Interestingly, a switch from short to long p120ctn isoforms is seen during epithelial-to-mesenchymal transition (EMT), which is induced by expression of c-Fos (23), Snail (24), SIP1/ZEB2 (25, 26), E47 (26), Slug (26) or Twist (27) (see Section 10.2. for more details).

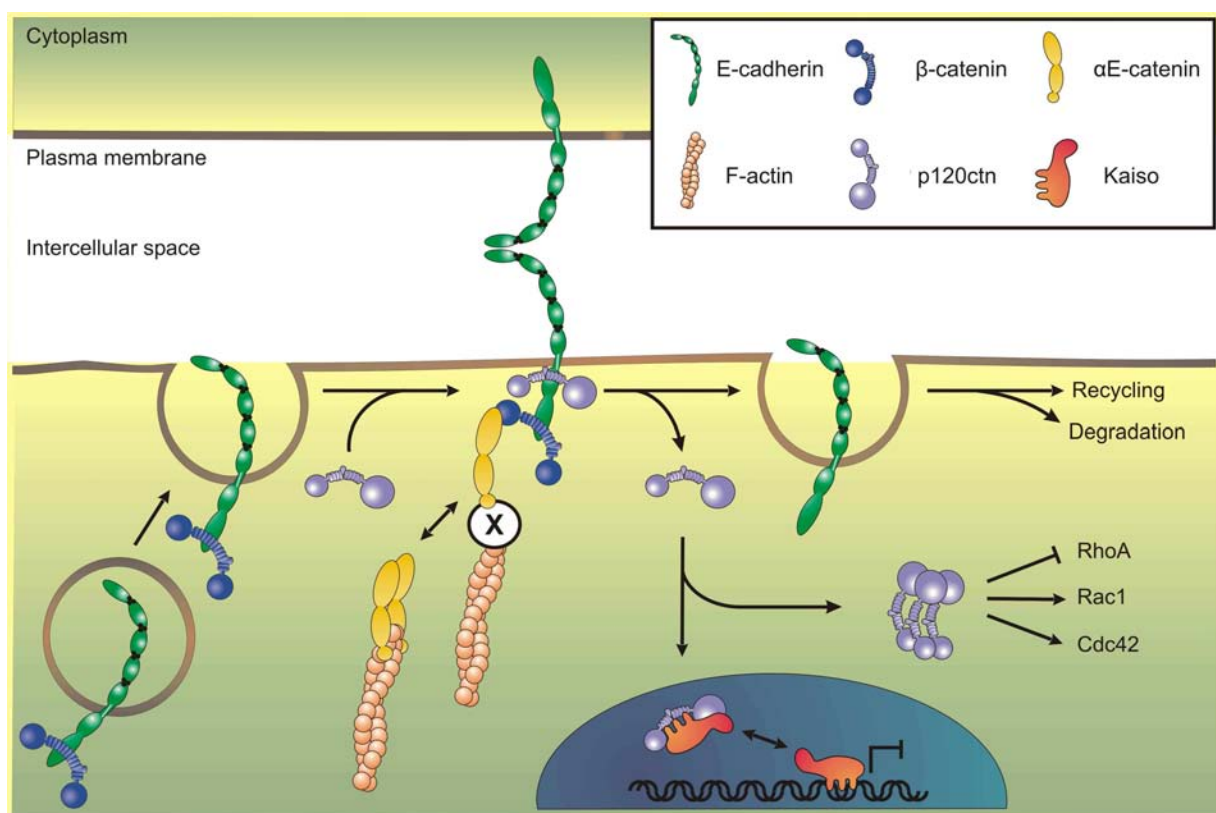


**Figure 2.** p120ctn performs different functions in different subcellular locations. Adherens junctions consist of transmembrane cadherins, which can bind to beta-catenin and p120ctn via their cytoplasmic tails. Beta-catenin binds to alpha-catenin, which can link to the actin cytoskeleton via an adaptor (e.g. Epln) or as an unbound dimeric complex. p120ctn binds to the juxtamembrane domain of cadherins and prevents their endocytosis. Internalized cadherin molecules can be recycled or targeted for degradation. Cytoplasmic p120ctn can regulate RhoGTPase activity, whereas nuclear p120ctn can inhibit Kaiso-mediated transcriptional repression.

**Table 1.** Expression of long and short p120ctn isoforms in cell lines, normal tissues and tumors.

Cell or tissue	Species	Cell type	Cadherin type	p120ctn isoform		Detection method	Reference
				long	short		
<b>Normal tissues</b>							
	M	mammary gland		+	+++	a	(5)
	M	small intestine		+	+++	a	(5)
	H	brain		+		a	(15)
	H	heart		+++	+	a	(15)
	H	kidney		+	+++	a	(15)
	H	liver		+	++	a	(15)
	H	lung		+	+++	a	(15)
	H	skelatal muscle			+	a	(15)
	H	spleen		+++	+	a	(15)
	H	thymus		+	++	a	(15)
	H	pancreas			+++	a	(15)
	H	colon			+++	a	(15)
	H	small intestine			+++	a	(15)
	H	prostate			+++	a	(15)
	H	testis		+++	+	a	(15)
	H	ovary		+++	+	a	(15)
	H	placenta		+	+++	a	(15)
	H	leukocyte		+		a	(15)
	H	keRinocyte			+	a	(15)
	R	isolated enterocytes		+	+++	b	(20)
	R	tongue mucosa		++	++	b	(20)
	R	pancreas		+	+++	b	(20)
	R	kidney		++	+	b	(20)
	R	seminiferous tubules of testis		+		b	(20)
	R	liver		++	++	b	(20)
	R	heart		++		b	(20)
	R	retina		+++		b	(20)
	R	cerebellum		+++		b	(20)
	M	eye		+++	++	c	(21)
	M	skin		+++	+++	c	(21)
	M	calvaria		+++		c	(21)
	M	fore stomach		++	+	c	(21)
	M	back stomach		++	+	c	(21)
	M	bladder		+++	+	c	(21)
	M	thymus		++	++	c	(21)
	M	spleen		+++	+	c	(21)
	M	brain		+++	+	c	(21)
	M	skeletal muscle		+		c	(21)
	M	heart		+++	+	c	(21)
	M	lung		+++	+++	c	(21)
	M	kidney			++	c	(21)
	M	testis		+++	++	c	(21)
<b>Tumors</b>							
GI-112	H	colon adenocarcinoma			++	a	(15)
CX-1	H	colon adenocarcinoma				a	(15)
GI-103	H	pancreatic adenocarcinoma		++	+	a	(15)
PC-3	H	prostatic adenocarcinoma			+++	a	(15)
GI-117	H	lung carcinoma		++	+++	a	(15)
LX-1	H	lung carcinoma			+++	a	(15)
GI-101	H	breast carcinoma				a	(15)
GI-102	H	ovarian carcinoma			+	a	(15)

## p120ctn in normal development and tumorigenesis

<b>Cell lines</b>							
NIH3T3	M	fibroblast	N	+++	+	d	(4)
Swiss3T3	M	fibroblast	N	+++	+	d	(7, 19)
C3H 10T1/2	M	fibroblast	N	+++		d	(7)
WEG-1	M	fibroblast-like cells derived from uterine epithelium (SV40 T-antigen, E-cadherin deficient)		+++		d	(7)
Bac1.2F5	M	macrophage cell line		+++	+	d	(7)
VA13	M	SV40 virus transformed lung fibroblasts		+++	++	a	(5)
32 D	M	myeloid cells				d	(7)
Ag 8	M	B lymphocyte				d	(7)
MDCK	D	epithelial cells derived from kidney	E	+	+++	d	(4, 19)
MDBK	B	epithelial cells derived from kidney		+++	+++	d	(19)
EVC304	H	endothelial cells derived from umbilical vein endothelial cells		++	+++	d	(19)
LLC-PK1	P	epithelial cells derived from kidney		+++	+++	d	(19)
RBE4	R	immortalized brain endothelial cells		+++	+	d	(19)
brain EC	B	primary brain endothelial cells		+++	+++	d	(19)
TM4	M	epithelial sertoli cells derived from testis		++	+++	d	(7)
CommaD	M	epithelial mammary cell line		++	+++	d	(7)
<b>Tumor cell lines</b>							
caco-2	H	epithelial cells derived from colonic tumor		+	+++	d	(19)
HCT116	H	epithelial cells derived from colon carcinoma	P, E		+++	d	(6, 7)
SW480	H	epithelial cells derived from colon carcinoma	P, little E	+	+++	d, a	(6, 7) (5)
DLD-1	H	epithelial cells derived from colon adenocarcinoma	E, P	+	+++	d	(7)
SW620	H	epithelial cells derived from colon carcinoma	P, little E	+	+++	d	(7)
Lovo	H	epithelial cells derived from colon carcinoma	P, E	++	+	d	(7)
Colo 205	H	epithelial cells derived from colon carcinoma (dispersed)	E	++		d	(7)
Va-2	H	epithelial cells derived from forskin fibroblast cells		+++	++	d	(7)
A-431	H	epithelial cells derived from cervical carcinoma			+++	d	(7)
Hela	H	epithelial cells derived from cervical carcinoma		+++	+++	d	(7)
Hep G2	H	epithelial cells derived from liver carcinoma		++	+++	d	(7)
PC3	H	prostate cancer epithelial cells ( $\alpha$ -catenin deficient)	N, E, P		+++	d	(6, 7)
Bewo	H	epithelial cells derived from choriocarcinoma			++	d	(7)
Capan 2	H	epithelial cells derived from pancreatic adenocarcinoma		++	+++	d	(7)
ZR75B	H	epithelial cells derived from breast carcinoma	E, P		+++	d	(7)
MCF-7	H	epithelial cells derived from breast ductal carcinoma	E, P		++	d	(7)
SKB-3	H	epithelial cells derived from breast carcinoma	E, P neg		+++	d	(7)
MDA 231	H	epithelial cells derived from breast carcinoma	E, P neg	+	+++	d	(7)
MDA468	H	epithelial cells derived from breast carcinoma	P, E		+++	d	(7)
BT 474	H	epithelial cells derived from breast carcinoma	E, P	+++	+++	d	(7)
T470	H	epithelial cells derived from breast carcinoma	E, P	+++	+++	d	(7)
Fekete	H	trophectodermal carcinoma cell line (weak adherence)				d	(7)
Molt 4	H	T-lymphocyte				d	(7)
Raji	H	B-lymphocyte				d	(7)
MKN45	H	gastric carinoma			+++	a	(5)
KATOIII	H	gastric carinoma			+++	a	(5)
HT29	H	colon adenocarcinoma			+++	a	(5)
SK-LMS1	H	leiomyosarcoma cells		++	++	a	(5)
SK-ES1	H	osteosarcoma cells		++	++	a	(5)
GLC34	H	small cell lung carcinomas		+++	+++	a	(5)
GLC8	H	small cell lung carcinomas		+++		a	(5)
HCT8	H	ileocecical adenocarcinoma			+++	a	(5)

PC AA/C1	H	colon adenocarcinoma			+++	a	(5)
LICR-HN2	H	squamous carcinoma cells derived from larynx			+++	a	(5)
LICR-HN6	H	squamous carcinoma cells derived from larynx			++	a	(5)
<b>p120ctn isoform switch in EMT</b>							
IMEp-1	M	mammary epithelial cells	E		+++	+	b (23)
IMEp-1	M	mammary epithelial cells + c-Fos	E neg			+++	b (23)
MDCK	D	epithelial cells derived from kidney	E		+++	+	b (24)
MDCK	D	epithelial cells derived from kidney + Snail	E neg			+++	b (24)
MDCK	D	epithelial cells derived from kidney + Snail + E-cadh				+++	b (24)
DLD1	H	colon cancer cell line	E			+++	b (25)
DLD1	H	colon cancer cell line + SIP1	E neg		+++	++	b (25)
MDCK	D	epithelial cells derived from kidney	E		+++		c (26)
MDCK	D	epithelial cells derived from kidney + Snail	E neg		+	++	c (26)
MDCK	D	epithelial cells derived from kidney + E47	E neg		+	++	c (26)
MDCK	D	epithelial cells derived from kidney + Slug	E neg		+	+++	c (26)
HMLE	H	mammary epithelial cells				+++	a (27)
HMLE	H	mammary epithelial cells			++	++	a (27)
LIM1863	H	colon carcinoma (highly differentiated)	E		+++	+++	b (114)
LIM1863	H	colon carcinoma + TGF- $\beta$ - and TNF- $\alpha$ -	E neg		+++	+++	b (114)
MDCK	D	epithelial cells derived from kidney			++	+++	d (7)
MDCK	D	epithelial cells derived from kidney + Src			+++	+	d (7)
<b>p120ctn isoform switch in cancer</b>							
LNCaP	H	epithelial prostate carcinoma cells	E			+++	b (224)
DU145	H	epithelial prostate carcinoma cells	E		+	++	b (224)
PC3N	H	mesenchymal prostate carcinoma cells	N		++	+	b (224)
PC3	H	mesenchymal prostate carcinoma cells	N, little E		++	++	b (224)
JCA1	H	mesenchymal prostate carcinoma cells	N		++	+	b (224)
-	H	prostate stromal fibroblasts	N		+++	+	b (224)
-	H	non-neoplastic thyrocytes	E			+++	b (225)
HTh7	H	anaplastic thyroid carcinoma cells	N		++	+	b (225)
C643	H	anaplastic thyroid carcinoma cells	N		++		b (225)
SW1736	H	anaplastic thyroid carcinoma cells	N		++	+	b (225)
HTh4	H	anaplastic thyroid carcinoma cells	N		+++	+	b (225)
HaCat	H	benign immortalized keRinocytes				+++	a (216)
DJM-1	H	malignant skin carcinoma cells				+++	a (216)
BSCC-93	H	malignant skin carcinoma cells				+++	a (216)
HSC-1	H	malignant skin carcinoma cells				+++	a (216)
HSC-5	H	malignant skin carcinoma cells				+++	a (216)
A431	H	malignant skin carcinoma cells				+++	a (216)
NHK	H	neonatal H keRinocytes			+	+++	c (22)
HaCat	H	immortalized aneuploid keRinocyte cells			+++	+	c (22)
A431	H	squamous cell carcinoma			+++		c (22)
A253	H	squamous cell carcinoma			+++		c (22)
FADU	H	squamous cell carcinoma			++		c (22)
SCC12	H	squamous cell carcinoma			++		c (22)
DET562	H	squamous cell carcinoma			++		c (22)
FM51	H	immortalized melanocytes			++	+	c (22)
6SV3/3	H	immortalized melanocytes			++	+	c (22)
WM793	H	malignant melanoma cells			+++	+	c (22)
1205-LU	H	malignant melanoma cells			+++	+	c (22)
WM164	H	malignant melanoma cells			++	+	c (22)
451-LU	H	malignant melanoma cells			+++	+	c (22)

a: RT-PCR, b: pp120 antibody, c: pp120 and 6H11 antibodies, d: pp120 and 2B12 antibodies; B: bovine, P: porcine, H: human, M: mouse, R: rat, D: dog.

## p120ctn in normal development and tumorigenesis

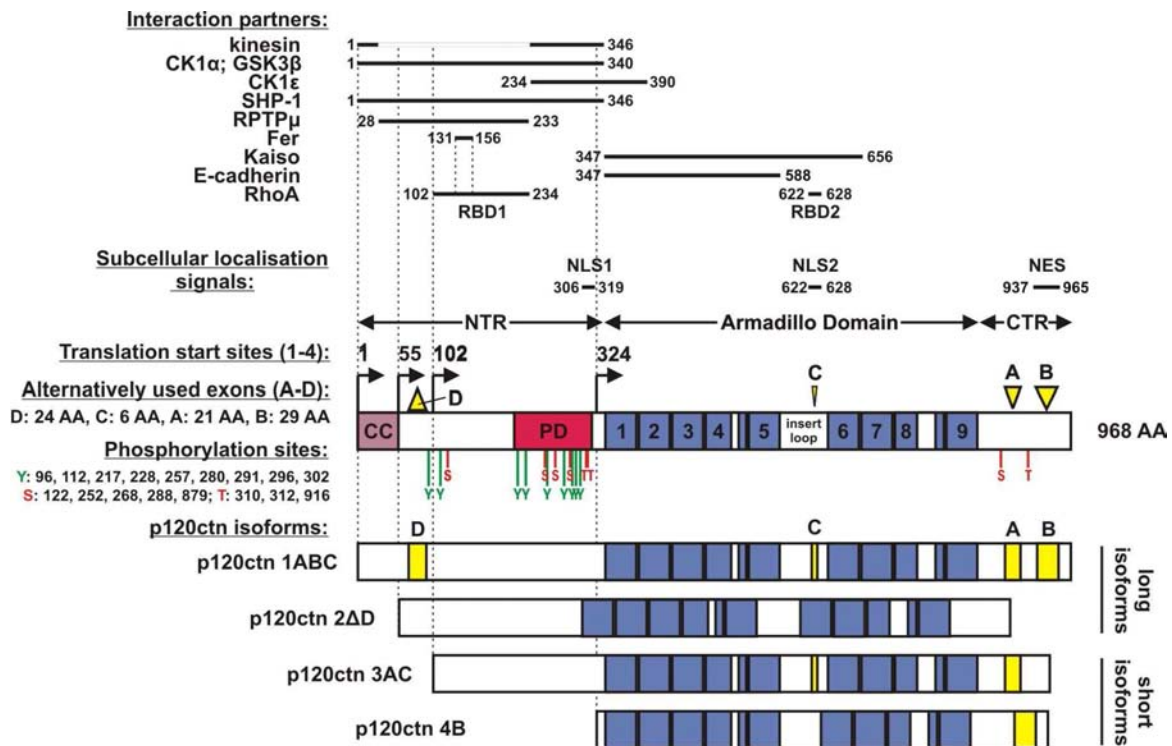


**Figure 3.** p120ctn structure. p120ctn structural features include interaction domains, subcellular localization signals, phosphorylation sites and alternative splice forms. The p120ctn domains for binding different interaction partners are shown. p120ctn contains two conventional nuclear localization signals (NLS) and a nuclear export sequence (NES), but armadillo repeats (ARM) 3, 5 and 8 have also been implicated in nuclear trafficking. As a result of alternative splicing, four translation start site (1 to 4) can be used. Alternatively spliced exons A, B and C, encoding 21, 29 and 6 amino acid residues (AA), respectively, can be included, whereas exon D (encoding 24 AA) is rarely excluded. p120ctn isoform 1ABC is the longest isoform, employs the first start codon, and contains all alternatively spliced exons. CC, coiled coil domain; CTR, carboxy-terminal (non-armadillo) region; NTR, amino-terminal (non-armadillo) region; PD, phosphorylation domain, comprising many Ser, Thr and Tyr residues for which phosphorylation under particular conditions has been demonstrated; RBD, RhoA-binding domain.

It is not clear how the splicing events generating these isoforms are regulated. However, two epithelial splicing regulatory proteins (ESRP1 and ESRP2) favoring the expression of epithelial isoforms of various proteins, including the short ‘epithelial’ p120ctn isoform, were recently identified (27). Reduction of ESRP1 and ESRP2 levels by RNAi-mediated knockdown or by Twist-induced EMT resulted in a switch from short to long p120ctn isoforms. Expression of ‘epithelial’ p120ctn in mesenchymal cells could be induced by introducing ESRP1, which causes a switch toward the epithelial splicing pathway (27). Identification of these epithelial splicing factors has been an important breakthrough in understanding the molecular regulation of different splice variants of p120ctn. However, many questions remain unanswered. Is the expression of epithelial splicing factors sufficient for expression of short ‘epithelial’ p120ctn

isoforms? Is there a default ‘mesenchymal’ splicing setting? Or are there also mesenchymal splicing factors, which somehow compete with the epithelial splice factors for generation of long and short p120ctn isoforms?

The transcript diversity of p120ctn is increased by alternative splicing of internal exons. In man or mouse, exon A encodes a 21-AA sequence that is ubiquitously expressed in various cell lines and tissues (Fig. 3) (5). Exon B encodes a putative nuclear export signal (NES) with a characteristic leucine motif that counteracts the nuclear localization of p120ctn isoform 3A (28). Exon C encodes six AA that interrupt the second nuclear localization signal (NLS2) of p120ctn, which coincides with the second RhoA-binding domain (RBD2) (Fig. 3). Expression of exon C blocks at the same time nuclear localization and inhibits dendritic-like branching (Pieters et al., in preparation). Exon C is strongly expressed in brain (5) (Pieters et al., in preparation). A rare deletion of a fourth alternatively spliced internal exon, exon D, was reported in fetal and adult brain tissue (15). In conclusion, alternative exon usage regulates the subcellular localization of p120ctn isoforms and therefore directs their functionality.

#### 4. P120CTN GENE FAMILY

The family of armadillo catenins consists of three subfamilies: the p120ctn subfamily (p120ctn, ARVCF, p0071 and delta-catenin), the plakophilin subfamily (plakophilins 1 to 3) and the beta-catenin subfamily (beta-catenin and plakoglobin) (8, 29). The p120ctn subfamily members associate with cadherins to form proper adherens junctions, while members of the plakophilin subfamily support desmosomal adhesion. We will not discuss the beta-catenin and plakophilin subfamilies; they have been extensively reviewed elsewhere (30-32).

Invertebrates, such as *Caenorhabditis elegans* and *Drosophila melanogaster*, have only a few catenin genes. Only one beta-catenin and one p120ctn ancestor have been identified in *Drosophila*, whereas *C. elegans* contains four highly divergent beta-catenins and only one p120ctn subfamily member (33-36). Interestingly, sequence analysis revealed that invertebrate p120ctn resembles most the vertebrate delta-catenin and not p120ctn (9). In vertebrates and in particular in mammals, the diversity of the p120ctn family has increased throughout evolution. This has led to the emergence of two evolutionarily conserved clusters, on the one hand the p120ctn and ARVCF branch, and on the other hand the p0071 and delta-catenin branch (9).

All p120ctn family members have similar overall structures, with a central armadillo repeat domain containing nine armadillo repeats (Fig. 4) (16, 17). This central armadillo repeat domain enables all p120ctn subfamily members to bind the juxtamembrane domain (JMD) of classical cadherins (37-42). Upon overexpression ARVCF and delta-catenin can compete with p120ctn for JMD binding (38, 43) and they can restore cadherin-based junctions in p120ctn-depleted cells (44). However, at endogenous levels apparently none of them can substitute for



## p120ctn in normal development and tumorigenesis

p120ctn. Indeed, endogenous ARVCF and delta-catenin fail to stabilize classical cadherins in tissue-specific p120ctn knockout mice (45-47).

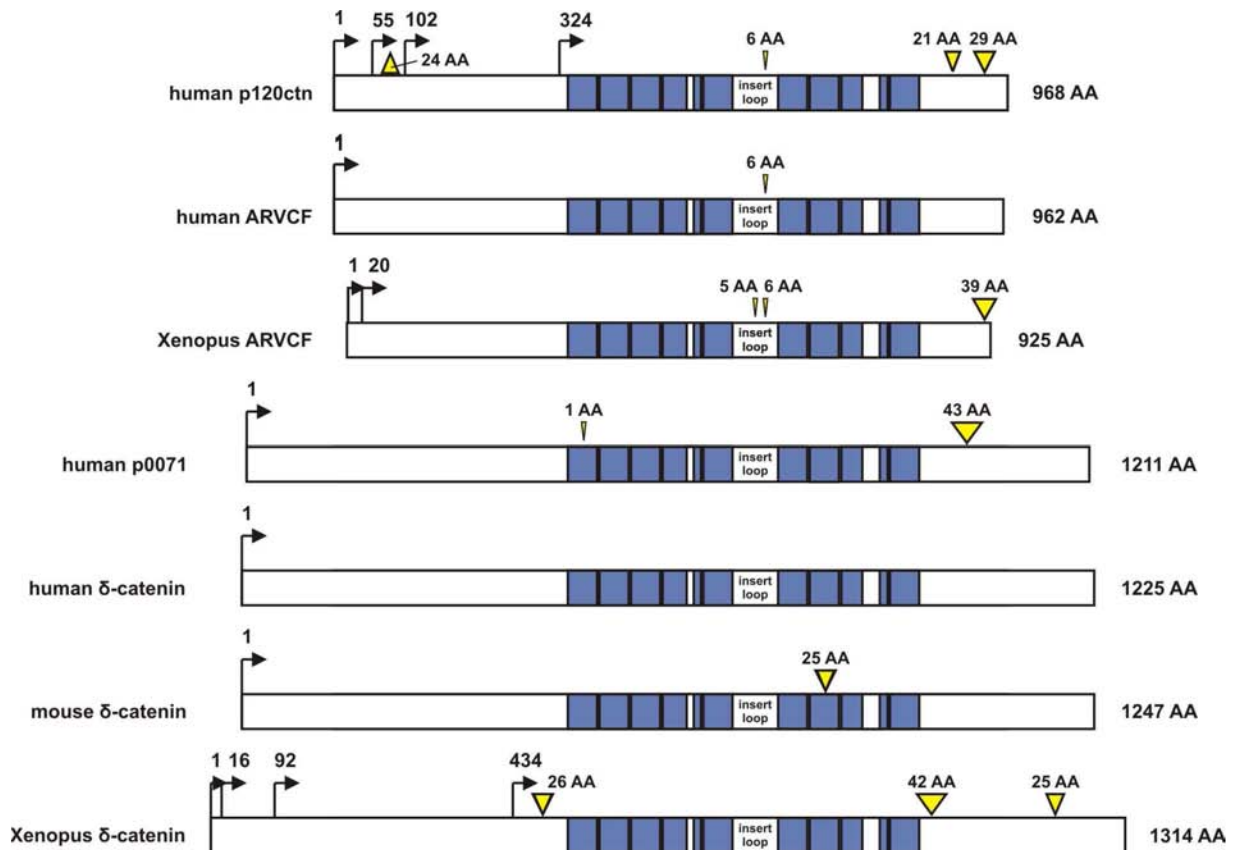


**Figure 4.** Overview of isoforms of p120ctn subfamily members. Yellow triangles indicate sequences, encoded by alternatively spliced exons. In case of alternatively used start codons, the multiple translation start sites are also indicated. Armadillo repeats are represented by blue boxes. The protein sizes for the longest forms are indicated at the right. AA: amino acid residues.

ARVCF was identified as an armadillo repeat gene that is deleted in the velo-cardio-facial syndrome. It encodes 962 AA and is most closely related to p120ctn (39). Like p120ctn, ARVCF is ubiquitously expressed in different tissues, but ARVCF is much less abundant (38). Also like p120ctn, ARVCF localizes to the nucleus in some cell types (38). Multiple isoforms of *Xenopus* ARVCF have been reported (Fig. 4), including the use of two different translation initiation sites and three alternatively spliced inserts of 15, 18 and 117 bp (41). This 18-bp insert has also been found in human ARVCF (39) and corresponds to p120ctn exon C (5). Exon C of *Xenopus* ARVCF is expressed strongest in brain (41). Human ARVCF too is expressed as multiple isoforms, which points to extensive alternative splicing like that observed for p120ctn (38).

The p0071 protein is officially known as plakophilin-4, encoded by the *PKP4/Pkp4* gene, but this is actually a misnomer, as it shows higher homology with delta-catenin and p120ctn than with any of the genuine plakophilins (Pkp-1 to -3). The p0071/Pkp4 protein is ubiquitously expressed and localizes in adherens junctions by means of its central armadillo repeat domain, and in desmosomes by virtue of its N-terminus (37, 48). However, using novel antibodies, Hofmann *et al.* (49) localized p0071 in non-desmosomal adherens junctions but not in desmosomes of MCF-7 human breast carcinoma cells, human skeletal muscle and lung epithelium, and bovine pancreas, tongue, thymus and lymphatics. In addition, p0071 is targeted to the midbody by the kinesin-II family member, KIF3, but it is also located at the centrosomes and spindle bodies of mitotic cells, and at composite junctions (*areae compositae*) of the intercalated disks of cardiomyocytes (49-51). p0071 is larger than p120ctn (1211 AA versus 981 AA) and has a more extended N-terminus and C-terminus (48). Splice variants of p0071 have been reported (Fig. 4), including a large variant, found in a brain cDNA library and a smaller variant, detected in A431 and HeLa cells (48). The long and short variant mRNAs encode, respectively, a long isoform (1212 AA) that lacks valine residue 488, and a shorter isoform that lacks a stretch of 43 AA (Fig. 4).

Delta-catenin was discovered as a presenilin-1-binding protein (52). It is expressed almost exclusively in the nervous system (52-55). The human and mouse delta-catenins encompass 1225 and 1247 AA, respectively, and the mouse delta-catenin has a 25-AA insert in armadillo repeat 7 (new nomenclature based on (16, 17)) possibly due to alternative splicing (Fig. 4) (40, 56). The insert loop of delta-catenin contains a polylysine stretch similar to the NLS of p120ctn (Fig. 3, AA 622-628) (40). Four translation initiation sites have been identified in *Xenopus* delta-catenin in combination with three alternatively used sequence elements (A-C) (Fig. 4) (57). *In vitro*, several tyrosine residues in the N-terminal domain of delta-catenin can be phosphorylated by tyrosine kinase Abl (58) or by Src family members (59). In humans, loss of delta-catenin can result in the Cri du Chat syndrome, featured by severe mental retardation (60).

## 5. P120CTN AND E-CADHERIN REGULATION

### 5.1. p120ctn interacts with cadherins and modulates adherens junctions

The role of p120ctn in regulating cadherin stability and turnover has been studied intensively (61-65). In vertebrates, the armadillo repeat domain of p120ctn interacts with the JMD of E-cadherin, and together with beta-catenin and alpha-E-catenin they make up the adherens junction complex (Fig. 2) (4, 42). Armadillo repeats 1 to 5 of p120ctn are essential for this interaction (17, 18), and the exact stoichiometry of the cadherin-catenin complex has been determined (6, 19, 66). Interestingly, both long and short p120ctn isoforms (isoforms 1 and 3, respectively) can bind E-cadherin but they cannot bind each other in a higher order molecular complex (19). Cadherin-binding is essential for the membrane localization of p120ctn: introducing exogenous E-cadherin in E-cadherin-negative cells relocalized p120ctn from the cytoplasm to the membrane (67). Minimal mutations in the JMD selectively uncoupled p120ctn from E-cadherin, disabled p120ctn phosphorylation, and interfered with cell-cell adhesion (67).

## p120ctn in normal development and tumorigenesis

In contrast to this evidence for a supportive role for p120ctn in cadherin-mediated adhesion (see also Sections 5.2 and 5.3), some reports postulated p120ctn as a negative regulator of cadherin function (68, 69). Phosphorylation was proposed as a probable explanation for this discrepancy because E-cadherin-mediated cell aggregation could be induced by treatment with the kinase inhibitor staurosporine, and by expression of N-terminal p120ctn mutants lacking the phosphorylation domain. However, the negative regulation of cell-cell adhesion might not be p120ctn-specific, but may be the consequence of a shift in overall phosphorylation levels of cadherin-based junctions, which ultimately affects their adhesive strength (see also Section 8). Alternatively, differential expression of p120ctn isoforms might explain why p120ctn can act both as a positive and negative regulator. In both instances in which p120ctn acted as a negative regulator, the authors used a ‘mesenchymal’ p120ctn isoform 1 construct, which is predominantly expressed in non-epithelial cell types, in order to induce cell-cell adhesion. Colo-205 cells express only p120ctn isoform 1 (68). Expressing p120ctn isoform 1 in E-cadherin-deficient mouse fibroblastic L-cells probably stabilizes their mesenchymal phenotype rather than transforming it to an adherent one. A better option could have been to co-transfect L-cells with E-cadherin cDNA and a construct encoding and the ‘epithelial’ p120ctn isoform 3, which is expressed in junctions of epithelial tissues and cell lines.

### 5.2. p120ctn regulates cadherin turnover: evidence from genetic and knockdown studies

The positive regulatory effect of p120ctn on cadherin expression levels was further underscored in several studies that used RNAi-mediated or genetic depletion of p120ctn in, respectively, cells and laboratory animals. The first clue that p120ctn is critical for cadherin function emerged from analysis of SW48 colon carcinoma cells bearing mutations in the p120ctn gene (18). Due to p120ctn insufficiency, these poorly differentiated cells failed to form compact colonies and displayed less E-cadherin protein but not reduced E-cadherin mRNA (18). The epithelial morphology and the cadherin levels could be restored by expressing p120ctn isoform 1, 3 or 4, or by using a RhoA-uncoupled variant of p120ctn isoform 1 (*delta662-628*), but not by using an E-cadherin-uncoupled p120ctn mutant. Pulse chase experiments revealed that p120ctn expression increased the E-cadherin half-life (18).

Stable RNAi-mediated knockdown of p120ctn in mammalian cells resulted in a drastic and dose-dependent decrease of classical cadherins, such as E-, N-, P-, and VE-cadherin (44, 70, 71), as well as mesenchymal cadherins (72). Furthermore, the absence of p120ctn also resulted in decreased expression of beta- and alpha-E-catenin due to decreased cadherin levels (44, 70). Human cells depleted of p120ctn became dispersed, but introduction of a murine p120ctn cDNA rescued both morphology and cadherin levels (44). Cadherin chimeras, comprising the extracellular domain of interleukin-2 receptor and the cytoplasmic tail of VE-cadherin that still binds p120ctn, reduce endogenous VE-cadherin levels due to increased internalization of cell surface VE-cadherin, whereas p120ctn-uncoupled variants of such chimeras do not show such an effect (71).

In *Drosophila melanogaster* and *Caenorhabditis elegans*, p120ctn is dispensable for the formation of cadherin-based junctions and exerts merely a supportive role (34, 35, 73). In contrast, p120ctn has been shown to stabilize cadherin levels *in vivo* both in amphibians and in mammals. Knockdown of p120ctn (74, 75) or of its family members ARVCF (75) or delta-catenin (57) in *Xenopus* embryos reduces the levels of classical cadherins. Moreover, gastrulation defects seen upon p120ctn or delta-catenin depletion in *Xenopus* could be rescued by ectopic expression of C-cadherin (57, 75). Tissue-specific p120ctn depletion in mice decreases levels of E-cadherin (45-47, 76), N-cadherin (76-78), P-cadherin (46) and VE-cadherin (78). In conclusion, p120ctn regulates cadherin turnover at the cell membrane both *in vitro* and *in vivo*.

### 5.3. p120ctn and cadherin biogenesis, endocytosis and degradation

How does p120ctn regulate cadherin trafficking? Cadherin-based junctions are highly dynamic, and cadherin complexes are constantly assembled and disassembled. The process of cadherin trafficking involves cadherin synthesis in the Golgi, transport to the cell surface, stabilization at the cell surface or internalization, followed by recycling or proteasomal or lysosomal degradation (Fig. 2) (79, 80). When newly synthesized E-cadherin is transported from the Golgi complex to the plasma membrane, its basolateral targeting depends on a membrane-proximal dileucine motif in the cadherin tail and on its association with beta-catenin (81, 82). Unlike beta-catenin, p120ctn does not interact with E-cadherin during its biogenesis (83), and p120ctn-uncoupled E-cadherin is indeed properly targeted to the plasma membrane (67). In contrast, p120ctn has been reported to associate with N-cadherin early during its biogenesis (84), and both N-cadherin and p120ctn move along microtubule tracks towards cell-cell contacts (85, 86). p120ctn isoform 1 colocalizes and interacts with microtubules and the motor protein kinesin, which transports cargos towards the plus ends of microtubules (towards the plasma membrane) (86-88). The N-terminus of p120ctn binds to the heavy chain of kinesin, whereas both an N-terminal deletion mutant and native p120ctn isoform 4 do not bind kinesin (86, 87, 89). p120ctn isoform 1 containing the entire N-terminal domain binds to kinesin with a higher affinity than p120ctn isoform 3, which lacks 100 AA of the N-terminus (87). p120ctn might therefore play a role in delivering N-cadherins to the plasma membrane, and disassembly of the N-cadherin/p120ctn/kinesin complex indeed delayed the delivery of N-cadherin to cell-cell contacts (86). In contrast, delivery of newly synthesized E-cadherin to the plasma membrane was not delayed by depletion of p120ctn (44).

Cell surface cadherins can be internalized *via* different pathways, including clathrin-dependent endocytosis (90-94), caveolae-mediated endocytosis (95, 96), lipid-raft-mediated endocytosis (97, 98) and micropinocytosis (99, 100). The decision to enter a certain endocytotic pathway is highly cell-specific and depends on the microenvironment. p120ctn blocks clathrin-mediated endocytosis of VE-cadherin, and this inhibition depends on the binding of p120ctn to the JMD of VE-cadherin (92). On the other hand, increased E-cadherin endocytosis was observed in cells expressing a p120ctn-uncoupled E-cadherin mutant as well as in cells in which p120ctn was depleted by RNAi (101). It is not clear how p120ctn prevents endocytosis, but several possibilities have been proposed. First, a dileucine motif in the cytoplasmic tail of E-cadherin

## **p120ctn in normal development and tumorigenesis**

(close to the JMD) is responsible for clathrin-mediated internalization of E-cadherin (101). If the dileucine motif is mutated or if the cadherin tail is completely deleted, E-cadherin fails to undergo endocytosis (101, 102). p120ctn might regulate E-cadherin endocytosis by masking the dileucine motif to prevent interaction with adaptor proteins, such as AP-2, which are required for clathrin-mediated endocytosis (103). Second, p120ctn competes with presenilin-1 and Hakai for binding to the JMD of classical cadherin. Presenilin-1 favors E-cadherin degradation by proteolytic cleavage of the cadherin cytoplasmic tail (104, 105). During synapse maturation, p120ctn dissociates from N-cadherin and is replaced by presenilin-1 (106). Hakai is an E3 ubiquitin ligase and binds to the phosphorylated tyrosine motifs in the JMD of E-cadherin (but does not bind other classical cadherins). This leads to ubiquitination and endocytosis of E-cadherin (Figs. 2 and 6D) (Section 8) (107, 108). To conclude, p120ctn seems to act as a cap that binds cadherin and prevents its endocytosis. In view of this, one may expect major pathological effects in case of p120ctn defects.

## **6. P120CTN AND RHO GTPASES**

### **6.1 p120ctn and dendritic-like branching**

The early hints about the role of cytoplasmic p120ctn came from p120ctn overexpression studies. Expressing large amounts of exogenous p120ctn saturated cadherin-binding sites, and the excess of p120ctn translocated to the cytoplasm and caused a neuron-like cellular morphology similar to dendritic branching (10). This phenotype was due to p120ctn-mediated RhoA inhibition, as the phenotype could be mimicked by adding a RhoA inhibitor (C3 exotransferase) or by expressing p190RhoGAP (Table 2) (11, 109). On the other hand, the dendritic-like branching could be blocked by coexpressing a constitutively active (CA) RhoA variant (11-13), or by mutating one of the RhoA-binding sites (11, 22). An N-terminal deletion including RBD1 diminishes p120ctn-induced branching (22), but branching is completely blocked by deleting a second RhoA-binding domain (containing AA 622-628; Fig. 3) (11). Is this branching phenotype RhoA-specific? Or are there other RhoGTPases involved? Activation of Rac1 and Cdc42 also influences p120ctn-mediated branching because branching was blocked by dominant negative forms of Rac1 and Cdc42 in two studies (12, 13). However, this was not seen in another study (11). In addition, p120ctn binds to Vav2, a specific guanine nucleotide exchange factor for RhoGTPases, and overexpression of a dominant-negative Vav2 construct decreases p120ctn-induced dendritic-like branching (13). It would be interesting to investigate whether expression of full-length or dominant active Vav2 alone could phenocopy the p120ctn-induced branched morphology.

Do cadherins modulate p120ctn-mediated branching? dendritic-like branching could be blocked by sequestering p120ctn by co-transfection of E- or C-cadherin (11, 13). Blocking could occur by either the complete transmembrane domain of E- or C-cadherin or by its JMD only, but not by its beta-catenin binding domain CBD only (11, 13). On the other hand, E-cadherin binding is dispensable for this p120ctn-induced branching because E-cadherin-uncoupled p120ctn mutants lacking either Armadillo repeat 1 (ARM1) or Armadillo repeats 1-3 (ARM1-3) can still

elicit a branched morphology (10, 72). Like cadherins, microtubules can tether away p120ctn from cytoplasmic pools and thereby prevent p120ctn-induced dendritic-like branching. Coexpression of the kinesin heavy chain reduced the branching elicited by p120ctn isoform 1 but not this elicited by p120ctn isoform 3, which means that isoform 1 has a higher affinity for kinesin (87).

In this paragraph we describe how p120ctn isoforms influence p120ctn-mediated dendritic-like branching and discuss the link between branching and nuclear localization of p120ctn. In an initial report of Reynolds *et al.* (4), p120ctn isoform 1A was shown to induce dendritic-like branching. A follow up study revealed that p120ctn isoform 2A and 3A, but not 4A, also elicit dendritic-like branching. Remarkably, there seems to be a correlation between nuclear localization of p120ctn and the ability to elicit branching. p120ctn isoform 1 is localized in the nucleus and induces dendritic-like branching, while isoform 4, which lacks the N-terminal domain, did not induce branching and was not localized either in the nucleus (22). Because p120ctn isoform 4 lacks the phosphorylation domain (Fig. 3), there might also be a link between phosphorylation and dendritic-like branching. In addition, both p120ctn isoforms 1AB and 3AB have 29 additional AA that are encoded by the alternatively spliced exon B and contain a NES (Fig. 3). p120ctn isoforms 1AB and 3AB can both block branching morphogenesis and promote nuclear export (22, 28). Mutational analysis revealed a second NES in armadillo repeat 7 (new nomenclature based on (16, 17)) (88). Full-length p120ctn contains two conventional nuclear localization sequences, NLS1 and NLS2 (Fig. 3). Deleting NLS1 does not prevent branching (22). However, branching is abolished by mutation (110) or deletion (11) of NLS2. Interrupting NLS2 by expression of six AA encoded by the alternatively spliced exon C disrupts both dendritic-like branching and nuclear translocation (Pieters *et al.*, in preparation). NLS2 comprises AA 622-628, which coincide with the second RhoA binding domain RBD2 (Fig. 3). Remarkably, nuclear import is not fully blocked by mutating the two conventional NLSs, and an additional role has been proposed for the armadillo domain in nucleocytoplasmic shuttling (88). Armadillo repeats 3 and 5 of p120ctn turned out to be essential for nuclear import (88), and deleting them both by removing either ARM3-5 or ARM3-9 blocks the neuron-like morphogenesis (10, 12). Interestingly, the p120ctn $\Delta$ ARM3-5 construct retains both RhoA-binding domains but nevertheless fails to induce branching (10, 12). Is nuclear import of p120ctn *per se* enough to induce branching? No, because forced nuclear translocation of p120ctn (*via* Leptomycin B administration or *via* coupling of an SV40 NLS) does not trigger dendritic-like branching (110). To conclude, the different p120ctn isoforms vary in their ability to elicit a branched morphology and this is often correlated with their ability to translocate to the nucleus.

## p120ctn in normal development and tumorigenesis

**Table 2.** p120ctn-mediated 'dendritic branching': effects of p120ctn isoforms, p120ctn mutants, cadherins and RhoGTPases

constructs	cell type(s)	branching	references
<b>p120ctn isoforms</b>			
isoform 1A	NIH3T3, Swiss3T3, C3H10T1/2, COS, MDCK, HeLa, LMTK, BHK, SV-80, CHO, 1205-Lu, HaCaT	Yes	(10-13, 22, 258)
isoform 1AB ( contains NES)	1205-Lu, HaCaT	No	(22)
isoform 1AC (interrupts RBD2)	NIH3T3, HeLa	No	(258)
isoform 1A	NIH3T3 (retroviral transduction)	No	(12)
isoform 2A	1205-Lu, HaCaT	Yes	(22)
isoform 3A	1205-Lu, HaCaT, MDCK, NIH3T3, HeLa	Yes	(22, 28, 258)
isoform 3AB	MDCK	No	(28)
isoform 3AC (interrupts RBD2)	NIH3T3, HeLa	No	(258)
isoform 4A (lacks RBD1, NLS1 and PD)	1205-Lu, HaCaT	No	(22)
<b>p120ctn mutants</b>			
isoform 1AΔN-terminus (lacks RBD1 and NLS1)	SV-80	No	(12)
isoform 1AΔ1-158 (lacks FBD and partly RBD1)	NIH3T3	Yes	(10)
isoform 1AΔ26-233 (lacks RBD1 partly PD)	NIH3T3, SV-80	Yes	(10, 12)
isoform 1AΔARM (Ecadherin-uncoupled)	NIH3T3	Yes	(72)
isoform 1AΔARM 1-3 (lacks NLS1 and partly PD)	NIH3T3	Yes, less	(10)
isoform 1AΔARM 3-5	NIH3T3, SV-80	No	(10, 12)
isoform 1AΔARM 3-11 (lacks RBD2)	NIH3T3	No	(10)
isoform 1AΔ622-628 (lacks RBD2)	NIH3T3, HeLa	No	(11, 258)
isoform 1AΔC-terminus	NIH3T3, SV-80	No	(10, 12)
isoform 1A8F			
isoform 2AΔNS (lacks RBD1)	1205-Lu	Yes, less	(22)
isoform 2AΔNLS1	1205-Lu	Yes	(22)
isoform 3AΔNLS1	1205-Lu	Yes	(22)
isoform 3AΔAK (lacks PD and NLS1)	1205-Lu, HaCaT	No	(22)
isoform 3AΔ622-628 (lacks RBD2)	NIH3T3, HeLa	No	(258)
<b>p120ctn and cadherins</b>			
isoform 1 + E-cadherin (cyto)	NIH3T3	No	(11)
isoform 1 + E-cadherin (JMD only)	NIH3T3	No	(11)
isoform 1 + E-cadherin (CBD only)	NIH3T3	Yes	(11)
isoform 1 + C-cadherin	NIH3T3	No	(13)
isoform 1 + C-cadherinΔcyto	NIH3T3	Yes	(13)
isoform 1 + C-cadherinΔCBD	NIH3T3	No	(13)
isoform 1 + C-cadherinΔJMD	NIH3T3	Yes	(13)
<b>p120ctn and RhoGTPases</b>			
isoform 1 + V14RhoA (CA)	NIH3T3	No	(11-13)
isoform 1 + N19RhoA (DN)	NIH3T3	Yes	(11)
isoform 1 + V12Rac1 (CA)	NIH3T3	Yes	(11)
isoform 1 + N17Rac1 (DN)	NIH3T3	Yes	(11)
isoform 1 + N17Rac1 (DN)	NIH3T3	No	(13)
isoform 1 + V12Cdc42 (CA)	NIH3T3	Yes	(11, 12)
isoform 1 + N17Cdc42 (DN)	NIH3T3	Yes	(11)
isoform 1 + N17Cdc42 (DN)	NIH3T3	No	(12, 13)
isoform 1 + C-terminus Vav2 (Rho family GEF)	NIH3T3	No	(13)
<b>p120ctn family members</b>			
ARVCF (Xenopus)	NIH3T3	yes	(75)
ARVCF (human)	NIH3T3	no	(38)
p0071		little	(129)
δ-catenin	MDCK, NIH3T3, PC12	yes	(40, 59, 131)
DN-PKP1 (lacks N-terminus)	Hacat, HeLa, L6	yes	(130)

## 6.2. p120ctn mediates RhoA inhibition and activation of both Rac1 and Cdc42

There are several ways of showing that p120ctn modulates RhoA activity. p120ctn overexpression results in RhoA inhibition, whereas knockdown or genetic ablation of endogenous p120ctn in mice results in increased RhoA activity. First, expression of p120ctn isoform 1A inhibits RhoA activation in 293T and CHO cells (11, 13). However, RhoA activity was not found to be altered by stable expression of lower levels of p120ctn isoform 1A fused to GFP (details in Table 3) (12). Also, a mutant p120ctn isoform, 1 $\Delta$ delta622-628, lacking RBD2 failed to inhibit RhoA activity and to induce dendritic-like branching (11). Based on this link between p120ctn-mediated branching and RhoA inhibition, one might expect that other AA encoded by the alternatively used exons B and C, which inhibit branching, might also interfere with RhoA activation. Due to the low activity of RhoA, cells transfected with p120ctn isoform 1A did not form actin stress fibers (11-13). In a second approach, stable knockdown of endogenous p120ctn in different cell lines resulted in RhoA activation (70, 72, 112-114) and strongly enhanced formation of actin stress fibers (70, 112). These p120ctn-depleted cell lines are also suitable for testing the ability of various p120ctn isoforms (originating from another species and therefore unaffected by shRNA) to affect RhoA activity (Table 3). Re-expression of p120ctn isoform 1, but not p120ctn isoform 4, rescued p120-mediated RhoA inhibition (72, 113). Finally, modulation of RhoA activity by p120ctn is also observed *in vivo*, as genetic ablation of p120ctn in mouse skin and dorsal forebrain result in increased RhoA activation (46, 77).

**Table 3.** Effect of p120ctn expression, knockdown and knockout on RhoGTPase activity

experimental setup					RhoGTPase activity		Reference
<b>Overexpression</b>							
cell type	transfection/ transduction	vector	promoter	p120ctn isoform (activator)	RhoA activity	Rac1 and Cdc42 activity	
293T	cytofectene (Biorad)	pRcCMV	CMV	m1A (LPA)	decreased		(11)
CHO	Lipofectamine Plus retroviral transduction	pEGFP-N1	CMV	m1A - GFP fusion	decreased	increased	(13)
NIH3T3		pBAbE-puro (pEGFP-C1)	SV40	m1A - GFP fusion	unaltered	increased	(12)
<b>Knockdown (KD)</b>							
cell type	Stable p120ctn KD	vector		p120ctn isoform (stable rescue)	RhoA activity	Rac1 activity	
NIH3T3	mouse p120ctn	pRS mp120ctn siRNA			increased		(112)
MDCK	canine p120ctn	pRS hp120ctn siRNA			increased		(70)
MDA-231	human p120ctn	pRS hp120ctn siRNA			increased	decreased	(72, 113, 115)
MDA-231	human p120ctn	pRS hp120ctn siRNA		mp120ctn m1A	decreased	increased	(72, 113, 115)
MDA-231	human p120ctn	pRS hp120ctn siRNA		mp120ctn m4A	increased	increased	(113, 115)
MCF7	human p120ctn	pRS hp120ctn siRNA				increased	(115)
MCF7	human p120ctn	pRS hp120ctn siRNA		mp120ctn m1A		decreased	(115)
<b>Knockout</b>							
cell type	cells analyzed	floxed p120ctn allele		Tissue-specific Cre recombinase expression	RhoA activity	Rac1 activity	
skin	epidermis	exon 3-8 floxed (45)		K14-Cre (239)	increased		(46)
forebrain	hippocampus	exon 7 floxed		Emx1-Cre (240)	increased	decreased	(77)

CHO: Chinese hamster ovary; CMV: cytomegaly virus; EGFP: enhanced green fluorescent protein; LPA:Lysophosphatidic acid; m: mouse; h: human



## p120ctn in normal development and tumorigenesis

p120ctn expression also results in increased Rac1 and Cdc42 activity (12, 13). In line with this, knockdown or knockout of p120ctn results in decreased activity of Rac1 (Table 3) (72, 77, 113). Re-expression of both p120ctn isoforms 1 and 4 in stable p120ctn-knockdown lines results in reactivation of Rac1 (113, 115). Remarkably, p120ctn isoform 4 can restore Rac1 activity but fails to inhibit RhoA activity, indicating that a single p120ctn isoform can differentially regulate the activity of different RhoGTPases. Overall, p120ctn regulates RhoGTPase activity by inhibiting RhoA and activating Rac1 and Cdc42, and this alters cytoskeletal dynamics and increases cell migration (13).

### 6.3. Interaction between p120ctn and RhoA

Does p120ctn bind to RhoA or is it involved in indirectly regulating its activity? In *Drosophila*, p120ctn binds directly to Rho1, the RhoA homolog (33). Remarkably, also alpha-catenin binds to Rho1 in *Drosophila*, although alpha-catenin and p120ctn bind to distinct regions of the N-terminus of Rho1 (33). One RhoA binding domain (RBD1) was identified in the N-terminus of mouse p120ctn (AA 102-234) (111). Binding of this p120ctn domain to RhoA is regulated by tyrosine phosphorylation of RBD1 by the action of Src family members. Fyn-mediated phosphorylation of Y112 or introduction of a phosphomimetic Y112E mutation inhibits the interaction of p120ctn with RhoA and prevents p120ctn-mediated dendritic-like branching and RhoA inhibition. On the other hand, Fer- or Src-mediated phosphorylation of Y217 and Y228 increases the affinity between p120ctn and RhoA, resulting in inhibition of RhoA activity (111). Alternatively, RhoA activity was also inhibited by expressing a Y112F mutant of p120ctn that can not be phosphorylated by Fyn (111). The RBD1 on its own does not have RhoGDI activity, indicating that additional sequences in p120ctn are required for RhoA stabilization and RhoGDI functionality (111). The second RhoA binding domain (RBD2, AA622-628) coincides with NLS2 of p120ctn, and the isoform 1 $\Delta$ 622-628 mutation activates RhoA and does not elicit dendritic-like branching (11). Deleting either RBD1 or RBD2 does not prevent RhoA from binding to p120ctn isoform 4 or to p120ctn isoform 1 $\Delta$ 622-628, respectively (113). However, deleting both RBDs of p120ctn, as in isoform 4 $\Delta$ 622-628, completely abrogates its ability to bind RhoA (113). Thus, both p120ctn RBD1 and RBD2 need to be present for high affinity RhoA binding, which results in RhoA inhibition.

### 6.4. Mechanism of p120ctn-mediated RhoA inhibition

The mechanism by which p120ctn inhibits RhoA is still unclear, but several modes of action have been postulated. Either p120ctn can bind to RhoA (see above) and act as a Rho guanine nucleotide dissociation inhibitor (GDI), or it can activate Rac1 what leads to p190RhoGTPase activating protein (p190RhoGAP)-mediated RhoA inhibition (Fig. 5A). In the first proposed mechanism, p120ctn binds to RhoA and prevents its activation by Rho Guanine exchange factors (GEFs). p120ctn has been shown to specifically inhibit the intrinsic GDP/GTP exchange activity of RhoA, what resembles the mode of action of GDIs (11, 111). Also *in vitro*

translated and purified *Drosophila* p120ctn preferentially binds to GDP-bound Rho1 (33). In addition, p120ctn binds dominant-negative (DN) Rho1, but not constitutively active (CA) Rho1 (33). The p120ctn-binding region of Rho1 adopts different conformations depending on which nucleotide is bound, and this might explain the binding preference of p120ctn for GDP-bound Rho1 (33). Although p120ctn has no sequence similarity to GDI, it interacts with the same face of RhoA protein (33, 116). The second proposed mechanism involves interplay between several RhoGTPases. Rac1 and Cdc42 can inhibit RhoA activity in NIH3T3 cells (117), and p120ctn can interact with Vav2, a RhoGEF, which might account for the p120ctn-mediated activation of Rac1 and Cdc42 (13). Therefore, p120ctn-mediated Rac1 activation may indirectly inhibit RhoA through a pathway that involves low molecular weight (LMW) phosphatase and p190RhoGAP (Fig. 5A) (112, 118, 119).

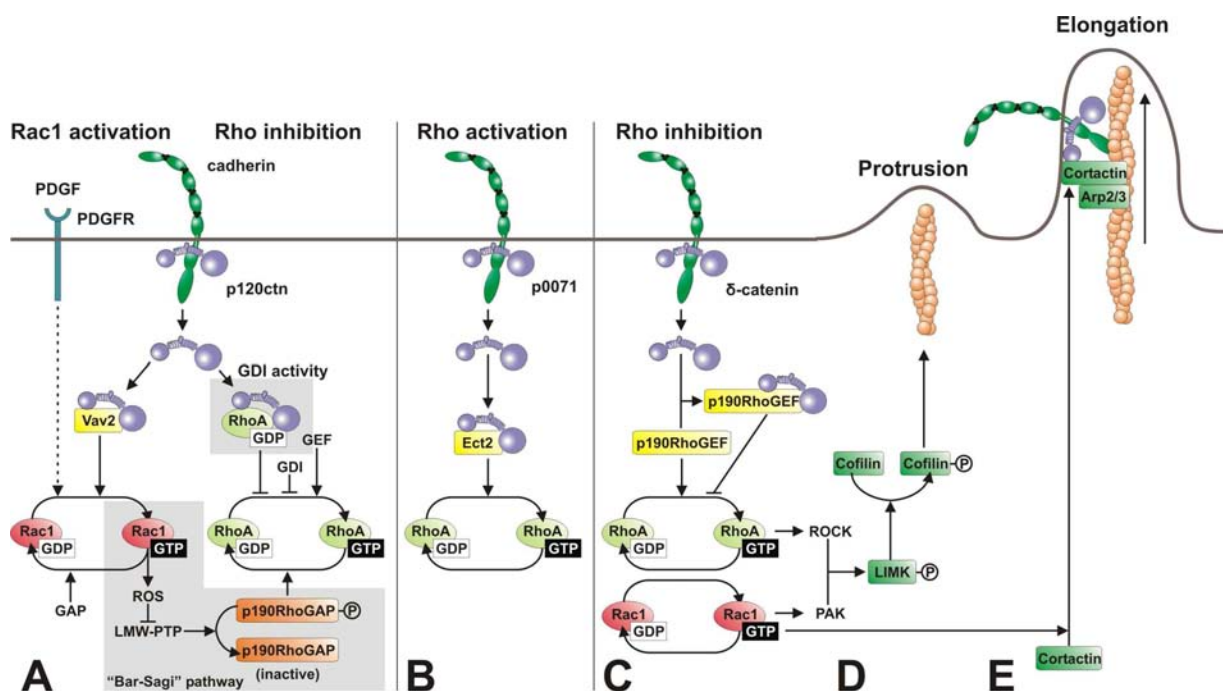


**Figure 5.** p120ctn family members regulate RhoGTPase activity. (A) RhoGTPases are molecular switches that alternate between an active (GTP-bound) and an inactive (GDP-bound) state. Guanine exchange factors (GEFs) promote RhoGTPase activation, whereas GTPase activating proteins (GAPs) and Rho guanine dissociation inhibitor (GDI) result in RhoGTPase inactivation. p120ctn inhibits RhoA activity and activates Rac1 (and Cdc42). p120ctn can inhibit RhoA either by its RhoGDI activity or by Rac1-mediated activation of the ‘Bar-Sagi’ pathway. p120ctn interacts with RhoGEF Vav2, which can activate Rac1, which in turn activates p190RhoGAP via the ‘Bar-Sagi’ pathway. (B) p0071 activates RhoA by binding to RhoGEF Ect2. (C) Delta-catenin inhibits RhoA activity by binding and sequestering p190RhoGEF away from RhoA. (D) Activated RhoA or Rac1 results in LIMK1-mediated phosphorylation of cofilin at serine residue 3 (S<sub>3</sub>), which inactivates cofilin by preventing its binding to actin. Inactivation of cofilin promotes actin protrusive activity by reducing actin dynamics. (E) p120ctn recruits the cortactin/Arp2/3 complex to the protrusions, where the cortactin/Arp2/3 complex stimulates actin polymerization and this results in branch elongation. GTP: guanine triphosphate, GDP: guanine diphosphate, PDGFR: platelet-derived growth factor receptor.

### 6.5. RhoGTPases and cadherin-based junctions

RhoGTPases and cadherin-based junctions have a common denominator: the actin cytoskeleton. RhoGTPases are key mediators of actin dynamics and can modulate formation of adherens junctions, and on the other hand, they can become activated upon the formation of adherens junctions (120, 121). Activated RhoGTPases can promote cell adhesion, and inhibition of RhoA by C3 exotransferase disrupts cell adhesion and removes E-cadherin from the contact sites (122-124). RhoA inhibition can also affect the composition of the cadherin complex (125). On the other hand, Rac1 activation disrupts cadherin-dependent cell–cell adhesion in human keratinocytes (96, 126). Furthermore, cadherin recycling is important both during the formation of new contacts and in the maintenance of stable junctions (64). RhoGTPases regulate many stages of vesicular trafficking, but they also have effects on cadherin-based junctions that vary with the cellular environment (64, 109, 127, 128). RhoGTPases have been shown to be important for cadherin-based adhesion *in vivo*. Rho1, the *Drosophila* RhoA homolog, colocalizes with DE-cadherin in embryos, and DE-cadherin is mislocalized in Rho1 mutants (33). Also fibroblasts depleted of p190RhoGAP, which is normally recruited to adherens junctions by p120ctn, fail to form proper adherens junctions (112). In conclusion, an intricate relationship exists between RhoGTPases and the formation and maintenance of cadherin-based junctions.

### 6.6. p120ctn subfamily members and RhoGTPases

Dendritic-like branching and RhoA inhibition represent a general theme among p120ctn family members. Expression of *Xenopus* ARVCF, but not human ARVCF, induces dendritic-like branching (38, 75). Although human ARVCF is quite similar to p120ctn isoform 1A, it does not induce branching (38). In contrast, p0071 can also induce branching but to a lower extent compared to p120ctn-mediated branching (129). p0071 is involved in cytokinesis and cell division, and its knockdown results in multinucleated cells and multipolar cells (50). During cytokinesis p0071 is required for RhoA activation, and defects in p0071 knockdown cells can be reduced by expression of a constitutively active RhoA mutant (50). p0071 can bind directly to RhoA or to Ect2 (a RhoGEF), and expression of both p0071 and Ect2 result in RhoA activation (Fig. 5B) (50). Surprisingly, p120ctn and p0071 have opposite effects on RhoA activity. Finally, a dominant negative plakophilin 1 mutant, which lacks the N-terminal binding domain that interacts with desmosomal proteins, can also elicit dendritic-like branching (130).

Overexpression of delta-catenin also induces neuron-like morphological alterations (40, 59, 131, 132). Neuronal morphogenesis can be divided into formation of new processes (branching) and elongation of existing branches (Figs. 5D, E). Branching is enhanced by RhoA inhibition in the presence of delta-catenin, and can be blocked by expression of constitutively active RhoA mutant (59), as well as by presenilin-1 or E-cadherin (133, 134). On the other hand, branch elongation depends on the interaction between delta-catenin and cortactin, which is regulated by tyrosine phosphorylation (Fig. 5E) (59). Interestingly, growth factor-induced Rac1 activation increases transport of cortactin towards the cell surface (135), where cortactin can interact with the Arp2/3 complex and initiate actin nucleation (136). So, both initiation and elongation of branches are regulated directly or indirectly by RhoGTPases, which in turn are

regulated by p120ctn family members. Interestingly, also p120ctn binds to cortactin, and knockdown of p120ctn decreases the presence of cortactin and Arp3 at leading edges and diminishes lamellipodial dynamics (137). Like E-cadherin binding, cortactin binding might be a general feature of p120ctn family members, and the neuron-like phenotypes, induced by overexpression of p120ctn family members, might be explained by cytoskeletal rearrangements mediated by cortactin and Arp2/3.

Like p120ctn, delta-catenin can inhibit RhoA activity, and it does so by interacting with p190RhoAGEF and sequestering this GEF away from RhoA (Fig. 5C) (138). The interaction between delta-catenin and p190RhoAGEF depends on Akt1-mediated phosphorylation of the residue T454 of delta-catenin. Indeed, a T454A mutant of delta-catenin fails to induce dendritic-like branching and RhoA inhibition (138). Like p120ctn, E-cadherin can sequester cytoplasmic delta-catenin and thereby prevent delta-catenin-mediated branching and RhoA inhibition (134). E-cadherin competes with p190RhoAGEF for binding to delta-catenin, and in confluent cell layers E-cadherin binds the majority of available delta-catenin protein. This binding results in increased levels of unbound p190RhoAGEF, which can activate RhoA (134). However, in contrast to these findings in delta-catenin overexpression studies, the activities RhoA or Rac1 are not altered in delta-catenin-deficient hippocampal neurons (139). In one study, delta-catenin expression also increased Rac1 and Cdc42 activity, and coexpression of *delta*-catenin with dominant negative Rac1 or Cdc42 prevented its protrusive activity in hippocampal neurons (132). In another study, however, delta-catenin expression did not affect Rac1 or Cdc42 activity (138). Rac1 and RhoA activation results in phosphorylation and activation of LIMK1, which in turn phosphorylates cofilin. Phosphorylated cofilin cannot bind actin but promotes its protrusive activity by reducing actin dynamics (Fig. 5D). Interestingly, activated LIMK1 and cofilin phenocopy the increased protrusive activity, whereas a LIMK1 kinase-dead mutant or a constitutively active cofilin S3A mutant (which cannot be phosphorylated) failed to elicit branching (132). Delta-catenin also regulates RhoGTPase activity *in vivo*, as knockdown of delta-catenin in *Xenopus* results in RhoA activation and Rac1 inhibition (57). In addition, both DN RhoA and CA Rac1 were able to rescue the developmental defect in *Xenopus* embryos depleted of delta-catenin (57). In mice, genetic or RNAi-mediated delta-catenin depletion in hippocampal neurons results in reduced dendritic complexity (132, 139). Knockdown of delta-catenin in hippocampal cultures results in loss of N-cadherin and alphaN-catenin (132). So, though all members of the p120ctn gene family can regulate RhoA, their modes of action differ.

## 7. P120CTN INTERACTS WITH TRANSCRIPTION FACTORS IN THE NUCLEUS

Like beta-catenin, p120ctn acts both as a component of adherens junctions and as a transcriptional regulator in the nucleus. p120ctn is localized in the nucleus (22, 28, 88, 110, 140) and interacts with transcription factors Kaiso (14) and Glis2 (141). Interestingly, Kaiso coprecipitates efficiently with p120ctn isoform 3 in epithelial lines, but not with p120ctn isoform 1 in fibroblasts (14). Nuclear trafficking of p120ctn depends on conventional NLS and NES signals (Fig. 2) (22, 28, 110), as well as on its armadillo repeat domain (88) and on the microenvironment (142). Kaiso also contains a functional NLS for its nuclear import (143).

## p120ctn in normal development and tumorigenesis

p120ctn and its relation to transcription factor Kaiso have been studied extensively (144-146). The armadillo domain of p120ctn binds to the C-terminal zinc finger domain of Kaiso and thereby inhibits the interaction between the zinc finger domain of Kaiso and DNA (14). Kaiso has a dual specificity for DNA: it can bind to sequence-specific Kaiso binding sites (KBS) and to methylated CpG-dinucleotides (147, 148). Remarkably, the function of Kaiso that involves binding to sequence-specific KBSs is dispensable *in vivo* (149). The binding of Kaiso to methylated DNA is evolutionarily conserved (149) and allows histone-deacetylase-dependent transcriptional repression. This involves the recruitment of chromatin co-repressor components, such as nuclear co-repressor 1 (NCOR) (150), to the N-terminal poxvirus and zinc finger (POZ) domain of Kaiso. The POZ domain also enables Kaiso to homodimerize (14, 151). Kaiso acts as a transcriptional repressor and p120ctn can bind to Kaiso and block its repressor activity, resulting in activation of the target genes of Kaiso, such as *Siamois*, *c-Fos*, *Myc*, *Ccnd1* (encodes Cyclin D1) (152), *xWnt11* (153), and *Mmp7* (encodes Matrilysin) (154). There is significant overlap between the target genes of p120ctn/Kaiso and the beta-catenin/TCF signaling pathways. The synergism between these pathways was observed both in cell lines (154) and in *Xenopus* embryos (152). The promoter of the matrilysin gene contains two KBSs, and Kaiso can repress beta-catenin-induced activation of the *Mmp7* gene, but this Kaiso-mediated transcriptional repression of *Mmp7* can be reversed by p120ctn expression (154). Several other beta-catenin target genes contain KBSs, and in *Xenopus* embryos they can be either repressed by Kaiso or activated by either beta-catenin activity or Kaiso depletion (152). The highest transcriptional activation of *Siamois* was obtained by beta-catenin expression in Kaiso-depleted *Xenopus* embryos (152). p120ctn relieves the Kaiso-mediated repression of beta-catenin target genes, and its ablation in *Xenopus* embryos increases the repression of these genes (152). Frodo physically links the p120ctn/Kaiso and beta-catenin/TCF pathways by binding to both p120ctn and Dishevelled (155). Frodo acts upstream of both signaling pathways and stabilizes p120ctn, which relieves Kaiso-mediated transcriptional repression of beta-catenin target genes (155). An additional link between p120ctn/Kaiso and the beta-catenin/TCF pathways is provided by the interaction between Kaiso and TCF3 in *Xenopus* (156). Although Kaiso acts as a genome wide transcriptional repressor in *Xenopus* embryos (157), no increased gene expression was observed in Kaiso-deficient mice (158). Morpholino-mediated depletion of Kaiso in *Xenopus* embryos results in severe defects in gastrulation and in convergent extension, and these phenotypes can be rescued by re-expression of Kaiso (152, 153). In contrast, Kaiso-deficient mice are viable (158). The discrepancy between the findings in mice and in *Xenopus* concerning the developmental requirement of Kaiso and its gene regulatory activity might be explained by functional redundancy of Kaiso-like family members (144). Indeed, Kaiso is part of a small protein family that contains two other Kaiso-like proteins, namely ZBTB4 (Kaiso-like 1) and ZBTB38 (ZENON). Like Kaiso, these proteins bind methylated DNA and act as transcriptional repressors (159). Like Kaiso, ZBTB4 exerts bimodal DNA binding, whereas ZBTB38 binds only methylated DNA (159). ZBTB4 has been implicated in p53 activation (160). Interestingly, no ZBTB4 homolog could be identified in *Xenopus*, which indicates that ZBTB4 might substitute for Kaiso in mouse but not in frog.

In addition, recent reports point at interesting interactions between the Wnt signaling pathway and p120ctn in the cell junctions or the cytoplasm (155, 261, 262). A recent report of the McCrea group showed that p120ctn is targeted for proteasomal degradation via the same pathway as beta-catenin (262). This degradation involves a series of steps including its association with axin and APC proteins, its phosphorylation by kinases of the CK1 family and by GSK3beta, eventually followed by its ubiquitination and proteasomal degradation. The long isoform-1 of p120ctn can associate with CK1alpha and GSK3beta, and that it is prone to phosphorylation by these kinases, as well as to axin binding, ubiquitination and proteasomal degradation (262). Moreover, the related armadillo subfamily members ARVCF and delta-catenin of *Xenopus* bind likewise to axin and are responsive to the axin-containing destruction complex (262), in line with a previous report on vulnerability of human delta-catenin to GSK3beta-triggered degradation (263). In another recent report, p120ctn was shown to bind to CK1epsilon *via* an amino-terminal domain (Fig. 3) (261). In this model, p120ctn functions as an essential but subtle regulator of Wnt signaling by recruiting CK1epsilon to the E-cadherin/LRP/Fz receptor complex, and by counteracting this phenomenon upon Wnt-induced activation of CK1epsilon.

## 8. P120CTN AND PHOSPHORYLATION

In this section we address two main questions. First, how does tyrosine phosphorylation affect cadherin-based adhesion in general? We give an overview of the kinases and phosphatases that are involved, and either physically interact or phosphorylate and dephosphorylate members of the cadherin-catenin complex. Furthermore, we try to give mechanistic insight by pinpointing key residues to be phosphorylated upon cadherin-based junctional disassembly. Second, how is p120ctn phosphorylated and how does this affect the adhesive properties of the cadherin catenin complex? We discuss the p120ctn phosphorylation sites, the difference between tyrosine and serine/threonine phosphorylation, the regulatory role of phosphatases and the effect of different p120ctn isoforms on the phosphorylation status and junctional stability.

### 8.1. Phosphorylation of the cadherin-catenin complex

Several lines of evidence suggest that cadherin-based junctions, like integrin-mediated adhesion plaques, are regulated by phosphorylation. In fact, all members of the cadherin catenin complex, except alpha-catenin, are prone to phosphorylation on tyrosine, serine or threonine residues (Table 4). Tyrosine phosphorylation of cadherins and catenins has been studied extensively. This phosphorylation is executed by receptor tyrosine kinases (RTKs) and non-receptor tyrosine kinases (nRTK). On the other hand, protein tyrosine phosphatases (PTPs) reverse this phosphorylation and allow dynamic protein modification in response to internal and external cues (reviewed in 161). The presence of multiple phosphorylation sites in cadherins and catenins and the multitude of different kinases and phosphatases located at the membrane reveal the complexity of protein phosphorylation and its effects on adhesion. Several tools, such as Src transformation, phosphotyrosine-specific antibodies, specific kinase or phosphatase inhibitors and a few mouse knockout models have been generated to investigate tyrosine phosphorylation.

## p120ctn in normal development and tumorigenesis

These tools allow only general interpretation of tyrosine phosphorylation events, whereas individual tyrosine mutations provide a rather narrow view.

**Table 4.** Overview of kinases and phosphatases binding and/or modifying the phosphorylation status of cadherins and catenins

	kinases		phosphatases	
	non Receptor kinase	Receptor-associated kinase	non Receptor phosphatase	Receptor-associated phosphatase
cadherins				
E-cadherin	v-Src (164)	<i>EGFR</i> (241)	<i>PTP1B</i> (242), <i>PP2A</i> (S/T)(243)	<i>PTPμ</i> (244)
N-cadherin	v-Src (165)	<i>FGFR-4</i> (245)	<i>PTP1B</i> (246)	<i>PTPμ</i> (244)
VE-cadherin	c-Src (247)	<i>VEGFR-2</i> (197, 247, 248)	<i>PTP1B</i> (249)	<i>VE-PTP</i> (171)
R-cadherin				<i>PTPμ</i> (244)
catenins				
α-catenin				
β-catenin	Fer (179), Fyn (179), Yes (179), c-Src (179), v-Src (4, 164, 203)	<i>EGFR</i> (241), TrkA (173), <i>VEGFR-2</i> (197), c-Met (190)	<i>PTP1B</i> (242, 246), <i>SHP2</i> (250), <i>PP2A</i> (S/T)(243)	<i>DEP1</i> (200, 201), <i>PTPκ</i> (251), <i>PTP-LAR</i> (252, 253), <i>PTPλ</i> (254), <i>PCP-2</i> (255), <i>PTPβ/ζ</i> (256),
γ-catenin	v-Src (4)	<i>EGFR</i> (241), <i>VEGFR-2</i> (197), c-Met (66)	<i>SHP2</i> (250), <i>PP2A</i> (S/T)(243)	<i>DEP1</i> (200, 201), <i>PTPκ</i> (251), <i>PTP-LAR</i> (252)
p120ctn	v-Src (4, 181), Fer (167, 179, 195), Fyn (179), Yes (179), GSK3β (S/T)(185)	TrkA (173), c-Met (66, 173), <i>EGFR</i> (196), <i>PDGFR</i> (196), <i>CSFR</i> (196), <i>VEGFR-2</i> (197)	<i>SHP2</i> (250), <i>PKC*</i> (S/T)(191)	<i>DEP1</i> (200, 201), <i>VEGFR-2*</i> (S/T)(190), <i>PTPμ</i> (202)

How does phosphorylation affect cadherin-based adhesion? Tyrosine phosphorylation of cadherins and catenins has been studied extensively and is thought to modulate adhesive strength (Fig 6A). The underlying mechanism is not clear and there is evidence for both a positive role and a negative role for tyrosine phosphorylation. One way to investigate the phosphorylation of cadherin-catenin structures is by using Src-mediated cellular transformation, which leads to constitutive phosphorylation on tyrosines of all membrane-bound Src-substrates, including cadherins and catenins. When cells are transformed with Src or Ras, they become loosely attached and fibroblast-like (70, 162-166). So, forced tyrosine phosphorylation of mature confluent cell layers causes cell dispersal. The reverse is also true, because in human endothelial cells, p120 is transiently tyrosine-phosphorylated in nascent cell-cell contacts, but this phosphorylation is lost in stable confluent layers (168). Loose cells might be more accessible for growth factors and therefore show an increased phosphotyrosine status.

Another way to investigate phosphorylation is by using specific inhibitors of phosphatases and kinases to keep proteins phosphorylated or unphosphorylated, respectively. Treatment with an inhibitor specific for phosphotyrosine phosphatases (pervanadate) keeps cadherins and catenins (except alpha-catenin) phosphorylated and results in the dissociation of alpha-catenin from the cadherin-catenin complex (169). In contrast to these findings, knockout of Fyn or a double knockout of Fyn and Src in mouse revealed that phosphorylation has a positive role on adhesion. Fyn-deficient keratinocytes lack tyrosine-phosphorylation of catenins, and this causes a defect in cell adhesion. The same was observed in the skin of mice deficient in both Fyn and Src (172).

normal writing denotes (de)phosphorylation only; underlined text denotes both binding and (de)phosphorylation; italics denotes binding only; S/T denotes (de)phosphorylation on serine or threonine residues. TrkA = receptor for nerve growth factor (NGF); c-Met = receptor for Hepatocyte growth factor (HGF)

How does phosphorylation affect the affinity between members of the cadherin–catenin complex? A Src tyrosine phosphorylation residue was identified in beta-catenin (Y654) that is important for binding to E-cadherin. Src-induced phosphorylation of Y654 or introduction of a phosphomimetic mutation (Y654E) decreased the affinity between beta-catenin and E-cadherin and disrupted the cadherin-based junctions (Figs. 6C, D) (174). Like E-cadherin, N-cadherin does not bind tyrosine-phosphorylated beta-catenin (175). The presence of p120ctn does not influence the binding of phosphorylated or unphosphorylated beta-catenin to E-cadherin (174). Beta-catenin binds the acidic E-cadherin sequence via a long, positively charged groove and adding a negative charge in this groove by phosphorylation might disrupt intermolecular binding (177).

Binding of beta-catenin to alpha-catenin involves 29 AA, only one of which is a tyrosine, Y142 (178). Phosphorylation of this Tyr residue in beta-catenin by the non-receptor tyrosine kinases Fer or Fyn (but not Src and or Yes) or by applying a tyrosine phosphatase inhibitor (perovanadate) uncoupled alpha-catenin from beta-catenin (Figs. 6B, C) (179-181). Keeping tyrosine residues Y142 and Y654 of beta-catenin unphosphorylated is critical for the integrity of cadherin-based adhesion. PTP1B, a non-receptor tyrosine phosphatase, associates with N-cadherin and can dephosphorylate beta-catenin and thereby stabilize cadherin-mediated adhesion (reviewed in 182). The binding of PTP1B to cadherin requires phosphorylation of PTP1B on tyrosine residue Y152 by Fer, which in turn is recruited to the cadherin–catenin complex by binding to p120ctn (Fig. 6B) (183). Cell-permeable peptides that disrupt the Fer–p120ctn interaction cause Fer to dissociate from N-cadherin complexes, after which PTP1B, beta-catenin and eventually p120ctn are lost (183).

Tyrosine phosphorylation not only affects the binding efficacy of catenins, but also determines the amount of membrane-localized E-cadherin. Src-mediated disruption of cell-cell contacts is accompanied by increased ubiquitination of E-cadherin, which causes its endocytosis (107). Src- or HGF-mediated tyrosine phosphorylation of E-cadherin on Tyrosine residues 755 and 756 (which are situated in the JMD) is a prerequisite for the binding of Hakai, an E3 ubiquitin-ligase. p120ctn binds to phosphorylated and unphosphorylated E-cadherin equally, but it has to compete with Hakai for binding of tyrosine phosphorylated E-cadherin (Fig. 6D) (107).



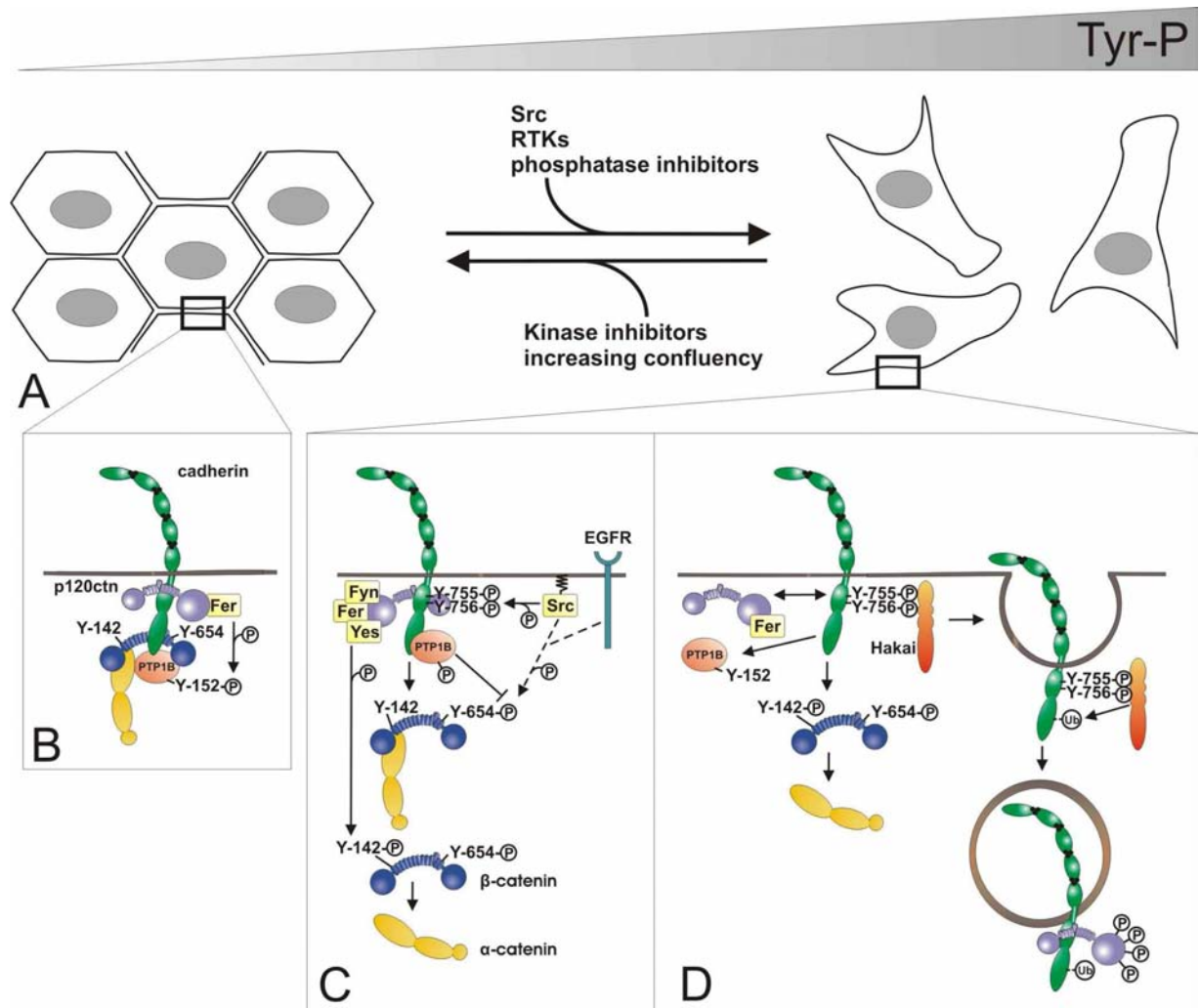


**Figure 6.** Constitutive tyrosine phosphorylation of the cadherin–catenin complex results in disassembly of junctions. (A) Src transformation, growth factor receptor signaling and phosphatase inhibition cause tyrosine phosphorylation of cadherins and catenins, which leads to dissociation of adherent cell layers (*left, blowup in B*) into non-adherent spindle-shaped cells (*right, blowup in C, D*). Tyrosine phosphorylation in cadherin-based structures is lost by kinase inhibition and upon junctional maturation and formation of confluent layers. (B) In adherent cells, p120ctn recruits Fer to the cadherin–catenin complex, which activates the protein tyrosine phosphatase PTP1B. Dephosphorylation of key tyrosine residues (Y142 and Y654) in beta-catenin by PTP1B promotes junctional integrity. (C) The phosphorylation status of Y142 and Y654 in beta-catenin can be shifted by growth factor signaling and by Src family members, which can be recruited by p120ctn. Phosphorylation of Y142 and Y654 results in disassembly of the beta-catenin/alpha-catenin and cadherin/beta-catenin complexes, respectively. (D) Dissociation of p120ctn from the cadherin tail results in removal of PTP1B, which causes dissociation of cadherin-based junctions. Hakai can bind to phosphorylated tyrosine residues Y755 and Y756 in the tail of E-cadherin, which results in its ubiquitilation and internalization. EGFR: epidermal growth factor receptor.

## 8.2. Phosphorylation of p120ctn

What are the phosphorylation sites of p120ctn? Over the previous decade, the laboratory of Reynolds has been trying to decipher how phosphorylation affects the diverse functions of p120ctn by using two approaches. First, two-dimensional tryptic mapping allowed the identification of eight tyrosine and eight serine/threonine phosphorylation sites in p120ctn (Fig. 3) (184, 185). A ninth tyrosine phosphorylation site was identified by mutational analysis. In comparison with v-Src transformed L-cells expressing WT p120ctn and exogenous E-cadherin, the Y217F mutation of p120ctn increased cell aggregation of such cells (181). All tyrosine sites and most of the serine and threonine sites are located in the N-terminal domain. The two remaining phosphorylation sites, S879 and T916, flank the sequence encoded by the alternatively spliced exon A nearby the C-terminus. S879 and T916 correspond to the previously reported S873 and T910, respectively: the new numbering is due to the inclusion of the six amino acids encoded by the alternatively used exon C. Remarkably, no phosphorylation sites are present in the Armadillo repeat domain. Second, panels of p120ctn phospho-specific monoclonal antibodies were generated against specific tyrosine, serine and threonine residues: Y228 (186), S879 (187), S268, S288, T310, and T916 (188). These antibodies have been helpful in identifying the residues in p120ctn that are phosphorylated in response to EGF (186) or PDGF (189), namely Y228 and S879, respectively (Table 5).

**Table 5.** Phosphorylation and dephosphorylation of Y/S/T residues of p120ctn

residue	action	phospho-specific antibody
Y228	phosphorylated in response to EGF	yes
Y296	efficiently dephosphorylated by SHP-1	no
S268	dephosphorylated by PKC stimulation and CA RhoA	yes
S288	dephosphorylated by CA RhoA and DA Galpha12	yes
S879	phosphorylated in response to PDGF and PKC activation	yes
T310	dephosphorylated by CA RhoA and DA Galpha12	yes
T916	-	yes

Cells that were not transformed by Src are mainly phosphorylated on serine, with a relatively small amount of phosphorylation on threonine and tyrosine (68, 69, 184). Src-transformed cells have higher phosphotyrosine content while mutating all eight Src-phosphorylation sites to Phe (p120ctn-8F) prevents phosphorylation of p120ctn and its binding to SHP-1 (184). Physiological tyrosine phosphorylation of p120 occurs transiently in response to growth factor signaling and is rapidly terminated (186). In contrast, all serine or threonine (S/T) phosphorylation appears to be constitutive, with the exception of S873, which is phosphorylated by phorbol ester-activated PKC (185) or PDGF (189). Basal S/T phosphorylation is transiently down-regulated in response to several cellular stimuli, such as VEGF (190) and PKC (191), and the inflammatory stimuli histamine (H1), thrombin and lysophosphatidic acid (LPA) (192). This is thought to modulate a variety of cadherin-associated activities, such as vascular permeability and leukocyte transcytosis.

## p120ctn in normal development and tumorigenesis

Which kinases phosphorylate p120ctn? This armadillo protein, which was initially identified as a substrate for the non-receptor tyrosine kinase Src (1), is also phosphorylated by Src-family members Fyn and Yes. Fyn interacts with tyrosine-phosphorylated and -unphosphorylated p120ctn protein equally (179). p120ctn is also a good substrate for the tyrosine kinase Yes, which interacts with p120ctn in an activation-dependent manner and subsequently activates Fer and Fyn (179). Tyrosine kinase Fer is constitutively associated with p120ctn (167, 195). The N-terminus of p120ctn serves as a docking protein facilitating interaction of Fer (and Fyn) with the cadherin-catenin complex (Fig. 3). p120ctn-bound Fer can phosphorylate PTP1B on tyrosine 152, and this phosphorylation event is essential for the binding of PTP1B to cadherin (183). In addition, p120ctn is phosphorylated in response to PDGF, CSF-1, EGF, NGF, HGF and VEGF (Table 4) (66, 173, 196, 197).

Which phosphatases dephosphorylate p120ctn? Since tyrosine phosphorylation of p120ctn is transient, a feedback mechanism must exist for reversing this phosphorylation. Indeed, several phosphatases have been reported to bind and to dephosphorylate p120ctn (Table 4). Src homology 2 (SH2) domain-containing protein tyrosine phosphatase 1 (SHP-1) binds to p120ctn following EGFR activation (198). SHP-1 is activated by Src-mediated phosphorylation at the C-terminus and is very effective in dephosphorylating Src substrates, including p120ctn Y296 (199). Using substrate trapping mutants of receptor protein tyrosine phosphatase DEP1 revealed that DEP1 interacts with p120ctn, as well as with beta-catenin and plakoglobin (200, 201). p120ctn might interact with DEP1 in a phosphorylation-dependent manner, whereas beta-catenin and plakoglobin might interact with DEP1 constitutively (201). The receptor-like protein tyrosine phosphatase RPTPmu specifically binds and dephosphorylates p120ctn (but not beta-catenin) independently of cadherins and of the phosphorylation status of p120ctn (202). The RPTPmu binding site in p120ctn is in the N-terminal domain, and deletion of AA 28-233 of p120ctn abrogates its interaction with RPTPmu (202). In conclusion, the N-terminus of p120ctn acts as a scaffold for a multitude of kinases and phosphatases that can interact with cadherin-bound p120ctn. In that way, p120ctn enables the modulation of the cadherin-catenin complex by phosphorylation.

How does phosphorylation of p120ctn affect cadherin-based adhesion? In Src-transformed MDCK and L-cells, constitutive tyrosine phosphorylation of p120ctn and beta-catenin weakens cadherin-based junctions (181, 203). Phosphorylation of p120ctn is dependent on its association with E-cadherin, as L-cells expressing an E-cadherin mutant lacking the cytoplasmic domain failed to phosphorylate p120ctn. However, membrane localization of p120ctn, but not via E-cadherin ligation *per se*, is essential for its ability to become phosphorylated on Ser or Thr residues. Both a chimeric cadherin-containing extracellular part of the IL-2R fused to the cytoplasmic cadherin part and CAAX-anchored p120ctn localize p120ctn to the membrane and allow its phosphorylation in the absence of E-cadherin (207). Serine/threonine (S/T) phosphorylation of p120ctn does not affect the p120ctn-cadherin binding affinity and stability of the cadherin complex, because mutating either individual S/T phosphorylation sites to alanine or mutating six major S/T sites together to alanine does not interfere with the capacity of mutated p120ctn to rescue the phenotypes of p120ctn-deficient cells

(207). In contrast, the presence of cadherin-bound beta-catenin is not essential for p120ctn phosphorylation, as an E-cadherin–alpha-catenin fusion is equally potent in phosphorylating p120ctn junctions (181, 203). In conclusion, increased Tyr phosphorylation of p120ctn is leading to disruption of junctions, while constitutive Ser/Thr phosphorylation of p120ctn does not affect the integrity of adherens junctions.

It is not clear how phosphorylation of p120ctn affects its binding to E-cadherin. Several groups reported that tyrosine phosphorylation of p120ctn increases binding affinity for E-cadherin (162, 163, 167, 172, 174), while others found no change in binding affinity between E-cadherin and p120ctn upon Src-mediated phosphorylation (4, 181). Increased binding of phosphorylated p120ctn to E-cadherin during junctional disassembly in Src-transformed cells implies that p120ctn blocks the key residues for Hakai-binding (Y755 and Y756) (Fig. 6C) and that E-cadherin internalization is not mediated by ubiquitination. In contrast, phosphorylated p120ctn has also been reported to dissociate from E-cadherin, allowing in this way the Hakai-mediated ubiquitination and endocytosis of E-cadherin (Fig. 6D) (205). A recent report shows that CK1epsilon can be recruited to the cadherin-catenin complex, resulting in the dissociation of p120ctn and beta-catenin from membrane-localized cadherins (261).

### 8.3. p120ctn isoforms and phosphorylation

Alternative splicing determines the extent of phosphorylation of different p120ctn isoforms by restricting the number of available phosphorylation sites or by the isoform-specific binding of kinases and phosphatases. The N-terminal domain is essential for the phosphorylation of p120ctn, and different p120ctn isoforms that can be generated from the four translation initiation sites exhibit variable truncations of this N-terminal domain (Fig. 3). p120ctn isoform 1 has the longest N-terminal domain and contains all the tyrosine, serine and threonine sites that may be phosphorylated. p120ctn isoform 3 lacks the first tyrosine residue (S96), which is indeed present only in the long isoforms. p120ctn isoform 4 is translated from the fourth translation initiation site and lacks almost the entire N-terminal domain, including all nine tyrosine sites and six serine and threonine sites. Hence, p120ctn isoform 4 is not regulated by phosphorylation and can be viewed as a dominant-negative p120ctn variant in this context.

Besides the role of isoforms in determining the potential phosphorylation sites, some kinases and phosphatases preferentially bind to certain p120ctn isoforms. p120ctn interacts with tyrosine kinase Fer in Rat-2 embryonic fibroblasts and in epithelial A431 cells. Although both cell types express long and short isoforms, Fer predominantly binds and phosphorylates long isoforms (167, 195). The Fer binding domain in p120ctn is confined to a 26-AA region (131 to 156) present in both long and short isoforms (183). This is odd, because only long p120ctn isoforms seem to bind to Fer (195). Different isoforms of p120ctn interact to different extents with the tyrosine phosphatase SHP-1, and this seems to be partly related to their susceptibility to EGF-dependent phosphorylation (198). p120ctn isoform 3A was very efficiently phosphorylated

## p120ctn in normal development and tumorigenesis

on tyrosine in response to EGF stimulation and bound SHP-1 strongly. Although p120ctn isoform 1A contains all tyrosine phosphorylation sites, it was less efficiently phosphorylated after EGF stimulation. This resulted in a weaker interaction with SHP-1. Strangely, both p120ctn isoform 1A and 3A contain the EGF-specific phosphorylation site Y228, but they show different degrees of phosphorylation. p120ctn isoform 1A can probably dock an additional phosphatase via its exclusive Y96 site, which would diminish overall tyrosine phosphorylation. p120ctn isoform 4A has no tyrosine phosphorylation sites and interacts with SHP-1 very weakly. Remarkably, the presence of six AA encoded by the alternatively spliced exon C led to a strong reduction in both tyrosine phosphorylation and SHP-1 binding (198). RPTPmu interacts with p120ctn isoform 1A but fails to bind to a mutant lacking much of the N-terminus (202). However, the different binding capacities of the long and short p120ctn isoforms have not been tested. In summary, the length of the N-terminal domain differs amongst p120ctn isoforms and determines the number of phosphorylation sites and the spectra of kinases and phosphatases that can be bound. p120ctn isoforms might promote divergent overall phosphorylation states, which might ultimately result in differential junctional strength.

## 9. THE p120CTN FAMILY IN ANIMAL MODELS

### 9.1. Animal models for p120ctn

The knockout and depletion of p120ctn in invertebrates (*C. elegans* and *Drosophila*), amphibians (*Xenopus*) and mouse was recently reviewed (9). Although *C. elegans* and *Drosophila* have only one p120ctn subfamily member (JAC-1 and *Drosophila* p120ctn, respectively), genetic or RNAi-mediated reduction of p120ctn levels in *C. elegans* and *Drosophila* did not affect normal development (Table 6) (34, 35, 208). In contrast, RNAi depletion of both zygotic and maternal p120ctn in *Drosophila* embryos resulted in severe morphogenetic defects, particularly in head involution (33). Although *Drosophila* p120ctn interacts with Rho1 (the *Drosophila* RhoA homolog) (33), Rho1 maintains proper localization of DE-cadherin and catenins independently of p120ctn (208). In addition, mutants of *Drosophila* DE-cadherin could be rescued by p120ctn-uncoupled but not by beta-catenin-uncoupled DE-cadherin mutants, indicating that p120ctn in invertebrates is not a core component of adherens junctions and only has a supportive role (34, 73).

In contrast, morpholino-mediated p120ctn knockdown in *Xenopus* resulted in severe developmental defects; the nature of the defects depended on which cells of early cleavage embryos were injected with morpholinos (Table 6) (74, 75). On the other hand, induced expression of murine p120ctn isoform 1A or 1N during amphibian development leads to gastrulation defects and head malformation, respectively, in contrast to the secondary body axis abnormality caused by overexpression of beta-catenin (209, 210). So, in *Xenopus*, normal development is contingent on maintenance of p120ctn expression levels within a physiological range. Also in mice proper p120ctn levels are a prerequisite for normal development and embryos with total knockout of p120ctn results in early embryonic lethality (mentioned in refs. 45, 77). According to a personal communication by Walter Birchmeier (Berlin), embryonic death is seen

at E10. Despite seemingly normal mesoderm formation, embryos do not turn at E8.5 to 9.0. The notochord is interrupted, and cell adhesion in the notochord and to the endoderm is weakened. Embryos stop growing at the 10-somite stage while closure of the neural tube is not completed. Several tissue-specific p120ctn knockouts have been reported by using the Cre/LoxP system. Two types of floxed p120ctn alleles were generated. In one of them, p120ctn exons 3 to 8, encoding all four possible start codons (M1-4), were flanked by LoxP sites to prevent any natural initiation of translation after Cre-mediated recombination (45). In the other approach, exon 7 of p120ctn was floxed, and Cre-mediated recombination resulted in a frameshift leading to degradation of mRNA by non-sense mediated decay (77).

**Table 6.** Knockout and knockdown of p120ctn family members in different species

Catenin	Organism	Tissue/cell type	Knockout (KO) or knockdown (KD)	Phenotype	References
JAC-1	C. elegans	whole animal	KD (RNAi)	No obvious developmental defects	(35)
p120ctn	Drosophila	whole animal	zygotic and maternal KO	No obvious developmental defects; except delayed dorsal closure	(34)
		whole animal	KD (RNAi)	No obvious developmental defects	(208)
		whole animal	KO (includes several genes)	Severe dorsal open phenotype	(33)
		whole animal	KD (RNAi)	Severe morphogenic effect including head involution	(33)
		whole animal	KO and KD (RNAi)	Reduced numbers and density of spine-like neuronal protrusions	(257)
p120ctn	Xenopus	whole animal	KD (Morpholino)	Disrupted gastrulation and axial elongation; reduced C-cadherin levels	(75)
		Anterior neural ectoderm	KD (Morpholino)	Impaired evagination of optic vesicles and defective eye formation; perturbed cranial neural crest cell; migration and malformations in craniofacial cartilage	(74)
p120ctn	mouse	whole animal	KO	Embryonic lethality around gastrulation Die at 10,5 dpc; defects in notochord formation, weakened cell adhesion between notochord and embryonic endoderm	(45, 77) W.B.
		Salivary gland	KO (MMTV-Cre)	Die shortly after parturition; blocked acinar differentiation; reduced E-cadherin levels; formation of neoplasias; abnormal epithelial polarity and morphology	(45)
		Skin	KO (K14-Cre)	Viable; reduced adherens junction components; increased RhoA activity; epidermal hyperplasia and chronic inflammation in aged mice; NFκB activation; skin neoplasias; mitotic defects	(46, 220)
		Teeth	KO (K14-Cre)	Viable; reduced E- and N-cadherin; dysplastic hypo-mineralized enamel; disrupted ameloblast polarity and morphology	(76)
		Vascular endothelium	KO (Tie2-Cre)	Die at 11,5 dpc; disorganized embryonic and extraembryonic vasculature; decreased microvascular density and hemorrhages; proliferation defect; reduced VE- and N-cadherin	(78)
		Dorsal forebrain	KO (Emx1-Cre)	Viable; reduced spine and synapse densities; decreased N-cadherin levels; increased RhoA activity	(77)
		Small intestine; colon	KO (Villin-Cre)	Die within 3 weeks; disruption of epithelial barrier; mucosal erosion; reduced adherens junction components; increased inflammation and neurophil binding	(47)
		liver	KO (Albumin-Cre)	Viable; severely impaired intrahepatic bile duct development; normal hepatocyte differentiation; unaltered cell-cell adhesion; accelerated initiation of hepatocarcinogenesis by diethylnitrosamine	van Hengel et al., unpublished
ARVCF	Xenopus	Whole animal	KD (Morpholino)	Disrupted gastrulation and axial elongation; reduced C-cadherin levels	(75)
		Anterior neural ectoderm	KD (Morpholino)	Perturbed cranial neural crest cell migration and malformations in craniofacial cartilage	K.V. & M.D.
	mouse	whole animal		Viable; no obvious phenotype	R.K.
δ-catenin	Xenopus	Whole animal; anterior neural ectoderm	KD (Morpholino)	Defects in gastrulation and axial elongation; reduced cadherin levels; RhoA activation; malformations in eye and craniofacial skeleton	(57)
		mouse	Whole animal	Impaired cognitive functions; abnormal synaptic plasticity; reduced N-cadherin and PSD-95 levels	(211)

W.B.: Walter Birchmeier, personal communication; K.V. & M.D.: Kris Vleminckx and Mieke Delvaeye, personal communication; R.K.: Raju Kucherlapati, personal communication.

## p120ctn in normal development and tumorigenesis

The importance of p120ctn during development is further demonstrated by Cre-mediated ablation of p120ctn in endothelial tissues at 7.5 dpc, causing death at 11.5 dpc (78). In other studies, developmental defects in tissue-specific p120ctn knockouts are mostly avoided by employing Cre-lines that are expressed near the end of embryonic development. Nevertheless, ablating p120ctn after midgestation in salivary gland and intestine can still result in perinatal death (45, 47), whereas its ablation in the skin, teeth or dorsal forebrain does not affect viability (46, 76, 77). Though these conditional p120ctn knockout mice show a wide range of tissue-specific phenotypes (listed in Table 6) (9), reduction of cadherin levels seems to be a common underlying mechanism (Section 5.2).

### 9.2. Animal models for p120ctn family members

Like p120ctn, ARVCF and delta-catenin are essential during *Xenopus* development. For instance, gastrulation defects are caused by generalized or localized knockdown of delta-catenin (Table 6) (57, 75). However, ARVCF and delta-catenin seem to be dispensable in mice, because both ARVCF and delta-catenin knockout mice are viable (R. Kucherlapati, personal communication) (211). Delta-catenin-deficient mice display cognitive dysfunctions, including severe learning defects and abnormal synaptic plasticity (211). p120ctn can probably substitute for ARVCF and delta-catenin in knockout mice, whereas p120ctn family members ARVCF, p0071 and delta-catenin cannot rescue the lethal phenotypes in p120ctn knockout mice. This further illustrates that p120ctn family members ARVCF, p0071 and delta-catenin are not functionally redundant. Alternatively, ARVCF, p0071 and delta-catenin might be intrinsically redundant, although they have spacial and temporal restricted expression patterns.

## 10. P120CTN AND CANCER

### 10.1. Altered expression of p120ctn in tumors

The role of p120ctn in tumors has been reviewed (212, 213). In general, p120ctn is either absent or altered in most human tumors, and its derangement is often correlated with poor prognosis. Alterations in p120ctn expression include decreased levels, translocation to the cytoplasm, and occasionally to the nucleus. These alterations remove p120ctn from the cell membrane and disable p120ctn-mediated stabilization of E-cadherin. p120ctn can act as a proto-oncogene or as an invasion-suppressor, depending on the order in which p120ctn and E-cadherin are down-regulated. Loss of p120ctn results in decreased E-cadherin levels, and E-cadherin is indeed frequently down-regulated in epithelial cancers where it acts as a tumor-suppressor (214, 215). On the other hand, E-cadherin loss results in translocation of p120ctn to the cytoplasm, where p120ctn modulates RhoGTPases in a way that favors cell motility. Like overexpression of dominant active Rac1, p120ctn-mediated Rac1 activation might promote cellular transformation. p120ctn also acts as a proto-oncogene by relieving the Kaiso-mediated repression of beta-catenin target genes, such as *c-Fos*, *Myc*, *Ccnd1* (encodes Cyclin D1) and *Mmp7* (encodes Matrylisin) (152, 154), and this favors tumor formation and invasion. In addition, Kaiso-deficient mice are more resistant to intestinal tumorigenesis when bred into an APC<sup>Min/+</sup> genetic background (158). Heterozygous APC<sup>Min</sup> mice are used as a model for human familial adenomatous polyposis

caused by a mutation of the *Apc* (adenomatous polyposis coli) gene that leads to nuclear localization of beta-catenin and activation of the canonical Wnt pathway. In contrast to tumor-associated nuclear beta-catenin, nuclear localization of p120ctn is observed only rarely in human tumors (140, 216).

Only a few mutations in the *CTNND1* gene have been reported, in breast cancer (217) and in SW48 colon carcinomacells (18). It is noteworthy that p120ctn expression might be compromised by mutating a single p120ctn allele. Indeed, expression of p120ctn can be monoallelic in some cell types (218). Perhaps other mechanisms are involved in p120ctn downregulation in tumors, such as transcriptional downregulation, epigenetic modifications or microRNA-mediated silencing, but this is poorly documented. p120ctn is transcriptionally downregulated by FOXC2 in non-small cell lung cancer cells (NSCLC) (219). FOXC2 binds to the p120ctn promoter and reduces its activity. On the other hand, RNAi-mediated silencing of FOXC2 increases p120ctn promoter activity as well as p120ctn mRNA and protein levels. p120ctn stabilizes cadherins at the cell membrane and RNAi-mediated depletion of its transcriptional repressor, FoxC2, enhances E-cadherin levels in NSCLC cells (219). The role of p120ctn in cancer was further investigated in animal models. Ablation of p120ctn in salivary gland resulted in morphological abnormalities, which closely resemble high-grade intraepithelial neoplasia, a precancerous condition in humans that typically progresses to invasive cancer (45). Ablation of p120ctn in skin caused hyperproliferation (46) and p120ctn-deficient skin grafts displayed signs of epidermal hyperkeratosis and dysplastic keratinocytes (220). In addition, p120ctn regulates several processes involved in tumorigenesis, such as RhoGTPase activity, cell proliferation, motility, invasion, anchorage-independent growth (AIG), and inflammatory conditions (see below).

## 10.2. p120ctn isoforms in EMT and cancer

Epithelial-to-mesenchymal transition (EMT) is an orchestrated series of events that allows epithelial sheets to dissociate, lose cell-cell interactions and cell-extracellular matrix interactions, and reorganize the cytoskeleton and transcriptional program in order to induce a mesenchymal phenotype (221). During EMT, E-cadherin downregulation in epithelial cells is accompanied by upregulation of mesenchymal cadherins (e.g. N-cadherin), a phenomenon called cadherin switching (222). Cadherin switching has been observed during normal development, such as primitive streak formation and neural crest delamination, and also during tumorigenesis (222, 223). Interestingly, a switch from short to long p120ctn isoforms has been observed during the EMT process, induced by expression of c-Fos (23), Snail (24), SIP1/ZEB2 (25, 26), E47 (26), Slug (26) or Twist (27) (Table 1). The downregulation of short ‘epithelial’ p120ctn isoforms during EMT is due to decreased expression of epithelial splicing regulatory proteins 1 and 2 (ESRP1 and ESRP2), what favors skipping of exon 3 (encoding the first two translation initiation sites) and translation initiation from the third start codon (encoded by exon 5) (27). Also Src transformation of MDCK cells induces an EMT-like process (164) associated with a switch from short to long p120ctn isoforms (7). This switch during EMT is consistent with the expression pattern of long and short p120ctn isoforms in fibroblasts and epithelial cell types, respectively (Table 1) (Section 3). Re-expression of E-cadherin in Snail-induced mesenchymal cells failed to



## p120ctn in normal development and tumorigenesis

restore the epithelial morphology and expression of 'epithelial' short p120ctn isoforms (24). This confirms that the abundance of the different p120ctn isoforms is regulated by cell type-specific splice factors and not necessarily by the expression of certain cadherin types (27). In contrast, the p120ctn isoform switch was not observed during EMT induced in highly differentiated colon cancer cells by TGF-beta and TNF-alpha (114). This discrepancy might be explained by the high expression levels of long p120ctn isoforms in non-induced cells, which can not be augmented even further during EMT. Increased RhoA inhibition is observed during EMT induced by TGF-beta and TNF-alpha, which coincides with increased binding of p120ctn to RhoA (114).

Similar EMT-like processes have been observed during tumor progression in prostate carcinoma cells and in anaplastic thyroid carcinomas, and these changes coincide with a switch from short to long p120ctn isoforms and from E- to N-cadherin (Table 1) (224, 225). Forced expression of E-cadherin in the pancreatic carcinoma cell line MIA PaCa-2 restored the epithelial phenotype and suppressed cell migration and invasion, but this did not occur upon N-cadherin expression (226). Interestingly, tyrosine-phosphorylated p120ctn isoform 1 interacted exclusively with N-cadherin, whereas E-cadherin predominantly bound to unphosphorylated p120ctn isoform 3 (226). There exists a controversy concerning p120ctn isoform switching in skin cancer (Table 1). One RT-PCR study reported the predominant expression of short p120ctn isoforms both in normal skin tissue and in benign and malignant skin cancer cells (216). In squamous cell carcinomas (SCCs), the p120ctn levels were consistently reduced while this was not the case for E-cadherin. Any remaining p120ctn was detected in the cytoplasm or sometimes the nuclei instead of the cell-cell boundaries (216). Another study (22) used antibodies with different p120ctn isoform specificity and this revealed the expression of p120ctn isoform 2, 3 and 4 in neonatal human keratinocytes and in HaCaT cells (immortalized but non-tumorigenic keratinocytes), whereas SCCs expressed predominantly p120ctn isoform 2 but not isoform 3 or 4. Both studies indicated that there is no striking difference in expression of p120ctn isoforms between benign (immortalized human keratinocytes) and malignant epithelial skin tumors (SCCs). In addition, no p120ctn isoform switch is observed in melanomas compared to normal melanocytes, although both express primarily p120ctn isoform 1 in contrast to the epithelial cell types (22). E-cadherin is expressed by both keratinocytes and melanocytes, allowing their mutual heterotypic and homophilic interaction. However, melanomas switch to N-cadherin during tumorigenesis and this facilitates dissociation from the keratinocyte layers and heterotypic interactions with stromal cells including fibroblasts and endothelial cells (227). In melanomas, p120ctn can compete with RhoA for binding to p190RhoGAP, which leads to RhoA activation. Reintroducing E-cadherin in melanomas blocked chemokine-induced invasion and sequestered p120ctn away from p190RhoGAP, leading to increased p190RhoGAP association with RhoA what results in RhoA inactivation (228). Melanocytes are quite interesting because they express the mesenchyme-associated long p120ctn isoforms in combination with E-cadherin. This shows that specific p120ctn isoforms are not invariably restricted to a certain cadherin type.

In lung SCC and adenocarcinomas, abnormal expression of p120ctn, including downregulation of both long and short isoforms, is associated with tumor progression and poor prognosis (230). Abnormal p120ctn expression, including complete loss, downregulation or mislocalization of p120ctn, correlated with abnormal E-cadherin expression (including reduced

or absent membrane expression of E-cadherin besides increased cytoplasmic expression of E-cadherin) and overexpression of RhoGTPases. Abnormal expression of p120ctn, E-cadherin and overexpression of RhoGTPases were associated with malignant human lung cancer *in vitro* and *in vivo* (231). E-cadherin and p120ctn isoform 3 are expressed in normal bronchial epithelium, but p120ctn isoform 1 is upregulated and localized in the cytoplasm of squamous cell lung cancers and lung adenocarcinomas (232). Further analysis revealed that overexpression of p120ctn isoform 1 mRNA correlated significantly with abnormal E-cadherin expression, with lymph node metastasis and poor differentiation (232). Another study confirmed a significant reduction of both long and short p120ctn isoforms in lung carcinomas compared to normal lung tissues (233). More recently these investigators reported that expression of p120ctn isoform 3 in lung cancer cells inhibited *in vivo* tumor growth in nude mice but failed to block invasion (234). On the other hand, p120ctn isoform 1 effectively blocked invasion but not tumor growth (234). All together, p120ctn isoforms 1 and 3 appear to have opposing effects on invasion and proliferation in lung cancer cells due to differential regulation of RhoGTPase activity (see also Section 10.3.) and differential stabilization of cadherin-based junctions (234, 235).

Little is known about the effects of the alternatively spliced internal exons of p120ctn on tumorigenesis. Exon B encodes a NES and is expressed in some human tissues, such as kidney, pancreas, colon, small intestine and prostate. Interestingly, expression of exon B is lost in the corresponding tumorigenic tissues (22), suggesting that during tumor progression p120ctn is shifted towards the nucleus, which relieves the repression of oncogenic target genes of Kaiso.

### 10.3. Differential regulation of RhoGTPases by p120ctn in cancer

In contrast to the dogma stating that p120ctn isoform 1 inhibits RhoA activity and activates Rac1 and Cdc42 (see Section 6.2.), in lung cancer cells p120ctn isoform 1 has been found to block Rac1 activity and p120ctn isoform 3 to activate RhoA and inhibit Cdc42 activity (234). Knockdown of p120ctn in lung cancer cell lines results in inhibition of RhoA and activation of Rac1 and Cdc42 (235). Activated RhoA has also been observed in a mouse model for invasive lobular carcinoma (Patrick Derksen, Utrecht, personal communication). Treatment of these mice with the clinically approved Rock inhibitor Fasudil inhibited tumor growth *in vivo* (P. Derksen, personal communication). Activation of the RhoA/Rock pathway in cells derived from primary mouse invasive lobular carcinomas results in phosphorylation of cofilin. Phosphorylated cofilin was also found in human invasive lobular carcinoma samples (P. Derksen, personal communication). A possible explanation for the discrepancy between the dogma and RhoGTPase regulation in lung and breast cancer might be the persistence or not of E-cadherin. Indeed, the effect of p120ctn on Rac1 activity depends on E-cadherin expression: knockdown of p120ctn results in Rac1 inhibition in E-cadherin-negative cells, but in Rac1 activation in E-cadherin positive cells (115). The lung cancer cells used in the study of Liu *et al.* (2009a) were still expressing E-cadherin, and this might explain the inhibition of Rac1 induced by p120ctn isoform 1. However, since the mouse model for invasive lobular carcinoma involves genetic inactivation of E-cadherin, the deviant RhoA activity in these tumors can not be explained by E-cadherin expression but must be caused by an unidentified mechanism.

## p120ctn in normal development and tumorigenesis

### 10.4. p120ctn isoforms: effects on proliferation and tumor growth

p120ctn can regulate cell proliferation in different ways. Several lines of evidence show that (high levels of) p120ctn promote cell proliferation and tumor growth. This promotes transformed growth of both E-cadherin negative and positive cells, and knockdown of p120ctn reduces the growth rate, as evidenced by a reduction in the proportion of cells in the S-phase (70, 115). Ras/MAPK signaling is important for the p120ctn-mediated growth effect, because RNAi-mediated depletion of p120ctn inactivates MAPK signaling in E-cadherin-negative cells (115). Both p120ctn isoforms 1 and 4 as well as constitutively active Rac1 can reactivate MAPK signaling (115). On the other hand, AIG mediated by p120ctn isoform 1 could be blocked by a MEK inhibitor (115). In addition, primary keratinocytes deficient in p120ctn grow more slowly than their wild-type counterparts due to defects in mitosis and cytokinesis, including the generation of binucleate cells (220). A similar phenotype was observed upon knockdown of p0071, another p120ctn family member (50). The defects seen in cells devoid of either p0071 or p120ctn could be rescued by constitutively active RhoA and dominant negative RhoA, respectively (50, 220). This discrepancy depends on the different abilities of p0071 and p120ctn to regulate RhoA activity (Fig. 5) (Section 6).

On the other hand, p120ctn can also block proliferation. p120 knockdown in NIH3T3 cells promotes serum-free cell proliferation and partial cell transformation (112). In E-cadherin-positive breast cancer cells, p120ctn depletion results in increased proliferation and activation of Ras-MAPK signaling (115). Expression of p120ctn isoform 3 in E-cadherin-positive cells blocks cell proliferation, DNA synthesis and *in vivo* tumor growth (234, 236). Cells expressing p120ctn isoform 3 are arrested in the G1-S phase and this transition from G1 to S phase depends on the cyclin-dependent kinase 2/CyclinE complex. p120ctn isoform 3 associates with this complex and prevents its proteasomal degradation. This leads to S-phase lengthening, centrosome overduplication, and genomic instability (236). In contrast to p120ctn deficient keratinocytes in culture (see above), genetic ablation of p120ctn in skin results in hyperproliferation and increased MAPK signaling (46). Cell proliferation is also increased in p120ctn-deficient colon and small intestine (47). These observations indicate that p120ctn might have different effects on cell growth *in vitro* and *in vivo*, and that the effects also depend on the cell type and the microenvironment.

### 10.5. p120ctn isoforms: effects on motility and invasion

p120ctn overexpression can activate Rac1 and Cdc42 and enhance migration (12, 13). Cells devoid of p120ctn fail to repopulate the wounded area in a scratch assay (112). On the other hand, a stable knockdown of p120ctn in E-cadherin-deficient cells resulted in decreased migration and invasiveness. These deficiencies could be rescued by reexpression of p120ctn isoform 1, but not by reexpression of cadherin-uncoupled p120ctn isoform 1 (72). Moreover, p120ctn induces invasiveness by its association with mesenchymal cadherins, such as N-cadherin or cadherin 11, whereas knockdown of these mesenchymal cadherins and the use of p120ctn-uncoupled mutants blocks invasiveness (72). Invasiveness can also be blocked by constitutively

active RhoA, dominant negative Rac1 and E-cadherin expression, but it is enhanced by inhibition of ROCK, a downstream effector of RhoA (72). The p120ctn-depleted cells have been employed for testing the potential of different p120ctn isoforms to induce invasion. Invasiveness is strongest upon expression of p120ctn isoform 1A, it is unaffected by p120ctn isoform 3A, and is blocked by p120ctn isoform 4 (113). In clear renal cell carcinomas, E-cadherin is downregulated and p120ctn is translocated to the cytoplasm. Furthermore, p120ctn undergoes an isoform switch from predominantly short to long p120ctn isoforms. This switch is correlated with micrometastasis, which indicates that, at least for this cancer type, p120ctn isoform 1 simulates invasiveness *in vivo* (113). p120ctn can also block invasion because p120ctn depletion in lung cancer cell lines enhances invasion and metastasis due to differential regulation of RhoGTPase activity (see Section 10.3) (235). To conclude, p120ctn isoforms affect migration and invasion in different ways by inducing RhoGTPase-mediated rearrangements of the actin cytoskeleton.

### 10.6. p120ctn and anchorage-independent growth (AIG)

AIG is a hallmark of tumor formation and is dependent on endogenous p120ctn. Stable knockdown of p120ctn in E-cadherin negative MDA-MB-231 cells abolished their ability to grow anchorage-independently *in vitro* (colony formation in soft agar) and *in vivo* (xenografts), but this effect could be rescued by re-expression of p120ctn isoform 1 (115). Similarly, knockdown of p120ctn in E-cadherin-negative mouse breast cancer cell lines blocked anoikis-resistance (P. Derksen, personal communication). p120ctn promotes tumor growth *via* Rac1 activation, and expression of a constitutively active Rac1 mutant reverses the cell cycle defect and can rescue AIG *in vitro* and xenograft growth *in vivo* (115). E-cadherin, but not p120ctn-uncoupled cadherin, can block both AIG and Rac1 and Ras activation in the presence of p120ctn (115). Stable knockdown of p120ctn in E-cadherin positive MCF7 cells results in reciprocal effects on AIG, Rac1 activity and MAPK signaling (115). However, it is not clear what the real molecular mechanism is, because p120ctn knockdown also affects the E-cadherin expression levels. Depletion of endogenous E-cadherin in MCF7 cells phenocopies the effect of p120ctn knockdown, indicating that under normal conditions E-cadherin blocks AIG by inhibiting both Rac and Ras-mediated signaling (115).

p120ctn ablation blocked AIG in cells transformed with Rac1 or Src, but not in cells transformed with H-Ras (70). AIG in cells transformed with Rac1 or Src is dependent on p120ctn-mediated RhoA inhibition because ablation of p120ctn in these transformed cells is rescued by inhibition of ROCK, a downstream RhoA effector (70). Activating the RhoA pathway by adding LIMK1, which is downstream of ROCK, also blocks AIG in transformed cells (70). RhoA activation results in phosphorylation and inactivation of cofilin at serine residue 3 (S3), whereas p120ctn-mediated RhoA inhibition results in cofilin activation (Fig. 5). Strangely, in contrast to ROCK inhibition, AIG is not rescued by a dominant active S3A cofilin mutant, which can no longer be phosphorylated. So, other RhoA effectors might be involved in the regulation of AIG (70).

## **p120ctn in normal development and tumorigenesis**

The finding in the abovementioned studies in which AIG depends on either Rac1 activation or RhoA inhibition, may be explained by the 'Bar-Sagi' pathway, in which Rac1 activation results in RhoA inhibition (Section 6, Fig. 4) (112).

### **10.7. p120ctn in inflammation and cancer**

A strong connection exists between inflammation and tumor progression (237). p120ctn depletion in mouse skin caused hyperproliferation and chronic inflammation due to increased NF- $\kappa$ B activation (46). Both general immunosuppressive drugs (Dexamethasone) and a NF- $\kappa$ B inhibitor (IKK2 inhibitor) reduced the hyperproliferation in p120ctn-deficient skin grafts (46, 220). The NF- $\kappa$ B activation in p120ctn-depleted keratinocytes is dependent on RhoA activity. Constitutively active RhoA and ROCK mutants result in nuclear translocation of NF- $\kappa$ B in wild-type keratinocytes, whereas nuclear NF- $\kappa$ B expression can be reverted in p120ctn-deficient keratinocytes by expression of dominant-negative RhoA or by treatment with ROCK inhibitor (46). Moreover, nuclear NF- $\kappa$ B can also be reverted by introducing a cadherin-uncoupled p120ctn mutant, but not by a RhoA-uncoupled (*delta622-628*) mutant (46). So, NF- $\kappa$ B activation depends on RhoA activity, which in turn might be influenced by expression of the alternatively spliced exon C (see Section 3). Poorly differentiated human squamous cell carcinomas also showed nuclear NF- $\kappa$ B and perturbed expression and/or localization of p120ctn (220). Finally, genetic ablation of intestinal p120ctn also results in increased infiltration of COX-2-positive neutrophils, which is commonly seen in inflammatory bowel disease (47). This disease predisposes intestinal tissue to cancer (238).

## **11. ACKNOWLEDGEMENTS**

This work was supported by grants from the Queen Elisabeth Medical Foundation (G.S.K.E.), Belgium, and from the Geconcerteerde Onderzoeksacties of Ghent University. Tim Pieters has been supported by the Instituut voor de Aanmoediging van Innovatie door Wetenschap en Technologie in Vlaanderen (IWT). We acknowledge Dr. Amin Bredan for critical reading of the manuscript, , and the members of our research group for valuable discussions.

**12. REFERENCES**

1. A. B. Reynolds, D. J. Roesel, S. B. Kanner and J. T. Parsons: Transformation-specific tyrosine phosphorylation of a novel cellular protein in chicken cells expressing oncogenic variants of the avian cellular src gene. *Mol Cell Biol* 9, 629-638 (1989)
2. J. M. Daniel and A. B. Reynolds: Tyrosine phosphorylation and cadherin/catenin function. *Bioessays* 19, 883-891 (1997)
3. A. B. Reynolds, L. Herbert, J. L. Cleveland, S. T. Berg and J. R. Gaut: p120, a novel substrate of protein tyrosine kinase receptors and of p60v-src, is related to cadherin-binding factors beta-catenin, plakoglobin and armadillo. *Oncogene* 7, 2439-2445 (1992)
4. A. B. Reynolds, J. Daniel, P. D. McCrea, M. J. Wheelock, J. Wu and Z. Zhang: Identification of a new catenin: the tyrosine kinase substrate p120cas associates with E-cadherin complexes. *Mol Cell Biol* 14, 8333-8342 (1994)
5. A. Keirsebilck, S. Bonne, K. Staes, J. van Hengel, F. Nollet, A. Reynolds and F. van Roy: Molecular cloning of the human p120ctn catenin gene (CTNND1): expression of multiple alternatively spliced isoforms. *Genomics* 50, 129-146 (1998)
6. J. M. Daniel and A. B. Reynolds: The tyrosine kinase substrate p120cas binds directly to E-cadherin but not to the adenomatous polyposis coli protein or alpha-catenin. *Mol Cell Biol* 15, 4819-4824 (1995)
7. Y. Y. Mo and A. B. Reynolds: Identification of murine p120 isoforms and heterogeneous expression of p120cas isoforms in human tumor cell lines. *Cancer Res* 56, 2633-2640 (1996)
8. P. Z. Anastasiadis and A. B. Reynolds: The p120 catenin family: complex roles in adhesion, signaling and cancer. *J Cell Sci* 113 ( Pt 8), 1319-1334 (2000)
9. P. D. McCrea and J. I. Park: Developmental functions of the P120-catenin sub-family. *Biochim Biophys Acta* 1773, 17-33 (2007)
10. A. B. Reynolds, J. M. Daniel, Y. Y. Mo, J. Wu and Z. Zhang: The novel catenin p120cas binds classical cadherins and induces an unusual morphological phenotype in NIH3T3 fibroblasts. *Exp Cell Res* 225, 328-337 (1996)
11. P. Z. Anastasiadis, S. Y. Moon, M. A. Thoreson, D. J. Mariner, H. C. Crawford, Y. Zheng and A. B. Reynolds: Inhibition of RhoA by p120 catenin. *Nat Cell Biol* 2, 637-644 (2000)
12. I. Grosheva, M. Shtutman, M. Elbaum and A. D. Bershadsky: p120 catenin affects cell motility via modulation of activity of Rho-family GTPases: a link between cell-cell contact formation and regulation of cell locomotion. *J Cell Sci* 114, 695-707 (2001)

## p120ctn in normal development and tumorigenesis

13. N. K. Noren, B. P. Liu, K. BurrIDGE and B. Kreft: p120 catenin regulates the actin cytoskeleton via Rho family GTPases. *J Cell Biol* 150, 567-580 (2000)
14. J. M. Daniel and A. B. Reynolds: The catenin p120(ctn) interacts with Kaiso, a novel BTB/POZ domain zinc finger transcription factor. *Mol Cell Biol* 19, 3614-3623 (1999)
15. S. Aho, K. Rothenberger and J. Uitto: Human p120ctn catenin: tissue-specific expression of isoforms and molecular interactions with BP180/type XVII collagen. *J Cell Biochem* 73, 390-399 (1999)
16. H. J. Choi and W. I. Weis: Structure of the armadillo repeat domain of plakophilin 1. *J Mol Biol* 346, 367-376 (2005)
17. N. Ishiyama, S. H. Lee, S. Liu, G. Y. Li, M. J. Smith, L. F. Reichardt and M. Ikura: Dynamic and static interactions between p120 catenin and E-cadherin regulate the stability of cell-cell adhesion. *Cell* 141, 117-128 (2010)
18. R. C. Ireton, M. A. Davis, J. van Hengel, D. J. Mariner, K. Barnes, M. A. Thoreson, P. Z. Anastasiadis, L. Matrisian, L. M. Bundy, L. Sealy, B. Gilbert, F. van Roy and A. B. Reynolds: A novel role for p120 catenin in E-cadherin function. *J Cell Biol* 159, 465-476 (2002)
19. J. M. Staddon, C. Smales, C. Schulze, F. S. Esch and L. L. Rubin: p120, a p120-related protein (p100), and the cadherin/catenin complex. *J Cell Biol* 130, 369-381 (1995)
20. N. Golenhofen and D. Drenckhahn: The catenin, p120ctn, is a common membrane-associated protein in various epithelial and non-epithelial cells and tissues. *Histochem Cell Biol* 114, 147-155 (2000)
21. O. Montonen, M. Aho, J. Uitto and S. Aho: Tissue distribution and cell type-specific expression of p120ctn isoforms. *J Histochem Cytochem* 49, 1487-1496 (2001)
22. S. Aho, L. Levansuo, O. Montonen, C. Kari, U. Rodeck and J. Uitto: Specific sequences in p120ctn determine subcellular distribution of its multiple isoforms involved in cellular adhesion of normal and malignant epithelial cells. *J Cell Sci* 115, 1391-1402 (2002)
23. A. Eger, A. Stockinger, B. Schaffhauser, H. Beug and R. Foisner: Epithelial mesenchymal transition by c-Fos estrogen receptor activation involves nuclear translocation of beta-catenin and upregulation of beta-catenin/lymphoid enhancer binding factor-1 transcriptional activity. *J Cell Biol* 148, 173-188 (2000)
24. T. Ohkubo and M. Ozawa: The transcription factor Snail downregulates the tight junction components independently of E-cadherin downregulation. *J Cell Sci* 117, 1675-1685 (2004)
25. C. Vandewalle, J. Comijn, B. De Craene, P. Vermassen, E. Bruyneel, H. Andersen, E. Tulchinsky, F. Van Roy and G. Berx: SIP1/ZEB2 induces EMT by repressing genes of different epithelial cell-cell junctions. *Nucleic Acids Res* 33, 6566-6578 (2005)

26. D. Sarrio, B. Perez-Mies, D. Hardisson, G. Moreno-Bueno, A. Suarez, A. Cano, J. Martin-Perez, C. Gamallo and J. Palacios: Cytoplasmic localization of p120ctn and E-cadherin loss characterize lobular breast carcinoma from preinvasive to metastatic lesions. *Oncogene* 23, 3272-3283 (2004)
27. C. C. Warzecha, T. K. Sato, B. Nabet, J. B. Hogenesch and R. P. Carstens: ESRP1 and ESRP2 are epithelial cell-type-specific regulators of FGFR2 splicing. *Mol Cell* 33, 591-601 (2009)
28. J. van Hengel, P. Vanhoenacker, K. Staes and F. van Roy: Nuclear localization of the p120(ctn) Armadillo-like catenin is counteracted by a nuclear export signal and by E-cadherin expression. *Proc Natl Acad Sci U S A* 96, 7980-7985 (1999)
29. P. D. McCrea and D. Gu: The catenin family at a glance. *J Cell Sci* 123, 637-642 (2010)
30. W. J. Nelson and R. Nusse: Convergence of Wnt, beta-catenin, and cadherin pathways. *Science* 303, 1483-1487 (2004)
31. J. Heuberger and W. Birchmeier: Interplay of cadherin-mediated cell adhesion and canonical Wnt signaling. *Cold Spring Harb Perspect Biol* 2, a002915 (2010)
32. M. Hatzfeld: Plakophilins: Multifunctional proteins or just regulators of desmosomal adhesion? *Biochim Biophys Acta* (2007)
33. C. R. Magie, D. Pinto-Santini and S. M. Parkhurst: Rho1 interacts with p120ctn and alpha-catenin, and regulates cadherin-based adherens junction components in *Drosophila*. *Development* 129, 3771-3782 (2002)
34. S. H. Myster, R. Cavallo, C. T. Anderson, D. T. Fox and M. Peifer: *Drosophila* p120catenin plays a supporting role in cell adhesion but is not an essential adherens junction component. *J Cell Biol* 160, 433-449 (2003)
35. J. Pettitt, E. A. Cox, I. D. Broadbent, A. Flett and J. Hardin: The *Caenorhabditis elegans* p120 catenin homologue, JAC-1, modulates cadherin-catenin function during epidermal morphogenesis. *J Cell Biol* 162, 15-22 (2003)
36. R. Tewari, E. Bailes, K. A. Bunting and J. C. Coates: Armadillo-repeat protein functions: questions for little creatures. *Trends Cell Biol* 20, 470-481 (2010)
37. M. Hatzfeld, K. J. Green and H. Sauter: Targeting of p0071 to desmosomes and adherens junctions is mediated by different protein domains. *J Cell Sci* 116, 1219-1233 (2003)
38. D. J. Mariner, J. Wang and A. B. Reynolds: ARVCF localizes to the nucleus and adherens junction and is mutually exclusive with p120(ctn) in E-cadherin complexes. *J Cell Sci* 113 ( Pt 8), 1481-1490 (2000)



## p120ctn in normal development and tumorigenesis

39. H. Sirotkin, H. O'Donnell, R. DasGupta, S. Halford, B. St Jore, A. Puech, S. Parimoo, B. Morrow, A. Skoultchi, S. M. Weissman, P. Scambler and R. Kucherlapati: Identification of a new human catenin gene family member (ARVCF) from the region deleted in velo-cardio-facial syndrome. *Genomics* 41, 75-83 (1997)
40. Q. Lu, M. Paredes, M. Medina, J. Zhou, R. Cavallo, M. Peifer, L. Orecchio and K. S. Kosik: delta-catenin, an adhesive junction-associated protein which promotes cell scattering. *J Cell Biol* 144, 519-532 (1999)
41. A. F. Paulson, E. Mooney, X. Fang, H. Ji and P. D. McCrea: Xarvcf, Xenopus member of the p120 catenin subfamily associating with cadherin juxtamembrane region. *J Biol Chem* 275, 30124-30131 (2000)
42. A. S. Yap, C. M. Niessen and B. M. Gumbiner: The juxtamembrane region of the cadherin cytoplasmic tail supports lateral clustering, adhesive strengthening, and interaction with p120ctn. *J Cell Biol* 141, 779-789 (1998)
43. I. Yang, O. Chang, Q. Lu and K. Kim: Delta-catenin affects the localization and stability of p120-catenin by competitively interacting with E-cadherin. *Mol Cells* 29, 233-237 (2010)
44. M. A. Davis, R. C. Ireton and A. B. Reynolds: A core function for p120-catenin in cadherin turnover. *J Cell Biol* 163, 525-534 (2003)
45. M. A. Davis and A. B. Reynolds: Blocked acinar development, E-cadherin reduction, and intraepithelial neoplasia upon ablation of p120-catenin in the mouse salivary gland. *Dev Cell* 10, 21-31 (2006)
46. M. Perez-Moreno, M. A. Davis, E. Wong, H. A. Pasolli, A. B. Reynolds and E. Fuchs: p120-catenin mediates inflammatory responses in the skin. *Cell* 124, 631-644 (2006)
47. W. G. Smalley-Freed, A. Efimov, P. E. Burnett, S. P. Short, M. A. Davis, D. L. Gumucio, M. K. Washington, R. J. Coffey and A. B. Reynolds: p120-catenin is essential for maintenance of barrier function and intestinal homeostasis in mice. *J Clin Invest* 120, 1824-1835 (2010)
48. M. Hatzfeld and C. Nachtsheim: Cloning and characterization of a new armadillo family member, p0071, associated with the junctional plaque: evidence for a subfamily of closely related proteins. *J Cell Sci* 109 ( Pt 11), 2767-2778 (1996)
49. I. Hofmann, C. Kuhn and W. W. Franke: Protein p0071, a major plaque protein of non-desmosomal adhering junctions, is a selective cell-type marker. *Cell Tissue Res* 334, 381-399 (2008)
50. A. Wolf, R. Keil, O. Gotzl, A. Mun, K. Schwarze, M. Lederer, S. Huttelmaier and M. Hatzfeld: The armadillo protein p0071 regulates Rho signalling during cytokinesis. *Nat Cell Biol* (2006)

51. R. Keil, C. Kiessling and M. Hatzfeld: Targeting of p0071 to the midbody depends on KIF3. *J Cell Sci* 122, 1174-1183 (2009)
52. J. Zhou, U. Liyanage, M. Medina, C. Ho, A. D. Simmons, M. Lovett and K. S. Kosik: Presenilin 1 interaction in the brain with a novel member of the Armadillo family. *Neuroreport* 8, 2085-2090 (1997)
53. R. Paffenholz and W. W. Franke: Identification and localization of a neurally expressed member of the plakoglobin/armadillo multigene family. *Differentiation* 61, 293-304 (1997)
54. C. Ho, J. Zhou, M. Medina, T. Goto, M. Jacobson, P. G. Bhide and K. S. Kosik: delta-catenin is a nervous system-specific adherens junction protein which undergoes dynamic relocalization during development. *J Comp Neurol* 420, 261-276 (2000)
55. K. S. Kosik, C. P. Donahue, I. Israely, X. Liu and T. Ochiishi: Delta-catenin at the synaptic-adherens junction. *Trends Cell Biol* 15, 172-178 (2005)
56. Y. Kawamura, Q. W. Fan, H. Hayashi, M. Michikawa, K. Yanagisawa and H. Komano: Expression of the mRNA for two isoforms of neural plakophilin-related arm-repeat protein/delta-catenin in rodent neurons and glial cells. *Neurosci Lett* 277, 185-188 (1999)
57. D. Gu, A. K. Sater, H. Ji, K. Cho, M. Clark, S. A. Stratton, M. C. Barton, Q. Lu and P. D. McCrea: Xenopus delta-catenin is essential in early embryogenesis and is functionally linked to cadherins and small GTPases. *J Cell Sci* 122, 4049-4061 (2009)
58. Q. Lu, N. K. Mukhopadhyay, J. D. Griffin, M. Paredes, M. Medina and K. S. Kosik: Brain armadillo protein delta-catenin interacts with Abl tyrosine kinase and modulates cellular morphogenesis in response to growth factors. *J Neurosci Res* 67, 618-624 (2002)
59. M. C. Martinez, T. Ochiishi, M. Majewski and K. S. Kosik: Dual regulation of neuronal morphogenesis by a delta-catenin-cortactin complex and Rho. *J Cell Biol* 162, 99-111 (2003)
60. M. Medina, R. C. Marinescu, J. Overhauser and K. S. Kosik: Hemizyosity of delta-catenin (CTNND2) is associated with severe mental retardation in cri-du-chat syndrome. *Genomics* 63, 157-164 (2000)
61. M. Peifer and A. S. Yap: Traffic control: p120-catenin acts as a gatekeeper to control the fate of classical cadherins in mammalian cells. *J Cell Biol* 163, 437-440 (2003)
62. A. B. Reynolds and R. H. Carnahan: Regulation of cadherin stability and turnover by p120ctn: implications in disease and cancer. *Semin Cell Dev Biol* 15, 657-663 (2004)
63. A. B. Reynolds and A. Rocznik-Ferguson: Emerging roles for p120-catenin in cell adhesion and cancer. *Oncogene* 23, 7947-7956 (2004)

## p120ctn in normal development and tumorigenesis

64. K. Xiao, R. G. Oas, C. M. Chiasson and A. P. Kowalczyk: Role of p120-catenin in cadherin trafficking. *Biochim Biophys Acta* 1773, 8-16 (2007)
65. A. P. Kowalczyk and A. B. Reynolds: Protecting your tail: regulation of cadherin degradation by p120-catenin. *Curr Opin Cell Biol* 16, 522-527 (2004)
66. S. Shibamoto, M. Hayakawa, K. Takeuchi, T. Hori, K. Miyazawa, N. Kitamura, K. R. Johnson, M. J. Wheelock, N. Matsuyoshi, M. Takeichi and et al.: Association of p120, a tyrosine kinase substrate, with E-cadherin/catenin complexes. *J Cell Biol* 128, 949-957 (1995)
67. M. A. Thoreson, P. Z. Anastasiadis, J. M. Daniel, R. C. Ireton, M. J. Wheelock, K. R. Johnson, D. K. Hummingbird and A. B. Reynolds: Selective uncoupling of p120(ctn) from E-cadherin disrupts strong adhesion. *J Cell Biol* 148, 189-202 (2000)
68. S. Aono, S. Nakagawa, A. B. Reynolds and M. Takeichi: p120(ctn) acts as an inhibitory regulator of cadherin function in colon carcinoma cells. *J Cell Biol* 145, 551-562 (1999)
69. T. Ohkubo and M. Ozawa: p120(ctn) binds to the membrane-proximal region of the E-cadherin cytoplasmic domain and is involved in modulation of adhesion activity. *J Biol Chem* 274, 21409-21415 (1999)
70. M. R. Dohn, M. V. Brown and A. B. Reynolds: An essential role for p120-catenin in Src- and Rac1-mediated anchorage-independent cell growth. *J Cell Biol* 184, 437-450 (2009)
71. K. Xiao, D. F. Allison, K. M. Buckley, M. D. Kottke, P. A. Vincent, V. Faundez and A. P. Kowalczyk: Cellular levels of p120 catenin function as a set point for cadherin expression levels in microvascular endothelial cells. *J Cell Biol* 163, 535-545 (2003)
72. M. Yanagisawa and P. Z. Anastasiadis: p120 catenin is essential for mesenchymal cadherin-mediated regulation of cell motility and invasiveness. *J Cell Biol* 174, 1087-1096 (2006)
73. A. Pacquelet, L. Lin and P. Rorth: Binding site for p120/delta-catenin is not required for Drosophila E-cadherin function in vivo. *J Cell Biol* 160, 313-319 (2003)
74. M. Ciesiolka, M. Delvaeye, G. Van Imschoot, V. Verschuere, P. McCrea, F. van Roy and K. Vleminckx: p120 catenin is required for morphogenetic movements involved in the formation of the eyes and the craniofacial skeleton in Xenopus. *J Cell Sci* 117, 4325-4339 (2004)
75. X. Fang, H. Ji, S. W. Kim, J. I. Park, T. G. Vaught, P. Z. Anastasiadis, M. Ciesiolka and P. D. McCrea: Vertebrate development requires ARVCF and p120 catenins and their interplay with RhoA and Rac. *J Cell Biol* 165, 87-98 (2004)
76. J. D. Bartlett, J. M. Dobeck, C. E. Tye, M. Perez-Moreno, N. Stokes, A. B. Reynolds, E. Fuchs and Z. Skobe: Targeted p120-catenin ablation disrupts dental enamel development. *PLoS One* 5 (2010)

77. L. P. Elia, M. Yamamoto, K. Zang and L. F. Reichardt: p120 catenin regulates dendritic spine and synapse development through Rho-family GTPases and cadherins. *Neuron* 51, 43-56 (2006)
78. R. G. Oas, K. Xiao, S. Summers, K. B. Wittich, C. M. Chiasson, W. D. Martin, H. E. Grossniklaus, P. A. Vincent, A. B. Reynolds and A. P. Kowalczyk: p120-Catenin is required for mouse vascular development. *Circ Res* 106, 941-951 (2010)
79. D. M. Bryant and J. L. Stow: The ins and outs of E-cadherin trafficking. *Trends Cell Biol* 14, 427-434 (2004)
80. E. Delva and A. P. Kowalczyk: Regulation of cadherin trafficking. *Traffic* 10, 259-267 (2009)
81. K. C. Miranda, T. Khromykh, P. Christy, T. L. Le, C. J. Gottardi, A. S. Yap, J. L. Stow and R. D. Teasdale: A dileucine motif targets E-cadherin to the basolateral cell surface in Madin-Darby canine kidney and LLC-PK1 epithelial cells. *J Biol Chem* 276, 22565-22572 (2001)
82. Y. T. Chen, D. B. Stewart and W. J. Nelson: Coupling assembly of the E-cadherin/beta-catenin complex to efficient endoplasmic reticulum exit and basal-lateral membrane targeting of E-cadherin in polarized MDCK cells. *J Cell Biol* 144, 687-699 (1999)
83. K. C. Miranda, S. R. Joseph, A. S. Yap, R. D. Teasdale and J. L. Stow: Contextual binding of p120ctn to E-cadherin at the basolateral plasma membrane in polarized epithelia. *J Biol Chem* 278, 43480-43488 (2003)
84. J. K. Wahl, 3rd, Y. J. Kim, J. M. Cullen, K. R. Johnson and M. J. Wheelock: N-cadherin-catenin complexes form prior to cleavage of the proregion and transport to the plasma membrane. *J Biol Chem* 278, 17269-17276 (2003)
85. S. Mary, S. Charrasse, M. Meriane, F. Comunale, P. Travo, A. Blangy and C. Gauthier-Rouviere: Biogenesis of N-cadherin-dependent cell-cell contacts in living fibroblasts is a microtubule-dependent kinesin-driven mechanism. *Mol Biol Cell* 13, 285-301 (2002)
86. X. Chen, S. Kojima, G. G. Borisy and K. J. Green: p120 catenin associates with kinesin and facilitates the transport of cadherin-catenin complexes to intercellular junctions. *J Cell Biol* 163, 547-557 (2003)
87. M. Yanagisawa, I. N. Kaverina, A. Wang, Y. Fujita, A. B. Reynolds and P. Z. Anastasiadis: A novel interaction between kinesin and p120 modulates p120 localization and function. *J Biol Chem* 279, 9512-9521 (2004)
88. A. Rocznik-Ferguson and A. B. Reynolds: Regulation of p120-catenin nucleocytoplasmic shuttling activity. *J Cell Sci* 116, 4201-4212 (2003)

## p120ctn in normal development and tumorigenesis

89. T. Ichii and M. Takeichi: p120-catenin regulates microtubule dynamics and cell migration in a cadherin-independent manner. *Genes Cells* 12, 827-839 (2007)
90. T. L. Le, A. S. Yap and J. L. Stow: Recycling of E-cadherin: A potential mechanism for regulating cadherin dynamics. *Journal of Cell Biology* 146, 219-232 (1999)
91. A. I. Ivanov, A. Nusrat and C. A. Parkos: Endocytosis of epithelial apical junctional proteins by a clathrin-mediated pathway into a unique storage compartment. *Mol Biol Cell* 15, 176-188 (2004)
92. K. Xiao, J. Garner, K. M. Buckley, P. A. Vincent, C. M. Chiasson, E. Dejana, V. Faundez and A. P. Kowalczyk: p120-Catenin regulates clathrin-dependent endocytosis of VE-cadherin. *Mol Biol Cell* 16, 5141-5151 (2005)
93. F. Palacios, L. Price, J. Schweitzer, J. G. Collard and C. D'Souza-Schorey: An essential role for ARF6-regulated membrane traffic in adherens junction turnover and epithelial cell migration. *Embo J* 20, 4973-4986 (2001)
94. G. Izumi, T. Sakisaka, T. Baba, S. Tanaka, K. Morimoto and Y. Takai: Endocytosis of E-cadherin regulated by Rac and Cdc42 small G proteins through IQGAP1 and actin filaments. *J Cell Biol* 166, 237-248 (2004)
95. Z. Lu, S. Ghosh, Z. Wang and T. Hunter: Downregulation of caveolin-1 function by EGF leads to the loss of E-cadherin, increased transcriptional activity of beta-catenin, and enhanced tumor cell invasion. *Cancer Cell* 4, 499-515 (2003)
96. N. Akhtar and N. A. Hotchin: RAC1 regulates adherens junctions through endocytosis of E-cadherin. *Mol Biol Cell* 12, 847-862 (2001)
97. F. Palacios, J. S. Tushir, Y. Fujita and C. D'Souza-Schorey: Lysosomal targeting of E-cadherin: a unique mechanism for the down-regulation of cell-cell adhesion during epithelial to mesenchymal transitions. *Mol Cell Biol* 25, 389-402 (2005)
98. A. D. Paterson, R. G. Parton, C. Ferguson, J. L. Stow and A. S. Yap: Characterization of E-cadherin endocytosis in isolated MCF-7 and chinese hamster ovary cells: the initial fate of unbound E-cadherin. *J Biol Chem* 278, 21050-21057 (2003)
99. D. M. Bryant, M. C. Kerr, L. A. Hammond, S. R. Joseph, K. E. Mostov, R. D. Teasdale and J. L. Stow: EGF induces macropinocytosis and SNX1-modulated recycling of E-cadherin. *J Cell Sci* 120, 1818-1828 (2007)
100. M. Sharma and B. R. Henderson: IQ-domain GTPase-activating protein 1 regulates beta-catenin at membrane ruffles and its role in macropinocytosis of N-cadherin and adenomatous polyposis coli. *J Biol Chem* 282, 8545-8556 (2007)

101. Y. Miyashita and M. Ozawa: Increased internalization of p120-uncoupled E-cadherin and a requirement for a dileucine motif in the cytoplasmic domain for endocytosis of the protein. *J Biol Chem* 282, 11540-11548 (2007)
102. Y. Miyashita and M. Ozawa: A dileucine motif in its cytoplasmic domain directs beta-catenin-uncoupled E-cadherin to the lysosome. *J Cell Sci* 120, 4395-4406 (2007)
103. C. M. Chiasson, K. B. Wittich, P. A. Vincent, V. Faundez and A. P. Kowalczyk: p120-catenin inhibits VE-cadherin internalization through a Rho-independent mechanism. *Mol Biol Cell* 20, 1970-1980 (2009)
104. L. Baki, P. Marambaud, S. Efthimiopoulos, A. Georgakopoulos, P. Wen, W. Cui, J. Shioi, E. Koo, M. Ozawa, V. L. Friedrich, Jr. and N. K. Robakis: Presenilin-1 binds cytoplasmic epithelial cadherin, inhibits cadherin/p120 association, and regulates stability and function of the cadherin/catenin adhesion complex. *Proc Natl Acad Sci U S A* 98, 2381-2386 (2001)
105. P. Marambaud, J. Shioi, G. Serban, A. Georgakopoulos, S. Sarner, V. Nagy, L. Baki, P. Wen, S. Efthimiopoulos, Z. Shao, T. Wisniewski and N. K. Robakis: A presenilin-1/gamma-secretase cleavage releases the E-cadherin intracellular domain and regulates disassembly of adherens junctions. *Embo J* 21, 1948-1956 (2002)
106. M. E. Rubio, C. Curcio, N. Chauvet and J. L. Bruses: Assembly of the N-cadherin complex during synapse formation involves uncoupling of p120-catenin and association with presenilin 1. *Mol Cell Neurosci* 30, 118-130 (2005)
107. Y. Fujita, G. Krause, M. Scheffner, D. Zechner, H. E. Leddy, J. Behrens, T. Sommer and W. Birchmeier: Hakai, a c-Cbl-like protein, ubiquitinates and induces endocytosis of the E-cadherin complex. *Nat Cell Biol* 4, 222-231 (2002)
108. S. Pece and J. S. Gutkind: E-cadherin and Hakai: signalling, remodeling or destruction? *Nat Cell Biol* 4, E72-74 (2002)
109. P. Z. Anastasiadis: p120-ctn: A nexus for contextual signaling via Rho GTPases. *Biochim Biophys Acta* 1773, 34-46 (2007)
110. K. F. Kelly, C. M. Spring, A. A. Otchere and J. M. Daniel: NLS-dependent nuclear localization of p120ctn is necessary to relieve Kaiso-mediated transcriptional repression. *J Cell Sci* 117, 2675-2686 (2004)
111. J. Castano, G. Solanas, D. Casagolda, I. Raurell, P. Villagrasa, X. R. Bustelo, A. Garcia de Herreros and M. Dunach: Specific phosphorylation of p120-catenin regulatory domain differently modulates its binding to RhoA. *Mol Cell Biol* 27, 1745-1757 (2007)
112. G. A. Wildenberg, M. R. Dohn, R. H. Carnahan, M. A. Davis, N. A. Lobdell, J. Settleman and A. B. Reynolds: p120-catenin and p190RhoGAP regulate cell-cell adhesion by coordinating antagonism between Rac and Rho. *Cell* 127, 1027-1039 (2006)

## p120ctn in normal development and tumorigenesis

113. M. Yanagisawa, D. Huvelde, P. Kreinest, C. M. Lohse, J. C. Cheville, A. S. Parker, J. A. Copland and P. Z. Anastasiadis: A p120 catenin isoform switch affects Rho activity, induces tumor cell invasion, and predicts metastatic disease. *J Biol Chem* 283, 18344-18354 (2008)
114. D. I. Bellovin, R. C. Bates, A. Muzikansky, D. L. Rimm and A. M. Mercurio: Altered localization of p120 catenin during epithelial to mesenchymal transition of colon carcinoma is prognostic for aggressive disease. *Cancer Res* 65, 10938-10945 (2005)
115. E. Soto, M. Yanagisawa, L. A. Marlow, J. A. Copland, E. A. Perez and P. Z. Anastasiadis: p120 catenin induces opposing effects on tumor cell growth depending on E-cadherin expression. *J Cell Biol* 183, 737-749 (2008)
116. G. R. Hoffman, N. Nassar and R. A. Cerione: Structure of the Rho family GTP-binding protein Cdc42 in complex with the multifunctional regulator RhoGDI. *Cell* 100, 345-356 (2000)
117. E. E. Sander, J. P. ten Klooster, S. van Delft, R. A. van der Kammen and J. G. Collard: Rac downregulates Rho activity: reciprocal balance between both GTPases determines cellular morphology and migratory behavior. *J Cell Biol* 147, 1009-1022 (1999)
118. A. S. Nimnual, L. J. Taylor and D. Bar-Sagi: Redox-dependent downregulation of Rho by Rac. *Nat Cell Biol* 5, 236-241 (2003)
119. C. M. Niessen and A. S. Yap: Another job for the talented p120-catenin. *Cell* 127, 875-877 (2006)
120. V. M. Braga and A. S. Yap: The challenges of abundance: epithelial junctions and small GTPase signalling. *Curr Opin Cell Biol* 17, 466-474 (2005)
121. V. M. Braga: Cell-cell adhesion and signalling. *Curr Opin Cell Biol* 14, 546-556 (2002)
122. V. M. Braga, L. M. Machesky, A. Hall and N. A. Hotchin: The small GTPases Rho and Rac are required for the establishment of cadherin-dependent cell-cell contacts. *J Cell Biol* 137, 1421-1431 (1997)
123. K. Takaishi, T. Sasaki, H. Kotani, H. Nishioka and Y. Takai: Regulation of cell-cell adhesion by rac and rho small G proteins in MDCK cells. *J Cell Biol* 139, 1047-1059 (1997)
124. E. Calautti, M. Grossi, C. Mammucari, Y. Aoyama, M. Pirro, Y. Ono, J. Li and G. P. Dotto: Fyn tyrosine kinase is a downstream mediator of Rho/PRK2 function in keratinocyte cell-cell adhesion. *J Cell Biol* 156, 137-148 (2002)
125. E. Sahai and C. J. Marshall: ROCK and Dia have opposing effects on adherens junctions downstream of Rho. *Nat Cell Biol* 4, 408-415 (2002)

126. V. M. Braga, M. Betson, X. Li and N. Lamarche-Vane: Activation of the small GTPase Rac is sufficient to disrupt cadherin-dependent cell-cell adhesion in normal human keratinocytes. *Mol Biol Cell* 11, 3703-3721 (2000)
127. S. Ellis and H. Mellor: Regulation of endocytic traffic by rho family GTPases. *Trends Cell Biol* 10, 85-88 (2000)
128. M. Symons and N. Rusk: Control of vesicular trafficking by Rho GTPases. *Curr Biol* 13, R409-418 (2003)
129. M. Hatzfeld: The p120 family of cell adhesion molecules. *Eur J Cell Biol* 84, 205-214 (2005)
130. M. Hatzfeld, C. Haffner, K. Schulze and U. Venzens: The function of plakophilin 1 in desmosome assembly and actin filament organization. *J Cell Biol* 149, 209-222 (2000)
131. K. Kim, A. Sirota, Y. H. Chen Yh, S. B. Jones, R. Dudek, G. W. Lanford, C. Thakore and Q. Lu: Dendrite-like process formation and cytoskeletal remodeling regulated by delta-catenin expression. *Exp Cell Res* 275, 171-184 (2002)
132. K. Abu-Elneel, T. Ochiishi, M. Medina, M. Remedi, L. Gastaldi, A. Caceres and K. S. Kosik: A delta-catenin signaling pathway leading to dendritic protrusions. *J Biol Chem* 283, 32781-32791 (2008)
133. J. S. Kim, S. Bareiss, K. K. Kim, R. Tatum, J. R. Han, Y. H. Jin, H. Kim, Q. Lu and K. Kim: Presenilin-1 inhibits delta-catenin-induced cellular branching and promotes delta-catenin processing and turnover. *Biochem Biophys Res Commun* 351, 903-908 (2006)
134. H. Kim, M. Oh, Q. Lu and K. Kim: E-Cadherin negatively modulates delta-catenin-induced morphological changes and RhoA activity reduction by competing with p190RhoGEF for delta-catenin. *Biochem Biophys Res Commun* 377, 636-641 (2008)
135. S. A. Weed, Y. Du and J. T. Parsons: Translocation of cortactin to the cell periphery is mediated by the small GTPase Rac1. *J Cell Sci* 111 ( Pt 16), 2433-2443 (1998)
136. S. A. Weed, A. V. Karginov, D. A. Schafer, A. M. Weaver, A. W. Kinley, J. A. Cooper and J. T. Parsons: Cortactin localization to sites of actin assembly in lamellipodia requires interactions with F-actin and the Arp2/3 complex. *J Cell Biol* 151, 29-40 (2000)
137. S. Boguslavsky, I. Grosheva, E. Landau, M. Shtutman, M. Cohen, K. Arnold, E. Feinstein, B. Geiger and A. Bershadsky: p120 catenin regulates lamellipodial dynamics and cell adhesion in cooperation with cortactin. *Proc Natl Acad Sci U S A* 104, 10882-10887 (2007)
138. H. Kim, J. R. Han, J. Park, M. Oh, S. E. James, S. Chang, Q. Lu, K. Y. Lee, H. Ki, W. J. Song and K. Kim: Delta-catenin-induced dendritic morphogenesis. An essential role of



## p120ctn in normal development and tumorigenesis

p190RhoGEF interaction through Akt1-mediated phosphorylation. *J Biol Chem* 283, 977-987 (2008)

139. J. Arikath, I. Israely, Y. Tao, L. Mei, X. Liu and L. F. Reichardt: Erbin controls dendritic morphogenesis by regulating localization of delta-catenin. *J Neurosci* 28, 7047-7056 (2008)

140. J. Mayerle, H. Friess, M. W. Buchler, J. Schnekenburger, F. U. Weiss, K. P. Zimmer, W. Domschke and M. M. Lerch: Up-regulation, nuclear import, and tumor growth stimulation of the adhesion protein p120 in pancreatic cancer. *Gastroenterology* 124, 949-960 (2003)

141. C. R. Hosking, F. Ulloa, C. Hogan, E. C. Ferber, A. Figueroa, K. Gevaert, W. Birchmeier, J. Briscoe and Y. Fujita: The transcriptional repressor Glis2 is a novel binding partner for p120 catenin. *Mol Biol Cell* 18, 1918-1927 (2007)

142. A. Soubry, J. van Hengel, E. Parthoens, C. Colpaert, E. Van Marck, D. Waltregny, A. B. Reynolds and F. van Roy: Expression and nuclear location of the transcriptional repressor Kaiso is regulated by the tumor microenvironment. *Cancer Res* 65, 2224-2233 (2005)

143. K. F. Kelly, A. A. Otchere, M. Graham and J. M. Daniel: Nuclear import of the BTB/POZ transcriptional regulator Kaiso. *J Cell Sci* 117, 6143-6152 (2004)

144. F. M. van Roy and P. D. McCrea: A role for Kaiso-p120ctn complexes in cancer? *Nat Rev Cancer* 5, 956-964 (2005)

145. K. F. Kelly and J. M. Daniel: POZ for effect - POZ-ZF transcription factors in cancer and development. *Trends Cell Biol* (2006)

146. J. M. Daniel: Dancing in and out of the nucleus: p120(ctn) and the transcription factor Kaiso. *Biochim Biophys Acta* 1773, 59-68 (2007)

147. J. M. Daniel, C. M. Spring, H. C. Crawford, A. B. Reynolds and A. Baig: The p120(ctn)-binding partner Kaiso is a bi-modal DNA-binding protein that recognizes both a sequence-specific consensus and methylated CpG dinucleotides. *Nucleic Acids Res* 30, 2911-2919 (2002)

148. A. Prokhortchouk, B. Hendrich, H. Jorgensen, A. Ruzov, M. Wilm, G. Georgiev, A. Bird and E. Prokhortchouk: The p120 catenin partner Kaiso is a DNA methylation-dependent transcriptional repressor. *Genes Dev* 15, 1613-1618 (2001)

149. A. Ruzov, E. Savitskaya, J. A. Hackett, J. P. Reddington, A. Prokhortchouk, M. J. Madej, N. Chekanov, M. Li, D. S. Dunican, E. Prokhortchouk, S. Pennings and R. R. Meehan: The non-methylated DNA-binding function of Kaiso is not required in early *Xenopus laevis* development. *Development* 136, 729-738 (2009)

150. H. G. Yoon, D. W. Chan, A. B. Reynolds, J. Qin and J. Wong: N-CoR mediates DNA methylation-dependent repression through a methyl CpG binding protein Kaiso. *Mol Cell* 12, 723-734 (2003)

151. S. W. Kim, X. Fang, H. Ji, A. F. Paulson, J. M. Daniel, M. Ciesiolka, F. van Roy and P. D. McCrea: Isolation and characterization of XKaiso, a transcriptional repressor that associates with the catenin Xp120(ctn) in *Xenopus laevis*. *J Biol Chem* 277, 8202-8208 (2002)
152. J. I. Park, S. W. Kim, J. P. Lyons, H. Ji, T. T. Nguyen, K. Cho, M. C. Barton, T. Deroo, K. Vleminckx, R. T. Moon and P. D. McCrea: Kaiso/p120-catenin and TCF/beta-catenin complexes coordinately regulate canonical Wnt gene targets. *Dev Cell* 8, 843-854 (2005)
153. S. W. Kim, J. I. Park, C. M. Spring, A. K. Sater, H. Ji, A. A. Otchere, J. M. Daniel and P. D. McCrea: Non-canonical Wnt signals are modulated by the Kaiso transcriptional repressor and p120-catenin. *Nat Cell Biol* 6, 1212-1220 (2004)
154. C. M. Spring, K. F. Kelly, I. O'Kelly, M. Graham, H. C. Crawford and J. M. Daniel: The catenin p120ctn inhibits Kaiso-mediated transcriptional repression of the beta-catenin/TCF target gene matrilysin. *Exp Cell Res* 305, 253-265 (2005)
155. J. I. Park, H. Ji, S. Jun, D. Gu, H. Hikasa, L. Li, S. Y. Sokol, P. D. McCrea, M. Perez-Moreno and E. Fuchs: Frodo Links Dishevelled to the p120-Catenin/Kaiso Pathway: Distinct Catenin Subfamilies Promote Wnt Signals  
Catenins: keeping cells from getting their signals crossed. *Dev Cell* 11, 683-695 (2006)
156. A. Ruzov, J. A. Hackett, A. Prokhortchouk, J. P. Reddington, M. J. Madej, D. S. Dunican, E. Prokhortchouk, S. Pennings and R. R. Meehan: The interaction of xKaiso with xTcf3: a revised model for integration of epigenetic and Wnt signalling pathways. *Development* 136, 723-727 (2009)
157. A. Ruzov, D. S. Dunican, A. Prokhortchouk, S. Pennings, I. Stancheva, E. Prokhortchouk and R. R. Meehan: Kaiso is a genome-wide repressor of transcription that is essential for amphibian development. *Development* 131, 6185-6194 (2004)
158. A. Prokhortchouk, O. Sansom, J. Selfridge, I. M. Caballero, S. Salozhin, D. Aithozhina, L. Cerchietti, F. G. Meng, L. H. Augenlicht, J. M. Mariadason, B. Hendrich, A. Melnick, E. Prokhortchouk, A. Clarke and A. Bird: Kaiso-deficient mice show resistance to intestinal cancer. *Mol Cell Biol* 26, 199-208 (2006)
159. G. J. Filion, S. Zhenilo, S. Salozhin, D. Yamada, E. Prokhortchouk and P. A. Defossez: A family of human zinc finger proteins that bind methylated DNA and repress transcription. *Mol Cell Biol* 26, 169-181 (2006)
160. A. Weber, J. Marquardt, D. Elzi, N. Forster, S. Starke, A. Glaum, D. Yamada, P. A. Defossez, J. Delrow, R. N. Eisenman, H. Christiansen and M. Eilers: Zbtb4 represses transcription of P21CIP1 and controls the cellular response to p53 activation. *Embo J* 27, 1563-1574 (2008)

## p120ctn in normal development and tumorigenesis

161. S. Alema and A. M. Salvatore: p120 catenin and phosphorylation: Mechanisms and traits of an unresolved issue. *Biochim Biophys Acta* 1773, 47-58 (2007)
162. A. Skoudy, M. D. Llosas and A. Garcia de Herreros: Intestinal HT-29 cells with dysfunction of E-cadherin show increased pp60src activity and tyrosine phosphorylation of p120-catenin. *Biochem J* 317 ( Pt 1), 279-284 (1996)
163. M. S. Kinch, G. J. Clark, C. J. Der and K. Burridge: Tyrosine phosphorylation regulates the adhesions of ras-transformed breast epithelia. *J Cell Biol* 130, 461-471 (1995)
164. J. Behrens, L. Vakaet, R. Friis, E. Winterhager, F. Van Roy, M. M. Mareel and W. Birchmeier: Loss of epithelial differentiation and gain of invasiveness correlates with tyrosine phosphorylation of the E-cadherin/beta-catenin complex in cells transformed with a temperature-sensitive v-SRC gene. *J Cell Biol* 120, 757-766 (1993)
165. M. Hamaguchi, N. Matsuyoshi, Y. Ohnishi, B. Gotoh, M. Takeichi and Y. Nagai: p60v-src causes tyrosine phosphorylation and inactivation of the N-cadherin-catenin cell adhesion system. *Embo J* 12, 307-314 (1993)
166. N. Matsuyoshi, M. Hamaguchi, S. Taniguchi, A. Nagafuchi, S. Tsukita and M. Takeichi: Cadherin-mediated cell-cell adhesion is perturbed by v-src tyrosine phosphorylation in metastatic fibroblasts. *J Cell Biol* 118, 703-714 (1992)
167. R. Rosato, J. M. Veltmaat, J. Groffen and N. Heisterkamp: Involvement of the tyrosine kinase fer in cell adhesion. *Mol Cell Biol* 18, 5762-5770 (1998)
168. M. G. Lampugnani, M. Corada, P. Andriopoulou, S. Esser, W. Risau and E. Dejana: Cell confluence regulates tyrosine phosphorylation of adherens junction components in endothelial cells. *J Cell Sci* 110 ( Pt 17), 2065-2077 (1997)
169. M. Ozawa and R. Kemler: Altered cell adhesion activity by pervanadate due to the dissociation of alpha-catenin from the E-cadherin.catenin complex. *J Biol Chem* 273, 6166-6170 (1998)
170. D. W. Owens, G. W. McLean, A. W. Wyke, C. Paraskeva, E. K. Parkinson, M. C. Frame and V. G. Brunton: The catalytic activity of the Src family kinases is required to disrupt cadherin-dependent cell-cell contacts. *Mol Biol Cell* 11, 51-64 (2000)
171. R. Nawroth, G. Poell, A. Ranft, S. Kloep, U. Samulowitz, G. Fachinger, M. Golding, D. T. Shima, U. Deutsch and D. Vestweber: VE-PTP and VE-cadherin ectodomains interact to facilitate regulation of phosphorylation and cell contacts. *Embo J* 21, 4885-4895 (2002)
172. E. Calautti, S. Cabodi, P. L. Stein, M. Hatzfeld, N. Kedersha and G. Paolo Dotto: Tyrosine phosphorylation and src family kinases control keratinocyte cell-cell adhesion. *J Cell Biol* 141, 1449-1465 (1998)

173. M. Cozzolino, B. Giovannone, A. Serafino, K. Knudsen, A. Levi, S. Alema and A. Salvatore: Activation of TrkA tyrosine kinase in embryonal carcinoma cells promotes cell compaction, independently of tyrosine phosphorylation of catenins. *J Cell Sci* 113 ( Pt 9), 1601-1610 (2000)
174. S. Roura, S. Miravet, J. Piedra, A. Garcia de Herreros and M. Dunach: Regulation of E-cadherin/Catenin association by tyrosine phosphorylation. *J Biol Chem* 274, 36734-36740 (1999)
175. J. Balsamo, T. Leung, H. Ernst, M. K. Zanin, S. Hoffman and J. Lilien: Regulated binding of PTP1B-like phosphatase to N-cadherin: control of cadherin-mediated adhesion by dephosphorylation of beta-catenin. *J Cell Biol* 134, 801-813 (1996)
176. T. Shibata, A. Ochiai, Y. Kanai, S. Akimoto, M. Gotoh, N. Yasui, R. Machinami and S. Hirohashi: Dominant negative inhibition of the association between beta-catenin and c-erbB-2 by N-terminally deleted beta-catenin suppresses the invasion and metastasis of cancer cells. *Oncogene* 13, 883-889 (1996)
177. A. H. Huber, W. J. Nelson and W. I. Weis: Three-dimensional structure of the Armadillo repeat region of beta-catenin. *Cell* 90, 871-882 (1997)
178. H. Aberle, H. Schwartz, H. Hoschuetzky and R. Kemler: Single amino acid substitutions in proteins of the armadillo gene family abolish their binding to alpha-catenin. *J Biol Chem* 271, 1520-1526 (1996)
179. J. Piedra, S. Miravet, J. Castano, H. G. Palmer, N. Heisterkamp, A. Garcia de Herreros and M. Dunach: p120 Catenin-associated Fer and Fyn tyrosine kinases regulate beta-catenin Tyr-142 phosphorylation and beta-catenin-alpha-catenin Interaction. *Mol Cell Biol* 23, 2287-2297 (2003)
180. P. Hu, E. J. O'Keefe and D. S. Rubenstein: Tyrosine phosphorylation of human keratinocyte beta-catenin and plakoglobin reversibly regulates their binding to E-cadherin and alpha-catenin. *J Invest Dermatol* 117, 1059-1067 (2001)
181. M. Ozawa and T. Ohkubo: Tyrosine phosphorylation of p120(ctn) in v-Src transfected L cells depends on its association with E-cadherin and reduces adhesion activity. *J Cell Sci* 114, 503-512 (2001)
182. J. Lilien, J. Balsamo, C. Arregui and G. Xu: Turn-off, drop-out: functional state switching of cadherins. *Dev Dyn* 224, 18-29 (2002)
183. G. Xu, A. W. Craig, P. Greer, M. Miller, P. Z. Anastasiadis, J. Lilien and J. Balsamo: Continuous association of cadherin with beta-catenin requires the non-receptor tyrosine-kinase Fer. *J Cell Sci* 117, 3207-3219 (2004)
184. D. J. Mariner, P. Anastasiadis, H. Keilhack, F. D. Bohmer, J. Wang and A. B. Reynolds: Identification of Src phosphorylation sites in the catenin p120ctn. *J Biol Chem* 276, 28006-28013 (2001)

## p120ctn in normal development and tumorigenesis

185. X. Xia, D. J. Mariner and A. B. Reynolds: Adhesion-associated and PKC-modulated changes in serine/threonine phosphorylation of p120-catenin. *Biochemistry* 42, 9195-9204 (2003)
186. D. J. Mariner, M. A. Davis and A. B. Reynolds: EGFR signaling to p120-catenin through phosphorylation at Y228. *J Cell Sci* 117, 1339-1350 (2004)
187. M. H. Vaughan, X. Xia, X. Wang, E. Chronopoulou, G. J. Gao, R. Campos-Gonzalez and A. B. Reynolds: Generation and characterization of a novel phospho-specific monoclonal antibody to p120-catenin serine 879. *Hybridoma (Larchmt)* 26, 407-415 (2007)
188. X. Xia, J. Brooks, R. Campos-Gonzalez and A. B. Reynolds: Serine and threonine phospho-specific antibodies to p120-catenin. *Hybrid Hybridomics* 23, 343-351 (2004)
189. M. V. Brown, P. E. Burnett, M. F. Denning and A. B. Reynolds: PDGF receptor activation induces p120-catenin phosphorylation at serine 879 via a PKC $\alpha$ -dependent pathway. *Exp Cell Res* 315, 39-49 (2009)
190. E. Y. Wong, L. Morgan, C. Smales, P. Lang, S. E. Gubby and J. M. Staddon: Vascular endothelial growth factor stimulates dephosphorylation of the catenins p120 and p100 in endothelial cells. *Biochem J* 346 Pt 1, 209-216 (2000)
191. M. J. Ratcliffe, L. L. Rubin and J. M. Staddon: Dephosphorylation of the cadherin-associated p100/p120 proteins in response to activation of protein kinase C in epithelial cells. *J Biol Chem* 272, 31894-31901 (1997)
192. M. J. Ratcliffe, C. Smales and J. M. Staddon: Dephosphorylation of the catenins p120 and p100 in endothelial cells in response to inflammatory stimuli. *Biochem J* 338 ( Pt 2), 471-478 (1999)
193. A. W. Craig, R. Zirngibl, K. Williams, L. A. Cole and P. A. Greer: Mice devoid of fer protein-tyrosine kinase activity are viable and fertile but display reduced cortactin phosphorylation. *Mol Cell Biol* 21, 603-613 (2001)
194. P. L. Stein, H. M. Lee, S. Rich and P. Soriano: pp59fyn mutant mice display differential signaling in thymocytes and peripheral T cells. *Cell* 70, 741-750 (1992)
195. L. Kim and T. W. Wong: The cytoplasmic tyrosine kinase FER is associated with the catenin-like substrate pp120 and is activated by growth factors. *Molecular and Cellular Biology* 15, 4553-4561 (1995)
196. J. R. Downing and A. B. Reynolds: PDGF, CSF-1, and EGF induce tyrosine phosphorylation of p120, a pp60src transformation-associated substrate. *Oncogene* 6, 607-613 (1991)

197. S. Esser, M. G. Lampugnani, M. Corada, E. Dejana and W. Risau: Vascular endothelial growth factor induces VE-cadherin tyrosine phosphorylation in endothelial cells. *J Cell Sci* 111 (Pt 13), 1853-1865 (1998)
198. H. Keilhack, U. Hellman, J. van Hengel, F. van Roy, J. Godovac-Zimmermann and F. D. Bohmer: The protein-tyrosine phosphatase SHP-1 binds to and dephosphorylates p120 catenin. *J Biol Chem* 275, 26376-26384 (2000)
199. C. Frank, C. Burkhardt, D. Imhof, J. Ringel, O. Zschornig, K. Wieligmann, M. Zacharias and F. D. Bohmer: Effective dephosphorylation of Src substrates by SHP-1. *J Biol Chem* 279, 11375-11383 (2004)
200. L. J. Holsinger, K. Ward, B. Duffield, J. Zachwieja and B. Jallal: The transmembrane receptor protein tyrosine phosphatase DEP1 interacts with p120(ctn). *Oncogene* 21, 7067-7076 (2002)
201. H. L. Palka, M. Park and N. K. Tonks: Hepatocyte growth factor receptor tyrosine kinase met is a substrate of the receptor protein-tyrosine phosphatase DEP-1. *J Biol Chem* 278, 5728-5735 (2003)
202. G. C. Zondag, A. B. Reynolds and W. H. Moolenaar: Receptor protein-tyrosine phosphatase RPTPmu binds to and dephosphorylates the catenin p120(ctn). *J Biol Chem* 275, 11264-11269 (2000)
203. H. Takeda, A. Nagafuchi, S. Yonemura, S. Tsukita, J. Behrens and W. Birchmeier: V-src kinase shifts the cadherin-based cell adhesion from the strong to the weak state and beta catenin is not required for the shift. *J Cell Biol* 131, 1839-1847 (1995)
204. R. Y. Huang, S. M. Wang, C. Y. Hsieh and J. C. Wu: Lysophosphatidic acid induces ovarian cancer cell dispersal by activating Fyn kinase associated with p120-catenin. *Int J Cancer* 123, 801-809 (2008)
205. Y. Chen, C. H. Chen, P. Y. Tung, S. H. Huang and S. M. Wang: An acidic extracellular pH disrupts adherens junctions in HepG2 cells by Src kinases-dependent modification of E-cadherin. *J Cell Biochem* 108, 851-859 (2009)
206. K. H. Chen, P. Y. Tung, J. C. Wu, Y. Chen, P. C. Chen, S. H. Huang and S. M. Wang: An acidic extracellular pH induces Src kinase-dependent loss of beta-catenin from the adherens junction. *Cancer Lett* 267, 37-48 (2008)
207. X. Xia, R. H. Carnahan, M. H. Vaughan, G. A. Wildenberg and A. B. Reynolds: p120 serine and threonine phosphorylation is controlled by multiple ligand-receptor pathways but not cadherin ligation. *Exp Cell Res* 312, 3336-3348 (2006)
208. D. T. Fox, C. C. Homem, S. H. Myster, F. Wang, E. E. Bain and M. Peifer: Rho1 regulates Drosophila adherens junctions independently of p120ctn. *Development* 132, 4819-4831 (2005)

## p120ctn in normal development and tumorigenesis

209. A. F. Paulson, X. Fang, H. Ji, A. B. Reynolds and P. D. McCrea: Misexpression of the catenin p120(ctn)1A perturbs *Xenopus* gastrulation but does not elicit Wnt-directed axis specification. *Dev Biol* 207, 350-363 (1999)
210. K. Geis, H. Aberle, M. Kuhl, R. Kemler and D. Wedlich: Expression of the Armadillo family member p120cas1B in *Xenopus* embryos affects head differentiation but not axis formation. *Dev Genes Evol* 207, 471-481 (1998)
211. I. Israely, R. M. Costa, C. W. Xie, A. J. Silva, K. S. Kosik and X. Liu: Deletion of the neuron-specific protein delta-catenin leads to severe cognitive and synaptic dysfunction. *Curr Biol* 14, 1657-1663 (2004)
212. J. van Hengel and F. van Roy: Diverse functions of p120ctn in tumors. *Biochim Biophys Acta* (2006)
213. M. A. Thoreson and A. B. Reynolds: Altered expression of the catenin p120 in human cancer: implications for tumor progression. *Differentiation* 70, 583-589 (2002)
214. A. Bonnomet, M. Polette, K. Strumane, C. Gilles, V. Dalstein, C. Kileztky, G. Berx, F. van Roy, P. Birembaut and B. Nawrocki-Raby: The E-cadherin-repressed hNanos1 gene induces tumor cell invasion by upregulating MT1-MMP expression. *Oncogene* 27, 3692-3699 (2008)
215. G. Berx and F. van Roy: Involvement of members of the cadherin superfamily in cancer. *Cold Spring Harb Perspect Biol* 1, a003129 (2009)
216. Y. Ishizaki, Y. Omori, M. Momiyama, Y. Nishikawa, T. Tokairin, M. Manabe and K. Enomoto: Reduced expression and aberrant localization of p120catenin in human squamous cell carcinoma of the skin. *J Dermatol Sci* 34, 99-108 (2004)
217. L. D. Wood, D. W. Parsons, S. Jones, J. Lin, T. Sjoblom, R. J. Leary, D. Shen, S. M. Boca, T. Barber, J. Ptak, N. Silliman, S. Szabo, Z. Dezso, V. Ustyanksky, T. Nikolskaya, Y. Nikolsky, R. Karchin, P. A. Wilson, J. S. Kaminker, Z. Zhang, R. Croshaw, J. Willis, D. Dawson, M. Shipitsin, J. K. Willson, S. Sukumar, K. Polyak, B. H. Park, C. L. Pethiyagoda, P. V. Pant, D. G. Ballinger, A. B. Sparks, J. Hartigan, D. R. Smith, E. Suh, N. Papadopoulos, P. Buckhaults, S. D. Markowitz, G. Parmigiani, K. W. Kinzler, V. E. Velculescu and B. Vogelstein: The genomic landscapes of human breast and colorectal cancers. *Science* 318, 1108-1113 (2007)
218. A. A. Gimelbrant, A. W. Ensminger, P. Qi, J. Zucker and A. Chess: Monoallelic expression and asynchronous replication of p120 catenin in mouse and human cells. *J Biol Chem* 280, 1354-1359 (2005)
219. F. Mortazavi, J. An, S. Dubinett and M. Rettig: p120-catenin is transcriptionally downregulated by FOXC2 in non-small cell lung cancer cells. *Mol Cancer Res* 8, 762-774 (2010)

220. M. Perez-Moreno, W. Song, H. A. Pasolli, S. E. Williams and E. Fuchs: Loss of p120 catenin and links to mitotic alterations, inflammation, and skin cancer. *Proc Natl Acad Sci U S A* 105, 15399-15404 (2008)
221. D. C. Radisky: Epithelial-mesenchymal transition. *J Cell Sci* 118, 4325-4326 (2005)
222. M. J. Wheelock, Y. Shintani, M. Maeda, Y. Fukumoto and K. R. Johnson: Cadherin switching. *J Cell Sci* 121, 727-735 (2008)
223. S. Nakagawa and M. Takeichi: Neural crest cell-cell adhesion controlled by sequential and subpopulation-specific expression of novel cadherins. *Development* 121, 1321-1332 (1995)
224. N. L. Tran, R. B. Nagle, A. E. Cress and R. L. Heimark: N-Cadherin expression in human prostate carcinoma cell lines. An epithelial-mesenchymal transformation mediating adhesion with Stromal cells. *Am J Pathol* 155, 787-798 (1999)
225. J. Husmark, N. E. Heldin and M. Nilsson: N-cadherin-mediated adhesion and aberrant catenin expression in anaplastic thyroid-carcinoma cell lines. *Int J Cancer* 83, 692-699 (1999)
226. B. Seidel, S. Braeg, G. Adler, D. Wedlich and A. Menke: E- and N-cadherin differ with respect to their associated p120ctn isoforms and their ability to suppress invasive growth in pancreatic cancer cells. *Oncogene* 23, 5532-5542 (2004)
227. M. Herlyn, C. Berking, G. Li and K. Satyamoorthy: Lessons from melanocyte development for understanding the biological events in naevus and melanoma formation. *Melanoma Res* 10, 303-312 (2000)
228. I. Molina-Ortiz, R. A. Bartolome, P. Hernandez-Varas, G. P. Colo and J. Teixido: Overexpression of E-cadherin on melanoma cells inhibits chemokine-promoted invasion involving p190RhoGAP/p120ctn-dependent inactivation of RhoA. *J Biol Chem* 284, 15147-15157 (2009)
229. M. Maeda, E. Johnson, S. H. Mandal, K. R. Lawson, S. A. Keim, R. A. Svoboda, S. Caplan, J. K. Wahl, 3rd, M. J. Wheelock and K. R. Johnson: Expression of inappropriate cadherins by epithelial tumor cells promotes endocytosis and degradation of E-cadherin via competition for p120(ctn). *Oncogene* 25, 4595-4604 (2006)
230. E. H. Wang, Y. Liu, H. T. Xu, S. D. Dai, N. Liu, C. Y. Xie and X. M. Yuan: Abnormal expression and clinicopathologic significance of p120-catenin in lung cancer. *Histol Histopathol* 21, 841-847 (2006)
231. Y. Liu, Y. Wang, Y. Zhang, Y. Miao, Y. Zhao, P. X. Zhang, G. Y. Jiang, J. Y. Zhang, Y. Han, X. Y. Lin, L. H. Yang, Q. C. Li, C. Zhao and E. H. Wang: Abnormal expression of p120-catenin, E-cadherin, and small GTPases is significantly associated with malignant phenotype of human lung cancer. *Lung Cancer* 63, 375-382 (2009)



## p120ctn in normal development and tumorigenesis

232. Y. Miao, N. Liu, Y. Zhang, Y. Liu, J. H. Yu, S. D. Dai, H. T. Xu and E. H. Wang: p120ctn isoform 1 expression significantly correlates with abnormal expression of E-cadherin and poor survival of lung cancer patients. *Med Oncol* 27, 880-886
233. Y. Liu, H. T. Xu, S. D. Dai, Q. Wei, X. M. Yuan and E. H. Wang: Reduction of p120(ctn) isoforms 1 and 3 is significantly associated with metastatic progression of human lung cancer. *APMIS* 115, 848-856 (2007)
234. Y. Liu, Q. Z. Dong, Y. Zhao, X. J. Dong, Y. Miao, S. D. Dai, Z. Q. Yang, D. Zhang, Y. Wang, Q. C. Li, C. Zhao and E. H. Wang: P120-catenin isoforms 1A and 3A differently affect invasion and proliferation of lung cancer cells. *Exp Cell Res* 315, 890-898 (2009)
235. Y. Liu, Q. C. Li, Y. Miao, H. T. Xu, S. D. Dai, Q. Wei, Q. Z. Dong, X. J. Dong, Y. Zhao, C. Zhao and E. H. Wang: Ablation of p120-catenin enhances invasion and metastasis of human lung cancer cells. *Cancer Sci* 100, 441-448 (2009)
236. N. T. Chartier, C. I. Oddou, M. G. Laine, B. Ducarouge, C. A. Marie, M. R. Block and M. R. Jacquier-Sarlin: Cyclin-dependent kinase 2/cyclin E complex is involved in p120 catenin (p120ctn)-dependent cell growth control: a new role for p120ctn in cancer. *Cancer Res* 67, 9781-9790 (2007)
237. W. E. Naugler and M. Karin: The wolf in sheep's clothing: the role of interleukin-6 in immunity, inflammation and cancer. *Trends Mol Med* 14, 109-119 (2008)
238. M. L. Hermiston and J. I. Gordon: Inflammatory bowel disease and adenomas in mice expressing a dominant negative N-cadherin. *Science* 270, 1203-1207 (1995)
239. V. Vasioukhin, L. Degenstein, B. Wise and E. Fuchs: The magical touch: Genome targeting in epidermal stem cells induced by tamoxifen application to mouse skin. *Proceedings of the National Academy of Sciences of the United States of America* 96, 8551-8556 (1999)
240. J. A. Gorski, T. Talley, M. Qiu, L. Puelles, J. L. Rubenstein and K. R. Jones: Cortical excitatory neurons and glia, but not GABAergic neurons, are produced in the Emx1-expressing lineage. *J Neurosci* 22, 6309-6314 (2002)
241. H. Hoschuetzky, H. Aberle and R. Kemler: Beta-catenin mediates the interaction of the cadherin-catenin complex with epidermal growth factor receptor. *J Cell Biol* 127, 1375-1380 (1994)
242. P. Sheth, A. Seth, K. J. Atkinson, T. Gheyi, G. Kale, F. Giorgianni, D. M. Desiderio, C. Li, A. Naren and R. Rao: Acetaldehyde dissociates the PTP1B-E-cadherin-beta-catenin complex in Caco-2 cell monolayers by a phosphorylation-dependent mechanism. *Biochem J* 402, 291-300 (2007)
243. B. T. Jamal, M. Nita-Lazar, Z. Gao, B. Amin, J. Walker and M. A. Kukuruzinska: N-glycosylation status of E-cadherin controls cytoskeletal dynamics through the organization of

distinct beta-catenin- and gamma-catenin-containing AJs. *Cell Health Cytoskelet* 2009, 67-80 (2009)

244. S. M. Brady-Kalnay, T. Mourton, J. P. Nixon, G. E. Pietz, M. Kinch, H. Chen, R. Brackenbury, D. L. Rimm, R. L. Del Vecchio and N. K. Tonks: Dynamic interaction of PTPmu with multiple cadherins in vivo. *J Cell Biol* 141, 287-296 (1998)

245. U. Cavallaro, J. Niedermeyer, M. Fuxa and G. Christofori: N-CAM modulates tumour-cell adhesion to matrix by inducing FGF-receptor signalling. *Nat Cell Biol* 3, 650-657 (2001)

246. J. Balsamo, C. Arregui, T. Leung and J. Lilien: The nonreceptor protein tyrosine phosphatase PTP1B binds to the cytoplasmic domain of N-cadherin and regulates the cadherin-actin linkage. *J Cell Biol* 143, 523-532 (1998)

247. N. Lambeng, Y. Wallez, C. Rampon, F. Cand, G. Christe, D. Gulino-Debrac, I. Vilgrain and P. Huber: Vascular endothelial-cadherin tyrosine phosphorylation in angiogenic and quiescent adult tissues. *Circ Res* 96, 384-391 (2005)

248. M. G. Lampugnani, A. Zanetti, F. Breviario, G. Balconi, F. Orsenigo, M. Corada, R. Spagnuolo, M. Betson, V. Braga and E. Dejana: VE-cadherin regulates endothelial actin activating Rac and increasing membrane association of Tiam. *Mol Biol Cell* 13, 1175-1189 (2002)

249. Y. Nakamura, N. Patrushev, H. Inomata, D. Mehta, N. Urao, H. W. Kim, M. Razvi, V. Kini, K. Mahadev, B. J. Goldstein, R. McKinney, T. Fukai and M. Ushio-Fukai: Role of protein tyrosine phosphatase 1B in vascular endothelial growth factor signaling and cell-cell adhesions in endothelial cells. *Circ Res* 102, 1182-1191 (2008)

250. J. A. Ukropec, M. K. Hollinger, S. M. Salva and M. J. Woolkalis: SHP2 association with VE-cadherin complexes in human endothelial cells is regulated by thrombin. *J Biol Chem* 275, 5983-5986 (2000)

251. M. Fuchs, T. Muller, M. M. Lerch and A. Ullrich: Association of human protein-tyrosine phosphatase kappa with members of the armadillo family. *J Biol Chem* 271, 16712-16719 (1996)

252. B. Aicher, M. M. Lerch, T. Muller, J. Schilling and A. Ullrich: Cellular redistribution of protein tyrosine phosphatases LAR and PTPsigma by inducible proteolytic processing. *J Cell Biol* 138, 681-696 (1997)

253. R. M. Kypta, H. Su and L. F. Reichardt: Association between a transmembrane protein tyrosine phosphatase and the cadherin-catenin complex. *J Cell Biol* 134, 1519-1529 (1996)

254. J. Cheng, K. Wu, M. Armanini, N. O'Rourke, D. Dowbenko and L. A. Lasky: A novel protein-tyrosine phosphatase related to the homotypically adhering kappa and mu receptors. *J Biol Chem* 272, 7264-7277 (1997)

## p120ctn in normal development and tumorigenesis

255. H. X. Yan, Y. Q. He, H. Dong, P. Zhang, J. Z. Zeng, H. F. Cao, M. C. Wu and H. Y. Wang: Physical and functional interaction between receptor-like protein tyrosine phosphatase PCP-2 and beta-catenin. *Biochemistry* 41, 15854-15860 (2002)
256. K. Meng, A. Rodriguez-Pena, T. Dimitrov, W. Chen, M. Yamin, M. Noda and T. F. Deuel: Pleiotrophin signals increased tyrosine phosphorylation of beta beta-catenin through inactivation of the intrinsic catalytic activity of the receptor-type protein tyrosine phosphatase beta/zeta. *Proc Natl Acad Sci U S A* 97, 2603-2608 (2000)
257. W. Li, Y. Li and F. B. Gao: Abelson, enabled, and p120 catenin exert distinct effects on dendritic morphogenesis in *Drosophila*. *Dev Dyn* 234, 512-522 (2005)
258. T. Pieters, P. D'Hooge, P. Hulpiau, M. P. Stemmler, F. Van Roy and J. Van Hengel: p120ctn isoform C knockout and knock-in mice rescue E-cadherin loss and embryonic lethality in p120ctn-deficient embryos. *Manuscript in preparation*
259. A. B. Reynolds, N. A. Jenkins, D. J. Gilbert, N. G. Copeland, D. N. Shapiro, J. Wu and J. M. Daniel: The gene encoding p120cas, a novel catenin, localizes on human chromosome 11q11 (CTNND) and mouse chromosome 2 (Catns). *Genomics*, 31(1), 127-9 (1996)
260. S. Bonne, J. van Hengel and F. van Roy: Chromosomal mapping of human armadillo genes belonging to the p120(ctn)/plakophilin subfamily. *Genomics*, 51(3), 452-4 (1998)
261. D. Casagolda, B. Del Valle-Perez, G. Valls, E. Lugalde, M. Vinyoles, J. Casado-Vela, G. Solanas, E. Batlle, A. B. Reynolds, J. I. Casal, A. G. de Herreros and M. Dunach: A p120-catenin-CK1epsilon complex regulates Wnt signaling. *J Cell Sci* 123, 2621-2631 (2010)
262. J. Y. Hong, J. I. Park, K. Cho, D. Gu, H. Ji, S. E. Artandi and P. D. McCrea: Shared molecular mechanisms regulate multiple catenin proteins: canonical Wnt signals and components modulate p120-catenin isoform-1 and additional p120 subfamily members. *J Cell Sci* 123, 4351-4365 (2010)
263. M. Oh, H. Kim, I. Yang, J. H. Park, W. T. Cong, M. C. Baek, S. Bareiss, H. Ki, Q. Lu, J. No, I. Kwon, J. K. Choi and K. Kim: GSK-3 phosphorylates delta-catenin and negatively regulates its stability via ubiquitination/proteosome-mediated proteolysis. *J Biol Chem* 284, 28579-28589 (2009)

## Chapter 2

---

### MOUSE DEVELOPMENT

**TABLE OF CONTENTS**

INTRODUCTION ..... 71

    Mice as animal model system ..... 71

    Overview of mouse development ..... 72

PREIMPLANTION DEVELOPMENT IN MOUSE ..... 72

    Fertilization and early cleavage cycles ..... 72

    Morula compaction and polarization ..... 73

    Blastocyst formation and the first cell type diversification: TE and ICM ..... 76

    Late blastocyst stage and establishment of epiblast and primitive endoderm lineages .... 77

TRANSCRIPTION FACTORS GOVERNING BLASTOCYST LINEAGE ALLOCATION ... 79

    ICM-specific transcription factors ..... 79

    TE-specific transcription factors ..... 84

    PE-specific transcription factors ..... 86

IMPLANTATION AND GASTRULATION ..... 86

REFERENCES ..... 91

## INTRODUCTION

### Mice as animal model system

Mice have become the preferred mammalian research model for several reasons. First, they are small, robust, fecund and cheap to maintain. They thrive and breed under a wide range of environmental conditions (including laboratory conditions), have a short gestation, produce large litters, and develop rapidly. In addition, most laboratory mice are quite tame and easy to handle. Second, mice are very interesting from a genetic perspective. They are evolutionarily close to humans (only primates are closer), with whom they share 95% of coding sequences, and display considerable synteny. Mice share many physiological and anatomical features with humans, and they have many syndromes that resemble human inherited diseases. In addition, some mice lineages survive inbreeding depression, which makes it possible to generate inbred strains to obtain genetic standardization (Corrigan et al., 2009). Third, pluripotent mouse embryonic stem (ES) cell lines can be established (Evans and Kaufman, 1981; Martin, 1981), which contribute to the germ line after injection in host blastocysts (Bradley et al., 1984). Homologous recombination in these ES cells enables the generation of mice with genetically modified alleles (Thomas and Capecchi, 1987) displaying Mendelian inheritance (Chénot, 1902). This technique has revolutionized biomedical research and permits to assay the functionality of individual genes. Over the last decades, thousands of transgenic mouse strains, including knock-out mice, have been generated by different laboratories and by international consortia (The international Mouse Knockout Consortium, 2007). In the end, functional information obtained in mice could be extrapolated to humans to provide insight into human disease and to enable knowledge-based drug discovery.

## **Mouse Development**

### **Overview of mouse development**

The short gestation of mice (19 days) makes them suitable for studying mammalian embryonic development. Mouse development can be subdivided into four major periods: preimplantation (0-4.5 dpc), implantation, gastrulation and turning (5-8.5 dpc), organogenesis (9-13.5 dpc) and fetal growth (14-19 dpc) (Fig.1A). In brief, oocyte fertilization is followed by successive cleavages to generate totipotent blastomeres. Increased blastomere adhesion transforms the loosely attached blastomeres into a compacted morula (2.5 dpc) that develops into a blastocyst (3.5 dpc) (Fig.1B). Blastocysts hatch from their zona pellucida and attach to the uterine wall, after which they implant. Gastrulation (6-7.5 dpc) sets the stage for the establishment of the primary germ layers, namely endoderm, mesoderm and ectoderm. After gastrulation, the mouse embryo initiates somitogenesis and undergoes a complex movement, called turning. This process inverts the germ layers and repositions the endoderm, which was exposed to the outside, towards the inside. These basic layers are the groundwork for generating various tissues during organogenesis. The ectoderm develops into epidermis and neurons, which are critical for protection from and sensing of the environment. The endoderm is the precursor of the gastrointestinal tract. The mesoderm gives rise to muscle and blood cells. During organogenesis, several organ primordia arise, including limbs, olfactory pit, lens vesicle, gonads, heart, lung buds, and thymus. After establishment of the body plan, the fetal organs grow and develop further until parturition on day 19 (Hogan et al., 1994; Kaufman, 1992).

The research described in this doctoral dissertation involves analysis of mouse embryos during preimplantation and gastrulation. Therefore, these two topics are explained below in detail.

### **PREIMPLANTION DEVELOPMENT IN MOUSE**

#### **Fertilization and early cleavage cycles**

The unfertilized mouse egg is arrested at metaphase II of meiosis and is much smaller compared to eggs of chick or frog. Therefore, it lacks the massive maternal contribution of freely developing eggs and, like other mammalian eggs, mouse oocytes need to develop a machinery to exploit their nutritive environment. So, in contrast to other animals, in which the first step of cell type diversification is the creation of the primary germ layers, mammals

produce extraembryonic structures first. The first cell differentiation event in mammalian development is not the formation of the three germ layers but the establishment of two distinct cell lineages: the trophoctoderm (TE) and the inner cell mass (ICM). The TE is important for embryo attachment to and implantation in the uterus, and is a key contributor to the placenta. Only when this supportive frame is set up do the three germ layers, which ultimately generate all the tissues in the embryonic and adult body, arise from the ICM (Hogan et al., 1994; Marikawa and Alarcon, 2009; O'Farrell et al., 2004).

Mouse embryonic development starts with fertilization of the egg in the oviduct. Thereafter, the egg resumes and completes meiosis with the emission of the second polar body (Hogan et al., 1994). This second polar body often remains attached to the egg and serves as a landmark of the animal pole during later development (Fig.1C) (Gardner, 1997). Sperm binds to the glycoprotein ZP3, present in the zona surrounding the oocyte, and triggers the acrosomal reaction, which enables the sperm head to fuse with the egg membrane. Nuclear membranes form around the maternal and paternal chromosomes, forming separate haploid male and female pronuclei, which migrate to the centre of the egg and undergo DNA replication. After breakdown of the pronuclear membranes, both sets of chromosomes assemble on the spindle and the first cleavage occurs (Hogan et al., 1994). Successive cleavages generate totipotent blastomeres. However, in contrast to free developing eggs, these cleavage divisions are rather slow, as the first cleavage occurs 16 to 20 hours after fertilization and the following cleavages take place at intervals of about 12 hours (Marikawa and Alarcon, 2009). Cell cycle length varies among embryos and even among blastomeres in the same embryo. This asynchronous cell division has been shown by time-lapse recording and labeling of developing embryos *in vitro* (Bischoff et al., 2008; Fujimori et al., 2009; Kurotaki et al., 2007). Due to asynchronous cell division in blastomeres, the total blastomere number of an embryo at a given time point is sometimes other than  $2^n$ . For example, after four rounds of cleavage ( $2^4$ ) the total blastomere number is not always 16. Three rounds of cleavage result in eight blastomeres that are morphologically similar to each other and retain the ability to form all cell lineages (Gardner, 1998; Johnson and McConnell, 2004)(Fig. 1Bb).

### **Morula compaction and polarization**

The eight clearly demarcated blastomeres undergo compaction into a sphere in which individual blastomeres are no longer visible (Fig. 1Bc). During morula compaction, blastomeres flatten, increase their cell contacts and establish apical-basal polarity.



## Mouse Development

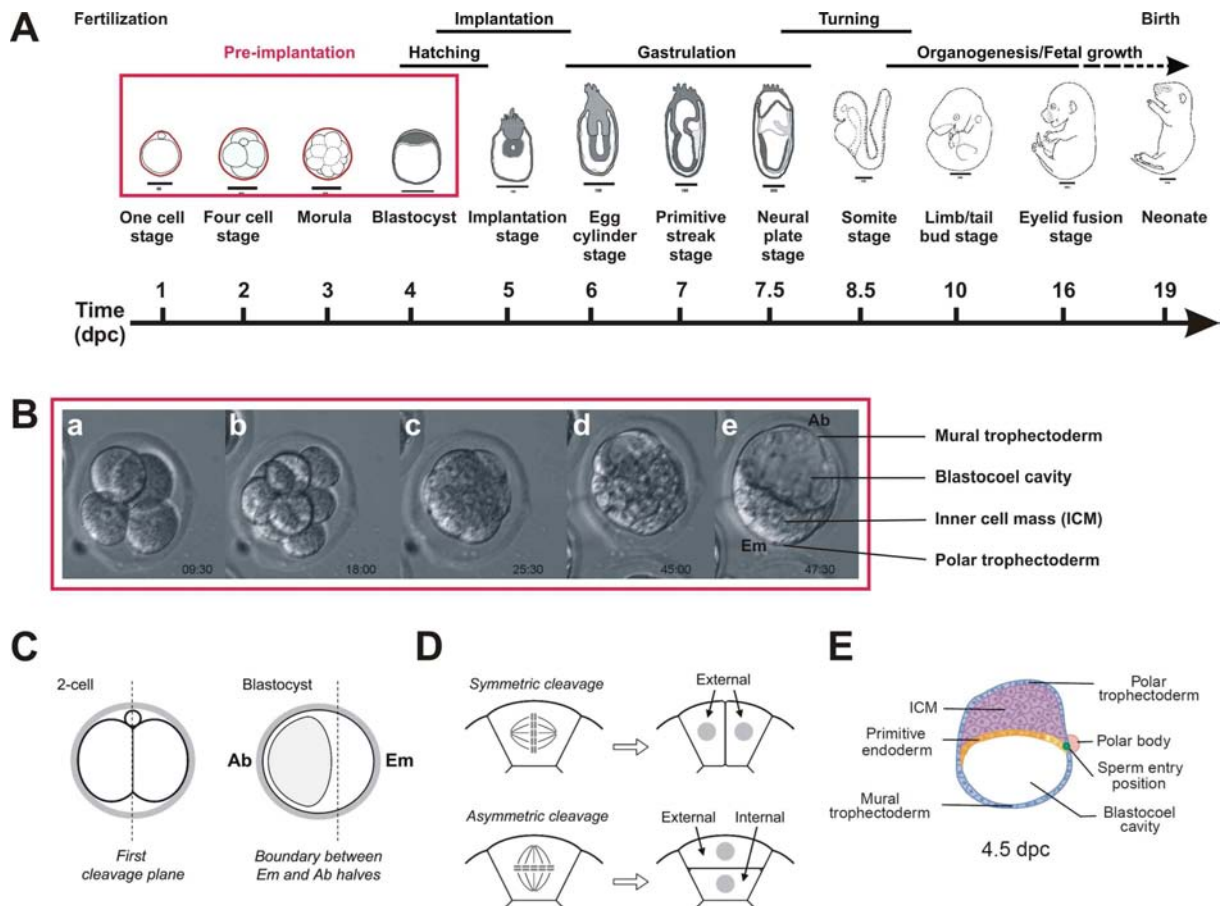


**Figure 1. Overview of preimplantation development.** (A) A general overview of mouse development and its different stages. The stages of preimplantation are marked by a red box. Diagrams of Theiler stage embryos were adapted from the Edinburgh Mouse Atlas (<http://genex.hgu.mrc.ac.uk/Atlas>). (B) Overview of preimplantation development. *In vitro* preimplantation development monitored by time lapse recording reveals progression of a four-cell embryo (a) into an uncompacted morula (b), a compacted morula (c) and finally into a blastocyst (e). Time is indicated at the bottom of each recording. (C) Diagram of the cleavage model, which postulates that the first cleavage plane corresponds with the boundaries of embryonic and abembryonic regions. (D) Diagram of symmetric and asymmetric cleavages generating two external blastomeres or one external and one internal blastomere, respectively. (E) Diagram of a late blastocyst consisting of trophectoderm, primitive endoderm and inner cell mass (ICM). Ab: abembryonic pole, Em: embryonic pole. Diagrams in C and D were taken from Marikawa et al. (2009). The diagram in E was taken from Lu et al. (2001).

Compaction depends on the cell-cell adhesion molecule E-cadherin (also called uvomorulin), which switches from a homogeneous to a basolateral distribution during compaction. Compaction is completely inhibited by antibodies against E-cadherin or by calcium depletion (Hyafil et al., 1981; Hyafil et al., 1980; Johnson et al., 1986; Peyrieras et al., 1983; Reeve and

Ziomek, 1981; Vestweber and Kemler, 1985). E-cadherin mutants lacking both maternal and zygotic E-cadherin also fail to compact (Stephenson et al., 2010). Polarization of eight-cell morulas was evident when they were decompacted under low  $\text{Ca}^{2+}$  conditions. Decompacted blastomeres showed numerous microvilli on their apical surfaces, but the inner surfaces remained smooth (Reeve and Ziomek, 1981).

The partition-defective (PAR)-atypical protein kinase C (aPKC) system is responsible for the establishment of cell polarity in most epithelial tissues. The PAR-aPKC system might also contribute to polarity in the TE, since many of its components become localized asymmetrically along the apical-basal axis of cells after compaction (Vinot et al., 2005; Yamanaka et al., 2006). Moreover, knockdown of PAR3 or expression of a dominant negative aPKC leads to increased ICM formation and diminished number of TE cells (Plusa et al., 2005). RhoGTPases are also important for polarization, because overexpression of a constitutive active RhoA mutant in four-cell embryos results in loss of apical polar microvilli and reduced blastomere adhesion. Inhibition of RhoA mediated by C3-transferase results in decompaction (Clayton et al., 1999). In addition to cadherin-based adherens junctions, also tight junctions and gap junctions emerge, allowing the creation of an impermeable outer epithelial layer and enabling ionic coupling between blastomeres, respectively. E-cadherin null embryos fail to form trophectoderm epithelium (Larue et al., 1994) and displace apical polarity and tight junction marker ZO-1 (Ohsugi et al., 1997). In contrast, the expression pattern of Connexin43, which is a constituent of gap junctions, was not altered E-cadherin null embryos. Mouse embryos lacking both maternal and zygotic E-cadherin exhibit a disorganized epithelial polarity lacking demarcated apical and basolateral domains, but are still capable of producing normal trophectoderm (TE) and inner cell mass allocation (ICM) (Stephenson et al., 2010). The trophectoderm is the first differentiated cell type and resembles epithelium, with polarized cell adhesion systems. The compacted morula can also decompact transiently during the fourth cleavage, which increases the number of cells to 16. The fourth cleavage generates two types of blastomeres, those positioned on the surface of the embryo ( $n=10$ ) and those entirely surrounded by neighboring blastomeres ( $n=6$ ) (Fig.1D). The outer blastomeres retain apical-basal polarity and eventually give rise to the TE lineage, whereas the inner blastomeres do not exhibit polarity and later form the ICM (Marikawa and Alarcon, 2009; Yamanaka et al., 2006).

### **Blastocyst formation and the first cell type diversification: TE and ICM**

The fifth cleavage yields 32 cells and increases both the number of external (n=20) and internal cells (n=12). From this point on, small cavities start to form in between blastomeres that continuously expand and fuse with each other to form a single large cavity, called the blastocoel (Fig. 1Bd,e). The blastocoel provides a space for the mesoderm and the endoderm to move into during the morphogenesis of gastrulation. When the blastocoel appears, the embryo is referred to as a blastocyst, which is characterized by cell type diversification into TE and ICM. The ICM is a pluripotent non-polarized compact cell layer that gives rise to all the embryonic lineages and can be used to derive mouse embryonic stem (mES) cell lines. The TE is an epithelial monolayer surrounding both the blastocoel and the ICM. The ICM marks the embryonic pole, which delineates the embryonic–abembryonic (Em–Ab) axis, which persists throughout further development, including gastrulation. The TE overlaying the ICM is called the polar TE, whereas TE overlaying the blastocoel is called mural TE (Fig. 1Be). At the time of implantation, the mural TE cells differentiate into primary trophoblast giant cells that undergo endoreplication and initiate endometrium invasion (Dickson, 1963; Kirby et al., 1967). The polar TE remains diploid due to signals from the adjacent ICM, such as fibroblast growth factor (FGF) 4 (Chai et al., 1998; Tanaka et al., 1998). After implantation, polar TE contributes to the extraembryonic ectoderm and the ectoplacental cone, which give rise to the chorion and the placenta, respectively (Gardner et al., 1973).

For proper blastocyst and blastocoels formation, the TE needs to acquire two features: establishment of mature tight junctions to seal the blastocoel cavity and polarized expression of ion channels to pump fluid into the cavity. Tight junctions are composed of transmembrane proteins, such as claudins and occludins, and zonula occludens (ZO) proteins, such as ZO-1, -2 and -3, which provide linkage to the actin cytoskeleton (Matter and Balda, 2003). Mature tight junctions are present in the TE of blastocysts sealing the blastocoel and creating a barrier that is almost impermeable to fluid (Eckert and Fleming, 2008; Johnson and McConnell, 2004). Inhibition of claudin 4 and 6 (Moriwaki et al., 2007) and knockdown of ZO-1 or ZO-2 (Sheth et al., 2008; Wang et al., 2008) in blastomeres results in defective or delayed blastocoel formation. Osmotic pressure is the major force driving water influx from the apical side to the basal side of TE and is generated by an increased concentration of sodium ions on the basal side of the epithelium. At the apical membrane,  $\text{Na}^+/\text{H}^+$  exchangers transport sodium ions into TE cells, while sodium efflux is mediated by  $\text{Na}^+/\text{K}^+$ -ATPases at the basal

membrane (Barcroft et al., 2004; Kawagishi et al., 2004). In addition, aquaporins contribute to water movements across the TE, which leads to expansion of the blastocoel (Barcroft et al., 2003). Knockdown of the  $\beta 1$  subunit of  $\text{Na}^+/\text{K}^+$ -ATPase not only prevents blastocoel formation, but also displaces tight junction components ZO-1 and occluding (Madan et al., 2007). This last finding reveals a putative link between pumping of fluid and providing an impermeable seal by tight junctions.

What causes this first differentiation event in the blastocyst? One hypothesis states that differentiation might arise as the result of cellular polarization about the time of compaction. The fourth cleavage generates external and internal cells having different compositions of membrane and cytosolic factors, which leads to different cell fates (Johnson and Ziomek, 1981). A second hypothesis states that different microenvironments of inside and outside blastomeres drive the differentiation into TE and ICM lineages (Tarkowski and Wroblewska, 1967). A last cleavage-driven hypothesis proposes that blastocyst polarity can be traced back to asymmetries generated during the early cleavage of the embryo (Zernicka-Goetz, 2002). This model is based on findings that the first cleavage separates the fertilized eggs in two blastomeres that follow different destinies (Deb et al., 2006; Gardner, 2001; Piotrowska et al., 2001)(Fig. 1C). In this model, the first dividing (leading) blastomere at the two cell stage is thought to make up the ICM, while the lagging blastomere will form the TE. However, this model is contested by several studies (Alarcon and Marikawa, 2003; Alarcon and Marikawa, 2005; Hiiragi and Solter, 2004; Motosugi et al., 2006). In particular, when two-cell embryos are dual labeled and transferred back into oviducts of female mice to allow *in vivo* development to the blastocyst stage, the two initial blastomeres give rise to both embryonic and abembryonic regions (Kurotaki et al., 2007).

### **Late blastocyst stage and establishment of epiblast and primitive endoderm lineages**

Twenty-four hours after blastocyst formation, a second cell type diversification occurs. In this process, the ICM gives rise to two morphologically distinct populations, namely the epiblast (primitive ectoderm) and hypoblast (primitive endoderm, PE) lineages. The epiblast represents the embryonic lineage, while the primitive endoderm will give rise to extraembryonic tissues, namely the parietal and visceral endoderm, which will form the yolk sac. The primitive endoderm forms as a monolayer on the surface of the ICM directly facing the blastocoel, while the epiblast is encapsulated by primitive endoderm and polar trophectoderm (Fig. 1E). The primitive endoderm plays important roles not only in supporting

## Mouse Development

fetal development but also in patterning and in the establishment of the anterior/posterior (A/P) axis of the embryo (Beddington and Robertson, 1999; Lu et al., 2001; Rossant and Tam, 2009). Cells from late blastocysts originating either from the epiblast or primitive endoderm seem to be lineage-restricted, because they contribute only to their respective lineages in chimeric embryos (Gardner, 1982; Gardner and Rossant, 1979).

There are two models to explain the cell type allocation between epiblast and primitive endoderm (Yamanaka et al., 2006). One model proposes that ICM cells of the early blastocyst are a homogeneous population of bipotential cells, each with the ability to become either epiblast or primitive endoderm, and the fate of the cells within the ICM is determined by their position in the ICM. The surface cells facing the blastocoel cavity differentiate into primitive endoderm, while the cells enclosed inside become the epiblast. Evidence for this model was provided by the presence of a single layer of primitive endoderm on the surface of embryoid bodies from embryonal carcinoma cells (Becker et al., 1992; Martin and Evans, 1975) and embryonic stem cells (Murray and Edgar, 2001). A second model proposes that ICM cells are a heterogeneous mixture of both primitive endoderm and epiblast cells, and that the primitive endoderm cells are sorted out to form a monolayer separating the epiblast from the blastocoel cavity. This model is consistent with the non-overlapping expression pattern of epiblast and primitive endoderm markers (*nanog* and *Gata6*, respectively) in 3.5-dpc blastocysts (Chazaud et al., 2006). Single ICM cells exhibit distinct epiblast-like or primitive endoderm-like expression profiles (Kurimoto et al., 2006) and contribute to either the epiblast or the primitive endoderm lineage, but rarely to both (Chazaud et al., 2006). So, the ICM of the late blastocyst consists of a mixed population of cells with different fates (epiblast or primitive endoderm).

But what drives this cell lineage diversification? Live cell lineage tracing starting at the eight-cell stage revealed that there is no clear linkage between developmental history of individual ICM cells and later cell fate (Yamanaka et al., 2010). Instead, FGF signaling might be involved in cell fate determination of ICM, because blocking the receptor/MAP kinase pathway steers towards the epiblast fate, whereas adding exogenous FGF steers towards the primitive endoderm fate (Yamanaka et al., 2010). The late blastocyst contains three lineages, namely trophoblast, hypoblast, and epiblast, and from each lineage progenitor cells can be isolated and propagated to give rise to three types of cells: trophectoderm stem cells (TS) (Tanaka et al., 1998), extraembryonic endoderm cells (XEN) (Kunath et al., 2005), and ES cells (Evans and Kaufman, 1981; Martin, 1981), respectively. These observations emphasize the stem cell character of these late blastocyst progenitor cells (Rossant, 2008).

## **TRANSCRIPTION FACTORS GOVERNING BLASTOCYST LINEAGE ALLOCATION**

Cell fate determination in early and late blastocysts is mostly accompanied by lineage-specific transcription factor repertoires. A number of transcription factors have been identified as essential for the establishment of the ICM (such as Oct4, nanog and sox2), TE (such as Cdx2 and Tead4), and primitive endoderm lineage (such as Gata 6) (Table 1, Fig. 2) (Niwa, 2007).

### **ICM-specific transcription factors**

A first set of transcription factors is expressed in ICM cells (after segregation of the TE and ICM lineages) and/or cells of the epiblast (after differentiation of ICM cells into epiblast and primitive endoderm). Oct4 (also known as Pou5f1 and Oct3) is a POU-domain transcription factor expressed in blastomeres, pluripotent early embryo cells, germ cells, ES cells, embryonal carcinoma (EC) cells and embryonic germ (EG) cells (Okamoto et al., 1990; Rosner et al., 1990; Scholer et al., 1990). During blastocyst formation, Oct4 becomes gradually restricted to the ICM (Palmieri et al., 1994). In late blastocysts, Oct4 is expressed in the epiblast (primitive ectoderm) and is transiently upregulated in the hypoblast (primitive endoderm), but after implantation all extraembryonic cells are devoid of Oct4 (Palmieri et al., 1994). After birth, Oct4 is absent in most adult tissues and is confined to pluripotent compartments, such as the germ cells (Rosner et al., 1990). Oct4-depleted embryos can form normal cavitated blastocysts having both TE and ICM like cell populations, which indicates that the initial generation of the ICM does not depend on Oct4 (Nichols et al., 1998). However, the ICM cells of Oct4-null blastocysts express TE-specific intermediate filaments (Nichols et al., 1998). Oct4-null blastocysts can implant, which indicates that the TE is functional, but they die because they fail to form ICM derivatives, such as epiblast and yolk sac (Nichols et al., 1998) (Table 1). In addition, no ES cell lines could be derived from Oct4 null blastocysts, which only formed trophoblast giant cells (Nichols et al., 1998). Similar to Oct4 null blastocysts, Oct4 repression in ES cell lines induces differentiation towards the TE lineages, whereas Oct4 overexpression induces differentiation mainly into extraembryonic endoderm (Niwa et al., 2000).

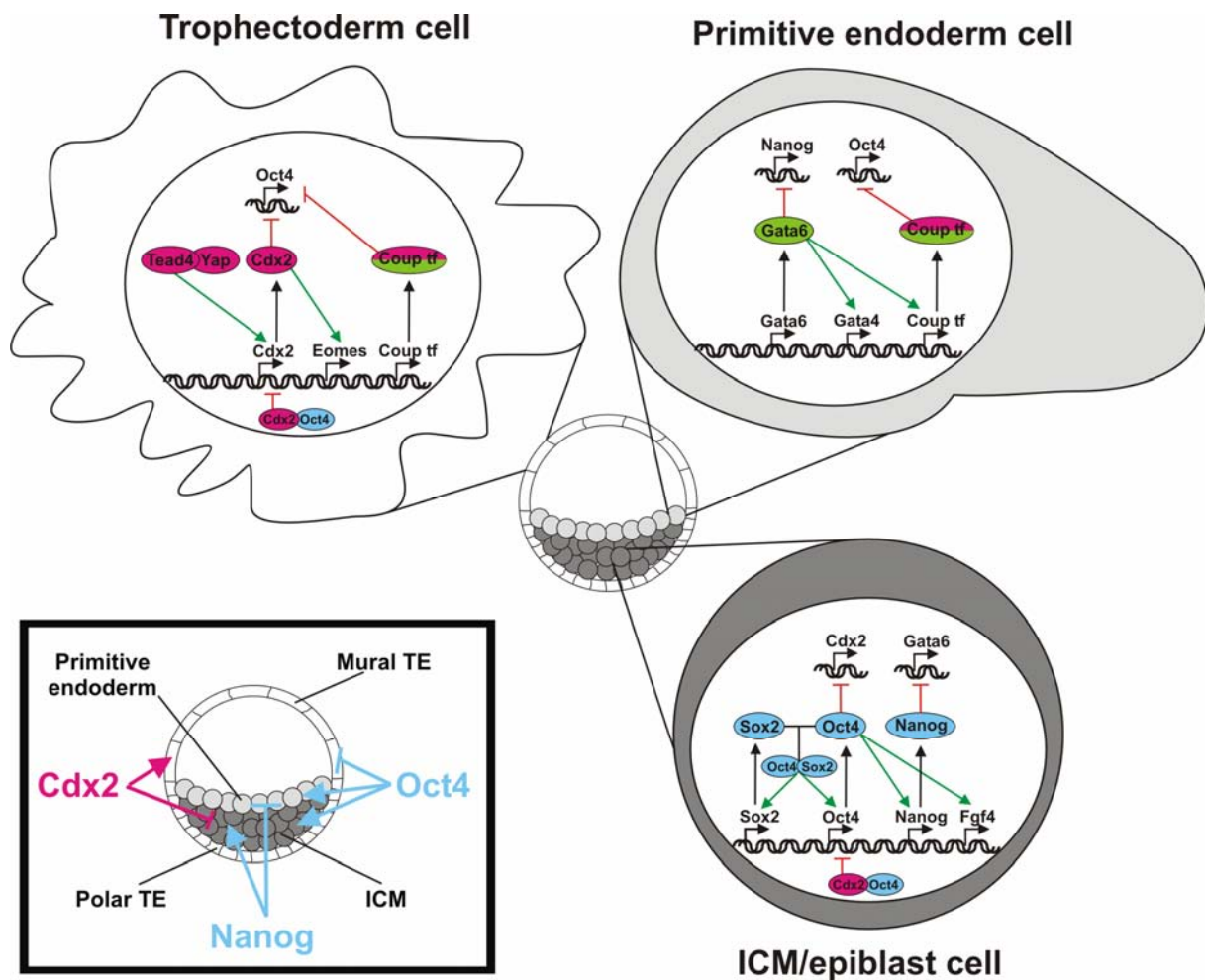


**Figure 2. Transcription factors govern lineage allocation in late blastocysts.** Diagram of a late blastocyst consisting of three cell lineages: ICM/epiblast, trophectoderm and primitive endoderm. The cell fate of these three cell types is determined by distinct sets of transcription factors. In epiblast cells, Oct4, Sox2 and Nanog induce expression of genes (including themselves) involved in self-renewal and repress genes that favor differentiation into trophectoderm (Cdx2) and primitive endoderm (Gata6). Tead4-induced Cdx2 expression enables differentiation into trophectoderm while blocking commitment to the ICM lineage by inhibiting Oct4 expression. ICM cells that express Gata6 become primitive endoderm due to inhibition of stemness genes Oct4 and Nanog by Gata6 and its target genes. Green arrows indicate gene activation, red lines indicate gene inhibition. (Inset) Oct4 is expressed in both ICM derivatives and is downregulated in the trophectoderm. A reciprocal expression pattern is seen for Cdx2, which becomes restricted to trophectoderm cells. Nanog is an epiblast-specific transcription factor that blocks commitment to the primitive endoderm lineage. The result of gene targeting of these transcription factors is in line with their expression pattern: trophectoderm cells be isolated from Oct4<sup>-/-</sup> blastocysts but ES cells cannot, Cdx2<sup>-/-</sup> embryos can establish ES cells but TS cells cannot, and only endoderm cells can be isolated from Nanog<sup>-/-</sup> embryos.

Therefore, Oct4 expression is essential for steering cell fate towards epiblast and primitive endoderm lineages, while preventing commitment to the TE lineage. One well studied transcriptional target of Oct4 is the Fgf4 gene, which induces differentiation of ES cells by activating the RAS-MAPK pathway and in this way provides a negative feedback loop for self-renewal. On the other hand, Fgf4 can be secreted from the ICM and induces proliferation in the adjacent polar TE (Tanaka et al., 1998).

Sox2 is a member of the Sox (SRY-related HMG box) gene family that encodes transcription factors with a single HMG DNA-binding domain. Sox2 is expressed in morulas, ICM of blastocysts and epiblasts. During gastrulation, Sox2 becomes restricted to the neuroectoderm and ectoplacental cone, and in adults it is present in both male and female germ cells (Avilion et al., 2003). Sox2 is known to co-operate with Oct4 in activating Oct4 target genes, such as FGF4 (Yuan et al., 1995). Both Oct4 and Sox2 expression can be regulated by binding of the Oct4-Sox2 complex to an enhancer in their corresponding promoters (Okumura-Nakanishi et al., 2005). This provides a positive feedback loop for expression of these stem cell markers in the ICM or epiblast cells (Fig. 2). But also other transcription factors can bind to the promoters of Oct4 and Sox2 and regulate their expression (Niwa, 2007). Foxd3 (a member of the forkhead family of transcriptional regulators) and Sox2 are essential for the establishment of ICM derivatives and for maintaining pluripotency in mouse embryos (Avilion et al., 2003; Hanna et al., 2002) (Table 1).

Nanog, a homeodomain transcription factor, is also essential for maintenance of pluripotency in ICM and ES cells, but unlike Oct4, it prevents ICM cells from giving rise to the primitive endoderm lineage (Chambers et al., 2003; Mitsui et al., 2003). Nanog mRNA and protein are first expressed in compacted morulas, are confined to the ICM in blastocysts and demarcate the epiblast in late blastocysts and in blastocysts in diapause (Chambers et al., 2003; Mitsui et al., 2003; Silva et al., 2009). After implantation of the blastocyst, Nanog is downregulated and becomes restricted to the genital ridges, and it is completely absent in adult tissues (Chambers et al., 2003; Mitsui et al., 2003). Ectopic expression of Nanog allowed growth of LIF-independent mouse ES cells (Chambers et al., 2003; Mitsui et al., 2003). Using a floxed Nanog transgenic mouse, LIF independence could be reversed after Cre-mediated recombination (Chambers et al., 2003). Nanog-deficient embryos form normal blastocysts but die shortly after implantation (Mitsui et al., 2003)(Table 1). Nanog-deficient late blastocysts have fewer ICM cells and decreased Oct4 levels, and they fail elicit epiblast-specific reactivation of silenced female X chromosomes (Silva et al., 2009). After immunosurgery, which selectively destroys trophectoderm cells *via* complement-dependent



## Mouse Development

antibody cytotoxicity (Solter and Knowles, 1975), isolated Nanog-deficient ICM failed to give rise to ES cells but differentiated into parietal endoderm (Mitsui et al., 2003), but not into cells of the trophectoderm lineage, as is seen in Oct4-deficient ICM cultures (Nichols et al., 1998). Stem cell markers, such as Oct4 and Rex1, are downregulated in Nanog-deficient cells but expression of Gata6, a marker for visceral endoderm, is induced, which is consistent with the endoderm-like morphology (Mitsui et al., 2003). Recent studies concerning the role for Nanog in lineage commitment yielded controversial results. Silva and colleagues (2009) showed that Nanog-deficient ICM cells are capable only of TE differentiation or, otherwise, apoptosis (Silva et al., 2009). On the other hand, Messerschmidt and colleagues (2010) showed that Nanog-ablated embryos retain the capacity to form primitive endoderm *in vivo* (Messerschmidt and Kemler, 2010). In addition, Nanog can directly repress Gata6 expression through its binding to the proximal promoter region of the Gata6 gene (Mitsui et al., 2003; Singh et al., 2007). Nanog expression fluctuates in wild type ES cell cultures, and a transient and inducible downregulation of Nanog in ES cells predisposes them to differentiation but does not mark commitment (Chambers et al., 2007). These Nanog-deficient cells contribute in chimeras (obtained by injecting Nanog-deficient cells in wild-type blastocysts) to somatic tissues, but not to the germ line (Chambers et al., 2007).

In retrospect, neither Oct4 nor Nanog can be considered a master regulator of stemness and pluripotency. Oct4 fails to sustain self-renewal of ES cells upon LIF withdrawal, whereas Nanog is not sufficient to sustain pluripotency in Oct4-depleted embryos and ES cell cultures (Boiani and Scholer, 2005). Instead, Oct4, Sox2 and Nanog work together as a core transcriptional circuitry by co-occupying a substantial portion of their target genes in human ES cells and by forming a regulatory circuitry consisting of autoregulatory and feedforward loops (Boyer et al., 2005). Oct4 and Sox2 have been shown to bind to elements in the promoter of Nanog to induce its expression (Kuroda et al., 2005; Rodda et al., 2005). The core transcription factors, Oct4, Sox2 and Nanog, constitute a positive feedback loop to maintain their expression and to promote continuous ES cell self-renewal (Fig.2)(Niwa, 2007).

Table. Gene targeting of transcription factors involved in lineage allocation in blastocysts

knockout	blastocyst	implantation	embryonic death	Stem cell derivatives from late blastocyst			reference
				ICM/ES cells	TE	PE	
<b>ICM markers</b>							
Oct4 <sup>-/-</sup>	normal	yes, but lack ICM derivatives	5,5 dpc	no	yes, TG	no	Nichols et al., 1998
Nanog <sup>-/-</sup>	normal	yes, but lack ICM derivatives	5,5 dpc	no	no	yes, PaE	Mitsui et al., 2003
Sox2 <sup>-/-</sup>	normal	yes, but lack ICM derivatives	6,0 dpc	no	yes, TG	yes, PaE	Avilion et al., 2003
FoxD3 <sup>-/-</sup>	normal	yes, normal epiblast (5,5 dpc) but replaced by ExE (6,5 dpc)	6,5 dpc	no	yes, TG		Hanna et al., 2002
<b>TE markers</b>							
Cdx2 <sup>-/-</sup>	normal, but fail to maintain blastocoel cavity and epithelial integrity; misexpression of ICM makers in TE	No, no postimplantation mutants or empty decidia	3,5-5,5 dpc	yes	no TS or TG		Chawengsakophak et al., 1997 Strumpf et al., 2005
Tead4 <sup>-/-</sup>	no blastocoel cavity formation, failure to induce TE-specific genes	No, no postimplantation mutants or empty decidia	3,5 dpc	yes	no TS or TG		Yagi et al., 2007 Nishioka et al., 2008
Tomes <sup>-/-</sup>	normal, proper expression of ICM and TE markers	Yes, but fail to form egg cylinder	6,5-7,5 dpc	yes	no TS or TG		Russ et al., 2000 Strumpf et al., 2005
<b>PE markers</b>							
Gata4 <sup>-/-</sup>	normal	Yes, but disrupted ventral body pattern lacked a primitive heart tube	7,5-10,5 dpc			No, VE	Molkenin et al., 1997 Kuro et al 1997
Gata6 <sup>-/-</sup>	normal	Yes, defective endoderm differentiation	6,5-7,5 dpc			No, VE	Soudais et al., 1995 Morrisey et al., 1998

ExE: extraembryonic ectoderm; PaE: parietal endoderm; PE: primitive endoderm; TE: trophectoderm; TG: Trophectoderm Giant Cells; TS: trophectoderm stem cells; VE: visceral endoderm ES: Embryonic stem cells

## Mouse Development

Sox2 and Oct4, but not Nanog, are essential for reprogramming somatic cells into mouse and human induced pluripotent stem (iPS) cells (Takahashi et al., 2007; Takahashi and Yamanaka, 2006). Klf4, another factor involved in reprogramming somatic cells, bridges LIF/STAT3 signaling with the core transcriptional regulators (Niwa et al., 2009). Both Klf4 and Nanog can revert epistemic cells (epiSC, derived from postimplantation epiblast) to a ground state pluripotency (Guo et al., 2009; Silva et al., 2009). Another way of reprogramming somatic cells is to fuse them with ES, whereby somatic cells erase the epigenetic signatures and reset to a ground state pluripotency. This type of somatic reprogramming is enhanced by expression of Nanog (Silva et al., 2006). In conclusion, Nanog expression is essential for reprogramming somatic-ES cell fusions, epiSCs and ICM cells towards a ground state pluripotency and contributes to a coherent gene regulatory network (Silva et al., 2009).

### **TE-specific transcription factors**

Cdx2 is a caudal-type homeodomain transcription factor expressed specifically in the TE of blastocysts and in extra-embryonic tissues, such as the placenta (Beck et al., 1995). Cdx2 protein is first seen in all the nuclei of eight-cell stage morulas (Niwa et al., 2005), but it becomes restricted to outside cells of the late morulas and blastocysts (Niwa et al., 2005; Strumpf et al., 2005). Blastocysts of Cdx2 mutant embryos appear normal, but they fail to maintain the blastocoels cavity due to loss of epithelial integrity, as evidenced by disturbed adherens and tight junctions (Strumpf et al., 2005). Cdx2 mutant blastocysts were unable to repress ICM markers, such as Oct4 and Nanog, in the TE, which points to a defect in restriction of the ICM/TE lineage (Strumpf et al., 2005). Cdx2 mutant TE eventually collapses and undergoes apoptosis at the peri-implantation stage (between 3.5 and 5.5 dpc) (Table 1) (Chawengsaksophak et al., 1997; Strumpf et al., 2005). Overexpression of Cdx2 in ES cells induces TE differentiation (Niwa et al., 2005), whereas Cdx2-deficient blastocysts could give rise to ES cell lines but not to trophoblast giant cells or trophectoderm stem (TS) cell lines (Strumpf et al., 2005). The Cdx2 mutant phenotype resembles the Oct4 mutant phenotype: both mutants form morphologically normal blastocysts but exhibit defects in segregation of the ICM and TE lineages. Depletion of both zygotic and maternal Cdx2 results in a more drastic phenotype. The abnormalities include defects in polarization and compaction of morulas, and failure to establish a functional trophectoderm lineage (Jedrusik et al., 2010).

Cdx2 and Oct4 can form a repressor complex that allows inhibition of the expression of both Oct4 and Cdx2, and this repressor complex provides a negative feedback loop and prevents cell commitment (Niwa et al., 2005)(Fig. 2). The smallest change in expression levels of Oct4 or Cdx2 can thus shift the balance and determine allocation of cell fate to either TE or ICM (Niwa, 2007).

Tead4 is a transcription factor containing a TEA domain (TEAD). This factor is expressed in two-cell embryos, morulas and blastocysts (Yagi et al., 2007). Tead4 is expressed in the nuclei of both TE and ICM cells in blastocysts (Nishioka et al., 2008), but its levels are higher in cultured TS and trophoblast giant (TG) cells than in ES cells or embryoid bodies (Yagi et al., 2007). After embryo implantation, Tead4 is preliminary expressed in trophectoderm-derived cell lineages (Yagi et al., 2007). Tead4-deficient embryos can undergo compaction and have intact adherens junctions, but they can not establish a functional trophectoderm and consequently fail to form a blastocoel and die before implantation (Nishioka et al., 2008; Yagi et al., 2007). The phenotypic abnormality of *Tead4*-deficient embryos is more severe than that of *Cdx2*-deficient embryos. This means that Tead4 target genes other than Cdx2 might be essential in epithelialization and cavity formation. Like *Cdx2*-deficient embryos, ES cells, but not TS cells, can be derived from Tead4-deficient embryos, indicating that Tead4 is essential for TE but dispensable for ICM (Table 1)(Nishioka et al., 2008; Yagi et al., 2007). Remarkably, the expression of TE markers, such as Cdx2 and Eomesodermin, is virtually absent in Tead4-deficient embryos, whereas ICM-markers, such as Oct4 and Nanog, are ectopically expressed in external cells at the late blastocyst stage (Nishioka et al., 2008; Yagi et al., 2007). Like Cdx2, Tead4 expression in ES cells promotes trophoblast differentiation, but Cdx2 expression in Tead4-deficient ES cell lines was not sufficient to maintain TS cell lines, indicating that Cdx2 cannot fully substitute for Tead4 in the TE lineage (Nishioka et al., 2009). On the other hand, Tead4 expression in *Cdx2*-deficient ES cells induces trophoblast differentiation but does not allow the establishment of TS lines (Nishioka et al., 2009). Yap, a Tead co-activator, is also expressed during preimplantation, and its nuclear expression becomes restricted in the outside cells of blastocysts (Nishioka et al., 2009). Hippo signaling suppresses nuclear accumulation of Yap in inside cells. Both cell-cell contact and Lats-mediated phosphorylation of Yap causes its translocation to the cytoplasm, separating Tead4 from its co-activator and causing a drop in Cdx2 expression in inside cells (Nishioka et al., 2009).

Eomesodermin (Eomes), a T-box TF, is also expressed specifically in the TE at the blastocyst stage, and, like Cdx2, it is expressed at later stages in the ExE (Ciruna and Rossant,

## Mouse Development

1999; Hancock et al., 1999; Russ et al., 2000). *Eomes* mutants have also been reported to show early defects in trophoblast proliferation (Table 1)(Russ et al., 2000). Overexpression of *Eomes*, like *Cdx2* overexpression, also induces TE differentiation (Niwa et al., 2005). Unlike *Cdx2*-null embryos, *Eomes*-null embryos form morphologically normal blastocysts with an expanded cavity and the proper lineage-specific expression patterns for Oct4 and *Cdx2* (Strumpf et al., 2005). Like *Cdx2*-null embryos, *Eomes*-null embryos are unable to generate trophoblast giant cells and TS cell lines (Russ et al., 2000; Strumpf et al., 2005). Overexpression of *Eomes* in ES cells also induces TE differentiation (Strumpf et al., 2005) even in the absence of *Cdx2* (Niwa et al., 2005). However, *Cdx2* is required for normal expression of *Eomes* in the trophectoderm of blastocysts (Ralston and Rossant, 2008).

### PE-specific transcription factors

Expression of *Gata4* or *Gata6* in ES cells induces differentiation into parietal endoderm, and this coincides with upregulation of chicken ovalbumin upstream promoter-transcription factors (Coup-tf) and downregulation of Oct4 (Fujikura et al., 2002). Expression of coup-tf in ES cells is sufficient to inhibit stem cell markers, such as Oct4 (Fig.2)(Fujikura et al., 2002). *Gata6*-knockout embryos fail to form visceral endoderm *in vivo* and *in vitro*, show a decrease in *Gata4* expression levels, and die during the onset of gastrulation (Table 1)(Morrisey et al., 1998). *Gata4*-deficient embryos die during midgestation due to abnormal ventral morphogenesis and heart tube formation (Kuo et al., 1997; Molkenin et al., 1997). *Gata4*-knockout ES cells are unable to differentiate in culture into visceral endoderm, suggesting that *Gata4* is necessary for the differentiation of this cell lineage (Soudais et al., 1995). *Gata* factors and *Nanog* show a mutual exclusive localization pattern in late blastocysts and are confined to primitive endoderm and epiblast, respectively. Based on a computational model, reprogramming from an endoderm state into a stem cell state is best achieved by over-expressing *Nanog* rather than by suppressing differentiation genes such as *Gata-6* (Chickarmane and Peterson, 2008).

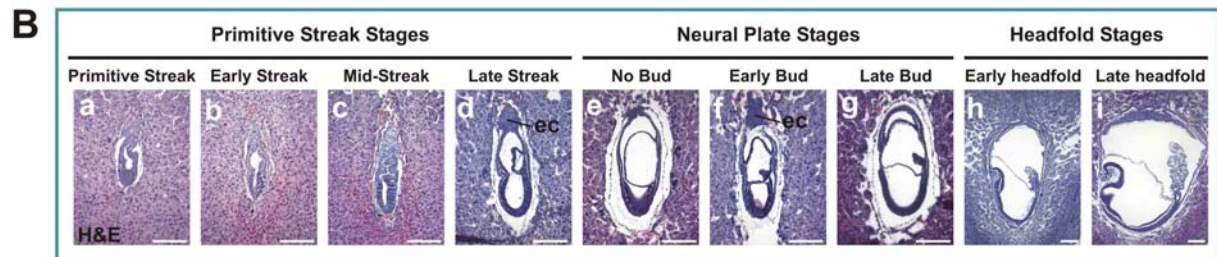
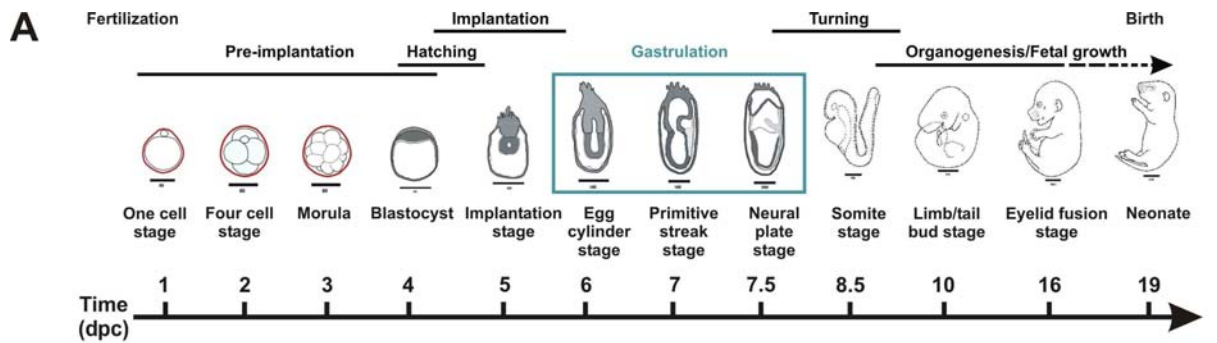
## IMPLANTATION AND GASTRULATION

On the fifth day of mouse development, the blastocyst hatches from its zona pellucida. Trypsin-like enzyme produced by mural TE digests the glycoprotein matrix of the zona pellucida and the blastocyst escapes by rhythmic expansion and contraction. During onset of implantation, the walls of the uterus become tightly apposed and get ready for attachment of

blastocysts by their mural TE. Blastocyst adhesion is dependent on estrogen (absence induces diapause) and induces the formation of a uterine crypt and decidual tissue (deciduum) consisting of a spongy mass of decidual cells surrounding a single embryo. The decidual reaction causes a rapid increase in permeability, which causes the uterine stroma to become swollen and edematous. Trophoblast giant cells invade the stroma by passing through the eroded epithelium that was separating the uterine stroma from the blastocyst. TE cells that are not near the ICM become polyploid giant cells, which can invade but not proliferate, which prevents them from attaining features of metastatic cancer cells (Hogan et al., 1994).

Late blastocysts contain three lineages, of which the epiblast is the smallest population, consisting of only 20–25 cells enclosed between the polar TE and PE. After implantation, these apolar epiblast cells become polarized and organize into a simple epithelium surrounding a small central cavity, called the proamniotic cavity (Fig. 3Ba, pre-streak). During gastrulation (5.5 – 7.5 dpc) the primitive ectoderm divides extremely rapidly. This proliferation is accompanied by rapid morphological changes ultimately leading to the transformation of a bilaminar egg cylinder into a multilayered, three-chambered conceptus (Fig. 3). The time window during which gastrulation occurs differs among strains and even between littermates. Therefore, gastrulating embryos are classified according to a staging system based on morphological landmarks rather than according to time (Fig. 3B)(Downs and Davies, 1993). Mesoderm cells are derived from the epiblast following ingression through the primitive streak, which marks the posterior side of the embryo (Fig. 3C). Epithelial continuity is lost near the primitive streak as cells from the epiblast undergo an epithelial to mesenchymal transition and emerge as a new intermediate mesoderm layer between the epiblast and the visceral endoderm (Fig. 3Bb,c; insets). Depending on the proportion of mesoderm on the posterior side of the gastrula, embryos are scored as early streak (Fig. 3Bb) or as mid-streak (Fig. 3Bc). Nascent mesoderm moves in two directions. Mesoderm cells move anteriorward and can intercalate with visceral endoderm cells to make up the first cohort of definitive endoderm. Posterior mesoderm pushes and displaces extraembryonic ectoderm towards the ectoplacental cone. Mesoderm in the posterior (and to a lesser extent in the anterior) extraembryonic region accumulates due to the acquisition of intercellular openings, and fusion of this extraembryonic mesoderm results in a mesoderm-lined exocoelom. The expanding extraembryonic mesoderm pushes the extraembryonic ectoderm towards the centre of the proamniotic cavity, forming distinct bulges called amniotic folds. These amniotic folds fuse and form a new chamber separated from the embryonic region by amnion and from the ectoplacental cone by chorion (Fig. 3C). The mesodermal and visceral

## Mouse Development



### Primitive Streak Stages

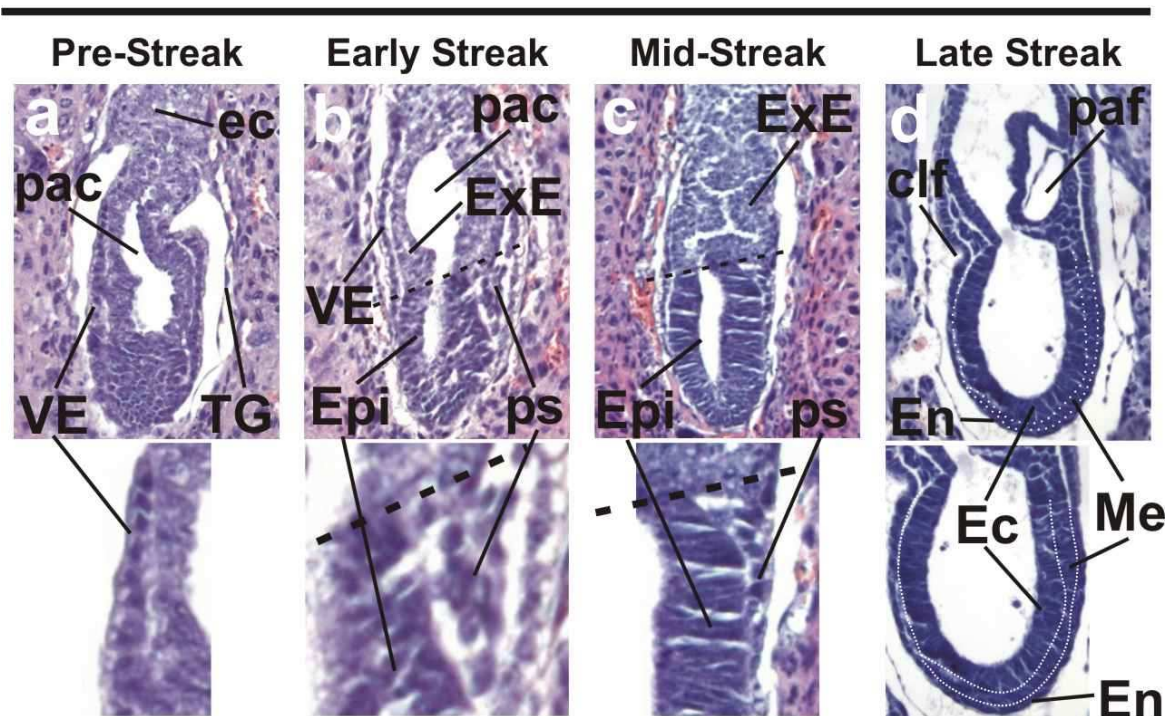


**Figure 3. Overview of gastrulation.** (A) A general overview of mouse development and its different stages. The stages of gastrulation are marked by a green box. Diagrams of Theiler stage embryos were adapted from the Edinburgh Mouse Atlas (<http://genex.hgu.mrc.ac.uk/Atlas>). (B) Overview of gastrulation. Hematoxylin and eosin (H&E)-stained sagittal paraffin sections of the different stages of gastrulation according to the staging system of Downs and Davies (1993), including pre-streak (a), early streak (b), mid streak (c), late streak (d), no bud (e), early bud (f), late bud (g), early headfold (h) and late headfold (i) stages. Scale bar: 200  $\mu$ m.



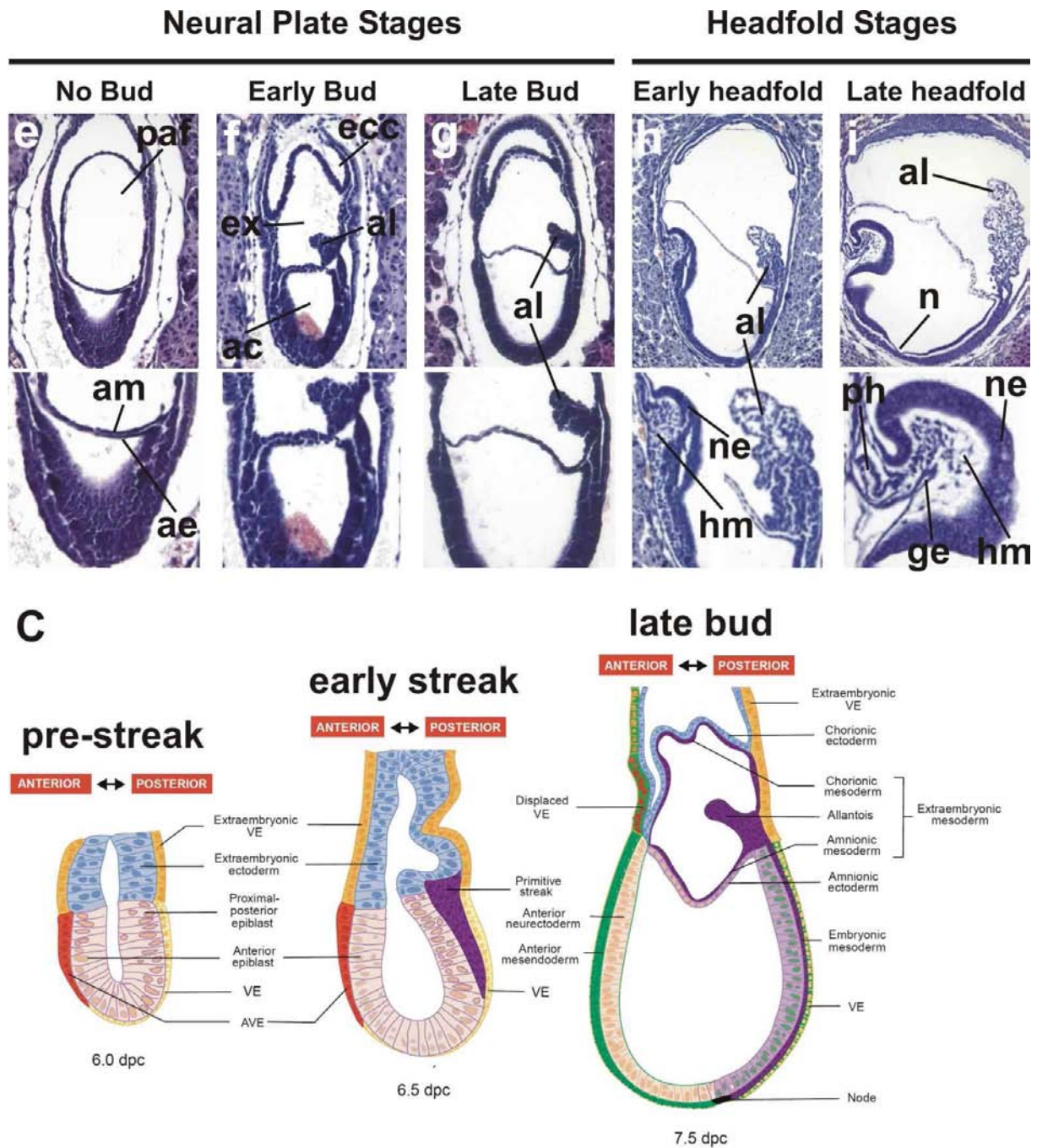


**Figure 3 (continued).** Middle and bottom panels contain magnifications from the top panel. (C) Diagram of pre-streak, early streak and late streak stage embryos, are taken from Lu et al. (2001). ac: amniotic cavity, ae: amniotic ectoderm, al: allantois, am: amniotic mesoderm, AVE: anterior visceral endoderm, clf: cranial limiting furrow, ec: ectoplacental cone, ecc: ectoplacental cavity, Ec: ectoderm, En: endoderm, Epi: epiblast, ex: exocoelom, ExE: extraembryonic ectoderm, ge: gut endoderm, hm: head mesenchyme, Me: mesoderm, n: node, ne: neural ectoderm, paf: posterior amniotic fold, ph: primitive heart tube, ps: primitive streak, VE: visceral endoderm.



## Mouse Development

endoderm walls of this chamber will form the visceral yolk sac. Late streak gastrulas are identified by the presence of a posterior amniotic fold, an indentation at the cranial limiting furrow and the node on the distal tip (Fig. 3Bd). In no bud stage embryos, the amniotic folds have fused to generate three cavities, namely the amniotic cavity, the exocoelom and the ectoplacental cavity (Fig. 3Be,f). Extraembryonic mesoderm keeps emerging from the posterior streak and bulges into the exocoelom to form a discrete structure, the allantois. The allantois eventually fuses with the chorion and will be detrimental for nutrient and waste exchange between the embryo and the placenta. Early and late stage embryos can be distinguished by the amount of allantois formed (Fig. 3Bf,g). The most anterior aspect of the streak is the node, a specialized structure of about 20 cells that is equivalent to Hensen's node in chick and is important for organizing and patterning the midline axis of the embryo. The node region is recognized by a slight indentation of the tip of the egg cylinder (Fig. 3Bi) and lacks visceral endoderm. The layers of this bilaminar structure are intimately associated, in contrast to the trilaminar layers in the embryonic region, which are separated from each other by basal lamina. Late headfold gastrula can be distinguished from early headfold embryos by the presence of well-defined headfolds and foregut invagination (Fig. 3Bh,i). Late headfold embryos contain primordia of forebrain, gut and heart and therefore demarcate the onset of organogenesis (Hogan et al., 1994; Downs and Davies, 1993).

## REFERENCES

- Alarcon, V.B., and Y. Marikawa. 2003. Deviation of the blastocyst axis from the first cleavage plane does not affect the quality of mouse postimplantation development. *Biol Reprod.* 69:1208-12.
- Alarcon, V.B., and Y. Marikawa. 2005. Unbiased contribution of the first two blastomeres to mouse blastocyst development. *Mol Reprod Dev.* 72:354-61.
- Avilion, A.A., S.K. Nicolis, L.H. Pevny, L. Perez, N. Vivian, and R. Lovell-Badge. 2003. Multipotent cell lineages in early mouse development depend on SOX2 function. *Genes Dev.* 17:126-40.
- Barcroft, L.C., A.E. Moseley, J.B. Lingrel, and A.J. Watson. 2004. Deletion of the Na/K-ATPase alpha1-subunit gene (*Atp1a1*) does not prevent cavitation of the preimplantation mouse embryo. *Mech Dev.* 121:417-26.
- Barcroft, L.C., H. Offenberg, P. Thomsen, and A.J. Watson. 2003. Aquaporin proteins in murine trophectoderm mediate transepithelial water movements during cavitation. *Dev Biol.* 256:342-54.
- Beck, F., T. Erler, A. Russell, and R. James. 1995. Expression of *Cdx-2* in the mouse embryo and placenta: possible role in patterning of the extra-embryonic membranes. *Dev Dyn.* 204:219-27.
- Becker, S., J. Casanova, and L. Grabel. 1992. Localization of endoderm-specific mRNAs in differentiating F9 embryoid bodies. *Mech Dev.* 37:3-12.
- Beddington, R.S., and E.J. Robertson. 1999. Axis development and early asymmetry in mammals. *Cell.* 96:195-209.
- Bischoff, M., D.E. Parfitt, and M. Zernicka-Goetz. 2008. Formation of the embryonic-abembryonic axis of the mouse blastocyst: relationships between orientation of early cleavage divisions and pattern of symmetric/asymmetric divisions. *Development.* 135:953-62.
- Boiani, M., and H.R. Scholer. 2005. Regulatory networks in embryo-derived pluripotent stem cells. *Nat Rev Mol Cell Biol.* 6:872-84.
- Boyer, L.A., T.I. Lee, M.F. Cole, S.E. Johnstone, S.S. Levine, J.P. Zucker, M.G. Guenther, R.M. Kumar, H.L. Murray, R.G. Jenner, D.K. Gifford, D.A. Melton, R. Jaenisch, and R.A. Young. 2005. Core transcriptional regulatory circuitry in human embryonic stem cells. *Cell.* 122:947-56.
- Bradley, A., M. Evans, M.H. Kaufman, and E. Robertson. 1984. Formation of germ-line chimaeras from embryo-derived teratocarcinoma cell lines. *Nature.* 309:255-6.
- Chai, N., Y. Patel, K. Jacobson, J. McMahan, A. McMahan, and D.A. Rappolee. 1998. FGF is an essential regulator of the fifth cell division in preimplantation mouse embryos. *Dev Biol.* 198:105-15.
- Chambers, I., D. Colby, M. Robertson, J. Nichols, S. Lee, S. Tweedie, and A. Smith. 2003. Functional expression cloning of *Nanog*, a pluripotency sustaining factor in embryonic stem cells. *Cell.* 113:643-55.
- Chambers, I., J. Silva, D. Colby, J. Nichols, B. Nijmeijer, M. Robertson, J. Vrana, K. Jones, L. Grotewold, and A. Smith. 2007. *Nanog* safeguards pluripotency and mediates germline development. *Nature.* 450:1230-4.
- Chawengsaksophak, K., R. James, V.E. Hammond, F. Kontgen, and F. Beck. 1997. Homeosis and intestinal tumours in *Cdx2* mutant mice. *Nature.* 386:84-7.
- Chazaud, C., Y. Yamanaka, T. Pawson, and J. Rossant. 2006. Early lineage segregation between epiblast and primitive endoderm in mouse blastocysts through the Grb2-MAPK pathway. *Dev Cell.* 10:615-24.

## Mouse Development

- Chénot. 1902. La loi de Mendel et l'hérédité de la pigmentation chez les souris *Arch. Zool. Exp. Gen.* 3:27-30.
- Chickarmane, V., and C. Peterson. 2008. A computational model for understanding stem cell, trophoctoderm and endoderm lineage determination. *PLoS One.* 3:e3478.
- Ciruna, B.G., and J. Rossant. 1999. Expression of the T-box gene Eomesodermin during early mouse development. *Mech Dev.* 81:199-203.
- Clayton, L., A. Hall, and M.H. Johnson. 1999. A role for Rho-like GTPases in the polarisation of mouse eight-cell blastomeres. *Dev Biol.* 205:322-31.
- Corrigan, J., D. Corrow, J.M. Currer, P. Danneman, M. Davisson, K. Flurkey, D.E. Harrison, J. Merriam, M. Strobel, R. Vonder Haar, B. Witham, C. Linder, and K. Pritchett-Corning. 2009. The Jackson Laboratory Handbook on Genetically Standardized Mice. The Jackson Laboratory.
- Deb, K., M. Sivaguru, H.Y. Yong, and R.M. Roberts. 2006. Cdx2 gene expression and trophoctoderm lineage specification in mouse embryos. *Science.* 311:992-6.
- Dickson, A.D. 1963. Trophoblastic Giant Cell Transformation of Mouse Blastocysts. *J Reprod Fertil.* 6:465-6.
- Downs, K.M., and T. Davies. 1993. Staging of gastrulating mouse embryos by morphological landmarks in the dissecting microscope. *Development.* 118:1255-66.
- Eckert, J.J., and T.P. Fleming. 2008. Tight junction biogenesis during early development. *Biochim Biophys Acta.* 1778:717-28.
- Evans, M.J., and M.H. Kaufman. 1981. Establishment in culture of pluripotential cells from mouse embryos. *Nature.* 292:154-6.
- Fujikura, J., E. Yamato, S. Yonemura, K. Hosoda, S. Masui, K. Nakao, J. Miyazaki Ji, and H. Niwa. 2002. Differentiation of embryonic stem cells is induced by GATA factors. *Genes Dev.* 16:784-9.
- Fujimori, T., Y. Kurotaki, K. Komatsu, and Y. Nabeshima. 2009. Morphological organization of the mouse preimplantation embryo. *Reprod Sci.* 16:171-7.
- Gardner, R.L. 1982. Investigation of cell lineage and differentiation in the extraembryonic endoderm of the mouse embryo. *J Embryol Exp Morphol.* 68:175-98.
- Gardner, R.L. 1997. The early blastocyst is bilaterally symmetrical and its axis of symmetry is aligned with the animal-vegetal axis of the zygote in the mouse. *Development.* 124:289-301.
- Gardner, R.L. 1998. Contributions of blastocyst micromanipulation to the study of mammalian development. *Bioessays.* 20:168-80.
- Gardner, R.L. 2001. Specification of embryonic axes begins before cleavage in normal mouse development. *Development.* 128:839-47.
- Gardner, R.L., V.E. Papaioannou, and S.C. Barton. 1973. Origin of the ectoplacental cone and secondary giant cells in mouse blastocysts reconstituted from isolated trophoblast and inner cell mass. *J Embryol Exp Morphol.* 30:561-72.
- Gardner, R.L., and J. Rossant. 1979. Investigation of the fate of 4-5 day post-coitum mouse inner cell mass cells by blastocyst injection. *J Embryol Exp Morphol.* 52:141-52.
- Guo, G., J. Yang, J. Nichols, J.S. Hall, I. Eyres, W. Mansfield, and A. Smith. 2009. Klf4 reverts developmentally programmed restriction of ground state pluripotency. *Development.* 136:1063-9.
- Hancock, S.N., S.I. Agulnik, L.M. Silver, and V.E. Papaioannou. 1999. Mapping and expression analysis of the mouse ortholog of Xenopus Eomesodermin. *Mech Dev.* 81:205-8.
- Hanna, L.A., R.K. Foreman, I.A. Tarasenko, D.S. Kessler, and P.A. Labosky. 2002. Requirement for Foxd3 in maintaining pluripotent cells of the early mouse embryo. *Genes Dev.* 16:2650-61.

- Hiiragi, T., and D. Solter. 2004. First cleavage plane of the mouse egg is not predetermined but defined by the topology of the two apposing pronuclei. *Nature*. 430:360-4.
- Hogan, B., R. Beddington, F. Constantini, and E. Lacy. 1994. *Manipulating the Mouse Embryo*. Cold Spring Harbor Press. 1-88 pp.
- Hyafil, F., C. Babinet, and F. Jacob. 1981. Cell-cell interactions in early embryogenesis: a molecular approach to the role of calcium. *Cell*. 26:447-54.
- Hyafil, F., D. Morello, C. Babinet, and F. Jacob. 1980. A cell surface glycoprotein involved in the compaction of embryonal carcinoma cells and cleavage stage embryos. *Cell*. 21:927-34.
- Jedrusik, A., A.W. Bruce, M.H. Tan, D.E. Leong, M. Skamagki, M. Yao, and M. Zernicka-Goetz. 2010. Maternally and zygotically provided Cdx2 have novel and critical roles for early development of the mouse embryo. *Dev Biol*. 344:66-78.
- Johnson, M.H., B. Maro, and M. Takeichi. 1986. The role of cell adhesion in the synchronization and orientation of polarization in 8-cell mouse blastomeres. *J Embryol Exp Morphol*. 93:239-55.
- Johnson, M.H., and J.M. McConnell. 2004. Lineage allocation and cell polarity during mouse embryogenesis. *Semin Cell Dev Biol*. 15:583-97.
- Johnson, M.H., and C.A. Ziomek. 1981. The foundation of two distinct cell lineages within the mouse morula. *Cell*. 24:71-80.
- Kaufman, M. 1992. *The Atlas Of Mouse Development*. Academic Press.
- Kawagishi, R., M. Tahara, K. Sawada, K. Morishige, M. Sakata, K. Tasaka, and Y. Murata. 2004. Na<sup>+</sup> / H<sup>+</sup> exchanger-3 is involved in mouse blastocyst formation. *J Exp Zool A Comp Exp Biol*. 301:767-75.
- Kirby, D.R., D.M. Potts, and I.B. Wilson. 1967. On the orientation of the implanting blastocyst. *J Embryol Exp Morphol*. 17:527-32.
- Kunath, T., D. Arnaud, G.D. Uy, I. Okamoto, C. Chureau, Y. Yamanaka, E. Heard, R.L. Gardner, P. Avner, and J. Rossant. 2005. Imprinted X-inactivation in extra-embryonic endoderm cell lines from mouse blastocysts. *Development*. 132:1649-61.
- Kuo, C.T., E.E. Morrisey, R. Anandappa, K. Sigrist, M.M. Lu, M.S. Parmacek, C. Soudais, and J.M. Leiden. 1997. GATA4 transcription factor is required for ventral morphogenesis and heart tube formation. *Genes Dev*. 11:1048-60.
- Kurimoto, K., Y. Yabuta, Y. Ohinata, Y. Ono, K.D. Uno, R.G. Yamada, H.R. Ueda, and M. Saitou. 2006. An improved single-cell cDNA amplification method for efficient high-density oligonucleotide microarray analysis. *Nucleic Acids Res*. 34:e42.
- Kuroda, T., M. Tada, H. Kubota, H. Kimura, S.Y. Hatano, H. Suemori, N. Nakatsuji, and T. Tada. 2005. Octamer and Sox elements are required for transcriptional cis regulation of Nanog gene expression. *Mol Cell Biol*. 25:2475-85.
- Kurotaki, Y., K. Hatta, K. Nakao, Y. Nabeshima, and T. Fujimori. 2007. Blastocyst axis is specified independently of early cell lineage but aligns with the ZP shape. *Science*. 316:719-23.
- Larue, L., M. Ohsugi, J. Hirchenhain, and R. Kemler. 1994. E-cadherin null mutant embryos fail to form a trophectoderm epithelium. *Proc Natl Acad Sci U S A*. 91:8263-7.
- Lu, C.C., J. Brennan, and E.J. Robertson. 2001. From fertilization to gastrulation: axis formation in the mouse embryo. *Curr Opin Genet Dev*. 11:384-92.
- Madan, P., K. Rose, and A.J. Watson. 2007. Na/K-ATPase beta1 subunit expression is required for blastocyst formation and normal assembly of trophectoderm tight junction-associated proteins. *J Biol Chem*. 282:12127-34.
- Marikawa, Y., and V.B. Alarcon. 2009. Establishment of trophectoderm and inner cell mass lineages in the mouse embryo. *Mol Reprod Dev*. 76:1019-32.

## Mouse Development

- Martin, G.R. 1981. Isolation of a pluripotent cell line from early mouse embryos cultured in medium conditioned by teratocarcinoma stem cells. *Proc Natl Acad Sci U S A.* 78:7634-8.
- Martin, G.R., and M.J. Evans. 1975. Differentiation of clonal lines of teratocarcinoma cells: formation of embryoid bodies in vitro. *Proc Natl Acad Sci U S A.* 72:1441-5.
- Matter, K., and M.S. Balda. 2003. Signalling to and from tight junctions. *Nat Rev Mol Cell Biol.* 4:225-36.
- Messerschmidt, D.M., and R. Kemler. 2010. Nanog is required for primitive endoderm formation through a non-cell autonomous mechanism. *Dev Biol.* 344:129-37.
- Mitsui, K., Y. Tokuzawa, H. Itoh, K. Segawa, M. Murakami, K. Takahashi, M. Maruyama, M. Maeda, and S. Yamanaka. 2003. The homeoprotein Nanog is required for maintenance of pluripotency in mouse epiblast and ES cells. *Cell.* 113:631-42.
- Molkentin, J.D., Q. Lin, S.A. Duncan, and E.N. Olson. 1997. Requirement of the transcription factor GATA4 for heart tube formation and ventral morphogenesis. *Genes Dev.* 11:1061-72.
- Moriwaki, K., S. Tsukita, and M. Furuse. 2007. Tight junctions containing claudin 4 and 6 are essential for blastocyst formation in preimplantation mouse embryos. *Dev Biol.* 312:509-22.
- Morrisey, E.E., Z. Tang, K. Sigrist, M.M. Lu, F. Jiang, H.S. Ip, and M.S. Parmacek. 1998. GATA6 regulates HNF4 and is required for differentiation of visceral endoderm in the mouse embryo. *Genes Dev.* 12:3579-90.
- Motosugi, N., J.E. Dietrich, Z. Polanski, D. Solter, and T. Hiragi. 2006. Space asymmetry directs preferential sperm entry in the absence of polarity in the mouse oocyte. *PLoS Biol.* 4:e135.
- Murray, P., and D. Edgar. 2001. The regulation of embryonic stem cell differentiation by leukaemia inhibitory factor (LIF). *Differentiation.* 68:227-34.
- Nichols, J., B. Zevnik, K. Anastassiadis, H. Niwa, D. Klewe-Nebenius, I. Chambers, H. Scholer, and A. Smith. 1998. Formation of pluripotent stem cells in the mammalian embryo depends on the POU transcription factor Oct4. *Cell.* 95:379-91.
- Nishioka, N., K. Inoue, K. Adachi, H. Kiyonari, M. Ota, A. Ralston, N. Yabuta, S. Hirahara, R.O. Stephenson, N. Ogonuki, R. Makita, H. Kurihara, E.M. Morin-Kensicki, H. Nojima, J. Rossant, K. Nakao, H. Niwa, and H. Sasaki. 2009. The Hippo signaling pathway components Lats and Yap pattern Tead4 activity to distinguish mouse trophoctoderm from inner cell mass. *Dev Cell.* 16:398-410.
- Nishioka, N., S. Yamamoto, H. Kiyonari, H. Sato, A. Sawada, M. Ota, K. Nakao, and H. Sasaki. 2008. Tead4 is required for specification of trophoctoderm in pre-implantation mouse embryos. *Mech Dev.* 125:270-83.
- Niwa, H. 2007. How is pluripotency determined and maintained? *Development.* 134:635-46.
- Niwa, H., J. Miyazaki, and A.G. Smith. 2000. Quantitative expression of Oct-3/4 defines differentiation, dedifferentiation or self-renewal of ES cells. *Nat Genet.* 24:372-6.
- Niwa, H., K. Ogawa, D. Shimosato, and K. Adachi. 2009. A parallel circuit of LIF signalling pathways maintains pluripotency of mouse ES cells. *Nature.* 460:118-22.
- Niwa, H., Y. Toyooka, D. Shimosato, D. Strumpf, K. Takahashi, R. Yagi, and J. Rossant. 2005. Interaction between Oct3/4 and Cdx2 determines trophoctoderm differentiation. *Cell.* 123:917-29.
- O'Farrell, P.H., J. Stumpff, and T.T. Su. 2004. Embryonic cleavage cycles: how is a mouse like a fly? *Curr Biol.* 14:R35-45.
- Ohsugi, M., L. Larue, H. Schwarz, and R. Kemler. 1997. Cell-junctional and cytoskeletal organization in mouse blastocysts lacking E-cadherin. *Dev Biol.* 185:261-71.

- Okamoto, K., H. Okazawa, A. Okuda, M. Sakai, M. Muramatsu, and H. Hamada. 1990. A novel octamer binding transcription factor is differentially expressed in mouse embryonic cells. *Cell*. 60:461-72.
- Okumura-Nakanishi, S., M. Saito, H. Niwa, and F. Ishikawa. 2005. Oct-3/4 and Sox2 regulate Oct-3/4 gene in embryonic stem cells. *J Biol Chem*. 280:5307-17.
- Palmieri, S.L., W. Peter, H. Hess, and H.R. Scholer. 1994. Oct-4 transcription factor is differentially expressed in the mouse embryo during establishment of the first two extraembryonic cell lineages involved in implantation. *Dev Biol*. 166:259-67.
- Peyrieras, N., F. Hyafil, D. Louvard, H.L. Ploegh, and F. Jacob. 1983. Uvomorulin: a nonintegral membrane protein of early mouse embryo. *Proc Natl Acad Sci U S A*. 80:6274-7.
- Piotrowska, K., F. Wianny, R.A. Pedersen, and M. Zernicka-Goetz. 2001. Blastomeres arising from the first cleavage division have distinguishable fates in normal mouse development. *Development*. 128:3739-48.
- Plusa, B., S. Frankenberg, A. Chalmers, A.K. Hadjantonakis, C.A. Moore, N. Papalopulu, V.E. Papaioannou, D.M. Glover, and M. Zernicka-Goetz. 2005. Downregulation of Par3 and aPKC function directs cells towards the ICM in the preimplantation mouse embryo. *J Cell Sci*. 118:505-15.
- Ralston, A., and J. Rossant. 2008. Cdx2 acts downstream of cell polarization to cell-autonomously promote trophoderm fate in the early mouse embryo. *Dev Biol*. 313:614-29.
- Reeve, W.J., and C.A. Ziomek. 1981. Distribution of microvilli on dissociated blastomeres from mouse embryos: evidence for surface polarization at compaction. *J Embryol Exp Morphol*. 62:339-50.
- Rodda, D.J., J.L. Chew, L.H. Lim, Y.H. Loh, B. Wang, H.H. Ng, and P. Robson. 2005. Transcriptional regulation of nanog by OCT4 and SOX2. *J Biol Chem*. 280:24731-7.
- Rosner, M.H., M.A. Viganò, K. Ozato, P.M. Timmons, F. Poirier, P.W. Rigby, and L.M. Staudt. 1990. A POU-domain transcription factor in early stem cells and germ cells of the mammalian embryo. *Nature*. 345:686-92.
- Rossant, J. 2008. Stem cells and early lineage development. *Cell*. 132:527-31.
- Rossant, J., and P.P. Tam. 2009. Blastocyst lineage formation, early embryonic asymmetries and axis patterning in the mouse. *Development*. 136:701-13.
- Russ, A.P., S. Wattler, W.H. Colledge, S.A. Aparicio, M.B. Carlton, J.J. Pearce, S.C. Barton, M.A. Surani, K. Ryan, M.C. Nehls, V. Wilson, and M.J. Evans. 2000. Eomesodermin is required for mouse trophoblast development and mesoderm formation. *Nature*. 404:95-9.
- Scholer, H.R., G.R. Dressler, R. Balling, H. Rohdewohld, and P. Gruss. 1990. Oct-4: a germline-specific transcription factor mapping to the mouse t-complex. *Embo J*. 9:2185-95.
- Sheth, B., R.L. Nowak, R. Anderson, W.Y. Kwong, T. Papenbrock, and T.P. Fleming. 2008. Tight junction protein ZO-2 expression and relative function of ZO-1 and ZO-2 during mouse blastocyst formation. *Exp Cell Res*. 314:3356-68.
- Silva, J., I. Chambers, S. Pollard, and A. Smith. 2006. Nanog promotes transfer of pluripotency after cell fusion. *Nature*. 441:997-1001.
- Silva, J., J. Nichols, T.W. Theunissen, G. Guo, A.L. van Oosten, O. Barrandon, J. Wray, S. Yamanaka, I. Chambers, and A. Smith. 2009. Nanog is the gateway to the pluripotent ground state. *Cell*. 138:722-37.
- Singh, A.M., T. Hamazaki, K.E. Hankowski, and N. Terada. 2007. A heterogeneous expression pattern for Nanog in embryonic stem cells. *Stem Cells*. 25:2534-42.

## Mouse Development

- Solter, D., and B.B. Knowles. 1975. Immunosurgery of mouse blastocyst. *Proc Natl Acad Sci U S A.* 72:5099-102.
- Soudais, C., M. Bielinska, M. Heikinheimo, C.A. MacArthur, N. Narita, J.E. Saffitz, M.C. Simon, J.M. Leiden, and D.B. Wilson. 1995. Targeted mutagenesis of the transcription factor GATA-4 gene in mouse embryonic stem cells disrupts visceral endoderm differentiation in vitro. *Development.* 121:3877-88.
- Stephenson, R.O., Y. Yamanaka, and J. Rossant. 2010. Disorganized epithelial polarity and excess trophoblast cell fate in preimplantation embryos lacking E-cadherin. *Development.*
- Strumpf, D., C.A. Mao, Y. Yamanaka, A. Ralston, K. Chawengsaksophak, F. Beck, and J. Rossant. 2005. Cdx2 is required for correct cell fate specification and differentiation of trophoblast in the mouse blastocyst. *Development.* 132:2093-102.
- Takahashi, K., K. Tanabe, M. Ohnuki, M. Narita, T. Ichisaka, K. Tomoda, and S. Yamanaka. 2007. Induction of pluripotent stem cells from adult human fibroblasts by defined factors. *Cell.* 131:861-72.
- Takahashi, K., and S. Yamanaka. 2006. Induction of pluripotent stem cells from mouse embryonic and adult fibroblast cultures by defined factors. *Cell.* 126:663-76.
- Tanaka, S., T. Kunath, A.K. Hadjantonakis, A. Nagy, and J. Rossant. 1998. Promotion of trophoblast stem cell proliferation by FGF4. *Science.* 282:2072-5.
- Tarkowski, A.K., and J. Wroblewska. 1967. Development of blastomeres of mouse eggs isolated at the 4- and 8-cell stage. *J Embryol Exp Morphol.* 18:155-80.
- The international Mouse Knockout Consortium. 2007. A mouse for all reasons. *Cell.* 128:9-13.
- Thomas, K.R., and M.R. Capecchi. 1987. Site-directed mutagenesis by gene targeting in mouse embryo-derived stem cells. *Cell.* 51:503-12.
- Vestweber, D., and R. Kemler. 1985. Identification of a putative cell adhesion domain of uvomorulin. *Embo J.* 4:3393-8.
- Vinot, S., T. Le, S. Ohno, T. Pawson, B. Maro, and S. Louvet-Vallee. 2005. Asymmetric distribution of PAR proteins in the mouse embryo begins at the 8-cell stage during compaction. *Dev Biol.* 282:307-19.
- Wang, H., T. Ding, N. Brown, Y. Yamamoto, L.S. Prince, J. Reese, and B.C. Paria. 2008. Zonula occludens-1 (ZO-1) is involved in morula to blastocyst transformation in the mouse. *Dev Biol.* 318:112-25.
- Yagi, R., M.J. Kohn, I. Karavanova, K.J. Kaneko, D. Vullhorst, M.L. DePamphilis, and A. Buonanno. 2007. Transcription factor TEAD4 specifies the trophoblast lineage at the beginning of mammalian development. *Development.* 134:3827-36.
- Yamanaka, Y., F. Lanner, and J. Rossant. 2010. FGF signal-dependent segregation of primitive endoderm and epiblast in the mouse blastocyst. *Development.* 137:715-24.
- Yamanaka, Y., A. Ralston, R.O. Stephenson, and J. Rossant. 2006. Cell and molecular regulation of the mouse blastocyst. *Dev Dyn.* 235:2301-14.
- Yuan, H., N. Corbi, C. Basilico, and L. Dailey. 1995. Developmental-specific activity of the FGF-4 enhancer requires the synergistic action of Sox2 and Oct-3. *Genes Dev.* 9:2635-45.
- Zernicka-Goetz, M. 2002. Patterning of the embryo: the first spatial decisions in the life of a mouse. *Development.* 129:815-29.

# Research Aims

---



## Research Aims

The human p120ctn gene (*CTNND1*) was cloned in our laboratory more than a decade ago, and revealed that multiple human p120ctn isoforms could be generated as a result of alternative splicing. Forty-eight putative p120ctn isoforms can be generated by employing four different translation initiation sites (M1-4) combined with four alternatively spliced exons (A to D). Different p120ctn isoforms exert tissue-specific and cell-specific expression patterns and p120ctn isoforms can have opposing effects on tumor growth, RhoGTPase activity and invasiveness *in vitro*. However, the significance of all these p120ctn isoforms *in vivo* remains unknown. Several tissue-specific p120ctn knockout mice have been reported, but in these studies all p120ctn isoforms are removed. To gain functional data on p120ctn isoforms *in vivo*, a panel of p120ctn isoform-specific knock-out and knock-in mice were generated in our laboratory.

The aim of this project was to generate and analyze mice harboring a constitutive knockout allele or a constitutive knockin allele of the alternatively spliced exon C of p120ctn. These mice are referred to as p120ctn knockout of exon C (p120ctn KOC) or p120ctn knockin of exon C (p120ctn KIC) mice. The alternatively spliced exon C of p120ctn encodes only six amino acid residues, which interrupt a nuclear localization signal and a RhoA binding domain. Because of its interesting location, expression of exon C-encoded amino acids might have functional consequences, making the evolutionarily conserved exon C of p120ctn an interesting research target. The inclusion of exon C-encoded amino acids interferes with nuclear translocation and 'dendritic branching' *in vitro*. Three lines of research were pursued to analyze these p120ctn KOC and KIC mice.

First, I wanted to determine the phenotype of p120ctn KOC and KIC mice. Surprisingly, homozygous p120ctn KOC and homozygous KIC embryos died during preimplantation, while completely p120ctn-deficient (p120ctn<sup>-/-</sup>) embryos formed normal blastocysts. To further elaborate on this discrepancy I generated p120ctn<sup>KOC/-</sup> and p120ctn<sup>KIC/-</sup> mice. In addition, I also aimed at analyzing *in vitro* preimplantation development of these embryos *via* time lapse monitoring.

Second, I intended to derive embryonic stem (ES) cells from homozygous p120ctn KOC and homozygous p120ctn KIC embryos. To do so, I generated a highly efficient pluripotin-based ES cell derivation protocol.

Third, I wanted to obtain functional information of p120ctn KOC and KIC mice beyond the developmental stage. This was achieved by combining the p120ctn KOC or KIC allele with a liver- or brain-specific p120ctn null allele, resulting in mice with liver or brains that express only p120ctn transcripts with (KIC) or without (KOC) exon C. I aimed at analyzing these transgenic brains in detail *via* histological and MRI analysis, and to study neuronal morphogenesis in hippocampal cultures that were derived from these brains.

# **Results and Discussion**

---

## Chapter 3

---

EXPRESSION OF p120CTN DURING EARLY MOUSE  
DEVELOPMENT

## **p120ctn expression in early mouse development**

## Expression of p120ctn during early mouse development

Tim Pieters<sup>1,2</sup>, Marc P. Stemmler<sup>3</sup>, Frans van Roy<sup>1,2</sup>, Jolanda van Hengel<sup>1,2,4</sup>

<sup>1</sup> Department for Molecular Biomedical Research, Technologiepark 927, VIB, B-9052 Ghent, Belgium

<sup>2</sup> Department of Biomedical Molecular Biology, Ghent University, Technologiepark 927, B-9052 Ghent, Belgium

<sup>3</sup> Department of Molecular Embryology, Max-Planck Institute of Immunobiology, Stuebeweg 51, 79108 Freiburg, Germany

<sup>4</sup> corresponding author: Jolanda.vanhengel@dmbr.VIB-UGent.be or Frans.Vanroy@dmbr.VIB-UGent.be

### TABLE OF CONTENTS

ABSTRACT .....	108
INTRODUCTION.....	109
MATERIAL AND METHODS .....	110
Immunofluorescence .....	110
Confocal microscopy.....	110
Histology and immunohistochemistry .....	110
RT-PCR.....	111
Western blot analysis .....	111
RESULTS.....	112
p120ctn expression in wild-type preimplantation embryos .....	112
p120ctn expression in gastrulating embryos .....	115
Cadherin expression in gastrulating embryos .....	117
DISCUSSION .....	121
ACKNOWLEDGEMENTS .....	124
REFERENCES.....	124

### ABSTRACT

p120 catenin (p120ctn) is a versatile member of the armadillo family, and has different functions in different subcellular compartments. Cytoplasmatic p120ctn regulates the activity of RhoGPTases, nuclear p120ctn inhibits Kaiso-mediated transcriptional repression, while membrane-localized p120ctn binds and stabilizes E-cadherin on the cell surface and supports cadherin-mediated adhesion. In addition, the cadherin-catenin complex consists of  $\beta$ -catenin, which binds to a second domain in the cytoplasmic tail of E-cadherin, and  $\alpha$ E-catenin, which can interact with both  $\beta$ -catenin and the actin cytoskeleton. Genetic depletion studies have shown that E-cadherin and  $\alpha$ E-catenin are essential for proper preimplantation development and stem cell formation. We analysed the expression of p120ctn during preimplantation development and gastrulation via RT-PCR, immunoblotting and immunostainings. p120ctn was ubiquitously expressed throughout the first half of mouse development and colocalized with other members of the cadherin-catenin complex. Although cadherin expression becomes restricted to specific germ layers (e.g. E- to N-cadherin switching in mesoderm), the expression pattern of p120ctn remains ubiquitous in all germ layers. Multiple p120ctn isoforms are generated as a result of alternative splicing, but gastrulas mainly expressed p120ctn isoform 3, which is abundant in epithelial tissues and cell lines.

## INTRODUCTION

p120ctn is a versatile Armadillo protein and is a part of adherens junctions. Adherens junctions consist of cadherin-catenin complexes in which single-span transmembrane cadherin molecules mediate calcium-dependent homophilic interactions via their extracellular domains. Mammalian genomes contain over 100 genes belonging to the cadherin superfamily (Hulpiau and van Roy, 2009). E-cadherin is the prototypic member of the classic cadherin family. This family is characterized by the presence of five tandem extracellular cadherin repeats (EC1-5) which allow calcium-dependent homophilic adhesion (van Roy and Berx, 2008). The cytoplasmic domain of E-cadherin serves as a scaffold for catenins that link cadherin-mediated cell adhesion to the actin cytoskeleton, either directly or indirectly (Meng and Takeichi, 2009). Two conserved catenin-binding domains are present, a membrane proximal domain or juxtamembrane domain (JMD) for binding p120catenin (p120ctn) and a  $\beta$ -catenin binding domain (CBD). Beta-catenin binds to alpha-catenin, which can link to the actin cytoskeleton via an adaptor (e.g. Eplin) (Abe and Takeichi, 2008) or as an unbound dimeric complex (Drees et al., 2005; Yamada et al., 2005). p120ctn binds to cadherins and regulates their turnover (Reynolds and Roczniak-Ferguson, 2004; Xiao et al., 2007). In addition, p120ctn modulates RhoGTPase activity (Anastasiadis, 2007) and regulates gene transcription by binding to Kaiso, and preventing its transcriptional repression (Daniel, 2007; van Roy and McCrea, 2005).

E-cadherin,  $\beta$ -catenin and  $\alpha$ E-catenin are expressed during mouse embryonic development (Haegel et al., 1995; Larue et al., 1994; Torres et al., 1997). E-cadherin (also called uvomorulin) on the cell surface of loosely attached blastomeres is involved in their transformation into a compacted morula (Hyafil et al., 1981; Johnson et al., 1986; Vestweber and Kemler, 1985). The cadherin-catenin complex is important during early mouse development because embryos with ablated E-cadherin or  $\alpha$ E-catenin do not form proper blastocysts and fail to form trophectoderm (Larue et al., 1994; Torres et al., 1997). However,  $\beta$ -catenin does not seem to be essential for preimplantation development, probably due to compensation by plakoglobin (Haegel et al., 1995). In addition, cadherins and catenins are indispensable for the formation of normal ES cell colonies, as depleting E-cadherin,  $\alpha$ E-catenin or  $\beta$ -catenin results in dispersed ES cell colonies with loosely adherent cells (Haegel et al., 1995; Larue et al., 1996; Larue et al., 1994; Torres et al., 1997). The role of p120ctn in ES cell derivation and preimplantation development has not yet to been investigated.



## **p120ctn expression in early mouse development**

We examined the expression of p120ctn during preimplantation development and gastrulation.

## **MATERIAL AND METHODS**

### **Immunofluorescence**

The staining procedure for preimplantation embryos is carried out in 24-well plates at room temperature according to a published procedure (Kan et al., 2007). In brief, embryos were washed twice in phosphate buffered saline (PBS) containing 0.05% Tween 20 (PBT) and fixed for 10 min in 2% paraformaldehyde (PFA). After permeabilization for 10 min with 0.25% Triton X-100 in PBS and two washes in PBT, embryos were blocked for 30 min with 1% goat serum in PBT (GS-PBT) and then incubated for 1 h with primary antibodies. After three washes with GS-PBT, embryos were incubated for 30 min with secondary antibodies, washed. One-microliter drops of PBS, each containing an embryo, were placed on a glass-bottom dish (WillCo Wells) and covered with mineral oil before examination by confocal microscopy (see below). The following antibodies were used: mouse monoclonal anti-p120ctn (pp120, 1/500, BD Transduction Laboratories), polyclonal rabbit anti-p120ctn isoform C (pAbexC, 1/50, see below), polyclonal rabbit anti- $\beta$ -catenin (1/2000, Sigma), polyclonal rabbit anti- $\alpha$ -catenin (1/1000, Sigma), mouse monoclonal anti-E-cadherin (1/300, BD Transduction Laboratories), rat monoclonal anti-E-cadherin (DECMA-1, 1/100, Sigma), mouse monoclonal anti-Oct-4 (1/100, Santa Cruz Biotechnology), mouse monoclonal anti-Cdx2 (1/100, Biogenex). Secondary species-specific Alexa-fluorochrome-conjugated antibodies were used at a dilution of 1/500 (Molecular Probes).

### **Confocal microscopy**

Confocal microscopy was performed using a Leica TCS SP5 confocal scan head attached to a Leica DM IRE2 inverted microscope and a PC running Leica AF software version 2.5. Optical sections were taken every 2  $\mu$ m. Three-dimensional reconstructions of Z-stacks were made using Volocity software (Perkin Elmer).

### **Histology and immunohistochemistry**

Decidua containing gastrulating embryos were fixed overnight in 4% paraformaldehyde in phosphate-buffered saline (PBS), embedded in paraffin wax, and

sectioned at 6 to 8  $\mu\text{m}$ . Sections were deparaffinated using HistoClearII (National Diagnostics). For histology, tissue sections were rehydrated and stained with hematoxylin and eosin. For immunohistochemistry, tissue sections were rehydrated and pretreated with 0.3%  $\text{H}_2\text{O}_2$  in methanol for 45 min. The sections were then transferred to 10 mM citrate buffer (pH 6.0) and the antigen was exposed in a Retriever (PickCell Laboratories, Amsterdam, The Netherlands). The sections were covered with blocking buffer (10% goat serum, 1% BSA in PBS) for 20 min and then incubated with appropriate antibodies (diluted in 1% BSA in PBS) overnight at 4°C. Staining was completed with a biotinylated secondary antibody (Dako, Glostrup, Denmark), avidin-peroxidase (Dako) and 3,3'-diamino-benzidine (Biogenex, San Roman, CA). The following antibodies were used: mouse monoclonal anti-p120ctn (pp120, 1/500, BD Transduction Laboratories), mouse monoclonal anti-E-cadherin (1/500, BD Transduction Laboratories), mouse monoclonal anti-N-cadherin (1/600, Zymed, San Fransisco, CA), rat monoclonal anti-Ki67 (1/30, Dako).

### RT-PCR

RNA was isolated from individual or pooled embryos using the PicoPure RNA Isolation Kit (Arcturus, cat no. KIT0204). cDNA was produced with Superscript III reverse transcriptase according to the manufacturer's instructions (Invitrogen). Specific transcripts were detected with primers for p120ctn, p120ctn exon C, Oct-4 or mGAPDH (Table 1).

**Table 1. Primers for RT-PCR**

allele	primers for RT-PCR	size (bp)
p120ctn	forward 5'-CCACAGGCAGAGCGTTACCAG-3', reverse 5'-AGCAGGACTAGTTCCTTTTAG-3	177
Oct-4	forward 5'-GTTGGAGAAGGTGGAACCAA-3', reverse 5'-CTCCTTCTGCAGGGCTTTC-3	350
GAPDH	forward 5'-ACCACAGTCCATGCCATCAC-3', reverse 5'-TCCACCACCCTGTTGCTGTA-3	470

### Western blot analysis

Individual embryos were washed in PBS, frozen in a minimal amount of PBS, thawed, supplemented with 10  $\mu\text{l}$  Laemmli buffer (Laemmli, 1970), mixed by pipetting, and boiled for 5 min. Proteins were separated by SDS-PAGE on a 8% polyacrylamide gel, electroblotted onto polyvinylidene fluoride (PVDF) membranes (Millipore), and incubated with antibodies. NBT/BCIP was used for detection (Zymed Laboratories).

## RESULTS

### p120ctn expression in wild-type preimplantation embryos

Weak expression of p120ctn transcripts has been reported in mouse preimplantation embryos (Na et al., 2006), but no data exist on the p120ctn protein level. We also performed reverse transcriptase polymerase chain reaction (RT-PCR) analysis on single and pooled morulas and blastocyst. In agreement with previously published data, only faint p120ctn expression was observed in single preimplantation embryos (Fig. 1) (Na et al., 2006). However, expression of p120ctn transcripts could be readily detected in pooled morulas and in pooled blastocyst.

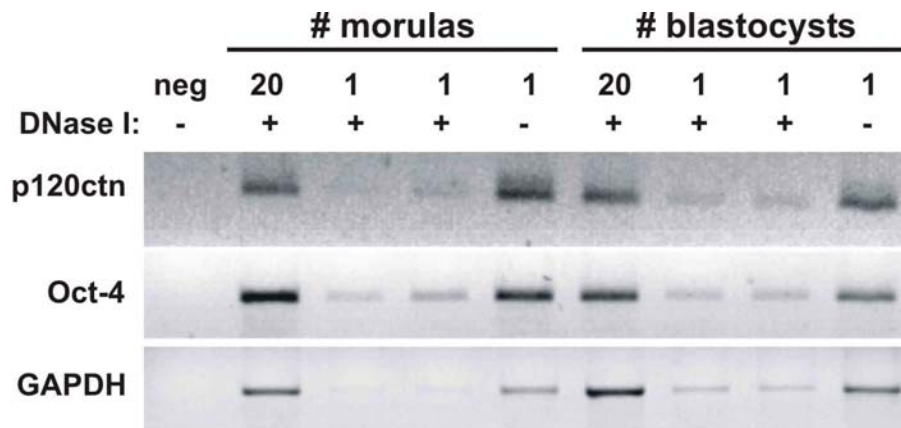


**Figure 1. Expression of p120ctn transcripts in wild-type preimplantation embryos.** RT-PCR to detect all p120ctn transcripts and Oct-4-specific transcripts present in single and pooled wild-type mouse morulas and blastocysts. GAPDH was used as a loading control. RNA was treated with DNase I or not.

To investigate the expression of p120ctn protein in mouse preimplantation embryos, we performed double immunolabeling for p120ctn and other members of the cadherin-catenin complex on wild-type mouse embryos ranging from the two-cell stage to blastocysts (Fig. 2). Several members of the cadherin-catenin complex, such as E-cadherin and  $\alpha$ E-catenin, are indispensable during blastocyst formation and the establishment of the trophectoderm lineage (Larue et al., 1994; Torres et al., 1997). p120ctn is localized at the cell surface of blastomeres of two- to eight-cell embryos, where it co-localizes with  $\beta$ -catenin, especially at cell-cell contacts (Fig. 2A). In compacted morulas and blastocysts, p120ctn is seen at the cell-cell contacts together with  $\beta$ -catenin (Fig. 2A).

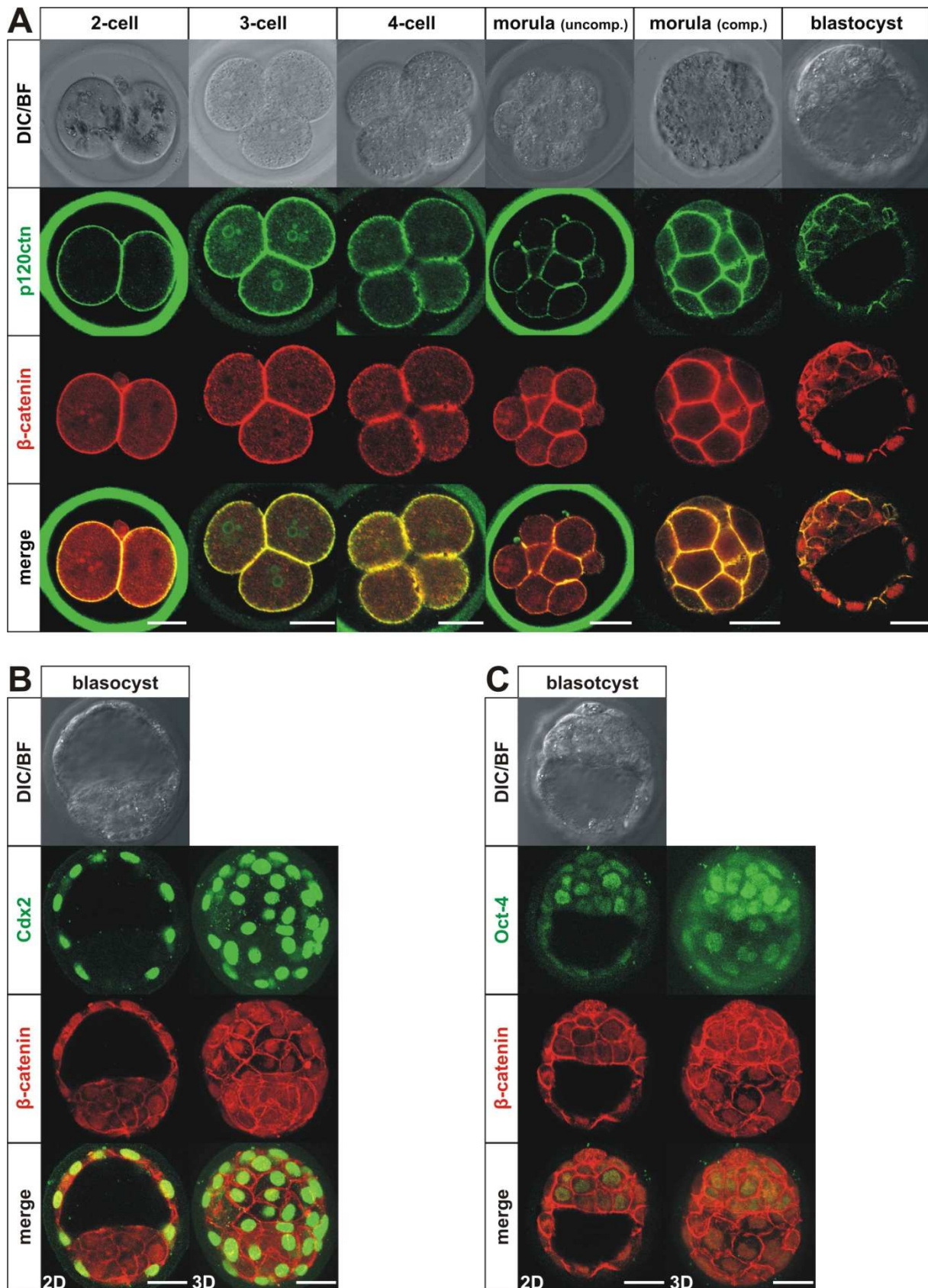


**Figure 2. Expression of p120ctn and  $\beta$ -catenin in wild-type preimplantation embryos.** Transmitted light micrographs, either differential interference contrast (DIC) or bright field (BF), and immunofluorescence of wild-type embryos from two-cell stage to blastocysts.

## p120ctn expression in early mouse development

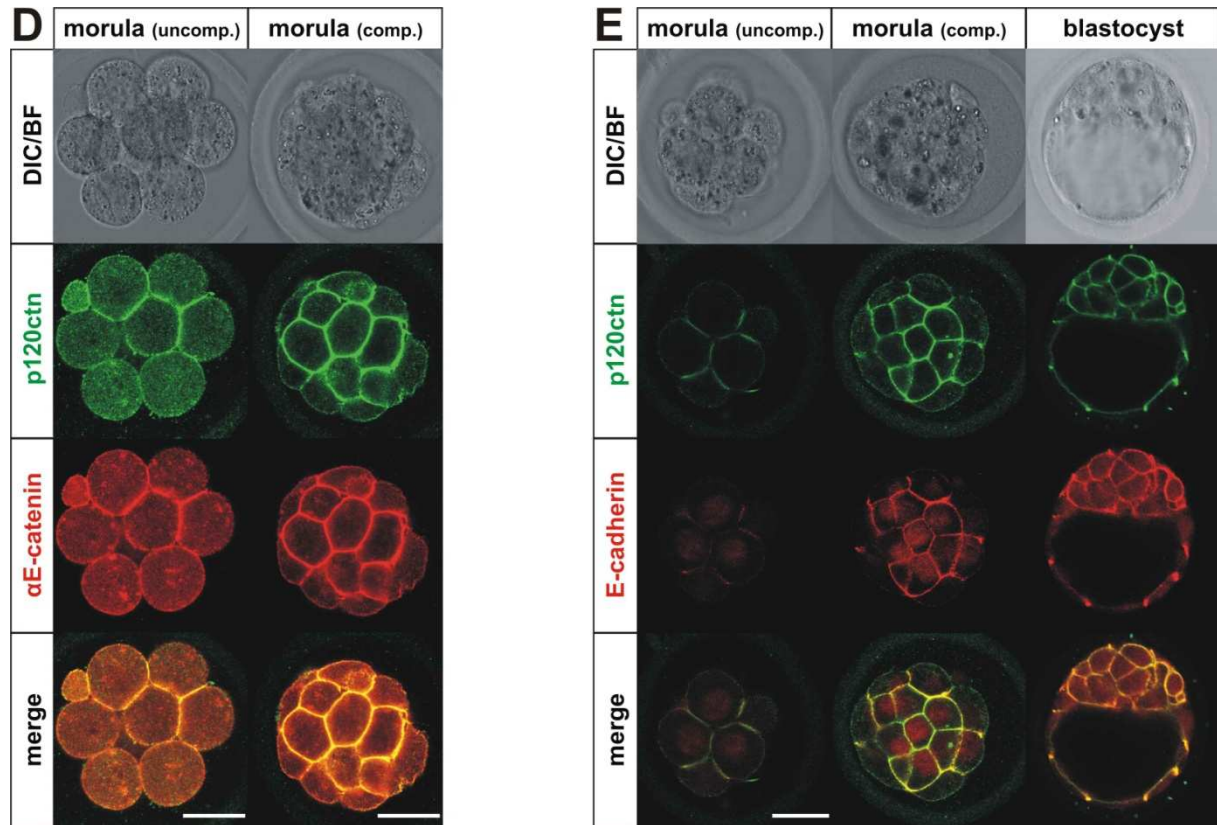


**Figure 2 (continued).** (A) Double immunofluorescence for p120ctn and  $\beta$ -catenin. p120ctn co-localizes with  $\beta$ -catenin at the cell surface of blastomeres (two- to eight-cell stage), morulas and blastocysts. Non-specific staining was observed in the zona pellucida. In blastocysts p120ctn protein is expressed exclusively at the plasma membrane, whereas  $\beta$ -catenin also shows nuclear staining, predominantly in the trophectoderm. (B,C) Marker analysis reveals that nuclear  $\beta$ -catenin is predominantly expressed in the trophectoderm of wild-type blastocysts. (B) A trophectoderm-specific marker (Cdx2) colocalizes with strong nuclear  $\beta$ -catenin staining in the trophectoderm. (C) An inner cell mass (ICM)-specific marker (Oct-4) shows only little colocalization with the weak nuclear  $\beta$ -catenin staining in the ICM. (D) Double immunofluorescence for p120ctn and  $\alpha$ E-catenin. p120ctn co-localizes with  $\alpha$ E-catenin at the cell surface of uncompact and compacted morulas and blastocysts. (E) Double immunofluorescence for p120ctn and E-cadherin (DECMA-1 antibody). p120ctn co-localizes with E-cadherin at the cell surface of uncompact and compacted morulas and blastocysts. Single confocal sections (2D) and three-dimensional (3D) reconstructions of wild-type blastocysts are shown. Scale bar: 25  $\mu$ m.

However, in blastocysts,  $\beta$ -catenin is expressed not only at the cell surface but also in the nucleus (Fig. 2A, blastocyst), which is indicative of active Wnt signaling. By using lineage-specific markers, we showed that  $\beta$ -catenin is expressed predominantly in the nuclei of trophectodermal cells (Figs. 2B,C). These data indicate that  $\beta$ -catenin mediated Wnt signaling is inactive until the blastocyst stage, which is in line with previously published results (Na et al., 2006). p120ctn also co-localizes with  $\alpha$ E-catenin (Figs. 2D) and E-cadherin



(Fig. 2E) at the cell-cell junctions in uncompacted and compacted morulas and blastocysts. In conclusion, p120ctn is expressed throughout preimplantation development and is enriched at cell-cell contacts, where it co-localizes with other members of the cadherin-catenin complex.

p120ctn binds to the transcription factor Kaiso and is able to block its transcriptional repression (Daniel and Reynolds, 1999; Spring et al., 2005). There exists considerable interplay between the p120ctn/Kaiso pathway and the  $\beta$ -catenin/TCF pathway (Park et al., 2005; Spring et al., 2005). We wanted to know whether the p120ctn/Kaiso pathway is functional in mouse preimplantation embryos, like it is the case in *Xenopus* embryos (Kim et al., 2004; Park et al., 2005). In blastocysts, Kaiso was only expressed in a limited number of cells and no Kaiso expression was observed in ES cells (data not shown).

In addition, p120ctn also binds to RhoA (Magie et al., 2002; Yanagisawa et al., 2008), and inhibits its activity (Anastasiadis et al., 2000; Noren et al., 2000). p120ctn colocalized with RhoA both in preimplantation embryos and in ES cells (data not shown).

### **p120ctn expression in gastrulating embryos**

To evaluate the expression of p120ctn during gastrulation, sagittal paraffin sections of embryos were selected at the beginning (Fig. 3A), the middle (Fig. 3B) and near the end (Fig. 3C) of gastrulation. In pre-streak stage embryos, p120ctn is expressed at cell-cell contacts of both embryonic tissue (epiblast) and extraembryonic tissues, such as the extraembryonic ectoderm, the ectoplacental cone and the visceral endoderm (Fig. 3A).

In late streak embryos, p120ctn is ubiquitously expressed at the cell membrane of the three germ layers, namely embryonic ectoderm, endoderm and mesoderm (Fig. 3B). p120ctn is also expressed in the primitive streak region, where cells disseminate from the ectoderm layer and make up mesoderm and endoderm layers. In addition, membrane staining for p120ctn is evident in the visceral endoderm, the ectoplacental cone and the posterior amniotic fold (Fig. 3B).

Near the end of gastrulation, in late headfold stage embryos, p120ctn is expressed in all embryonic tissues, including newly emerging neuroectoderm, head mesenchyme, gut endoderm and the primitive heart tube (Fig. 3C). p120ctn is predominantly localized at the cell surface in most embryonic tissues, except for the head mesenchyme, which shows cytoplasmic p120ctn localization, and its intensity varies substantially among different head mesenchyme cells. p120ctn is also ubiquitously expressed in extraembryonic tissues, such as allantoic, amniotic and chorionic mesoderm, the amniotic ectoderm, and the ectoplacental

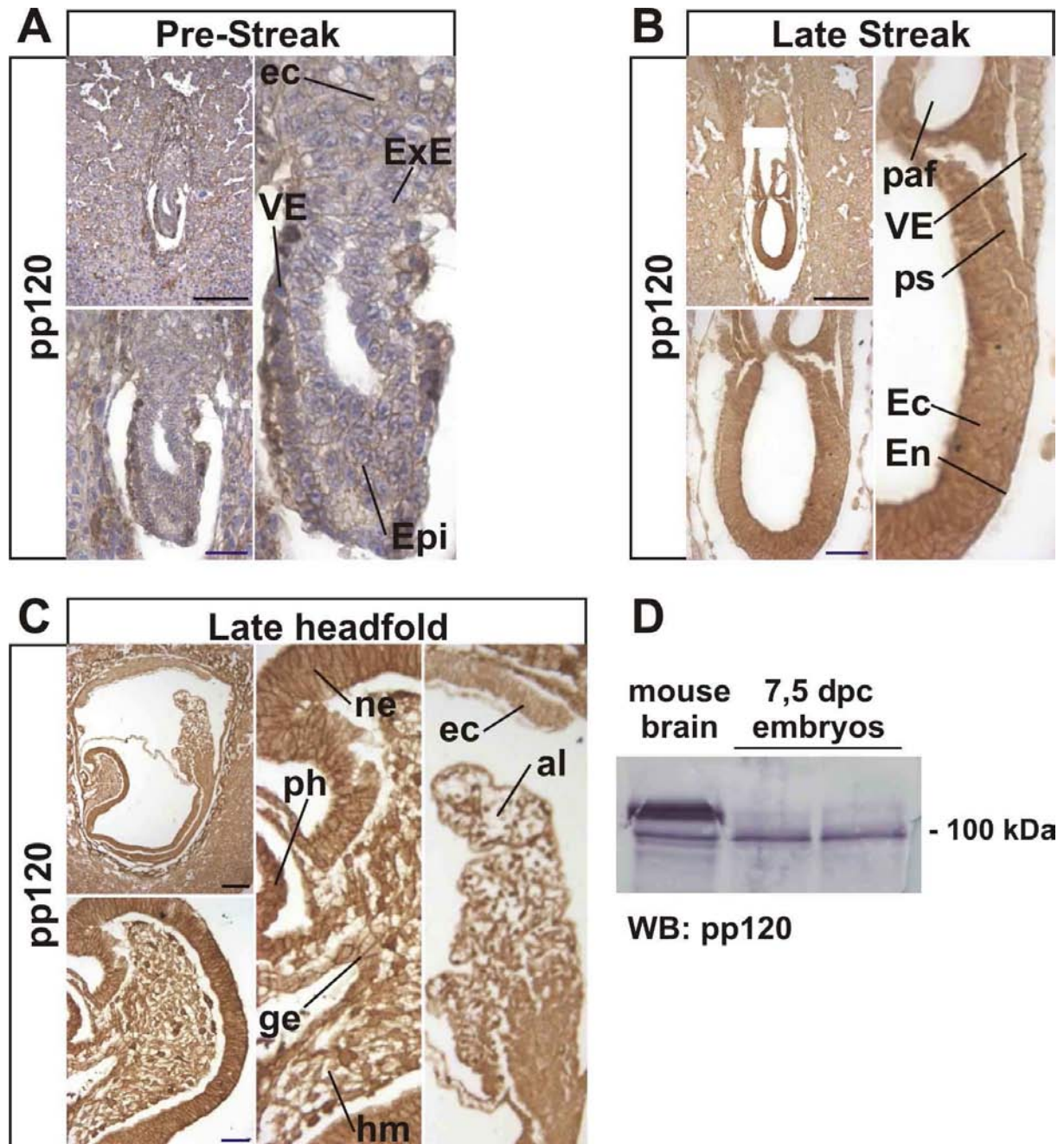


**Figure 3. p120ctn expression in gastrulating embryos.** Immunohistochemical analysis of p120ctn in sagittal paraffin sections of embryos at the stages of pre-streak (A), late streak (B) and late headfold (C). p120ctn is ubiquitously expressed in both embryonic and extraembryonic tissue. (D) Western blot analysis of two wild-type gastrulating embryos (7.5 dpc) in which all p120ctn isoforms were detected with pp120-antibody and p120ctn isoform C was detected with pAbexC. Mouse brain was taken as a positive control because it is rich in isoform C of p120ctn. ae: amniotic ectoderm, al: allantois, am: amniotic mesoderm, ec: ectoplacental cone, Ec: ectoderm, En: endoderm, Epi: epiblast, ExE: extraembryonic ectoderm, ge: gut endoderm, hm: head mesenchyme, Me: mesoderm, ne: neural ectoderm, paf: posterior amniotic fold, ph: primitive heart tube, ps: primitive streak, VE: visceral endoderm. Black scale bar: 200  $\mu$ m, purple scale bar: 50  $\mu$ m.

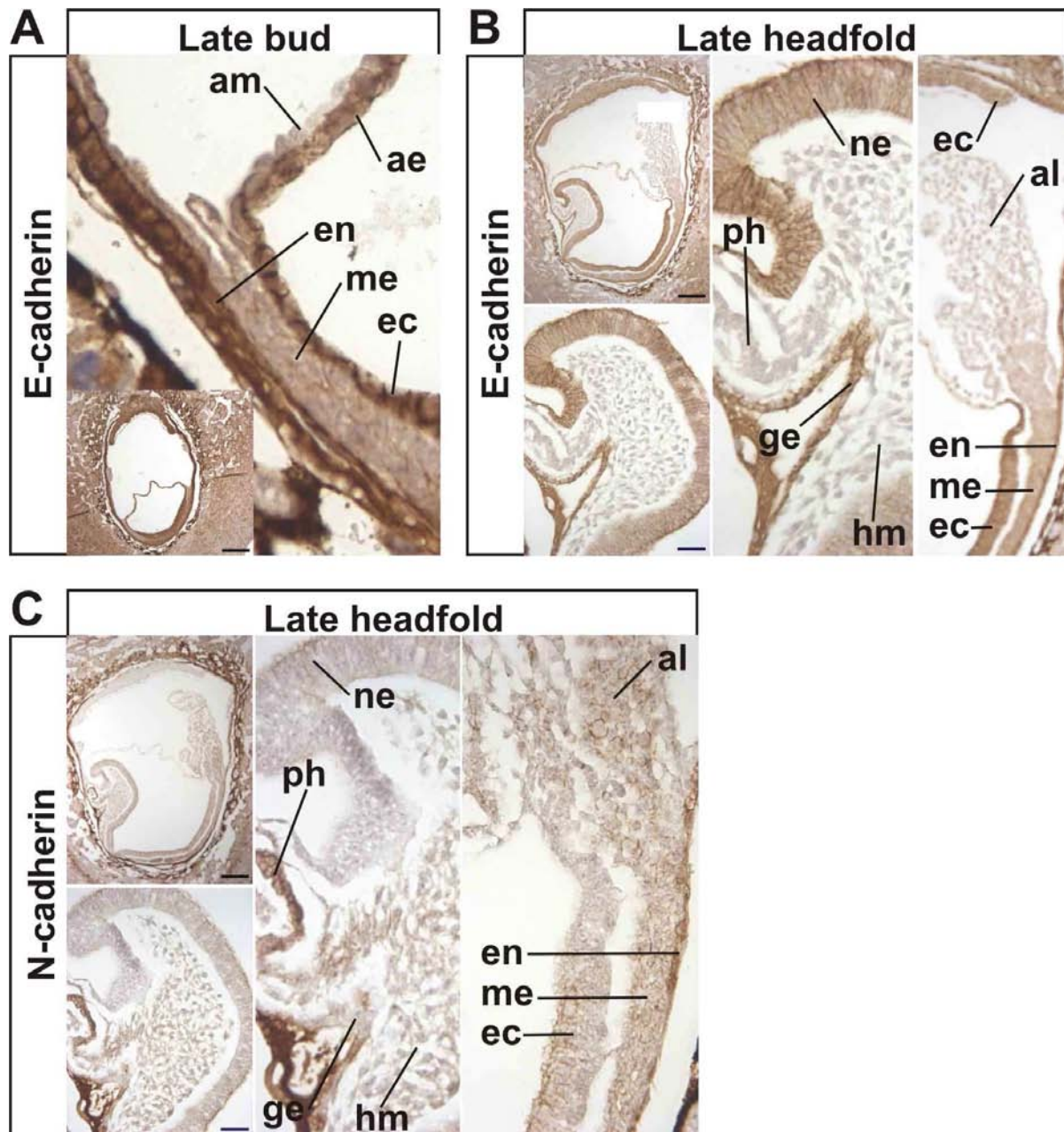
cone (Fig. 3C). To conclude, p120ctn is expressed throughout gastrulation in both embryonic and extraembryonic tissues.

Multiple p120ctn isoforms have been identified. These isoforms result from alternative splicing, which allows the translation of p120ctn isoforms from four start codons and enables the inclusion of four alternatively used exons (Keirsebilck et al., 1998). Alternative start codons usage allows the generation of p120ctn isoforms, differing from each other by the extension of their N-termini. Long p120ctn isoforms (p120ctn isoform 1, 120 kDa) contain the full-length N-terminus, whereas short p120ctn isoforms (p120ctn isoform 3, 100 kDa) have a truncated N-terminus and lack 100 AA. We wanted to determine which p120ctn isoforms are expressed during gastrulation. To do so, protein lysates from 7,5 dpc embryos were immunoblotted with pp120, an monoclonal antibody that detects all p120ctn isoforms. In contrast to mouse brain, which mainly expressed p120ctn isoform 1, gastrulas expressed predominantly p120ctn isoform 3 (Fig. 3D).

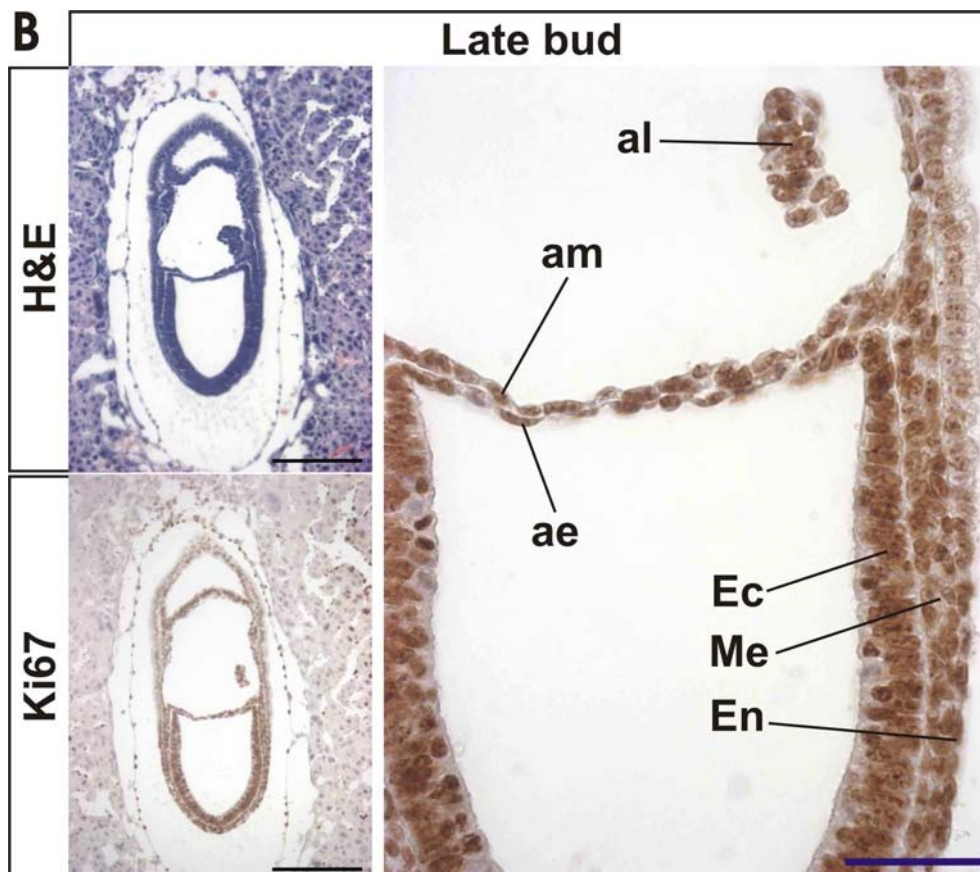
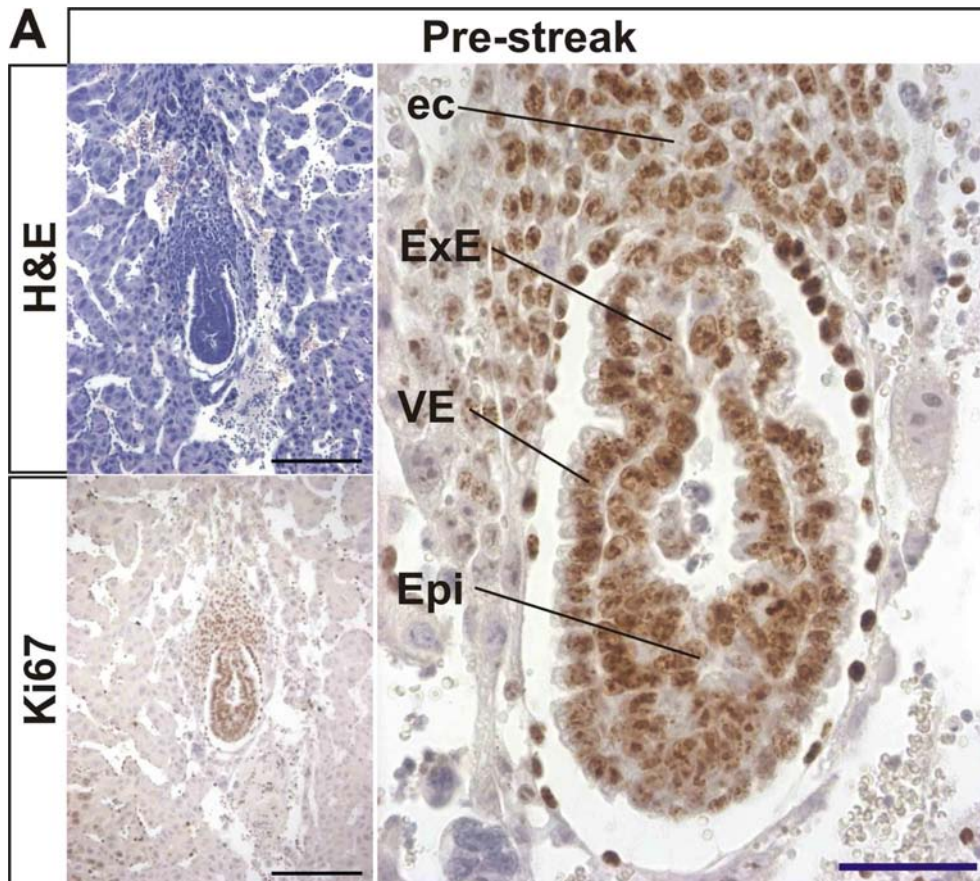
### **Cadherin expression in gastrulating embryos**

p120ctn binds and stabilize cadherins both *in vitro* and *in vivo* (Reynolds and Carnahan, 2004; Xiao et al., 2007). Therefore, we were interested in the localization of E- and N-cadherin in gastrulating embryos. In late streak embryos, E-cadherin is expressed at the cell surface of embryonic ectoderm and endoderm, but it is downregulated in embryonic mesoderm and amniotic mesoderm (Fig. 4A). These data are consistent with previously published results (Shibata et al., 2004). Shibata and colleagues (2004) found that next to E-cadherin, also  $\beta$ -catenin is decreased in mesoderm. Remarkably, ingressing mesoderm cells with reduced E-cadherin and  $\beta$ -catenin levels displayed occasionally cytoplasmic staining for p120ctn (Shibata et al., 2004). In the late headfold gastrula, E-cadherin is expressed in the neural ectoderm and primitive gut epithelium but is absent in the primitive heart, head mesenchyme and allantoic mesoderm (Fig. 4B). E-cadherin and N-cadherin displayed a reciprocal expression pattern in late headfold embryos. N-cadherin is absent in neural ectoderm and primitive gut endoderm but showed a discrete membrane localization in head mesenchyme and allantoic mesoderm, and the primitive heart shows strong cell surface staining (Fig. 4C). This is in line with reports on persistence of N-cadherin expression in precardiac (splanchnic) mesoderm during early heart development and its downregulation in somatic mesoderm (Linask, 1992).

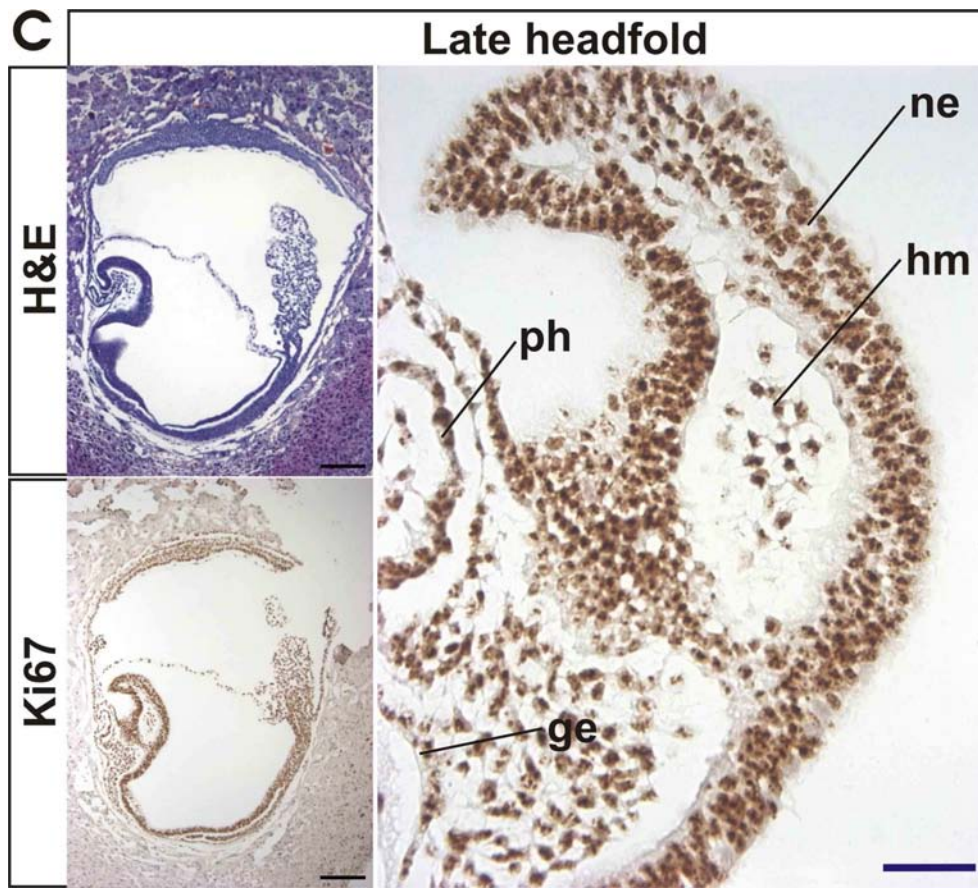




**Figure 4. Cadherin expression in gastrulating embryos.** Immunohistochemical analysis of E-cadherin in sagittal paraffin sections of late bud (A) and late headfold (B) embryos. E-cadherin is expressed in embryonic ectoderm and endoderm layers, neural ectoderm and gut epithelium. However, E-cadherin is downregulated in embryonic mesoderm, head mesenchyme, primitive heart and mesoderm from amnion and allantois. Immunohistochemical examination of N-cadherin in sagittal paraffin sections of late headfold stage embryos (C). N-cadherin is absent in gut endoderm and is expressed at low levels in embryonic ectoderm and mesoderm and in neural ectoderm. N-cadherin is expressed moderately in allantoic mesoderm and head mesenchyme and is strongly expressed in embryonic endoderm and in the primitive heart. ae: amniotic ectoderm, al: allantois, am: amniotic mesoderm, ec: ectoplacental cone, ecc, ectoplacental cavity, Ec: ectoderm, En: endoderm, ge: gut endoderm, hm: head mesenchyme, Me: mesoderm, ne: neural ectoderm, ph: primitive heart tube, ps: primitive streak.







**Supplementary Figure 1. Mouse embryos exhibit rapid cell proliferation during gastrulation.** Pre-streak stage (A), late bud stage (B) and late headfold stage (C) embryos containing a large proportion of dividing cells in both embryonic and extraembryonic regions, as evidenced by Ki67 immunohistochemistry. ae: amniotic ectoderm, al: allantois, am: amniotic mesoderm, ec: ectoplacental cone, Ec: ectoderm, En: endoderm, Epi: epiblast, ExE: extraembryonic ectoderm, ge: gut endoderm, H&E: hematoxylin and eosin, hm: head mesenchyme, Me: mesoderm, ne: neural ectoderm, ph: primitive heart tube, VE: visceral endoderm. Black scale bar: 200  $\mu$ m, purple scale bar: 50  $\mu$ m.

N-cadherin expression is also found in mouse precardiac mesoderm, and N-cadherin-deficient embryos exhibit aberrant heart morphogenesis (Radice et al., 1997). During gastrulation all three germ layers, but particularly the primitive ectoderm divide extremely fast (Hogan et al., 1994). This was evident when sections of gastrulating embryos were stained with a marker for proliferation, Ki67 (Fig. S1).

## DISCUSSION

The cadherin-catenin complex plays an important role in development by maintaining tissue integrity via adhesion and by conveying proper signals to various developmental pathways (Lien et al., 2006). All members of the classic cadherin-catenin complex have been found at the membrane of oocytes and early preimplantation embryos (Haegel et al., 1995; Larue et al., 1994; Torres et al., 1997). We report on the presence of p120ctn on the membrane of embryos from the two-cell stage until the blastocyst stage. p120ctn was localized at the free edges of uncompact blastomeres and p120ctn was progressively enriched at cell-cell borders from morula on, and especially in compacted morulas. Furthermore, in each of these early embryonic stages p120ctn colocalizes with E-cadherin and  $\alpha$ - and  $\beta$ -catenin. This implies that fully functional cadherin-based cell-cell junctions can be made during preimplantation development. In these early developmental stages, p120ctn seems to be expressed predominantly at the membrane, which supports the notion that p120ctn in the cadherin-catenin complex participates in adhesion. Other p120ctn functions, such as regulation of the activity of RhoGTPases in the cytoplasm or inhibition of Kaiso-mediated transcriptional repression in the nuclei, are less likely.

The presence of RhoGTPases and their correct spatiotemporal activation is essential in preimplantation development (Heasman and Ridley, 2008; Wang and Zheng, 2007). Conventional gene targeting of the classic RhoGTPase family members RhoA, Rac1 and Cdc42 causes early death in mouse embryos (Chen et al., 2000; Sugihara et al., 1998), whereas knockout mice for other RhoGTPase family members do not show major developmental abnormalities (Wang and Zheng, 2007). Also, injection of a siRNA against Cdc42 in mouse oocytes, did not affect the cleavage stage development, but decreased the formation of blastocysts (Cui et al., 2007). Overexpression of a constitutive active RhoA mutant in four-cell embryos results in reduced blastomere adhesion, whereas inhibition of RhoA mediated by C3-transferase results in decompaction (Clayton et al., 1999). In addition, culturing cleavage-stage embryos while inhibiting ROCK, a downstream effector of RhoA, affected the cavity formation in blastocysts. Expression of p120ctn inhibits RhoA expression and Rac1 activation (Anastasiadis and Reynolds, 2001), whereas genetic or RNAi-mediated depletion of p120ctn results in increased RhoA activity and decreased Rac1 activity (Elia et al., 2006; Perez-Moreno et al., 2006; Wildenberg et al., 2006; Yanagisawa and Anastasiadis, 2006). It has been shown that ectopic expression of classical cadherins prevents p120ctn-

## p120ctn expression in early mouse development

mediated dendritic-like branching, RhoA inhibition, and Rac1 activation (Anastasiadis et al., 2000; Noren et al., 2000; Soto et al., 2008). This indicates that cadherins can sequester the available p120ctn to cadherin-based junctions and this prevents the modulation of RhoGTPase activity by p120ctn. In addition, E-cadherin depletion in MCF7 cells releases p120ctn from the membrane and this results in increased Rac1 activity (Soto et al., 2008). Strangely, p120ctn knockdown also results in Rac1 activation (Soto et al., 2008). p120ctn depletion also affects E-cadherin levels, but Rac1 activation must occur then via a p120ctn-independent pathway. So, although p120ctn can influence RhoGTPases in early development, this will probably not occur because p120ctn is sequestered to the membrane by E-cadherin.

In contrast to p120ctn,  $\beta$ -catenin is not expressed exclusively at the cell membrane but also in the nuclei of blastocysts, which indicates active Wnt signaling. Secreted Wnt ligands bind to Frizzled and LPR receptors and prevent phosphorylation, ubiquitination and degradation of cytoplasmic  $\beta$ -catenin, which translocates to the nucleus and transactivates Wnt target genes (MacDonald et al., 2009). Wnt signaling is essential in multiple developmental processes, and its derailment has been associated with many diseases, including cancer (Logan and Nusse, 2004; Reya and Clevers, 2005). Active  $\beta$ -catenin can be detected by using antibodies specific for unphosphorylated  $\beta$ -catenin or antibodies that detect nuclear  $\beta$ -catenin. Several studies investigated Wnt activity in mouse preimplantation embryos. Several studies showed Wnt activation only in the late morula and blastocyst stages (Li et al., 2005; Na et al., 2006). Our findings are in line with these observation, as we detected nuclear  $\beta$ -catenin only in blastocysts (Fig. 2). Since Wnt is only activated in late blastocyst, the presence of nuclear  $\beta$ -catenin might depend on the time that blastocysts are collected. Similar to the findings of Xie and colleagues, active  $\beta$ -catenin is mainly located in nuclei of the trophectoderm lineage (Xie et al., 2008).

The p120ctn/Kaiso and the  $\beta$ -catenin/TCF pathways are physically connected via Frodo (Park et al., 2006) and there is significant overlap between the target genes of these pathways (Kim et al., 2004; Park et al., 2005; Spring et al., 2005). Cytoplasmic p120ctn relieves the Kaiso-mediated transcriptional repression of these mutual target genes, and thus results in their activation. But, if cadherins are able to sequester p120ctn away from cytoplasmic or nuclear pools, this would prevent p120ctn to inhibit the transcriptional repression of Kaiso in preimplantation embryos. Currently, it has not been tested whether expression of cadherins could block the ability of p120ctn to relieve the Kaiso-mediated transcriptional repression. Based on current knowledge, expression cadherins would result in repression of  $\beta$ -catenin target genes. This hypothesis requires a functional p120ctn/Kaiso

complex to be present in preimplantation development. We showed that both p120<sup>ctn</sup> and E-cadherin are present during preimplantation development. Kaiso is expressed in oocytes (Soubry et al., 2005) and Kaiso transcripts have been found in cleavage stage embryos and in blastocysts but are downregulated in expanded blastocysts (Na et al., 2007). Downregulation of Kaiso, a repressor of  $\beta$ -catenin target genes, in expanded blastocysts is accompanied with increased expression of Dishevelled, which is important for activation of Wnt signaling (Na et al., 2007). The expression pattern of Kaiso is in line with our observation that  $\beta$ -catenin becomes only activated in late blastocysts.

However, several lines of evidence state that  $\beta$ -catenin and Wnt signalling is not essential in preimplantation development. Both  $\beta$ -catenin null mice and mice expressing a stabilized form of  $\beta$ -catenin (deletion of exon 3; removes serine/threonine residues that are phosphorylated by GSK3 $\beta$ ) exhibit a normal preimplantation development (Haegel et al., 1995; Kemler et al., 2004). In addition, no evidence was found of functional Wnt activity in cleavage-stage embryos using a Wnt-reporter line (Kemler et al., 2004). On the other hand, the presence of nuclear  $\beta$ -catenin might also be dependent on the mouse strain. Clear nuclear  $\beta$ -catenin could be observed reproducibly in blastocysts from wild-type and transgenic mouse strains on the C57BL/6 background, but this was not seen in blastocyst on a mixed background (data not shown). The preimplantation embryos with genetic ablation or activation of  $\beta$ -catenin were on a mixed background, and this might explain why active  $\beta$ -catenin was not seen in these systems. Nevertheless, the fact that nuclear  $\beta$ -catenin is strain-specific, hints that Wnt signalling might not be an essential feature of preimplantation biology. Analysis of blastocysts with genetic ablation or activation of  $\beta$ -catenin, but on the C57BL/6 background may provide clarity in this matter. To conclude, we report the simultaneous detection of both membrane-bound and nuclear pools of  $\beta$ -catenin in blastocysts on the C57BL/6 background.

## ACKNOWLEDGEMENTS

This work was supported by grants from the Queen Elisabeth Medical Foundation (G.S.K.E.), Belgium, and from the Geconcerteerde Onderzoeksacties of Ghent University. Tim Pieters has been supported by the Instituut voor de Aanmoediging van Innovatie door Wetenschap en Technologie in Vlaanderen (IWT). Tim Pieters conducted all experiments and wrote this manuscript. Dr. Marc Stemmler provided excellent training in handling and immunostaining of preimplantation embryos. Prof. Dr. Frans Van Roy and Dr. Jolanda van Hengel were instructive in the experimental design and editing of the manuscript. We acknowledge Dr. Amin Bredan and Dr. Marc Stemmler for critical reading of the manuscript, and the members of our research group for valuable discussions.

## REFERENCES

- Abe, K., and M. Takeichi. 2008. EPLIN mediates linkage of the cadherin catenin complex to F-actin and stabilizes the circumferential actin belt. *Proc Natl Acad Sci U S A*. 105:13-9.
- Anastasiadis, P.Z. 2007. p120-ctn: A nexus for contextual signaling via Rho GTPases. *Biochim Biophys Acta*. 1773:34-46.
- Anastasiadis, P.Z., S.Y. Moon, M.A. Thoreson, D.J. Mariner, H.C. Crawford, Y. Zheng, and A.B. Reynolds. 2000. Inhibition of RhoA by p120 catenin. *Nat Cell Biol*. 2:637-44.
- Anastasiadis, P.Z., and A.B. Reynolds. 2001. Regulation of Rho GTPases by p120-catenin. *Curr Opin Cell Biol*. 13:604-10.
- Chen, F., L. Ma, M.C. Parrini, X. Mao, M. Lopez, C. Wu, P.W. Marks, L. Davidson, D.J. Kwiatkowski, T. Kirchhausen, S.H. Orkin, F.S. Rosen, B.J. Mayer, M.W. Kirschner, and F.W. Alt. 2000. Cdc42 is required for PIP(2)-induced actin polymerization and early development but not for cell viability. *Curr Biol*. 10:758-65.
- Clayton, L., A. Hall, and M.H. Johnson. 1999. A role for Rho-like GTPases in the polarisation of mouse eight-cell blastomeres. *Dev Biol*. 205:322-31.
- Cui, X.S., X.Y. Li, and N.H. Kim. 2007. Cdc42 is implicated in polarity during meiotic resumption and blastocyst formation in the mouse. *Mol Reprod Dev*. 74:785-94.
- Daniel, J.M. 2007. Dancing in and out of the nucleus: p120(ctn) and the transcription factor Kaiso. *Biochim Biophys Acta*. 1773:59-68.
- Daniel, J.M., and A.B. Reynolds. 1999. The catenin p120(ctn) interacts with Kaiso, a novel BTB/POZ domain zinc finger transcription factor. *Mol Cell Biol*. 19:3614-23.
- Drees, F., S. Pokutta, S. Yamada, W.J. Nelson, and W.I. Weis. 2005. Alpha-catenin is a molecular switch that binds E-cadherin-beta-catenin and regulates actin-filament assembly. *Cell*. 123:903-15.
- Elia, L.P., M. Yamamoto, K. Zang, and L.F. Reichardt. 2006. p120 catenin regulates dendritic spine and synapse development through Rho-family GTPases and cadherins. *Neuron*. 51:43-56.

- Haegel, H., L. Larue, M. Ohsugi, L. Fedorov, K. Herrenknecht, and R. Kemler. 1995. Lack of beta-catenin affects mouse development at gastrulation. *Development*. 121:3529-37.
- Heasman, S.J., and A.J. Ridley. 2008. Mammalian Rho GTPases: new insights into their functions from in vivo studies. *Nat Rev Mol Cell Biol*. 9:690-701.
- Hulpiau, P., and F. van Roy. 2009. Molecular evolution of the cadherin superfamily. *Int J Biochem Cell Biol*. 41:349-69.
- Hyafil, F., C. Babinet, and F. Jacob. 1981. Cell-cell interactions in early embryogenesis: a molecular approach to the role of calcium. *Cell*. 26:447-54.
- Johnson, M.H., B. Maro, and M. Takeichi. 1986. The role of cell adhesion in the synchronization and orientation of polarization in 8-cell mouse blastomeres. *J Embryol Exp Morphol*. 93:239-55.
- Kan, N.G., M.P. Stemmler, D. Junghans, B. Kanzler, W.N. de Vries, M. Dominis, and R. Kemler. 2007. Gene replacement reveals a specific role for E-cadherin in the formation of a functional trophectoderm. *Development*. 134:31-41.
- Keirsebilck, A., S. Bonne, K. Staes, J. van Hengel, F. Nollet, A. Reynolds, and F. van Roy. 1998. Molecular cloning of the human p120ctn catenin gene (CTNND1): expression of multiple alternatively spliced isoforms. *Genomics*. 50:129-46.
- Kemler, R., A. Hierholzer, B. Kanzler, S. Kuppig, K. Hansen, M.M. Taketo, W.N. de Vries, B.B. Knowles, and D. Solter. 2004. Stabilization of beta-catenin in the mouse zygote leads to premature epithelial-mesenchymal transition in the epiblast. *Development*. 131:5817-24.
- Kim, S.W., J.I. Park, C.M. Spring, A.K. Sater, H. Ji, A.A. Otchere, J.M. Daniel, and P.D. McCrea. 2004. Non-canonical Wnt signals are modulated by the Kaiso transcriptional repressor and p120-catenin. *Nat Cell Biol*. 6:1212-20.
- Laemmli, U.K. 1970. Cleavage of structural proteins during the assembly of the head of bacteriophage T4. *Nature*. 227:680-5.
- Larue, L., C. Antos, S. Butz, O. Huber, V. Delmas, M. Dominis, and R. Kemler. 1996. A role for cadherins in tissue formation. *Development*. 122:3185-94.
- Larue, L., M. Ohsugi, J. Hirchenhain, and R. Kemler. 1994. E-cadherin null mutant embryos fail to form a trophectoderm epithelium. *Proc Natl Acad Sci U S A*. 91:8263-7.
- Li, J., J.V. Zhang, Y.J. Cao, J.X. Zhou, W.M. Liu, X.J. Fan, and E.K. Duan. 2005. Inhibition of the beta-catenin signaling pathway in blastocyst and uterus during the window of implantation in mice. *Biol Reprod*. 72:700-6.
- Lien, W.H., O. Klezovitch, and V. Vasioukhin. 2006. Cadherin-catenin proteins in vertebrate development. *Curr Opin Cell Biol*. 18:499-506.
- Linask, K.K. 1992. N-cadherin localization in early heart development and polar expression of Na<sup>+</sup>,K<sup>(+)</sup>-ATPase, and integrin during pericardial coelom formation and epithelialization of the differentiating myocardium. *Dev Biol*. 151:213-24.
- Logan, C.Y., and R. Nusse. 2004. The Wnt signaling pathway in development and disease. *Annu Rev Cell Dev Biol*. 20:781-810.
- MacDonald, B.T., K. Tamai, and X. He. 2009. Wnt/beta-catenin signaling: components, mechanisms, and diseases. *Dev Cell*. 17:9-26.
- Magie, C.R., D. Pinto-Santini, and S.M. Parkhurst. 2002. Rho1 interacts with p120ctn and alpha-catenin, and regulates cadherin-based adherens junction components in *Drosophila*. *Development*. 129:3771-82.
- Meng, W., and M. Takeichi. 2009. Adherens junction: molecular architecture and regulation. *Cold Spring Harb Perspect Biol*. 1:a002899.
- Na, J., K. Lykke-Andersen, M.E. Torres Padilla, and M. Zernicka-Goetz. 2006. Dishevelled proteins regulate cell adhesion in mouse blastocyst and serve to monitor changes in Wnt signaling. *Dev Biol*.



## p120ctn expression in early mouse development

- Na, J., K. Lykke-Andersen, M.E. Torres Padilla, and M. Zernicka-Goetz. 2007. Dishevelled proteins regulate cell adhesion in mouse blastocyst and serve to monitor changes in Wnt signaling. *Dev Biol.* 302:40-9.
- Noren, N.K., B.P. Liu, K. Burrige, and B. Kreft. 2000. p120 catenin regulates the actin cytoskeleton via Rho family GTPases. *J Cell Biol.* 150:567-80.
- Park, J.I., H. Ji, S. Jun, D. Gu, H. Hikasa, L. Li, S.Y. Sokol, P.D. McCrea, M. Perez-Moreno, and E. Fuchs. 2006. Frodo Links Dishevelled to the p120-Catenin/Kaiso Pathway: Distinct Catenin Subfamilies Promote Wnt Signals
- Catenins: keeping cells from getting their signals crossed. *Dev Cell.* 11:683-95.
- Park, J.I., S.W. Kim, J.P. Lyons, H. Ji, T.T. Nguyen, K. Cho, M.C. Barton, T. Deroo, K. Vleminckx, R.T. Moon, and P.D. McCrea. 2005. Kaiso/p120-catenin and TCF/beta-catenin complexes coordinately regulate canonical Wnt gene targets. *Dev Cell.* 8:843-54.
- Perez-Moreno, M., M.A. Davis, E. Wong, H.A. Pasolli, A.B. Reynolds, and E. Fuchs. 2006. p120-catenin mediates inflammatory responses in the skin. *Cell.* 124:631-44.
- Reya, T., and H. Clevers. 2005. Wnt signalling in stem cells and cancer. *Nature.* 434:843-50.
- Reynolds, A.B., and R.H. Carnahan. 2004. Regulation of cadherin stability and turnover by p120ctn: implications in disease and cancer. *Semin Cell Dev Biol.* 15:657-63.
- Reynolds, A.B., and A. Rocznik-Ferguson. 2004. Emerging roles for p120-catenin in cell adhesion and cancer. *Oncogene.* 23:7947-56.
- Shibata, T., A. Kokubu, S. Sekine, Y. Kanai, and S. Hirohashi. 2004. Cytoplasmic p120ctn regulates the invasive phenotypes of E-cadherin-deficient breast cancer. *Am J Pathol.* 164:2269-78.
- Soto, E., M. Yanagisawa, L.A. Marlow, J.A. Copland, E.A. Perez, and P.Z. Anastasiadis. 2008. p120 catenin induces opposing effects on tumor cell growth depending on E-cadherin expression. *J Cell Biol.* 183:737-49.
- Soubry, A., J. van Hengel, E. Parthoens, C. Colpaert, E. Van Marck, D. Waltregny, A.B. Reynolds, and F. van Roy. 2005. Expression and nuclear location of the transcriptional repressor Kaiso is regulated by the tumor microenvironment. *Cancer Res.* 65:2224-33.
- Spring, C.M., K.F. Kelly, I. O'Kelly, M. Graham, H.C. Crawford, and J.M. Daniel. 2005. The catenin p120ctn inhibits Kaiso-mediated transcriptional repression of the beta-catenin/TCF target gene matrilysin. *Exp Cell Res.* 305:253-65.
- Sugihara, K., N. Nakatsuji, K. Nakamura, K. Nakao, R. Hashimoto, H. Otani, H. Sakagami, H. Kondo, S. Nozawa, A. Aiba, and M. Katsuki. 1998. Rac1 is required for the formation of three germ layers during gastrulation. *Oncogene.* 17:3427-33.
- Torres, M., A. Stoykova, O. Huber, K. Chowdhury, P. Bonaldo, A. Mansouri, S. Butz, R. Kemler, and P. Gruss. 1997. An alpha-catenin gene trap mutation defines its function in preimplantation development. *Proceedings of the National Academy of Sciences of the United States of America.* 94:901-906.
- van Roy, F., and G. Berx. 2008. The cell-cell adhesion molecule E-cadherin. *Cell Mol Life Sci.* 65:3756-88.
- van Roy, F.M., and P.D. McCrea. 2005. A role for Kaiso-p120ctn complexes in cancer? *Nat Rev Cancer.* 5:956-64.
- Vestweber, D., and R. Kemler. 1985. Identification of a putative cell adhesion domain of uvomorulin. *Embo J.* 4:3393-8.
- Wang, L., and Y. Zheng. 2007. Cell type-specific functions of Rho GTPases revealed by gene targeting in mice. *Trends Cell Biol.* 17:58-64.
- Wildenberg, G.A., M.R. Dohn, R.H. Carnahan, M.A. Davis, N.A. Lobdell, J. Settleman, and A.B. Reynolds. 2006. p120-catenin and p190RhoGAP regulate cell-cell adhesion by coordinating antagonism between Rac and Rho. *Cell.* 127:1027-39.

- Xiao, K., R.G. Oas, C.M. Chiasson, and A.P. Kowalczyk. 2007. Role of p120-catenin in cadherin trafficking. *Biochim Biophys Acta*. 1773:8-16.
- Xie, H., S. Tranguch, X. Jia, H. Zhang, S.K. Das, S.K. Dey, C.J. Kuo, and H. Wang. 2008. Inactivation of nuclear Wnt-beta-catenin signaling limits blastocyst competency for implantation. *Development*. 135:717-27.
- Yamada, S., S. Pokutta, F. Drees, W.I. Weis, and W.J. Nelson. 2005. Deconstructing the cadherin-catenin-actin complex. *Cell*. 123:889-901.
- Yanagisawa, M., and P.Z. Anastasiadis. 2006. p120 catenin is essential for mesenchymal cadherin-mediated regulation of cell motility and invasiveness. *J Cell Biol*. 174:1087-96.
- Yanagisawa, M., D. Huveldt, P. Kreinest, C.M. Lohse, J.C. Cheville, A.S. Parker, J.A. Copland, and P.Z. Anastasiadis. 2008. A p120 catenin isoform switch affects Rho activity, induces tumor cell invasion, and predicts metastatic disease. *J Biol Chem*. 283:18344-54.

## Chapter 4

---

p120CTN ISOFORM C KNOCKOUT AND KNOCKIN MICE  
RESCUE E-CADHERIN LOSS AND EMBRYONIC LETHALITY  
IN p120CTN-DEFICIENT EMBRYOS

## Mice harboring a knockout or knockin of exon C of p120ctn

## **p120ctn isoform C knockout and knockin mice rescue E-cadherin loss and embryonic lethality in p120ctn-deficient embryos**

Tim Pieters <sup>1,2</sup>, Petra D'hooge <sup>1,2</sup>, Tino Hochpied <sup>1,2</sup>, Paco Hulpiau <sup>1,2</sup>, Marc P. Stemmler <sup>3</sup>, Albert Reynolds <sup>4</sup>, Frans van Roy <sup>1,2</sup>, Jolanda van Hengel <sup>1,2,5</sup>

<sup>1</sup> Department for Molecular Biomedical Research, Technologiepark 927, VIB, B-9052 Ghent, Belgium

<sup>2</sup> Department of Biomedical Molecular Biology, Ghent University, Technologiepark 927, B-9052 Ghent, Belgium

<sup>3</sup> Department of Molecular Embryology, Max-Planck Institute of Immunobiology, Stuebeweg 51, 79108 Freiburg, Germany

<sup>4</sup> Department of Cancer Biology, Vanderbilt University, Nashville, Tennessee, United States of America

<sup>5</sup> Corresponding author: Jolanda.vanhengel@dmbr.VIB-UGent.be or Frans.Vanroy@dmbr.VIB-UGent.be

### **TABLE OF CONTENTS**

ABSTRACT .....	133
INTRODUCTION.....	134
MATERIAL AND METHODS .....	137
Immunofluorescence .....	137
Confocal microscopy.....	137
Histology and immunohistochemistry .....	137
Bioinformatic analyses .....	138
RT-PCR.....	138
Production and purification of a polyclonal antibody against p120ctn isoform C.....	139
Plasmid construction and cell culture.....	139
Western blot analysis .....	140
Generating p120ctn <sup>KOC/+</sup> and p120ctn <sup>KIC/+</sup> mice .....	140
Southern blot analysis .....	141
Generating p120ctn <sup>+/-</sup> , p120ctn <sup>KOC/-</sup> and p120ctn <sup>KIC/-</sup> mice .....	142
Generating p120ctn <sup>fl/fl</sup> ; Alb-Cre, p120ctn <sup>KOC/fl</sup> ; Alb-Cre and p120ctn <sup>KIC/fl</sup> ; Alb-Cre mice	142
Mouse breeding, embryo isolation and genotyping .....	142
ES cell isolation and culture.....	143
RhoA Activity assay.....	143

## Mice harboring a knockout or knockin of exon C of p120ctn

RESULTS.....	144
p120ctn exon C encoded amino acids inhibit nuclear translocation and dendritic-like branching <i>in vitro</i> .....	145
Homozygous p120ctn KOC and KIC embryos die very early in development .....	149
Homozygous p120ctn KOC and KIC embryos fail to implant .....	153
Evolutionarily conserved p120ctn exon C is expressed during early development.....	158
Blastocysts from homozygous p120ctn knockout mice fail to stabilize E-cadherin at the cell membrane .....	162
p120ctn <sup>KOC/-</sup> and p120ctn <sup>KIC/-</sup> mice are viable and can stabilize E-cadherin at the cell membrane of blastocysts .....	164
Generation and characterization of p120ctn <sup>KOC/-</sup> and p120ctn <sup>KIC/-</sup> ES cell lines .....	167
Both the p120ctn KOC and KIC allele can rescue defects seen in p120ctn-deficient livers. ....	170
DISCUSSION .....	173
Interplay between p120ctn and E-cadherin <i>in vivo</i> .....	173
p120ctn isoform C: essential for life, conserved in evolution.....	175
ACKNOWLEDGEMENTS .....	178
REFERENCES.....	179

**ABSTRACT**

p120 catenin (p120ctn) is a versatile member of the armadillo family, and has different functions in different subcellular compartments. Cytoplasmic p120ctn regulates the activity of RhoA GPTases, nuclear p120ctn inhibits Kaiso-mediated transcriptional repression, while membrane-localized p120ctn stabilizes E-cadherin on the cell surface and supports cadherin-mediated adhesion. Multiple human p120ctn isoforms are generated as a result of alternative splicing, however, the significance of all these p120ctn isoforms *in vivo* remains unknown. Several tissue-specific p120ctn knockout mice have been reported, but in these studies all p120ctn isoforms are removed. We report for the first time on the generation of p120ctn isoform-specific knockout and knockin mice to analyze the *in vivo* function of alternatively spliced exon C of p120ctn. This resulted in mice in which exon C of p120ctn is either constitutively ablated (p120ctn<sup>KOC</sup>) or constitutively expressed (p120ctn<sup>KIC</sup>). Surprisingly, homozygous p120ctn KOC and homozygous KIC embryos died during preimplantation, while completely p120ctn-deficient (p120ctn<sup>-/-</sup>) embryos formed normal blastocysts. The absence of p120ctn in blastocysts resulted in a drastic drop of membrane-localized E-cadherin. This confirms that p120ctn is the rate limiting factor for stabilizing cell surface E-cadherin *in vivo*. Both isoform C-deficient and isoform-C containing p120ctn variants could rescue the E-cadherin levels in blastocysts and could overcome the embryonic lethality in p120ctn-deficient mice. In addition, both p120ctn isoforms with or without the exon C-encoded amino acids can rescue the phenotypes that were seen in a liver-specific total p120ctn knockout. Expression of p120ctn isoform C inhibited nuclear translocation and the typical dendritic-like branching *in vitro*. Both isoform C-deficient and isoform C-expressing ES cell lines form proper cadherin catenin complexes, and RhoA activity wasn't affected. Thus both p120ctn KOC and p120ctn KIC mice were equally potent in rescuing the phenotypes seen in p120ctn-deficient (p120ctn<sup>-/-</sup>) mice.

### INTRODUCTION

p120ctn is a versatile Armadillo protein and has different functions in distinct subcellular compartments. The p120ctn protein consists of a central Armadillo repeat domain flanked by a short carboxy-terminal domain and an amino-terminus containing a coiled-coil domain and a phosphorylation domain (Reynolds and Rocznik-Ferguson, 2004). The central Armadillo repeat domain of p120ctn and that of its subfamily member plakophilin 1 consists of nine 42 amino-acid Armadillo-repeats (Choi and Weis, 2005; Ishiyama et al.). Structural and mutational analysis revealed that the first five Armadillo-repeats are essential for binding to the JMD of classic cadherins (Ireton et al., 2002; Ishiyama et al.). A core function of p120ctn is to stabilize cadherins at the plasma membrane by modulating cadherin trafficking and degradation (Reynolds and Carnahan, 2004; Xiao et al., 2007). In addition, p120ctn regulates RhoGTPase activity in the cytoplasm (Anastasiadis, 2007) and modulates gene expression by interacting with various transcription factors in the nucleus (Daniel and Reynolds, 1999; Hosking et al., 2007). In addition, p120ctn is also the prototypic member of the p120ctn subfamily, which consists of four members: p120ctn (CTNND1), armadillo repeat gene deleted in velocardiofacial syndrome (ARVCF),  $\delta$ -catenin (CTNND2) and p0071 (PKP4) (McCrea and Park, 2007).

Besides the existence of multiple p120ctn family members, the complexity is further increased by the presence of different p120ctn isoforms. Due to extensive splicing up to 48 possible human p120ctn isoforms can be generated: in that way up to four different start codons (M1-M4) can be used as well as four alternatively used internal exons (A-D) (Keirsebilck et al., 1998). A p120ctn isoform of approximately 120 kDa uses the first startcodon, M1 (p120ctn isoform 1) and has a longer amino-terminal region compared to the shorter 100-kDa p120ctn isoform that uses the third startcodon, M3 (p120ctn isoform 3). Short p120ctn isoforms are expressed mainly in epithelia (Keirsebilck et al., 1998; Montonen et al., 2001), whereas long p120ctn isoforms are expressed in motile mesenchymal cell types (Aho et al., 2002; Aho et al., 1999; Golenhofen and Drenckhahn, 2000; Mo and Reynolds, 1996). During epithelial-to-mesenchymal transition (EMT), a switch from short to long p120ctn isoforms occurs (Husmark et al., 1999; Vandewalle et al., 2005). In addition, different p120ctn isoforms exert tissue-specific and cell-specific expression patterns and p120ctn isoforms can have opposing effects on tumor growth, RhoGTPase activity and invasiveness *in vitro* (Yanagisawa et al., 2008). However, the significance of all these p120ctn isoforms *in vivo* remains unknown.



The subcellular localization of p120ctn can also be affected by its isoform expression pattern. The alternatively used exon B codes for p120ctn isoform B, which contains a nuclear export signal (NES) (van Hengel et al., 1999). p120ctn also contains two nuclear localization sequence (NLS) signals, one in the N-terminal phosphorylation domain and a second in the central armadillo repeat domain (Aho et al., 2002; Roczniak-Ferguson and Reynolds, 2003). The first NLS is absent in p120ctn isoform 4. The second NLS is situated in the large insert loop between arm repeats 5 and 6 of the central armadillo repeat domain (Choi and Weis, 2005; Ishiyama et al., 2010). This second NLS can be interrupted and inactivated by six amino acids, encoded by the alternatively used exon C. The insert loop itself is not essential for binding to classical cadherins (Ireton et al., 2002; Ishiyama et al., 2010).

Furthermore, p120ctn isoforms have different effects on RhoGTPase activity and cell invasion (Yanagisawa et al., 2008). p120ctn has two RhoA-binding domains, one in the N-terminal domain (amino acids 102 to 234) and a second, coinciding with the sequence of the second NLS (amino acids 622 to 628) in the insert loop of the armadillo repeat domain (Castano et al., 2007; Yanagisawa et al., 2008). In analogy to the NLS signals, the first RhoA-binding domain is absent in p120ctn isoform 4 and the second RhoA-binding domain can be interrupted by six amino acids, encoded by the alternatively used exon C. However, this second RhoA-binding domain is also essential for RhoGTPase activity because deleting this sequence (p120ctn  $\Delta$ 622-628) leads to loss of the ability to inhibit RhoA activity (Anastasiadis et al., 2000). By interrupting the sequence, important for both nuclear import and RhoA inhibition, expression of exon C- encoded amino acids may regulate p120ctn localization and function. But the function of the alternative spliced exon C has not been investigated *in vitro*, nor *in vivo*.

Two strategies have been used for tissue-specific removal p120ctn in mice, but both strategies ablate all p120ctn isoforms and no isoform-specific information can be deduced from them. In the first strategy, exons 3 to 8 (containing all four start codons) were floxed (Davis and Reynolds, 2006). Cre-mediated recombination was then used to selectively remove p120ctn from salivary gland, skin and gastrointestinal tract (Davis and Reynolds, 2006; Perez-Moreno et al., 2006; Smalley-Freed et al., 2010). The second strategy uses nonsense-mediated decay to remove truncated p120ctn transcripts after Cre-mediated removal of exon 7, which is flanked by LoxP sites. In this way, p120ctn could be ablated from the forebrain (Elia et al., 2006).

So far, no *in vivo* tools for investigating the function of different p120ctn isoforms have been reported. We report on the generation of p120ctn exon C-specific knock-out

### Mice harboring a knockout or knockin of exon C of p120ctn

(p120ctn KOC) and knock-in (p120ctn KIC) mice. Homozygous p120ctn KOC and p120ctn KIC mice both die very early in development, probably due to a deletion of highly conserved sequence present in the intronic regions flanking exon C. We also generated total p120ctn knock-out mice (p120ctn<sup>-/-</sup>), by crossing floxed p120ctn mice (Davis and Reynolds, 2006) with mice expressing the Cre-recombinase in a tissue-wide manner (Betz et al., 1996). By crossing p120ctn KOC or p120ctn KIC mice with the p120ctn null mice we could obtain blastocysts and ES cells expressing either always p120ctn isoform C or not, and could show that both isoforms can stabilize cadherins *in vivo*.

## MATERIAL AND METHODS

### Immunofluorescence

The staining procedure for preimplantation embryos is carried out in 24-well plates at room temperature according to a published procedure (Kan et al., 2007). In brief, embryos were washed twice in phosphate buffered saline (PBS) containing 0.05% Tween 20 (PBT) and fixed for 10 min in 2% paraformaldehyde (PFA). After permeabilization for 10 min with 0.25% Triton X-100 in PBS and two washes in PBT, embryos were blocked for 30 min with 1% goat serum in PBT (GS-PBT) and then incubated for 1 h with primary antibodies. After three washes with GS-PBT, embryos were incubated for 30 min with secondary antibodies, washed. One-microliter drops of PBS, each containing an embryo, were placed on a glass-bottom dish (WillCo Wells) and covered with mineral oil before examination by confocal microscopy (see below). Staining cultured cells involved methanol-fixation, incubation for 2 h with primary antibody and 1 h with the secondary antibody, each dissolved in 1:4 mixture of 2% gelatin and PBS. The following antibodies were used: mouse monoclonal anti-p120ctn (pp120, 1/500, BD Transduction Laboratories), polyclonal rabbit anti-p120ctn isoform C (pAbexC, 1/50, see below), polyclonal rabbit anti- $\beta$ -catenin (1/2000, Sigma), polyclonal rabbit anti- $\alpha$ -catenin (1/1000, Sigma), mouse monoclonal anti-E-cadherin (1/300, BD Transduction Laboratories), rat monoclonal anti-E-cadherin (DECMA-1, 1/100, Sigma), mouse monoclonal anti-Oct-4 (1/100, Santa Cruz Biotechnology), mouse monoclonal anti-Cdx2 (1/100, Biogenex). Secondary species-specific Alexa-fluorochrome-conjugated antibodies were used at a dilution of 1/500 (Molecular Probes).

### Confocal microscopy

Confocal microscopy was performed using a Leica TCS SP5 confocal scan head attached to a Leica DM IRE2 inverted microscope and a PC running Leica AF software version 2.5. Optical sections were taken every 2  $\mu$ m. Three-dimensional reconstructions of Z-stacks were made using Volocity software (Perkin Elmer).

### Histology and immunohistochemistry

Decidua containing gastrulating embryos were dissected from the uterus. Livers were dissected from five week old mice. Tissues were washed several times in phosphate-buffered saline (PBS) fixed overnight in 4% paraformaldehyde in PBS, embedded in paraffin wax, and

## Mice harboring a knockout or knockin of exon C of p120ctn

sectioned at 6 to 8  $\mu\text{m}$ . Sections were deparaffinated using HistoClearII (National Diagnostics). For histology, tissue sections were rehydrated and stained with hematoxylin and eosin. For immunohistochemistry, tissue sections were rehydrated and pretreated with 0.3%  $\text{H}_2\text{O}_2$  in methanol for 45 min. The sections were then transferred to 10 mM citrate buffer (pH 6.0) and the antigen was exposed in a Retriever (PickCell Laboratories, Amsterdam, The Netherlands). The sections were covered with blocking buffer (10% goat serum, 1% BSA in PBS) for 20 min and then incubated with appropriate antibodies (diluted in 1% BSA in PBS) overnight at 4°C. Staining was completed with a biotinylated secondary antibody (Dako, Glostrup, Denmark), avidin-peroxidase (Dako) and 3,3'-diamino-benzidine (Biogenex, San Roman, CA). The following antibodies were used: mouse monoclonal anti-p120ctn (pp120, 1/500, BD Transduction Laboratories), mouse monoclonal anti-E-cadherin (1/500, BD Transduction Laboratories), mouse monoclonal anti-N-cadherin (1/600, Zymed, San Francisco, CA), rat monoclonal anti-Ki67 (1/30, Dako).

## Bioinformatic analyses

Genomic details of p120ctn and ARVCF and the multiple sequence alignments were retrieved from the UCSC Genome Browser (Miller et al., 2007). The alignments were shaded using BoxShade ([http://www.ch.embnet.org/software/BOX\\_form.html](http://www.ch.embnet.org/software/BOX_form.html)) and Neighbor-Joining trees were constructed using ClustalX2 (Larkin et al., 2007). The conserved Roaz binding sites were identified using the ConTra tool (Hooghe et al., 2008). A BLASTn search at the miRBase website (Griffiths-Jones et al., 2008) of the conserved block containing p120ctn exon C and flanking intron sequence, both human (chr2:84452570-84452790) and mouse (chr11:57330338-57330652), retrieved mmu-miR-141\* as top scoring match. The MicroCosm resource (formerly miRBase Targets) listed several olfactory receptor transcripts as putative targets of mouse miR-141 (mmu-miR-141\*).

## RT-PCR

RNA was isolated from individual or pooled embryos using the PicoPure RNA Isolation Kit (Arcturus, cat no. KIT0204). cDNA was produced with Superscript III reverse transcriptase according to the manufacturer's instructions (Invitrogen). Specific transcripts were detected with primers for p120ctn, p120ctn exon C, Oct-4 or mGAPDH (Table 1).

Table 1. Primers for genotyping and RT-PCR

allele	primers for genotyping	size (bp)
p120ctn KOC	forward 5'-GTGTGAGGATGGTGACGAT-3', reverse 5'-TAAATGATAGACAGCCGAGAT-3	1220 (wt), 981 (KOC)
p120ctn KOC (nested)	forward 5'-GTGTGAGGATGGTGACGAT-3', reverse 5'-AGCAGGACTAGTTCTTTAG-3	723 (wt), 485 (KOC)
p120ctn KIC	forward 5'-GTGCTGTTAATGACTAAGCCATCC-3', reverse 5'-GGAAGGGCCTCTGGTTAACG-3	576 (KIC), 450 (wt)
p120ctn KIC (nested)	forward 5'-GTGCTGTTAATGACTAAGCCATCC-3', reverse 5'-CCGAGGAGGCAAACACA-3	504 (KIC), 408 (wt)
p120ctn loxP	forward 5'-TTGAACTCAGGACCGTCAGAGGAG-3', reverse 5'-AAAGCAAGCCACCACCAACC-3	564 (loxP), 450 (wt)
p120ctn -	forward 5'-TTGAACTCAGGACCGTCAGAGGAG-3', reverse 5'-TCAGCACCCACACAAAGGTTG-3	550
Cre recombinase	forward 5'-AACATGCTTCATCGTCGG-3', reverse 5'-TTCGGATCATCAGCTACACC-3	470
allele	primers for RT-PCR	size (bp)
p120ctn	forward 5'-CCACAGGCAGAGCGTTACCAG-3', reverse 5'-AGCAGGACTAGTTCTTTAG-3	177
p120ctn exon C	forward 5'-GGAGGAAACTTCGGGAATGTGA-3', reverse 5'-TTTTCCCTCTGAGAACTCAT-3	262
Oct-4	forward 5'-GTTGGAGAAGGTGGAACCAA-3', reverse 5'-CTCCTTCTGCAGGGCTTTC-3	350
GAPDH	forward 5'-ACCACAGTCCATGCCATCAC -3', reverse 5'-TCCACCACCCTGTTGCTGTA-3	470

### Production and purification of a polyclonal antibody against p120ctn isoform C

An antibody specific for p120ctn isoform C (pAbexC) was generated by injecting rabbits with a peptide containing the six amino acids, encoded by alternative exon C (GKDEWFSRGKGAC), fused to keyhole limpet hemocyanin (KLH, Sigma), together with Titermax gold adjuvant (Sigma). Two bleedings from three rabbits were characterized by western blotting and immunofluorescence in cells, that were transiently transfected with either pEFBOS hp120ctn 3A or 3AC (data not shown). The most promising serum was peptide-purified on affinity columns, using the SulfoLink kit (Pierce Biotechnology) according to the manufacturer's instructions. After Elisa, the antibody-containing fractions were pooled, supplemented with glycerol, aliquoted and frozen at  $-70^{\circ}\text{C}$ .

### Plasmid construction and cell culture

The mammalian expression vector pHM829 was designed for expression of the protein of interest fused to  $\beta$ -galactosidase ( $\beta$ -gal) at its N-terminus and to green fluorescent protein (GFP) at its C-terminus (Sorg and Stamminger, 1999). pHM829 vectors containing either the second NLS of p120ctn (NLS) or a mutated NLS (NLSmut) were described previously (Kelly et al., 2004). To create a pHM829 construct containing the second p120ctn NLS interrupted by exon C-encoded amino acids, two complimentary oligonucleotides were designed to incorporate a 5' *Sac*II site and a 3' *Xba*I site (underlined) flanking the NLS sequence, which is interrupted by p120ctn exon C (italics): 5'-CCGCGGAAGAAGGGCAAAGATGAGTGGTCTCCAGAGGGAAAAAGCCTTCTAGA-3' 3'-GGCGCCCGCCGCCCGTTTCTACTCACCAAGAGGTCTCCCTTTTTTCGGAAGATCT -5'. The oligonucleotides were annealed, digested with *Sac*II and *Xba*I, and ligated in pHM829 pre-digested with the same enzymes. cDNA coding for different human p120ctn isoforms (1A,

## Mice harboring a knockout or knockin of exon C of p120ctn

3A, 3AC, 4A, 4AC) were cloned in a eukaryotic expression vector (pEFBOS). This has been described partly (van Hengel et al., 1999). pEFBOS hp120ctn 1AΔ622-628 was generated using a QuikChange® II Site-Directed Mutagenesis Kit (Stratagene).

HeLa (human cervical carcinoma), MCF7/AZ (human breast adenomacarcinoma), Cos1 (SV40 immortalized simian kidney cells), HEK293T (human embryonic kidney), and mouse fibroblast NIH3T3 cells were grown at 37°C, 5% CO<sub>2</sub> in Dulbecco's minimal essential medium (DMEM) supplemented with 10% fetal bovine serum, 4 mM L-glutamine, penicillin (100 U/ml) and streptomycin (100 mg/ml). Cells were transfected either by the calcium phosphate precipitation method (293T) or by using Fugene reagent (Roche Applied Science) according to the manufacturer's instructions. For the branching assay, at least 100 transiently transfected HeLa or NIH3T3 cells were and scored for each construct for normal or branched cellular phenotype. The percentage of branched versus normal phenotype was plotted graphically.

### Western blot analysis

Individual embryos were washed in PBS, frozen in a minimal amount of PBS, thawed, supplemented with 10 µl Laemmli buffer (Laemmli, 1970), mixed by pipetting, and boiled for 5 min. Proteins were separated by SDS-PAGE on a 8% polyacrylamide gel, electroblotted onto polyvinylidene fluoride (PVDF) membranes (Millipore), and incubated with antibodies. NBT/BCIP was used for detection (Zymed Laboratories).

### Generating p120ctn<sup>KOC/+</sup> and p120ctn<sup>KIC/+</sup> mice

The mouse p120ctn gene *Ctnd1* was cloned from a genomic DNA cosmid library from the 129/Ola strain. Two cosmids, comprising exons 1 to 17 and exons 13 to 21 respectively, contain the full genomic DNA sequence of the p120ctn gene. All targeting vector were generated by standard cloning techniques. A genomic fragment (*NheI-EagI*) containing exon 7 to 13 was cloned in the pBlue vector. For the p120ctn<sup>KOC</sup> targeting vector, a fragment of exon C and flanking sequences was replaced by a floxed selection cassette containing a neomycin resistance gene and a thymidine kinase gene from herpes simplex virus (Neo<sup>r</sup>-TK, Fig. 3A). To do that, a *NotI* site (161bp downstream of exon 11) and a *ClaI* site (197bp upstream of exon 11) were generated by Stratagene kit 2 primers. The floxed Neo<sup>r</sup>-TK cassette was cloned in the pBlue vector by digesting the pBSloxPneotkloxP vector with *NotI* and *ClaI* and ligating it into the pBlue mp120ex3-7 vector pre-digested with the same enzymes. For the p120ctn<sup>KIC</sup> targeting vector, the genomic sequence of exons 10 to 12 was

replaced by its corresponding cDNA sequence (Fig. 3B), by using a *BspEI* site (present in exon10) and a *XhoI* site (present in exon12). A mouse p120ctn cDNA fragment was digested with *BspEI* and *XhoI* and ligated in the pBlue mp120ctnex3-7 vector pre-digested with the same enzymes. In addition, a floxed neomycin resistance gene from the pGK-loxP vector (Genebridges) was inserted in intron 9 via Red/ET recombination. Homologous recombination at the p120ctn locus was achieved by electroporation of *PvuI*-linearized p120ctn<sup>KOC</sup> targeting vector or *ApaI*-linearized p120ctn<sup>KIC</sup> targeting vector into E14 ES cells. Electroporated cells were subjected to positive selection using G418. Positive clones were screened by Southern blot analysis for correct and unique homologous recombination events using internal and external 5' and 3' probes (Figs. 3C,D). Correctly targeted p120ctn<sup>KOC</sup> NeoFL/+ ES cells were electroporated with a Cre-recombinase expression plasmid, selected with Gancyclovir and screened by Southern blotting. Correct ES cell clones of each construct were used for injection into host C57BL/6 blastocysts. Chimeric males, identified by their coat color, were mated to C57BL/6 females to generate p120ctn<sup>KOC/+</sup> and <sup>KIC</sup> NeoFL/+ mouse lines. The neomycin resistance cassette in p120ctn<sup>KIC</sup> NeoFL/+ mice was removed by mating with deleter<sup>Cre</sup> mice (Betz et al., 1996), resulting in p120ctn<sup>KIC/+</sup> mice. p120ctn<sup>KOC/+</sup> and p120ctn<sup>KIC/+</sup> mice were backcrossed on C57BL/6 nine and eighth times, respectively. p120ctn KOC and KIC alleles could be discriminated from the wild-type allele by performing PCR on tail genomic DNA (Figs. 3E,F). Mice were housed in individually ventilated cages either in specific pathogen-free or in conventional animal facilities. All experiments on mice were conducted according to institutional, national, and European animal regulations. Animal protocols were approved by the ethics committee of Ghent University.

### Southern blot analysis

For ES cell selection, genomic DNA was digested for KOC with *BgIII* to differentiate between the 19 kb and 12 kb fragments of the WT and KOC-modified alleles, respectively. DNA from positive clones was further checked by *BamHI* digest to differentiate between either 5.1 kb or 4.5 kb fragments for the WT and KOC-modified alleles. For KIC ES cell selection we used *BgIII* or *EcoRV*, which generate bands of 19 kb and 13 kb for the WT and KIC-modified alleles, respectively. DNA was separated on agarose gels and transferred to Hybond-N<sup>+</sup> membranes (Amersham), which were hybridized with <sup>32</sup>P-labeled probes.

## Mice harboring a knockout or knockin of exon C of p120ctn

### Generating p120ctn<sup>+/-</sup>, p120ctn<sup>KOC/-</sup> and p120ctn<sup>KIC/-</sup> mice

Mice harboring a floxed region in the p120ctn gene (containing exon 3 till 8, including all four start codons) have been described (Davis and Reynolds, 2006). Crossing these mice with deleter<sup>Cre</sup> mice (Betz et al., 1996) resulted in p120ctn<sup>+/-</sup> mice which were backcrossed to C57BL/6 to remove the Cre-recombinase from the genome.

### Generating p120ctn<sup>fl/fl</sup>; Alb-Cre, p120ctn<sup>KOC/fl</sup>; Alb-Cre and p120ctn<sup>KIC/fl</sup>; Alb-Cre mice

Mice harboring a floxed region in the p120ctn gene (containing exon 3 till 8, including all four start codons) have been described (Davis and Reynolds, 2006). Crossing p120ctn<sup>fl/fl</sup> mice with mice expressing the Cre recombinase under control of a rat albumin promoter (Postic and Magnuson, 2000) resulted in p120ctn<sup>fl/+</sup>; Alb-Cre mice. These mice were crossed again with p120ctn<sup>fl/fl</sup> mice to obtain p120ctn<sup>fl/fl</sup>; Alb-Cre mice, which lack p120ctn specifically in the liver. In addition, p120ctn<sup>fl/fl</sup>; Alb-Cre mice can be crossed with p120ctn<sup>KOC/+</sup> and p120ctn<sup>KIC/+</sup> mice, giving rise to p120ctn<sup>KOC/fl</sup>; Alb-Cre and p120ctn<sup>KIC/fl</sup>; Alb-Cre mice, respectively (Table 2).

**Table 2. Crossing p120ctn KOC or KIC mice with liver specific p120ctn knock-out mice**

Genotyping offspring from p120ctn <sup>KOC/wt</sup> x p120ctn <sup>fl/fl</sup> ; Alb-Cre mating						
KOC/fl; Alb-Cre (25%)	KOC/fl (25%)	fl/wt; Alb-Cre (25%)	fl/wt (25%)	total	recombination	
4 (44,4%)	1 (11,1%)	3 (33,3%)	1 (11,1%)	9		
0/2	0/1	0/1		0/4	tail gDNA	
2/2	0/1	1/1		3/4	liver gDNA	
Genotyping offspring from p120ctn <sup>KIC/wt</sup> x p120ctn <sup>fl/fl</sup> ; Alb-Cre mating						
KIC/fl; Alb-Cre (25%)	KIC/fl (25%)	fl/wt; Alb-Cre (25%)	fl/wt (25%)	total	recombination	
3 (25,0%)	3 (25,0%)	4 (33,3%)	2 (16,7%)	12		
0/2	0/1	0/1		0/4	tail gDNA	
2/2	0/1	1/1		3/4	liver gDNA	

### Mouse breeding, embryo isolation and genotyping

Female mice at the age of 6-8 weeks were put together with male studs and copulation plugs were checked the following morning. Preimplantation embryos were obtained by crossing or intercrossing heterozygous p120ctn<sup>+/-</sup>, p120ctn<sup>KOC/+</sup> and p120ctn<sup>KIC/+</sup> mice. Embryos were flushed with M2 medium (Sigma) from oviducts at E1.5 and E2.5 using a 32G needle (Popper & Sons Inc., Cat. No. 7400) and 5 ml Luer-Lok syringe (B&D). For flushing



from the uterus at E3.5, a G23 needle and a 1 ml syringe were used. Genotyping was performed by PCR on genomic DNA isolated from mouse tail snips and ES cells (Laird et al., 1991). Genomic DNA from individual embryos was isolated by boiling for 5 min in 5  $\mu$ l of 50 mM KOH, followed by neutralization with 5  $\mu$ l of 50 mM Tris HCl pH 8. PCR primers are depicted in table 1.

### **ES cell isolation and culture**

The ES cell isolation procedure has been described before (Pieters et al., in preparation). ES cells were grown on MEFs in SR-ES cell medium, composed of DMEM (Gibco) and F12 (Gibco) mixed in a 1:1 ratio and supplemented with 15% knock-out serum replacement (SR, Gibco), L-glutamine (2 mM, Gibco), penicillin (100 U/ml, Gibco), streptomycin (100 mg/ml, Gibco),  $\beta$ -mercaptoethanol (0.1 mM, Gibco), and 2000 U/ml recombinant mouse LIF (DMBR/VIB Protein Service facility, [www.dnbr.ugent.be](http://www.dnbr.ugent.be)).

### **RhoA Activity assay**

ES cells were treated for 3 min with 4  $\mu$ M lysophosphatidic acid (LPA, Sigma) or were stimulated for 48 h with 10  $\mu$ M ROCK inhibitor Y-27632 (CalBiochem). RhoA activity was determined by a G-LISA kit (Cytoskeleton) according to the manufacturer's instructions. In brief, individual lysates are snap-frozen, and collectively thawed, and equal amounts of protein lysates are incubated on an ELISA plate, coated with RhoA-GTP-binding protein. After several washes, bound active RhoA is detected with a RhoA-specific antibody, following colorimetric analysis.

## RESULTS

p120ctn is composed of a central armadillo repeat domain consisting of nine armadillo repeats, and with each repeat consisting of three helices (H1,H2, and H3) (Fig. 1A) (Ishiyama et al., 2010). The alternatively spliced exon C encodes six amino acids which are situated in the insert loop within the armadillo repeat domain of p120ctn (Fig. 1A).

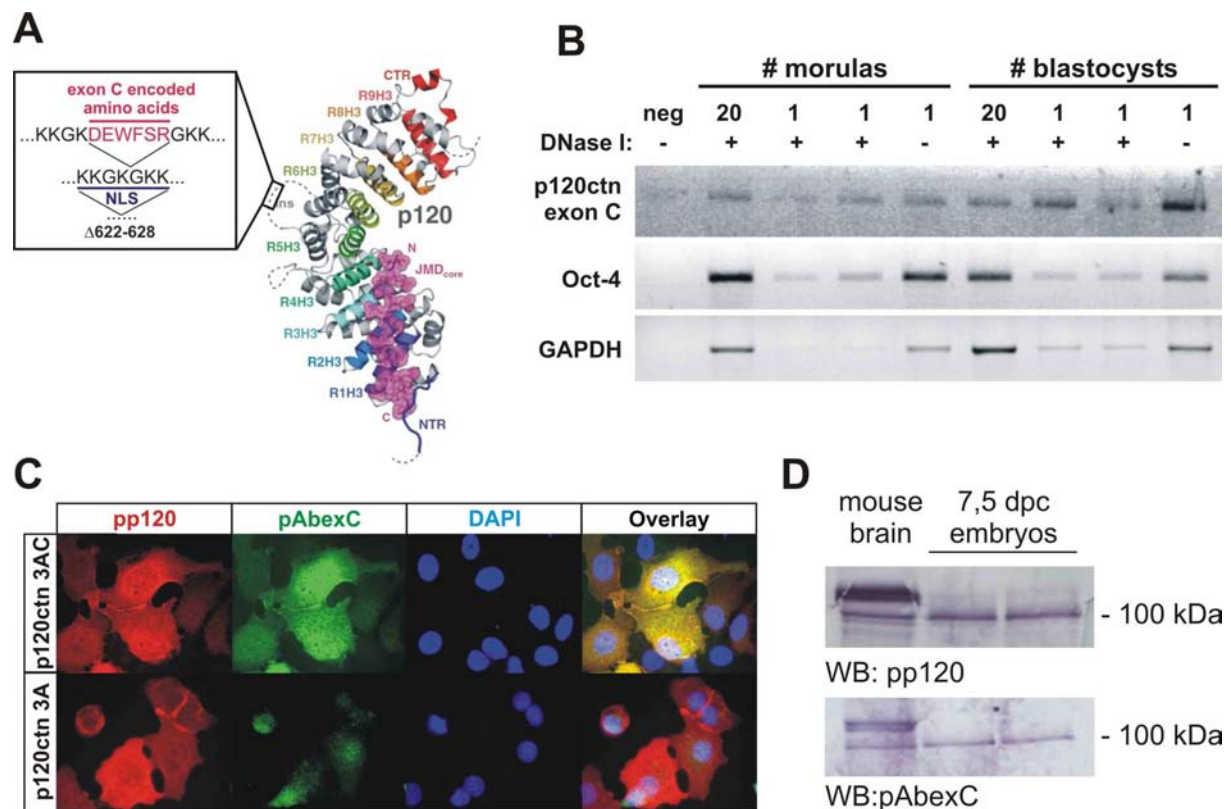


**Figure 1. Expression of evolutionarily conserved p120ctn exon C in wild-type preimplantation and gastrulating embryos.** (A) Crystal structure of the p120ctn isoform 4/JMDcore complex. p120ctn contains nine ARM repeats (R<sub>1</sub>–9) with each repeat consisting of three helices (H<sub>1</sub>,H<sub>2</sub>, and H<sub>3</sub>). The JMDcore is shown in magenta. Between p120ctn ARM repeat 5 and 6 lies an unstructured insert loop, which contains a nuclear localization signal (NLS, coincides with a RhoA binding domain). The NLS is interrupted upon expression of the exon C-encoded amino acids and this NLS is deleted in the p120ctn Δ622-628 mutant. (B) RT-PCR to detect all p120ctn transcripts (p120ctn), p120ctn transcripts containing exon C (p120ctn exon C), and Oct-4-specific transcripts present in single and pooled wild-type mouse morulas and blastocysts. RNA was treated with DNase I or not. (C) Immunostaining to characterize an antibody specific for isoform C of p120ctn (pAbexC). This antibody recognizes transiently transfected p120ctn isoform 3AC, but not 3A in MCF7/AZ cells. (D) Western blot analysis of two wild-type gastrulating embryos (7.5 dpc) in which all p120ctn isoforms were detected with pp120-antibody and p120ctn isoform C was detected with pAbexC. Mouse brain was taken as a positive control because it is rich in isoform C of p120ctn. Scale bar: 25 μm.

To examine whether p120ctn exon C is expressed in preimplantation development, we performed reverse transcriptase polymerase chain reaction (RT-PCR) analysis on single and pooled morulas and blastocyst. Weak expression of p120ctn exon C-containing transcripts was observed in both morulas and blastocysts (Fig. 1B). To investigate p120ctn isoform C expression in more detail, we generated a polyclonal antibody specific for p120ctn isoform C (pAbexC). This antibody can detect exogenous p120ctn isoform C in western blots (data not shown) and by immunofluorescence (Fig. 1C). pAbexC is specific for detecting p120ctn isoform C, as exogenous expression of p120ctn isoform 3AC is readily detected (Fig. 1C, top), but no signal is observed for p120ctn isoform 3A, lacking exon C-encoded amino acids (Fig. 1C, bottom). As human fetal brain was previously described to be rich of p120ctn exon C-containing transcripts (Keirsebilck et al., 1998), we checked whether pAbexC could also detect endogenous p120ctn isoform C in mouse brain. Indeed, also endogenous p120ctn isoform 1AC could be detected in mouse brain lysates (Fig. 1D). pAbexC detects both human and mouse p120ctn isoform C (Figs. 1C, D), as expected from the fully conserved exon C sequences (Fig. 9). Using our pAbexC antibody we also found expression of p120ctn isoform 3 and isoform C in gastrulating embryos (7.5 dpc) (Fig. 1D). Unfortunately, the pAbexC antibody could not be used for immunohistochemistry on tissue sections. To conclude, p120ctn exon C is expressed during both preimplantation development and gastrulation.

### **p120ctn exon C encoded amino acids inhibit nuclear translocation and dendritic-like branching *in vitro***

The exon C-encoded amino acids interrupt an nuclear localization signal and a RhoA-binding domain, but its functional implications are currently unknown. All p120ctn isoforms, except for p120ctn isoform 4, contain 2 NLS signals, one in the N-terminal phosphorylation domain and a second in the insert loop between arm repeats 5 and 6 of the central armadillo repeat domain (Aho et al., 2002; Choi and Weis, 2005; Ishiyama et al., 2010; Rocznik-Ferguson and Reynolds, 2003). p120ctn exon C encodes six amino acids (DEWFSR) that interrupt the basic motif (KKGKGGKK) from the second NLS (Fig. 1A). To elucidate the functional relevance of p120ctn isoform C, we performed several *in vitro* studies, such as nuclear localization and dendritic-like branching assay. We reproduced a reported strategy (Kelly et al., 2004), showing that this second NLS, if isolated and fused to a N-terminal  $\beta$ -galactosidase ( $\beta$ -gal) and a C-terminal green fluorescent protein (GFP), allows nuclear translocation, whereas a mutant NLS does not (Fig. 2A).

## Mice harboring a knockout or knockin of exon C of p120ctn

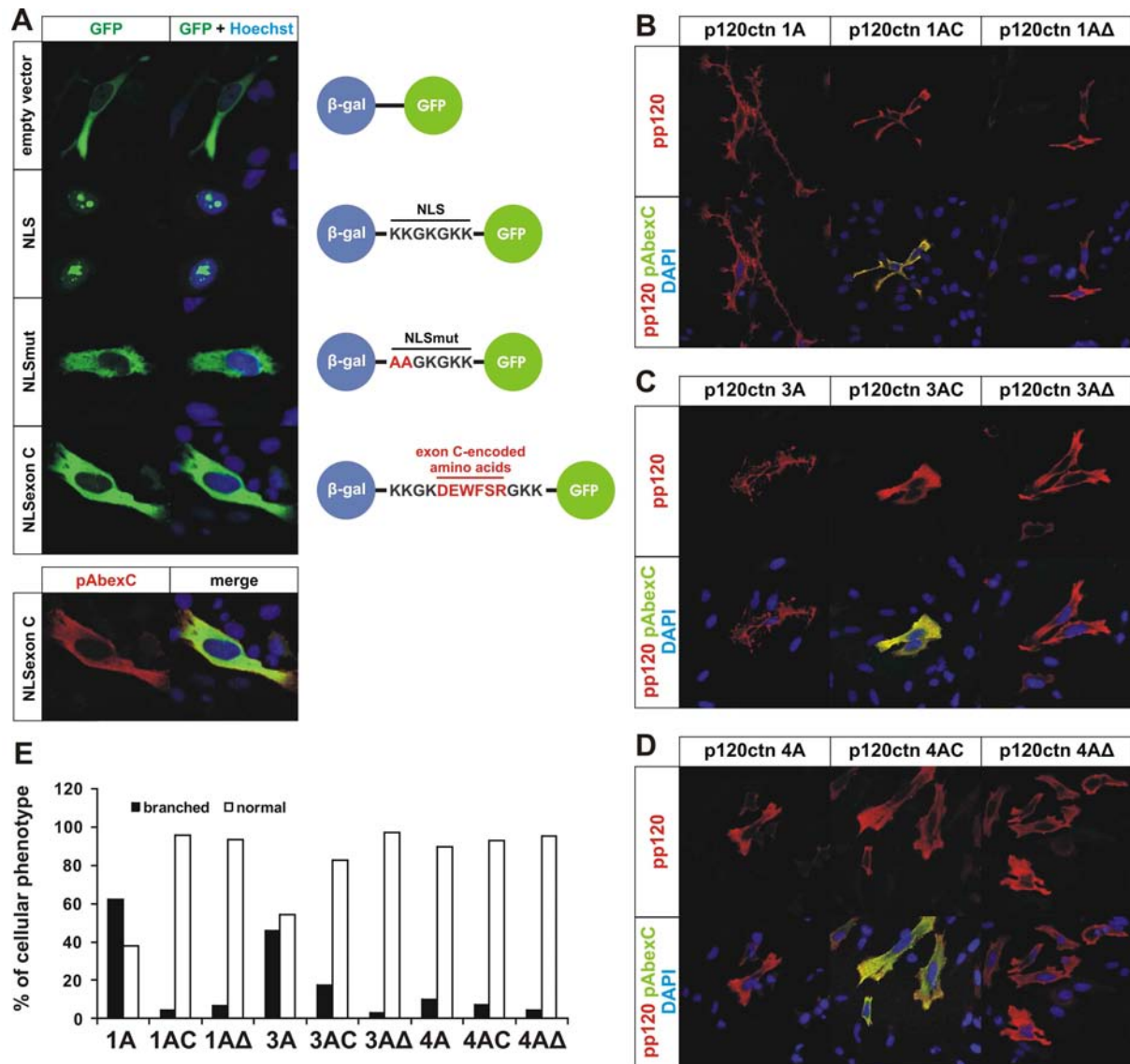


**Figure 2. p120ctn exon C-encoded amino acids inhibit nuclear translocation and dendritic-like branching.** (A) Nuclear translocation assay using constructs containing an N-terminal  $\beta$ -galactosidase ( $\beta$ -gal) and a C-terminal GFP. Between the  $\beta$ -gal and the GFP we cloned the second NLS of p120ctn (NLS), or a mutated version of this NLS (NLSmut), or the NLS interrupted by exon C-encoded amino acids (NLSexon C). These constructs were expressed in HeLa cells. Confocal analysis showed that both NLSmut and NLSexon C could prevent the nuclear GFP expression seen with the NLS construct. The exon C-encoded amino acids, expressed by the NLSexon C construct were detected by pAbexC (bottom panel). (B-D) Branching assay in HeLa cells transiently transfected with p120ctn isoform 1A (B), 3A (C), or 4A (D), or with p120ctn isoform C variants (p120ctn isoform 1AC, 3AC and 4AC), or with the corresponding mutants lacking amino acids 622-628 (p120ctn isoform 1A $\Delta$ , 3A $\Delta$  and 4A $\Delta$ ). Following double immunostaining for all p120ctn isoforms (pp120) and p120ctn isoform C (pAbexC), single confocal sections were made. (E) Diagram showing the percentage of branched versus normal cellular phenotypes for the different p120ctn isoforms in figure B,C and D.

We next investigated if exon C-encoded amino acids, as a result of alternative splicing, can regulate nuclear import. To address this, we made a construct in which the basic NLS is interrupted by exon C-encoded amino acids. Upon expression of this construct in HeLa cells, only cytoplasmic GFP staining was observed, showing that exon C-encoded amino acids can block nuclear import (Fig. 2A). Our pAbexC antibody nicely recognized the exon C-encoded amino acids upon expression of the NLS<sub>exon C</sub> construct (Fig. 2A, bottom). Similar results were obtained in NIH3T3 cells (data not shown). Next, we wanted to see if p120ctn isoform C expression can affect the nuclear localization of full length p120ctn isoforms, however, confocal analysis revealed that neither of these isoforms localized in the nucleus (Fig. 2B-D). So, although expression of the six amino acids encoded by exon C inhibits nuclear import of an isolated NLS, its effect on the subcellular localization of full-length p120ctn isoforms remains unclear.

Expression of p120ctn isoform 1A, 2A or 3A resulted in a marked branched phenotype in different cell lines (Aho et al., 2002; Reynolds et al., 1996). Overexpression of p120ctn isoform 1A saturates the p120ctn-binding sites on cadherins, causing the excess of p120ctn isoform 1A to inhibit RhoA activity in the cytoplasm (Anastasiadis et al., 2000). Deletion of second RhoA-binding domain ( $\Delta 622-628$ ) in the armadillo repeat domain, inhibits both cellular branching and RhoA activation (Anastasiadis et al., 2000). Therefore, we wanted to investigate the effect of p120ctn isoform C on cellular branching. Transient transfection of p120ctn isoform 1A in HeLa cells resulted in extensive cellular branching, which was absent upon expression of p120ctn 1A $\Delta 622-628$  (p120ctn 1A $\Delta$ , Figs. 2B,E). Expression of p120ctn isoform p120ctn 1AC was equally potent in the inhibition of this cellular branching compared to the p120ctn 1A $\Delta$  deletion construct (Figs. 2B,E). Also p120ctn isoform 3A induces the branching phenotype, but to a lesser extent than p120ctn isoform 1A (Figs. 2C,E). This result agrees with previously reported results (Aho et al., 2002). Either deleting the second NLS/RhoA-binding domain in p120ctn isoform 3 (p120ctn 3A $\Delta$ ) or interrupting it by exon C-encoded amino acids (p120ctn 3AC) resulted in a drastic reduction of branched cells (Figs. 2C,E). However, p120ctn isoform 3AC is less potent in inhibiting branching compared to p120ctn 3A $\Delta$  (Fig. 2E). In line with previous reports, p120ctn isoform 4A, which lacks the first NLS and the first RhoA-binding domain in the N-terminus, does not induce branching (Aho et al., 2002), and deleting the second NLS/RhoA-binding domain or interrupting it by exon C-encoded amino acids does not have any effect (Figs. 2D,E). To conclude, expression of p120ctn isoform C can block the typical cellular branching caused by overexpression of p120ctn isoforms 1A or 3A.

## Mice harboring a knockout or knockin of exon C of p120ctn

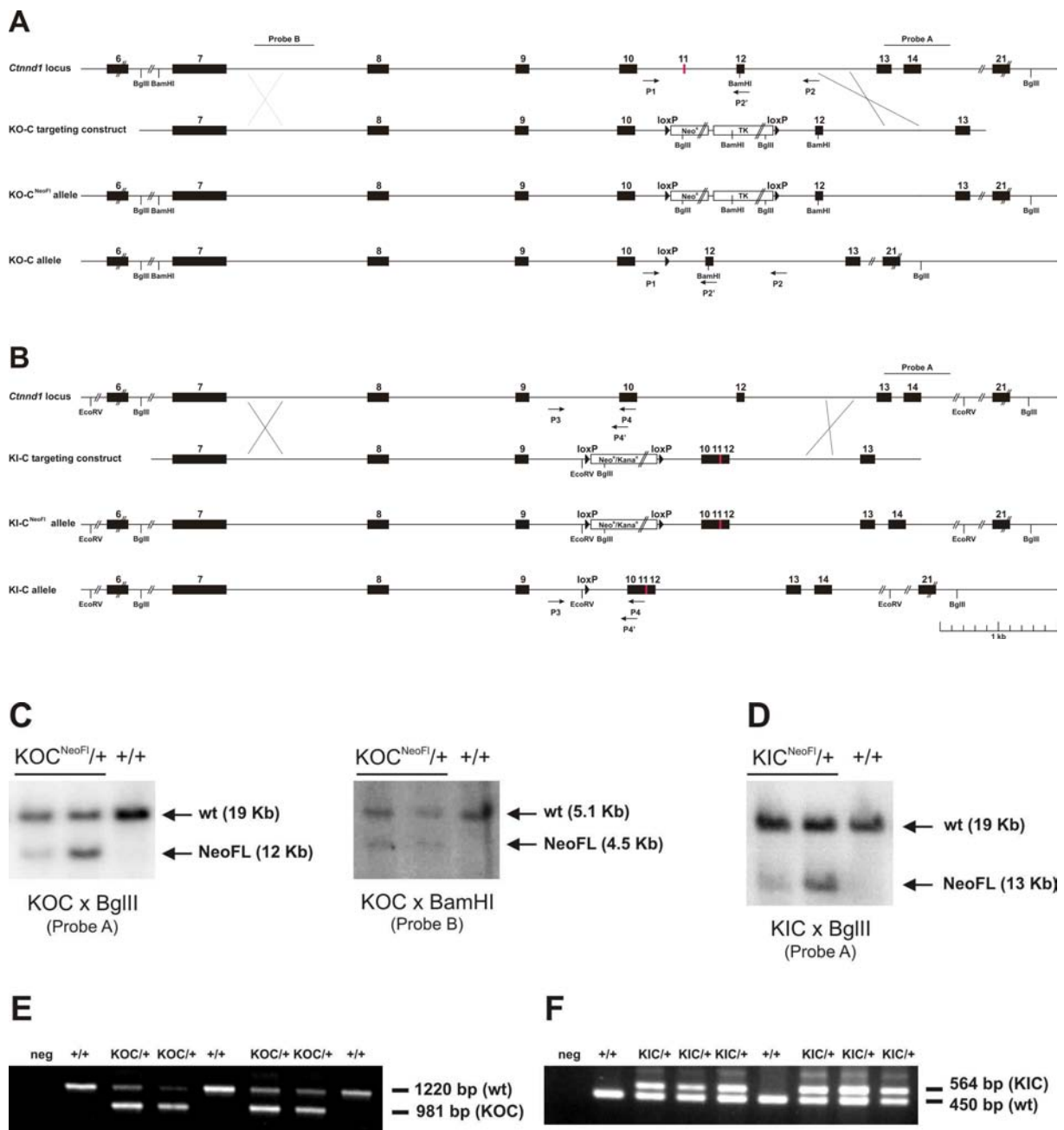


**Figure 3. Generation of mice with a knock-out ( $p120ctn^{KOC}$ ) or knock-in ( $p120ctn^{KIC}$ ) of the alternatively spliced exon C of p120ctn.** Schematic representation of the targeting strategy for the generation of  $p120ctn^{KOC/+}$  (A) and  $p120ctn^{KIC/+}$  ES cells (B). The diagram shows  $p120ctn$  KOC and KIC alleles with a loxP flanked neomycin resistance ( $Neo^R$ ) gene. Restriction enzyme sites and the location of the probe used for Southern blot analysis are depicted. (C) Southern blot analysis from wt (+/+) and homologous recombinant  $p120ctn^{KOC NeoFL/+}$  ES cells. (D) Southern blot analysis from wt (+/+) and homologous recombinant  $p120ctn^{KIC NeoFL/+}$  ES cells. (E) PCR primers P1 and P2 were used for genotyping offspring derived from  $p120ctn^{KOC/+}$  intercrosses. (F) PCR primers P3 and P4 were used for genotyping offspring derived from  $p120ctn^{KIC/+}$  intercrosses.

### Homozygous p120ctn KOC and KIC embryos die very early in development

To analyze the *in vivo* function of p120ctn isoform C, we generated p120ctn<sup>KOC/+</sup> and p120ctn<sup>KIC/+</sup> mice with constitutive ablation or expression of p120ctn isoform C, respectively. In the p120ctn KOC targeting vector, a fragment of exon C and flanking sequences was replaced by a floxed selection cassette (Fig. 3A, 4A). Heterozygous p120ctn KOC (p120ctn<sup>KOC/+</sup>) mice, which are phenotypically normal, were intercrossed to obtain homozygous p120ctn KOC (p120ctn<sup>KOC/KOC</sup>) mice. However, no such p120ctn<sup>KOC/KOC</sup> offspring were found (Table 3). Time matings were set up to identify the developmental stage at which p120ctn<sup>KOC/KOC</sup> embryos die. Homozygous p120ctn KOC embryos were identified by genotyping (Fig. 4B) and could only be found at the preimplantation stages, but never in the normal Mendelian ratio (Table 3). Most p120ctn<sup>KOC/KOC</sup> embryos were not morphologically normal but were fragmented, condensed or degraded (data not shown). However, in some rare occasions normal p120ctn<sup>KOC/KOC</sup> embryos were recovered between the two-cell (n=2, Fig. 4C) and the blastocyst stage (n=4, Figs. 4D,E). Double immunolabeling for p120ctn with  $\beta$ -catenin or Oct-4 revealed a similar expression pattern for both proteins in p120ctn isoform-C-deficient and littermate controls (Figs. 4C-E). These limited data on normal appearing p120ctn<sup>KOC/KOC</sup> embryos shows that p120ctn isoform C has not necessarily an effect on Wnt activity in the trophectoderm or on stemness in the ICM of blastocysts. Unfortunately, we failed to gain further insight in the abnormal phenotypes of p120ctn<sup>KOC/KOC</sup> embryos by performing time lapse monitoring experiments with these embryos (see Chapter 5).

In the p120ctn KIC targeting vector, the genomic sequence of exons 10 to 12 was replaced by its corresponding cDNA sequence (Fig. 3B, 5A). Heterozygous p120ctn KIC (p120ctn<sup>KIC/+</sup>) mice are, like p120ctn<sup>KOC/+</sup> mice, similar to wild-type littermate controls and the phenotype of p120ctn<sup>KIC/KIC</sup> mice strongly resembles that of p120ctn<sup>KOC/KOC</sup> mice. No p120ctn<sup>KIC/KIC</sup> offspring were born, and p120ctn<sup>KIC/KIC</sup> embryos, identified by genotyping (Fig. 5B), were also found only at preimplantation stages but not in the expected Mendelian ratio (Table 3). Also, most of the p120ctn<sup>KIC/KIC</sup> embryos were phenotypically abnormal (Fig. 5C), and only very few p120ctn<sup>KIC/KIC</sup> morulas (n=1, Fig. 5D) and blastocysts were found (n=1, Fig. 5D).

## Mice harboring a knockout or knockin of exon C of p120ctn

**Table 3. Offspring and embryos from intercrosses and backcrosses**

<b>Offspring and embryos from p120ctn<sup>KOC/+</sup> intercrosses</b>				
stage	+/+ (25%)	KOC/+ (50%)	KOC/KOC (25%)	total
offspring Ledeganck	80 (31%)	176 (69%)	0 (0%)	256
offspring FVMS	119 (27%)	327 (73%)	0 (0%)	446
organogenesis (9,5 - 18,5 dpc)	20 (23%)	66 (77%)	0 (0%)	86
gastrulation (6,5 - 8,5 dpc)	8 (7%)	102 (93%)	0 (0%)	110
blastocyst (3,5 dpc)	26 (19%)	100 (72%)	13 (9%)	139
morula (2,5 dpc)	17 (18%)	59 (63%)	17 (18%)	93
2cell - 16cell (0,5-1,5 dpc)	19 (19%)	70 (71%)	9 (9%)	98
junk	25 (27%)	42 (45%)	27 (29%)	94

<b>Offspring from p120ctn<sup>KOC/+</sup> backcrosses (n=9) to c57Bl6</b>			
	+/+ (50%)	KOC/+ (50%)	total
	56 (47%)	63 (53%)	119

<b>Offspring and embryos from p120ctn<sup>KIC/+</sup> intercrosses</b>				
stage	+/+ (25%)	KIC/+ (50%)	KIC/KIC (25%)	total
offspring Ledeganck	9 (13,4%)	58 (87%)	0 (0%)	67
offspring FVMS	79 (17,1%)	384 (83%)	0 (0%)	463
organogenesis (9,5 - 18,5 dpc)	11 (25,0%)	33 (75%)	0 (0%)	44
gastrulation (6,5 - 8,5 dpc)	2 (7%)	27 (93%)	0 (0%)	29
blastocyst (3,5 dpc)	14 (12%)	95 (84%)	4 (4%)	113
morula (2,5 dpc)	6 (19%)	23 (74%)	2 (6%)	31
2cell - 16cell (1,5 dpc)	16 (32%)	31 (62%)	3 (6%)	50
junk	23 (33%)	34 (51%)	12 (17%)	69

<b>Offspring from p120ctn<sup>KIC/+</sup> backcrosses (n=8) to c57Bl6</b>			
	+/+ (50%)	KIC/+ (50%)	total
	94 (51%)	92 (50%)	186

<b>Offspring and embryos from p120ctn<sup>+/-</sup> intercrosses</b>				
stage	+/+ (25%)	+/- (50%)	-/- (25%)	total
offspring	27 (36%)	48 (63%)	0 (0%)	75
organogenesis (9,5 - 18,5 dpc)	3 (42,9%)	4 (57%)	0* (0%)	7
gastrulation (6,5 - 8,5 dpc)				
blastocyst (3,5 dpc)	4 (29%)	7 (50%)	3 (21%)	14

\* 2 out of 5 resorbed embryos were genotyped as p120<sup>-/-</sup>

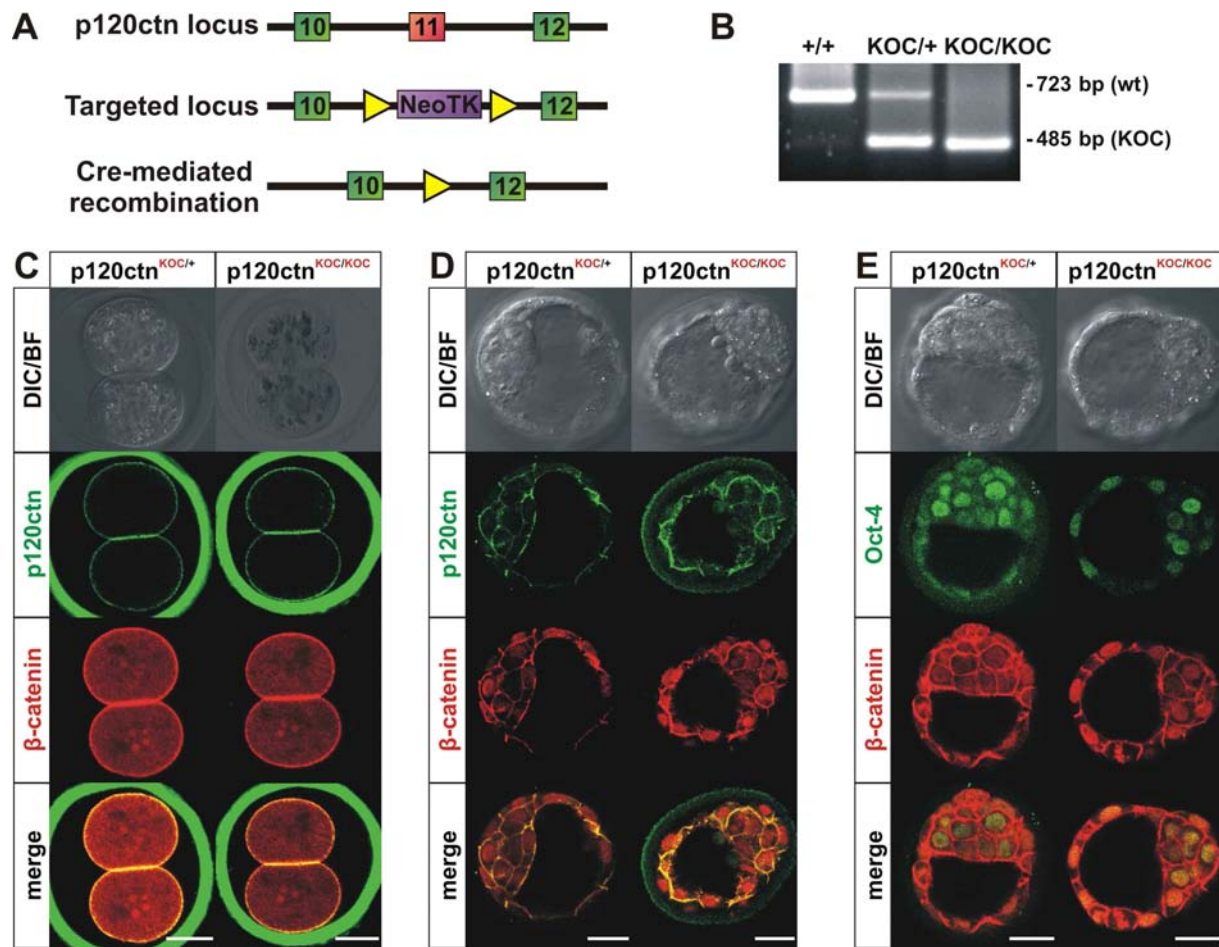
  

<b>Offspring and embryos from p120ctn<sup>KOC/+</sup> X p120ctn<sup>+/-</sup> crosses</b>					
stage	KOC/- (25%)	KOC/+ (25%)	+/- (25%)	+/+ (25%)	total
offspring	3 (38%)	0 (0%)	3 (38%)	2 (25%)	8
blastocyst (3,5 dpc)	5 (26%)	4 (21%)	4 (21%)	6 (32%)	12

<b>Offspring and embryos from p120ctn<sup>KIC/+</sup> X p120ctn<sup>+/-</sup> crosses</b>					
stage	KIC/- (25%)	KIC/+ (25%)	+/- (25%)	+/+ (25%)	total
offspring	6 (21%)	6 (21%)	7 (25%)	9 (32%)	28
blastocyst (3,5 dpc)	7 (41%)	8 (47%)	0 (0%)	2 (12%)	17





**Figure 4. p120ctn<sup>KOC/KOC</sup> embryos die during preimplantation.** (A) Schematic representation of the targeting strategy for the generation of p120ctn<sup>KOC/+</sup> ES cells. Exon 11 is the alternatively spliced exon C. (B) Genotyping of wild-type (+/+), heterozygous (KOC/+) and homozygous (KOC/KOC) p120ctn KOC blastocysts by nested PCR using primers P1 and P2' (Fig. 3A). (C-E) Transmitted light micrographs, with either differential interference contrast (DIC) or bright field (BF), and immunofluorescence of p120ctn<sup>KOC/KOC</sup> and control embryos at the two-cell stage (C) and blastocyst stage (D-E). Double immunofluorescence for p120ctn and  $\beta$ -catenin was performed at the two-cell stage (C) and blastocyst stage (D). p120ctn co-localizes with  $\beta$ -catenin at the cell surface of two-cell stage blastomeres and blastocysts. Double immunofluorescence for Oct-4 and  $\beta$ -catenin (E). Similar expression is seen in p120ctn<sup>KOC/KOC</sup> and littermate control embryos. Non-specific staining was observed in the zona pellucida (D-E, p120ctn). In blastocysts p120ctn protein is expressed exclusively at the plasma membrane,  $\beta$ -catenin also shows nuclear staining, predominantly in the trophectoderm (D,E). Scale bar: 25  $\mu$ m.

An optimized protocol to be reported elsewhere allowed ES cell lines to be derived with success rates of up to 100% (Pieters et al., in preparation). Using this protocol, we tried to generate homozygous p120ctn KOC and KIC ES cell lines. Blastocysts from p120ctn<sup>KOC/+</sup> and p120ctn<sup>KIC/+</sup> intercrosses gave rise to several ES cell lines (9 and 35, respectively) but no homozygous p120ctn<sup>KOC/KOC</sup> or p120ctn<sup>KIC/KIC</sup> ES cell lines could be obtained (Pieters et al.,

## Mice harboring a knockout or knockin of exon C of p120ctn

in preparation). To increase the chance of retrieving living homozygous p120ctn KOC or KIC embryos, we tried starting the ES cell isolation from morulas instead of blastocysts. Unfortunately, ES cell isolation from morulas turned out to be much less efficient and only four ES lines could be isolated from 28 morulas. Although morulas derived from p120ctn<sup>KOC/+</sup> and p120ctn<sup>KIC/+</sup> intercrosses gave rise to ES cell lines (three and one, respectively), no homozygous p120ctn<sup>KOC/KOC</sup> or p120ctn<sup>KIC/KIC</sup> ES cell lines were obtained (Pieters et al., in preparation). Together these data indicate that homozygous p120ctn KOC and KIC embryos show early phenotypic abnormalities and appear in a non-Mendelian ratio.

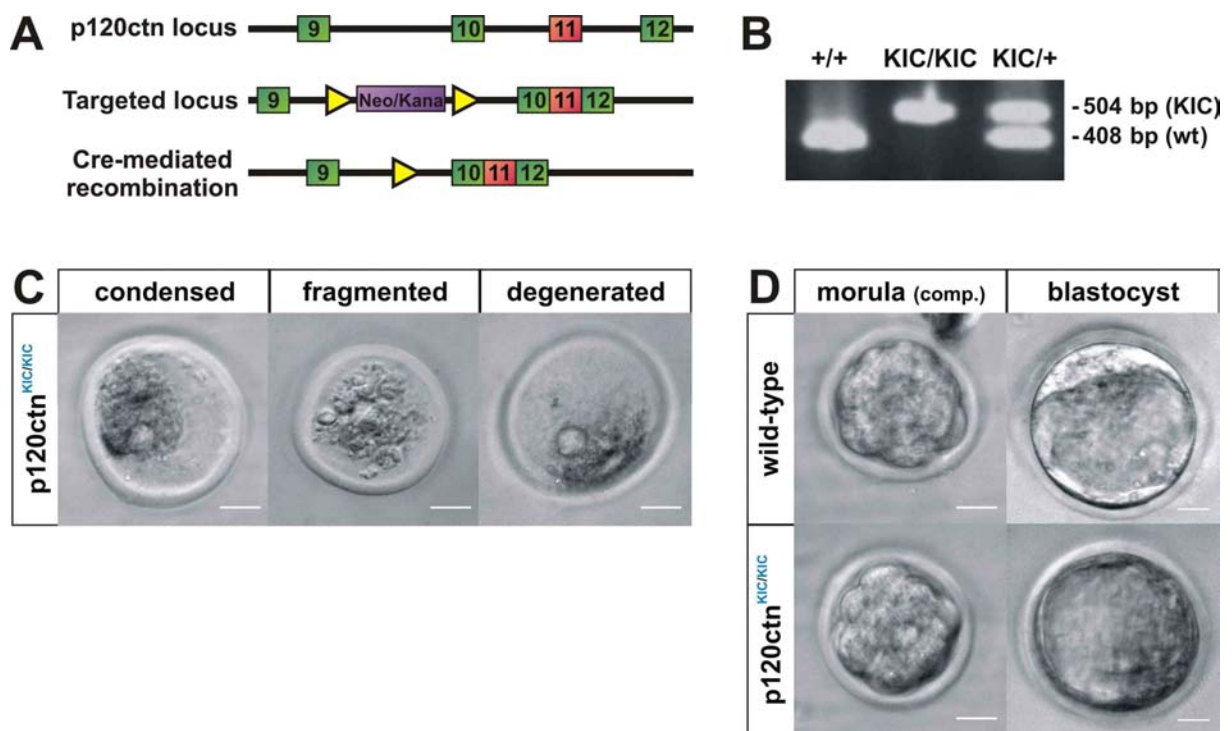


**Figure 5. p120ctn<sup>KIC/KIC</sup> embryos die during preimplantation.** (A) Schematic representation of the targeting strategy for the generation of p120ctn<sup>KIC/+</sup> ES cells. Exon 11 is the alternatively spliced exon C. (B) Genotyping of wild-type (+/+), heterozygous (KIC/+) and homozygous (KIC/KIC) p120ctn KIC blastocysts by nested PCR using primers P<sub>1</sub> and P<sub>2</sub>' (Fig. 3B). (C,D) Transmitted light micrographs of p120ctn<sup>KIC/KIC</sup> and control embryos. Most p120ctn<sup>KIC/KIC</sup> embryos were morphologically scored as condensed, fragmented or degenerated (C). Only one phenotypically normal p120ctn<sup>KIC/KIC</sup> morula and one blastocyst were recovered (D). Scale bar: 25 μm.

### **Homozygous p120ctn KOC and KIC embryos fail to implant**

Six pregnant females from p120ctn<sup>KOC/+</sup> intercrosses were sacrificed at various time points during gastrulation. All decidua obtained from each female were fixed, sectioned and examined histologically (Fig. 6). Embryos from each litter were staged according to the criteria proposed by Downs and Davies (1993). There was wide variation, as up to five different stages could be identified within a single litter (Figs. 6A,G). This is in line with previously published work (Downs and Davies, 1993). Of the 58 implantation sites that were examined, only one shows signs of embryo resorption (Figs. 6C,G). This corresponds to a normal frequency of naturally occurring resorption, and a similar ratio (1/52) was reported in control matings (Nichols et al., 1998). Therefore, no increase in implantation defects were observed in litters from p120ctn<sup>KOC/+</sup> intercrosses. This could indicate two things: either homozygous p120ctn<sup>KOC/KOC</sup> embryos implant normally, or they do not implant at all due to preimplantation mortality. The latter possibility is more likely because we could not identify any homozygous p120ctn<sup>KOC/KOC</sup> embryos during gastrulation by genotyping (n = 110, Table 3). We also performed histological analysis on implanting embryos (5.5 dpc) derived from p120ctn<sup>KOC/+</sup> intercrosses. From one litter, five embryos were identified, including an implanting blastocyst (Figs. 7A,B), three epiblast stage embryos (Figs. 7C-D), and a resorbed embryo (Fig. 7F). Our data are too preliminary to determine whether this resorption was caused by the genetic manipulation (homozygous p120ctn KOC embryos) or by natural decay. However, since there is no increase in the number of empty decidua during gastrulation (see above), the resorbed embryo is most likely a natural miscarriage.



Mice harboring a knockout or knockin of exon C of p120ctn

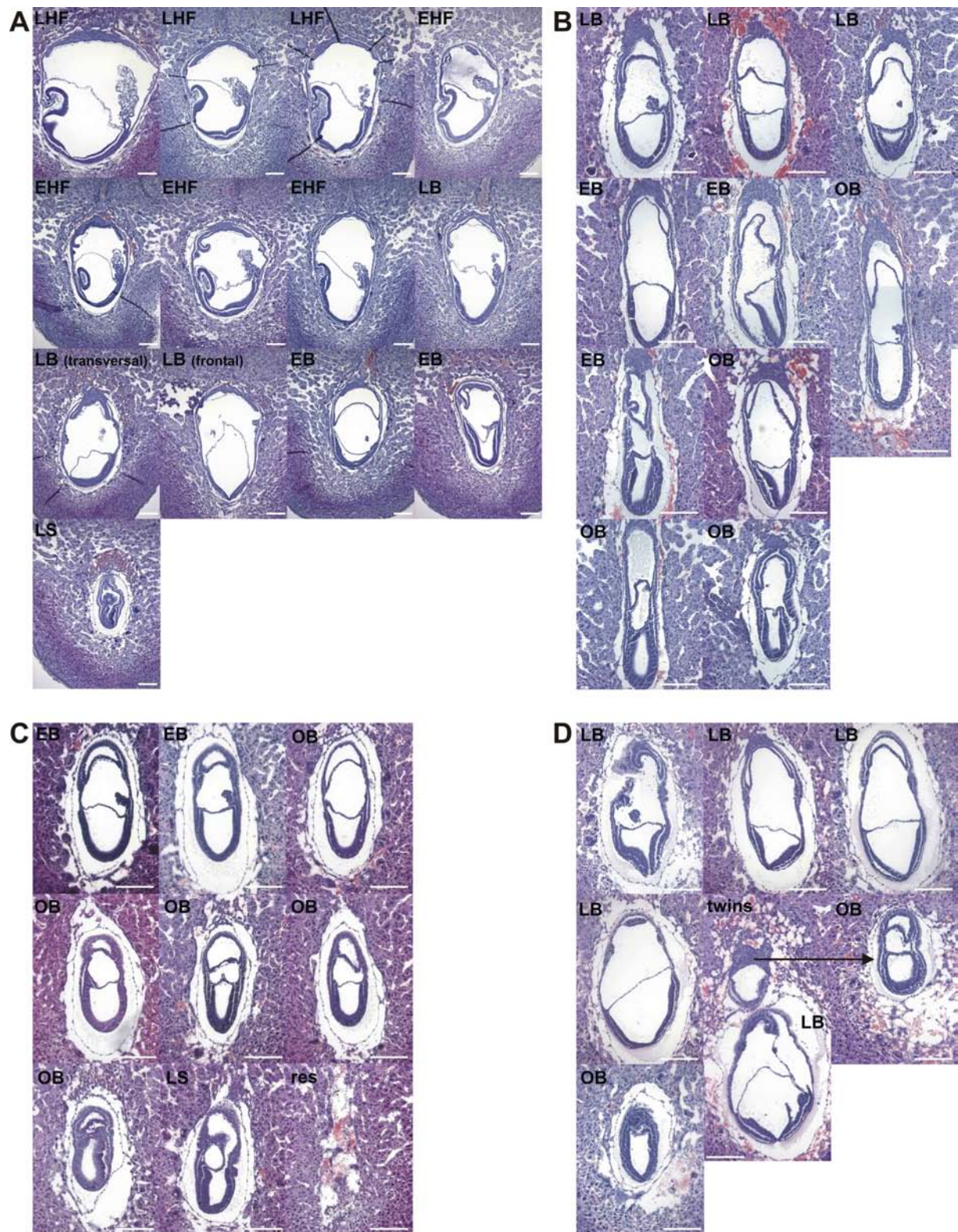


**Figure 6. Histological analysis of gastrulating embryos derived from  $p120ctn^{KOC/+}$  intercrosses.** Pregnant females were sacrificed at 8.75 dpc (A), 7.5 dpc (B-D), 7.0 dpc (E) and 6.5 dpc (F). All decidua from each offspring were sliced and stained with hematoxylin and eosin and a representative sagittal section is shown for each embryo. Non-sagittal section planes are indicated between brackets.



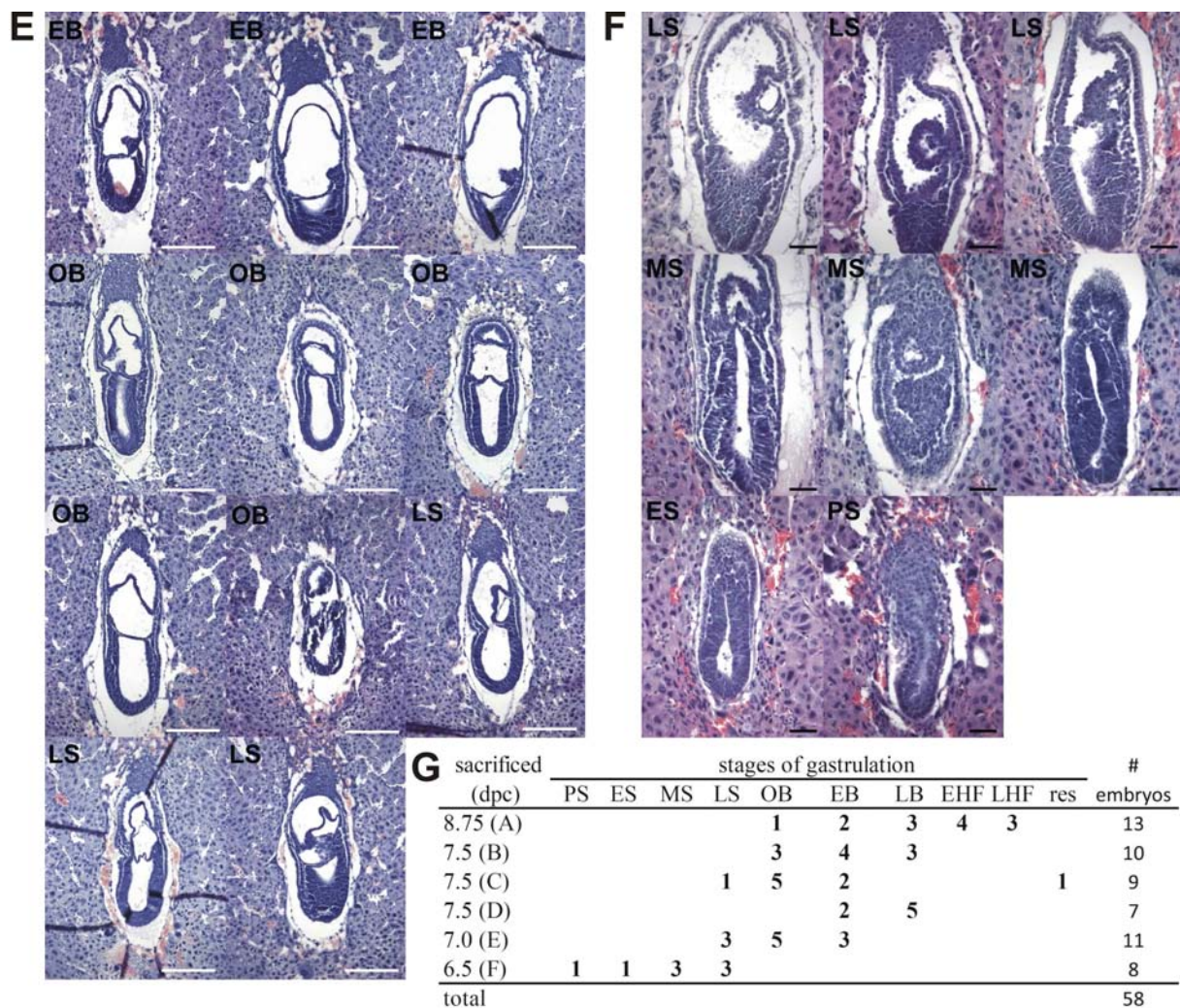


**Figure 6 (continued).** All gastrulating embryos were staged according the system of Downs and Davies (1993), including pre-streak (PS), early streak (ES), mid streak (MS), late streak (LS), no bud (OB), early bud (EB), late bud (LB), early headfold (EHF) and late headfold (LHF) stages. (G) Overview of the distribution of embryos according to their gastrulation stage in offspring that was sacrificed at different time points. res: resorbed. White scale bar: 200  $\mu$ m, black scale bar: 50  $\mu$ m.

Similar results were obtained for homozygous  $p120ctn^{KIC/KIC}$  mice. Two pregnant females from  $p120ctn^{KIC/+}$  intercrosses were sacrificed at 7.5 and 6.5 dpc, respectively. All embryos examined histologically and staged (Fig. 8). Thirteen implantation sites were examined and no resorbed embryos were found. Also, no homozygous  $p120ctn^{KIC/KIC}$  gastrulating embryos were identified by genotyping ( $n = 29$ , Table 3), indicating that homozygous  $p120ctn^{KIC/KIC}$  embryos, like homozygous  $p120ctn^{KOC/KOC}$  embryos, fail to implant and die before implantation.

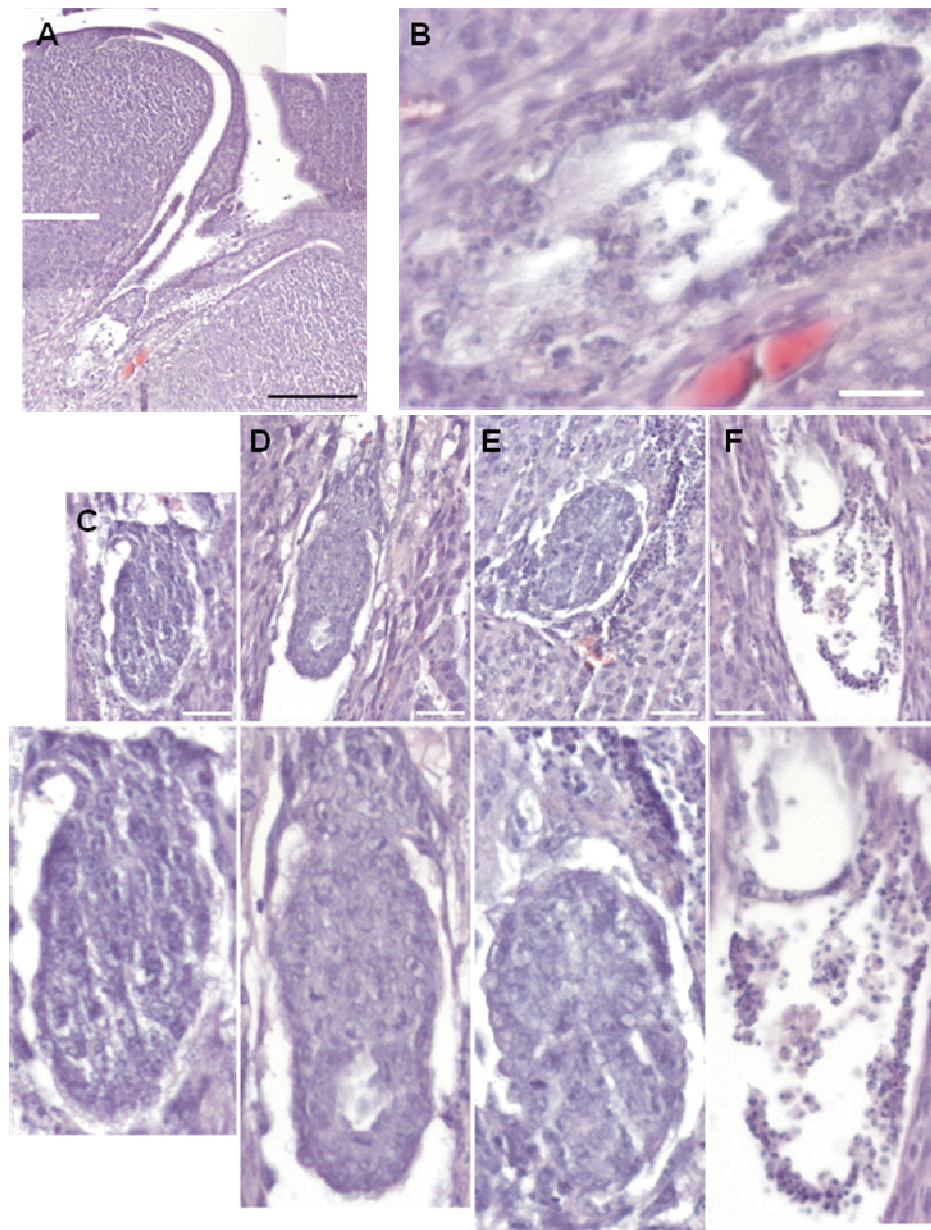


**Figure 7. Histological analysis of implantation stage embryos derived from  $p120ctn^{KOC/+}$  intercrosses.** Pregnant females were scarified at 5.5 dpc and decidua-containing uteri were fixed, sectioned, stained with hematoxylin and eosin and histologically analyzed. A representative section is shown for each embryo. This litter contained an implanting blastocyst (A, enlarged in B), several epiblast stage embryos (C-E) and one resorbed embryo (F). Black scale bar: 200  $\mu$ m, white scale bar: 50  $\mu$ m.



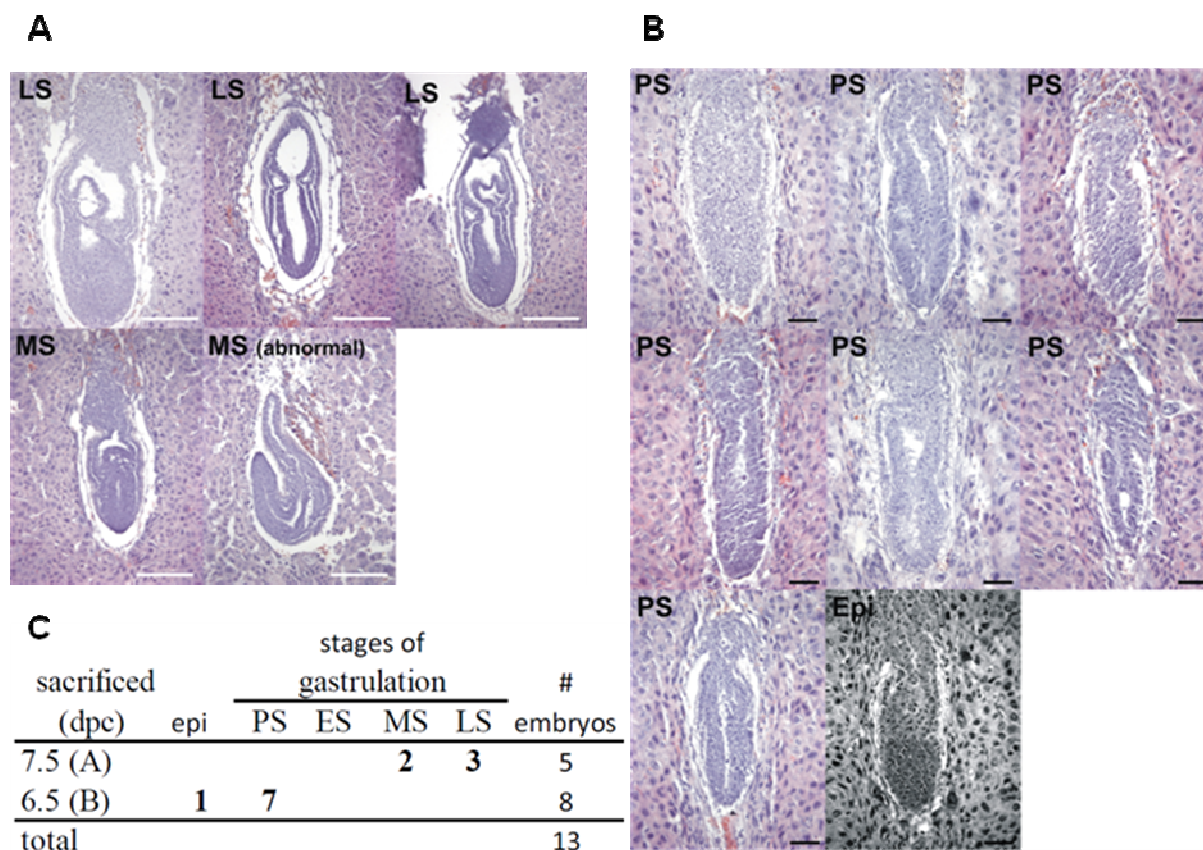


**Figure 8. Histological analysis of embryos derived of  $p12octn^{KIC/+}$  intercrosses during gastrulation.** Hematoxylin and eosin-stained sagittal paraffin sections of gastrulating embryos obtained from  $p12octn^{KIC/+}$  intercrosses. Pregnant females were sacrificed at 7.5 dpc (A) and 6.5 dpc (B). All decidua from each offspring were sectioned and a representative sagittal section is shown for each embryo. All gastrulating embryos were staged according the staging system of Downs and Davies (1993), including pre-streak (PS), early streak (ES), mid streak (MS) and late streak (LS). Epi: Epiblast stage. (C) Overview of the distribution of embryos according to their gastrulation stage in offspring that was sacrificed at different time points. White scale bar: 200  $\mu$ m, black scale bar: 50  $\mu$ m.

### Evolutionarily conserved p120ctn exon C is expressed during early development

What causes homozygous p120ctn KOC and KIC embryos to appear in a non-Mendelian ratio and how can their phenotypic abnormalities be explained? To address these matters, the p120ctn gene and its surrounding genomic region was analyzed in various species. p120ctn exon C (= exon 11) is one of the four alternatively used internal exons in the open reading frame of the human p120ctn gene (*CTNND1*) (Keirsebilck et al., 1998). Multiple sequence alignment of p120ctn orthologs ranging from humans to puffer fish revealed that p120ctn exon C is highly conserved amongst vertebrates (Fig. 9), which might indicate the putative functional importance of this alternatively used exon. Not only exon C is conserved but also the intronic flanking regions upstream (intron 10) and downstream (intron 11) of exon C have remained conserved during evolution, especially in mammals (Fig. 9,10). This conservation is not seen in the intronic sequences flanking the other p120cn exons. The intronic sequence flanking exon C is conserved for p120ctn, but to a lesser extent in its closest subfamily member, ARVCF (Fig. 11). The other two subfamily members CTNND2 and PKP4 do not have the exon C.

What is the function of this conserved intronic sequence flanking exon C? The highly conserved region could have a crucial functional or regulatory role that is affected in homozygous KOC and KIC embryos, as both p120ctn KOC and KIC alleles disrupt most of the conserved sequence (Fig. 10). Bioinformatic analysis revealed the presence of several features within this conserved block: two Rat O/E-1-associated zinc finger (Roaz) transcription factor binding sites, a lamin binding site and a miRNA-141 binding site (miR-141\*) (Fig. 10E). All these features are completely or partially compromised in both p120ctn KOC and KIC alleles (Fig. 10E). Interestingly, the abovementioned features are all involved in regulating gene expression, and altered gene expression might be causal for the early death in homozygous KOC and KIC embryos, which also appear in a non-Mendelian ratio. However, the underlying mechanism for these phenomena is still unknown.



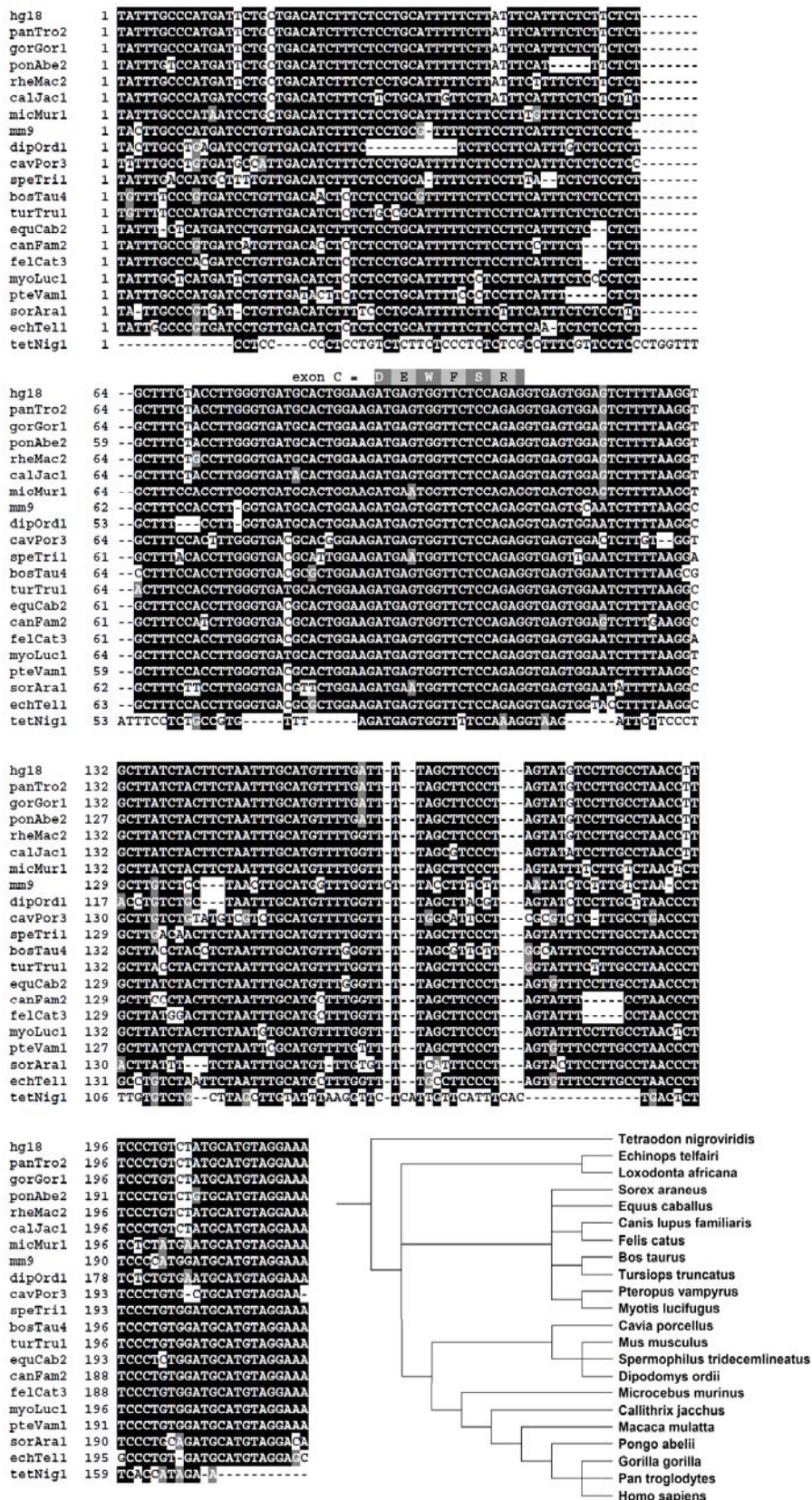
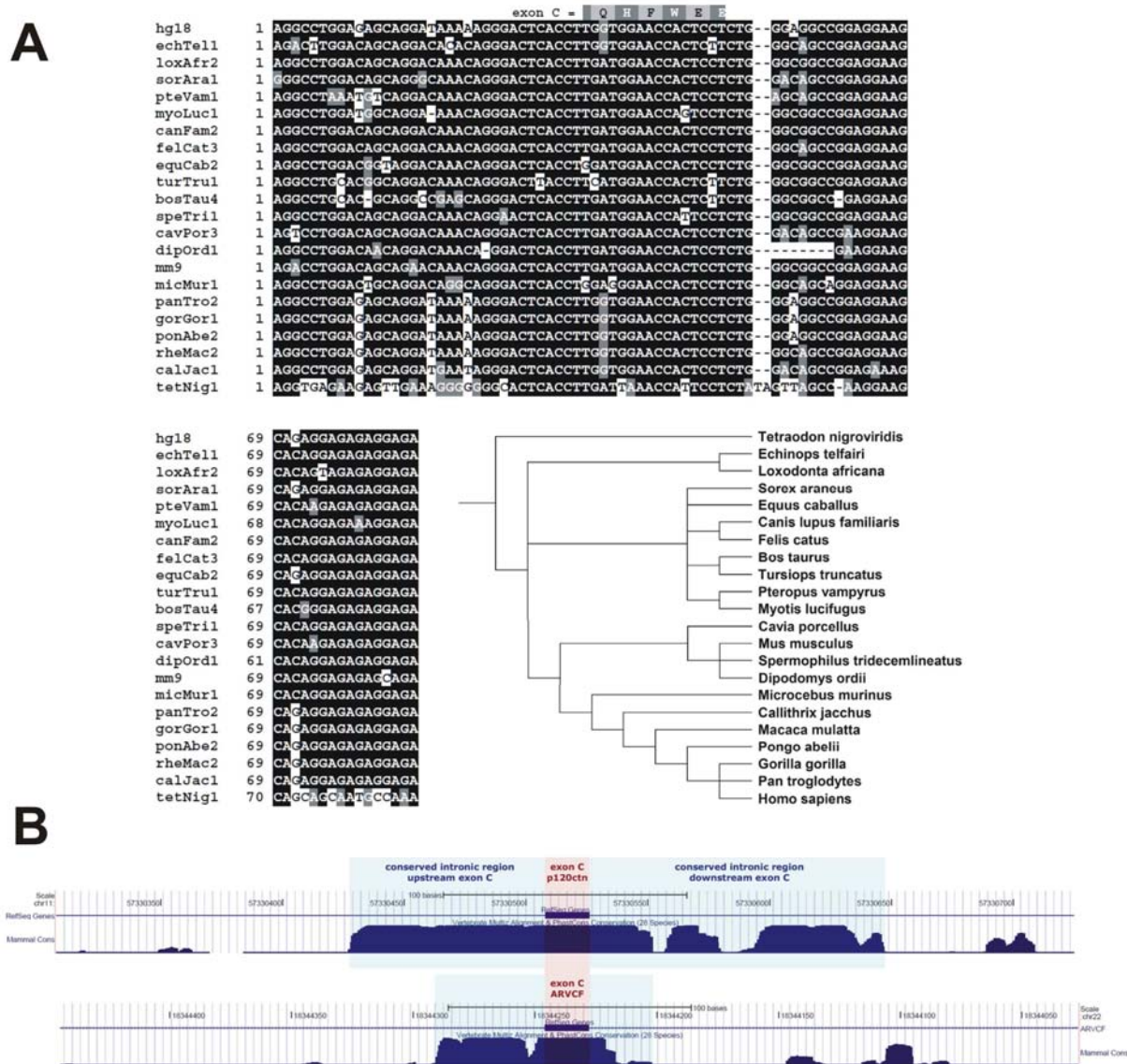


Figure 9. p12octn exon C and its surrounding intronic regions are highly conserved. Multiple sequence alignment of p12octn orthologs in vertebrates ranging from humans to puffer fish reveals that a 200 bp block, containing p12octn exon C and its flanking intronic sequences, are highly conserved amongst mammals.





**Figure 10. The conserved intronic region flanking p12octn exon C is compromised in both p12octn KOC and KIC alleles. UCSC diagrams. (A) A large cluster of olfactory receptor genes is situated upstream of the mouse *Ctnnd1* gene. (B) Ideogram of mouse chromosome 2, containing the *Ctnnd1* gene. (C) Full view of the *Ctnnd1* gene comprising 21 exons. (D) View of exons 10 to 14 of the *Ctnnd1* gene with 28 species alignment. The intronic sequences flanking exon C (= exon 11) are conserved, while the intronic sequences flanking of other exons are not conserved. p12octn KOC and KIC alleles both compromise the conserved sequence flanking exon C. (E) Detail of exon C and its flanking intronic sequence, showing the two Rat O/E-1-associated zinc finger (Roaz) transcription factor binding sites, a lamin-binding site and a miRNA-141 binding site (miR-141\*).**



**Figure 11. ARVCF exon C is also highly conserved but conservation of its surrounding intronic sequence is less prominent. (A) Multiple sequence alignment of ARVCF orthologs in vertebrates ranging from humans to puffer fish reveals that ARVCF exon C is also highly conserved in mammals, but its flanking intronic sequence is conserved to a lesser extent. (B) UCSC diagram showing a 28 species alignment for p12octn (top) and ARVCF (bottom) confirming that both p12octn exon C and are highly conserved, but the intronic sequence flanking ARVCF exon C is conserved to a lesser extent.**

### **Blastocysts from homozygous p120ctn knockout mice fail to stabilize E-cadherin at the cell membrane**

Strangely, the phenotypes of homozygous p120ctn KOC and KIC embryos (die before implantation, 3.5 dpc) are more severe than the phenotype of p120ctn null embryos, which die during gastrulation (7.5 dpc) (Davis and Reynolds, 2006; Elia et al., 2006). To bypass the early lethal phenotypes of homozygous p120ctn KOC and KIC embryos and their non-Mendelian inheritance, we wanted to combine the p120ctn null allele with the p120ctn KOC or KIC allele. First, we generated mice with heterozygous total p120ctn knock-out (p120ctn<sup>+/-</sup>) by removing floxed exons 3 to 8 (containing all four natural in-frame ATGs) by Cre-mediated recombination (Fig. 12B) (Betz et al., 1996; Davis and Reynolds, 2006). p120ctn<sup>+/-</sup> mice appeared indistinguishable from wild-type counterparts. However, no homozygous p120ctn knock-outs were found back in offspring of p120ctn<sup>+/-</sup> intercrosses (Table 3). This indicates that p120ctn<sup>-/-</sup> mice die during embryonic development, which corresponds to previously reported data (Davis and Reynolds, 2006; Elia et al., 2006). No p120ctn<sup>-/-</sup> embryos were found at 16.5 dpc (Table 3, Fig. 12A), but normal p120ctn<sup>-/-</sup> blastocysts could be recovered efficiently (Fig. 12C). p120ctn-deficient blastocysts were also E-cadherin negative (Fig. 12C, E-cadherin) compared to littermate control embryos, in which p120ctn and E-cadherin co-localized (Figs. 12C, merge). Only a small amount of membrane-localized E-cadherin is required for morula compaction *in vivo*, as maternal E-cadherin allows compaction in E-cadherin-deficient embryos (Larue et al., 1994) and de novo synthesized paternal E-cadherin allows compaction even in the absence of maternal E-cadherin (De Vries et al., 2004). So, we assumed that a limited amount of maternal p120ctn protein would also be present in p120ctn<sup>-/-</sup> embryos to allow stabilization of sufficient E-cadherin molecules at the cell membrane. Indeed, three-dimensional reconstruction of confocal images of p120ctn<sup>-/-</sup> blastocysts revealed a small amount of p120ctn staining above the background level, indicative of maternal p120ctn protein (Fig. 12D). This maternal p120ctn probably allows sufficient membrane expression of E-cadherin in p120ctn<sup>-/-</sup> embryos (Fig. 12D, arrowheads) to mediate morula compaction. This implies that p120ctn expression is the rate limiting factor for E-cadherin expression in young embryos. Together, these data confirm that p120ctn plays an important role by stabilizing E-cadherin levels at the cell membrane *in vivo* during embryonic development.

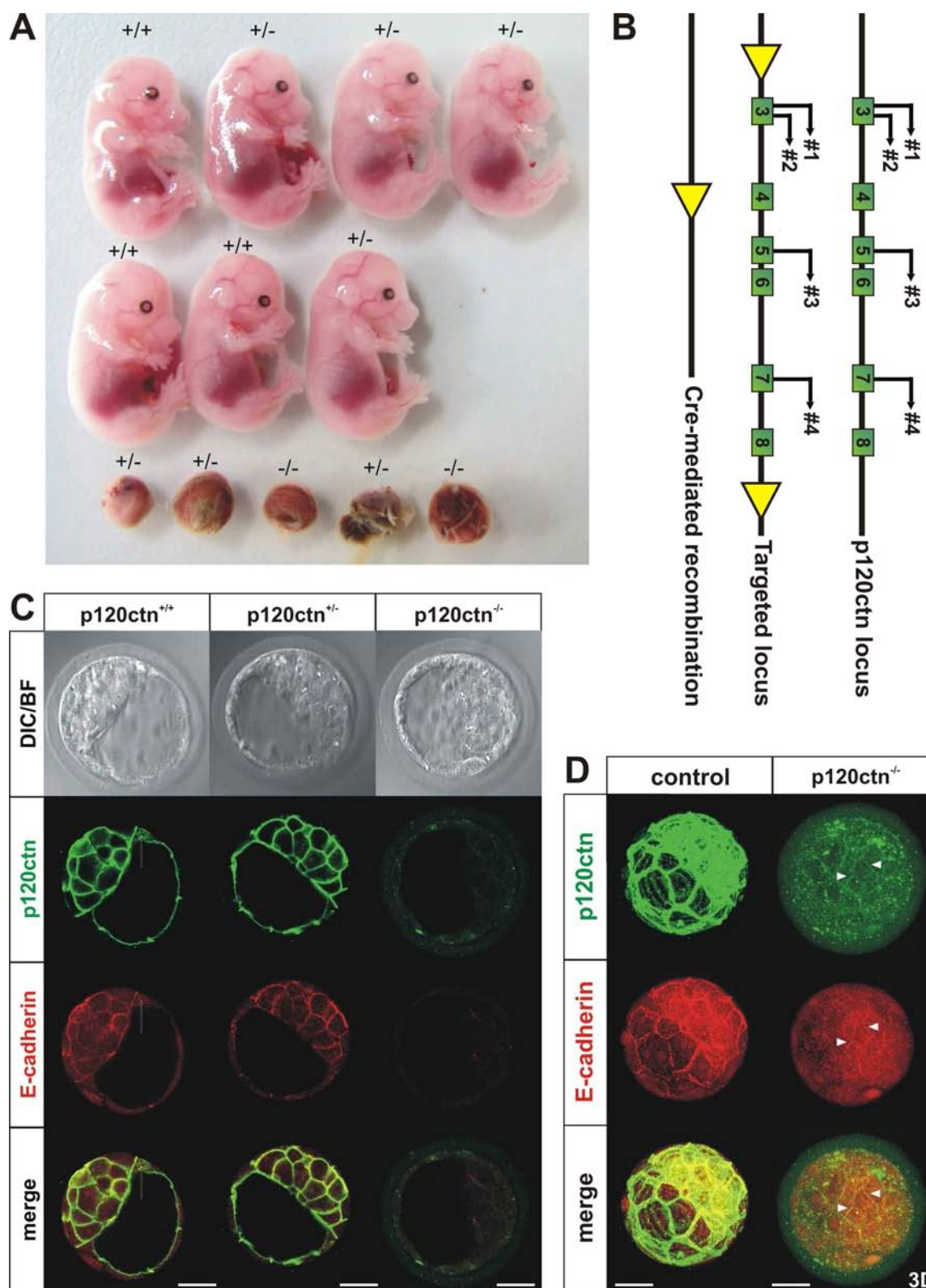


**Figure 12. A homozygous total p120ctn knock-out (p120ctn<sup>-/-</sup>) affects the E-cadherin levels in blastocyst.** (A) No normal p120ctn<sup>-/-</sup> embryos were found at 16.5 dpc in offspring derived from p120ctn<sup>+/-</sup> intercrosses. Two out of five resorbed embryos were genotyped as p120ctn<sup>-/-</sup>. (B) Diagram of wild-type, p120ctn floxed and p120ctn null alleles. Floxed p120ctn mice have loxP sites flanking a genomic region containing exons 3 to 8 (encoding for all 4 translation initiation sites).

**Figure 12 (continued).** (C) Transmitted light micrographs and immunostainings of wild-type (p120ctn<sup>+/+</sup>), heterozygous (p120ctn<sup>+/-</sup>) and homozygous (p120ctn<sup>-/-</sup>) p120ctn knock-out blastocysts. p120ctn-deficient embryos form normal blastocysts. Double immunofluorescence for p120ctn and E-cadherin (DECMA-1). Wild-type and heterozygous p120ctn knock-out blastocysts show membrane staining for p120ctn both in the trophoctoderm and in the inner cell mass. Only a very faint cell surface signal for p120ctn was seen in homozygous p120ctn knock-out blastocysts. Almost no E-cadherin staining could be observed in p120ctn<sup>-/-</sup> blastocysts compared to wild-type and heterozygous p120ctn mutant littermate controls. p120ctn co-localizes with E-cadherin at the membrane of wild-type and p120ctn<sup>+/-</sup> blastocysts. (D) Maternal p120ctn allows basal E-cadherin stabilization on the membrane of p120ctn-deficient blastocysts. Three-dimensional (3D) reconstruction using consecutive confocal sections of the blastocysts shown in C. The limited amount of maternal p120ctn in p120ctn-deficient embryos (p120ctn<sup>-/-</sup>, arrowheads) allows the stabilization of basal E-cadherin levels (arrowheads) on the membrane of blastocysts. This is sufficient for normal compaction and blastocyst formation. Scale bar: 25  $\mu$ m.

### **p120ctn<sup>KOC/-</sup> and p120ctn<sup>KIC/-</sup> mice are viable and can stabilize E-cadherin at the cell membrane of blastocysts**

To circumvent the biallelic removal of the conserved intronic sequence around exon 11 in homozygous p120ctn KOC and KIC mice, we crossed p120ctn<sup>KOC/+</sup> and p120ctn<sup>KIC/+</sup> mice with p120ctn<sup>+/-</sup> mice to produce p120ctn<sup>KOC/-</sup> and p120ctn<sup>KIC/-</sup> mice, respectively. In this way, an isoform-specific p120ctn KOC or KIC allele is combined with a p120ctn knock-out allele in which exons 3 to 8 are ablated but that still contains an unmodified version of the conserved intronic sequence flanking p120ctn exon C (= exon 11). Remarkably, both the p120ctn KOC and KIC alleles could rescue the lethal p120ctn<sup>-/-</sup> phenotype, as both p120ctn<sup>KOC/-</sup> and p120ctn<sup>KIC/-</sup> were viable (Table 3). Viable p120ctn<sup>KOC/-</sup> and p120ctn<sup>KIC/-</sup> embryos were also found at the level of blastocysts, and largely according to the Mendelian ratio (Table 3). In these blastocysts, p120ctn localized at cell-cell contacts (but not at the free membranes) together with other members of the cadherin-catenin complex, which was also seen in littermate controls (Figs. 13B,C and Figs. 14A,C,D). p120ctn isoforms, whether expressed as isoform C or not, could stabilize E-cadherin levels at the plasma membrane of blastocysts (Figs. 13B,C; E-cadherin) compared to p120ctn<sup>-/-</sup> blastocysts (Fig. 13A). Similar to findings with rare p120ctn<sup>KOC/KOC</sup> blastocysts (Fig. 5E), the number of pluripotent ICM cells in p120ctn<sup>KOC/-</sup> blastocysts (Fig. 14B) was similar to that in controls. In conclusion, in p120ctn<sup>KOC/-</sup> and p120ctn<sup>KIC/-</sup> mice the lethal phenotype of p120ctn is rescued as well as the failure to stabilize E-cadherin levels *in vivo*.



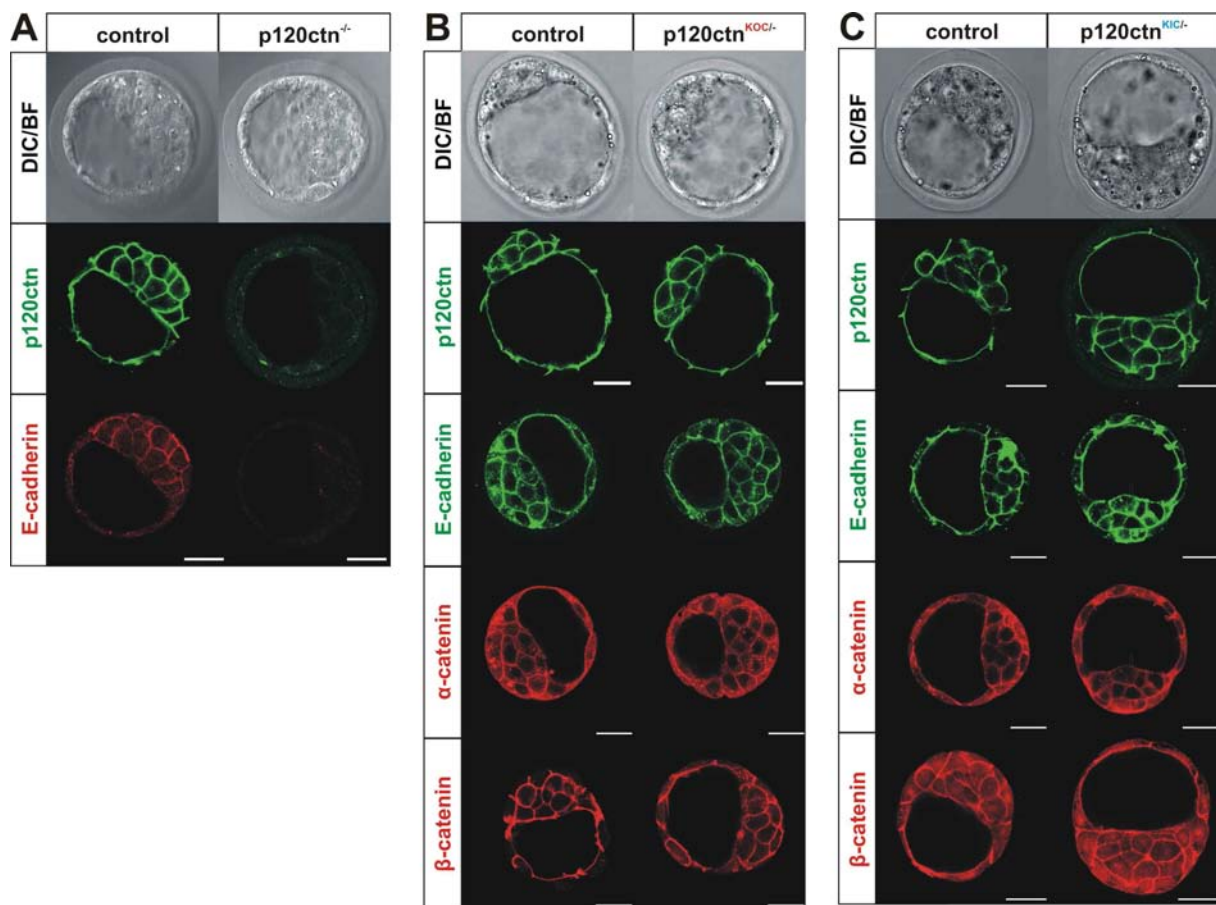


**Figure 13. p120ctn KOC or KIC alleles restored E-cadherin levels, which were affected in homozygous total p120ctn knock-out (p120ctn<sup>-/-</sup>) blastocysts.** Transmitted light micrographs and immunostainings homozygous (p120ctn<sup>-/-</sup>) p120ctn knock-out blastocysts and blastocysts containing one p120ctn knock-out allele, combined with either an p120ctn KOC allele (p120ctn<sup>KOC/-</sup>) or an p120ctn KIC allele (p120ctn<sup>KIC/-</sup>). **(A)** E-cadherin is reduced in p120ctn null blastocysts. **(B)** Isoform C-depleted p120ctn (p120ctn<sup>KOC/-</sup>) restores E-cadherin levels in blastocysts. Control and p120ctn<sup>KOC/-</sup> blastocysts show membrane staining of p120ctn protein in both the trophectoderm and the inner cell mass. Immunostaining for E-cadherin (BD antibody) shows that p120ctn depleted of isoform C (p120ctn<sup>KOC/-</sup>) stabilizes E-cadherin at the cell surface of blastocysts to a level similar to that in littermate controls. Also similar levels of αE-catenin and β-catenin were found in p120ctn<sup>KOC/-</sup> and control embryos. **(C)** Isoform C-containing p120ctn (p120ctn<sup>KIC/-</sup>) also restores E-cadherin levels in blastocysts, and the expression of catenins in p120ctn<sup>KIC/-</sup> mouse embryos is similar to that in controls. Scale bar: 25 μm.

Mice harboring a knockout or knockin of exon C of p120ctn

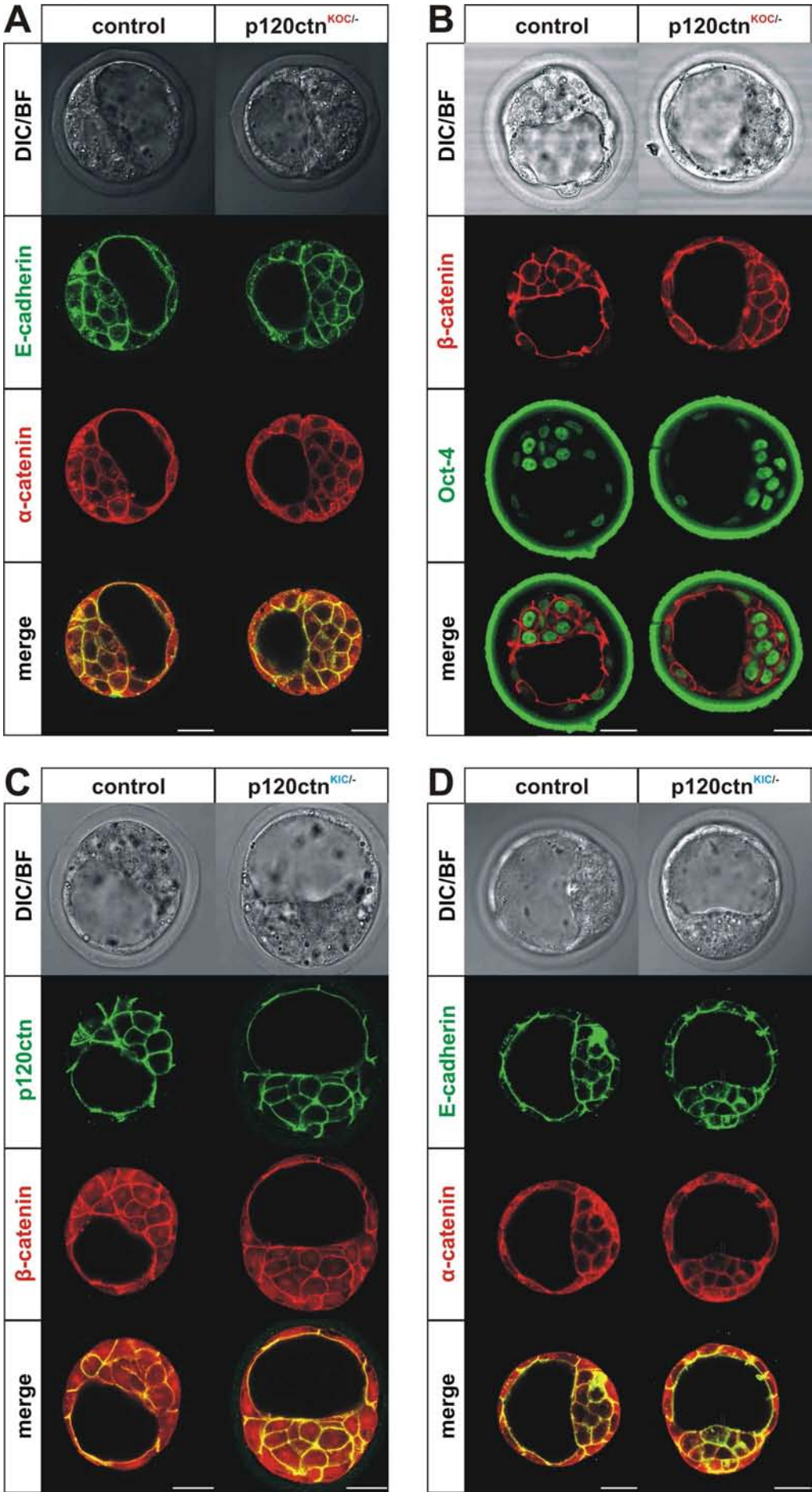




**Figure 18. Double immunostainings on p120ctn<sup>KOC/-</sup> (A,B), p120ctn<sup>KIC/-</sup> (C,D) and control blastocysts.** (A) Double immunofluorescence for E-cadherin (BD antibody) and  $\alpha$ E-catenin. E-cadherin co-localizes with  $\alpha$ E-catenin at the cell surface of control and p120ctn<sup>KOC/-</sup> blastocysts. (B) Double immunofluorescence for  $\beta$ -catenin and Oct-4. Similar cell surface expression pattern for  $\beta$ -catenin was found in both control and p120ctn<sup>KOC/-</sup> blastocysts. Nuclear Oct-4 staining was observed in the ICM and to a smaller extent in trophectoderm in both control and p120ctn<sup>KOC/-</sup> blastocysts. (C) Double immunofluorescence for p120ctn and  $\beta$ -catenin. p120ctn protein co-localizes with  $\beta$ -catenin at the membrane in control and p120ctn<sup>KIC/-</sup> blastocysts, both in ICM and trophectoderm. (D) Double immunofluorescence for E-cadherin (BD antibody) and  $\alpha$ E-catenin. E-cadherin co-localizes with  $\alpha$ E-catenin at the plasmamembrane of control and p120ctn<sup>KIC/-</sup> blastocysts. DIC: differential interference contrast, BF: bright field. Scale bar: 25  $\mu$ m.

### Generation and characterization of p120ctn<sup>KOC/-</sup> and p120ctn<sup>KIC/-</sup> ES cell lines

We generated ES cell lines from blastocysts derived from mating p120ctn<sup>KOC/+</sup> and p120ctn<sup>KIC/+</sup> mice with p120ctn<sup>+/-</sup> mice. For both matings, efficiency of ES cell derivation was 100% and the genotypes of the ES cells isolated followed a Mendelian distribution (Pieters et al., in preparation). This resulted in two p120ctn<sup>KOC/-</sup>, three p120ctn<sup>KIC/-</sup> and several littermate control ES cell lines. p120ctn<sup>KOC/-</sup>, p120ctn<sup>KIC/-</sup> and control ES cell lines were all positive for the stem cell marker Oct-4 (Fig. 15) and they showed staining for all members of the classic cadherin-catenin complex at the plasma membrane of ES cell colonies (Fig. 15). Since the six amino acids, encoded by exon C of p120ctn, interrupted internal sequence that is important for RhoA inhibition, we were interested in the active RhoA levels in p120ctn<sup>KOC/-</sup> and p120ctn<sup>KIC/-</sup> ES cell lines compared to control lines. Our hypotheses, based on literature and *in vitro* experiments, is that p120ctn<sup>KIC/-</sup> ES cell lines would have increased RhoA activity, as a result of blocking RhoA inhibition by interrupting the second RhoA-binding domain of p120ctn. p120ctn<sup>KOC/-</sup> and control ES cell lines would exhibit similar RhoA levels, since their second RhoA-binding domain is left untouched. However, no difference in basal or LPA-induced RhoA activity could be observed between p120ctn<sup>KOC/-</sup>, p120ctn<sup>KIC/-</sup> and control ES cell lines (Fig. 16). Inhibition of the downstream RhoA effector ROCK (Y-27632) in p120ctn<sup>KOC/-</sup>, p120ctn<sup>KIC/-</sup> and control ES cell lines did not affect the RhoA activity (Fig. 16) but showed a general and robust cell growth promoting effect. This proliferation effect caused by Y-27632-treatment is supported by increased protein content in Y-27632-treated ES cells (90.18 +/- 0.69), compared to untreated (80,92 +/- 0.72) or LPA-treated (80.30 +/- 0.97) ES cells (an equal amount of ES cells were seeded for each condition).

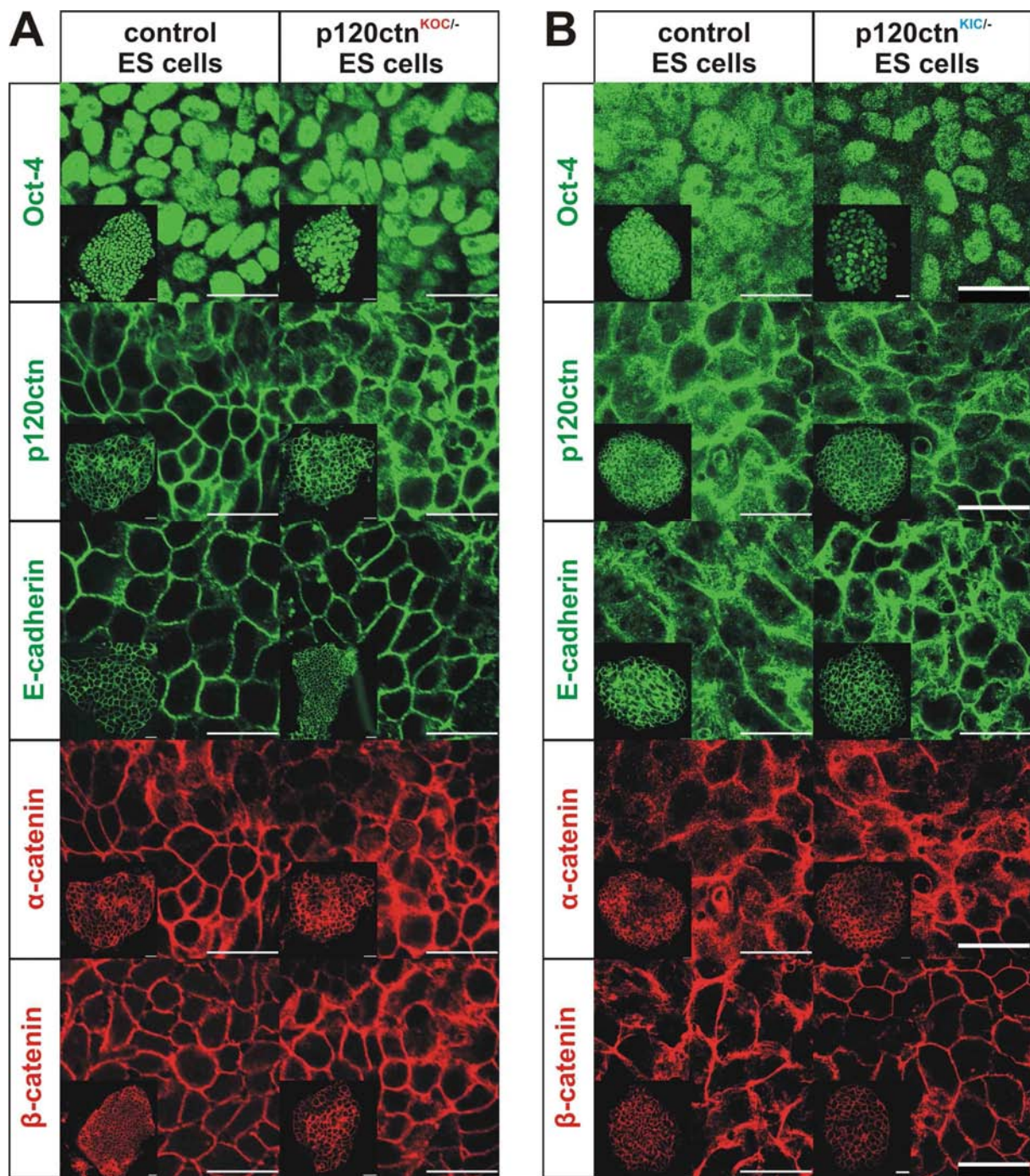


**Figure 15. Characterization of p120ctn<sup>KOC/-</sup> and p120ctn<sup>KIC/-</sup> ES cell lines.** Confocal sections of immunostainings for stem cell marker Oct-4 and for members of the cadherin-catenin complex in p120ctn<sup>KOC/-</sup> (A), p120ctn<sup>KIC/-</sup> (B) and control ES cell lines. A magnification and a complete view (inset) of single ES cell colonies are shown. p120ctn<sup>KOC/-</sup> ES (A), p120ctn<sup>KIC/-</sup> ES (B) and control cell lines show nuclear Oct-4 staining in all the cells. A similar honeycomb pattern was observed for p120ctn, E-cadherin, αE- and β-catenin at the membrane of p120ctn<sup>KOC/-</sup> ES (A), p120ctn<sup>KIC/-</sup> ES (B) and control cell lines. Scale bar: 25 μm.

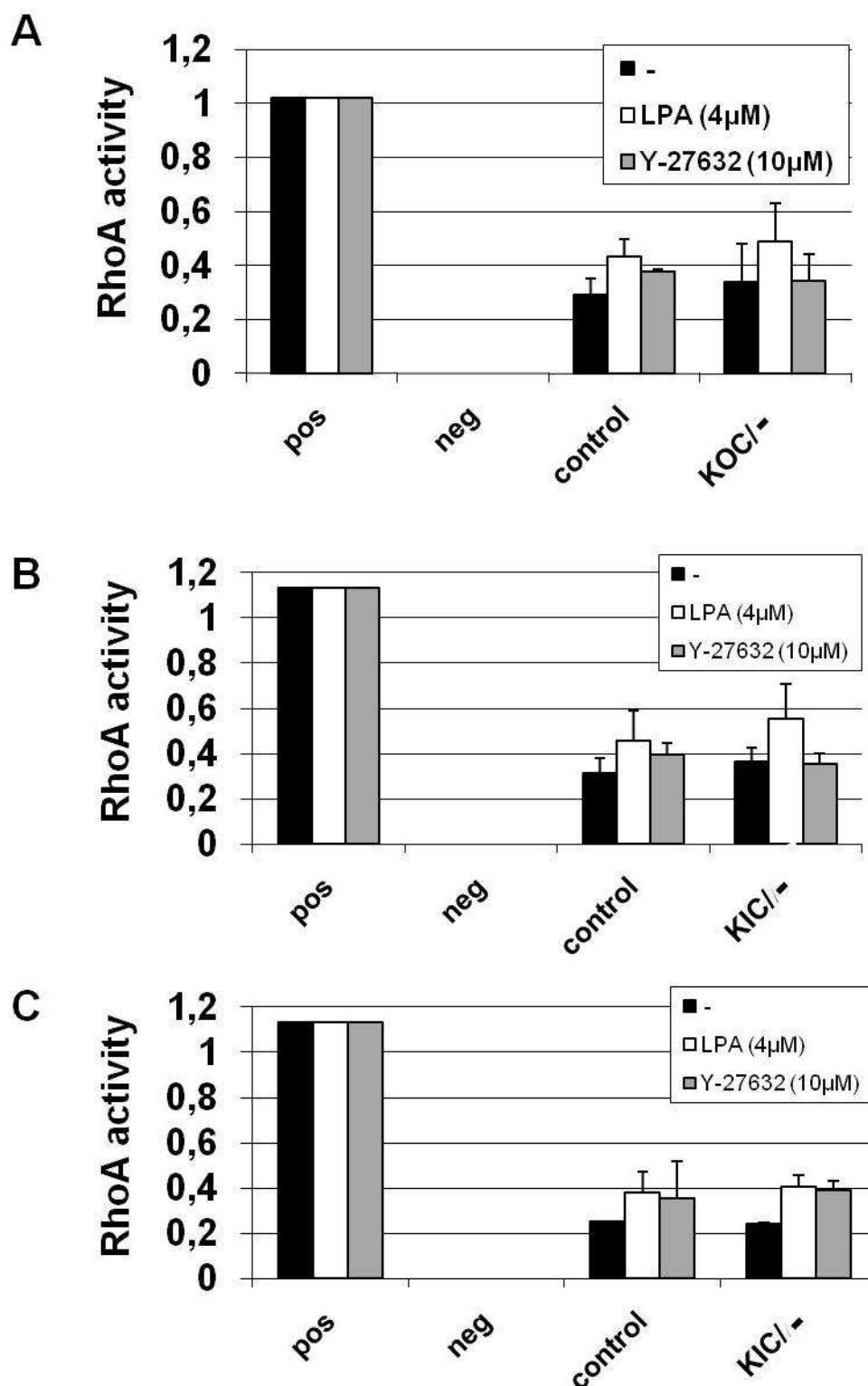


**Figure 16. p120ctn isoform C has no effect on RhoA activity in ES cells.** G-LISA based RhoA activity assays were performed on p120ctn<sup>KOC1<sup>-/-</sup></sup> (A), p120ctn<sup>KIC1<sup>-/-</sup></sup> (B,C) and littermate control ES cell lines. ES cells were either left untreated or treated with 4 µM lysophosphatidic acid (LPA) or 10 µM ROCK inhibitor Y-27632. No difference was observed in basal or LPA-induced RhoA activity between p120ctn<sup>KOC1<sup>-/-</sup></sup> (A) and p120ctn<sup>KIC1<sup>-/-</sup></sup> ES cell lines (B) compared to control ES cell lines. Similar results were obtained for p120ctn<sup>KIC1<sup>-/-</sup></sup> ES cell lines cultured in the absence of MEFs (C).

## Mice harboring a knockout or knockin of exon C of p120ctn

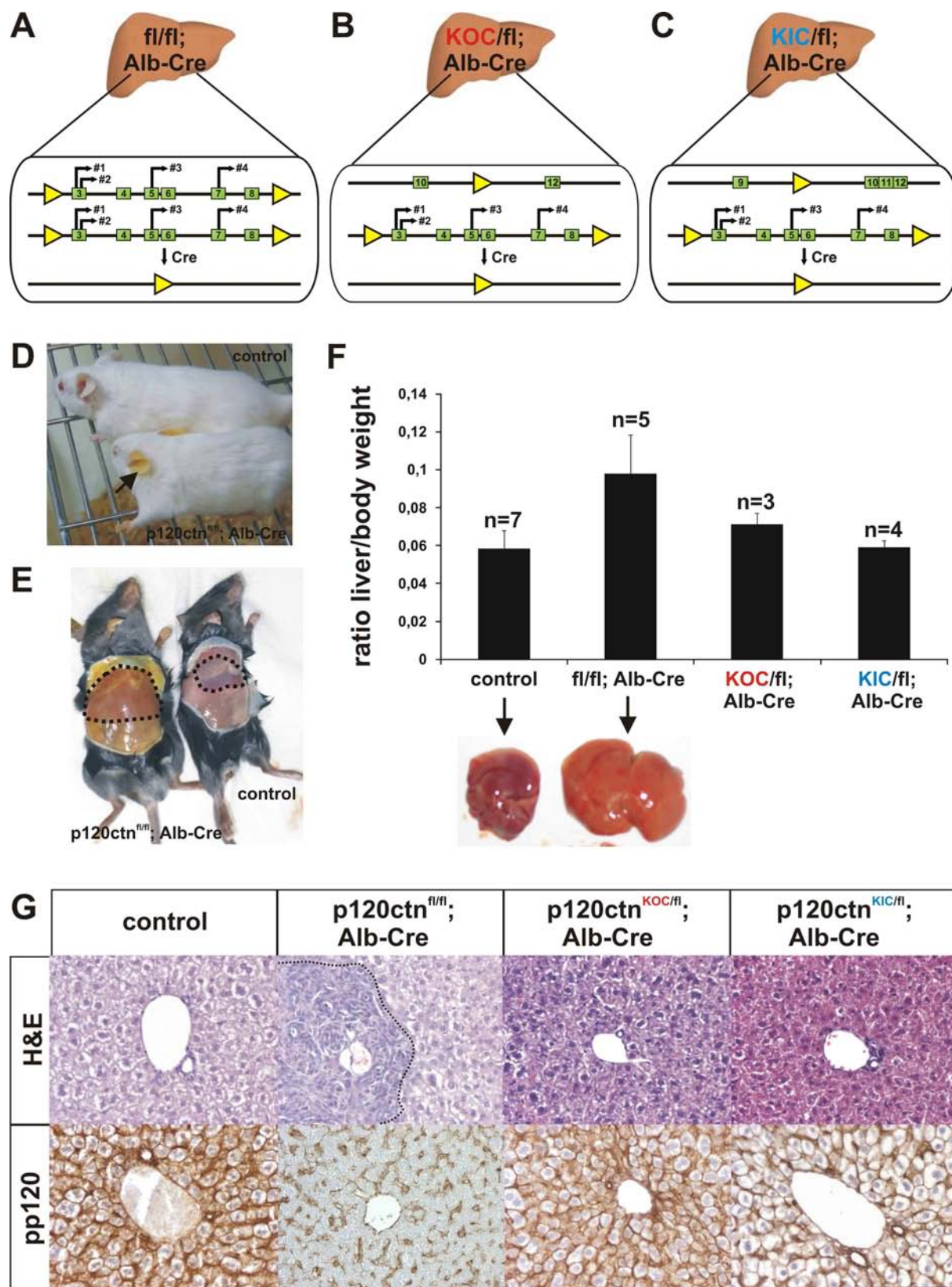
A similar Y-27632-mediated increase in proliferation was reported for the passaging of human ES cells (Gauthaman et al., 2010). We conclude that both isoform C-depleted ( $p120ctn^{KOC/-}$ ) and isoform C-deficient ( $p120ctn^{KIC/-}$ ) p120ctn proteins allow the assembly of normal cadherin-catenin complexes but do not have any influence on RhoA activity in ES cells.

### **Both the p120ctn KOC and KIC allele can rescue defects seen in p120ctn-deficient livers.**

To bypass the early death that was observed in homozygous  $p120ctn^{KOC/KOC}$  and  $p120ctn^{KIC/KIC}$  embryos, we used an additional strategy that involved a liver-specific ablation of p120ctn. By using the Cre-LoxP system we could obtain liver-specific p120ctn knock-out mice ( $p120ctn^{fl/fl}; Alb-Cre$ ) (Fig. 17A), which are viable and fertile but showed several macroscopic and microscopic phenotypes, including jaundice (Figs. 17D, E), hepatomegaly (Fig. 17F), and ductular reactions in the portal region (Fig. 17G). The liver weight to body weight ratio of  $p120ctn^{fl/fl}; Alb-Cre$  mice was about 2-fold higher than that of control littermates (Fig. 17F). Histological analysis revealed that bile duct cells, which are single layered and positive for p120ctn staining in control mice (Fig. 17G, inset) are dysplastic and multilayered in p120ctn-deficient livers (Fig. 17G, left from dotted line). p120ctn is ubiquitously expressed in all cell types of wild-type livers, whereas hepatocytes and bile duct cells do not show staining for p120ctn in  $p120ctn^{fl/fl}; Alb-Cre$  mice (Fig. 17G). Ductular reactions are seen in a variety of liver diseases and refer to an increased number of ductules, which are accompanied by immune cells (polymorphonuclear leukocytes) and matrix, leading to periportal fibrosis and eventually biliary cirrhosis (Roskams and Desmet, 1998). Ductular reactions thus are composed of a heterogenous mixture of different cell types, some of which still express p120ctn. These p120ctn-positive cells might be liver precursor cells, which have not undergone Cre-mediated recombination, or infiltrating immune cells.

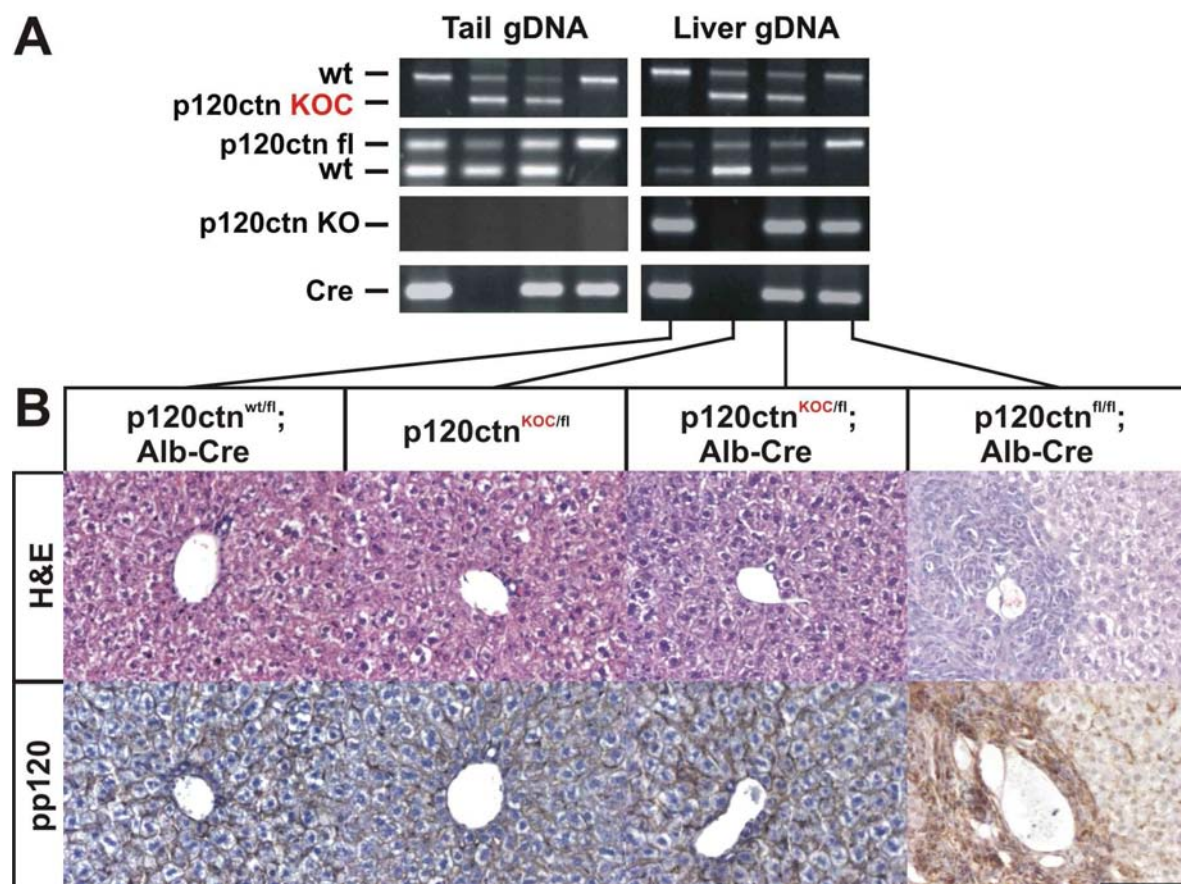
By crossing  $p120ctn^{fl/fl}; Alb-Cre$  mice with  $p120ctn^{KOC/+}$  or  $p120ctn^{KIC/+}$  mice we can obtain mice with livers in which every transcript excludes ( $p120ctn^{KOC/fl}; Alb-Cre$ ) or includes ( $p120ctn^{KIC/fl}; Alb-Cre$ ) the alternatively spliced exon C (Fig. 17B,C). p120ctn isoforms lacking or expressing the exon C-encoded amino acids are expressed from the p120ctn KOC and p120ctn KIC allele, respectively (Fig. 17G). Both p120ctn isoforms are capable of rescuing the phenotypes seen in  $p120ctn^{fl/fl}; Alb-Cre$  mice, including the jaundice, the hepatomegaly (Fig. 17F) and the ductular reactions (Fig. 17G).





**Figure 17. p120ctn ablation in mouse livers causes jaundice, hepatomegaly and ductular reactions.** (A) diagram of a liver-specific Cre-mediated excision of exons 3 to 8 of p120ctn containing all 4 start codons. (B) Jaundice in paws and ears (arrow) of p120ctn<sup>fl/fl</sup>; Alb-Cre mice. (C) Hepatomegaly and jaundice are apparent in p120ctn deficient livers. (D) graphic showing the liver weight/body weight ratio of control and p120ctn<sup>fl/fl</sup>; Alb-Cre mice and their corresponding dissected livers (inset). (E) Histology and p120ctn immunohistochemistry for control and p120ctn<sup>fl/fl</sup>; Alb-Cre liver sections. Scale bar: 200 μm.

Additional littermate controls and their corresponding genotypes for liver-specific p120ctn KOC (p120ctn<sup>KOC/+</sup> x p120ctn<sup>fl/fl</sup>; Alb-Cre) and p120ctn KIC (p120ctn<sup>KIC/+</sup> x p120ctn<sup>fl/fl</sup>; Alb-Cre) matings, respectively, are shown in Figure 18. Livers that constitutively express or lack the exon C-encoded amino acids provide a good model for testing our polyclonal antibody pAbexC that specifically recognizes p120ctn isoform C. However, we did not see an increased detection of p120ctn isoforms containing the exon C-encoded amino acids in p120ctn<sup>KIC/fl</sup>; Alb-Cre livers via western blotting or via immunohistochemistry (data not shown). In conclusion, both p120ctn KOC and KIC alleles can functionally rescue the genetic p120ctn inactivation in liver.





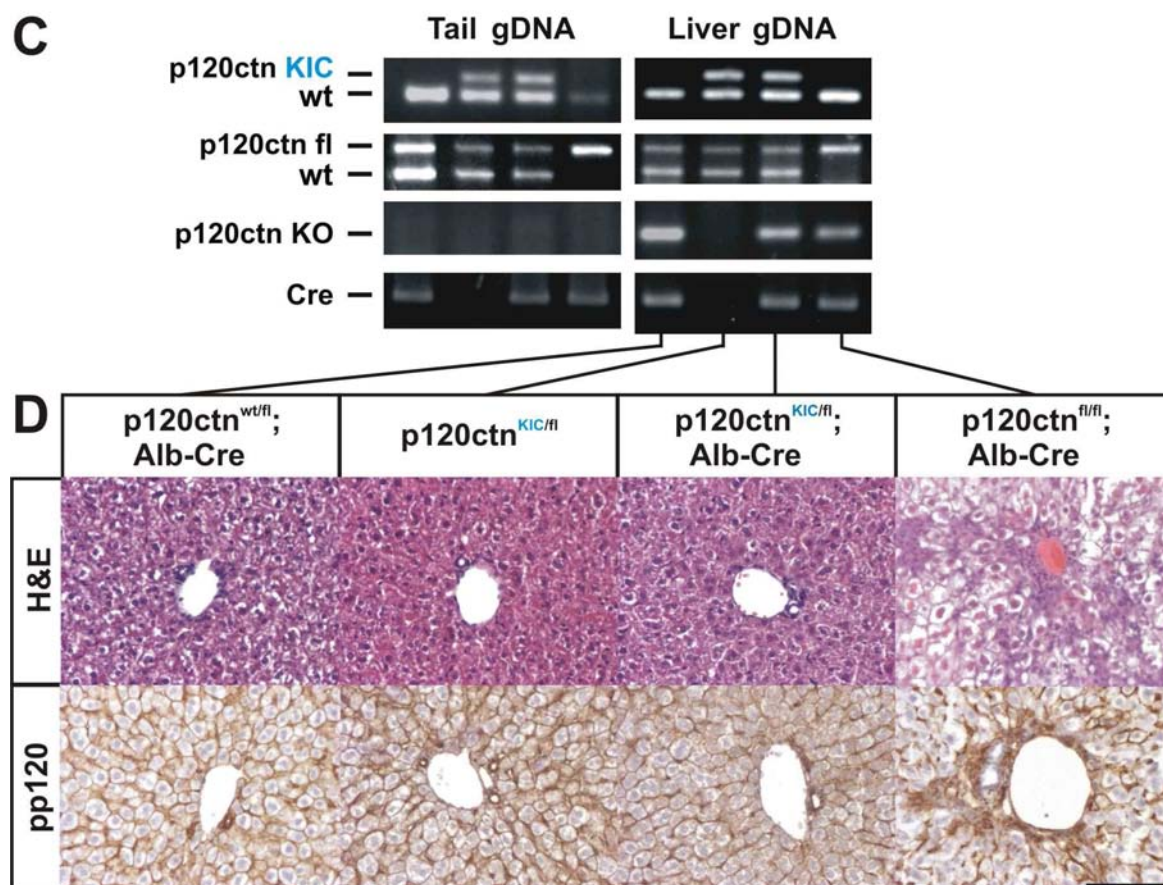


**Figure 18.** Genotype (A, C), histology and p120ctn immunohistochemistry (B, D) from offspring from crossing either p120ctn<sup>KOC/+</sup> mice (A, B) or p120ctn<sup>KIC/+</sup> mice (C, D) with p120ctn<sup>fl/fl</sup>; Alb-Cre mice. Liver-specific p120ctn knock-out mice (p120ctn<sup>fl/fl</sup>; Alb-Cre) mice were used as control. Five-week-old mice were analyzed. Scale bar: 200  $\mu$ m.

## DISCUSSION

### Interplay between p120ctn and E-cadherin *in vivo*

Several *in vitro* studies have revealed a role for p120ctn in the stabilization and turnover of classical cadherins, such as E-, VE- and N-cadherin on the cell membrane of epithelial (Davis et al., 2003), endothelial (Xiao et al., 2003) and fibroblast (Chen et al., 2003) cells, respectively. By tissue-specific ablation of p120ctn in salivary gland, skin, gastrointestinal tract and forebrain, the role of p120ctn in stabilizing cadherins could be reproduced *in vivo* in adult tissue (Davis and Reynolds, 2006; Elia et al., 2006; Perez-Moreno et al., 2006; Smalley-Freed et al., 2010). We show that p120ctn is important for proper levels of E-cadherin at the cell surface during early development because mice with a full knockout

## Mice harboring a knockout or knockin of exon C of p120ctn

of p120ctn (p120ctn<sup>-/-</sup>) fail to stabilize E-cadherin in blastocysts (Fig. 13A). We could rescue cell surface E-cadherin *in vivo* by crossing in p120ctn alleles that either constitutively deplete or constitutively express p120ctn isoform C (Figs. 13B,C). Because both p120ctn variants (with or without the six amino acids encoded by exon C) are equally competent in rescuing, expression or omission of p120ctn isoform C is not essential for cadherin stabilization. Considering this important early role of p120ctn, it would be interesting to investigate whether the embryonic mortality of p120ctn<sup>-/-</sup> mice is caused by E-cadherin displacement and destabilization, or via other pathways involving p120ctn, such as RhoGTPases, Src or Kaiso/Wnt signaling. For instance, a NLS and RhoA-binding domain are affected in p120ctn<sup>KIC/KIC</sup> mice, which may lead to activation of target genes of Kaiso or RhoA hyperactivation respectively. However, altered RhoA- and Kaiso-mediated signalling can not explain the early phenotypes in p120ctn<sup>KOC/KOC</sup> mice, that are similar to the abnormalities seen in p120ctn<sup>KIC/KIC</sup> mice.

In mouse liver, p120ctn is ubiquitously expressed, whereas E-cadherin and N-cadherin show a heterogeneous distribution in mouse livers (van Hengel et al., unpublished data). E-cadherin is expressed in bile ducts cells and in hepatocytes in the portal region but is absent in hepatocytes in the pericentral region. N-cadherin is present in all hepatocytes but is not expressed in bile duct cells. p120ctn ablation in mouse livers abrogates the regional E-cadherin expression in hepatocytes and confers to a weak homozygous expression pattern. N-cadherin levels are slightly diminished but its expression pattern is not altered (van Hengel et al., unpublished data). Remarkably, the regional E-cadherin expression was restored in both p120ctn<sup>KOC/fl</sup>; Alb-Cre and p120ctn<sup>KIC/fl</sup>; Alb-Cre mice (data not shown). This indicates that both p120ctn isoforms with or without the exon C-encoded amino acids are capable for maintaining the normal spatiotemporal expression of E-cadherin in mouse liver.

The first stages of preimplantation development are characterized by a period of transcriptional silence during which oocyte and embryo depend on stored maternal RNAs and proteins for successful completion of the first stages of embryonic development (Li et al., 2010). Knock-out studies have revealed that maternal protein of members of the cadherin-catenin complex, namely E-cadherin,  $\beta$ -catenin and  $\alpha$ -catenin, can persist until the blastocyst stage (Haegel et al., 1995; Larue et al., 1994; Torres et al., 1997). Maternal E-cadherin is responsible for compaction in homozygous E-cadherin knock-out morulas (Larue et al., 1994), and upon genetic ablation of maternal E-cadherin, blastomeres indeed fail to adhere to each other until the morula stage, when new E-cadherin is synthesized from the paternal allele (De Vries et al., 2004). We also found some p120ctn staining above the background level in



p120ctn<sup>-/-</sup> blastocysts, indicative of maternal p120ctn protein (Fig. 12). This maternal p120ctn probably allows sufficient membrane expression of E-cadherin for morula compaction.

### **p120ctn isoform C: essential for life, conserved in evolution**

The alternatively used exon C encodes six amino acids that are expressed in fetal brain (Keirsebilck et al., 1998). We show that transcripts of p120ctn containing exon-C encoded nucleotides can be detected in single morulas and blastocysts. The expression exon C-encoded amino acids is limited in time and space, and so it might have specialized functions. Surprisingly, homozygous constitutive knockout and knockin mice for p120ctn isoform C die very early during preimplantation. Mutant preimplantation embryos were not recovered in the Mendelian ratio, they were mostly in a bad state, and only a few of them were seemingly normal (Table 3).

Why are homozygous p120ctn KOC and KIC embryos not distributed according to the Mendelian ratio? To gain some genetic insight, we performed detailed bioinformatic analysis and found a highly conserved block of about 200 bp, consisting of exon C and its surrounding intronic sequence. The highly conserved region could have a crucial functional or regulatory role that is affected in homozygous KOC and KIC embryos, as both p120ctn KOC and KIC alleles disrupt most of the conserved sequence (Fig. 10). In contrast, p120ctn<sup>KOC/-</sup> and p120ctn<sup>KIC/-</sup> mice contain a p120ctn null allele that contains the normal conserved intronic sequence flanking exon C, and these mice are viable. To date, we do not know the exact function of this conserved sequence block in the middle of the *Ctnd1* gene, but we considered several possible explanations. First, two Rat O/E-1-associated zinc finger (Roaz) transcription factor binding sites are present in the conserved intronic region and are compromised in both p120ctn KOC and KIC alleles (Fig. 10E). Roaz regulates olfactory neuronal-specific gene expression during development (Tsai and Reed, 1997) and a huge cluster of more than 200 olfactory receptor (OR) genes is indeed situated upstream of the *Ctnd1* gene on mouse chromosome 2 (Fig. 10). Roaz-mediated regulation of OR genes and perhaps other genes might be altered in homozygous p120ctn KOC and KIC embryos, resulting in early mortality. Remarkably, also a small cluster of OR genes is situated downstream of the mouse ARVCF. Conservation of the intronic region flanking exon C seems to coincide with the proximity of OR genes because chicken, frog and zebrafish contain exon C but lack both conserved intronic sequences flanking exon C and proximal OR genes. A second explanation could be that a lamin binding site is spanning exon C, which is then lost

## Mice harboring a knockout or knockin of exon C of p120ctn

in p120ctn KOC and KIC alleles (Fig. 10E). This might influence the chromosomal positioning to the nuclear envelope and may affect global transcription levels, resulting in early lethal phenotypes. A last possibility is the interruption of a miRNA-141 binding site (miR-141\*), located between the two Roaz binding sites and partly present in exon C (Fig. 10E). This could be consistent with the first hypothesis as miR-141 is a member of the miRNA-200 family for which a regulatory role in olfactory neurogenesis has been reported (Choi et al., 2008). Although typically the seed strand of the RNA duplex is thought to be the biologically active one (mature miRNA) while the passenger or miRNA\* (“star”) strand is considered inactive and generally degraded, recent analysis also indicates a potential functional role for miRNA\* (Guo and Lu; Okamura et al., 2008).

Our conserved 200bp block, consisting of exon C and its flanking intronic sequence resembles ultraconserved region (UCRs). UCRs are a class of non-coding sequences (200-779 bp in length) that are absolutely conserved (100% identity) between orthologous regions of the human, rat, and mouse genomes. 481 UCRs were discovered in the human genome (Bejerano et al., 2004). These UCRs of the human genome are located either overlapping exons in genes involved in RNA processing or in introns, or nearby genes that are involved in the regulation of transcription or development. Therefore UCRs could serve as distal enhancers of these early developmental genes (Nobrega et al., 2003; Plaza et al., 1995). Interestingly, these elements are frequently found in genes post-transcriptionally regulated by alternative splicing events of exons with premature stop codons (Ni et al., 2007). The conserved ‘block’ of intronic sequence surrounding the alternatively spliced exon C of p120ctn has many characteristics of these UCRs, including its length and high conservation amongst orthologs. In addition, this ‘block’ might regulate expression of a huge cluster of olfactory receptor (OR) genes that are situated in the proximity of the *Ctnd1* and *CTNND1* genes. Nevertheless, the conserved ‘block’ that we identified is not one of 481 UCRs. And even when our ‘block’ would be considered as UCR, this would not fully account for the early phenotype in our homozygous KOC and KIC embryos. Recently, four non-coding UCRs, located near genes that are important for normal development, were removed from the mouse genome. Remarkably, all four resulting lines of mice lacking these ultraconserved elements were viable, fertile and did not show obvious abnormalities (Ahituv et al., 2007). So, although the UCRs are have been evolutionarily conserved for 300 million years, at least some of them, are not essential for normal development and homeostatis. These findings indicate that extreme sequence conservation is not necessarily indicative of an indispensable functional nature. The function of many UCRs remains elusive and might differ amongst UCRs. Because

Ahituv and colleagues (2007) selected four UCRs with a clear enhancer function, they might have targeted a specific ‘non-essential’ class of UCRs. Our conserved (UCR-like) ‘block’ may be a member of another class of conserved elements, which is essential for life.

Loss of non-coding RNA species might explain the phenotypes in  $p120ctn^{KOC/KOC}$  and  $p120ctn^{KIC/KIC}$  embryos. Traditionally, a gene is defined as a small genomic region encoding mRNAs that are translated into protein. However only 2% the mammalian genome encodes mRNAs, the vast majority is transcribed, largely as long and short non-protein-coding RNAs (ncRNAs) (Taft et al., 2010). These ncRNAs might form an additional layer of regulation in more complex organisms, such as mammals, which have roughly the same number of protein-coding genes as simple life form, such as the roundworm *Caenorhabditis elegans*. Plants and animals produce a dazzling array of small regulatory RNAs: endogenous small interfering RNAs (siRNAs), microRNAs (miRNAs) and PIWI interacting RNAs (piRNAs) (Taft et al., 2010). miRNAs are imperfect RNA hairpins encoded in long primary transcripts or short introns and dicer-mediated cleavage results in small RNAs of approximately 22 nt. miRNAs are primarily involved in post-transcriptional gene regulation. Interestingly, a miRNA-141 binding site (miR-141\*) is present and might be compromised in both  $p120ctn^{KOC/KOC}$  and  $p120ctn^{KIC/KIC}$  alleles. Failure of miR-141 to bind to this site might induce global changes in gene transcription, which ultimately will cause early death in  $p120ctn^{KOC/KOC}$  and  $p120ctn^{KIC/KIC}$  embryos. Altered gene transcription would also occur if the conserved ‘block’ flanking exon C of  $p120ctn$  would encode promoter-associated RNAs (PASRs) and transcription initiation RNAs (tiRNAs) that overlap promoters and TSSs. Another possibility is that the conserved ‘block’ encodes piRNAs which are lost in  $p120ctn^{KOC/KOC}$  and  $p120ctn^{KIC/KIC}$  embryos. piRNAs, which are 25 to 30 nt in length, are involved in, transposon defense. piRNAs are largely restricted to the germline, where active transposons could severely disrupt embryogenesis. Increased transposon activity in  $p120ctn^{KOC/KOC}$  and  $p120ctn^{KIC/KIC}$  germ cells (as a consequence of piRNA loss) may hamper early development. Long non-coding RNAs resemble protein-coding genes because they are generally long (between two and 100 kb), are bound by transcription factors and are epigenetically marked (Taft et al., 2010). Interestingly, long ncRNAs frequently associate with chromatin-modifying complexes. Aberrant expression of both short and long ncRNAs have been implicated in various types of diseases, including cancer and cardiovascular disease (Taft et al., 2010). On the other hand, complete loss of Dicer disrupts Dicer-dependent ncRNA biogenesis and results in early embryonic lethality (Bernstein et al., 2003). Non-coding RNA species are important for normal development and removal of any ncRNAs, which may be encoded by the conserved intronic sequence flanking

## Mice harboring a knockout or knockin of exon C of p120ctn

exon C of p120ctn, may explain the early lethal defects seen in p120ctn<sup>KOC/KOC</sup> and p120ctn<sup>KIC/KIC</sup> embryos.

Presently we lack the proper transgenic tools to analyze the function of this conserved 'block', as all available modified alleles for this conserved sequence are incompatible with life. On the other hand, all viable *in vivo* rescues realized in our studies so far have at least one intact p120ctn allele with an intact conserved sequence block. A powerful tool would be the generation of mice with loxP sites flanking the conserved sequence (including exon C), which would allow its temporal and conditional removal. But it will remain a daunting task to discriminate between p120ctn isoform C-specific functions and the presumptive regulatory potential of the conserved sequence block.

p120ctn isoforms, with or without the exon C-encoded amino acids, act similarly in respect to the early mortality in homozygous embryos, the rescue of the cell surface E-cadherin levels and the mortality in p120ctn-deficient embryos, and possibly the RhoA activity in ES cells. These data could indicate that the coding sequence of exon C by itself has no function in early development, while in combination with its flanking intronic sequences it is extremely important for embryo survival.

## ACKNOWLEDGEMENTS

This work was supported by grants from the Queen Elisabeth Medical Foundation (G.S.K.E.), Belgium, and from the Geconcerteerde Onderzoeksacties of Ghent University. Tim Pieters has been supported by the Instituut voor de Aanmoediging van Innovatie door Wetenschap en Technologie in Vlaanderen (IWT). Tim Pieters conducted all experiments and wrote this manuscript. Petra D'hooge screened targeted ES cell clones via Southern blotting. Dr. Tino Hochpied helped to establish an efficient ES cell derivation protocol for mouse blastocysts. Paco Hulpiau performed detailed bioinformatic analysis. Dr. Marc Stemmler provided excellent training in handling and immunostaining of preimplantation embryos. Prof. Dr. Albert Reynolds provided the floxed p120ctn mice. Prof. Dr. Frans Van Roy and Dr. Jolanda van Hengel were instructive in the experimental design and editing of the manuscript. We thank Dr. Karl Vandepoele for discovering the conserved intronic sequences flanking exon C. We acknowledge Dr. Amin Bredan and Dr. Marc Stemmler for critical reading of the manuscript, and the members of our research group for valuable discussions.

## REFERENCES

- Ahituv, N., Y. Zhu, A. Visel, A. Holt, V. Afzal, L.A. Pennacchio, and E.M. Rubin. 2007. Deletion of ultraconserved elements yields viable mice. *PLoS Biol.* 5:e234.
- Aho, S., L. Levansuo, O. Montonen, C. Kari, U. Rodeck, and J. Uitto. 2002. Specific sequences in p120ctn determine subcellular distribution of its multiple isoforms involved in cellular adhesion of normal and malignant epithelial cells. *J Cell Sci.* 115:1391-402.
- Aho, S., K. Rothenberger, and J. Uitto. 1999. Human p120ctn catenin: tissue-specific expression of isoforms and molecular interactions with BP180/type XVII collagen. *J Cell Biochem.* 73:390-9.
- Anastasiadis, P.Z. 2007. p120-ctn: A nexus for contextual signaling via Rho GTPases. *Biochim Biophys Acta.* 1773:34-46.
- Anastasiadis, P.Z., S.Y. Moon, M.A. Thoreson, D.J. Mariner, H.C. Crawford, Y. Zheng, and A.B. Reynolds. 2000. Inhibition of RhoA by p120 catenin. *Nat Cell Biol.* 2:637-44.
- Bejerano, G., M. Pheasant, I. Makunin, S. Stephen, W.J. Kent, J.S. Mattick, and D. Haussler. 2004. Ultraconserved elements in the human genome. *Science.* 304:1321-5.
- Bernstein, E., S.Y. Kim, M.A. Carmell, E.P. Murchison, H. Alcorn, M.Z. Li, A.A. Mills, S.J. Elledge, K.V. Anderson, and G.J. Hannon. 2003. Dicer is essential for mouse development. *Nat Genet.* 35:215-7.
- Betz, U.A., C.A. Voshenrich, K. Rajewsky, and W. Muller. 1996. Bypass of lethality with mosaic mice generated by Cre-loxP-mediated recombination. *Curr Biol.* 6:1307-16.
- Castano, J., G. Solanas, D. Casagolda, I. Raurell, P. Villagrasa, X.R. Bustelo, A. Garcia de Herreros, and M. Dunach. 2007. Specific phosphorylation of p120-catenin regulatory domain differently modulates its binding to RhoA. *Mol Cell Biol.* 27:1745-57.
- Chen, X., S. Kojima, G.G. Borisy, and K.J. Green. 2003. p120 catenin associates with kinesin and facilitates the transport of cadherin-catenin complexes to intercellular junctions. *J Cell Biol.* 163:547-57.
- Choi, H.J., and W.I. Weis. 2005. Structure of the armadillo repeat domain of plakophilin 1. *J Mol Biol.* 346:367-76.
- Choi, P.S., L. Zakhary, W.Y. Choi, S. Caron, E. Alvarez-Saavedra, E.A. Miska, M. McManus, B. Harfe, A.J. Giraldez, H.R. Horvitz, A.F. Schier, and C. Dulac. 2008. Members of the miRNA-200 family regulate olfactory neurogenesis. *Neuron.* 57:41-55.
- Daniel, J.M., and A.B. Reynolds. 1999. The catenin p120(ctn) interacts with Kaiso, a novel BTB/POZ domain zinc finger transcription factor. *Mol Cell Biol.* 19:3614-23.
- Davis, M.A., R.C. Ireton, and A.B. Reynolds. 2003. A core function for p120-catenin in cadherin turnover. *J Cell Biol.* 163:525-34.
- Davis, M.A., and A.B. Reynolds. 2006. Blocked acinar development, E-cadherin reduction, and intraepithelial neoplasia upon ablation of p120-catenin in the mouse salivary gland. *Dev Cell.* 10:21-31.
- De Vries, W.N., A.V. Evsikov, B.E. Haac, K.S. Fancher, A.E. Holbrook, R. Kemler, D. Solter, and B.B. Knowles. 2004. Maternal beta-catenin and E-cadherin in mouse development. *Development.* 131:4435-45.
- Downs, K.M., and T. Davies. 1993. Staging of gastrulating mouse embryos by morphological landmarks in the dissecting microscope. *Development.* 118:1255-66.

## Mice harboring a knockout or knockin of exon C of p120ctn

- Elia, L.P., M. Yamamoto, K. Zang, and L.F. Reichardt. 2006. p120 catenin regulates dendritic spine and synapse development through Rho-family GTPases and cadherins. *Neuron*. 51:43-56.
- Gauthaman, K., C.Y. Fong, and A. Bongso. 2010. Effect of ROCK inhibitor Y-27632 on normal and variant human embryonic stem cells (hESCs) in vitro: its benefits in hESC expansion. *Stem Cell Rev*. 6:86-95.
- Golenhofen, N., and D. Drenckhahn. 2000. The catenin, p120ctn, is a common membrane-associated protein in various epithelial and non-epithelial cells and tissues. *Histochem Cell Biol*. 114:147-55.
- Griffiths-Jones, S., H.K. Saini, S. van Dongen, and A.J. Enright. 2008. miRBase: tools for microRNA genomics. *Nucleic Acids Res*. 36:D154-8.
- Guo, L., and Z. Lu. The fate of miRNA\* strand through evolutionary analysis: implication for degradation as merely carrier strand or potential regulatory molecule? *PLoS One*. 5:e11387.
- Haegel, H., L. Larue, M. Ohsugi, L. Fedorov, K. Herrenknecht, and R. Kemler. 1995. Lack of beta-catenin affects mouse development at gastrulation. *Development*. 121:3529-37.
- Hooghe, B., P. Hulpiau, F. van Roy, and P. De Bleser. 2008. ConTra: a promoter alignment analysis tool for identification of transcription factor binding sites across species. *Nucleic Acids Res*. 36:W128-32.
- Hosking, C.R., F. Ulloa, C. Hogan, E.C. Ferber, A. Figueroa, K. Gevaert, W. Birchmeier, J. Briscoe, and Y. Fujita. 2007. The transcriptional repressor Glis2 is a novel binding partner for p120 catenin. *Mol Biol Cell*. 18:1918-27.
- Husmark, J., N.E. Heldin, and M. Nilsson. 1999. N-cadherin-mediated adhesion and aberrant catenin expression in anaplastic thyroid-carcinoma cell lines. *Int J Cancer*. 83:692-9.
- Ireton, R.C., M.A. Davis, J. van Hengel, D.J. Mariner, K. Barnes, M.A. Thoreson, P.Z. Anastasiadis, L. Matrisian, L.M. Bundy, L. Sealy, B. Gilbert, F. van Roy, and A.B. Reynolds. 2002. A novel role for p120 catenin in E-cadherin function. *J Cell Biol*. 159:465-76.
- Ishiyama, N., S.H. Lee, S. Liu, G.Y. Li, M.J. Smith, L.F. Reichardt, and M. Ikura. 2010. Dynamic and static interactions between p120 catenin and E-cadherin regulate the stability of cell-cell adhesion. *Cell*. 141:117-28.
- Kan, N.G., M.P. Stemmler, D. Junghans, B. Kanzler, W.N. de Vries, M. Dominis, and R. Kemler. 2007. Gene replacement reveals a specific role for E-cadherin in the formation of a functional trophectoderm. *Development*. 134:31-41.
- Keirsebilck, A., S. Bonne, K. Staes, J. van Hengel, F. Nollet, A. Reynolds, and F. van Roy. 1998. Molecular cloning of the human p120ctn catenin gene (CTNND1): expression of multiple alternatively spliced isoforms. *Genomics*. 50:129-46.
- Kelly, K.F., C.M. Spring, A.A. Otchere, and J.M. Daniel. 2004. NLS-dependent nuclear localization of p120ctn is necessary to relieve Kaiso-mediated transcriptional repression. *J Cell Sci*. 117:2675-86.
- Laemmli, U.K. 1970. Cleavage of structural proteins during the assembly of the head of bacteriophage T4. *Nature*. 227:680-5.
- Laird, P.W., A. Zijderveld, K. Linders, M.A. Rudnicki, R. Jaenisch, and A. Berns. 1991. Simplified mammalian DNA isolation procedure. *Nucleic Acids Res*. 19:4293.
- Larkin, M.A., G. Blackshields, N.P. Brown, R. Chenna, P.A. McGettigan, H. McWilliam, F. Valentin, I.M. Wallace, A. Wilm, R. Lopez, J.D. Thompson, T.J. Gibson, and D.G. Higgins. 2007. Clustal W and Clustal X version 2.0. *Bioinformatics*. 23:2947-8.
- Larue, L., M. Ohsugi, J. Hirchenhain, and R. Kemler. 1994. E-cadherin null mutant embryos fail to form a trophectoderm epithelium. *Proc Natl Acad Sci U S A*. 91:8263-7.

- Li, L., P. Zheng, and J. Dean. 2010. Maternal control of early mouse development. *Development*. 137:859-70.
- McCrea, P.D., and J.I. Park. 2007. Developmental functions of the P120-catenin sub-family. *Biochim Biophys Acta*. 1773:17-33.
- Miller, W., K. Rosenbloom, R.C. Hardison, M. Hou, J. Taylor, B. Raney, R. Burhans, D.C. King, R. Baertsch, D. Blankenberg, S.L. Kosakovsky Pond, A. Nekrutenko, B. Giardine, R.S. Harris, S. Tyekucheva, M. Diekhans, T.H. Pringle, W.J. Murphy, A. Lesk, G.M. Weinstock, K. Lindblad-Toh, R.A. Gibbs, E.S. Lander, A. Siepel, D. Haussler, and W.J. Kent. 2007. 28-way vertebrate alignment and conservation track in the UCSC Genome Browser. *Genome Res*. 17:1797-808.
- Mo, Y.Y., and A.B. Reynolds. 1996. Identification of murine p120 isoforms and heterogeneous expression of p120cas isoforms in human tumor cell lines. *Cancer Res*. 56:2633-40.
- Montonen, O., M. Aho, J. Uitto, and S. Aho. 2001. Tissue distribution and cell type-specific expression of p120ctn isoforms. *J Histochem Cytochem*. 49:1487-96.
- Ni, J.Z., L. Grate, J.P. Donohue, C. Preston, N. Nobida, G. O'Brien, L. Shiue, T.A. Clark, J.E. Blume, and M. Ares, Jr. 2007. Ultraconserved elements are associated with homeostatic control of splicing regulators by alternative splicing and nonsense-mediated decay. *Genes Dev*. 21:708-18.
- Nichols, J., B. Zevnik, K. Anastasiadis, H. Niwa, D. Klewe-Nebenius, I. Chambers, H. Scholer, and A. Smith. 1998. Formation of pluripotent stem cells in the mammalian embryo depends on the POU transcription factor Oct4. *Cell*. 95:379-91.
- Nobrega, M.A., I. Ovcharenko, V. Afzal, and E.M. Rubin. 2003. Scanning human gene deserts for long-range enhancers. *Science*. 302:413.
- Okamura, K., M.D. Phillips, D.M. Tyler, H. Duan, Y.T. Chou, and E.C. Lai. 2008. The regulatory activity of microRNA\* species has substantial influence on microRNA and 3' UTR evolution. *Nat Struct Mol Biol*. 15:354-63.
- Perez-Moreno, M., M.A. Davis, E. Wong, H.A. Pasolli, A.B. Reynolds, and E. Fuchs. 2006. p120-catenin mediates inflammatory responses in the skin. *Cell*. 124:631-44.
- Pieters, T., T. Hochepped, F. Van Roy, and J. Van Hengel. in preparation. Efficient and user-friendly pluripotin-based derivation of mouse embryonic stem cells
- Plaza, S., N. Turque, C. Dozier, M. Bailly, and S. Saule. 1995. C-Myb acts as transcriptional activator of the quail PAX6 (PAX-QNR) promoter through two different mechanisms. *Oncogene*. 10:329-40.
- Postic, C., and M.A. Magnuson. 2000. DNA excision in liver by an albumin-Cre transgene occurs progressively with age. *Genesis*. 26:149-150.
- Reynolds, A.B., and R.H. Carnahan. 2004. Regulation of cadherin stability and turnover by p120ctn: implications in disease and cancer. *Semin Cell Dev Biol*. 15:657-63.
- Reynolds, A.B., J.M. Daniel, Y.Y. Mo, J. Wu, and Z. Zhang. 1996. The novel catenin p120cas binds classical cadherins and induces an unusual morphological phenotype in NIH3T3 fibroblasts. *Exp Cell Res*. 225:328-37.
- Reynolds, A.B., and A. Rocznik-Ferguson. 2004. Emerging roles for p120-catenin in cell adhesion and cancer. *Oncogene*. 23:7947-56.
- Rocznik-Ferguson, A., and A.B. Reynolds. 2003. Regulation of p120-catenin nucleocytoplasmic shuttling activity. *J Cell Sci*. 116:4201-12.
- Roskams, T., and V. Desmet. 1998. Ductular reaction and its diagnostic significance. *Semin Diagn Pathol*. 15:259-69.
- Smalley-Freed, W.G., A. Efimov, P.E. Burnett, S.P. Short, M.A. Davis, D.L. Gumucio, M.K. Washington, R.J. Coffey, and A.B. Reynolds. 2010. p120-catenin is essential for

## Mice harboring a knockout or knockin of exon C of p120ctn

- maintenance of barrier function and intestinal homeostasis in mice. *J Clin Invest.* 120:1824-35.
- Sorg, G., and T. Stamminger. 1999. Mapping of nuclear localization signals by simultaneous fusion to green fluorescent protein and to beta-galactosidase. *Biotechniques.* 26:858-62.
- Taft, R.J., K.C. Pang, T.R. Mercer, M. Dinger, and J.S. Mattick. 2010. Non-coding RNAs: regulators of disease. *J Pathol.* 220:126-39.
- Torres, M., A. Stoykova, O. Huber, K. Chowdhury, P. Bonaldo, A. Mansouri, S. Butz, R. Kemler, and P. Gruss. 1997. An alpha-catenin gene trap mutation defines its function in preimplantation development. *Proceedings of the National Academy of Sciences of the United States of America.* 94:901-906.
- Tsai, R.Y., and R.R. Reed. 1997. Cloning and functional characterization of Roaz, a zinc finger protein that interacts with O/E-1 to regulate gene expression: implications for olfactory neuronal development. *J Neurosci.* 17:4159-69.
- van Hengel, J., P. Vanhoenacker, K. Staes, and F. van Roy. 1999. Nuclear localization of the p120(ctn) Armadillo-like catenin is counteracted by a nuclear export signal and by E-cadherin expression. *Proc Natl Acad Sci U S A.* 96:7980-5.
- Vandewalle, C., J. Comijn, B. De Craene, P. Vermassen, E. Bruyneel, H. Andersen, E. Tulchinsky, F. Van Roy, and G. Berx. 2005. SIP1/ZEB2 induces EMT by repressing genes of different epithelial cell-cell junctions. *Nucleic Acids Res.* 33:6566-78.
- Xiao, K., D.F. Allison, K.M. Buckley, M.D. Kottke, P.A. Vincent, V. Faundez, and A.P. Kowalczyk. 2003. Cellular levels of p120 catenin function as a set point for cadherin expression levels in microvascular endothelial cells. *J Cell Biol.* 163:535-45.
- Xiao, K., R.G. Oas, C.M. Chiasson, and A.P. Kowalczyk. 2007. Role of p120-catenin in cadherin trafficking. *Biochim Biophys Acta.* 1773:8-16.
- Yanagisawa, M., D. Huvelde, P. Kreinest, C.M. Lohse, J.C. Cheville, A.S. Parker, J.A. Copland, and P.Z. Anastasiadis. 2008. A p120 catenin isoform switch affects Rho activity, induces tumor cell invasion, and predicts metastatic disease. *J Biol Chem.* 283:18344-54.



## Chapter 5

---

### **TIME LAPSE MONITORING OF IN VITRO PREIMPLANTATION DEVELOPMENT**

**Time lapse monitoring of *in vitro* preimplantation development**

## Time lapse monitoring of *in vitro* preimplantation development

Tim Pieters<sup>1,2</sup>, Marc P. Stemmler<sup>3</sup>, Tino Hochpied<sup>1,2</sup>, Frans van Roy<sup>1,2</sup>, Jolanda van Hengel<sup>1,2,5</sup>

<sup>1</sup> Department for Molecular Biomedical Research, Technologiepark 927, VIB, B-9052 Ghent, Belgium

<sup>2</sup> Department of Biomedical Molecular Biology, Ghent University, Technologiepark 927, B-9052 Ghent, Belgium

<sup>3</sup> Department of Molecular Embryology, Max-Planck Institute of Immunobiology, Stuebeweg 51, 79108 Freiburg, Germany

<sup>4</sup> Department of Cancer Biology, Vanderbilt University, Nashville, Tennessee, United States of America

<sup>5</sup> Corresponding author: Jolanda.vanhengel@dmb.vib-ugent.be or Frans.Vanroy@dmb.vib-ugent.be

### TABLE OF CONTENTS

MATERIAL AND METHODS .....	188
Mouse breeding .....	188
Time lapse microscopy.....	188
RESULTS AND DISCUSSION .....	189
Time lapse monitoring of <i>in vitro</i> preimplantation development .....	189
Optimizing time lapse monitoring of <i>in vitro</i> preimplantation development.....	194
Rock inhibition delays blastocyst formation .....	196
ACKNOWLEDGEMENTS .....	198
REFERENCES.....	198

### MATERIAL AND METHODS

#### Mouse breeding

The generation of p120ctn<sup>KOC/+</sup> and p120ctn<sup>KIC/+</sup> mice, all backcrossed on the C57BL/6 background, will be reported elsewhere (Pieters et al., in preparation). p120ctn<sup>KOC/+</sup> and p120ctn<sup>KIC/+</sup> mice were intercrossed to obtain homozygous p120ctn KOC and KIC embryos. Female wild-type C57BL/6 mice at the age of 3–8 weeks were superovulated by intraperitoneal injection of 5 IU of pregnant mare serum gonadotropin (PMS), and 48 h later they were injected with 5 IU human chorionic gonadotropin (hCG). After the hCG injection, they were housed with male studs and copulation plugs were checked the following morning.

Embryos were flushed with M2 medium (Sigma-Aldrich Inc., St. Louis, MO) from oviducts at E1.5 and E2.5 by using a 32G needle (Popper & Sons Inc., New York, Cat. No. 7400) and a 5-ml Luer-Lok syringe. To flush blastocysts from the uterus at E3.5, a 23G needle and a 1-ml syringe were used. Mice were housed in individually ventilated cages in a specific pathogen-free animal facility. All experiments on mice were conducted according to institutional, national, and European animal regulations. Animal protocols were approved by the ethics committee of Ghent University.

#### Time lapse microscopy

Embryos were washed three times in M2 medium (Sigma) followed by three washes in the appropriate media used for time lapse recordings. Embryos were morphologically scored and only normal looking embryos were selected for time lapse recording. Embryos with an aberrant morphology were genotyped according to Pieters et al. (in preparation). Three types of media were used: KSOM (Sigma), GM 501 AIR (Gynemed, Lensahn, Germany) and FHM Embryomax (Chemicon, Billerica, MA). Embryos were cultured in eight-well chambered coverglass (Lab-Tek, Nunc, Roskilde, Denmark) or in 3-cm dishes containing microdrops (10  $\mu$ l) of the appropriate buffer covered with mineral oil (Sigma). Incubation was in 5% CO<sub>2</sub> at 37°C. Experiments were conducted either in Freiburg (Max-Planck Institute of Immunobiology) or in Ghent (DMBR, Ghent University and VIB). Experiments in Freiburg were conducted as previously described (Hiiragi and Solter, 2004). In brief, temperature was maintained by Tempcontrol 37-2 digital (Carl Zeiss, Oberkochen, Germany), a heating stage (E100 with ecoline RE106, LAUDA) and a plastic chamber Incubator XL (Zeiss, Jena, Germany), attached to Axiovert 200M (Zeiss) with Narishige

micromanipulators (London). Zeiss AxioVision Ver. 4.6 software was used to acquire and analyze the time-lapse images. The voltage of the halogen lamp was set below 2.6 V to minimize the embryo's exposure to the light. Images were recorded every 15 min for 24 or 48 h. Experiments in Ghent were conducted either in a Leica AS MDW live cell imaging system or in a system with only temperature control but with micromanipulators to align the embryos. The Leica AS MDW live cell imaging system (Leica Microsystems, Mannheim, Germany) includes a DM IRE2 inverted microscope, a 12-bit Coolsnap HQ camera and an incubation chamber, which keeps the cells at 37°C in a 5% CO<sub>2</sub> environment. Differential interference images were taken with a CPLAN 10x/0.22 objective every 30 min for 48 h. The DM IRE2 is equipped with an automated table enabling the monitoring of multiple positions. We monitored up to eight positions simultaneously using eight-well chambered coverglass slides (Lab-Tek, Nunc). The second system consists of a Nikon Eclipse TE200 microscope (Nikon, Amstelveen, The Netherlands) connected to a 1.3-megapixel CMOS Firewire camera (Bfi Optilas, Amsterdam, The Netherlands) with a thermo plate (Tokai Hit, Shizuoka, Japan) and Transferman NK micromanipulators (Eppendorf, Hamburg, Germany). Images were recorded every 15 min for 48 h using pixellink software (Bfi Optilas). This second system lacks CO<sub>2</sub> control and an automated shutter.

## RESULTS AND DISCUSSION

### Time lapse monitoring of *in vitro* preimplantation development

Preimplantation development takes place within the oviduct, but it can also be recapitulated *in vitro* in a chemically defined culture medium without adversely affecting the developmental potential of embryos (Summers and Biggers, 2003). Homozygous p120ctn<sup>KOC</sup> and KIC embryos die before implantation (Pieters et al., in preparation), and so we wanted to look for early defects in embryogenesis by monitoring preimplantation development *in vitro*. In the first experiment (KOC 1) 49 two-cell stage embryos (flushed at 1.5 dpc) derived from p120ctn<sup>KOC/+</sup> intercrosses were cultured in KSOM medium for up to 48 h and their developmental progress was scored. Some embryos developed into blastocysts (Chapter 2, Fig. 1B) but most embryos were morphologically abnormal (Fig. 1A). A similar experiment (KOC 2) starting from 34 two-cell stage embryos derived from p120ctn<sup>KOC/+</sup>

## Time lapse monitoring of *in vitro* preimplantation development

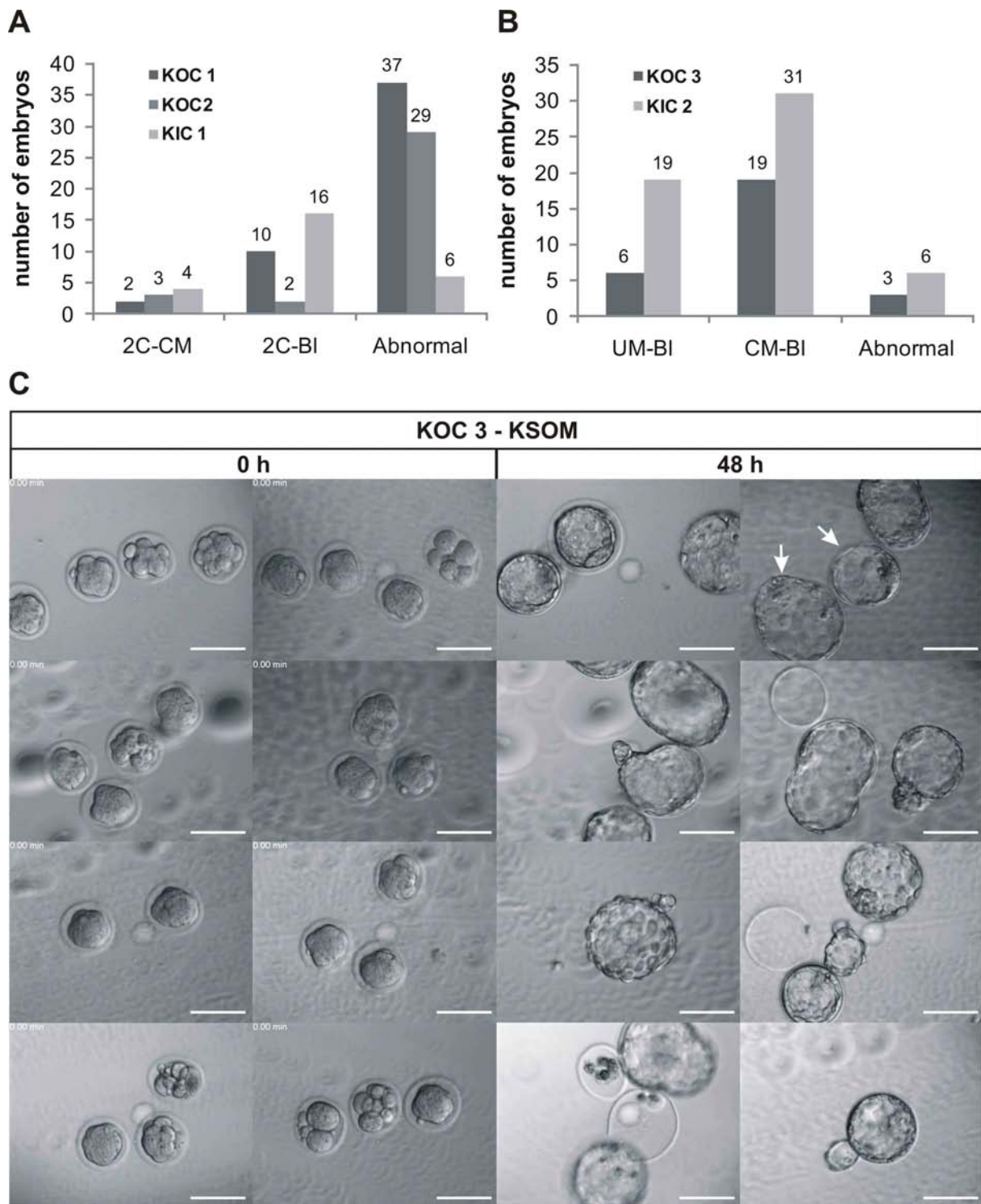


**Figure 1. Time lapse monitoring of *in vitro* preimplantation development in KSOM medium.** Diagram summarizing the developmental progress for time lapse experiments started either from two-cell (2C) embryos (A), or from compacted morulas (CM) or uncompact morulas (UM) (B). After 48 h of culture blastocysts (BI) and CM were formed. Experiments were performed on embryos derived either from  $p120ctn^{KOC/+}$  intercrosses (KOC) or  $p120ctn^{KIC/+}$  intercrosses (KIC). (C) The *in vitro* development of morula-stage embryos derived from  $p120ctn^{KOC/+}$  intercrosses and cultured in KSOM medium was monitored for 48 h. Eight positions corresponding to the wells of an eight-well chambered coverglass slide

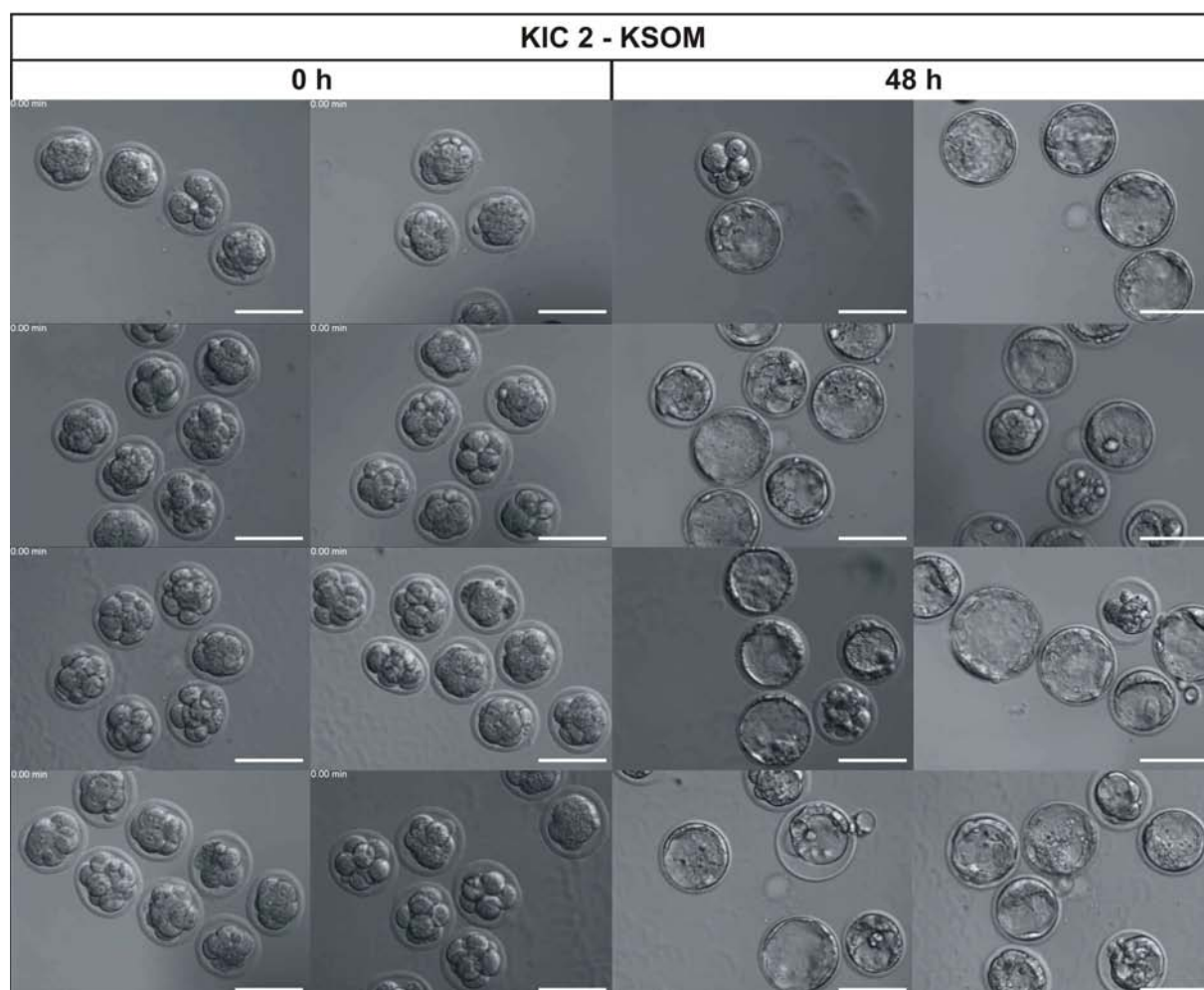
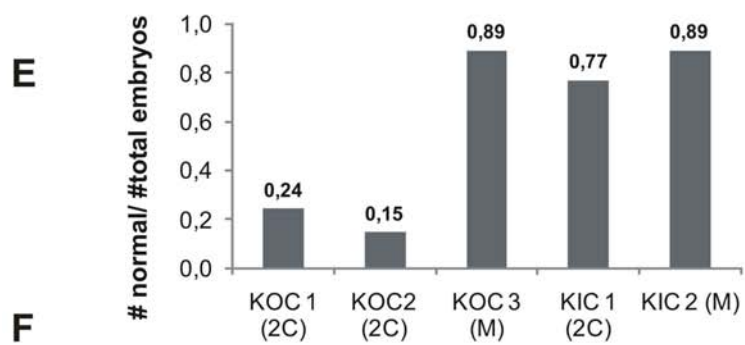
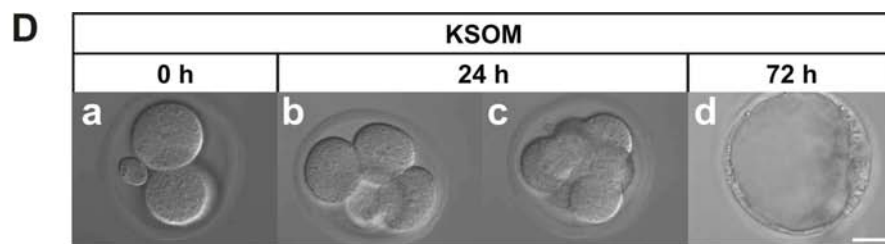


**Figure 1 (continued).** were monitored simultaneously. The first (0 h) and last (48 h) pictures from each time lapse movie are shown. White arrows point to  $p120ctn^{KOC/KOC}$  embryos. Scale bar: 100  $\mu\text{m}$ . (D) Two-cell embryos (a) were cultured in eight-well chambered coverglass filled with KSOM medium and developed into four-cell stage (b) to eight-cell stage (c) embryos after 24 h and into blastocysts (d) after 72 h. Scale bar: 25  $\mu\text{m}$ . (E) Diagram showing the ratio between the number of embryos developing normally compared to the total number of embryos for several experiments starting from two-cell embryos (2C) or morulas (M). (F) Same as in (C), but with morulas derived from  $p120ctn^{KIC/+}$  intercrosses. Scale bar: 100  $\mu\text{m}$ .

intercrosses yielded only three blastocysts and two morula stage embryos, but most of the embryos failed to develop (Fig. 1A). In a third experiment (KOC 3), compacted and uncompact morulas (flushed at 2.5 dpc) derived from  $p120ctn^{KOC/+}$  intercrosses were monitored by time lapse imaging. After 48 h of incubation in KSOM, almost 90% of the embryos developed into expanded blastocysts (Figs. 1B, C), and most blastocysts were hatching or did already hatch. Genotypic analysis of the 111 embryos that were analyzed by time lapse monitoring showed that only two embryos were homozygous KOC (Fig. 1C, white arrows). These mutants were morphologically indistinguishable from wild-type and heterozygous embryos.

Similar time lapse experiments were conducted with embryos derived from  $p120ctn^{KIC/+}$  intercrosses. These embryos too could be cultured in KSOM from two cell-stage to expanded blastocysts (Fig. 1D), but the percentage of embryos that developed normally in this experiment (KIC 1) was significantly higher compared to experiments performed with embryos from  $p120ctn^{KOC/+}$  intercrosses (Figs. 1A, E; compare KIC 1 with KOC 1 and 2).

A time lapse monitoring experiment (KIC 3) starting from morulas resulted in efficient formation of blastocysts *in vitro* (Figs. 1B, F). However, no homozygous  $p120ctn$  KIC embryos were identified by genotyping among the 82 embryos that were analyzed by time lapse analysis.

In summary, we monitored *in vitro* development starting from either two cell stage embryos or from morulas. However, the percentage of normal development varied substantially amongst experiments if the monitoring was performed using two cell stage embryos and did not exceed 89% in experiments that monitored development starting from the morula stage (Fig. 1E). That means that more than 10% of the embryos developed abnormally *in vitro*. Because the incidence of homozygous  $p120ctn$  KOC and KIC embryos is lower than the expected Mendelian ratio, we need an *in vitro* development method with an efficiency of about 95% to be able to discriminate genotype-based developmental defects from technique-based developmental abnormalities.



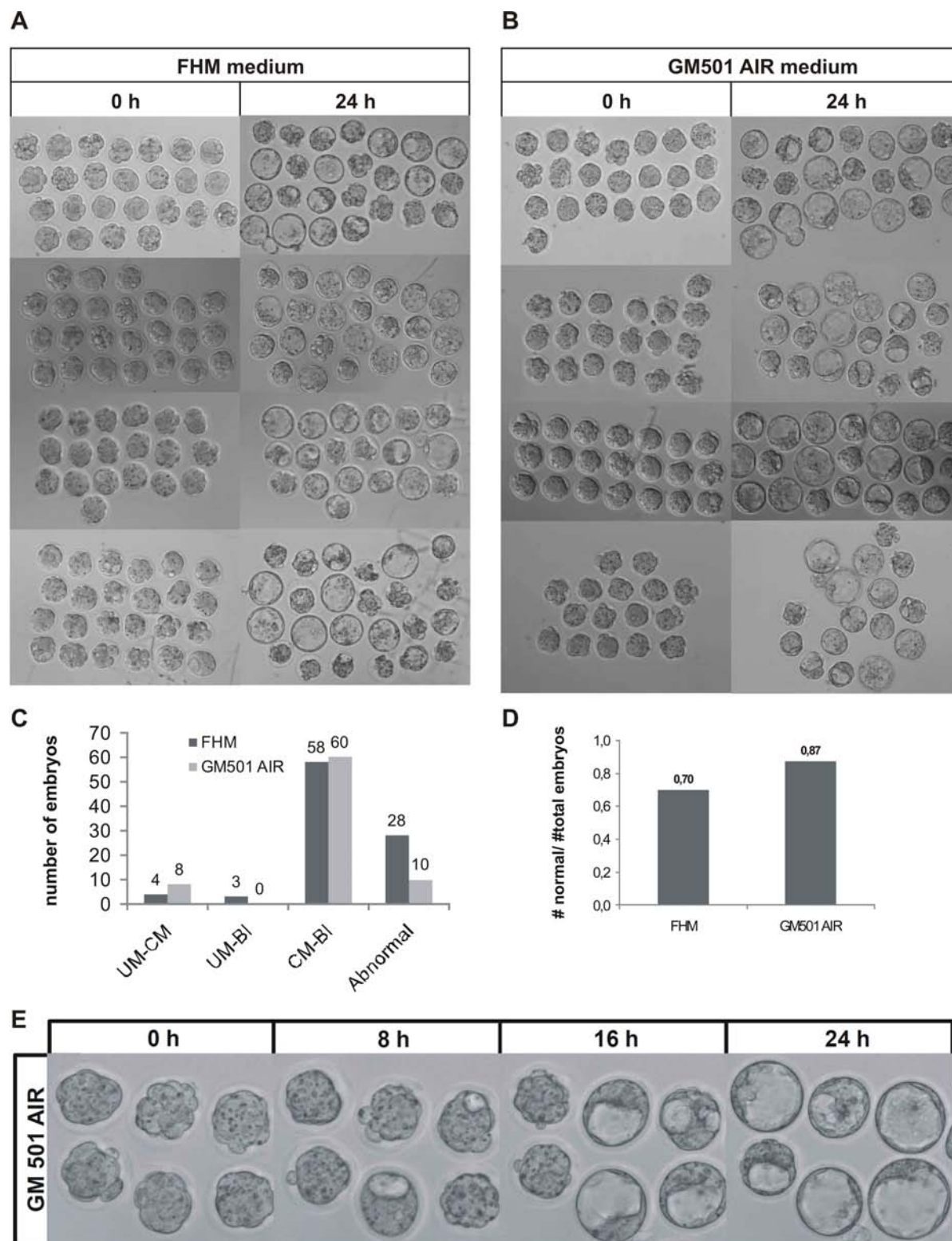


**Figure 2. Optimizing time lapse monitoring of *in vitro* preimplantation development (performed in Freiburg).** (A) Wild-type embryos were cultured *in vitro* in either FHM embryomax (A) or GM 501 AIR (B). Development was quantified and is depicted in a diagram (C). Most of the compacted morulas (CM) developed into blastocysts (BI). Abnormal embryos were morphologically abnormal or did not progress beyond their initial developmental stage. (D) Diagram showing the ratio between the number of normal developing embryos and the total number of embryos.

## Time lapse monitoring of *in vitro* preimplantation development

Another technical issue is the movement of the developing embryos during time lapse monitoring. By using eight-well chambered coverglass slides on a Leica AS MDW live cell imaging system, we were able to monitor up to eight positions simultaneously. However, the embryos could move around during the recordings and sometimes they moved out of focus (examples in Figs. 1C,F) causing developmental information to be lost. In conclusion, we need to increase the success rate of normal *in vitro* development and a way to group and fix embryos during the recordings.

## Optimizing time lapse monitoring of *in vitro* preimplantation development

Time lapse monitoring of *in vitro* preimplantation development has been used in the laboratories of Prof. Dr. Solter and Prof. Dr. Kemler in Freiburg, where they used it to investigate basic developmental biology (Hiiragi and Solter, 2004) and for morphological analysis of genetically engineered embryos (Kan et al., 2007). When I went to the Max-Planck Institute of Immunobiology in Freiburg to optimize our time lapse technique, I found that their time lapse analysis differed from ours in many ways. First, they used ordinary 3-cm Petri dishes rather than eight-well chambered coverglass slides like we do. The plastic surface of the Petri dishes reduces the movement of embryos in the dish. Second, embryos could be aligned and grouped by using micromanipulators, which makes it possible to monitor clusters of embryos that do not move. Third, they used Hepes-buffered media and thereby omitted the need for CO<sub>2</sub>. Fourth, they did not have an automated table, so that only one position could be monitored. Fifth, only 24-h time lapse experiments were performed, and so they monitored the development of either two-cell embryos (flushed at 1.5 dpc) into morulas, or uncompact morulas (flushed at 2,5 dpc) into blastocysts.

The developmental potential of 93 and 78 wild-type C57BL/6 embryos was assayed in FHM embryomax and in GM 501 AIR, respectively (Figs. 2A,B). Developmental progress after 24h was scored and is summarized in Fig. 2C. Embryos cultured in FHM showed a higher percentage of abnormalities compared to GM 501 AIR medium (Fig. 2C), which enabled almost 90% of the embryos to develop normally (Fig. 2D). However, due to the large scale of this experiment the maximal developmental efficiency may not be reached because of long time periods out of the incubator and possible damaging of embryos by micromanipulation. For this experiment approximately 250 embryos were flushed from 10 superovulated C57BL/6 mice. 171 (from 211) healthy looking embryos were selected

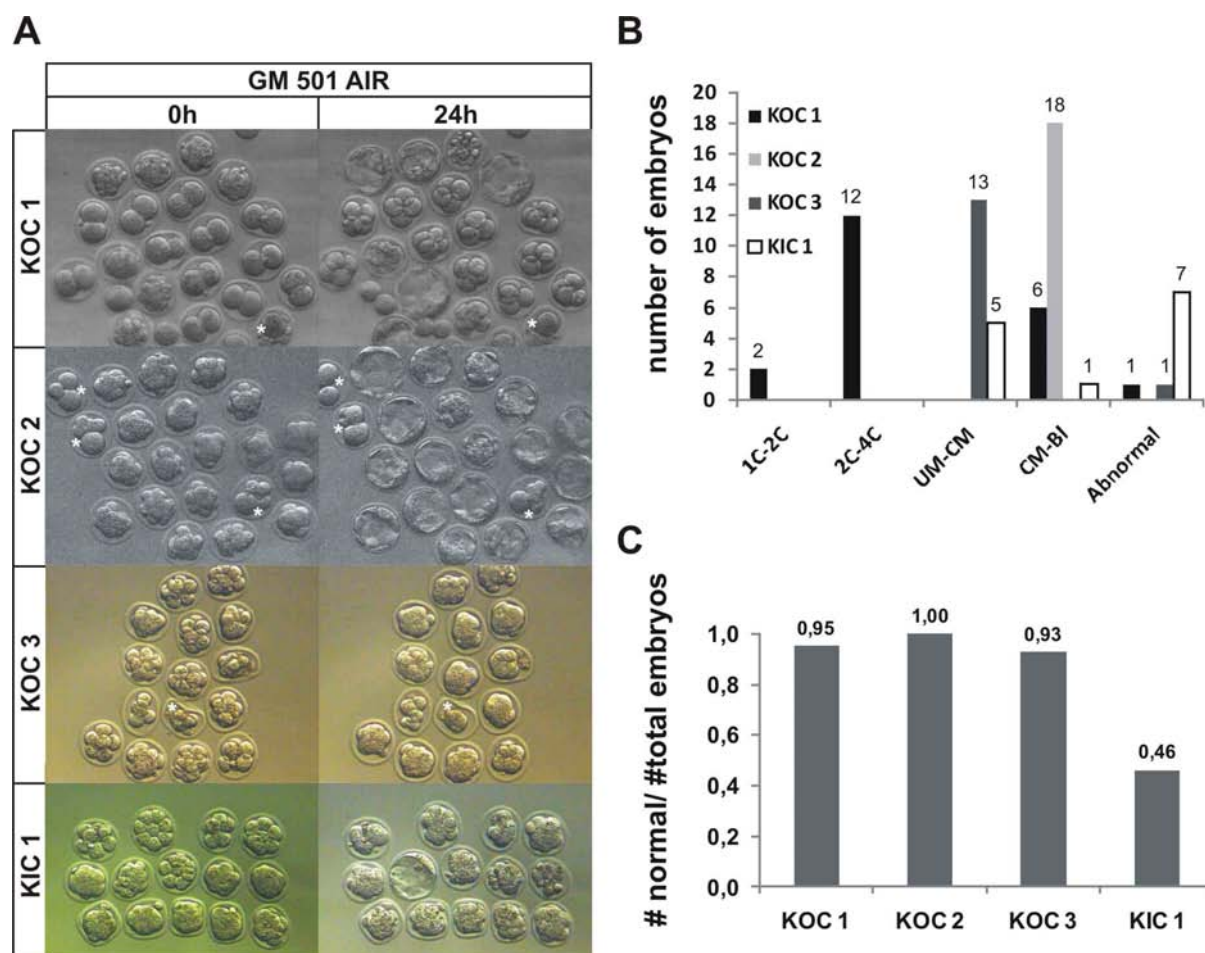


**Figure 3. Optimizing time lapse monitoring of *in vitro* preimplantation development (performed in Ghent).** (A) Development was scored following 24 h of time lapse monitoring of embryos derived from either  $p12octn^{KOC/+}$  intercrosses (KOC) or  $p12octn^{KIC/+}$  intercrosses (KIC) in GM 501 AIR. Embryos at the one-cell stage (1C) developed into two-cell embryos (2C). Uncompacted morulas (UM) could develop into compacted morulas (CM) or into blastocysts (BI). Abnormal embryos were morphologically aberrant or did not progress beyond their initial developmental stage. Embryos with aberrant morphology at the start of time-lapse monitoring are indicated with asterisks and are omitted from the analysis. (B) Diagram showing the development of embryos used in the experiments in A. (C) Diagram showing the ratio between the number of normal developing embryos and the total number of embryos.

and divided into two groups of 93 and 78 embryos. These groups were split again into four subgroups, each subgroup was transferred to a single well and all embryos were aligned and grouped using a micromanipulator (Fig. 2A). In addition, embryos derived from superovulated females tend to be less robust than embryos from natural matings. The maximal efficiency of *in vitro* development is probably close to 95%. A typical example of *in vitro* development of clustered embryos in GM 501 AIR is seen in Fig. 2E.

## Time lapse monitoring of *in vitro* preimplantation development

The next challenge was transferring this expertise to our laboratory in Ghent. This proved to be difficult, because it was nearly impossible to install micromanipulators on the Leica AS MDW live cell imaging system. So we used a Nikon Eclipse TE200 microscope connected to the Transferman NK micromanipulators that were used for blastocyst injection. However, this system has several drawbacks. First, we lacked an automated shutter, and so the light was always on, which might be harmful for the embryos. Second, this system lacked an incubation chamber, and so we could not provide CO<sub>2</sub> and the temperature was regulated by a thermo plate. Nevertheless, *in vitro* development could be monitored successfully by time lapse recordings (Figs. 3A,B). Although these experiments showed that development was quite normal (Fig. 3C), no homozygous p120ctn KOC or KIC embryos could be identified by genotyping.

## Rock inhibition delays blastocyst formation

Y-27632, a selective inhibitor of the Rho-associated coiled kinase (ROCK), enhances the survival of dissociated human ES cells (Watanabe et al., 2007) and improves the recovery from cryopreservation (Claassen et al., 2009; Li et al., 2009). In addition, Y27632-treatment results in increased proliferation and enables the expansion of undifferentiated human ES cells (Gauthaman et al., 2010). We wanted to test if the promoting growth and survival by inhibiting ROCK enhances the occurrence of homozygous p120ctn KOC and KIC embryos. So we monitored *in vitro* development of embryos derived from p120ctn<sup>KOC/+</sup> or p120ctn<sup>KIC/+</sup> intercrosses in either untreated medium (control) or in medium supplemented with 10 μM Y27632. In the first experiment (KOC 1), blastocyst formation was assayed starting from two-cell embryos, derived from p120ctn<sup>KOC/+</sup> intercrosses (Fig. 4A). After 24 h, both control and Y27632-treated embryos formed four- or eight-cell stage embryos, but after 48 h all control formed blastocysts but none of the Y27632-treated embryos did so. ROCK inhibition does not affect the developmental potential of cultured embryos because they develop into expanded blastocysts (Fig. 4A), but the blastocyst formation is delayed. This was confirmed in a second experiment (KOC 2, Fig. 4B) using embryos from p120ctn<sup>KOC/+</sup> intercrosses and in another experiment on embryos from p120ctn<sup>KIC/+</sup> intercrosses (KIC 1) (Fig. 4C). However, no homozygous p120ctn KOC or KIC embryos could be identified by genotyping.

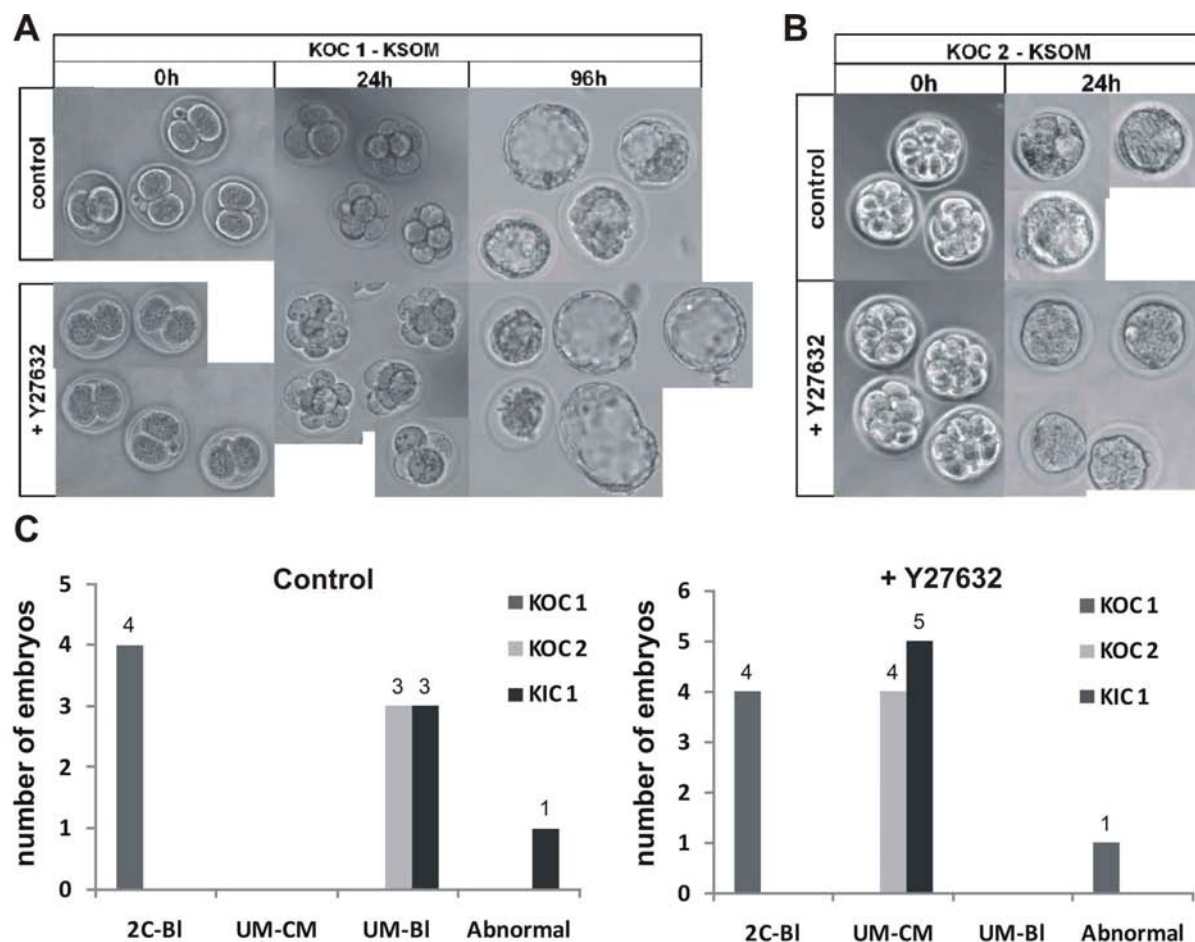


**Figure 4. ROCK inhibition delays blastocyst formation *in vitro*.** (A-B) Embryos derived from  $p120ctn^{KOC/+}$  or  $p120ctn^{KIC/+}$  intercrosses were cultured *in vitro* in normal medium (control) or in medium supplemented with the ROCK inhibitor Y27632. (C) Development was scored and is summarized in diagrams for control (left) and Y27632-treated embryos (right). Two-cell stage embryos (2C) and uncompact morulas (UM) could develop into compacted morulas (CM) or into blastocysts (BI). Abnormal embryos had an aberrant morphology or did not progress beyond their initial developmental stage.

### ACKNOWLEDGEMENTS

This work was supported by grants from the Queen Elisabeth Medical Foundation (G.S.K.E.), Belgium, and from the Geconcerteerde Onderzoeksacties of Ghent University. Tim Pieters has been supported by the Instituut voor de Aanmoediging van Innovatie door Wetenschap en Technologie in Vlaanderen (IWT). Dr. Marc Stemmler provided excellent training in handling and monitoring of preimplantation embryos. Dr. Tino Hocheplied was helpful in implementing time lapse monitoring of preimplantation embryos in the DMBR. Prof. Dr. Frans Van Roy and Dr. Jolanda van Hengel were instructive in the experimental design and editing of the manuscript. We thank the microscopy core for setting up image capture hardware and image analysis software. We acknowledge Dr. Amin Bredan for critical reading of the manuscript, and the members of our research group for valuable discussions.

### REFERENCES

- Claassen, D.A., M.M. Desler, and A. Rizzino. 2009. ROCK inhibition enhances the recovery and growth of cryopreserved human embryonic stem cells and human induced pluripotent stem cells. *Mol Reprod Dev.* 76:722-32.
- Gauthaman, K., C.Y. Fong, and A. Bongso. 2010. Effect of ROCK inhibitor Y-27632 on normal and variant human embryonic stem cells (hESCs) in vitro: its benefits in hESC expansion. *Stem Cell Rev.* 6:86-95.
- Hiiragi, T., and D. Solter. 2004. First cleavage plane of the mouse egg is not predetermined but defined by the topology of the two apposing pronuclei. *Nature.* 430:360-4.
- Kan, N.G., M.P. Stemmler, D. Junghans, B. Kanzler, W.N. de Vries, M. Dominis, and R. Kemler. 2007. Gene replacement reveals a specific role for E-cadherin in the formation of a functional trophectoderm. *Development.* 134:31-41.
- Li, X., R. Krawetz, S. Liu, G. Meng, and D.E. Rancourt. 2009. ROCK inhibitor improves survival of cryopreserved serum/feeder-free single human embryonic stem cells. *Hum Reprod.* 24:580-9.
- Pieters, T., P. D'Hooge, P. Hulpiau, M.P. Stemmler, F. Van Roy, and J. Van Hengel. in preparation. p120ctn isoform C knock-out and knock-in mice rescue E-cadherin loss and embryonic lethality in p120ctn-deficient embryos
- Summers, M.C., and J.D. Biggers. 2003. Chemically defined media and the culture of mammalian preimplantation embryos: historical perspective and current issues. *Hum Reprod Update.* 9:557-82.
- Watanabe, K., M. Ueno, D. Kamiya, A. Nishiyama, M. Matsumura, T. Wataya, J.B. Takahashi, S. Nishikawa, K. Muguruma, and Y. Sasai. 2007. A ROCK inhibitor permits survival of dissociated human embryonic stem cells. *Nat Biotechnol.* 25:681-6.

## Chapter 6

---

### **EFFICIENT AND USER-FRIENDLY PLURIPOTIN-BASED DERIVATION OF MOUSE EMBRYONIC STEM CELLS**

## Efficient pluripotin-based derivation of Mouse ES cells



## Efficient and user-friendly pluripotin-based derivation of mouse embryonic stem cells

Tim Pieters<sup>1,2</sup>, Tino Hochpied<sup>1,2</sup>, Jody Haigh<sup>1,2</sup>, Frans van Roy<sup>1,2</sup>, Jolanda van Hengel<sup>1,2,3</sup>

<sup>1</sup> Department for Molecular Biomedical Research, VIB, B-9052 Ghent, Belgium

<sup>2</sup> Department of Molecular Biology, Ghent University, Technologiepark 927, B-9052 Ghent, Belgium

<sup>3</sup> Corresponding author:

### TABLE OF CONTENTS

ABSTRACT .....	204
INTRODUCTION.....	205
MATERIAL AND METHODS .....	208
Mouse strains, breeding and genotyping.....	208
Classical ES cell derivation.....	208
Pluripotin-based ES cell isolation, ES cell culture, and embryoid body formation.....	209
Immunofluorescence .....	210
RESULTS.....	211
Classical derivation of ES cells for transgenic embryos in not efficient .....	211
Efficient pluripotin-based derivation of mouse ES cells.....	212
Characterization of newly established mouse ES cell lines .....	217
Attempt to generate homozygous p120ctn KOC, p120ctn KIC and p120ctn null ES cell lines .....	217
Generation and characterization of p120ctn <sup>KOC/-</sup> and p120ctn <sup>KIC/-</sup> ES cell lines .....	220
DISCUSSION .....	221
ACKNOWLEDGEMENTS .....	226
REFERENCES.....	226

### ABSTRACT

Classic derivation of mouse embryonic stem (ES) cells from blastocysts is inefficient, depends on the strain, and requires expert skills. Over recent years, several major improvements have greatly increased the success rate for deriving mouse ES cell lines. A first improvement was the establishment of a new, user-friendly and reproducible medium alternating protocol, allowing ES cell isolation of C57BL/6 transgenic mice with efficiencies of up to 75%. A recent report describes the use of this medium alternating protocol in combination with leukemia inhibitory factor and pluripotin treatment and made it possible to obtain embryonic stem cells from F1 strains (C57BL/6 transgenics X CD1) with high efficiency. Here we report modifications of these protocols which allowed user-friendly and reproducible derivation of mouse ES cells with efficiencies up to 100%. Our protocol describes a long initial incubation of primary outgrowths with pluripotin which resulted in big spherical outgrowth, that differ from classical inner cell mass (ICM) outgrowths, and can easily be picked and trypsinized. Pluripotin was omitted after the first trypsinization because pluripotin seems to block attachment of ES cells to the feeder layer and has to be removed to facilitate formation of ES cell colonies. We used our modified protocol to isolate 56 ES cell lines for C57BL/6 and five transgenic mouse strains (on C57BL/6 background) with an efficiency of up to 100%.

## INTRODUCTION

Embryonic stem (ES) cells are capable of self renewal and differentiation into all types of embryonic and adult cells, including the germ-cell lineage. Therefore, ES cells are a powerful tool in both regenerative medicine and biomedical research. Generation of genetically modified mice has been made possible by homologous recombination in mouse ES cells. The inventors of this ground-breaking technique were awarded the Nobel Prize in physiology or medicine in 2007 (Capecchi, 2008; Evans, 2008; Smithies, 2008). In addition, ES cells are instrumental in the analysis of transgenic mice if homozygous embryos die early during embryonic development.

Though leukemia inhibitory factor (LIF) was originally identified by its ability to induce differentiation of M1 leukemia cells (Gearing et al., 1987; Tomida et al., 1984), it prevents differentiation of mouse ES cells (Smith et al., 1988; Williams et al., 1988). Self-renewal of ES cells also depends on a second signal, which is produced by mouse embryonic fibroblasts (MEFs) or is a constituent of fetal bovine serum (FBS); this signal has been identified as BMP4 (Ying et al., 2003). On the other hand, ES cells can be propagated without differentiation in the absence of these external cues by inhibiting certain pathways that are important for self-renewal of ES cells (Ying et al., 2008).

Mouse ES cells are usually isolated from blastocysts. Blastocyst formation coincides with the first cell lineage specification in mouse embryogenesis, namely the formation of trophectoderm (TE) and inner cell mass (ICM) (Marikawa and Alarcon, 2009). The ICM is a pluripotent compact cell layer that gives rise to all the embryonic lineages and can be used to derive mouse ES cell lines. The first mouse ES cell lines were derived almost 30 years ago (Evans and Kaufman, 1981; Martin, 1981), but the classical way for isolating mouse ES cells is very inefficient, it is highly dependent on the strain, and it requires expert skills (Bryja et al., 2006b). The success rate for ES cell isolation is the highest (~30%) in favorable 129 strains, but it drops below 10% for C57BL/6 strains (Brook and Gardner, 1997; McWhir et al., 1996). There are many 129 substrains and their genetic variability is substantial. Although historically gene targeting has been performed mainly in ES cells from the 129 mouse strains, these strains are poor breeders and their anatomy and behavior are atypical (Nagy and Vintersten, 2006). Therefore, after gene targeting in 129 ES cells, the chimeric transgenic progeny is routinely backcrossed into the C57BL/6 background. C57BL/6 is considered the gold standard among reference strains (Rivera and Tessarollo, 2008). The C57BL/6 mouse is

## Efficient pluripotin-based derivation of Mouse ES cells

long-lived, breeds well, and its genome has been fully sequenced (Mouse Genome Sequencing Consortium, 2002). Moreover, the phenotypes of many mouse mutants have been studied in the C57BL/6J strain. However, classic ES cell isolation protocols are not efficient in this strain.

Several major improvements have greatly increased the success rate for deriving mouse ES cell lines. First, a defined serum-free medium (knockout serum replacement, SR) improved the generation of C57BL/6J embryonic stem cells (Cheng et al., 2004) and thereby increased the success rate to approximately 20%. Second, alternating between SR-containing medium and ES cell medium containing FBS allowed isolation of ES cells from C57BL/6 transgenic strains in an easy and reproducible manner and with efficiencies of up to 75% (Bryja et al., 2006b). Third, the use of pharmacological compounds in combination with LIF and MEFs has increased the efficiency of ES cell isolation. These compounds include PD98059 and U0126, which are inhibitors of mitogen-activated protein kinase (MAPK)/extracellular signal-related kinase (ERK) kinase (MEK) (Buehr and Smith, 2003; Lodge et al., 2005), the p38 inhibitor SB203580 (Qi et al., 2004), and BIO, an inhibitor of glycogen synthase kinase-3 (GSK-3) (Umehara et al., 2007). In addition, mouse ES cells could be isolated from 129 strains and the non-permissive CBA strain without the need for extrinsic stimuli, such as serum factors, MEFs, LIF or BMP4, but the efficiency of this method was not reported (Ying et al., 2008). The latter ES cell lines were obtained and maintained in a chemically defined medium containing three small-molecule inhibitors (3i) of, respectively, MEK 1/2 (PD98059), GSK-3 (CHIR99021) and fibroblast growth factor receptor (FGFR; SU5402) (Ying et al., 2008). The 3i method was also used to derive and propagate rat ES cells with success rates of 34% (Li et al., 2008) and 12% (Buehr et al., 2008). Using a system with two inhibitors (2i), PD0325901 for MEK and CHIR99021 for GSK-3, also allowed derivation of rat ES cells with an efficiency of 61% (Buehr et al., 2008). The 2i system, when supplemented with LIF, enabled derivation and propagation of mouse ES cells from the recalcitrant non-obese diabetic (NOD) strain with an efficiency of 53% (Nichols et al., 2009). Furthermore, adding only pluripotin, a small synthetic molecule, to the culture medium also allows the propagation of mouse ES cells in an undifferentiated state in the absence of LIF and MEFs (Chen et al., 2006). Finally, combining a reliable medium alternating protocol that switches between SR-containing and FBS-containing ES cell medium supplemented with MEFs, LIF and pluripotin eventually made it possible to derive

mouse ES cells from refractory strains with a success rate of up to 80% (57% for NOD-SCID) and from F1 strains (C57BL/6 transgenic x CD1) with 100% efficiency (Yang et al., 2009).

Here, we report the modifications of previously reported protocols (Bryja et al., 2006b; Yang et al., 2009) and the isolation of 69 ES cell lines from five transgenic strains on the C57Bl/6 background with an efficiency of up to 100%.

### MATERIAL AND METHODS

#### Mouse strains, breeding and genotyping

The generation of p120ctn<sup>KOC/+</sup>, p120ctn<sup>KIC/+</sup> and p120ctn<sup>+/-</sup> mice, all backcrossed on the C57BL/6 background, will be reported elsewhere (Pieters et al., in preparation). In brief, the p120ctn KOC allele lacks the alternatively spliced exon C (exon 11)(Keirsebilck et al., 1998) of the p120ctn gene (*Ctnd1*), while the p120ctn KIC allele constitutively incorporates exon C in all its transcripts. The p120ctn null allele was generated by Cre-mediated removal of a floxed region in the p120ctn gene (containing exons 3 to 8 and including all four possible start codons) (Betz et al., 1996; Davis and Reynolds, 2006). Preimplantation embryos were obtained by crossing or intercrossing heterozygous p120ctn<sup>+/-</sup>, p120ctn<sup>KOC/+</sup> and p120ctn<sup>KIC/+</sup> mice. Embryos were flushed with M2 medium (Sigma-Aldrich Inc., St. Louis, MO) from oviducts at E1.5 and E2.5 by using a 32G needle (Popper & Sons Inc., New York, Cat. No. 7400) and a 5-ml Luer-Lok syringe. For flushing from the uterus at E3.5, a 23G needle and a 1-ml syringe were used. Female mice at the age of 6–8 weeks were housed with male studs and copulation plugs were checked the following morning. Genotyping was performed by PCR on genomic DNA isolated from mouse tail snips or from ES cells, as described elsewhere (Pieters et al., in preparation). Mice were housed in individually ventilated cages in a specific pathogen-free animal facility. All experiments on mice were conducted according to institutional, national, and European animal regulations. Animal protocols were approved by the ethics committee of Ghent University.

#### Classical ES cell derivation

ES cells were isolated and cultured on feeder cells in either RESGRO medium (Chemicon) supplemented with L-glutamine (2 mM, Gibco) or in normal ES cell medium, consisting of DMEM (Gibco) with 15% FCS (PAN biotech, Aidenbach, Germany), supplemented with L-glutamine (2 mM, Gibco), sodium pyruvate (1 mM, Gibco), non-essential amino acids (Gibco), penicillin (100 U/ml, Gibco), streptomycin (100 mg/ml, Gibco),  $\beta$ -mercaptoethanol (0.1 mM, Gibco), 500 U/ml LIF (Chemicon). Embryos were seeded individually in separate wells of 96-well plates with inactivated MEFs and are cultured in 5% CO<sub>2</sub> at 37°C. On the fourth day, primary outgrowths were washed with PBS and were passaged in batch using a multichannel pipette with 50 $\mu$ l trypsin (Gibco) followed by an incubation for 5 min in 5% CO<sub>2</sub> at 37°C. Primary outgrowths were dissociated into small cell

clumps by pipetting up and down (ten times) and were transferred in (3 times 100  $\mu$ l) ES cell medium to new MEF-containing 96-well plates. After four days of culture, the ES cell like colonies were passaged again to new MEF-containing 96-well plates. After four days of culture, the ES cell-like colonies were passaged to 0,1% gelatin-coated 96-well plates. Newly established ES cell lines were passaged to MEF-containing 24-well and subsequently to 6-well plates.

### **Pluripotin-based ES cell isolation, ES cell culture, and embryoid body formation**

Basic ES cell medium consisted of Dulbecco's modified Eagle's medium (DMEM, Gibco, Grand Island, NY) and F12 (Gibco) mixed in a 1:1 ratio and supplemented with 15% knock-out serum replacement (SR, Gibco, Cat. No. 10828-028, for SR-ES cell medium) or 15% FBS (Hyclone, Logan, UT, Cat. No. SH30070.03E, for FBS-ES cell medium), L-glutamine (2 mM, Gibco), penicillin (100 U/ml, Gibco), streptomycin (100 mg/ml, Gibco),  $\beta$ -mercaptoethanol (0.1 mM, Gibco), and 2000 U/ml recombinant mouse LIF (DMBR/VIB Protein Service facility, [www.dnbr.ugent.be](http://www.dnbr.ugent.be)). Pluripotin (4  $\mu$ M, Cayman Chemical, Ann Arbor, MI, ) was added just before use. The procedure for ES cell isolation, schematized in figure 1, is a modified version of previously published protocols (Bryja et al., 2006a; Bryja et al., 2006b; Yang et al., 2009). In brief, blastocysts and morulas were collected and plated individually on 12-well mitomycin-C treated mouse embryonic feeder plates (MEF, TgN (DR4)1 Jae strain) with pluripotin-containing SR-ES cell medium (day 1). On days 6, 8 and 10, the pluripotin-containing SR-ES cell medium was refreshed, using a mouth pipette to prevent losing unattached or loosely attached outgrowths. Between days 12 and 16, big loosely attached spherical outgrowths from mouse embryos were picked, transferred to curved 96-well plates containing 30  $\mu$ l PBS (Gibco), and dissociated by incubation in 50  $\mu$ l of 0.25% trypsin (Gibco) for 3 min in 5% CO<sub>2</sub> at 37°C. Outgrowths were transferred in 100  $\mu$ l FBS-ES cell medium (preincubated for 1 h in 5% CO<sub>2</sub> at 37°C) to 96-well mitomycin C-treated MEF plates (containing 100  $\mu$ l preincubated FBS-ES cell medium) and dissociated into single cells and small-cell clumps by pipetting 10–15 times. Next day, the medium was changed to SR-ES cell medium. Newly established ES cell colonies were passaged two more times with a change of medium, scaling up from 96-well to 24-well and then 6-well plates using 30, 200 and 800  $\mu$ l of 0.25% trypsin, respectively. Dissociated cells were plated in FBS-ES medium, which was replaced next day by SR-ES medium. Established ES cell lines were propagated

## Efficient pluripotin-based derivation of Mouse ES cells

further using SR-ES medium and then frozen in 10% DMSO and 90% FCS in freeze containers (Nalgene, Rochester, NY) .

The embryoid body formation procedure was similar to that described before (Bibel et al., 2007; Bibel et al., 2004). In brief, highly proliferative ES cells were passaged at least twice in SR-ES cell medium on 0.1% gelatin-coated plates to get rid of the MEF cells and allow the ES cells to grow as flat monolayers. After trypsinization,  $4 \times 10^6$  cells were plated in non-adherent 10-cm bacterial grade Petri dishes containing cell aggregation (CA) medium composed of DMEM supplemented with 10% FCS, 2 mM L-glutamine, non-essential amino acids (Gibco) and 0.1 mM  $\beta$ -mercaptoethanol. Cell aggregates grow in suspension and are refreshed every other day after letting them settle spontaneously on the bottom of a 50-ml tube. After eight days, big embryoid bodies are readily visible.

### Immunofluorescence

The staining procedure for ES cells involved methanol fixation and incubation for 2 h with primary antibody and 1 h with secondary antibody, each of which was dissolved in a 1:4 mixture of 2% gelatin and PBS. The following antibodies were used: mouse monoclonal anti-p120ctn (pp120, 1/500, BD Transduction Laboratories, San Jose, CA), anti-Oct-4 (1/100, Santa Cruz Biotechnology, Santa Cruz, CA), Secondary species-specific Alexa-fluorochrome-conjugated antibodies (Molecular Probes, Eugene, OR) were used at a dilution of 1/500. Pictures were taken with an Olympus microscope or with a confocal microscope. Confocal microscopy was performed using a Leica TCS SP5 confocal scan head attached to a Leica DM IRE2 inverted microscope and a PC running Leica AF software version 2.5. Optical sections were taken every 2  $\mu$ m. Image analysis was performed using Volocity software (Perkin Elmer).



## RESULTS

## Classical derivation of ES cells for transgenic embryos in not efficient

By using a classical isolation procedure for ES cells with either normal or conditioned ES cell medium we failed to isolate ES cells in an efficient way (Table 1). We were able to establish ES cell lines for wild-type and transgenic C57BL/6 strains with an efficiency of only 4%. However, no ES cell lines were derived if we performed the classical ES cell isolation procedure on embryos obtained from p120ctn<sup>KOC/+</sup> or p120ctn<sup>KIC/+</sup> intercrosses (Table 1).

Table 1. Classical and RESGRO-mediated derivation of ES cells

Mating	Method	Embryonic stage	No. of embryos	Primary outgrowth (passage 0)	Lines derived (>passage 5)
<b>C57BL/7</b> <b>intercross</b>	classical	morula	24		1 (4%)
	(Freiburg)				
<b>Ncadh<sup>KI</sup></b> <b>intercross</b>	classical	morula	74	3 (4%)	3? (4%)
	(Freiburg)				
<b>p120ctn<sup>KOC/+</sup></b> <b>intercross</b>	Classical (Ghent)	morula	20		0 (0%)
	RESGRO*	blastocyst	89		1 (1%)
	RESGRO	morula	93		0 (0%)
	RESGRO	blastocyst	35	24 (69%)	0 (0%)
	RESGRO	morula	13	0 (0%)	0 (0%)
	pluripotin	morula	14	5 (36%)	0 (0%)
<b>p120ctn<sup>KIC/+</sup></b> <b>intercross</b>	Classical (Ghent)	blastocyst	9		0 (0%)
	Classical (Ghent)	morula	14		0 (0%)
	RESGRO	blastocyst	88		1 (1%)
	RESGRO	morula	36		0 (0%)
	RESGRO	blastocyst	17	4 (24%)	0 (0%)
	RESGRO	morula	55	14 (25%)	0 (0%)
	pluripotin	morula	33	7 (21%)	0 (0%)

\* Formerly TX-WES

Experiments were either performed in the Max-Planck institute for immunobiology in Freiburg or in Ghent (DMBR-UGent-VIB)

It has been reported that RESGRO ES cell medium, conditioned by a rabbit fibroblast cell line transduced with genomic rabbit leukemia inhibitory factor, allows efficient derivation and propagation of ES cell lines (Schoonjans et al., 2003). Using a classical ES cell procedure with RESGRO ES cell medium resulted only in one p120ctn<sup>KOC/+</sup> ES cell line and

## Efficient pluripotin-based derivation of Mouse ES cells

one p120ctn<sup>KIC/+</sup> ES cell line. The overall success rate of ES cell isolation in conditioned medium was still lower than 1% and in most cases no ES cell lines could be isolated at all (Table 1). In addition, we were also unable to derive ES cell lines from morulas, obtained from p120ctn<sup>KOC/+</sup> or p120ctn<sup>KIC/+</sup> intercrosses, when following a pluripotin-based protocol (Table 1)(Yang et al., 2009).

## Efficient pluripotin-based derivation of mouse ES cells

To increase the efficiency of mouse ES cell isolation from transgenic mice on a C57BL/6 background, we established an optimized pluripotin-based method based on the protocols of Bryja et al. (2006b) and Yang et al. (2009). By our modified procedure we isolated 56 mouse ES cell lines for C57BL/6 and five transgenic mouse strains (all on the C57BL/6 background) with an efficiency of 100% for C57BL/6, 67% for p120ctn<sup>KOC/+</sup> intercrosses, 90% for p120ctn<sup>KIC/+</sup> intercrosses, 100% for p120ctn<sup>+/-</sup> intercrosses, and 100% for both p120ctn<sup>KOC/-</sup> and p120ctn<sup>KIC/-</sup> strains (Table 2). The protocol was modified by culturing primary outgrowths for 12 days in pluripotin-containing SR-ES cell medium and by omitting pluripotin after the first trypsinization (Fig. 1).

**Table 2. The derivation efficiency of ES cells from blastocysts**

Strain/mating	No. of blastocysts	Primary outgrowth	Lines derived
		(passage 0)	(>passage 5)
<b>C57BL/6</b>	6	6 (100%)	6 (100%)
<b>p120ctn<sup>KOC/+</sup> intercross</b>	9	7 (78%)	6 (67%)
<b>p120ctn<sup>KIC/+</sup> intercross</b>	20	18 (90%)	18 (90%)
<b>p120ctn<sup>+/-</sup> intercross</b>	5	5 (100%)	5 (100%)
<b>p120ctn<sup>KOC/+</sup> x p120ctn<sup>+/-</sup></b>	13	13 (100%)	13 (100%)
<b>p120ctn<sup>KIC/+</sup> x p120ctn<sup>+/-</sup></b>	8	8 (100%)	8 (100%)
<b>total</b>	61	57 (93%)	56 (91%)

The prolonged cultivation of primary outgrowths in the presence of pluripotin allowed the formation of big spheres composed of pluripotent cells that do not much resemble the classical ICM outgrowths (Fig. 2, compare panel A to B or C). These spheres were mostly loosely attached to the underlying MEF layer but sometimes appeared in suspension; in both cases mouse ES cell lines could be readily isolated from them. In our hands the efficiency of initial mouse ES cell isolations (using our protocol) was not maximal due to the loss of non-attached spheres while changing medium, rather than to intrinsic failure of primary

outgrowths to form mouse ES cell lines. Omitting pluripotin during the first two days of initial culture allowed blastocysts to attach to the MEFs and form classical ICM outgrowths (Fig. 2B), which gave rise to ES cell lines with a lower efficiency (33%) (Table 3).

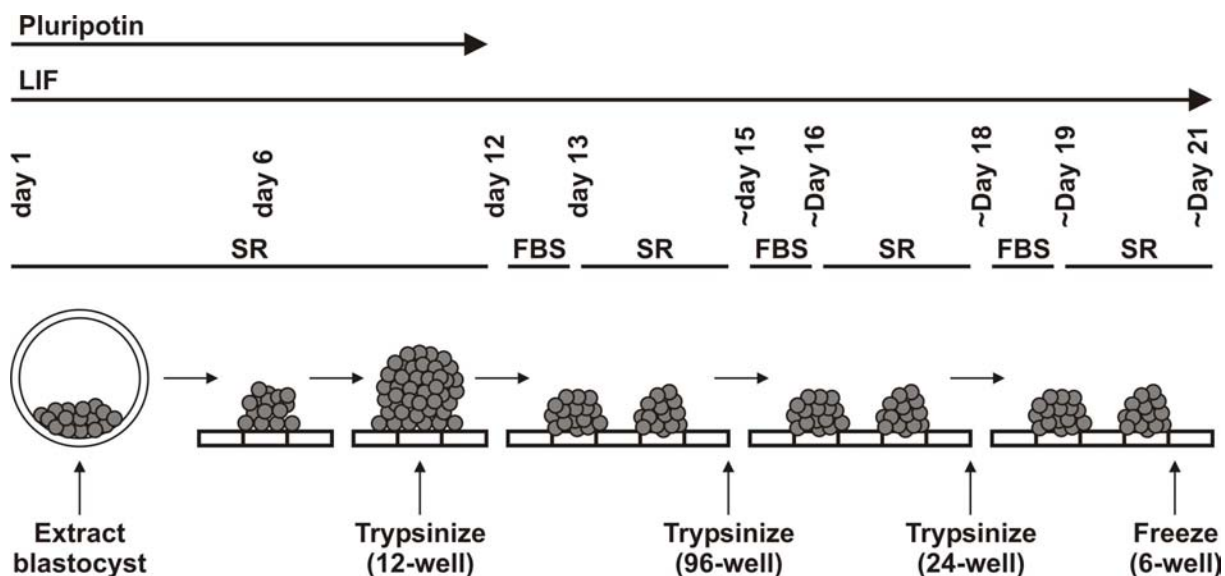


**Figure 1. Scheme of ES cell derivation with LIF and pluripotin.** Blastocysts are flushed on day 1 and seeded in 12-well plates coated with MEFs and with pluripotin-containing SR-ES cell medium (15% SR). Small spherical colonies, observed on day 6, grow rapidly to form big spherical cell aggregates that are loosely attached to the feeder layer on day 12. Big pluripotent cell aggregates are trypsinized with 0.25% trypsin and seeded in 96-well plates containing MEFs and FBS-ES cell medium (15% FBS) but no pluripotin. The next day, FBS-ES cell medium is replaced with SR-ES cell medium. After further incubation, ES cells appear. Newly established ES cell colonies are passaged two more times, changing the medium from FBS to SR-ES and scaling up from 96-well to 24-well and then 6-well plates. On about day 21, a confluent 6-well plate of newly established mouse ES cell line can be frozen. Adapted and modified after (Bryja et al., 2006b).

**Table 3. The derivation efficiency of ES cells from morulas and from blastocysts with pluripotin-treatment on day 3**

Strain/mating	No. of morulas	Primary outgrowth (passage 0)	Lines derived (>passage 5)
<b>p120ctn<sup>KOC+</sup> intercross</b>	19	6 (32%)	3 (16%)
<b>p120ctn<sup>KIC+</sup> intercross</b>	9	3 (33%)	1 (11%)
	28	9 (32%)	4 (14%)
Strain	No. of blastocysts	Primary outgrowth (passage 0)	Lines derived (>passage 5)
<b>C57BL/6</b>	9#	5 (55%)	0 (0%)
<b>C57BL/6</b>	7*	6 (85%)	0 (0%)
<b>p120ctn<sup>+/+</sup> intercross</b>	9*	4 (44%)	3 (33%)

# ES cell derivation according to Yang et al., (2009), \* pluripotin addition from day 3

Efficient pluripotin-based derivation of Mouse ES cells

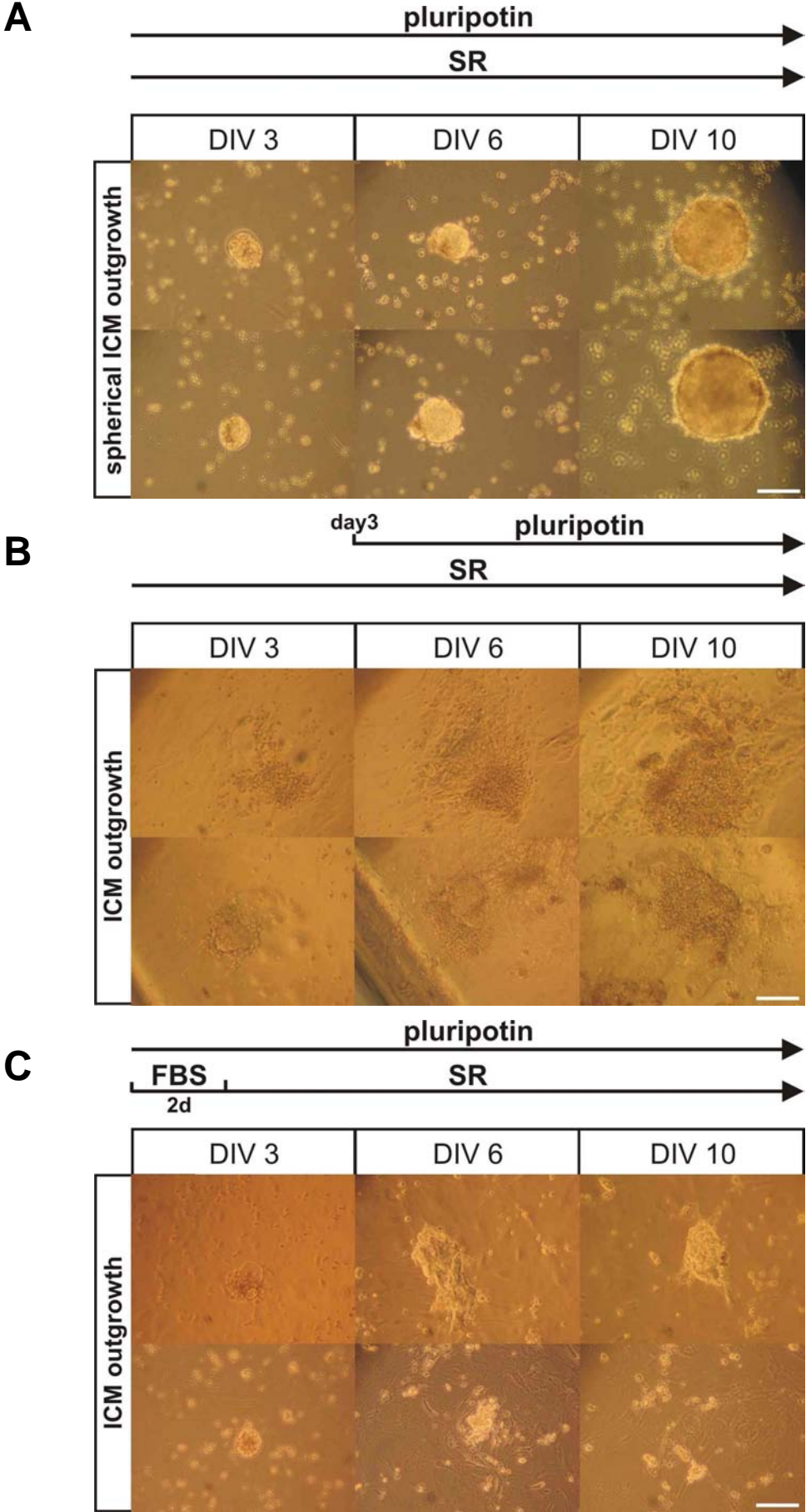


**Figure 2. Formation of non-classical spherical ICM outgrowths in SR medium supplemented with pluripotin and LIF.** Formation of ICM outgrowths from wild-type C57BL/6 blastocysts under different experimental conditions. (A) Two examples of non-classical, loosely attached, spherical ICM outgrowths formed after incubation in SR-ES medium supplemented with pluripotin and LIF. (B) Omitting pluripotin from the SR medium in the first two days allows attachment of blastocysts and formation of flat ICM outgrowths, which persist after pluripotin administration. Two examples are shown. (C) Two examples of ICM outgrowths formed according to Yang et al. (2009). Blastocysts were incubated for two days (2d) in FBS-ES medium supplemented with pluripotin and LIF, followed by incubation in SR-ES medium supplemented with pluripotin and LIF. DIV: days *in vitro*. Scale bar: 500  $\mu$ m.

After culturing the cells for 12 days with LIF and pluripotin, spherical colonies were readily visible by naked eye (Fig 2A, DIV10). The blastocyst outgrowths could be cultured up to 18 days without losing their ability to form ES cell lines. The big advantage of long initial culture in pluripotin-containing SR-ES cell medium is starting with a large amount of undifferentiated cells before the first trypsinization, which allows the establishment of ES cell lines with great confidence once large pluripotent spheres are obtained: 57 initial outgrowths gave rise to 56 ES cell lines (98%). The big spherical outgrowths were easy to pick and after trypsinization, cells were readily dissociated into single cells and plated on MEFs. When pluripotin was present in the FBS-containing ES cell medium, most of the cells failed to attach to the MEF layer and were lost upon changing the medium to SR-containing ES cell medium. By excluding pluripotin after the first trypsinization, dissociated cells became attached to the MEFs and formed primary ES cell colonies within days. These primary ES cell colonies were propagated in 96-well plates, then in 24-well plates and finally in six-well plates, after which they were frozen (Fig. 1).

Next, we compared the performance of our modified mouse ES cell derivation protocol with that of the protocol of Yang and colleagues (2009). Differences between these ES cell derivation protocols are listed in Table 4. Formation of ICM outgrowths and ES cell isolation from wild-type C57BL/6 blastocysts were performed according to our modified protocol or according to Yang and colleagues (2009). From the nine blastocysts that were processed with the latter protocol, only five formed small ICM outgrowths (Figs. 2C, 3A). Most outgrowths were dissociated after ten days of culture (Fig. 3A; DIV 10) and no ES cell lines could be derived from them (Table 3). In contrast, all six blastocysts, which were processed according to our modified protocol, formed big spherical ICM outgrowths after 10 days of culture (Figs. 2A, 3B; DIV 10). ES cell lines were established for all six outgrowths (Table 2). To conclude, our modified protocol allowed big spherical ICM outgrowths to be formed in a robust and reliable manner.

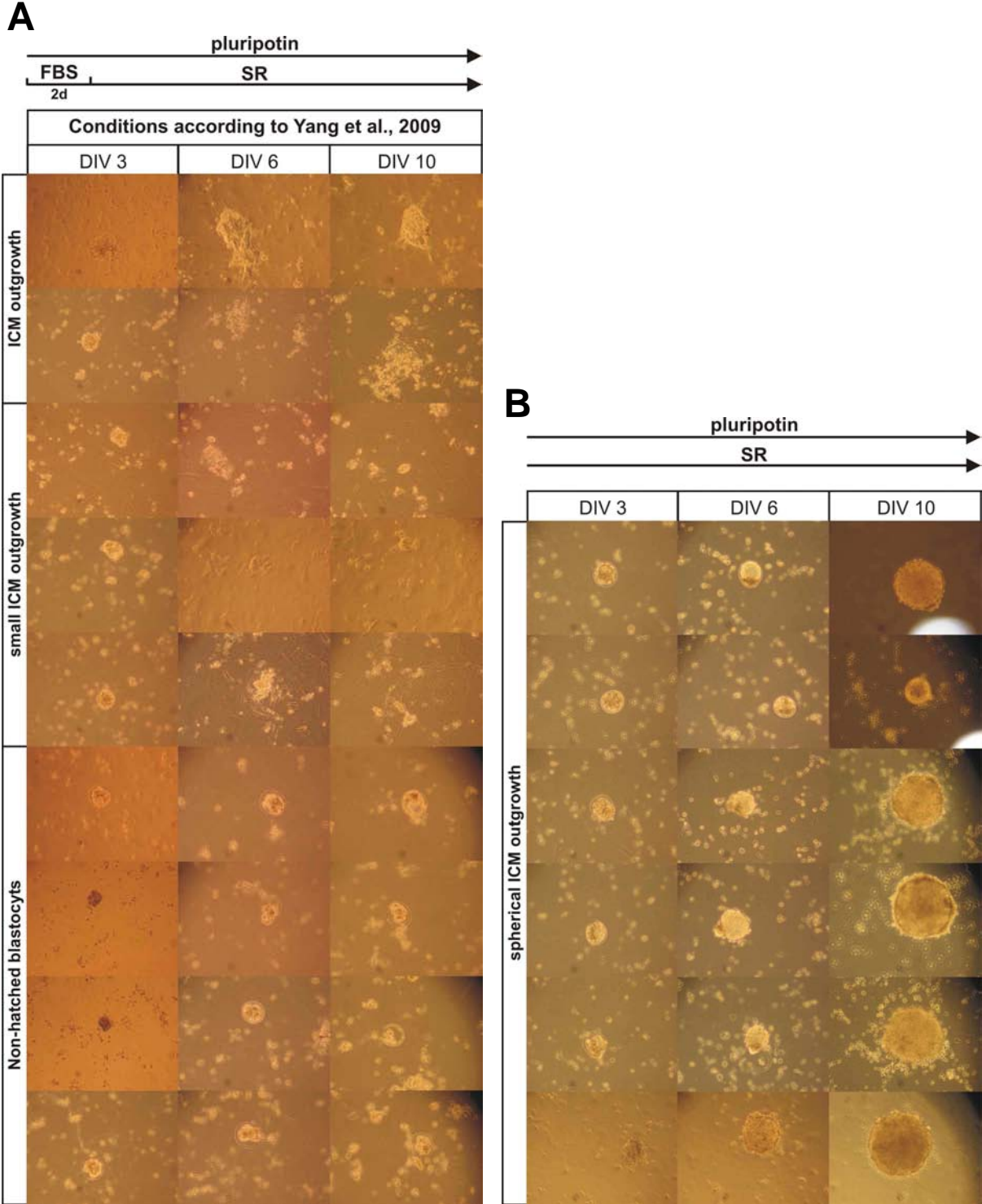


**Figure 3. Comparison between ES cell derivation protocols.** Formation of ICM outgrowths from wild-type C57BL/6 blastocysts under different experimental conditions. (A) Nine blastocyst were cultured according to Yang et al. (2009). Four blastocysts did not hatch from their zona pellucid. Only two ICM outgrowths were maintained after ten days of culture (top). (B) Six blastocysts were incubated in SR medium supplemented with pluripotin and LIF and all six blastocysts formed loosely attached, spherical ICM outgrowths after ten days of culture. Two outgrowths detached from the feeders and grew in suspension (top). DIV: days *in vitro*.



**Table 4. Comparison of different ES cell derivation protocols**

	ES cell derivation protocol			
	classical	Byrja et al. (2006b)	Yang et al. (2009)	Pieters et al.
Blastocysts seeded in	FBS-medium	SR-medium	FBS-medium	SR-medium
Incubation time of primary outgrowths	4-5 days	6 days	3-14 days	12-18 days
Medium alternating	no	yes	yes	yes
Pluripotin treatment	no	no	constant	till first trypsinization
Morphology of the outgrowth	ICM-like colony	ICM-like colony	ICM-like colony	big spheres
Attachment of outgrowths to feeders	strong	strong	strong	weak
Size outgrowths			500 $\mu$ m	900 $\mu$ m
Outgrowth dissociation	trypsin	trypsin	collagenase IV, trypsin	trypsin
User-friendly	no	yes	no	yes
Success rate (Strain)	30% (129)	50-75% (C57BL/6	100% (F1: C57BL/6	100% (C57BL/6
	10% (C57BL/6)	transgenics)	transgenics X CD1)	transgenics)

### Characterization of newly established mouse ES cell lines

Newly established ES cell lines could be maintained in a morphologically undifferentiated state for over 10 passages (Fig. 4A), and all ES cell colonies examined expressed the transcription factor Oct-4 (Fig. 4B), but not the trophectoderm-specific transcription factor Cdx2 (data not shown). The newly established ES cell lines proliferated rapidly and embryoid bodies could be readily formed (Fig. 4C). Those embryoid bodies could be differentiated into various cell types, including beating cardiomyocytes.

### Attempt to generate homozygous p120ctn KOC, p120ctn KIC and p120ctn null ES cell lines

Next, we tried to use the optimized protocol to generate homozygous ES lines for p120ctn KOC and KIC mice, both on the C57BL/6 background. This proved to be difficult since both homozygous p120ctn KOC and KIC embryos died before implantation (Pieters et al., in preparation). Blastocysts from p120ctn<sup>KOC/+</sup> and p120ctn<sup>KIC/+</sup> intercrosses gave rise to several ES cell lines (6 and 35, respectively), but no homozygous p120ctn<sup>KOC/KOC</sup> or p120ctn<sup>KIC/KIC</sup> ES cell lines could be obtained (Table 5). To increase the chance of retrieving viable homozygous p120ctn KOC or KIC embryos, we tried starting ES cell isolation from morulas instead of blastocysts. Unfortunately, ES cell isolation from morulas turned out to be much less efficient (14% compared to 91% for blastocysts) (Tables 2, 3) and only four ES lines could be isolated from 28 morulas (Table 5).

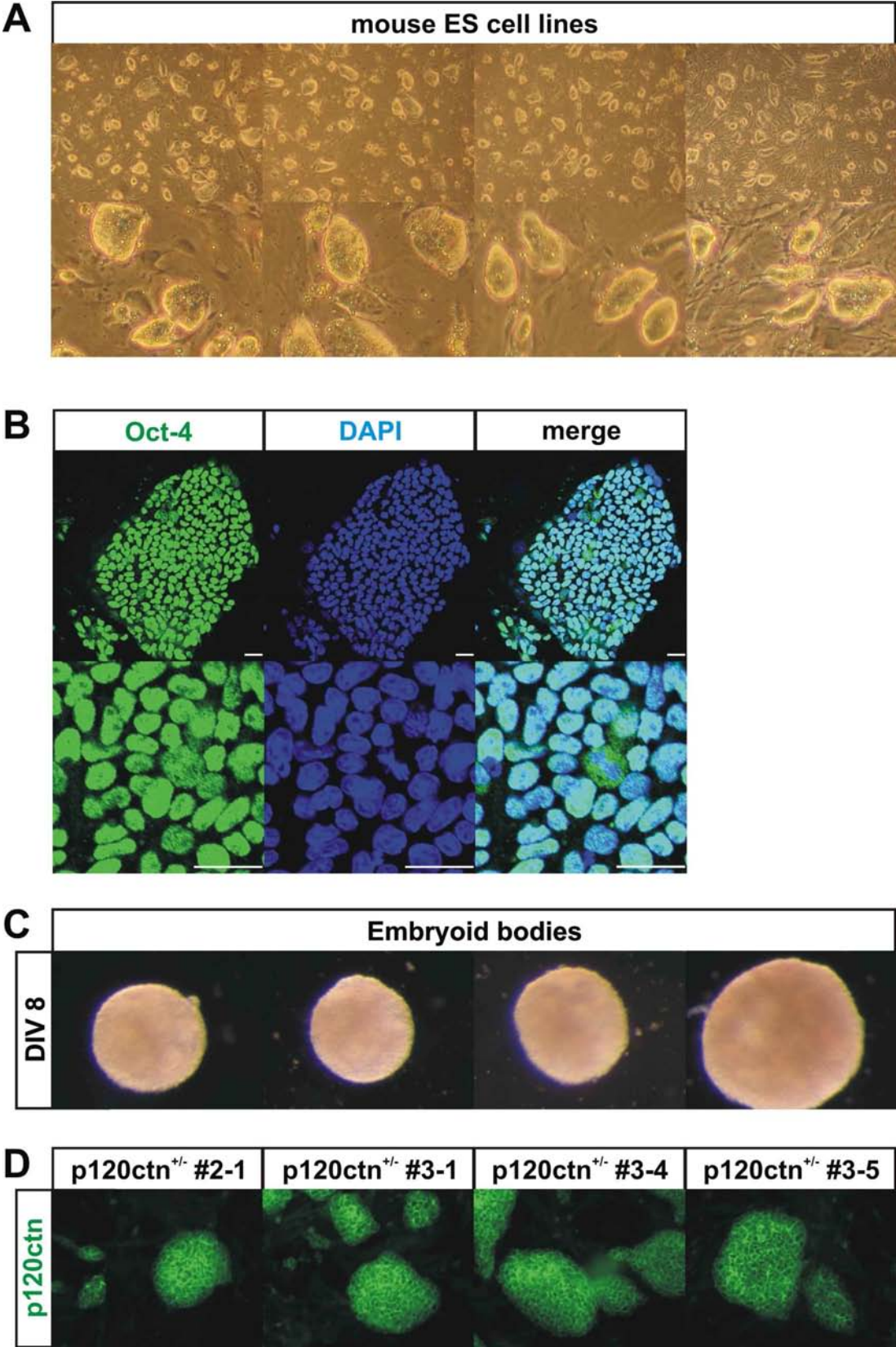


**Figure 4. Properties of ES cell lines derived from pluripotin-treated primary outgrowths.** (A) Morphology of newly established mouse ES cell lines, which are positive for stem cell marker Oct-4 (B) and form embryoid bodies after eight days of culture in suspension (C). p120ctn immunostainings of p120ctn<sup>+/-</sup> ES cell lines (D). Scale bar: 25 μm.



The lowered efficiency was due to decreased formation of primary outgrowths (32% compared to 93%) (Tables 2, 3). Although morulas derived from p120ctn<sup>KOC/+</sup> and p120ctn<sup>KIC/+</sup> intercrosses gave rise to ES cell lines (three and one, respectively), no homozygous p120ctn<sup>KOC/KOC</sup> or p120ctn<sup>KIC/KIC</sup> ES cell lines were obtained (Table 5). In conclusion, by using blastocysts from p120ctn<sup>KOC/+</sup> and p120ctn<sup>KIC/+</sup> intercrosses we established 41 new ES cell lines with efficiencies of 40 to 90%. However, no homozygous p120ctn KOC or KIC ES cell lines could be isolated due to the low frequency of homozygous p120ctn KOC and KIC embryos, which show abnormalities during preimplantation.

**Table 5. The derivation efficiency and genotype of ES cells**

Mating	Embryonic stage	No. of embryos	Primary outgrowth (passage 0)	Lines derived (>passage 5)	genotype			
					+/+ (25%)	KOC/+ (50%)	KOC/KOC (25%)	
<b>p120ctn<sup>KOC/+</sup></b>	blastocyst	9	7 (78%)	6 (67%)	2 (33,3%)	4 (66,7%)	0 (0%)	
<b>intercross</b>	morula	19	6 (32%)	3 (16%)	0 (0%)	3 (100%)	0 (0%)	
					genotype			
					+/+ (25%)	KIC/+ (50%)	KIC/KIC (25%)	
<b>p120ctn<sup>KIC/+</sup></b>	blastocyst	24	17 (71%)	13 (54%)	2 (15%)	11 (85%)	0 (0%)	
<b>intercross</b>	blastocyst	10	4 (40%)	4 (40%)	0 (0%)	4 (100%)	0 (0%)	
	blastocyst	20	18 (90%)	18 (90%)	0 (0%)	18 (100%)	0 (0%)	
	morula	9	3 (33%)	1 (11%)	0 (0%)	1 (100%)	0 (0%)	
					genotype			p120ctn staining
					+/+ (25%)	+/- (50%)	-/- (25%)	
<b>p120ctn<sup>+/-</sup></b>	blastocyst	5	3 (60%)	1 (20%)	1 (100%)	0 (0%)	0 (0%)	nd
<b>intercross</b>	blastocyst	5	2 (20%)	1 (20%)	0 (0%)	1 (100%)	0 (0%)	1/1
	blastocyst	5	5 (100%)	5 (100%)	2 (40%)	3 (60%)	0 (0%)	3/3
	blastocyst*	9	4 (44%)	3 (33%)	1 (33%)	2 (66%)	0 (0%)	2/2
					genotype			
					KOC/- (25%)	KOC/+ (25%)	+/- (25%)	+/+ (25%)
<b>p120ctn<sup>KOC/+</sup></b>	blastocyst	9	9 (100%)	9 (100%)	2 (22%)	1 (11%)	4 (44%)	2 (22%)
<b>X p120ctn<sup>+/-</sup></b>	blastocyst	4	4 (100%)	4 (100%)	0 (0%)	1 (25%)	2 (50%)	1 (25%)
					genotype			
					KIC/- (25%)	KIC/+ (25%)	+/- (25%)	+/+ (25%)
<b>p120ctn<sup>KIC/+</sup></b>	blastocyst	8	8 (100%)	8 (100%)	3 (38%)	5 (63%)	0 (0%)	0 (0%)
<b>X p120ctn<sup>+/-</sup></b>								
<b>C57BL/6</b>	blastocyst	6	6 (100%)	6 (100%)				

\* pluripotin addition from day 3; nd, not done

## Efficient pluripotin-based derivation of Mouse ES cells

We also tried to obtain p120ctn null (p120ctn<sup>-/-</sup>) ES cell lines. However, homozygous p120ctn null (p120ctn<sup>-/-</sup>) embryos die during early embryonic development (Davis and Reynolds, 2006; Elia et al., 2006). Since p120ctn<sup>-/-</sup> blastocysts appear morphologically normal (Pieters et al., in preparation), isolating ES cell lines with p120ctn<sup>-/-</sup> genotype should be feasible. p120ctn<sup>+/-</sup> intercrosses resulted in small numbers of embryos, but ES cells could still be derived with an efficiency of up to 100% (Table 5). From the embryos of p120ctn<sup>+/-</sup> intercrosses we isolated 10 ES cell lines, but no p120ctn<sup>-/-</sup> ES cell lines were identified by genotyping (Table 5). To exclude genotyping artefacts due to contamination by genomic DNA of wild-type MEFs, we performed immunostaining for p120ctn on all p120ctn<sup>+/-</sup> ES cell lines. All p120ctn<sup>+/-</sup> ES cells still expressed p120ctn (Fig. 4D; Table 5), which confirms that their genotypes were assigned correctly. This implies that p120ctn might be required for derivation and maintenance of ES cells, although more experiments may be performed in order to conclude this formally. All together, our modified pluripotin-based protocol enabled us to isolate more than 50 ES cell lines with an efficiency of up to 100%, but no homozygous p120ctn null ES cell lines were obtained.

### Generation and characterization of p120ctn<sup>KOC/-</sup> and p120ctn<sup>KIC/-</sup> ES cell lines

Next, we generated mouse ES cell lines from blastocysts derived from the mating of p120ctn<sup>KOC/+</sup> or p120ctn<sup>KIC/+</sup> mice with p120ctn<sup>+/-</sup> mice. For both matings, the efficiency of mouse ES cell derivation was 100% and the genotypes of the isolated ES cells followed a Mendelian distribution (Table 5). This resulted in two p120ctn<sup>KOC/-</sup>, three p120ctn<sup>KIC/-</sup>, and the same numbers of littermate control ES cell lines (Table 1). Together, these data show that our optimized pluripotin-based protocol is very efficient (with success rates of up to 100%) and generates both transgenic and littermate control ES cell lines. Thus, our protocol makes it possible to set up experiments with minimal genetic variation.

## DISCUSSION

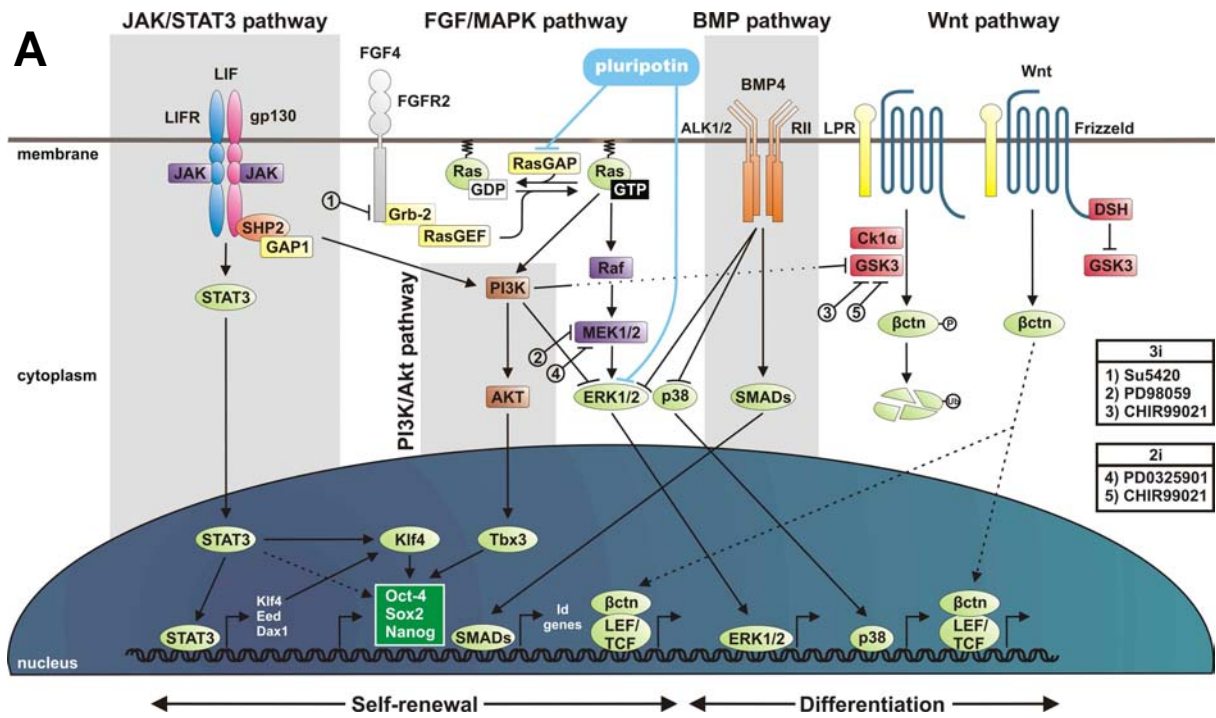
We describe a modified version of the protocols of Bryja et al. (2006b) and Yang et al. (2009). Our modified protocol enables easy and reproducible isolation of mouse ES cells from transgenic mice on a C57BL/6 background with an efficiency of up to 100%. With this protocol it should be possible, in theory, to isolate homozygous ES cell lines and littermate control ES lines from a single derivation. We combined the advantages of the two reported protocols: the ease, simplicity and reproducibility of the SR/FBS alteration protocol (Bryja et al., 2006b), and the protracted blastocyst outgrowth and the use of pluripotin in combination with LIF from the protocol of Yang et al. (2009). Our modified protocol yielded big, loosely attached, spherical outgrowths, which are easy to pick from a 12-well plate and can be readily dispersed in a single trypsinization step. Therefore, a sequential digestion procedure, as suggested by Yang et al. (2009) is not required. In addition, ES colonies could be established by us from both single cells and cell clumps which reduces the importance of the trypsinization step. The spherical outgrowths, which were formed with our protocol, were significantly bigger than outgrowths that were formed according to Yang et al. (2009). This resulted in a higher overall success rate of deriving mouse ES cell lines once the primary outgrowths were obtained compared to that of Yang et al. (2009) (98% and 85%, respectively). Once mouse ES cell lines are isolated, it is critical to keep them in an undifferentiated state. It can be argued that prolonged initial cultivation affects stemness. However, in our experience incubation of primary outgrowths with pluripotin for up to three weeks did not affect the ES cell derivation potential or ES cell characteristics such as morphology and Oct-4 positivity. In addition, using a transgenic Oct4-EGFP line (EGFP driven by the Oct4-promoter), Yang and colleagues (2009) showed EGFP expression for up to 14 days in outgrowths from Oct4-EGFP blastocysts. The ICM outgrowths, which are formed via our modified protocol are morphologically distinct from classical ICM outgrowths, do not adhere well to the feeder layer, and can sustain growth in suspension (Fig. 3A). Culturing blastocysts the first two days without pluripotin enabled formation of classical ICM outgrowths, which stay firmly attached to the underlying feeder and trophectoderm layer after pluripotin administration (Fig. 3B). However, these classical ICM outgrowths are smaller (on day 12), harder to pick and trypsinize, and less efficient (33%) in establishing ES cell lines. Remarkably, pluripotin was present in the ES medium during the entire isolation procedure of Yang and colleagues (2009) but still resulted in classic ICM outgrowths. This discrepancy

## Efficient pluripotin-based derivation of Mouse ES cells

between our results and those of Yang and colleagues (2009) might be explained by the use of different ES cell media in which blastocysts are seeded. On the first two days, Yang and colleagues (2009) used FBS-ES cell medium (Table 4), which might contain factors that stimulate substrate attachment of blastocyst outgrowths in the presence of pluripotin. These factors are probably not present in the chemically defined SR-ES cell medium that we used. It has been reported that MEFs, unlike ES cells, fail to adhere to gelatin-coated dishes in the presence of SR-ES cell medium (Gibco, data sheet Cat. No. 10828). Together, these data suggest that pluripotin blocks substrate attachment. Such a block might have a growth promoting effect and result in the formation of bigger but loosely attached outgrowths. To conclude, we believe that pluripotin acts as a strong brake that together with LIF prevents differentiation in primary outgrowths for up to three weeks. This brake has to be released (by omitting pluripotin) for proper substrate attachment and mouse ES cell line isolation and propagation in LIF-containing ES cell medium.

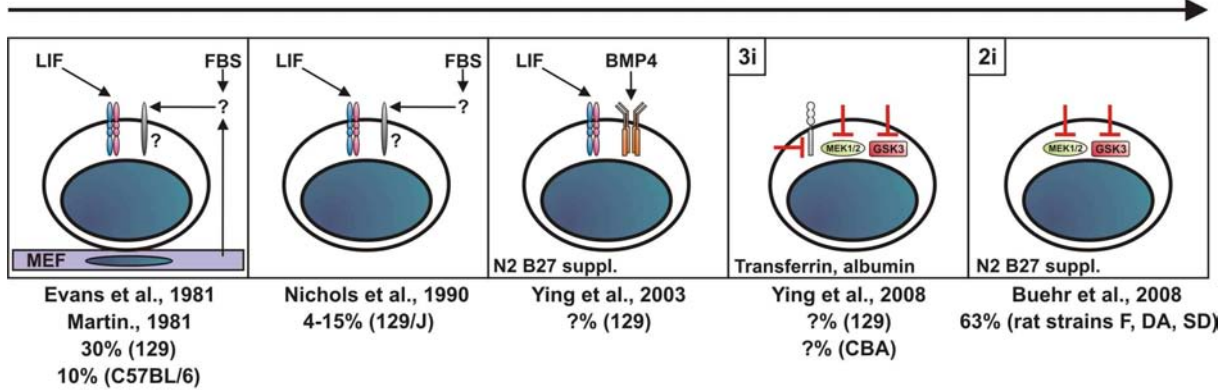
---

**Figure 5. Pluripotin modulates stemness pathways and allows efficient ES cell isolation, possibly using only a limited amount of defined factors.** (A) Different pathways are involved in maintaining self-renewal and differentiation during ES cell derivation and propagation. The leukemia inhibitory factor (LIF) activates STAT3, which can signal to the core transcription factor circuitry (including Oct-4, nanog and Sox2) via Klf4. Tbx3 can also activate the core transcription factors through the phosphatidylinositol 3 kinase (PI3K)–AKT pathway. Bone morphogenetic proteins (BMPs) induce expression of inhibitor of differentiation (Id) genes via SMADs and block mitogen-activated protein kinase (MAPK)-mediated signaling. Fibroblast growth factor (FGF) signaling activates Ras and MAPK signaling, resulting in ES cell commitment and differentiation. Although inhibiting glycogen synthase kinase 3 (GSK3) leads to activation of the Wnt/ $\beta$ -catenin ( $\beta$ ctn) pathway and increases ES cell derivation efficiency, its mode of action remains unclear. (B) Derivation of ES cells with an increasing number of defined medium constituents. (C) Derivation of ES cells with increasing efficiency. Alternation protocols switch between medium containing fetal bovine serum (FBS) (white) and medium containing serum replacement (SR) (pink). 2i: two small-molecule inhibitors; 3i: three inhibitors; CK1 $\alpha$ : casein kinase 1 $\alpha$ ; DA: Dark Agouti; DSH: dishevelled; ERK: extracellular signal-related kinase; FGFR: F: Fischer 344; FGF receptor; GAP: GTPase-activating protein; GAP1: Ras GTPase-Activating Protein; GEF: guanine exchange factor; Grb2: growth factor receptor-bound protein 2; JAK: Janus kinase; Klf4: kruppel-like factor 4; LEF/TCF: T-cell factor/lymphoid enhancer factor; LIFR: LIF receptor; MEK: MAPK/ERK kinase; SD: Sprague-Dawley; SHP2: Src homology 2 domain-containing protein-tyrosine phosphatase; STAT: signal transducer and activator of transcription.



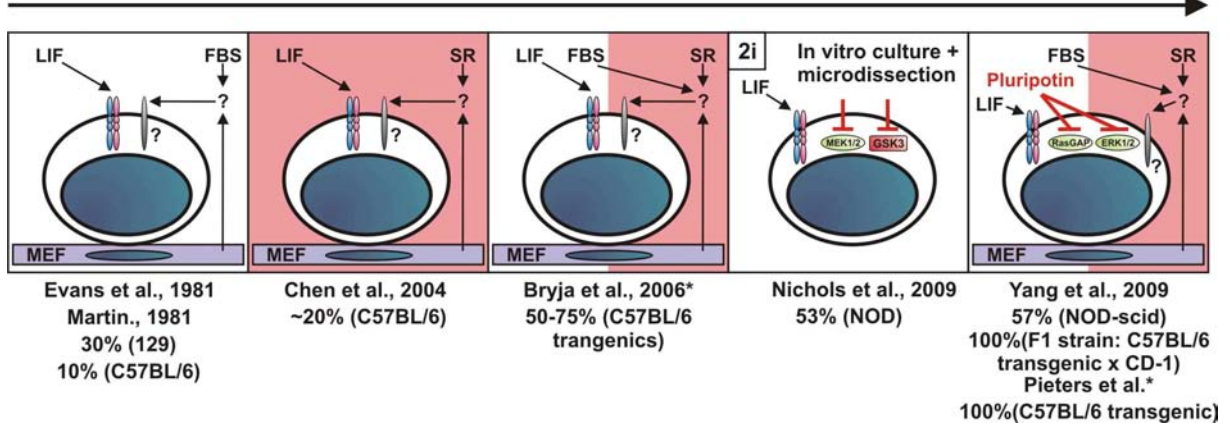
**B**

Defined medium constituents



**C**

ES cell derivatation efficiency



## Efficient pluripotin-based derivation of Mouse ES cells

How does pluripotin keep ICM outgrowths pluripotent while allowing long-lasting self-renewal? To gain mechanistic insight into how pluripotin works, we must identify the key signaling pathways involved in preserving stemness (Fig. 5A). Self-renewal of mouse cells largely depends on two key signaling molecules: LIF and bone morphogenic protein (BMP) 4. LIF, a cytokine belonging to the interleukin 6 family, blocks ES cell differentiation (Smith et al., 1988; Williams et al., 1988) and allows mouse ES cell isolation in the absence of MEFs, but it requires other serum factors (Nichols et al., 1990). LIF binds to a membrane-bound gp130-LIF receptor complex consisting of a general signal transducer and a LIF-specific receptor, and it activates STAT3 signaling (Niwa et al., 1998). It is not clear how LIF signals to the core circuitry of transcriptional regulators that govern pluripotency in ES cells, such as Oct-4 (Nichols et al., 1998), Nanog (Chambers et al., 2003; Mitsui et al., 2003) and Sox2 (Avilion et al., 2003). But recent data show that LIF signals to the core transcriptional circuitry *via* Krüppel-like factor 4 (Klf4) and Tbx3. Both factors, however, are not directly associated with the maintenance of pluripotency (Niwa et al., 2009). LIF-mediated Jak/Stat3 signaling induces Klf4 expression, while Oct4 induces Klf2 expression (Hall et al., 2009). Remarkably, Klf4 is also one of the four key factors that can convert a somatic differentiated cell into induced pluripotent stem cells (iPSCs) (Takahashi and Yamanaka, 2006). BMP4, on the other hand, induces expression of inhibitor of differentiation (Id) genes (Ying et al., 2003) and inhibits MAPK signaling (Qi et al., 2004). BMP4 and LIF are sufficient for maintaining self-renewal of mouse ES cells in the absence of both feeder cells and serum (Ying et al., 2003). Additionally, the phosphatidylinositol 3-kinase (PI3K)–AKT signaling pathway and the Wnt/ $\beta$ -catenin pathway are also involved in ES cell self-renewal (Paling et al., 2004; Sato et al., 2004; Watanabe et al., 2006). Pluripotin, a small synthetic compound, also enables the propagation of undifferentiated mouse ES cells in the absence of LIF and MEFs and works by dual inhibition of RasGAP and ERK1 signaling (Fig. 4A) (Chen et al., 2006). RasGAP inhibition keeps Ras in its active GTP-bound form and probably stimulates PI3K-mediated self-renewal while blocking MEK-mediated differentiation (Chen et al., 2006). ERK-mediated signaling is required for the development of trophoblast cells and primitive endoderm (Binetruy et al., 2007; Yang et al., 2006). Like MEK inhibition, pluripotin-mediated ERK1 inhibition causes a proliferation defect in trophectoderm cells (Fig. 2B). In conclusion, pluripotin preserves stemness by activating the core transcription factor circuitry *via* Ras/PI3K signaling and blocks MEK-mediated differentiation.

One could divide ES cell derivation research in two categories, the Yin(g) and the Yang, in analogy to the Chinese symbol and with reference to the authors who contributed to each category. The Yin(g) stands for attempting to isolate genuine ES cell lines using the smallest possible panel of chemically defined medium components regardless of the derivation efficiency. Using this approach, ES cells were derived in the absence of MEFs (Nichols et al., 1990), serum (Ying et al., 2003) or external stimuli (Ying et al., 2008) (Fig. 4B). This approach contributed to the unraveling of several stemness pathways. On the other hand, the Yang stands for isolating ES cell lines from different strains (including refractory strains) with the highest possible efficiency without paying attention to the medium constitution or underlying mechanism. Using this approach, the ES cell derivation efficiency for pure and transgenic C57BL/6 strains increased from less than 10% to about 20% (Cheng et al., 2004), to 50-75% (Bryja et al., 2006b), and to 100% for F1 strains (C57BL/6 transgenic x CD1) (Yang et al., 2009) (Fig. 4C). Here, we report the derivation of ES cells from C57BL/6 transgenics with a success rate of 100%. In addition, ES cell lines could be efficiently derived from refractory strains, such as NOD (Nichols et al., 2009) and NOD-scid (Yang et al., 2009), with an efficiency of 53% and 57%, respectively (Fig. 4C). This line of research provides user-friendly and highly efficient ES cell derivation protocols to the scientific community, enabling molecular analysis in recalcitrant strains and C57BL/6 transgenics with embryonically lethal phenotypes. The Yin(g) and the Yang research branches can merge, as knowledge of stemness pathways can also result in efficient ES cell derivation from, for example, the use of LIF + 2i (Nichols et al., 2009). While our pluripotin-based ES cell derivation protocol initially focused on efficiency, it would be interesting to test pluripotin in a MEF- and serum-free environment. ES cells can be propagated under these conditions (Chen et al., 2006), but ES cell derivation was not tested. In summary, we describe an alternative, simplified, pluripotin-based protocol that allows derivation of ES cells from C57BL/6 transgenics with an efficiency of up to 100%.

### ACKNOWLEDGEMENTS

This work was supported by grants from the Queen Elisabeth Medical Foundation (G.S.K.E.), Belgium, and from the Geconcerteerde Onderzoeksacties of Ghent University. Tim Pieters has been supported by the Instituut voor de Aanmoediging van Innovatie door Wetenschap en Technologie in Vlaanderen (IWT). Tim Pieters conducted all experiments and wrote this manuscript. Dr. Tino Hochpied supplied reagents, helped to establish an efficient ES cell derivation protocol for mouse blastocysts, reproduced results independently, and provided photographs. Dr. Jody Haigh was helped with analysis of embryoid bodies. Prof. Dr. Frans Van Roy and Dr. Jolanda van Hengel were instructive in the experimental design and editing of the manuscript. We acknowledge Dr. Amin Bredan for critical reading of the manuscript, and the members of our research group for valuable discussions.

### REFERENCES

- Avilion, A.A., S.K. Nicolis, L.H. Pevny, L. Perez, N. Vivian, and R. Lovell-Badge. 2003. Multipotent cell lineages in early mouse development depend on SOX2 function. *Genes Dev.* 17:126-40.
- Betz, U.A., C.A. Voshenrich, K. Rajewsky, and W. Muller. 1996. Bypass of lethality with mosaic mice generated by Cre-loxP-mediated recombination. *Curr Biol.* 6:1307-16.
- Bibel, M., J. Richter, E. Lacroix, and Y.A. Barde. 2007. Generation of a defined and uniform population of CNS progenitors and neurons from mouse embryonic stem cells. *Nat Protoc.* 2:1034-43.
- Bibel, M., J. Richter, K. Schrenk, K.L. Tucker, V. Staiger, M. Korte, M. Goetz, and Y.A. Barde. 2004. Differentiation of mouse embryonic stem cells into a defined neuronal lineage. *Nat Neurosci.* 7:1003-9.
- Binetruy, B., L. Heasley, F. Bost, L. Caron, and M. Aouadi. 2007. Concise review: regulation of embryonic stem cell lineage commitment by mitogen-activated protein kinases. *Stem Cells.* 25:1090-5.
- Brook, F.A., and R.L. Gardner. 1997. The origin and efficient derivation of embryonic stem cells in the mouse. *Proc Natl Acad Sci U S A.* 94:5709-12.
- Bryja, V., S. Bonilla, and E. Arenas. 2006a. Derivation of mouse embryonic stem cells. *Nat Protoc.* 1:2082-7.
- Bryja, V., S. Bonilla, L. Cajanek, C.L. Parish, C.M. Schwartz, Y. Luo, M.S. Rao, and E. Arenas. 2006b. An efficient method for the derivation of mouse embryonic stem cells. *Stem Cells.* 24:844-9.
- Buehr, M., S. Meek, K. Blair, J. Yang, J. Ure, J. Silva, R. McLay, J. Hall, Q.L. Ying, and A. Smith. 2008. Capture of authentic embryonic stem cells from rat blastocysts. *Cell.* 135:1287-98.



- Buehr, M., and A. Smith. 2003. Genesis of embryonic stem cells. *Philos Trans R Soc Lond B Biol Sci.* 358:1397-402; discussion 1402.
- Capecci, M.R. 2008. The making of a scientist II (Nobel Lecture). *Chembiochem.* 9:1530-43.
- Chambers, I., D. Colby, M. Robertson, J. Nichols, S. Lee, S. Tweedie, and A. Smith. 2003. Functional expression cloning of Nanog, a pluripotency sustaining factor in embryonic stem cells. *Cell.* 113:643-55.
- Chen, S., J.T. Do, Q. Zhang, S. Yao, F. Yan, E.C. Peters, H.R. Scholer, P.G. Schultz, and S. Ding. 2006. Self-renewal of embryonic stem cells by a small molecule. *Proc Natl Acad Sci U S A.* 103:17266-71.
- Cheng, J., A. Dutra, A. Takesono, L. Garrett-Beal, and P.L. Schwartzberg. 2004. Improved generation of C57BL/6J mouse embryonic stem cells in a defined serum-free media. *Genesis.* 39:100-4.
- Davis, M.A., and A.B. Reynolds. 2006. Blocked acinar development, E-cadherin reduction, and intraepithelial neoplasia upon ablation of p120-catenin in the mouse salivary gland. *Dev Cell.* 10:21-31.
- Elia, L.P., M. Yamamoto, K. Zang, and L.F. Reichardt. 2006. p120 catenin regulates dendritic spine and synapse development through Rho-family GTPases and cadherins. *Neuron.* 51:43-56.
- Evans, M. 2008. Embryonic stem cells: the mouse source--vehicle for mammalian genetics and beyond (Nobel lecture). *Chembiochem.* 9:1690-6.
- Evans, M.J., and M.H. Kaufman. 1981. Establishment in culture of pluripotential cells from mouse embryos. *Nature.* 292:154-6.
- Gearing, D.P., N.M. Gough, J.A. King, D.J. Hilton, N.A. Nicola, R.J. Simpson, E.C. Nice, A. Kelso, and D. Metcalf. 1987. Molecular cloning and expression of cDNA encoding a murine myeloid leukaemia inhibitory factor (LIF). *Embo J.* 6:3995-4002.
- Hall, J., G. Guo, J. Wray, I. Eyres, J. Nichols, L. Grotewold, S. Morfopoulou, P. Humphreys, W. Mansfield, R. Walker, S. Tomlinson, and A. Smith. 2009. Oct4 and LIF/Stat3 additively induce Kruppel factors to sustain embryonic stem cell self-renewal. *Cell Stem Cell.* 5:597-609.
- Keirsebilck, A., S. Bonne, K. Staes, J. van Hengel, F. Nollet, A. Reynolds, and F. van Roy. 1998. Molecular cloning of the human p120ctn catenin gene (CTNND1): expression of multiple alternatively spliced isoforms. *Genomics.* 50:129-46.
- Li, P., C. Tong, R. Mehrian-Shai, L. Jia, N. Wu, Y. Yan, R.E. Maxson, E.N. Schulze, H. Song, C.L. Hsieh, M.F. Pera, and Q.L. Ying. 2008. Germline competent embryonic stem cells derived from rat blastocysts. *Cell.* 135:1299-310.
- Lodge, P., J. McWhir, E. Gallagher, and H. Sang. 2005. Increased gp130 signaling in combination with inhibition of the MEK/ERK pathway facilitates embryonic stem cell isolation from normally refractory murine CBA blastocysts. *Cloning Stem Cells.* 7:2-7.
- Marikawa, Y., and V.B. Alarcon. 2009. Establishment of trophectoderm and inner cell mass lineages in the mouse embryo. *Mol Reprod Dev.* 76:1019-32.
- Martin, G.R. 1981. Isolation of a pluripotent cell line from early mouse embryos cultured in medium conditioned by teratocarcinoma stem cells. *Proc Natl Acad Sci U S A.* 78:7634-8.
- McWhir, J., A.E. Schnieke, R. Ansell, H. Wallace, A. Colman, A.R. Scott, and A.J. Kind. 1996. Selective ablation of differentiated cells permits isolation of embryonic stem cell lines from murine embryos with a non-permissive genetic background. *Nat Genet.* 14:223-6.

## Efficient pluripotin-based derivation of Mouse ES cells

- Mitsui, K., Y. Tokuzawa, H. Itoh, K. Segawa, M. Murakami, K. Takahashi, M. Maruyama, M. Maeda, and S. Yamanaka. 2003. The homeoprotein Nanog is required for maintenance of pluripotency in mouse epiblast and ES cells. *Cell*. 113:631-42.
- Mouse Genome Sequencing Consortium. 2002. Initial sequencing and comparative analysis of the mouse genome. *Nature*. 420:520-62.
- Nagy, A., and K. Vintersten. 2006. Murine embryonic stem cells. *Methods Enzymol*. 418:3-21.
- Nichols, J., E.P. Evans, and A.G. Smith. 1990. Establishment of germ-line-competent embryonic stem (ES) cells using differentiation inhibiting activity. *Development*. 110:1341-8.
- Nichols, J., K. Jones, J.M. Phillips, S.A. Newland, M. Roode, W. Mansfield, A. Smith, and A. Cooke. 2009. Validated germline-competent embryonic stem cell lines from nonobese diabetic mice. *Nat Med*. 15:814-8.
- Nichols, J., B. Zevnik, K. Anastasiadis, H. Niwa, D. Klewe-Nebenius, I. Chambers, H. Scholer, and A. Smith. 1998. Formation of pluripotent stem cells in the mammalian embryo depends on the POU transcription factor Oct4. *Cell*. 95:379-91.
- Niwa, H., T. Burdon, I. Chambers, and A. Smith. 1998. Self-renewal of pluripotent embryonic stem cells is mediated via activation of STAT3. *Genes Dev*. 12:2048-60.
- Niwa, H., K. Ogawa, D. Shimosato, and K. Adachi. 2009. A parallel circuit of LIF signalling pathways maintains pluripotency of mouse ES cells. *Nature*. 460:118-22.
- Paling, N.R., H. Wheadon, H.K. Bone, and M.J. Welham. 2004. Regulation of embryonic stem cell self-renewal by phosphoinositide 3-kinase-dependent signaling. *J Biol Chem*. 279:48063-70.
- Pieters, T., P. D'Hooge, P. Hulpiau, M.P. Stemmler, F. Van Roy, and J. Van Hengel. in preperation. p120ctn isoform C knockout and knockin mice rescue E-cadherin loss and embryonic lethality in p120ctn-deficient embryos.
- Qi, X., T.G. Li, J. Hao, J. Hu, J. Wang, H. Simmons, S. Miura, Y. Mishina, and G.Q. Zhao. 2004. BMP4 supports self-renewal of embryonic stem cells by inhibiting mitogen-activated protein kinase pathways. *Proc Natl Acad Sci U S A*. 101:6027-32.
- Rivera, J., and L. Tessarollo. 2008. Genetic background and the dilemma of translating mouse studies to humans. *Immunity*. 28:1-4.
- Sato, N., L. Meijer, L. Skaltsounis, P. Greengard, and A.H. Brivanlou. 2004. Maintenance of pluripotency in human and mouse embryonic stem cells through activation of Wnt signaling by a pharmacological GSK-3-specific inhibitor. *Nat Med*. 10:55-63.
- Schoonjans, L., V. Kreemers, S. Danloy, R.W. Moreadith, Y. Laroche, and D. Collen. 2003. Improved generation of germline-competent embryonic stem cell lines from inbred mouse strains. *Stem Cells*. 21:90-7.
- Smith, A.G., J.K. Heath, D.D. Donaldson, G.G. Wong, J. Moreau, M. Stahl, and D. Rogers. 1988. Inhibition of pluripotential embryonic stem cell differentiation by purified polypeptides. *Nature*. 336:688-90.
- Smithies, O. 2008. Turning pages (Nobel lecture). *Chembiochem*. 9:1342-59.
- Takahashi, K., and S. Yamanaka. 2006. Induction of pluripotent stem cells from mouse embryonic and adult fibroblast cultures by defined factors. *Cell*. 126:663-76.
- Tomida, M., Y. Yamamoto-Yamaguchi, and M. Hozumi. 1984. Purification of a factor inducing differentiation of mouse myeloid leukemic M1 cells from conditioned medium of mouse fibroblast L929 cells. *J Biol Chem*. 259:10978-82.
- Umehara, H., T. Kimura, S. Ohtsuka, T. Nakamura, K. Kitajima, M. Ikawa, M. Okabe, H. Niwa, and T. Nakano. 2007. Efficient derivation of embryonic stem cells by inhibition of glycogen synthase kinase-3. *Stem Cells*. 25:2705-11.

- Watanabe, S., H. Umehara, K. Murayama, M. Okabe, T. Kimura, and T. Nakano. 2006. Activation of Akt signaling is sufficient to maintain pluripotency in mouse and primate embryonic stem cells. *Oncogene*. 25:2697-707.
- Williams, R.L., D.J. Hilton, S. Pease, T.A. Willson, C.L. Stewart, D.P. Gearing, E.F. Wagner, D. Metcalf, N.A. Nicola, and N.M. Gough. 1988. Myeloid leukaemia inhibitory factor maintains the developmental potential of embryonic stem cells. *Nature*. 336:684-7.
- Yang, W., L.D. Klamann, B. Chen, T. Araki, H. Harada, S.M. Thomas, E.L. George, and B.G. Neel. 2006. An Shp2/SFK/Ras/Erk signaling pathway controls trophoblast stem cell survival. *Dev Cell*. 10:317-27.
- Yang, W., W. Wei, C. Shi, J. Zhu, W. Ying, Y. Shen, X. Ye, L. Fang, S. Duo, J. Che, H. Shen, S. Ding, and H. Deng. 2009. Pluripotin combined with leukemia inhibitory factor greatly promotes the derivation of embryonic stem cell lines from refractory strains. *Stem Cells*. 27:383-9.
- Ying, Q.L., J. Nichols, I. Chambers, and A. Smith. 2003. BMP induction of Id proteins suppresses differentiation and sustains embryonic stem cell self-renewal in collaboration with STAT3. *Cell*. 115:281-92.
- Ying, Q.L., J. Wray, J. Nichols, L. Battle-Morera, B. Doble, J. Woodgett, P. Cohen, and A. Smith. 2008. The ground state of embryonic stem cell self-renewal. *Nature*. 453:519-23.

## Chapter 7

---

### **KNOCKOUT AND KNOCKIN OF EXON C OF p120CTN IN THE BRAIN**



## Knockout and Knockin of exon C of p120ctn in brain

Tim Pieters<sup>1,2</sup>, Anja Lambrechts<sup>3,4</sup>, Annemie Van der Linden<sup>5</sup>, Frans van Roy<sup>1,2</sup>, Jolanda van Hengel<sup>1,2,6</sup>

<sup>1</sup> Department for Molecular Biomedical Research, Technologiepark 927, VIB, B-9052 Ghent, Belgium

<sup>2</sup> Department of Biomedical Molecular Biology, Ghent University, Technologiepark 927, B-9052 Ghent, Belgium

<sup>3</sup> Department of Medical Protein Research, VIB, B-9052 Ghent, Belgium

<sup>4</sup> Department of Biochemistry, Faculty of Medicine and Health Sciences, Ghent University, Albert Baertsoenkaai 3, B-9000 Ghent, Belgium

<sup>5</sup> Bio Imaging Lab, Antwerp University, Groene Groenenborgerlaan 171, B-2020 Antwerpen, Belgium

<sup>6</sup> corresponding author:

### TABLE OF CONTENTS

ABSTRACT .....	234
INTRODUCTION.....	235
MATERIAL AND METHODS .....	237
RESULTS AND DISCUSSION .....	241
p120ctn exon C is highly expressed in mouse brain .....	241
Brain-specific p120ctn knockout mice are viable .....	241
Sustained N-cadherin levels in p120ctn-deficient brains .....	245
Increased RhoA activity in p120ctn-deficient brains .....	246
NestinCre transgenic females and males show premature recombination .....	247
Revised mating strategy to obtain p120ctn <sup>KOC/fl</sup> ; Nes-Cre and p120ctn <sup>KIC/fl</sup> ; Nes-Cre mice .....	253
p120ctn <sup>KOC/fl</sup> ; Nes-Cre hippocampi display discrete medial abnormalities .....	255
Microcephaly in p120ctn <sup>KIC/fl</sup> ; Nes-Cre mice.....	261
p120ctn expression in hippocampal neurons.....	262
Fasciculation in p120ctn <sup>KIC/fl</sup> ; Nes-Cre hippocampal neurons .....	264
Transfection of transgenic hippocampal cultures.....	267
Immunohistochemistry with pAbexC on brain sections .....	269
CONCLUSION .....	271
ACKNOWLEDGEMENTS .....	271
REFERENCES.....	272

**ABSTRACT**

p120 catenin (p120ctn) is a versatile member of the armadillo family, and has different functions in different subcellular compartments. It stabilizes cadherins at the cell membrane, modulates RhoGTPase activity in the cytoplasm, and regulates nuclear transcription. p120ctn is a part of the cadherin catenin complex, and its components localize to synapses and are involved in both pre- and post-synaptic development. Genetic ablation of p120ctn in the dorsal forebrain resulted in reduced spine and synapse densities along dendrites, decreased N-cadherin levels and increased RhoA activity. Different p120ctn isoforms can be generated via alternative splicing, allowing translation initiation from four different start codons and incorporation of up to four alternatively spliced exons. The alternatively spliced exon C of p120ctn is highly expressed in brain, but homozygous p120ctn KOC or KIC embryos exhibit early lethal phenotypes. We combined a brain-specific p120ctn knockout allele with either a p120ctn KOC or KIC allele to generate mice with brains that exclusively express p120ctn transcripts without (p120ctn<sup>KOC/fl</sup>; Nes-Cre) or with (p120ctn<sup>KOC/fl</sup>; Nes-Cre) exon C. These mice showed discrete but different phenotypes. p120ctn<sup>KOC/fl</sup>; Nes-Cre mice exhibited aberrant morphology of the medial side of hippocampi and had a small reduction in total hippocampal volume. On the other hand, p120ctn<sup>KOC/fl</sup>; Nes-Cre mice displayed microcephaly and hippocampal cultures that were derived from them showed signs of fasciculation.

## INTRODUCTION

The formation of functional neuronal networks with synaptic contacts is established by sequential cellular events, such as the protrusion of filopodia from dendrites, contact between filopodia and axons, and maturation of filopodia into dendritic spines (Cohen-Cory, 2002). Dendritic spines are actin-rich protrusions that form the major postsynaptic sites of excitatory synaptic input. RhoGTPases regulate actin dynamics and allow spines to be highly motile structures. Aberrant spine distribution and morphology have been observed in many neurological disorders (Govek et al., 2005; Newey et al., 2005).

p120ctn is a versatile armadillo protein and regulates cadherin turnover (Kowalczyk and Reynolds, 2004; Xiao et al., 2007), RhoGTPase activity (Anastasiadis, 2007) and transcriptional regulation (Daniel, 2007). p120ctn is a component of the adherens junctions, which are composed of classical cadherins, such as N-cadherin, and catenins, including  $\alpha$ -catenin,  $\beta$ -catenin and p120ctn. Cadherins and catenins localize to synapses (Elste and Benson, 2006; Fannon and Colman, 1996; Uchida et al., 1996) and are important regulators of spine and synapse number and morphology (Abe et al., 2004; Bozdagi et al., 2004; Togashi et al., 2002). Neuronal systems with perturbed cadherins (Inoue and Sanes, 1997; Iwai et al., 2002) or genetic deletion of catenins (Abe et al., 2004; Bamji et al., 2003) have all defects in either spine or synapse formation. p120ctn is expressed in rat brain (Chauvet et al., 2003) and in chick ciliary neurons (Rubio et al., 2005). During synapse maturation in chick ciliary neurons, p120ctn and  $\beta$ -catenin are removed from N-cadherin complexes and are replaced by presenilin 1 and plakoglobin (Rubio et al., 2005). Genetic inactivation of p120ctn in the dorsal forebrain resulted in reduced spine and synapse densities along dendrites, decreased N-cadherin levels and increased RhoA activity (Elia et al., 2006). Interestingly, spine head width was dependent on its interaction with cadherins, whereas spine density was regulated by RhoA, independently of cadherin binding.

p120ctn is part of a small subfamily containing besides itself also ARVCF, p0071 and  $\delta$ -catenin (McCrea and Park, 2007).  $\delta$ -catenin is exclusively expressed in the nervous system (Kosik et al., 2005) and p120ctn and  $\delta$ -catenin share similar features. Expression of p120ctn or  $\delta$ -catenin both elicits dendritic-like branching (Abu-Elneel et al., 2008; Kim et al., 2002; Lu et al., 1999; Martinez et al., 2003; Reynolds et al., 1996) and both proteins are able to modulate RhoGTPase activity (Anastasiadis et al., 2000; Grosheva et al., 2001; Kim et al., 2008a; Kim et al., 2008b; Noren et al., 2000). Genetic ablation of  $\delta$ -catenin in mice results in



## p120ctn KOC and KIC in the brain

a mild cognitive phenotype (Israely et al., 2004) and in a reduced dendritic complexity in cultured hippocampal neurons (Arikkath et al., 2008).

Different p120ctn isoforms can be generated via alternative splicing, allowing translation initiation from four different start codons and incorporation of up to four alternatively spliced exons (Keirsebilck et al., 1998). So far, the relevance of these p120ctn isoforms *in vivo* is unknown. We generated mice harboring a knockout or a knockin of the alternatively spliced exon C of p120ctn, but homozygous p120ctn<sup>KOC/KOC</sup> or p120ctn<sup>KIC/KIC</sup> embryos die early during development (Pieters et al., in preparation). We found that the alternatively spliced exon C is highly expressed in brain and we devised a strategy allowing the analysis a knockout or a knockin of the alternatively used exon C of p120ctn in mouse brain.

## MATERIAL AND METHODS

### Generating p120ctn<sup>fl/fl</sup>; Nes-Cre, p120ctn<sup>KOC/fl</sup>; Nes-Cre and p120ctn<sup>KIC/fl</sup>; Nes-Cre mice

Mice harboring a floxed region in the p120ctn gene (containing exon 3 till 8, including all four start codons) have been described (Davis and Reynolds, 2006). Crossing p120ctn<sup>fl/fl</sup> mice with mice expressing the Cre recombinase under control of the rat nestin (Nes-Cre) promoter (Tronche et al., 1999) resulted in p120ctn<sup>fl/+</sup>; Nes-Cre mice. These mice were crossed again with p120ctn<sup>fl/fl</sup> mice to obtain p120ctn<sup>fl/fl</sup>; Nes-Cre mice, which lack p120ctn specifically in the brain. In addition, p120ctn<sup>fl/fl</sup>; Nes-Cre mice can be crossed with p120ctn<sup>KOC/+</sup> and p120ctn<sup>KIC/+</sup> mice (Pieters et al., in preparation) giving rise to p120ctn<sup>KOC/fl</sup>; Nes-Cre and p120ctn<sup>KIC/fl</sup>; Nes-Cre mice, respectively (Table 2). Genotyping was performed according to (Pieters et al., in preparation). Mice were housed in individually ventilated cages either in an specific pathogen-free animal facility. All experiments on mice were conducted according to institutional, national, and European animal regulations. Animal protocols were approved by the ethics committee of Ghent University.

### Nissl staining, immunostaining and immunohistochemistry

Brains were dissected from their skull and were washed several times in phosphate-buffered saline (PBS), fixed overnight in 4% paraformaldehyde in PBS, embedded in paraffin wax and sectioned at 6 to 8  $\mu$ m. Sections were deparaffinated using HistoClear II (two times 3 min, National Diagnostics). A Nissl body is a large granular body (rough endoplasmatic riculum) found in neurons. Nissl bodies can be visualized via a cresyl violet staining (Nissl staining), which labels extra-nuclear RNA present in the soma and dendrites of neurons. For histology, tissues sections were rehydrated and stained 30 min cresyl violet solution, consisting of 0,1% cresyl violet acetate (Sigma-Aldrich), 5,5% glacial acetic acid and 166 mM Natrium acetate. For immunohistochemistry, tissue sections were rehydrated and pretreated with 0.3% H<sub>2</sub>O<sub>2</sub> in methanol for 45 minutes. The sections were then transferred to 10mM citrate buffer (pH 6.0) and the antigen was exposed in a Retriever (PickCell Laboratories, Amsterdam, The Netherlands). The sections were covered with blocking buffer (10% goat serum, 1% BSA in PBS) for 20 min and then incubated with appropriate antibodies (diluted in 1% BSA in PBS) overnight at 4°C. Staining was completed with a biotinylated secondary antibody (Dako, Glostrup,Denmark), avidin-peroxidase (Dako) and 3,3'-diaminobenzidine (Biogenex, San Roman, CA). Coverslips with hippocampal cultures were fixed for

## **p120ctn KOC and KIC in the brain**

20 min in 4% paraformaldehyde in PHEM, composed of 120 mM PIPES (pH 7), 50 mM K-HEPES (pH 7), 20 mM EGTA, 4 mM MgCl<sub>2</sub> and 240 mM sucrose. The coverslips were washed 5 min in PBS, blocked 30 min with 3% BSA in PBS, permeabilized for 2 min with 0.2% Triton-X100 in PBS, washed 5 min in PBS, incubated 2 h with primary antibody in 1% BSA in PBS, washed 5 min in PBS, incubated 1 h with secondary antibody, washed and mounted. The following antibodies were used. Mouse monoclonal anti-p120ctn (pp120, 1/500, BD Transduction Laboratories), polyclonal rabbit anti- $\alpha$ -catenin (1/1000, Sigma), polyclonal rabbit anti- $\beta$ -catenin (1/2000, Sigma), mouse monoclonal anti- $\beta$ III tubulin (1/3000, Promega), mouse monoclonal anti-Tau-1 (1/200, Chemicon-Millipore), rabbit polyclonal anti-N-cadherin (1/500, Zymed), rabbit polyclonal pAbexC (1/20), rabbit polyclonal anti-Map2 (1/200, Covance, New Jersey), phalloidin-Alexa488 (Molecular Probes). Secondary species-specific Alexa-fluorochrome-conjugated antibodies were used at a dilution of 1/500 (Molecular Probes).

## **Hippocampal cultures**

Pregnant females were scarified and 16,5 dpc embryos were dissected and washed in sterile calcium- and magnesium-free Hanks' balanced salt solution (CMF-HBSS). Due to the heterogenic genotypes of the offspring, hippocampi from each embryo were dissected and processed separately. Hippocampi were transferred to 15 ml tubes containing 0.9 ml CMF-HBSS and were incubated with 0.1 ml 2.5% trypsin (10x) for 15 min at 37°C. After three washes with 1 ml CMF-HBSS, the hippocampi were triturated with a fire polished Pasteur pipette in the presence of 1 ml plating medium, composed of MEM with Earle's salts (Gibco), 10% fetal bovine serum, 10 mM sodium pyruvate (Gibco), 0.6% glucose, HEPES (Invitrogen), 0.5 mM Glutamine (Invitrogen) and 12.5  $\mu$ M glutamate (Sigma-Aldrich). Defined numbers ( $1 \times 10^5$ ) of cells were seeded in plating medium in 3.5 cm dishes containing poly-D-lysine (PDL) and laminin-coated coverslips. After 3 h of incubation at 37°C in 5% CO<sub>2</sub>, the plating medium is replaced by glia-conditioned growth medium, composed of Neurobasal (Gibco), B27 (Gibco), 0.5 mM Glutamine (Invitrogen) and 12.5  $\mu$ M glutamate (Sigma-Aldrich). At day 4, 7, 14 and 21 half of the medium is replaced by fresh glia-conditioned growth media without glutamate.

## RT-PCR and Q-PCR

For RT-PCR analysis of mouse tissues, RNA was prepared from different tissues via the RNAeasy (Qiagen) method. One microgram of total RNA was treated with the RQ1 RNase-free DNase according to the manufacturer's instructions (Promega), and treated RNA samples were desalted on Microcon-100 spin columns (Milipore, Bedford, USA). cDNA was prepared with Superscript II reverse transcriptase according to the manufacturer's instructions (Invitrogen). Q-PCR mixes contained 20 ng template cDNA, LightCycler 480 SYBR Green I Mastermix (Roche Diagnostics GmbH, Mannheim, Germany) and 300 nM forward and reverse primers. Reactions were performed on a LightCycler 480 (Roche Diagnostics) using the following protocol: incubation at 95°C for 5 min, then 50 cycles at 95°C for 10 sec, 60°C for 30 sec, and 72°C for 1 sec. Primers for RT-PCR and Q-PCR are listed in Table 1. Primer sequences for the reference genes are deposited in RTPrimerDB, a public database for real-time PCR primers (<http://medgen.ugent.be/rtpimerdb/>).

**Table 1. Primers for RT-PCR and Q-PCR**

allele	primers for RT-PCR	size (bp)
p120ctn transcripts with or without exon C	forward 5'-TTTGCCCTCTCCGGAAGCTTATCA-3' (primer in exon 10)	208 (with exon C)
	reverse 5'-CTTTTAGGGAAATCCACTGTATCA-3 (primer in exon 12)	190 (no exon C)
GAPDH	forward 5'-ACCACAGTCCATGCCATCAC -3'	470
	reverse 5'-TCCACCACCCTGTTGCTGTA-3	
allele	primers for Q-PCR	size (bp)
p120ctn exon 10-12 boundry	forward 5'-ATCCACAGGCAGAGCGTTA-3'	106
	reverse 5'-GCTTTTCCCTTTGCCCTTCT-3	
p120ctn exon 11-12 boundry	forward 5'-AGGGCAAAGATGAGTGGTCTC-3',	81
	reverse 5'-TTCTTTTAGGGAAATCCACTGTATCA-3	
p120ctn exon 9-10 boundry	forward 5'-AGACAGTAAGCTTGTGGAGAATTGTG-3',	101
	reverse 5'-GAAGGGCCTCTGGTAACG-3	

## Transfection of hippocampal cultures

Hippocampal cultures in 3.5 cm dishes were transfected on day *in vitro* (DIV) 8 or 11 with the Effectene transfection kit (Qiagen). We used transfection conditions optimized for rat hippocampal neurons. In brief, a DNA mix, consisting of 0.5 µg pmaxEGFP (Amaya), 1.6 µl enhancer (Qiagen) and 100 µl EC buffer (Qiagen) was briefly mixed (vortex 1 sec) and incubated for 5 min at room temperature. The DNA mix was supplemented with 2 µ Effectene (Qiagen), mixed briefly (vortex 10 sec) and incubated for 10 min at room temperature. The transfection mixture was transferred in 0.6 ml growth medium to the 3.5 cm dishes containing 1.6 ml glia conditioned growth medium.

**Western blot analysis**

Lysates from PBS-perfused brains were made with Laemmli buffer (Laemmli, 1970), mixed, and boiled for 5 min. Proteins were separated by SDS-PAGE on a 8% or 12% polyacrylamide gel, electroblotted onto polyvinylidene fluoride (PVDF) membranes (Millipore), and incubated with antibodies. Detection was performed by NBT/BCIP (Zymed Laboratories) or by an Odyssey infrared imaging system.

**RhoGTPase Activity assay**

RhoA activity was determined by a G-LISA kit (Cytoskeleton) according to the *manufacturer's* instructions. Alternatively, RhoA and Rac1 activity were determined by affinity precipitations (Ren et al., 1999). GTP-bound RhoA and GTP-bound Rac1 were affinity purified from brain or hippocampal lysates using glutathione beads coated with GST fusions of the RhoA binding domain of Rhotekin and the Rac1 binding domain of PAK, respectively. Bound proteins were resolved on 12% SDS-PAGE, after which rabbit polyclonal anti-RhoA (1/200, Santa Cruz) and mouse monoclonal anti-Rac1 (1/1000; upstate) antibodies were used to quantify active protein quantities. Whole brain or hippocampal lysates were fractionated by SDS-PAGE and blotted with the same antibodies to determine total amount of RhoA and Rac1. Detection was performed by an Odyssey infrared imaging system

## RESULTS AND DISCUSSION

### **p120ctn exon C is highly expressed in mouse brain**

The alternatively spliced exon C was first identified in human p120ctn transcripts and is highly expressed in human fetal brain, but is only a minor fraction of the mRNA pool in other tissues and cell lines (Keirsebilck et al., 1998). The sequence of human and murine p120ctn exon C is identical but no expression data exist for murine exon C. Therefore we analyzed the expression of p120ctn transcripts with or without exon C in a panel of wild-type CD1 mouse organs by RT-PCR (Fig. 1A) or by Q-PCR (Figs. 1C-D). Similar to the human situation, exon C was highly expressed in mouse brain (Figs. 1A,B). In addition, exon C-containing p120ctn transcripts were found in heart, muscle and testis, which exhibit a high degree of exon C inclusion in their p120ctn transcripts (Fig. 1D). All tissues with a high expression of exon C, except for muscle, showed also expression of exon C-encoded amino acids on the protein level (Fig. 1E, bottom). The pp120 antibody has a C-terminal epitope and recognizes all p120ctn isoforms. Brain, heart and testis expressed predominantly p120ctn isoform 1, liver expressed predominantly p120ctn isoform 3 and in lung both long and short p120ctn isoforms are equally expressed (Fig. 1E, top). The pAbexC antibody was generated against a peptide containing the exon C-encoded amino acids and specifically recognizes p120ctn isoform C (Pieters et al., in preparation). The exon C-encoded amino acids were detected in long p120ctn isoforms from brain, heart, lung and testis (Fig. 1E, bottom) and to a much lesser extent in short p120ctn isoforms from liver, lung and testis. To conclude, exon C of p120ctn and its corresponding amino acids are highly abundant in mouse brain.

### **Brain-specific p120ctn knockout mice are viable**

Because exon C of p120ctn is highly expressed in brain, we wanted to investigate the effect of a knockout or knockin of exon C in brain. However the constitutive knockout of exon C (p120ctn KOC) and knockin of exon C (p120ctn KIC) in mice, shows an early developmental defect before brain formation (Pieters et al., in preparation). Therefore, we created a strategy to combine an constitutive p120ctn KOC or KIC allele with a brain-specific p120ctn ablation (Figs. 9A and 14A). To generate a brain-specific p120ctn knockout (p120ctn<sup>fl/fl</sup>; Nes-Cre) mice, floxed p120ctn mice were crossed with mice expressing the Cre-

## p120ctn KOC and KIC in the brain

recombinase under the control of the rat nestin promoter (Davis and Reynolds, 2006; Tronche et al., 1999) (Fig. 2A).

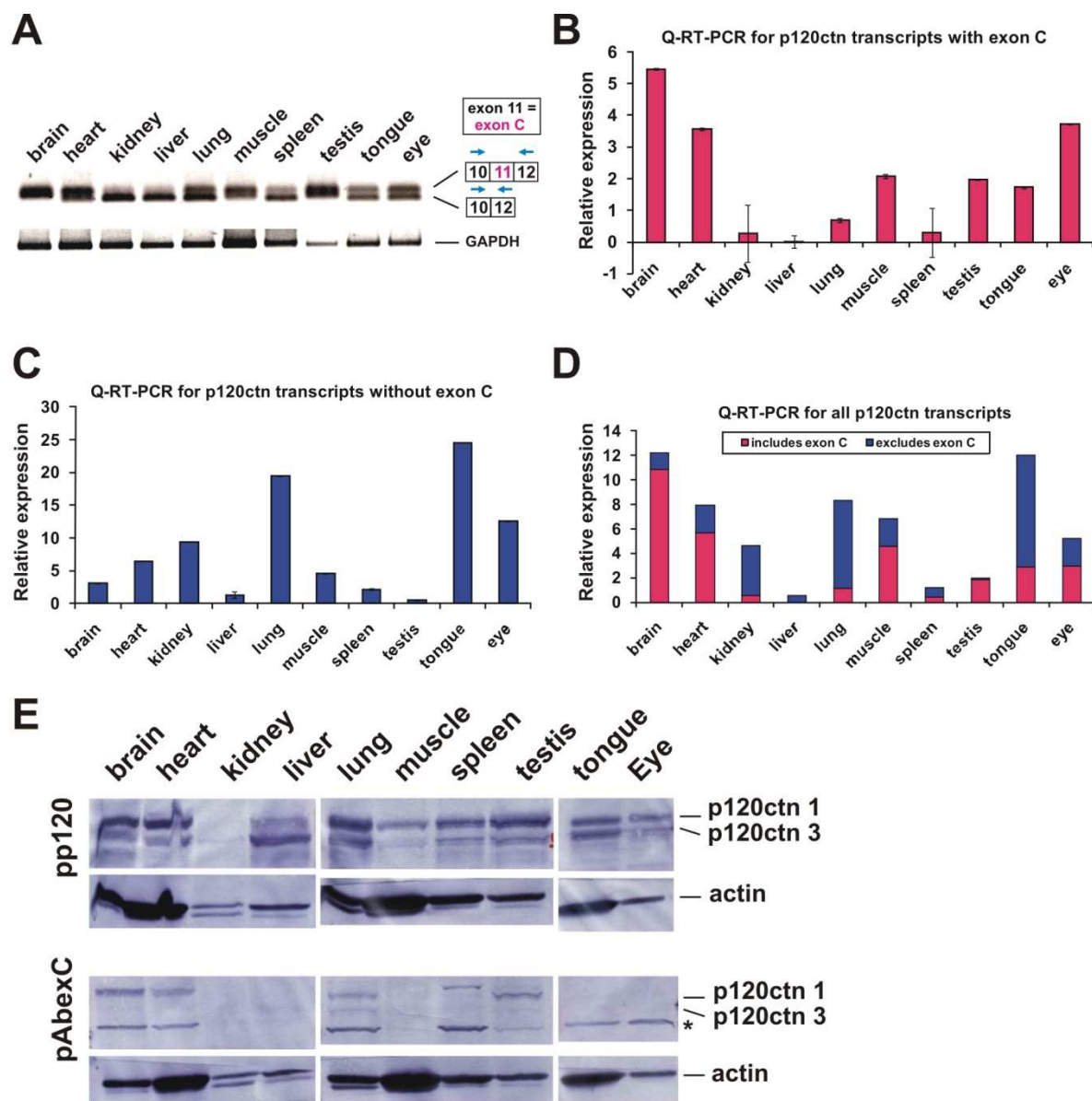


**Figure 1. p120ctn exon C is highly expressed in brain.** (A) RT-PCR for p120ctn transcripts with and without exon C in wild-type mouse tissues. GAPDH acts as a loading control. Q-RT-PCR for p120ctn transcripts with (B) or without exon C (C) or for all p120ctn transcripts (the proportion of exon C inclusion and exclusion is indicated) (D) in wild-type mouse tissues. Q-RT-PCR results were normalized with the expression of two reference genes TBP and B2M. (E) Immunoblot of lysates of wild-type mouse tissues detected with antibodies against all p120ctn isoforms (pp120), p120ctn isoform C (pAbexC) or actin (loading control). p120ctn 1: p120ctn isoform 1, p120ctn 3: p120ctn isoform 3. The asterisk indicates an aspecific band.

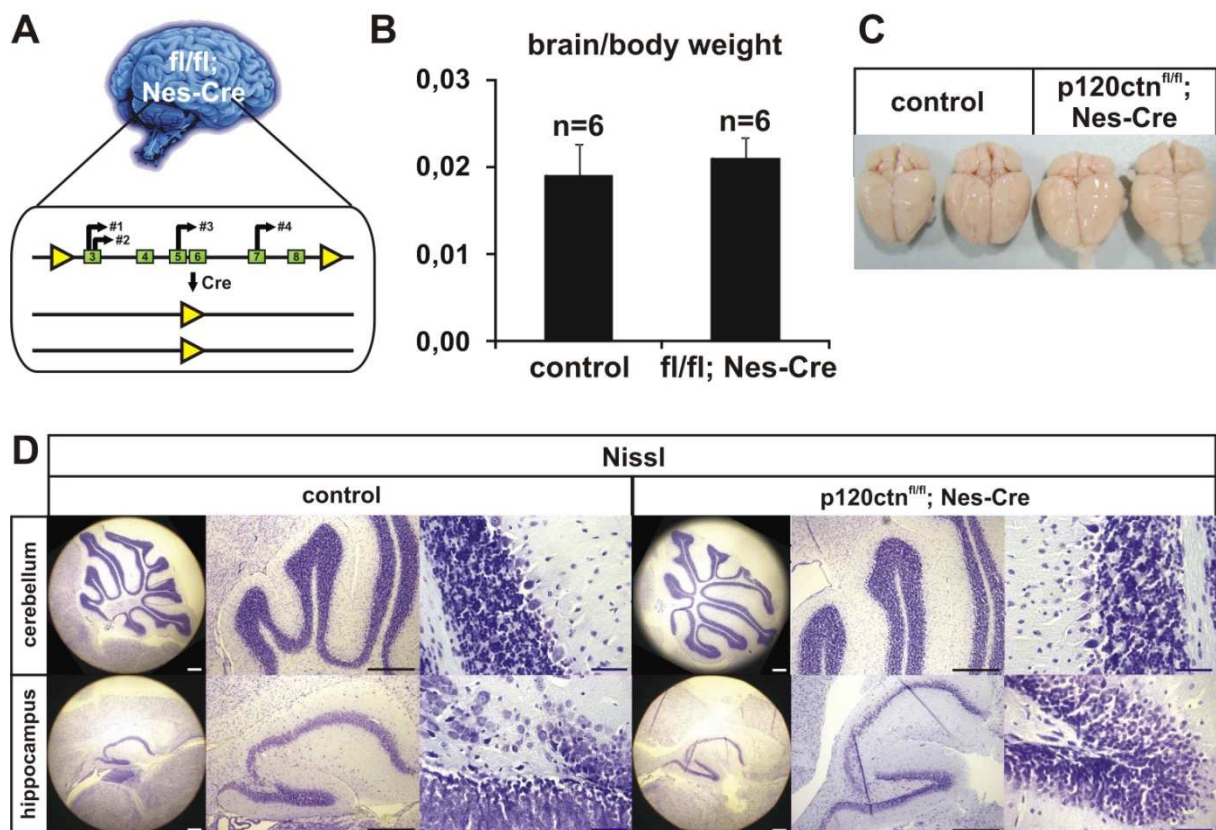


**Figure 2. p120ctn-deficient brains are normal.** (A) Diagram of brain-specific p120ctn knock out (*p120ctn<sup>fl/fl</sup>; Nes-Cre*) mice. Floxed p120ctn mice have loxP sites flanking a genomic region containing exons 3 to 8 (encoding for all 4 translation initiation sites). Cre is expressed under the control of the Nestin promoter, allowing recombination specifically in the brain. (B) Graphic depicting the brain to body ratio of control and *p120ctn<sup>fl/fl</sup>; Nes-Cre* mice. (C) Brains of control and *p120ctn<sup>fl/fl</sup>; Nes-Cre* mice. (D) Nissl-stained paraffin sections of control and *p120ctn<sup>fl/fl</sup>; Nes-Cre* brains. Black and white scale bar: 400  $\mu$ m, purple scale bar: 50  $\mu$ m.

In *p120ctn<sup>fl/fl</sup>; Nes-Cre* mice, the Cre-recombinase is expressed in both neuronal and glial precursors resulting in a p120ctn knockout in almost the entire brain, whereas the *emx-1* Cre only ablates p120ctn in the dorsal forebrain (Elia et al., 2006; Gorski et al., 2002).

Brain-specific p120ctn knockout mice are viable and fertile and exhibit a normal brain to body ratio (Fig. 2B). The p120ctn-deficient brains are macroscopically (Fig. 2C) and microscopically (Fig. 2D) indistinguishable from littermate controls. Immunohistochemical analysis reveals that p120ctn is depleted from the cerebellum, the hippocampus and the cortex, but p120ctn expression persists in glomerular layer of the olfactory bulb (Fig. 3A,B). In contrast, rat adult olfactory bulbs do not show strong staining for p120ctn in the glomerular layer (Chauvet et al., 2003).



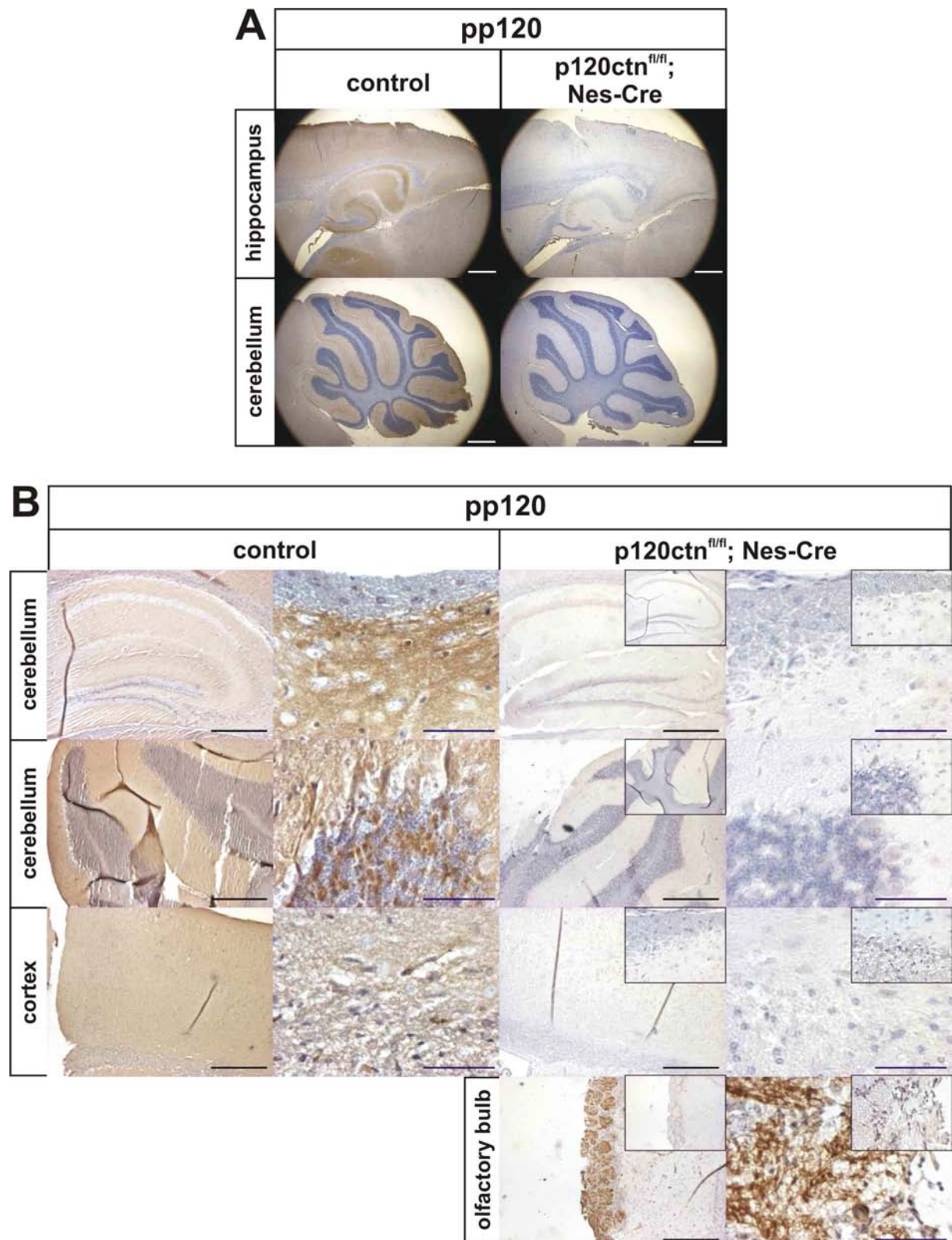


**Figure 3.** p120ctn immunohistochemistry on sagittal sections of p120ctn<sup>fl/fl</sup>; Nes-Cre and control brains at low (A) and high magnification (B). Inset: negative control, treated only with secondary antibody. Black and white scale bar: 400  $\mu$ m, purple scale bar: 50  $\mu$ m.

### Sustained N-cadherin levels in p120ctn-deficient brains

Brain lysates from p120ctn<sup>fl/fl</sup>; Nes-Cre and control mice were analyzed by immunoblotting and confirmed the loss of p120ctn protein in knockout brains (Fig. 4A). p120ctn has been shown to stabilize membrane-localized classical cadherins *in vitro* (Davis et al., 2003; Xiao et al., 2003) and *in vivo* (Davis and Reynolds, 2006; Perez-Moreno et al., 2006; Smalley-Freed et al., 2010). To determine if absence of p120ctn also reduced cadherin levels in the brain, we examined expression levels of N-cadherin in total brain lysates of control and p120ctn<sup>fl/fl</sup>; Nes-Cre mice.

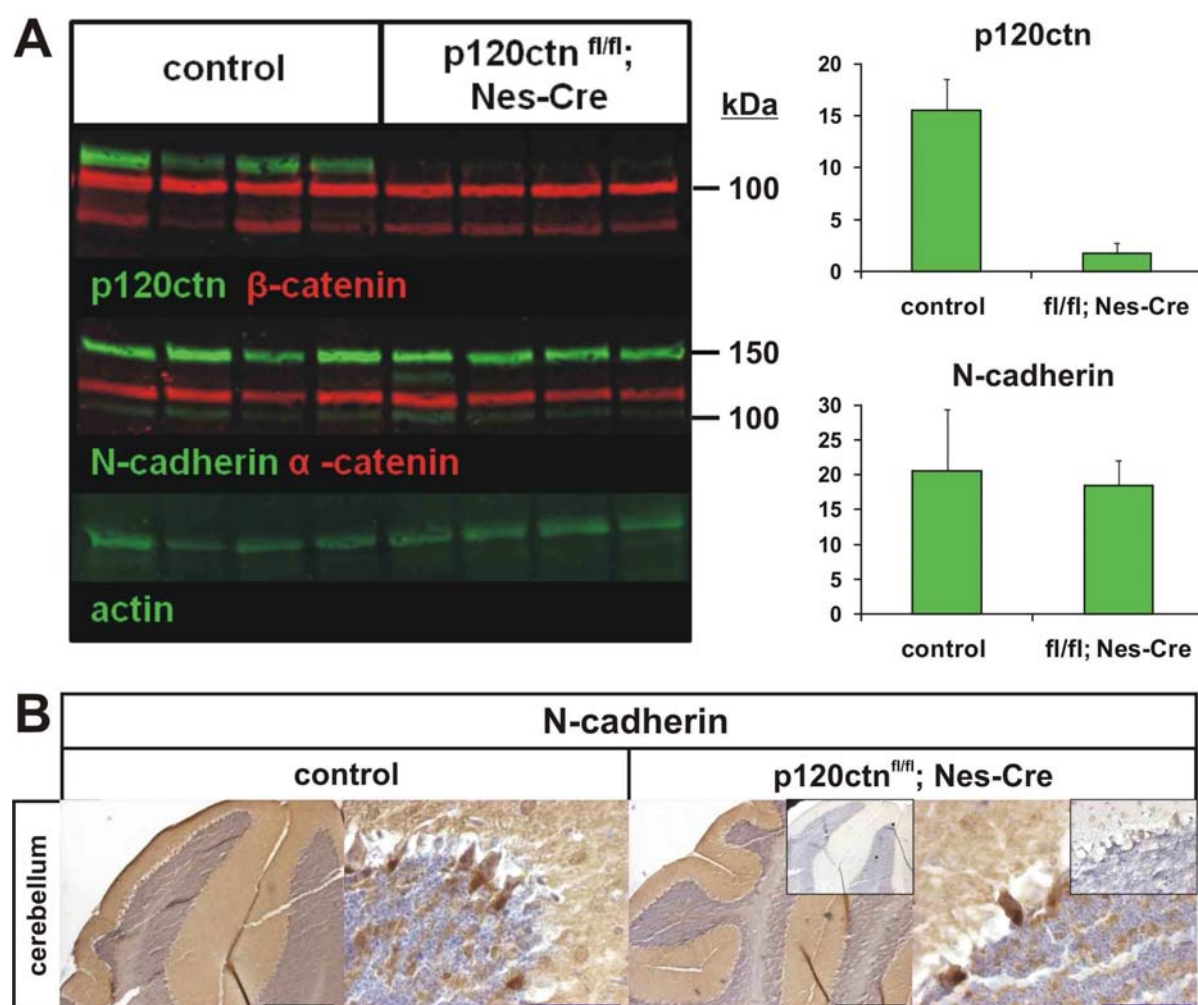


**Figure 4. Sustained N-cadherin levels in p120ctn<sup>fl/fl</sup>; Nes-Cre brains.** (A) Immunoblotting of lysates from control and p120ctn<sup>fl/fl</sup>; Nes-Cre brains with antibodies against p120ctn, β-catenin, N-cadherin and α-catenin. Actin acts as a loading control. Quantifications for p120ctn and N-cadherin are depicted on the right. (B) N-cadherin immunohistochemistry on sagittal sections of p120ctn<sup>fl/fl</sup>; Nes-Cre and control brains. Inset: negative control, treated only with secondary antibody. Black scale bar: 400 μm, purple scale bar: 50 μm.

## p120ctn KOC and KIC in the brain

However, p120ctn knockout brains show only a 10% to 35% reduction in N-cadherin expression levels (Figs. 4A and 12), which is comparable to the 32% reduction of N-cadherin that is seen in hippocampal lysates from dorsal forebrain-specific p120ctn knockout mice (Elia et al., 2006). Furthermore, immunohistochemical analysis shows a similar expression pattern for N-cadherin in brain sections of control and p120ctn<sup>fl/fl</sup>; Nes-Cre mice (Fig. 4B). The sustained N-cadherin expression in brain might be due to functional redundancy of  $\delta$ -catenin, a neuronal-specific p120ctn family member which is also implicated in stabilization of N-cadherin on the cell surface (Israely et al., 2004). Consistent with Elia et al. (2006), no significant difference in expression of  $\alpha$ - and  $\beta$ -catenin was observed in control and p120ctn knockout brains (Fig. 4A).

### Increased RhoA activity in p120ctn-deficient brains

RhoGTPases are biochemical switches that alternate between an active (GTP-bound) state and an inactive (GDP-bound) state. p120ctn has been shown to alter RhoGTPase activity. Overexpression of p120ctn isoform 1, which is predominantly expressed in brain, results in inhibition of RhoA activity and activates Rac1 and Cdc42 (Anastasiadis et al., 2000; Grosheva et al., 2001; Noren et al., 2000). Genetic of RNAi-mediated depletion of p120ctn causes increased RhoA activation and inhibits Rac1 activity (Elia et al., 2006; Perez-Moreno et al., 2006; Yanagisawa and Anastasiadis, 2006). To determine whether the absence of p120ctn affects the RhoAGTPase activity in brain, we performed affinity precipitations to measure RhoA and Rac1 activity (Ren et al., 1999). GST-fusion proteins containing the RhoA binding domain of rhotekin (GST-RBD) or the Rac1 binding domain of PAK (GST-PBD) were used to isolate active RhoA and Rac1, respectively. The active RhoGTPase fraction was then normalized to the total level of each protein. In agreement with previously published work, increased RhoA activity was observed in total brain lysates of p120ctn<sup>fl/fl</sup>; Nes-Cre mice (Figs. 5A, B) (Elia et al., 2006), however this increase in RhoA activity was not observed in all experiments (Fig. 13E). Decreased Rac1 activity was also observed in hippocampal lysates from dorsal forebrain-specific p120ctn knockout mice (Elia et al., 2006). In contrast, no difference in Rac1 activity was observed in lysates from p120ctn-deficient and control brains (Figs. 5C, D and 13C, D).

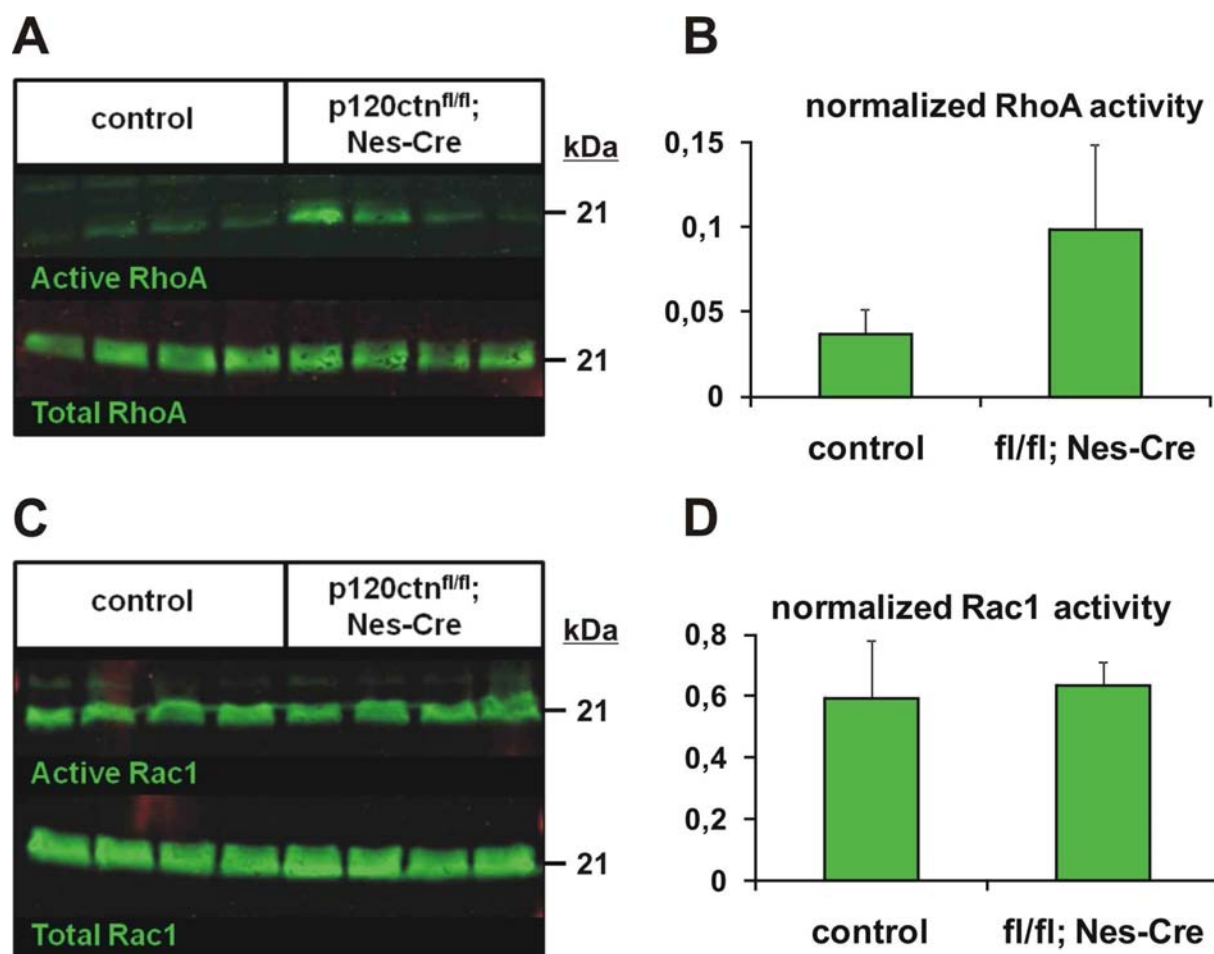


**Figure 5. Increased RhoA activity in  $p120ctn^{fl/fl}; Nes-Cre$  brains.** (A) Active and total RhoA levels in control and in  $p120ctn^{fl/fl}; Nes-Cre$  brains. (B) Active RhoA levels were normalized against total amounts of RhoA. (C) Active and total Rac1 levels in control and in  $p120ctn^{fl/fl}; Nes-Cre$  brains. (D) Active Rac1 levels were normalized against total amounts of Rac1.

### NestinCre transgenic females and males show premature recombination

Routine genotyping of litters derived from matings with second generation  $p120ctn^{fl/+}; Nes-Cre$  females revealed recombination events in tail genomic DNA (Table 2). Two different sets of primers are able to detect the floxed  $p120ctn$  allele (Fig. 6A, blue and red primer sets) and one set of primers can identify Cre-mediated excision of the floxed DNA fragment (Fig. 6A, blue forward primer and red reverse primer). PCR is very sensitive and it can detect a single recombination event in a single cell. On the other hand, if recombination occurred in all cells of a tissue than we can no longer detect the floxed  $p120ctn$  allele via PCR (Fig. 6A, blue primers).

## p120ctn KOC and KIC in the brain

**Table 2. Premature recombination in offspring derived from matings with female p120ctn floxed Nes-Cre mice**

Genotyping offspring from ♀ p120ctn <sup>fl/+</sup> ; Nes-Cre x ♂ p120ctn <sup>fl/fl</sup> mating					
fl/fl; Nes-Cre (25%)	fl/fl (25%)	fl/+; Nes-Cre (25%)	fl/+ (25%)	total	recombination
22 (19,1%)	29 (25,2%)	35 (30,4%)	29 (25,2%)	115	
3/4	3/9	6/6	0/10	6/16	tail
Genotyping offspring from ♀ p120ctn <sup>fl/fl</sup> ; Nes-Cre x ♂ p120ctn <sup>fl/fl</sup> mating					
fl/fl; Nes-Cre (50%)	fl/fl (50%)	total	recombination		
15 (44,1%)	19 (55,9%)	34			
16/16	4/8	20/24			tail
1/1	1/1	2/2			tail(skin)
1/1	1/1	2/2			tail(spine)
1/1	1/1	2/2			ear
1/1	1/1	2/2			toe
3/3	3/3	6/6			brain (Ectoderm)
3/3	3/3	6/6			liver (Endoderm)
1/1	1/1	2/2			kidney (Mesoderm)
1/1	1/1	2/2			lung (Endoderm)
Genotyping offspring from ♀ p120ctn <sup>KOC/fl</sup> ; Nes-Cre x ♂ p120ctn <sup>KOC/+</sup> mating					
KOC/fl; Nes-Cre (12,5%)	KOC/fl (12,5%)	KOC/+; Nes-Cre (12,5%)	KOC/+ (12,5%)	total	recombination
0 (0,0%)	2 (3,2%)	15 (24,2%)	22 (35,5%)		
	1/1	1/2	1/3		tail
fl/+; Nes-Cre (12,5%)	fl/+ (12,5%)	+/+; Nes-Cre (12,5%)	+/+ (12,5%)		recombination
1 (1,6%)	0 (0,0%)	9 (14,5%)	10 (21,0%)	62	
		0/1	1/2	4/9	tail
Genotyping offspring from ♀ p120ctn <sup>fl/fl</sup> ; Nes-Cre x ♂ p120ctn <sup>KOC/+</sup> mating					
KOC/fl; Nes-Cre (25%)	KOC/fl (25%)	fl/+; Nes-Cre (25%)	fl/+ (25%)	total	recombination
6 (20,7%)	11 (37,9%)	6 (20,7%)	6 (20,7%)	29	
6/6	11/11	6/6	4/6	27/29	tail
Genotyping offspring from ♀ p120ctn <sup>fl/fl</sup> ; Nes-Cre x ♂ p120ctn <sup>KIC/+</sup> mating					
KIC/fl; Nes-Cre (12,5%)	KIC/fl (12,5%)	KIC/+; Nes-Cre (12,5%)	KIC/+ (12,5%)	total	recombination
1 (2,9%)	2 (5,7%)	12 (34,5%)	22 (35,5%)		
1/1	0/1				tail
fl/+; Nes-Cre (12,5%)	fl/+ (12,5%)	+/+; Nes-Cre (12,5%)	+/+ (12,5%)		recombination
1 (2,9%)	2 (5,7%)	8 (22,9%)	6 (17,1%)	35	
	1/1		1/2	3/5	tail
Genotyping offspring from ♀ p120ctn <sup>fl/fl</sup> ; Nes-Cre x ♂ p120ctn <sup>KIC/+</sup> mating					
KIC/fl; Nes-Cre (25%)	KIC/fl (25%)	fl/+; Nes-Cre (25%)	fl/+ (25%)	total	recombination
1 (8,3%)	4 (33,3%)	1 (8,3%)	6 (50,0%)	12	
1/1	3/3	1/1	5/5	10/10	tail(skin)
1/1	1/1	1/1		3/3	tail(spine)
1/1	1/1	1/1		3/3	ear
1/1	1/1	1/1		3/3	toe
1/1	1/1	1/1		3/3	brain
1/1	1/1	1/1		3/3	liver

So, via PCR we can detect single or complete recombination events, however, via PCR we can not determine the degree of recombination and the corresponding loss of p120ctn protein. Normally we expect only recombination in brain cells, and not in tail cells, from p120ctn<sup>fl/fl</sup>; Nes-Cre mice, which express the Cre-recombinase from the Nestin promoter.



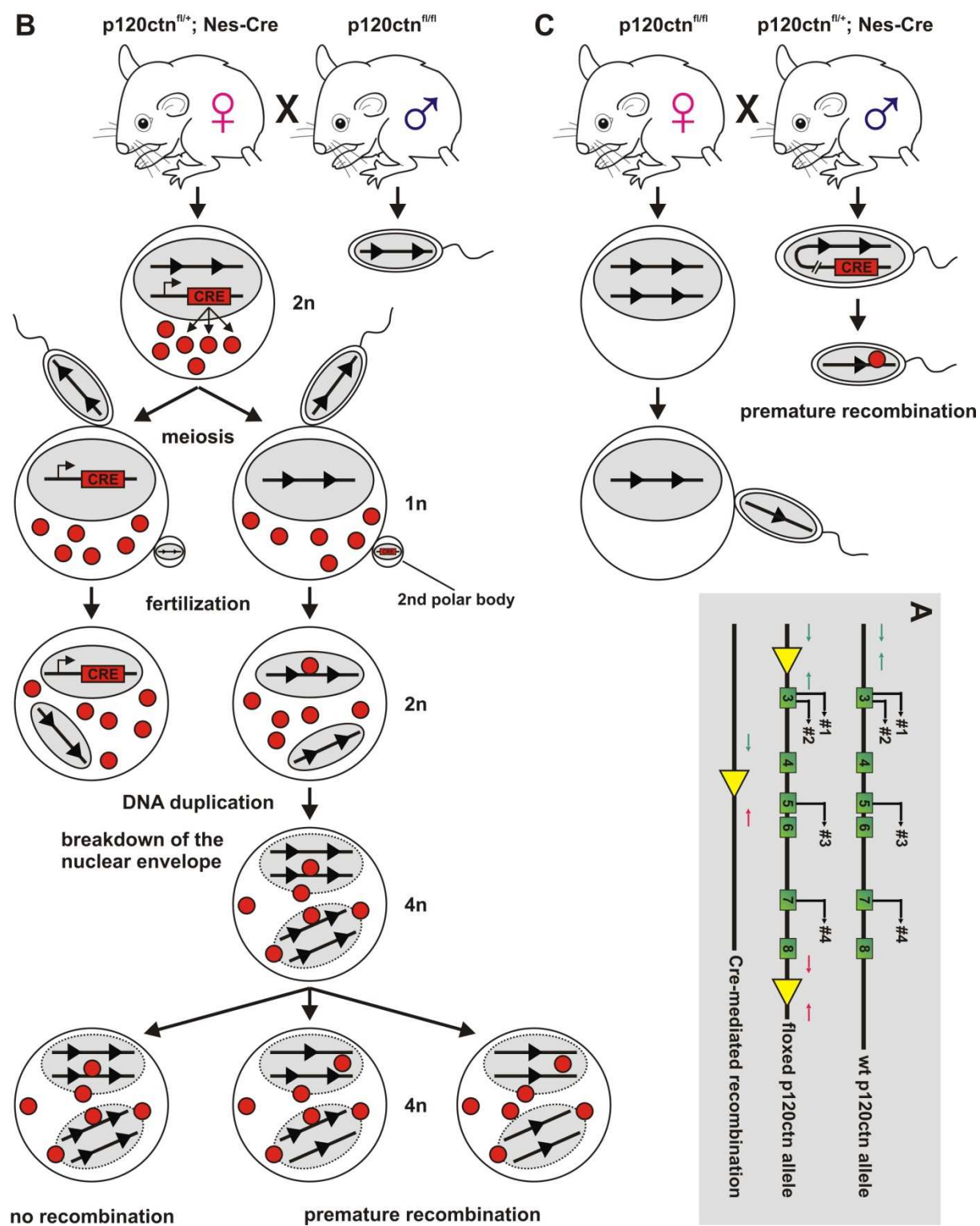


**Figure 6. Premature recombination in  $p120ctn$  floxed Nes-Cre female and males.** (A) PCR strategy to detect the floxed  $p120ctn$  allele (blue and red primer sets) and the recombined  $p120ctn$  allele (blue forward primer and red reverse primer). (B) Diagram depicting premature recombination when using Nes-Cre females. Diploid oocytes contain Cre-protein in their cytoplasm, resulting in premature recombination after fertilization with sperm that contains the floxed  $p120ctn$  allele. (C) Diagram depicting premature recombination of the floxed  $p120ctn$  allele during gametogenesis in Nes-Cre males.

## p120ctn KOC and KIC in the brain

However, recombination occurred in tail DNA from offspring, descending from a second generation Nes-Cre female, and recombination was even observed in tail DNA of progeny that did not have the Nes-Cre allele (Table 2). Recombination was also observed in genomic DNA from organs originating from all three germ layers (Table 2). This strange phenomenon has been described for another Cre-line (Lallemand et al., 1998) and can be explained by the presence of Cre-protein in diploid oocytes (Fig. 6B). During meiosis the second polar body is emitted from the haploid oocyte which contains Cre-protein in its cytoplasm. The female pronucleus can contain either a wild-type or a floxed p120ctn allele and possibly the Cre-transgene. After fertilization, the male and female pronuclei undergo DNA duplication and their nuclear membranes break down. From one-cell stage embryos on, premature recombination events can occur even though the embryo does not contain the Cre-transgene (Fig. 6B). In the first generation offspring the premature recombination will be mosaic and the degree of mosaicism depends on the embryonic stage in which premature recombination occurs. In the second generation offspring the recombined allele can be transmitted resulting in mice with a uniform tissue-wide recombination. Using floxed p120ctn Nes-Cre males is not a good alternative, since these mice express the Cre-recombinase during gametogenesis causing premature excision of floxed DNA fragments (Fig. 6C) (Table 3) (Haigh et al., 2003).

**Table 3. Premature recombination in offspring derived from matings with male p120ctn floxed Nes-Cre mice**

Genotyping offspring from ♀ p120ctn <sup>fl/fl</sup> x ♂ p120ctn <sup>fl/+</sup> ; Nes-Cre mating						
fl/fl; Nes-Cre (25%)	fl/fl (25%)	fl/+; Nes-Cre (25%)	fl/+ (25%)	total	recombination	
43 (24,7%)	47 (27,0%)	45 (25,8%)	39 (22,4%)	174		
16/16	4/6	5/5	1/3	26/30	tail	
2/2	0/2	1/1	0/1	3/6	brain	
1/1	0/2		0/1	1/4	liver	
1/1	0/2		0/1	1/4	kidney	
Genotyping offspring from ♀ p120ctn <sup>fl/fl</sup> x ♂ p120ctn <sup>fl/+</sup> ; Nes-Cre mating						
fl/fl; Nes-Cre (50%)	fl/fl (50%)	total	recombination			
32 (56,1%)	25 (43,9%)	57				
4/4	2/5	6/9	tail			
2/2	1/1	3/3	brain			
Genotyping offspring from ♀ p120ctn <sup>KOC/+</sup> x ♂ p120ctn <sup>fl/+</sup> ; Nes-Cre mating						
KOC/fl; Nes-Cre (25%)	KOC/fl (25%)	fl/+; Nes-Cre (25%)	fl/+ (25%)	total	recombination	
24 (20,7%)	22 (23,7%)	16 (17,2%)	31 (33,3%)	93		
7/8	4/5	4/4	3/4	18/21	tail	
2/2	0/1	1/1	1/2	4/6	brain	
Genotyping offspring from ♀ p120ctn <sup>KIC/+</sup> x ♂ p120ctn <sup>fl/+</sup> ; Nes-Cre mating						
KOC/fl; Nes-Cre (25%)	KOC/fl (25%)	fl/+; Nes-Cre (25%)	fl/+ (25%)	total	recombination	
15 (27,8%)	9 (16,7%)	17 (31,5%)	13 (24,1%)	54		
2/4	2/4	3/3	3/3	10/14	tail	
4/4	4/4	1/1	1/1	10/10	brain	

To address what the consequences are of these premature recombination events in tissues different from brain, protein lysates and tissue sections were made from organs from either p120ctn<sup>fl/fl</sup>; Nes-Cre and control mice. Crossing a p120ctn<sup>fl/fl</sup>; Nes-Cre female with a p120ctn<sup>fl/fl</sup>; male gave rise to offspring that had undergone premature recombination that could be detected on genomic level in various tissues. Western blotting revealed that p120ctn expression was lost in brain and kidney from p120ctn<sup>fl/fl</sup>; Nes-Cre mice (Fig. 7A). However these mice expressed similar levels of p120ctn in liver compared to control mice (Fig. 7B). Although recombination events were detected in genomic DNA from brain, kidney and liver of control mice (p120ctn<sup>fl/fl</sup>), they still express fairly normal p120ctn protein in these tissues (Figs. 7A,B). However in these experiments we lack a proper wild-type control, indicative for normal p120ctn expression. Matings with a p120ctn<sup>fl/+</sup>; Nes-Cre males gave rise to a p120ctn<sup>fl/fl</sup>; Nes-Cre offspring, which lost p120ctn expression in brain, but exhibited also diminished p120ctn protein in kidney and liver compared to control mice (Fig. 7C). However, no decrease in p120ctn expression was observed for these mice via immunohistochemistry (Fig. 7D). p120ctn protein was also diminished in kidney, but not in brain, from control mice that did not contain the Cre-transgene (Fig. 7E). To conclude, recombination events detected by PCR do not seem to have a large impact on protein level of p120ctn in control mice, however, p120ctn is often downregulated in organs different from brain in p120ctn<sup>fl/fl</sup>; mice.



p120ctn KOC and KIC in the brain

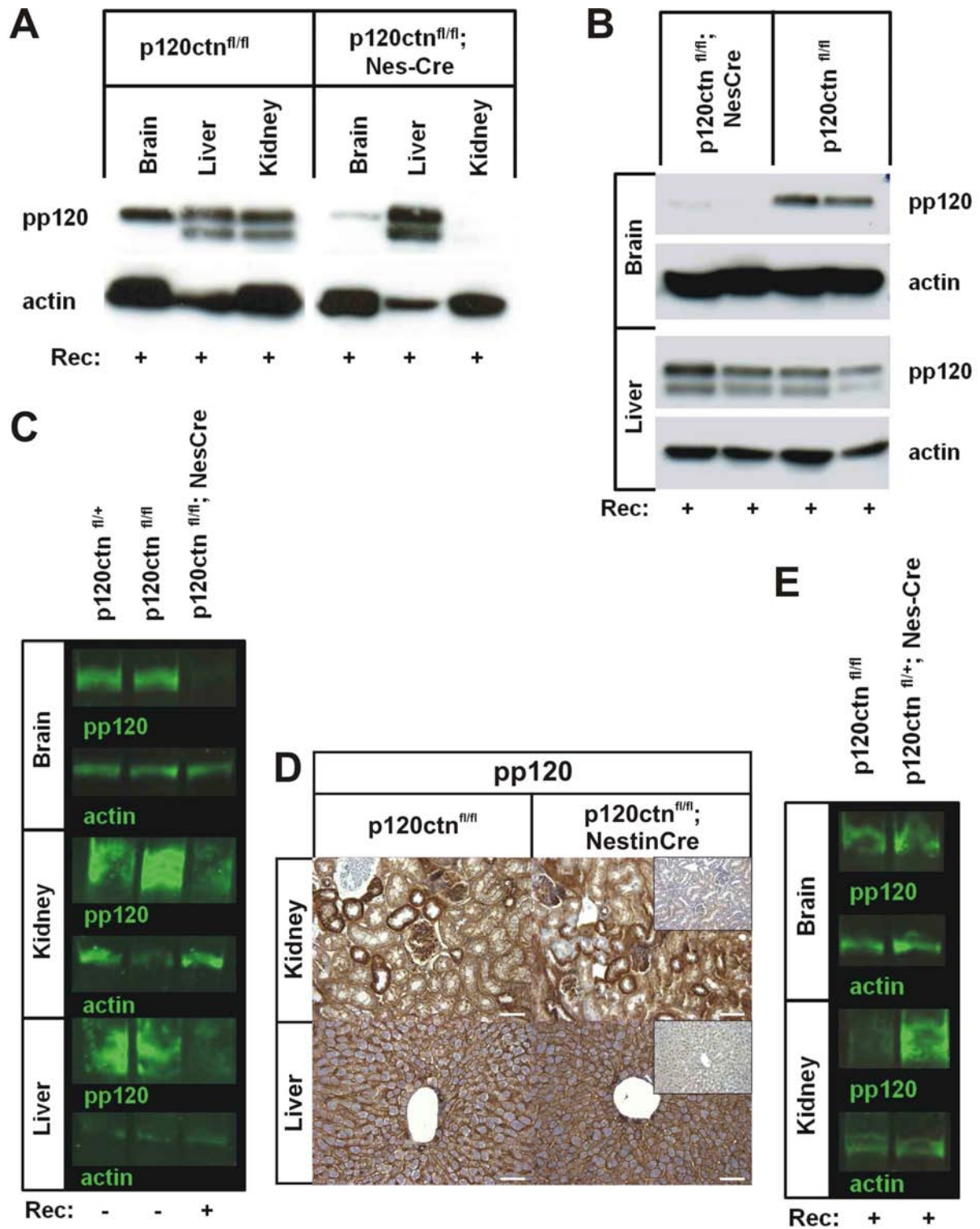


**Figure 7. Effect of premature recombination on p120ctn protein level.** (A,B) p120ctn expression in different organs of control and p120ctn<sup>fl/fl</sup>; Nes-Cre mice, descending from a mating between a p120ctn<sup>fl/fl</sup>; Nes-Cre female with a p120ctn<sup>fl/fl</sup>; male. (C-E) p120ctn expression in different organs of control and p120ctn<sup>fl/fl</sup>; Nes-Cre mice, descending from a mating between a p120ctn<sup>fl/+</sup>; Nes-Cre male with a p120ctn<sup>fl/fl</sup>; female. Immunoblotting (A-C, E) and immunohistochemistry (D) using an antibody that recognizes all p120ctn isoforms (pp120). Actin acts as a loading control. It is mentioned if recombination (Rec) was detected on genomic DNA by PCR. Scale bar: 50  $\mu$ m.

## Revised mating strategy to obtain p120ctn<sup>KOC/fl</sup>; Nes-Cre and p120ctn<sup>KIC/fl</sup>; Nes-Cre mice

To generate mice that never incorporate exon C in their p120ctn transcripts, brain-specific p120ctn knockout (p120ctn<sup>fl/fl</sup>; Nes-Cre) were mated with p120ctn<sup>KOC/+</sup> mice. However, as mentioned above, premature recombination was observed in matings with p120ctn<sup>fl/fl</sup>; Nes-Cre mice, resulting in a mozaic instead of a brain specific p120ctn deletion (Tables 2, 3). To avoid this, a new strategy was designed to prevent this premature recombination. In this strategy the Cre-transgene was combined with the p120ctn KOC allele, which has only one loxP site (the floxed selection cassette has already been removed) and therefore is not prone to premature recombination in gametes (Fig. 8). p120ctn<sup>KOC/+</sup> Nes-Cre males produce sperm, which can only carry very few Cre-proteins in their small cytoplasmic compartment. Therefore there is only a low probability of premature recombination after fertilization of oocytes containing a floxed p120ctn allele with sperm that contains both p120ctn KOC allele and the Cre-transgene (Fig. 8B). On the other hand, oocytes for p120ctn<sup>KOC/+</sup> Nes-Cre females can still accumulate a lot of Cre-protein in their cytoplasm, which can cause premature recombination events after fertilization with a sperm cell that contains a floxed p120ctn allele (Fig. 8A). Indeed, recombination events can be observed in genomic tail DNA of offspring bearing the Cre-transgene, if the p120ctn KOC Nes-Cre allele was transferred by the mother (Table 4). No recombination events were observed in genomic tail DNA of offspring descending from a p120ctn<sup>KOC/fl</sup>; male (Table 4).

**Table 4. Strategy to prevent premature recombination in p120ctn<sup>KOC/fl</sup>; Nes-Cre mice**

Genotyping offspring from ♀ Nes-Cre x ♂ p120ctn <sup>KOC/+</sup> mating					
KOC/+; Nes-Cre (25%)	KOC/+ (25%)	+/+; Nes-Cre (25%)	+/+ (25%)	total	recombination
23 (23,7%)	19 (19,6%)	24 (24,7%)	31 (32,0%)	97	
0/2	0/2		0/5	0/9	tail
Genotyping offspring from ♀ p120ctn <sup>KOC/+</sup> ; Nes-Cre x ♂ p120ctn <sup>fl/fl</sup> mating					
KOC/fl; Nes-Cre (25%)	KOC/fl (25%)	fl/+; Nes-Cre (25%)	fl/+ (25%)	total	recombination
9 (4,9%)	81 (40,0%)	67 (36,4%)	27 (14,7%)	184	
3/3	0/5	9/9	0/4	12/21	tail
2/2		2/2		4/4	brain
Genotyping offspring from ♀ p120ctn <sup>fl/fl</sup> x ♂ p120ctn <sup>KOC/+</sup> ; Nes-Cre mating					
KOC/fl; Nes-Cre (25%)	KOC/fl (25%)	fl/+; Nes-Cre (25%)	fl/+ (25%)	total	recombination
4 (4,8%)	40 (48,2%)	37 (44,6%)	2 (2,4%)	83	
0/3	0/3	0/3	0/2	0/11	tail

## p120ctn KOC and KIC in the brain

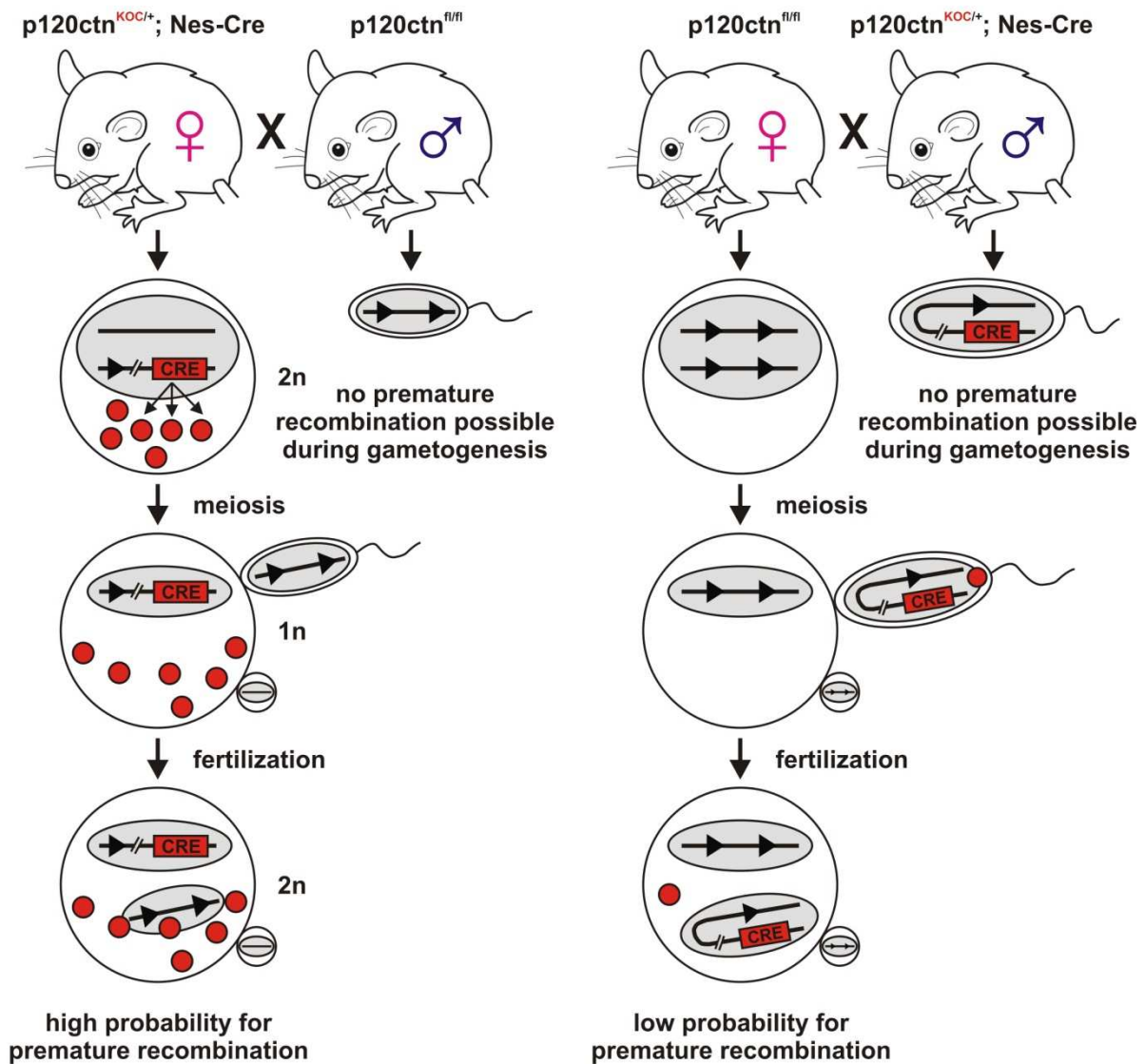


**Figure 8. Strategy to prevent premature recombination in  $p120ctn^{KOC/fl}; Nes-Cre$  and  $p120ctn^{KIC/fl}; Nes-Cre$  mice.** Combining the  $p120ctn$  KOC allele (has only one loxP site) with the Cre-transgene prevents premature during gametogenesis. (A)  $p120ctn^{KOC/+}; Nes-Cre$  females have a high probability for premature recombination in their offspring because the huge storage capacity for Cre-protein in the cytoplasm of their oocytes. (B)  $p120ctn^{KOC/+}; Nes-Cre$  males have a low probability for premature recombination in their offspring because sperm has only a small cytoplasmic compartment and a very limited storage capacity for Cre-protein.

Premature recombination was also observed in offspring from matings between  $p120ctn^{fl/fl}; Nes-Cre$  mice and  $p120ctn^{KIC/+}$  mice (Tables 2, 3). A similar strategy was employed to avoid premature recombination. The Cre-transgene was transferred along with the  $p120ctn$  KIC allele, which also has only one loxP site (the floxed selection cassette has already been removed). When  $p120ctn^{KIC/+}; Nes-Cre$  females were crossed to  $p120ctn^{fl/fl}; Nes-Cre$  mice,

males, recombination events could still be detected in genomic DNA from tail from offspring containing the Cre-recombinase (Table 5). However, control mice did not have any recombination in genomic DNA from tail and brain, indicating that these controls are ‘genetically clean’.

**Table 5. Strategy to prevent premature recombination in  $p120ctn^{KIC/fl}$ ; Nes-Cre mice**

Genotyping offspring from ♀ $p120ctn^{KIC/+}$ x ♂ Nes-Cre mating					
KIC/+; Nes-Cre (25%)	KIC/+ (25%)	+/+; Nes-Cre (25%)	+/+ (25%)	total	recombination
21 (42,2%)	21 (42,2%)	6 (11,8%)	3 (5,9%)	51	
0/5	0/3	0/3	0/3	0/14	tail
Genotyping offspring from ♀ $p120ctn^{KIC/+}$ ; Nes-Cre x ♂ $p120ctn^{fl/fl}$ mating					
KIC/fl; Nes-Cre (25%)	KIC/fl (25%)	fl/+; Nes-Cre (25%)	fl/+ (25%)	total	recombination
24 (25,3,6%)	21 (22,1%)	20 (21,1%)	30 (31,6,5%)	95	
4/4	0/5	4/4	0/5	8/18	tail
3/3			0/3	3/6	brain

To conclude, premature recombination is prevented during gametogenesis by combining the  $p120ctn$  KOC or  $p120ctn$  KIC allele (contain only one loxP site each) with the Cre-transgene. Furthermore,  $p120ctn^{KOC/+}$  Nes-Cre or  $p120ctn^{KIC/+}$  Nes-Cre males have to be crossed with  $p120ctn^{fl/fl}$ ; females to obtain offspring with a brain-specific  $p120ctn$  knockout in one allele and exclusive expression of  $p120ctn$  transcripts without (KOC) or with exon C (KIC), respectively, from the other allele.

### **$p120ctn^{KOC/fl}$ ; Nes-Cre hippocampi display discrete medial abnormalities**

$p120ctn^{KOC/fl}$ ; Nes-Cre mice combine a constitutive knockout of exon C of  $p120ctn$  with a brain-specific knockout of all  $p120ctn$  isoforms (Fig. 9A). These mice were viable and had normal brains, which were macroscopically indistinguishable from control brains (Figs. 10B,C). Detailed histological analysis revealed mild abnormalities in the medial side of both hippocampi of  $p120ctn^{KOC/fl}$ ; Nes-Cre mice (n=4) (Fig. 10A). This phenotype was also obvious in four-week-old mice. For an accurate comparison between control and  $p120ctn^{KOC/fl}$ ; Nes-Cre sections, similar sagittal planes were selected using a reference atlas (Allan brain atlas, <http://mouse.brain-map.org/atlas/ARA/Sagittal/browser.html>), and confirmed that the hippocampal abnormalities were restricted to the medial side (Fig. 11A,B). To get a global view on this medial defect in hippocampi, MRI analysis was performed on one  $p120ctn^{KOC/fl}$ ; Nes-Cre and one control mouse.



p120ctn KOC and KIC in the brain

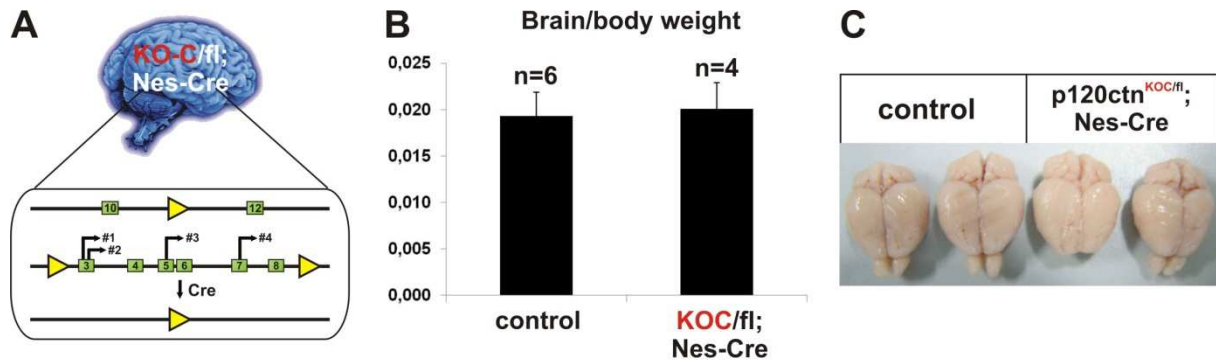


**Figure 9.** p120ctn<sup>KOC/fl</sup>; Nes-Cre mice have normal brain. (A) Diagram of p120ctn<sup>KOC/fl</sup>; Nes-Cre mice, containing a constitutive knockout of exon C of p120ctn and a brain-specific p120ctn knockout allele. (B) Graphic depicting the brain to body ratio of control and p120ctn<sup>KOC/fl</sup>; Nes-Cre mice. (C) Brains of control and p120ctn<sup>KOC/fl</sup>; Nes-Cre mice.

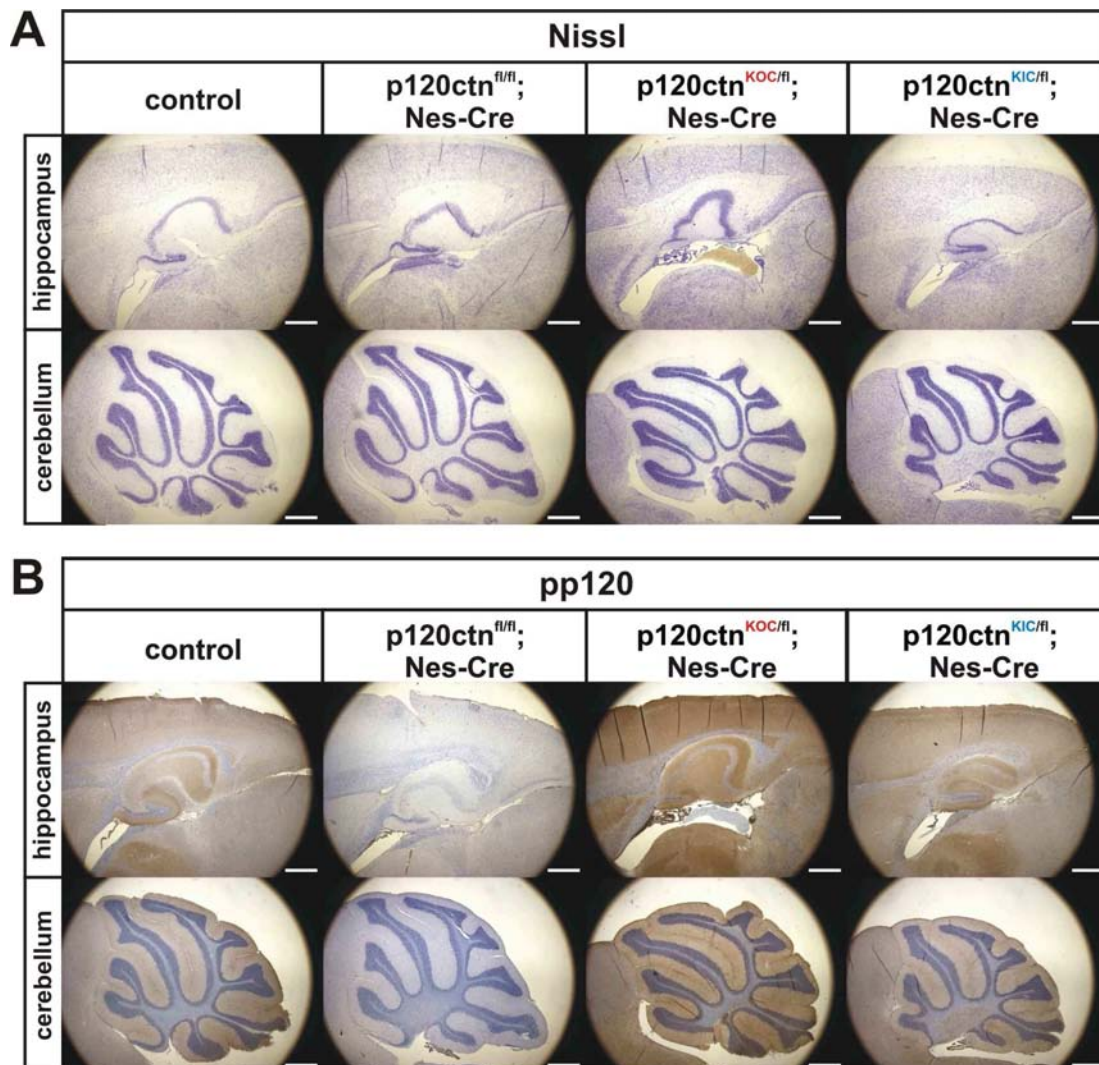


**Figure 10.** Histology and p120ctn immunohistochemistry for p120ctn<sup>KOC/fl</sup>; Nes-Cre and p120ctn<sup>KIC/fl</sup>; Nes-Cre brains. Nissl staining (A) and p120ctn immunohistochemistry (B) of sagittal brain sections of control, p120ctn<sup>fl/fl</sup>; Nes-Cre, p120ctn<sup>KOC/fl</sup>; Nes-Cre and p120ctn<sup>KIC/fl</sup>; Nes-Cre mice. Scale bar: 400  $\mu$ m.

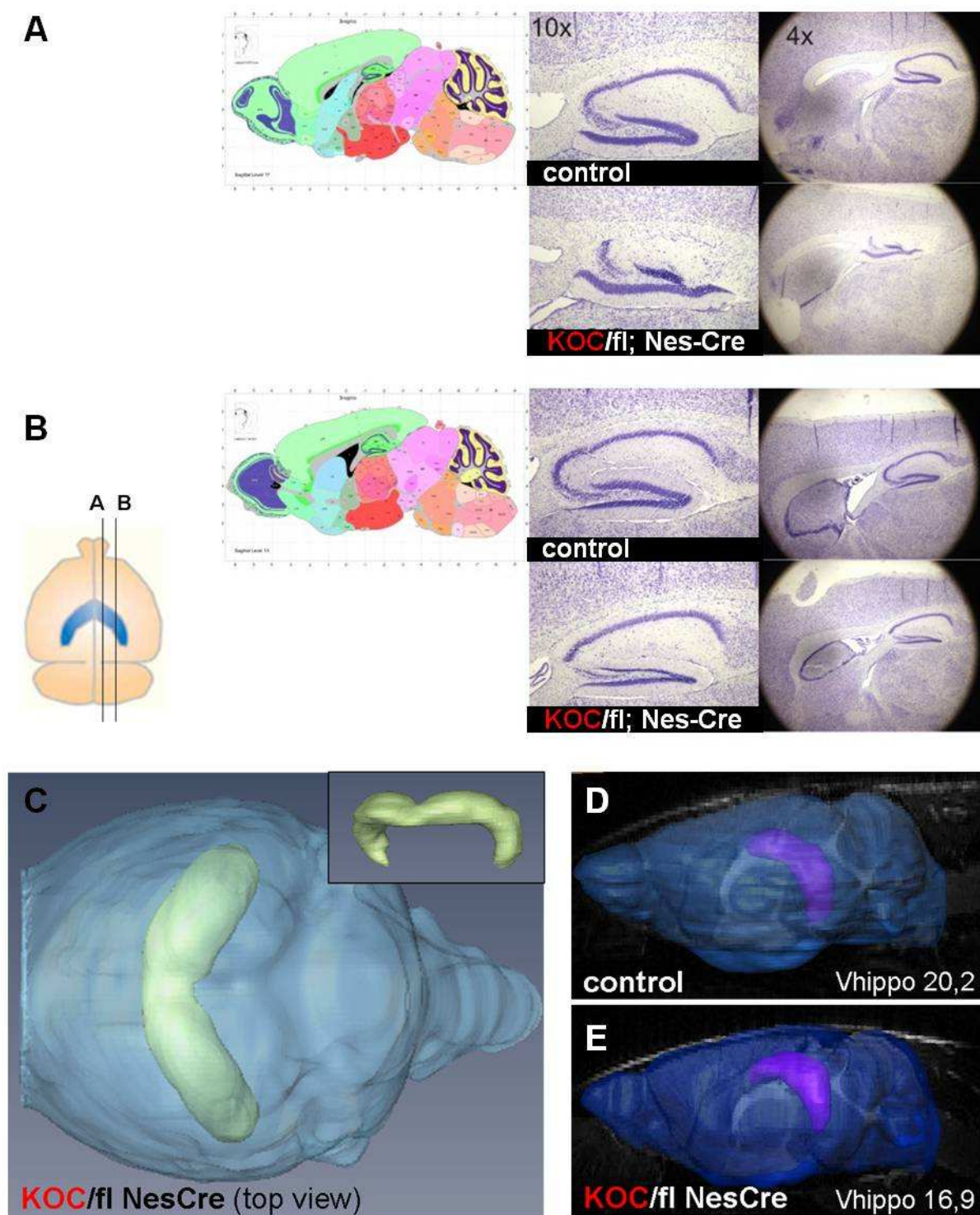


**Figure 11. Aberrant morphology in  $p120ctn^{KOC/fl}; Nes-Cre$  hippocampi.** (A, B) Nissl staining of brain sections from control and  $p120ctn^{KOC/fl}; Nes-Cre$  mice. Medial (A) and more lateral (B) sagittal sections were analyzed. Similar sagittal planes were selected based on a reference atlas (Allan brain atlas, <http://mouse.brain-map.org/atlas/ARA/Sagittal/browser.html>). (C-D) MRI-analysis of brains and hippocampi from control (D) and  $p120ctn^{KOC/fl}; Nes-Cre$  mice (C,E). Top view of brain and hippocampi of a  $p120ctn^{KOC/fl}; Nes-Cre$  mouse and a front view of hippocampi alone (inset). Side view from the brains and hippocampi of  $p120ctn^{KOC/fl}; Nes-Cre$  mice.

## p120ctn KOC and KIC in the brain

Although the overall morphology of p120ctn<sup>KOC/fl</sup>; Nes-Cre and control hippocampi was similar, a 16% decrease in hippocampal volume was observed in p120ctn<sup>KOC/fl</sup>; Nes-Cre mice compared to a littermate control. However, more mice need to be analyzed via MRI to confirm this preliminary finding. To ascertain that p120ctn protein is expressed from the p120ctn KOC allele, sagittal brain sections and brain lysates from p120ctn<sup>KOC/fl</sup>; Nes-Cre mice were stained or immunoblotted with an antibody that recognizes all p120ctn isoforms. Sections of p120ctn<sup>KOC/fl</sup>; Nes-Cre brains expressed comparable amounts of p120ctn protein compared to control brains (Fig. 10B), and this was confirmed by immunoblotting on whole brain lysates and hippocampal lysates from control and p120ctn<sup>KOC/fl</sup>; Nes-Cre mice (Figs. 12A, B, D). In addition, brain and hippocampal lysates from p120ctn<sup>KOC/fl</sup>; Nes-Cre mice expressed similar amounts of N-cadherin,  $\alpha$ -catenin and  $\beta$ -catenin (Fig. 12). Next we wondered if the absence of exon C in all p120ctn transcripts would affect the activity of RhoGTPases. p120ctn<sup>KOC/fl</sup>; Nes-Cre mice contain a pristine RhoA binding site, which is not interrupted by exon C-encoded amino acids, and does not interfere with RhoGTPase signaling. As expected, the RhoA and Rac1 activities in p120ctn<sup>KOC/fl</sup>; Nes-Cre brains are comparable to those of control brains (Fig 13).



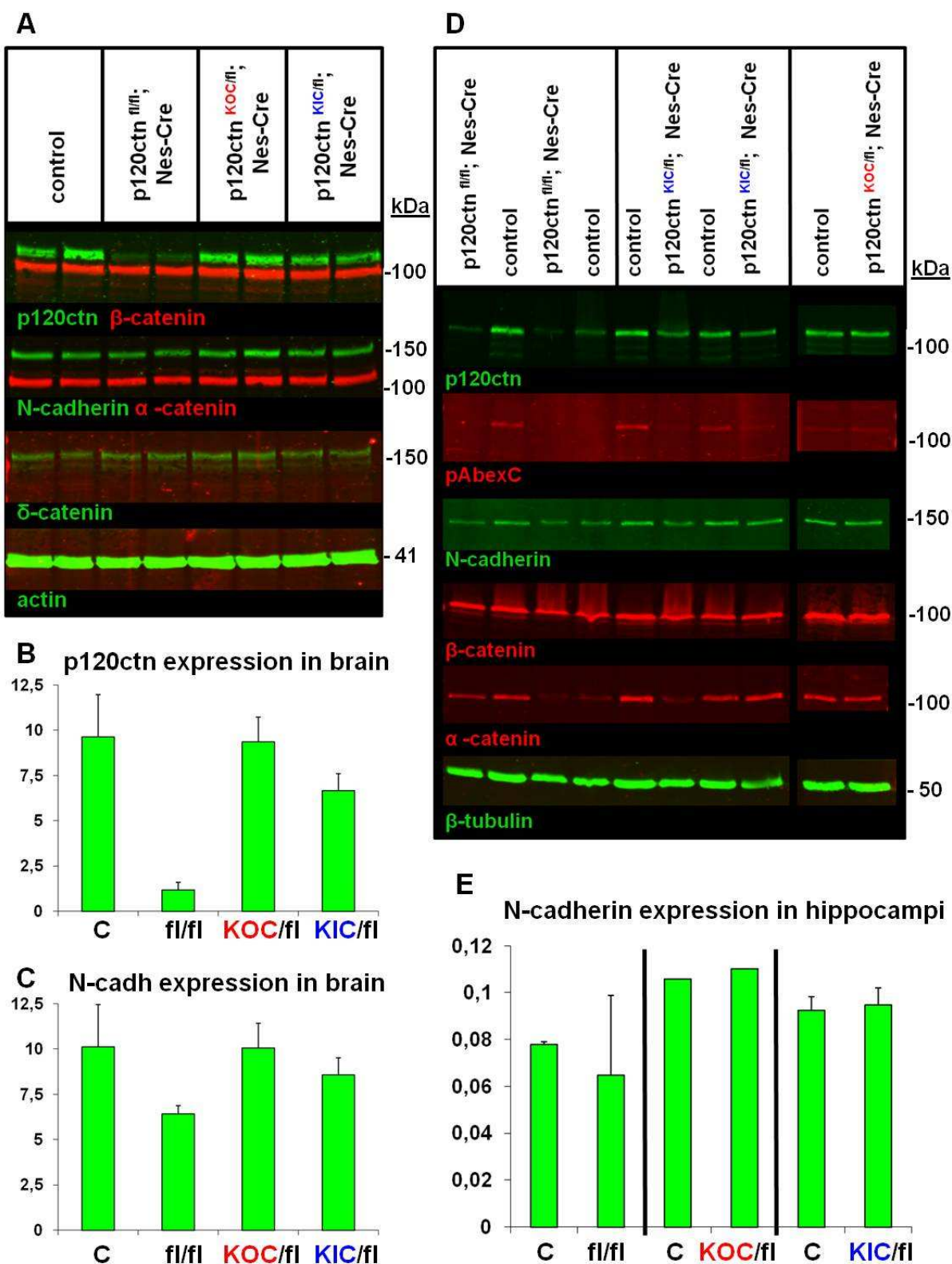


**Figure 12. Cadherin and catenins in p120ctn<sup>KOC/fl</sup>; Nes-Cre and p120ctn<sup>KIC/fl</sup>; Nes-Cre brains.** Immunoblotting with antibodies against cadherins and catenins on lysates of brains (A) and hippocampi (D), which are derived from control (letter C), p120ctn<sup>fl/fl</sup>; Nes-Cre (fl/fl), p120ctn<sup>KOC/fl</sup>; Nes-Cre (KOC/fl) and p120ctn<sup>KIC/fl</sup>; Nes-Cre (KIC/fl) mice. Graphics displaying normalized p120ctn (B) and N-cadherin (C) levels in brain or normalized N-cadherin levels in hippocampi (E).



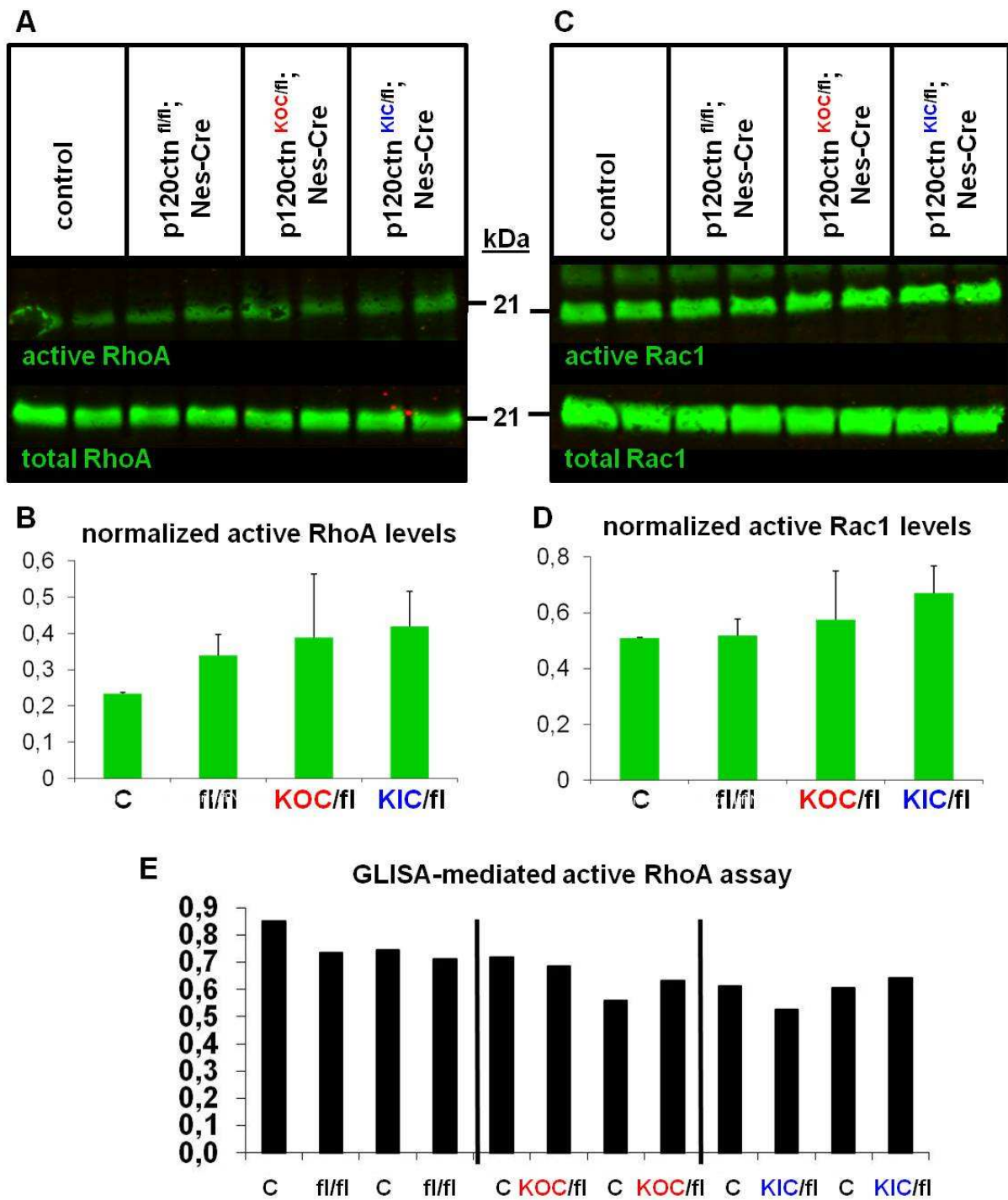


**Figure 13.** RhoGTPase activity in p120ctn<sup>KOC/fl</sup>; Nes-Cre and p120ctn<sup>KIC/fl</sup>; Nes-Cre brains . Affinity purification were performed to capture active RhoA (A) and active Rac1 (C) levels in brain lysates from control (letter C), p120ctn<sup>fl/fl</sup>; Nes-Cre (fl/fl), p120ctn<sup>KOC/fl</sup>; Nes-Cre (KOC/fl) and p120ctn<sup>KIC/fl</sup>; Nes-Cre (KIC/fl) mice. Graphics displaying normalized RhoA (B) and Rac1 (C) activity. RhoA activity in brain lysates was also assayed via GLISA (E).

### Microcephaly in p120ctn<sup>KIC/fl</sup>; Nes-Cre mice

Mice which only express exon C-containing p120ctn transcripts in their brain were generated by combining a brain-specific knockout of all p120ctn isoforms with a constitutive p120ctn KIC allele (Fig. 14A). p120ctn<sup>KIC/fl</sup>; Nes-Cre mice were viable and exhibited microcephaly (Figs. 14B ,C), with up to 35% reduction in brain weight. But this phenotype was not fully penetrant and was observed only in 6 out of 11 p120ctn<sup>KIC/fl</sup>; Nes-Cre mice. Histological analysis revealed that the brains of exon C knockin mice were proportionally smaller than littermate controls, as evidenced by a smaller hippocampus and cerebellum (Fig. 10A). Immunohistochemistry with an p120ctn antibody on sagittal sections from p120ctn<sup>KIC/fl</sup>; Nes-Cre and control brains revealed that normal levels of p120ctn were expressed from the p120ctn KIC allele (Fig. 10B). However, a 30% decrease in p120ctn expression was observed in brain lysates of p120ctn<sup>KIC/fl</sup>; Nes-Cre mice along with a 15% reduction in N-cadherin levels (Figs. 12A-C). Expression of p120ctn was also seen in hippocampal lysates from p120ctn<sup>KIC/fl</sup>; Nes-Cre mice (Figs. 12 D, E). p120ctn isoform 1A, which is predominantly expressed in brain, has been shown to inhibit RhoA activity and to activate Rac1 and Cdc42 (Anastasiadis et al., 2000; Grosheva et al., 2001; Noren et al., 2000). Like p120ctn-deficient brains, brains from p120ctn<sup>KIC/fl</sup>; Nes-Cre should also have elevated RhoA levels and reduced Rac1 activity because the exon C-encoded amino acids interrupt a RhoA binding domain of p120ctn and might interfere with its GDI activity. However, no reproducible increase in RhoA activity was observed in p120ctn<sup>KIC/fl</sup>; Nes-Cre mice compared to controls (Fig. 13). To conclude, p120ctn<sup>KIC/fl</sup>; Nes-Cre brains are smaller and express less p120ctn protein.

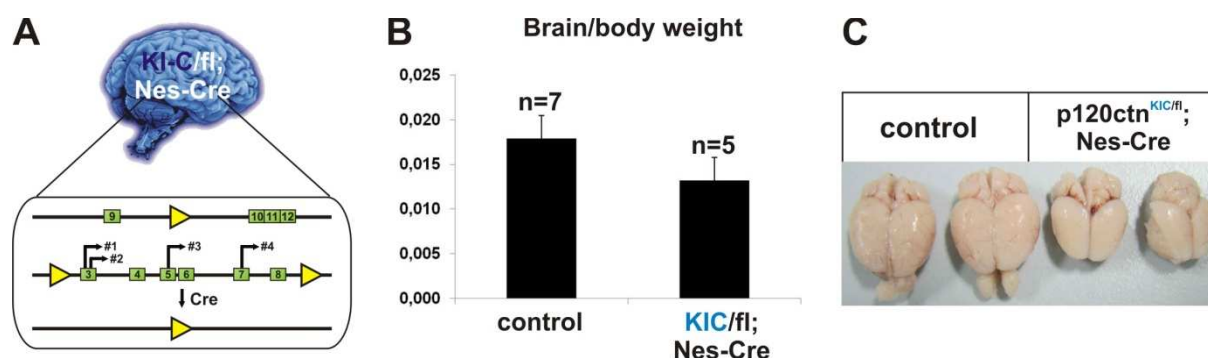


**Figure 14.** p120ctn<sup>KIC/fl</sup>; Nes-Cre mice display microcephaly. (A) Diagram of p120ctn<sup>KIC/fl</sup>; Nes-Cre mice, containing a constitutive knockin of exon C of p120ctn and a brain-specific p120ctn knock out allele. (B) Graphic depicting the brain to body ratio of control and p120ctn<sup>KIC/fl</sup>; Nes-Cre mice. (C) Brains of control and p120ctn<sup>KIC/fl</sup>; Nes-Cre mice.

### p120ctn expression in hippocampal neurons

Next we wanted to determine the morphology of neurons, that were derived from different transgenic mice. Hippocampal neurons, isolated from embryonic rats or mice, have been widely used for a number of reasons (Kaech and Banker, 2006). First, hippocampal neurons can be cultured at low density, allowing the manipulation and visualization of individual neurons. Morphological analysis of neurons with neural tissue is difficult, since the brain is composed of an intricate network of entangled neurons, which can only be visualized by Golgi staining or via complex transgenics. The Golgi silver stain was developed by the Spanish neuroscientist and Nobel laureate Ramón Cajal and stains only limited amount of neurons in their entirety. Complete neuronal circuits can be visualized in Brainbow transgenic mice by Cre/LoxP-based mosaic expression of fluorescent proteins (Livet et al., 2007). However, both approaches do not allow further fluorescence-based marker analysis of individual neurons. Second, the nerve cell population in the hippocampus is relatively simple and consists of mainly pyramidal neurons and a variety of interneurons. Pyramidal neurons develop extensive axonal and dendritic arbors, and form numerous functional synaptic connections *in vitro*. Third, hippocampal cultures are investigated extensively, and the stages of hippocampal development are well-characterized. Fourth, live cultures can be derived from transgenic animals. Expression of cadherins and catenins has been studied in hippocampal neurons (Abe et al., 2004; Benson and Tanaka, 1998).

The expression of p120ctn was analyzed in low-density mouse hippocampal cultures. In rat hippocampal cultures, p120ctn showed a redistribution over time from a global (DIV 2) to a punctuate expression pattern (DIV 7-12), and p120ctn colocalizes partially with N-cadherin and  $\beta$ -catenin (Chauvet et al., 2003). To obtain hippocampal neurons, hippocampi from 16.5 dpc embryos were dissected and cultured in glia conditioned medium. Two-week old cultures developed extensive dendritic and axonal arbors, as evidenced by the expression of markers for axons (Tau1) and dendrites (MAP2) (Fig. 15A). In contrast to rat hippocampal neurons, p120ctn showed a homogeneous expression pattern in mouse hippocampal neurons and colocalized with MAP2 (Fig. 15B). p120ctn also colocalized with  $\alpha$ -catenin in hippocampal neurons, but no punctuate staining for N-cadherin and  $\beta$ -catenin could be observed in dendritic spines as has been reported by Benson et al. (1998) (data not shown). The dendrites of our hippocampal cultures were not extensively decorated with actin-rich spines (Fig. 15C) and this may be due to our technical approach. We used glia-conditioned medium instead of a co-culture with astroglia. The latter has the advantage that supportive

factors are continuously produced *in situ*. These neuronal-specific factors may get exhausted in our glia-conditioned medium and this may hamper dendritic spine development. Therefore we were not able to quantify the number of spines and to analyze spine morphology in detail.

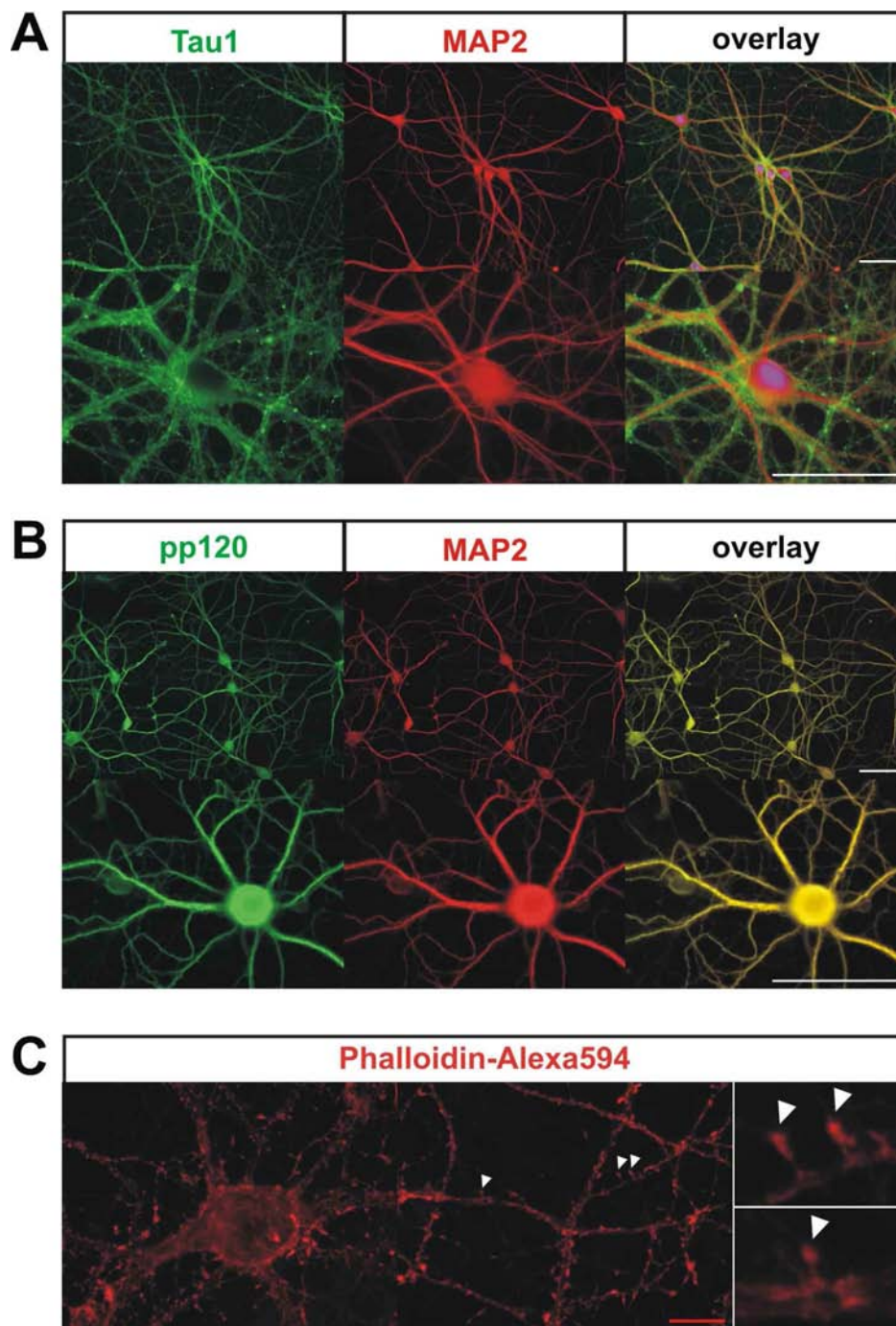


**Figure 15. p12octn immunostaining of wild-type mouse hippocampal neurons.** Two-week-old hippocampal neurons were stained with either an axon-specific marker (Tau1), a dendrite-specific marker (MAP2), an antibody recognizing all p12octn isoforms (pp120) and phalloidin-Alexa 594, which recognizes actin-rich spines (white arrowheads). Enlargements of individual spine are depicted (C, right). White scale bar: 25  $\mu$ m, red scale bar: 5  $\mu$ m.

**Fasciculation in p120ctn<sup>KIC/fl</sup>; Nes-Cre hippocampal neurons**

We wanted to isolate and culture primary hippocampal neurons from p120ctn<sup>KOC/fl</sup>; Nes-Cre and p120ctn<sup>KIC/fl</sup>; Nes-Cre brains to gain insight in their morphology. We failed to generate hippocampal cultures from p120ctn<sup>KOC/fl</sup>; Nes-Cre hippocampi and this might be because only 5% of the offspring were identified as p120ctn<sup>KOC/fl</sup>; Nes-Cre mice instead of the 25% which is expected theoretically (Tables 4, 6). To rule out that p120ctn<sup>KOC/fl</sup>; Nes-Cre embryos die during development, time matings were performed (Table 6). The Nestin-Cre transgene is activated early in development and Cre-expression has been reported from 9.5 dpc on (Haigh et al., 2003). No p120ctn<sup>KOC/fl</sup>; Nes-Cre embryos were identified at 12.5 and 9.5 dpc (Table 6), but no signs of resorption were found in five litters with an average of 10 embryos per litter. In addition, p120ctn KOC/- mice (bearing a constitutive knockout of all p120ctn isoforms combined with a constitutive knockout of exon C of p120ctn) are viable (see chapter 3), indicating that p120ctn<sup>KOC/fl</sup>; Nes-Cre mice should be viable as well. Currently we do not know what causes the non-Mendelian birth rate of p120ctn<sup>KOC/fl</sup>; Nes-Cre mice. One possibility is a Cre-mediated translocation between the p120ctn KOC allele and the floxed p120ctn allele, which both contain at least one loxP site.

**Table 6. genotyping hippocampal neurons en embryos**

Genotyping offspring from ♀ p120ctn <sup>KOC/+</sup> ; Nes-Cre x ♂ p120ctn <sup>fl/fl</sup> mating						
stage	KOC/fl; Nes-Cre (25%)	KOC/fl (25%)	fl/+; Nes-Cre (25%)	fl/+ (25%)	total	recombination
hippocampal culture (n=3)	1 (3,3%)	12 (40 %)	10 (33,3%)	7 (23,3%)	31	
16,5dpc		0/8	0/9	0/2	0/19	tail
		0/8	9/9		9/19	brain
13,5 dpc	0 (0,0%)	5 (50,0%)	4 (40,0%)	1 (10,0%)	10	
		0/5	0/4	0/1	0/10	yolk sac
9,5 dpc	0 (0,0%)	2 (28,5%)	3 (43,9%)	2 (28,5%)	7	
		0/2	0/3	0/2	0/7	yolk sac
Genotyping offspring from ♀ p120ctn <sup>KIC/+</sup> Nes-Cre x ♂ p120ctn <sup>fl/fl</sup> mating						
stage	KIC/fl; Nes-Cre (25%)	KIC/fl (25%)	fl/+; Nes-Cre (25%)	fl/+ (25%)	total	recombination
hippocampal culture (n=4)	11 (26,2%)	10 (23,8%)	9 (21,4%)	12 (28,6%)	21	
16,5dpc	0/5	0/4	0/6	0/7	0/9	tail
	5/5	0/4	6/6	7/7	6/9	brain

p120ctn<sup>KIC/fl</sup>; Nes-Cre mice are born according to the rules of Mendelian inheritance (Tables 5, 6). Neuronal cultures from p120ctn<sup>KIC/fl</sup>; Nes-Cre hippocampi showed signs of fasciculation after seven days of culture and this persisted till the third week of culture (Fig. 16). Fasciculation is a process in which ‘pioneering’ neurons extend their axons and axons from later differentiating ‘follower’ neurons migrate along the first axon, forming big mature axon bundles. Staining these cultures with a  $\beta$ III-tubulin marker, which detects both axons and dendrites, displayed thick bundles of neuronal protrusions and a less elaborate neuronal network in p120ctn<sup>KIC/fl</sup>; Nes-Cre cultures (Fig. 16). The fasciculation was apparent throughout the entire culture of p120ctn<sup>KIC/fl</sup>; Nes-Cre neurons but could also be detected sporadically in control cultures (data not shown). In a follow up experiment the fasciculation could be confirmed in p120ctn<sup>KIC/fl</sup>; Nes-Cre cultures, however, the fasciculation was less homogenous than in the first experiment and signs of fasciculation were also evident in small areas of control neuronal cultures (Fig. 17).

What causes fasciculation in p120ctn<sup>KIC/fl</sup>; Nes-Cre hippocampal cultures? Expression of amino acids encoded by the alternatively spliced exon C of p120ctn abrogates dendritic branching *in vitro* (Pieters et al., in preparation). Likewise, the exon C-encoded amino acids in p120ctn<sup>KIC/fl</sup>; Nes-Cre hippocampal neurons could reduce neuronal branches and might explain the reduced complexity of neuronal networks, which might stimulate fasciculation. Neuronal cell adhesion molecule (NCAM) is essential for fasciculation and pathfinding of axons of hippocampal neurons (Cremer et al., 1997) and might be upregulated in p120ctn<sup>KIC/fl</sup>; cultures. Fasciculation was also observed in hippocampal cultures upon Rac1 activation (Leemhuis et al., 2004). Interestingly, inhibition of ROCK, a downstream effector of RhoA also induces Rac1 activation and neurite clustering (Leemhuis et al., 2004). Rac1 activation leads to RhoA inhibition via the ‘Bar-Sagi’ pathway, (Nimnual et al., 2003; Sander et al., 1999), but in hippocampal neurons inhibition of a downstream RhoA effector seems to cause Rac1 activation via an unknown pathway. To analyze whether the fasciculation in p120ctn<sup>KIC/fl</sup>; Nes-Cre is the result of increased Rac1 activity, we performed affinity precipitations to measure Rac1 activity in brain lysates from control and p120ctn<sup>KIC/fl</sup>; Nes-Cre mice. But only a small (1.3 fold) increase in Rac1 activity was observed in p120ctn<sup>KIC/fl</sup>; Nes-Cre mice compared to controls (Figs. 13C, D).



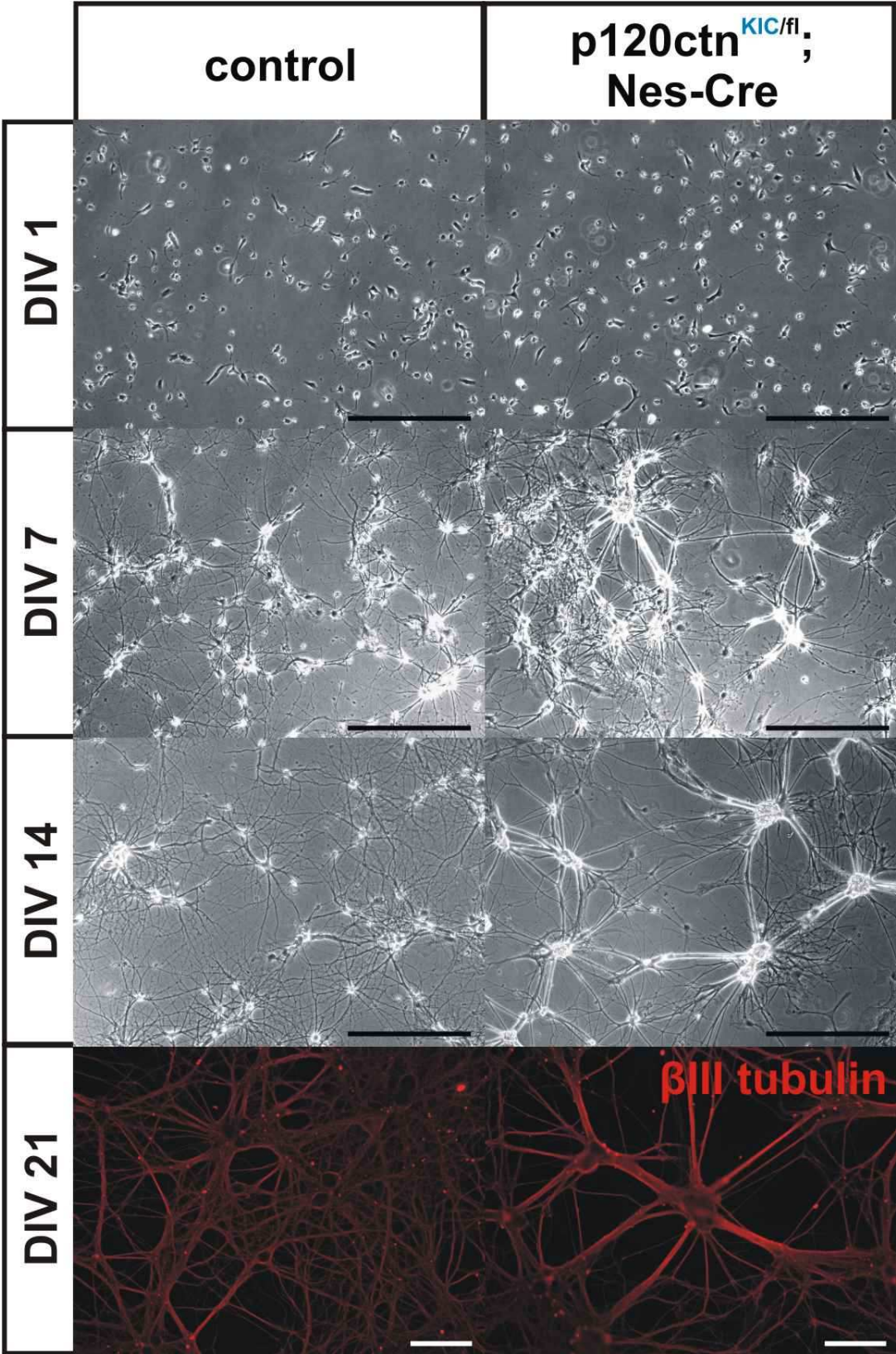


**Figure 16. Fasciculation in p120ctn<sup>KIC/fl</sup>; Nes-Cre hippocampal cultures.** Morphology of control and p120ctn<sup>KIC/fl</sup>; Nes-Cre hippocampal neurons at day *in vitro* (DIV) 1, 7 and 14. Three-week old hippocampal cultures were stained with a neuron marker,  $\beta$ III tubulin. Black scale bar: 50  $\mu$ m, white scale bar: 25  $\mu$ m.

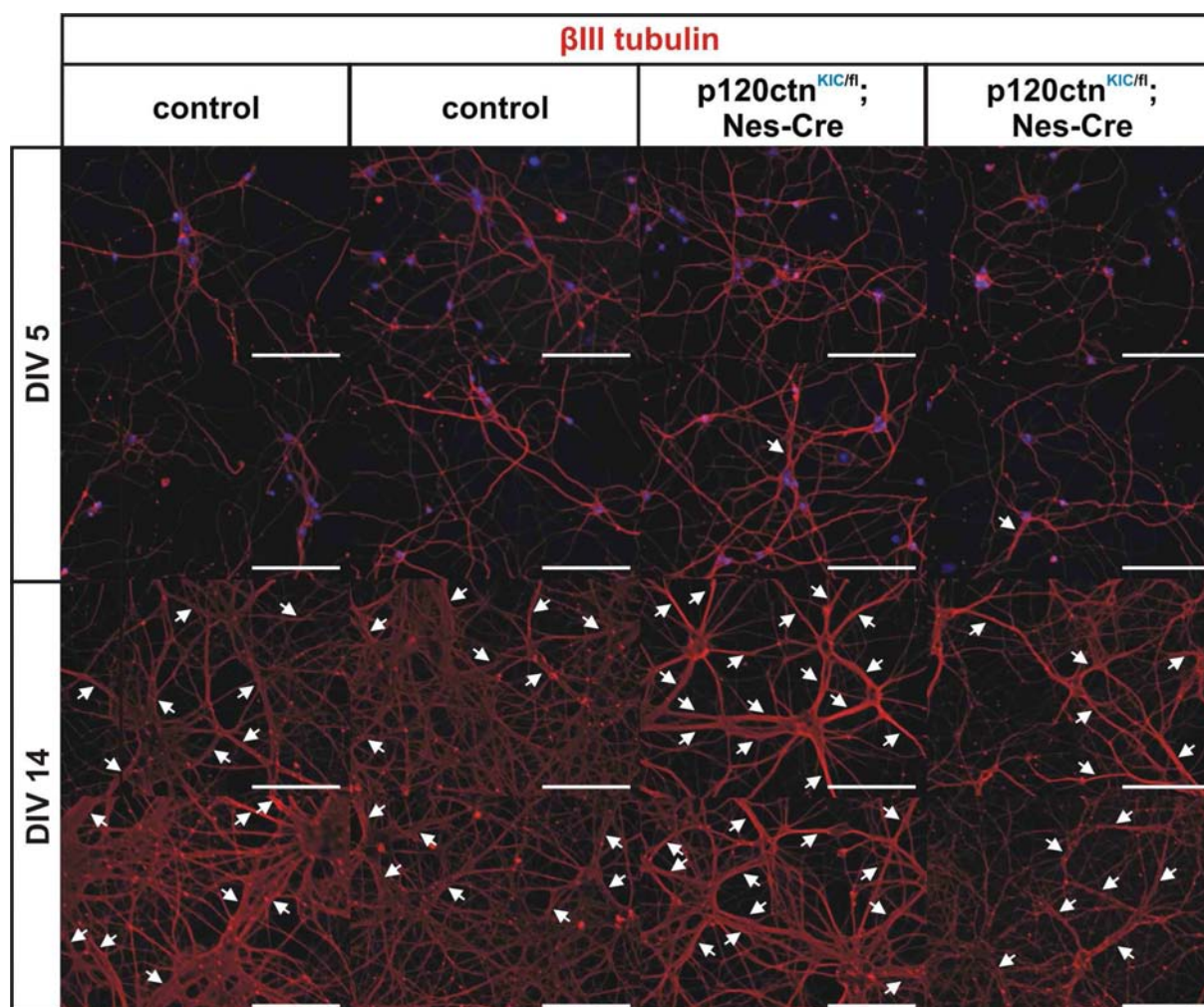


**Figure 17. Fasciculation in p120ctn<sup>KIC/fl</sup>; Nes-Cre hippocampal cultures.** Immunostaining of control and p120ctn<sup>KIC/fl</sup>; Nes-Cre hippocampal neurons at day *in vitro* (DIV) 5 and 14 with a neuron marker,  $\beta$ III tubulin. Arrows point to neurite bundles. Scale bar: 50  $\mu$ m.

### Transfection of transgenic hippocampal cultures

To visualize the morphology of neurons from p120ctn<sup>KIC/fl</sup>; Nes-Cre mice, hippocampal cultures were transfected with an EGFP plasmid. Transfection of hippocampal cultures is very inefficient (less than 1%) because neurons do no longer divide. In addition, hippocampal cultures are very sensitive and their viability may be affected by several manipulations. In a first step we tried to optimize the transfection procedure for hippocampal cultures. We tried using different transfection agents, such as Lipofectamine 2000, which did not affect their viability but only resulted in very few GFP-positive glial cells, but never in branched GFP-positive neurons (data not shown). An Effectene transfection protocol adapted with neuronal-specific conditions resulted in few GFP-positive neurons with elaborate neuronal protrusions (Fig. 18A). To optimize the time point of transfection, wild-type



## p120ctn KOC and KIC in the brain

neuronal cultures were transfected after two, four or eleven days *in vitro* (DIV). Transfections at early time points (DIV 2 or 4) resulted in an high initial transfection efficiency, but after two to three weeks of culture only small GFP-positive arbors were identified along with very weak GFP-positive neurons and remnants of dead neurons (Fig.18B). Transfection of older (DIV 11) hippocampal cultures is less efficient, however, GFP-positive neurons with extensive arbors could still be identified (Fig. 18B). So although the transfection efficiency drops in older cultures, transfection at later time points remains the best option to visualize the morphology of cultured hippocampal neurons.

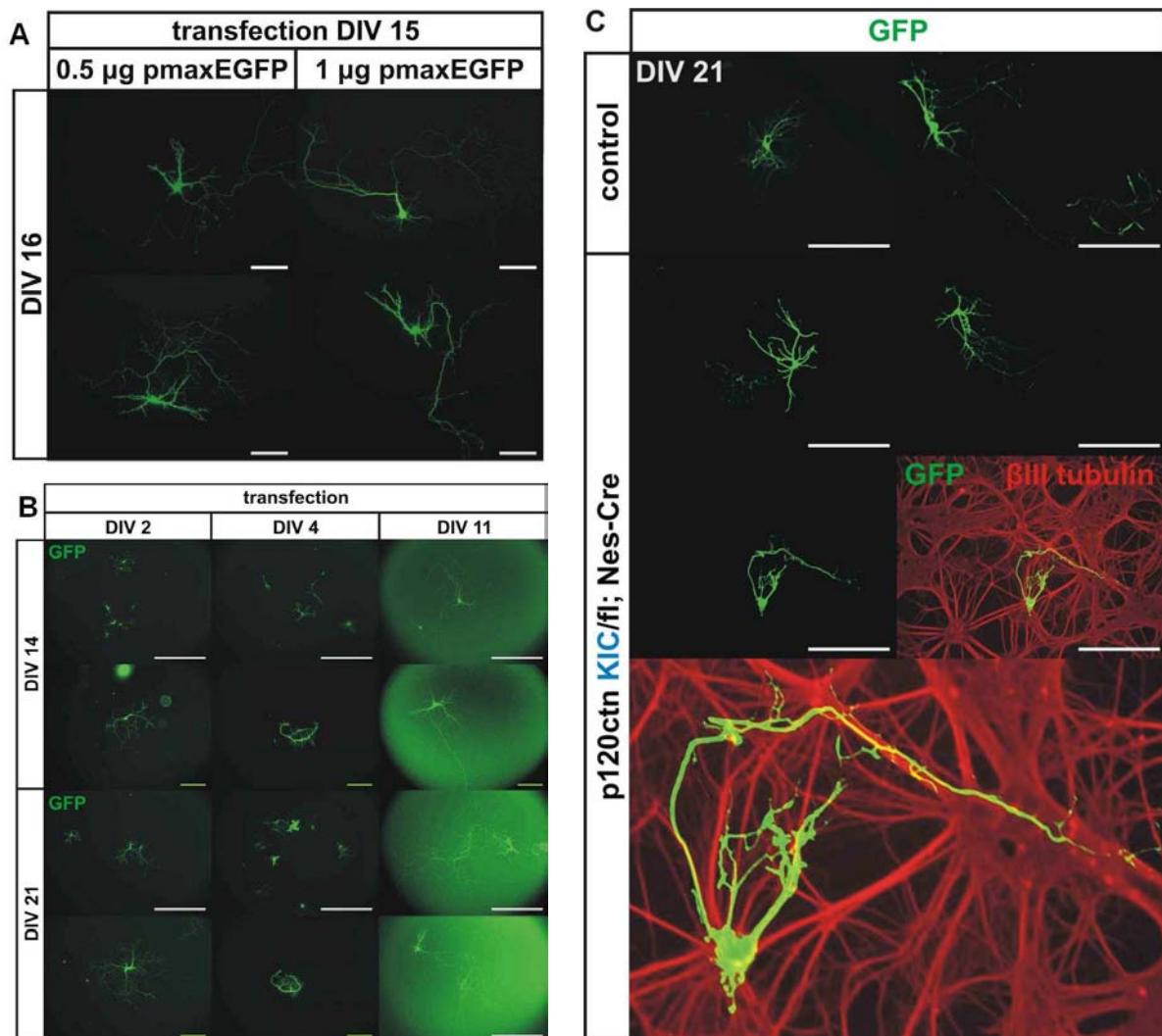


**Figure 18. Transfection procedure for hippocampal neurons.** (A) Primary hippocampal neurons were transfected with 0,5 or 1 µg vector at day *in vitro* (DIV) 15 and pictures were taken at DIV16. Scale bar: 25 µm (B) Hippocampal neurons were transfected at day *in vitro* (DIV) 2, 4 and 11 and pictures were taken at DIV 14 and 21. White scale bar: 100 µm, green scale bar: 25 µm. (C) Morphology of p120ctn<sup>KIC/fi</sup>; Nes-Cre cultures. Primary hippocampal neurons from control and p120ctn<sup>KIC/fi</sup>; were transfected at day *in vitro* (DIV) 15 and pictures from GFP-positive neurons were taken at DIV 21. Hippocampal cultures were stained with a neuronal marker, βIII tubulin. Scale bar: 100 µm.

In a next step we tried to compare the morphology of hippocampal neurons from control and p120ctn<sup>KIC/fl</sup>; Nes-Cre mice. Only few GFP-positive arbors could be identified for each setup and no obvious differences were seen in GFP-positive neurons from control and p120ctn<sup>KIC/fl</sup>; Nes-Cre mice (Fig. 18C). Staining of p120ctn<sup>KIC/fl</sup>; Nes-Cre cultures with a neuronal marker ( $\beta$ III tubulin) revealed that only one GFP-positive neuron was located in a region with a high degree of fasciculation. This neuron did not contain elaborate neuronal protrusions and its axon fasciculated along a cluster of axons (Fig. 18C). However, we need more GFP-positive neurons, which can be analyzed via automated tracing software (Meijering et al., 2004; Popko et al., 2009) in order to get more objective data on the number and length of primary, secondary and tertiary neurites.

As an alternative strategy we wanted to analyze the morphology of wild-type hippocampal cultures that have been transfected with different p120ctn isoforms. p120ctn isoform 3AC, expressing of the exon C-encoded amino acids, blocks cellular branching in several cell lines (Pieters et al., in preparation) and we wanted to investigate whether a p120ctn 3AC-GFP fusion would also inhibit neuronal complexity in hippocampal cultures. However after transfection of hippocampal cultures with constructs expressing either p120ctn 3A-GFP or p120ctn 3AC-GFP we could detect only GFP-positive remnants of dead neurons, indicating that p120ctn overexpression causes cytotoxicity in hippocampal neurons.

### **Immunohistochemistry with pAbexC on brain sections**

p120ctn-deficient brain provide a good tool to characterize our p120ctn isoform C-specific antibody (pAbexC). To analyze if this antibody can detect endogenous p120ctn isoforms containing the exon C-encoded amino acids, we performed immunohistochemistry on brain sections of control and p120ctn<sup>fl/fl</sup>; Nes-Cre mice (Fig. 19A). Staining control brain with pAbexC reveals that p120ctn isoform C is expressed in the cortex and in all layers of the cerebellum. However, in p120ctn-deficient brain sections some aspecific staining remains in the cortex, and in the granular layer and in purkinje cells from the cerebellum. Similar amounts of aspecific staining were also observed in brain sections from p120ctn<sup>KOC/fl</sup>; Nes-Cre and p120ctn<sup>KIC/fl</sup>; Nes-Cre mice, for one would expect pAbexC staining to be negative and highly positive, respectively (Fig. 19B). Probably our polyclonal pAbexC antibody recognizes other proteins, making the antibody unsuitable for detecting endogenous p120ctn isoforms containing the exon C-encoded amino acids via immunohistochemistry.

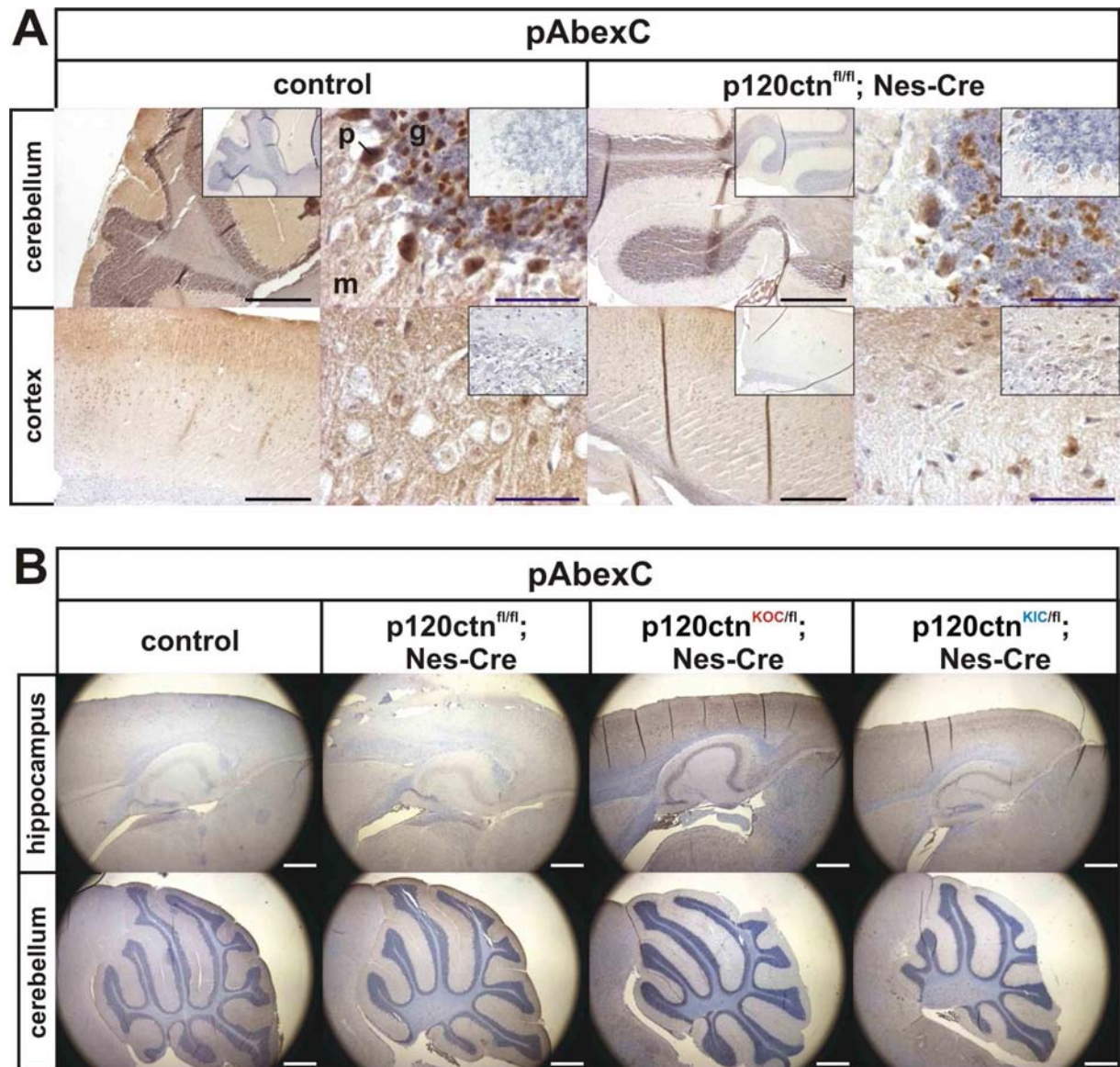


**Figure 19. Characterizing the pAbexC antibody in of p120ctn<sup>fl/fl</sup>; Nes-Cre cultures. (A)** Immunohistochemistry with the pAbexC antibody on sagittal brain sections form control and p120ctn<sup>fl/fl</sup>; Nes-Cre mice. Tissue section were counterstained with hematoxylin and eosin. The exon C-encoded amino acids are expressed in the molecular layer (m), granular layer (g) and purkinje cells (p) from control brain. **(B)** Immunohistochemistry with the pAbexC antibody on sagittal brain sections form control, p120ctn<sup>fl/fl</sup>; Nes-Cre, p120ctn<sup>KOC/fl</sup>; Nes-Cre and p120ctn<sup>KIC/fl</sup>; Nes-Cre mice. Black and white scale bar: 400  $\mu$ m, purple scale bar: 50  $\mu$ m.

## CONCLUSION

We showed that the alternatively spliced exon C of p120ctn is highly expressed in mouse brain. We also showed that mice with p120ctn-deficient brains (p120ctn fl/fl; Nes-Cre) are viable and have phenotypes similar to those of dorsal-forebrain specific p120ctn knockout (p120ctn fl/fl; Emx1-Cre) mice, including a small decrease in N-cadherin levels and increased RhoA activity (Elia et al., 2006). But no Rac1 activation could be observed in brains from our p120ctn fl/fl; Nes-Cre mice. Measuring RhoGTPase activity in mouse tissues is not straight forward, due to fast hydrolysis of GTP-bound RhoGTPase and contamination of blood and non-recombined cell types. In addition, premature recombination in mice expressing the Nes-Cre transgene and one or two floxed p120ctn alleles, can cause variable loss of p120ctn in these mice. This implicates that control mice are not really genetically ‘clean’. The abovementioned reason might explain why no reproducible changes in RhoGTPase activity could be detected in p120ctn<sup>KOC/fl</sup>; Nes-Cre and p120ctn<sup>KIC/fl</sup>; Nes-Cre. Perhaps p120ctn<sup>KOC/-</sup> and p120ctn<sup>KIC/-</sup> might be a better alternative to study the affect of the p120ctn KOC and KIC alleles *in vivo*. Nevertheless, mice with exclusive expression of p120ctn transcripts without the alternatively spliced exon C in the brain, exhibited discrete abnormalities in their hippocampi. On the other hand, forced expression of exon C in the brain resulted in microcephaly and in fasciculation.

## ACKNOWLEDGEMENTS

This work was supported by grants from the Queen Elisabeth Medical Foundation (G.S.K.E.), Belgium, and from the Geconcerteerde Onderzoeksacties of Ghent University. Tim Pieters has been supported by the Instituut voor de Aanmoediging van Innovatie door Wetenschap en Technologie in Vlaanderen (IWT). Tim Pieters conducted all experiments and wrote this manuscript. Dissection of hippocampi and culturing of hippocampal neurons was performed in the laboratory of Prof. Dr. Ampe and Dr. Anja Lambrechts. Dr. Anja Lambrechts provided reagents, training and was helpful with the experimental design. We thank Karima Bakkali for technical assistance. MRI analysis was done in the laboratory of Prof. Dr. Annemie Van der Linden. Prof. Dr. Frans Van Roy and Dr. Jolanda van Hengel were instructive in the experimental design and editing of the manuscript. We acknowledge Dr. Amin Bredan for critical reading of the manuscript, and the members of our research group for valuable discussions.

## REFERENCES

- Abe, K., O. Chisaka, F. Van Roy, and M. Takeichi. 2004. Stability of dendritic spines and synaptic contacts is controlled by alpha N-catenin. *Nat Neurosci.* 7:357-63.
- Abu-Elneel, K., T. Ochiishi, M. Medina, M. Remedi, L. Gastaldi, A. Caceres, and K.S. Kosik. 2008. A delta-catenin signaling pathway leading to dendritic protrusions. *J Biol Chem.* 283:32781-91.
- Anastasiadis, P.Z. 2007. p120-ctn: A nexus for contextual signaling via Rho GTPases. *Biochim Biophys Acta.* 1773:34-46.
- Anastasiadis, P.Z., S.Y. Moon, M.A. Thoreson, D.J. Mariner, H.C. Crawford, Y. Zheng, and A.B. Reynolds. 2000. Inhibition of RhoA by p120 catenin. *Nat Cell Biol.* 2:637-44.
- Arikkath, J., I. Israely, Y. Tao, L. Mei, X. Liu, and L.F. Reichardt. 2008. Erbin controls dendritic morphogenesis by regulating localization of delta-catenin. *J Neurosci.* 28:7047-56.
- Bamji, S.X., K. Shimazu, N. Kimes, J. Huelsken, W. Birchmeier, B. Lu, and L.F. Reichardt. 2003. Role of beta-catenin in synaptic vesicle localization and presynaptic assembly. *Neuron.* 40:719-31.
- Benson, D.L., and H. Tanaka. 1998. N-cadherin redistribution during synaptogenesis in hippocampal neurons. *J Neurosci.* 18:6892-904.
- Bozdagi, O., M. Valcin, K. Poskanzer, H. Tanaka, and D.L. Benson. 2004. Temporally distinct demands for classic cadherins in synapse formation and maturation. *Mol Cell Neurosci.* 27:509-21.
- Chauvet, N., M. Prieto, C. Fabre, N.K. Noren, and A. Privat. 2003. Distribution of p120 catenin during rat brain development: potential role in regulation of cadherin-mediated adhesion and actin cytoskeleton organization. *Mol Cell Neurosci.* 22:467-86.
- Cohen-Cory, S. 2002. The developing synapse: construction and modulation of synaptic structures and circuits. *Science.* 298:770-6.
- Cremer, H., G. Chazal, C. Goridis, and A. Represa. 1997. NCAM is essential for axonal growth and fasciculation in the hippocampus. *Mol Cell Neurosci.* 8:323-35.
- Daniel, J.M. 2007. Dancing in and out of the nucleus: p120(ctn) and the transcription factor Kaiso. *Biochim Biophys Acta.* 1773:59-68.
- Davis, M.A., R.C. Ireton, and A.B. Reynolds. 2003. A core function for p120-catenin in cadherin turnover. *J Cell Biol.* 163:525-34.
- Davis, M.A., and A.B. Reynolds. 2006. Blocked acinar development, E-cadherin reduction, and intraepithelial neoplasia upon ablation of p120-catenin in the mouse salivary gland. *Dev Cell.* 10:21-31.
- Elia, L.P., M. Yamamoto, K. Zang, and L.F. Reichardt. 2006. p120 catenin regulates dendritic spine and synapse development through Rho-family GTPases and cadherins. *Neuron.* 51:43-56.
- Elste, A.M., and D.L. Benson. 2006. Structural basis for developmentally regulated changes in cadherin function at synapses. *J Comp Neurol.* 495:324-35.
- Fannon, A.M., and D.R. Colman. 1996. A model for central synaptic junctional complex formation based on the differential adhesive specificities of the cadherins. *Neuron.* 17:423-34.
- Gorski, J.A., T. Talley, M. Qiu, L. Puelles, J.L. Rubenstein, and K.R. Jones. 2002. Cortical excitatory neurons and glia, but not GABAergic neurons, are produced in the Emx1-expressing lineage. *J Neurosci.* 22:6309-14.
- Govek, E.E., S.E. Newey, and L. Van Aelst. 2005. The role of the Rho GTPases in neuronal development. *Genes Dev.* 19:1-49.

- Grosheva, I., M. Shtutman, M. Elbaum, and A.D. Bershadsky. 2001. p120 catenin affects cell motility via modulation of activity of Rho-family GTPases: a link between cell-cell contact formation and regulation of cell locomotion. *J Cell Sci.* 114:695-707.
- Haigh, J.J., P.I. Morelli, H. Gerhardt, K. Haigh, J. Tsien, A. Damert, L. Miquerol, U. Muhlner, R. Klein, N. Ferrara, E.F. Wagner, C. Betsholtz, and A. Nagy. 2003. Cortical and retinal defects caused by dosage-dependent reductions in VEGF-A paracrine signaling. *Dev Biol.* 262:225-41.
- Inoue, A., and J.R. Sanes. 1997. Lamina-specific connectivity in the brain: regulation by N-cadherin, neurotrophins, and glycoconjugates. *Science.* 276:1428-31.
- Israely, I., R.M. Costa, C.W. Xie, A.J. Silva, K.S. Kosik, and X. Liu. 2004. Deletion of the neuron-specific protein delta-catenin leads to severe cognitive and synaptic dysfunction. *Curr Biol.* 14:1657-63.
- Iwai, Y., Y. Hirota, K. Ozaki, H. Okano, M. Takeichi, and T. Uemura. 2002. DN-cadherin is required for spatial arrangement of nerve terminals and ultrastructural organization of synapses. *Mol Cell Neurosci.* 19:375-88.
- Kaech, S., and G. Banker. 2006. Culturing hippocampal neurons. *Nat Protoc.* 1:2406-15.
- Keirsebilck, A., S. Bonne, K. Staes, J. van Hengel, F. Nollet, A. Reynolds, and F. van Roy. 1998. Molecular cloning of the human p120ctn catenin gene (CTNND1): expression of multiple alternatively spliced isoforms. *Genomics.* 50:129-46.
- Kim, H., J.R. Han, J. Park, M. Oh, S.E. James, S. Chang, Q. Lu, K.Y. Lee, H. Ki, W.J. Song, and K. Kim. 2008a. Delta-catenin-induced dendritic morphogenesis. An essential role of p190RhoGEF interaction through Akt1-mediated phosphorylation. *J Biol Chem.* 283:977-87.
- Kim, H., M. Oh, Q. Lu, and K. Kim. 2008b. E-Cadherin negatively modulates delta-catenin-induced morphological changes and RhoA activity reduction by competing with p190RhoGEF for delta-catenin. *Biochem Biophys Res Commun.* 377:636-41.
- Kim, K., A. Sirota, Y.H. Chen Yh, S.B. Jones, R. Dudek, G.W. Lanford, C. Thakore, and Q. Lu. 2002. Dendrite-like process formation and cytoskeletal remodeling regulated by delta-catenin expression. *Exp Cell Res.* 275:171-84.
- Kosik, K.S., C.P. Donahue, I. Israely, X. Liu, and T. Ochiishi. 2005. Delta-catenin at the synaptic-adherens junction. *Trends Cell Biol.* 15:172-8.
- Kowalczyk, A.P., and A.B. Reynolds. 2004. Protecting your tail: regulation of cadherin degradation by p120-catenin. *Curr Opin Cell Biol.* 16:522-7.
- Laemmli, U.K. 1970. Cleavage of structural proteins during the assembly of the head of bacteriophage T4. *Nature.* 227:680-5.
- Lallemand, Y., V. Luria, R. Haffner-Krausz, and P. Lonai. 1998. Maternally expressed PGK-Cre transgene as a tool for early and uniform activation of the Cre site-specific recombinase. *Transgenic Res.* 7:105-12.
- Leemhuis, J., U. Mayer, H. Barth, G. Schmidt, and D.K. Meyer. 2004. The small GTPase Rac is involved in clustering of hippocampal neurons and fasciculation of their neurites. *Naunyn Schmiedebergs Arch Pharmacol.* 370:211-22.
- Livet, J., T.A. Weissman, H. Kang, R.W. Draft, J. Lu, R.A. Bennis, J.R. Sanes, and J.W. Lichtman. 2007. Transgenic strategies for combinatorial expression of fluorescent proteins in the nervous system. *Nature.* 450:56-62.
- Lu, Q., M. Paredes, M. Medina, J. Zhou, R. Cavallo, M. Peifer, L. Orecchio, and K.S. Kosik. 1999. delta-catenin, an adhesive junction-associated protein which promotes cell scattering. *J Cell Biol.* 144:519-32.
- Martinez, M.C., T. Ochiishi, M. Majewski, and K.S. Kosik. 2003. Dual regulation of neuronal morphogenesis by a delta-catenin-cortactin complex and Rho. *J Cell Biol.* 162:99-111.



- McCrea, P.D., and J.I. Park. 2007. Developmental functions of the P120-catenin sub-family. *Biochim Biophys Acta*. 1773:17-33.
- Meijering, E., M. Jacob, J.C. Sarria, P. Steiner, H. Hirling, and M. Unser. 2004. Design and validation of a tool for neurite tracing and analysis in fluorescence microscopy images. *Cytometry A*. 58:167-76.
- Newey, S.E., V. Velamoor, E.E. Govek, and L. Van Aelst. 2005. Rho GTPases, dendritic structure, and mental retardation. *J Neurobiol*. 64:58-74.
- Nimnual, A.S., L.J. Taylor, and D. Bar-Sagi. 2003. Redox-dependent downregulation of Rho by Rac. *Nat Cell Biol*. 5:236-41.
- Noren, N.K., B.P. Liu, K. Burrige, and B. Kreft. 2000. p120 catenin regulates the actin cytoskeleton via Rho family GTPases. *J Cell Biol*. 150:567-80.
- Perez-Moreno, M., M.A. Davis, E. Wong, H.A. Pasolli, A.B. Reynolds, and E. Fuchs. 2006. p120-catenin mediates inflammatory responses in the skin. *Cell*. 124:631-44.
- Pieters, T., P. D'Hooge, P. Hulpiau, M.P. Stemmler, F. Van Roy, and J. Van Hengel. in preparation. p120ctn isoform C knockout and knockin mice rescue E-cadherin loss and embryonic lethality in p120ctn-deficient embryos.
- Popko, J., A. Fernandes, D. Brites, and L.M. Lanier. 2009. Automated analysis of NeuronJ tracing data. *Cytometry A*. 75:371-6.
- Ren, X.D., W.B. Kiosses, and M.A. Schwartz. 1999. Regulation of the small GTP-binding protein Rho by cell adhesion and the cytoskeleton. *Embo J*. 18:578-85.
- Reynolds, A.B., J.M. Daniel, Y.Y. Mo, J. Wu, and Z. Zhang. 1996. The novel catenin p120cas binds classical cadherins and induces an unusual morphological phenotype in NIH3T3 fibroblasts. *Exp Cell Res*. 225:328-37.
- Rubio, M.E., C. Curcio, N. Chauvet, and J.L. Bruses. 2005. Assembly of the N-cadherin complex during synapse formation involves uncoupling of p120-catenin and association with presenilin 1. *Mol Cell Neurosci*. 30:118-30.
- Sander, E.E., J.P. ten Klooster, S. van Delft, R.A. van der Kammen, and J.G. Collard. 1999. Rac downregulates Rho activity: reciprocal balance between both GTPases determines cellular morphology and migratory behavior. *J Cell Biol*. 147:1009-22.
- Smalley-Freed, W.G., A. Efimov, P.E. Burnett, S.P. Short, M.A. Davis, D.L. Gumucio, M.K. Washington, R.J. Coffey, and A.B. Reynolds. 2010. p120-catenin is essential for maintenance of barrier function and intestinal homeostasis in mice. *J Clin Invest*. 120:1824-35.
- Togashi, H., K. Abe, A. Mizoguchi, K. Takaoka, O. Chisaka, and M. Takeichi. 2002. Cadherin regulates dendritic spine morphogenesis. *Neuron*. 35:77-89.
- Tronche, F., C. Kellendonk, O. Kretz, P. Gass, K. Anlag, P.C. Orban, R. Bock, R. Klein, and G. Schutz. 1999. Disruption of the glucocorticoid receptor gene in the nervous system results in reduced anxiety. *Nat Genet*. 23:99-103.
- Uchida, N., Y. Honjo, K.R. Johnson, M.J. Wheelock, and M. Takeichi. 1996. The catenin/cadherin adhesion system is localized in synaptic junctions bordering transmitter release zones. *J Cell Biol*. 135:767-79.
- Xiao, K., D.F. Allison, K.M. Buckley, M.D. Kottke, P.A. Vincent, V. Faundez, and A.P. Kowalczyk. 2003. Cellular levels of p120 catenin function as a set point for cadherin expression levels in microvascular endothelial cells. *J Cell Biol*. 163:535-45.
- Xiao, K., R.G. Oas, C.M. Chiasson, and A.P. Kowalczyk. 2007. Role of p120-catenin in cadherin trafficking. *Biochim Biophys Acta*. 1773:8-16.
- Yanagisawa, M., and P.Z. Anastasiadis. 2006. p120 catenin is essential for mesenchymal cadherin-mediated regulation of cell motility and invasiveness. *J Cell Biol*. 174:1087-96.

# **General discussion and perspectives**

---



**TABLE OF CONTENTS**

INTRODUCTION..... 279  
*IN VITRO* ANALYSIS ..... 279  
     Effects on nuclear translocation ..... 279  
     Effects on RhoGTPase activity ..... 280  
*IN VIVO* ANALYSIS ..... 281  
     p120ctn KOC and KIC mice: ‘C’ stands for conserved intronic sequence..... 281  
     Effects on RhoGTPase activity ..... 284  
 REFERENCES..... 287

**INTRODUCTION**

In my PhD research I analyzed the function of the alternatively spliced exon C of p120ctn *in vitro* and *in vivo*. Due to extensive splicing, up to 48 possible human p120ctn isoforms can be generated: in that way up to four different start codons (M1-M4) can be used as well as four alternatively used internal exons (A-D) (Keirsebilck et al., 1998). Alternatively used exon C of p120ctn encodes 6 AA situated in the large insert loop between repeats ARM5 and ARM6 of the central armadillo repeat domain (Choi and Weis, 2005; Ishiyama et al., 2010). The AA sequence encoded by exon-C interrupts a nuclear localization signal (NLS), which coincides with a RhoA-binding domain.

***IN VITRO* ANALYSIS**

**Effects on nuclear translocation**

First, I will discuss the analysis of p120ctn isoform C *in vitro*. Expression of plasmids encoding exon-C blocked nuclear translocation and ‘dendritic branching’ *in vitro*. The interruption of this NLS by the AA sequence encoded by exon-C could either block this NLS or create a bi-partite NLS. I tested the functionality of the isolated NLS with or without the interspersed AA encoded by exon-C and found that inclusion of these 6 AA blocked its nuclear localization. It is less clear how the interruption of this NLS by those AAs affects the full-length p120ctn. I did not observe any nuclear localization when a panel of p120ctn

## General discussion and perspectives

isoforms, including p120ctn isoform C variants, was transfected. It has been shown that mutating both conventional NLSs in p120ctn has little effect on its nuclear localization (Kelly et al., 2004; Rocznik-Ferguson and Reynolds, 2003). Interestingly, like p120ctn, the nuclear import receptor,  $\alpha$ -importin, is a member of the armadillo family and is almost entirely composed of armadillo repeats (Conti et al., 1998; Gorlich, 1998). The armadillo repeat domain of p120ctn has also been implicated in nuclear transport (Rocznik-Ferguson and Reynolds, 2003). Although different signals for nuclear transport have been identified, determining the contribution of each signal present in full-length p120ctn isoforms is a daunting task. The absence of detectable p120ctn in the nucleus is somewhat problematic. Forced nuclear expression might be achieved by treating the cells with Leptomycin B to block nuclear export. In addition, membrane-localized classical cadherins sequester the available p120ctn protein. Therefore, it might be helpful to perform nuclear translocation experiment in cells deficient in classical cadherins. However, one may wonder whether strong or persistent nuclear expression of p120ctn ever occurs under physiological conditions.

### Effects on RhoGTPase activity

A correlation between nuclear localization of p120ctn isoforms and their ability to elicit 'dendritic branching' was reported (Aho et al., 2002). These neuron-like processes are the result of altered RhoGTPase activity and changes in actin dynamics in cells expressing p120ctn (Anastasiadis et al., 2000; Grosheva et al., 2001; Noren et al., 2000). p120ctn isoform 1, but not a RhoA-uncoupled mutant ( $\Delta 622-628$ ), inhibits RhoA activity and induces neuron-like arbors (Anastasiadis et al., 2000). p120ctn isoform 1AC, and to a lesser extent isoform 3AC, can block 'dendritic branching'. As the AAs encoded by exon-C interrupt a RhoA-binding domain (RBD), I speculated that p120ctn isoform 1AC could prevent 'dendritic branching' by interfering with the ability of p120ctn to inhibit RhoA. However, there was no reproducible increase in RhoA activity in cells that express p120ctn isoform 1AC. On the other hand, an increase in RhoA was evident in cells expressing a RhoA-uncoupled p120ctn mutant. Apparently, Rac1 activity was also unaltered in cells expressing p120ctn isoform 1AC. Maybe this isoform modulates RhoGTPases other than the prototypic family members RhoA, Rac1 and Cdc42. Over 20 mammalian Rho members have been identified and most of them are poorly studied (Boureaux et al., 2007).

**IN VIVO ANALYSIS****p120ctn KOC and KIC mice: ‘C’ stands for conserved intronic sequence**

To analyze the function of p120ctn isoform C *in vivo*, we generated mice harboring a knockout (KOC) or knockin (KIC) of the alternatively used exon C of p120ctn, by introducing small genomic changes around exon C. Surprisingly, homozygous p120ctn KOC and homozygous KIC embryos died before implantation. Although I optimized techniques to analyze preimplantation embryos in detail, such as time lapse monitoring and ES cell derivation, I could not unravel the phenotypes of p120ctn<sup>KOC/KOC</sup> and p120ctn<sup>KIC/KIC</sup> embryos in detail. This implies that both p120ctn KOC and p120ctn KIC alleles are detrimental for the viability of the embryo. In contrast, the p120ctn KOC and p120ctn KIC alleles could rescue p120ctn-null embryos from the lethality. To investigate this discrepancy, We used bioinformatic analysis, which revealed the presence of a highly conserved 200-bp block consisting of exon C and its surrounding intronic sequence. Generally, only exons, but not intronic sequences, have been strongly conserved during evolution. It is recommended (and may turn out to be worthwhile) to perform detailed analysis of the genomic sequence that is to be modified to prevent the deletion of conserved regulatory sequences in the targeting construct. The conserved intronic sequences flanking exon C are partly removed in the p120ctn KOC allele and completely removed in the KIC allele. Consequently, the biallelic deletion of that conserved intronic sequence, and not the deletion of p120ctn exon C *per se*, might be responsible for the early mortality and the non-Mendelian inheritance of homozygous p120ctn<sup>KOC/KOC</sup> and p120ctn<sup>KIC/KIC</sup> embryos. This would also explain why p120ctn<sup>KOC/-</sup> and p120ctn<sup>KIC/-</sup> mice are viable. Indeed, these mice contain a p120ctn-null allele featured by ablation of exons 3 to 8, but with retention of the conserved intronic sequence flanking exon C! These data imply that our p120ctn KOC and p120ctn KIC alleles can be considered as mutants of the highly conserved 200-bp block, and that the phenotypes of p120ctn<sup>KOC/KOC</sup> and p120ctn<sup>KIC/KIC</sup> mice can not be solely attributed to the presence or absence of the AAs encoded by exon-C.

Is it possible to generate ‘specific’ p120ctn KOC and p120ctn KIC alleles? As an alternative to generating mice lacking exon C, we could mutate key nucleotides in the splice acceptor site of exon C, which would result in the exclusion of exon C from all p120ctn transcripts. This exon-C skipping strategy could be achieved with minimal mutations and

## General discussion and perspectives

would preserve most of the intronic sequence. It is far more difficult to create KIC mice without interfering with the conserved intronic sequence. Although inclusion of exon C could be enhanced by modifying splicing enhancers, presently it is impossible to generate KIC alleles without removing these sequences. So, though we should have performed a detailed analysis of the genomic region around exon C before constructing our targeting vector, there is no straightforward alternative way for generating p120ctn KOC alleles, and for KIC alleles there is little if any alternative to the strategy we followed. Assuming that expression of our current p120ctn KOC and KIC alleles caused developmental effects due to loss of intronic sequences, these alleles can still be useful in combination with p120ctn-null alleles (p120ctn<sup>KOC/-</sup> and p120ctn<sup>KIC/-</sup>) for studying late embryogenesis and postnatal development. For instance, it would be interesting to see if the phenotypes of p120ctn<sup>KOC/fl</sup>; Nes-Cre and p120ctn<sup>KIC/fl</sup>; Nes-Cre mice are reproduced also in p120ctn<sup>KOC/-</sup> and p120ctn<sup>KIC/-</sup> mice, respectively. So, we speculate that the early lethal phenotypes were not caused by the KO and KI of the alternatively spliced exon C as such, but by the removal of its flanking conserved intronic sequence.

Both the p120ctn KOC and KIC allele are incompatible with life when they were crossed to homozygosity. Maybe we can learn something from a mouse model that combines the p120ctn KOC and KIC allele. Are these p120ctn<sup>KOC/KIC</sup> mice viable? Two hypothesis with a different outcome can be envisioned: a 'dosage-effect' theory and a 'conserved intronic sequence' theory. First, one could argue that a proper ratio of p120ctn transcripts with or without exon C is required to allow normal development and p120ctn-mediated signalling. This fragile balance would then be perturbed upon forced ablation and expression of exon C in p120ctn<sup>KOC/KOC</sup> and p120ctn<sup>KIC/KIC</sup> embryos, respectively. In compound p120ctn<sup>KOC/KIC</sup> mice, the ratio between p120ctn transcripts with or without exon C could be normalized, which would predispose these mice to be viable. A second theory involves the evolutionarily conserved 200bp 'block', consisting of exon C and its flanking intronic sequence. This conserved 'block' is deleted in both the p120ctn KOC and KIC allele, and could explain the early death of p120ctn<sup>KOC/KOC</sup> and p120ctn<sup>KIC/KIC</sup> embryos. This conserved 'block' would also be completely absent in compound p120ctn<sup>KOC/KIC</sup> embryos, and we would expect that these embryos to die very early as well. We performed the actual experiment and after crossing p120ctn<sup>KOC/+</sup> and p120ctn<sup>KIC/+</sup> mice, we obtained viable p120ctn<sup>KOC/KIC</sup> mice in which the intronic sequence is compromised in both alleles. These findings support our 'dosage-effect' theory. However, in several follow-up studies we could not validate these

p120ctn<sup>KOC/KIC</sup> mice. First, alleles did not segregate according to Mendelian inheritance when p120ctn<sup>KOC/KIC</sup> mice were intercrossed or crossed with C57BL/6 mice (Table 1). Second, a PCR screening of the genomic region of the *Ctnnd1* gene (exon 7 till exon 12) in p120ctn<sup>KOC/KIC</sup> mice did not yield the expected banding patterns.

**Table1. p120ctn<sup>KOC/KIC</sup> mice**

Genotyping offspring from p120ctn <sup>KOC/+</sup> X p120ctn <sup>KIC/+</sup> (n=5)				
+/+ (25%)	KOC/+ (25%)	KIC/+ (25%)	KOC/KIC (25%)	total
5 (10%)	3 (6%)	11 (22%)	31 (62%)	50
Genotyping offspring from p120ctn <sup>KIC/KOC</sup> X C57Bl6 (n=2)				
+/+ (0%)	KOC/+ (50%)	KIC/+ (50%)	KOC/KIC (0%)	total
5 (27,7%)	5 (27,7%)	2 (11,1%)	6 (33,3%)	18
Genotyping offspring from p120ctn <sup>KIC/KOC</sup> X p120ctn <sup>KIC/KOC</sup> (n=3)				
+/+ (0%)	KOC/+ (0%)	KIC/+ (0%)	KOC/KIC (100%*)	total
0 (0%)	6 (18,8%)	7 (21,9%)	19 (59,4%)	32

\* as KOC/KOC and KIC/KIC genotypes are lethal

At this moment, we can only speculate about the function of this conserved 200-bp block. This block might contain regulatory sequences that are indispensable during mouse development. *In silico* analysis (in collaboration with P. Hulpiau) identified two Rat O/E-1-associated zinc finger (Roaz) transcription factor binding sites in this conserved intronic region, and these sites are compromised in both p120ctn KOC and KIC alleles. The C2H2 zinc finger protein Roaz plays a role in the regulation of olfactory neuronal differentiation (Tsai and Reed, 1997), and a huge cluster of more than 200 olfactory receptor (OR) genes is indeed situated upstream of the *Ctnnd1* gene on mouse chromosome 2. Roaz-mediated regulation of OR genes and perhaps of other genes as well might be altered in homozygous p120ctn KOC and KIC embryos, resulting in early mortality. This would imply that during early development, OR genes are also involved in processes other than olfaction, for instance in transcription regulation. A second explanation could be that a lamin binding site spans exon C, which means that it is not present in p120ctn KOC and KIC alleles. The position of a chromosome within the nucleus is crucial for its gene expression, which is altered by chromosomal translocation (Harewood et al., 2010). Therefore, removal of the lamin binding site that spans exon C may influence the chromosomal positioning at the nuclear envelope and may affect global transcription levels, resulting in early lethal phenotypes.

## General discussion and perspectives

How can we study the role of this conserved intronic sequence? Currently we can not easily deduce functional information from this conserved 200-bp block because all the mice in which the intronic sequence is affected in both alleles die early in development, whereas all mice with at least one allele with the unmodified conserved sequence are viable. To study the function of this conserved block, we can flox the conserved intronic sequence. In this way, we would be able to attain functional data after spatial and temporal removal of this 200-bp block in ES cells or in gene manipulated mice. However, it would still be daunting to discriminate the effects caused by deletion of exon C from the effects caused by deletion of its flanking intronic sequence. To this end, we have to make knockin ES cells or mice, aiming at site-specific deletion of the splice acceptor site of exon C or at inactivating the NLS and/or RBD encoded by exon C.

### Effects on RhoGTPase activity

Since all *in vitro* studies describe changes in RhoGTPase activity as a consequence of p120ctn overexpression in cell lines, I wondered if RhoGTPase signaling is also regulated by p120ctn *in vivo*. Reported analyses of tissue-specific p120ctn KO mice have confirmed that p120ctn regulates RhoA activity *in vivo*, because increased RhoA activity was observed in skin and dorsal forebrain when p120ctn was ablated in these tissues (Elia et al., 2006; Perez-Moreno et al., 2006). To check whether p120ctn isoform C can modulate RhoGTPase activity *in vivo*, I used two approaches that involved the p120ctn KOC or p120ctn KIC allele. The p120ctn KOC allele still encodes two undisturbed RBDs and is able to regulate RhoGTPase activity. In contrast, the p120ctn KIC allele encodes six additional AAs that interrupt the second RBD of p120ctn. As both RBDs of p120ctn are required for its high-affinity binding to GDP-bound RhoA (Yanagisawa et al., 2008), the exon-C encoded AAs might abolish the GDI activity of p120ctn (Fig. 1). Therefore, I speculated that p120ctn isoform C might be unable to inhibit RhoA activity *in vivo*. The expression of the p120ctn KIC allele may activate RhoA, like a constitutively active RhoA mutant, but without the need for mutating RhoA. To conclude, I postulated that p120ctn KIC mice could be considered an activator of endogenous RhoA *in vivo*. Whether p120ctn isoform C can also regulate the activity of other Rho family members remains to be tested.

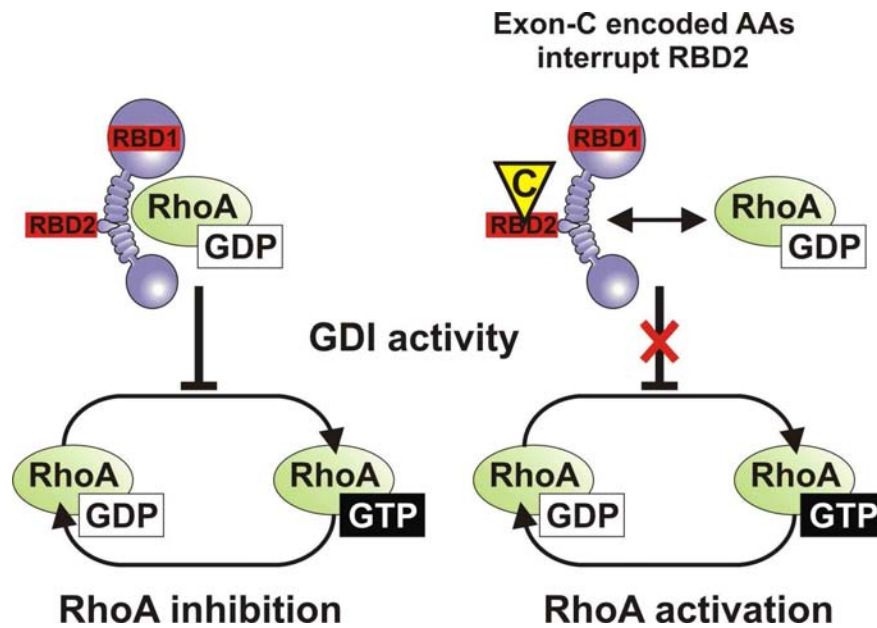


**Figure 1. Model for p120ctn isoform C-mediated RhoA activation *in vivo***

In a first approach, I isolated p120ctn<sup>KOC/-</sup> and p120ctn<sup>KIC/-</sup> ES cells and assayed the RhoA activity under basal and LPA induced conditions. Unfortunately, I could not observe increased RhoA activity in p120ctn<sup>KIC/-</sup> ES cells under these conditions. In addition, I only observed a small but reproducible increase in RhoA activity after LPA treatment of these ES cell cultures. The increase in RhoA activity might not have been optimal because the ES cells were grown in serum-replacement medium, which might contain factors that influence RhoA activity. This could result in a high basal RhoA activity that can not be elevated further. Perhaps serum starvation of ES cells would have resulted in lower basal RhoA activity, and would have allowed an increase in RhoA activity after LPA treatment or in p120ctn<sup>KIC/-</sup> ES cells. On the other hand, serum starved ES cells might start to differentiate and the observed RhoA activities might be determined more by the degree of differentiation than by the p120ctn isoform expression profile.

In a second approach we investigated the effect of p120ctn isoform C on RhoGTPase activity in brain. p120ctn isoform 1A is strongly expressed in brain and has been shown to inhibit RhoA activity *in vitro* (Anastasiadis et al., 2000). The fraction of GTP-bound RhoA was determined in lysates from p120ctn<sup>fl/fl</sup>; Nes-Cre, p120ctn<sup>KOC/fl</sup>; Nes-Cre and p120ctn<sup>KIC/fl</sup>; Nes-Cre mice. In line with previous work (Elia et al., 2006), we found increased active RhoA levels in fully p120ctn-deficient brains. However, we did not observe a reproducible increase

## General discussion and perspectives

in RhoA activity in p120ctn<sup>KIC/fl</sup>; Nes-Cre brain lysates. However, RhoGTPase measurements *in vivo* turned out to be tricky for a number of reasons. First, the brain is composed of various cell types, and some cell types, for example endothelial cells, do not express nestin and will therefore not undergo Nes-Cre-mediated p120ctn ablation. Whole brain lysates are thus a mixture of targeted p120ctn-null brain cells and non-targeted p120ctn-expressing cells. The latter cell types will influence and dampen the overall effect of p120ctn ablation on RhoGTPase activity. To eliminate blood cells, which would also interfere with RhoGTPase measurements, we perfused the mice with PBS just before lysates were made from their brains. However, RhoGTPase measurements of perfused p120ctn<sup>fl/fl</sup>; Nes-Cre, p120ctn<sup>KOC/fl</sup>; Nes-Cre and p120ctn<sup>KIC/fl</sup>; Nes-Cre brains were quite variable as well. A second major concern is the occurrence of premature recombination events in our brain-specific mouse model. These recombinations were detected on the genomic level and caused variable expression of p120ctn protein in different organs of both control and p120ctn<sup>fl/fl</sup>; Nes-Cre mice. All control mice, even those that do not contain the Nes-Cre transgene, are prone to premature recombinations. As a consequence, p120ctn levels in control mice might be reduced, which will also have an impact on the RhoGTPase levels measured. To avoid these problems, we might performed RhoGTPase measurements in brains from more suitable mouse models, such as p120ctn<sup>KOC/-</sup> and p120ctn<sup>KIC/-</sup> mice. These mice are viable and express exclusively p120ctn isoforms without (KOC) or with (KIC) the exon C-encoded AA in the entire mouse. In this context, mice expressing the p120ctn KIC allele could be a valuable tool for activating RhoA *in vivo*. Future experiments may reveal the validity of this model.



## REFERENCES

- Aho, S., L. Levansuo, O. Montonen, C. Kari, U. Rodeck, and J. Uitto. 2002. Specific sequences in p120ctn determine subcellular distribution of its multiple isoforms involved in cellular adhesion of normal and malignant epithelial cells. *J Cell Sci.* 115:1391-402.
- Anastasiadis, P.Z., S.Y. Moon, M.A. Thoreson, D.J. Mariner, H.C. Crawford, Y. Zheng, and A.B. Reynolds. 2000. Inhibition of RhoA by p120 catenin. *Nat Cell Biol.* 2:637-44.
- Boureux, A., E. Vignal, S. Faure, and P. Fort. 2007. Evolution of the Rho family of ras-like GTPases in eukaryotes. *Mol Biol Evol.* 24:203-16.
- Choi, H.J., and W.I. Weis. 2005. Structure of the armadillo repeat domain of plakophilin 1. *J Mol Biol.* 346:367-76.
- Conti, E., M. Uy, L. Leighton, G. Blobel, and J. Kuriyan. 1998. Crystallographic analysis of the recognition of a nuclear localization signal by the nuclear import factor karyopherin alpha. *Cell.* 94:193-204.
- Elia, L.P., M. Yamamoto, K. Zang, and L.F. Reichardt. 2006. p120 catenin regulates dendritic spine and synapse development through Rho-family GTPases and cadherins. *Neuron.* 51:43-56.
- Gorlich, D. 1998. Transport into and out of the cell nucleus. *Embo J.* 17:2721-7.
- Grosheva, I., M. Shtutman, M. Elbaum, and A.D. Bershadsky. 2001. p120 catenin affects cell motility via modulation of activity of Rho-family GTPases: a link between cell-cell contact formation and regulation of cell locomotion. *J Cell Sci.* 114:695-707.
- Harewood, L., F. Schutz, S. Boyle, P. Perry, M. Delorenzi, W.A. Bickmore, and A. Reymond. 2010. The effect of translocation-induced nuclear reorganization on gene expression. *Genome Res.* 20:554-64.
- Ishiyama, N., S.H. Lee, S. Liu, G.Y. Li, M.J. Smith, L.F. Reichardt, and M. Ikura. 2010. Dynamic and static interactions between p120 catenin and E-cadherin regulate the stability of cell-cell adhesion. *Cell.* 141:117-28.
- Keirsebilck, A., S. Bonne, K. Staes, J. van Hengel, F. Nollet, A. Reynolds, and F. van Roy. 1998. Molecular cloning of the human p120ctn catenin gene (CTNND1): expression of multiple alternatively spliced isoforms. *Genomics.* 50:129-46.
- Kelly, K.F., C.M. Spring, A.A. Otchere, and J.M. Daniel. 2004. NLS-dependent nuclear localization of p120ctn is necessary to relieve Kaiso-mediated transcriptional repression. *J Cell Sci.* 117:2675-86.
- Noren, N.K., B.P. Liu, K. Burrige, and B. Kreft. 2000. p120 catenin regulates the actin cytoskeleton via Rho family GTPases. *J Cell Biol.* 150:567-80.
- Perez-Moreno, M., M.A. Davis, E. Wong, H.A. Pasolli, A.B. Reynolds, and E. Fuchs. 2006. p120-catenin mediates inflammatory responses in the skin. *Cell.* 124:631-44.
- Roczniak-Ferguson, A., and A.B. Reynolds. 2003. Regulation of p120-catenin nucleocytoplasmic shuttling activity. *J Cell Sci.* 116:4201-12.
- Tsai, R.Y., and R.R. Reed. 1997. Cloning and functional characterization of Roaz, a zinc finger protein that interacts with O/E-1 to regulate gene expression: implications for olfactory neuronal development. *J Neurosci.* 17:4159-69.
- Yanagisawa, M., D. Huveltdt, P. Kreinest, C.M. Lohse, J.C. Cheville, A.S. Parker, J.A. Copland, and P.Z. Anastasiadis. 2008. A p120 catenin isoform switch affects Rho activity, induces tumor cell invasion, and predicts metastatic disease. *J Biol Chem.* 283:18344-54.

# Samenvatting

---

Het p120 catenine (p120ctn) behoort tot de familie van Armadillo-eiwitten en maakt deel uit van het cadherine-catenine complex. Het p120ctn vervult verscheidene functies naargelang zijn subcellulaire lokalisatie: het moduleert de expressie van klassieke cadherines aan het celmembraan, het reguleert de activiteit van RhoGTPasen in het cytoplasma, en het bepaalt de activiteit van transcriptiefactoren in de kern. Het p120ctn is onontbeerlijk voor een normale ontwikkeling en homeostase. In een deelaspect van mijn doctoraatsonderzoek heb ik aangetoond dat p120ctn alomtegenwoordig is in verschillende stadia van de normale ontwikkeling van de muis.

Er komen verschillende p120ctn-isovormen voor, die ontstaan als gevolg van alternative splicing. Hierbij kunnen p120ctn-isovormen vertaald worden van vier verschillende start-codons en kunnen er tot vier interne exonen al dan niet geïncorporeerd worden. Het alternatief gebruikte exon C codeert voor slechts voor zes aminozuurresten, die een nucleair lokalisatiesignaal (NLS) en een RhoA-bindingsdomein (RBD) onderbreken. De expressie van deze zes additionele aminozuurresten blokkeerde inderdaad zowel de nucleaire translocatie van p120ctn als de *in vitro* inductie in cellen van neuronachtige uitlopers. Tot op heden is het functioneel belang van al dan niet expressie *in vivo* van deze talrijke p120ctn-isovormen niet gekend. Enkele weefsel-specifieke p120ctn-knockout (KO) muizen werden gegenereerd, maar in deze muizen werden telkenmale alle p120ctn isovormen tegelijk verwijderd. Ik rapporteer hier voor de eerste maal over isovorm-specifieke KO en knockin (KI) muizen. Inderdaad hebben wij muizen gemaakt met een KO of een KI van het alternatief gebruikte exon C van p120ctn, respectievelijk KOC en KIC muizen genoemd. Hiervoor hebben we kleine aanpassingen gemaakt in het genoom ter hoogte van exon C van het p120ctn-gen. Tot onze grote verbazing stierven zowel homozygote p120ctn-KOC als homozygote p120ctn-KIC embryo's nog voor hun inplanting en gebeurde de overerving van de p120ctn-KOC en p120ctn KIC-allelen niet volgens de regels van de Mendeliaanse erfelijkheid.

Om de vastgestelde vroege sterfte in embryo's te omzeilen maakten we vervolgens gebruik van een strategie waarbij een allel van een totale p120ctn-KO gecombineerd werd met een p120ctn-KOC of een p120ctn-KIC allel. Daartoe kruisten we gefloxeerde p120ctn muizen (p120ctn<sup>fl/fl</sup>) met Deleter-Cre, Albumin-Cre (Alb-Cre) of Nestin-Cre (Nes-Cre) muizen om, respectievelijk, constitutieve (p120ctn<sup>-/-</sup>), leverspecifieke (p120ctn<sup>fl/fl</sup>; Alb-Cre) en hersenspecifieke (p120ctn<sup>fl/fl</sup>; Nes-Cre) p120ctn KO muizen te bekomen (Tabel 1).

## Samenvatting

Homozygote, totale p120ctn-KO embryo's sterven vroeg tijdens de ontwikkeling en p120ctn-deficiënte blastocysten brengen minder E-cadherine tot expressie ter hoogte van het celmembraan. Evenwel, in de door mij gegenereerde p120ctn<sup>KOC/-</sup> en p120ctn<sup>KIC/-</sup> embryo's, werd de embryonale sterfte verhinderd door de expressie van ofwel het p120ctn-KOC ofwel het p120ctn-KIC allel. De *in vivo* E-cadherine-expressieniveaus werden hierbij hersteld (Tabel 1). Leverspecifieke p120ctn-KO (p120ctn<sup>fl/fl</sup>; Alb-Cre) muizen vertoonden geelzucht, hepatomegalie en ductulaire reacties, en ook al deze defecten konden hersteld worden door de expressie van een p120ctn-KOC of p120ctn-KIC allel (Tabel 1). Hersenspecifieke p120ctn-KO muizen (p120ctn<sup>fl/fl</sup>; Nes-Cre) hadden geen opvallende macroscopische defecten. p120ctn<sup>KOC/fl</sup>; Nes-Cre en p120ctn<sup>KIC/fl</sup>; Nes-Cre muizen daarentegen vertoonden lichte maar onderling verschillende fenotypes (Tabel 1). p120ctn<sup>KOC/fl</sup>; Nes-Cre muizen hadden namelijk kleine morfologische defecten in de hippocampus. Anderzijds hadden <sup>KIC/fl</sup>; Nes-Cre muizen kleinere hersenen en vertoonden neuroncultures, die van deze hersenen afgeleid waren, tekenen van fasciculatie.

**Tabel 1. Overzicht van de muismodellen en hun fenotypes**

	Genotype	Verlies van geconserveerde intronsequenties	Embryonale letaliteit	Fenotype
	wild-type	nee nee	nee	Normaal
	p120ctn <sup>KOC/KOC</sup>	ja ja	ja	Sterven voor implantatie
	p120ctn <sup>KIC/KIC</sup>	ja ja	ja	Sterven voor implantatie
	p120ctn <sup>-/-</sup>	nee nee	ja	Sterven tijdens gastrulatie en somitogenese; verminderde E-cadherin niveaus in blastocysten
	p120ctn <sup>KOC/-</sup>	ja nee	nee	Normaal, het p120ctn KOC allel herstelt de E-cadherin-expressieniveaus en de leefbaarheid in p120ctn-deficiënte muizen
	p120ctn <sup>KIC/-</sup>	ja nee	nee	Normaal, het p120ctn KIC allel herstelt de E-cadherin-expressieniveaus en de leefbaarheid in p120ctn-deficiënte muizen
Levermodel	p120ctn <sup>fl/fl</sup> ; Alb-Cre	nee nee	nee	Geelzucht, hepatomegalie en ductulaire reactie
	p120ctn <sup>KOC/fl</sup> ; Alb-Cre	ja nee	nee	Normaal, het p120ctn KOC allel heft de geelzucht, hepatomegalie en ductulaire reacties op
	p120ctn <sup>KIC/fl</sup> ; Alb-Cre	ja nee	nee	Normaal, het p120ctn KIC allel heft de geelzucht, hepatomegalie en ductulaire reacties op
Hersenmodel	p120ctn <sup>fl/fl</sup> ; Nes-Cre	nee nee	nee	Normaal
	p120ctn <sup>KOC/fl</sup> ; Nes-Cre	ja nee	nee	Mild fenotype in de hippocampus
	p120ctn <sup>KIC/fl</sup> ; Nes-Cre	ja nee	nee	Microcefalie, fasciculatie in hippocampale neuronen

Deze observaties confronteren ons met een merkwaardige contradictie. Enerzijds zijn de p120ctn-KOC en -KIC allelen verantwoordelijk voor de vroege sterfte van homozygote p120ctn<sup>KOC/KOC</sup> en p120ctn<sup>KIC/KIC</sup> embryo's. Anderzijds kunnen de p120ctn-KOC en p120ctn-KIC allelen de vroege embryonale sterfte van totale p120ctn-KO embryo's verhinderen. (Tabel 1). Om deze ambiguïteit te ontrafelen hebben we met behulp van bioïnfomatica de genomische regio rond exon C van het p120ctn-gen geanalyseerd. We ontdekten een geconserveerd blok van 200 bp, dat exon C omvat alsook de flankerende intronsequenties. Deze laatste worden deels of volledig verwijderd in, respectievelijk, p120ctn-KOC of p120ctn-KIC allelen. Misschien is het verwijderen van deze geconserveerde intronsequenties, en niet zozeer het verlies van exon C op zich, verantwoordelijk voor de vroege sterfte van p120ctn<sup>KOC/KOC</sup> en p120ctn<sup>KIC/KIC</sup> embryo's. Dit zou tevens kunnen verklaren waarom p120ctn<sup>KOC/-</sup> en p120ctn<sup>KIC/-</sup> muizen wel levensvatbaar zijn. Deze muizen bevatten namelijk een p120ctn-KO allel waarin weliswaar exon 3 tot 8 gedeleteed zijn, maar waarin de geconserveerde intronsequentie rond exon C van p120ctn onaangetast is. Tot op heden kunnen we enkel gissen naar de functie van dit geconserveerde blok van 200 bp, maar wij speculeren dat het regulatorische sequenties bevat die essentieel zijn voor het leven.

# Summary

---

p120 catenin (p120ctn) belongs to the Armadillo family and is a component of the cadherin-catenin complex. It fulfills pleiotropic functions according to its subcellular localization: modulating the turnover rate of membrane-bound cadherins, regulating the activation of small RhoGTPases in the cytoplasm, and changing nuclear activity of transcription factors. p120ctn is essential for normal development and homeostasis in vertebrates such as mouse and *Xenopus*. I demonstrated that p120ctn is ubiquitously expressed in early preimplantation mouse embryos and in gastrula-stage embryos.

Multiple p120ctn isoforms have been identified. These isoforms result from alternative splicing, which allows the translation of p120ctn isoforms from four start codons and enables the inclusion of four alternatively used exons. The alternatively used exon C encodes only six amino acid residues (AA), which interrupt a nuclear localization signal and a RhoA binding domain. Consequently, inclusion of the AAs encoded by exon C interferes with nuclear translocation and ‘dendritic branching’ *in vitro*. The significance of these many p120ctn isoforms *in vivo* remains largely unknown. Several tissue-specific p120ctn knockout mice have been reported, but in these studies all p120ctn isoforms were removed. We report for the first time on p120ctn-isoform specific knockout and knockin mice. We generated mice harboring a knockout (KOC) or knockin (KIC) of the alternatively used exon C of p120ctn, by introducing small genomic changes around exon C. Surprisingly, homozygous p120ctn KOC and homozygous KIC embryos died before implantation and displayed a non-Mendelian inheritance (Table 1).

To bypass the early lethal phenotypes in homozygous p120ctn KOC and homozygous KIC embryos, we employed several strategies that combined a full p120ctn KO allele with either a p120ctn KOC or KIC allele. We crossed floxed p120ctn mice (p120ctn<sup>fl/fl</sup>) with Deleter-Cre, Albumin-Cre (Alb-Cre) and Nestin-Cre (Nes-Cre) mice to obtain constitutive (p120ctn<sup>-/-</sup>), liver-specific (p120ctn<sup>fl/fl</sup>; Alb-Cre) and brain-specific (p120ctn<sup>fl/fl</sup>; Nes-Cre) p120ctn KO mice, respectively (Table 1). p120ctn null embryos died around midgestation and p120ctn-deficient blastocysts failed to sustain proper levels of membrane-localized E-cadherin. We generated p120ctn<sup>KOC/-</sup> and p120ctn<sup>KIC/-</sup> mice, which rescue from the lethal phenotype of p120ctn null mice and their failure to stabilize E-cadherin levels *in vivo* (Table). Genetic ablation of p120ctn in the liver (p120ctn<sup>fl/fl</sup>; Alb-Cre) resulted in jaundice, hepatomegaly, and ductular reactions, and these defects could be rescued by introducing either the p120ctn KOC or KIC allele (Table 1). Brain-specific p120ctn knockout mice (p120ctn<sup>fl/fl</sup>; Nes-Cre) showed no obvious abnormality. In contrast, p120ctn<sup>KOC/fl</sup>; Nes-Cre

## Summary

and p120ctn<sup>KIC/fl</sup>; Nes-Cre mice showed discrete but different phenotypes (Table 1). p120ctn<sup>KOC/fl</sup>; Nes-Cre mice exhibited aberrant morphology of the medial side of the hippocampus and had a small reduction in total hippocampal volume. On the other hand, p120ctn<sup>KIC/fl</sup>; Nes-Cre mice displayed microcephaly, and hippocampal cultures that were derived from them showed signs of fasciculation.

**Table 1. Overview of the mouse models and their phenotypes**

	Genotype	Loss of conserved intronic sequence	Embryonic lethal phenotype	Phenotype
	wild-type	no no	no	Normal
	p120ctn <sup>KOC/KOC</sup>	yes yes	yes	Die before implantation
	p120ctn <sup>KIC/KIC</sup>	yes yes	yes	Die before implantation
	p120ctn <sup>-/-</sup>	no no	yes	Die during gastrulation and somitogenesis decreased E-cadherin levels blastocysts
	p120ctn <sup>KOC/-</sup>	yes no	no	No obvious phenotype, p120ctn KOC allele rescues E-cadherin levels and lethality of p120ctn null mice
	p120ctn <sup>KIC/-</sup>	yes no	no	No obvious phenotype, p120ctn KIC allele rescues E-cadherin levels and lethality of p120ctn null mice
Liver model	p120ctn <sup>fl/fl</sup> ; Alb-Cre	no no	no	Jaundice, hepatomegaly, ductular reactions
	p120ctn <sup>KOC/fl</sup> ; Alb-Cre	yes no	no	No obvious phenotype, p120ctn KOC allele rescues jaundice, hepatomegaly, ductular reactions
	p120ctn <sup>KIC/fl</sup> ; Alb-Cre	yes no	no	No obvious phenotype, p120ctn KIC allele rescues jaundice, hepatomegaly, ductular reactions
Brain model	p120ctn <sup>fl/fl</sup> ; Nes-Cre	no no	no	No obvious phenotype
	p120ctn <sup>KOC/fl</sup> ; Nes-Cre	yes no	no	Discrete hippocampal defect
	p120ctn <sup>KIC/fl</sup> ; Nes-Cre	yes no	no	Microcephaly, fasciculation in hippocampal neurons

The presence of p120ctn KOC and KIC alleles seems to be detrimental for the viability of homozygous p120ctn<sup>KOC/KOC</sup> and p120ctn<sup>KIC/KIC</sup> embryos, whereas the same alleles could rescue from the lethality in p120ctn null embryos (Table 1). To investigate this discrepancy, bioinformatic analysis was performed. This analysis revealed the presence of a highly conserved 200-bp block consisting of exon C and its surrounding intronic sequence. These sequences are partly or completely removed in, respectively, the p120ctn KOC and KIC alleles. Therefore, the biallelic deletion of that conserved intronic sequence, and not the deletion of p120ctn exon C *per se*, might be responsible for the early lethal phenotypes and the non-Mendelian inheritance of homozygous p120ctn<sup>KOC/KOC</sup> and p120ctn<sup>KIC/KIC</sup> embryos.



This also explains why p120ctn<sup>KOC/-</sup> and p120ctn<sup>KIC/-</sup> mice are viable. Indeed, they contain a p120ctn null allele featured by ablation of exons 3 to 8, but with retention of the conserved intronic sequence flanking exon C. At this moment, we can only speculate about the function of this 200-bp block, but we hypothesize that it contains regulatory features that are essential for early life.

## Curriculum vitae

### Personalialia

---

Name: Tim Pieters  
 Nationality: Belgian  
 Date of birth: 14/09/1979  
 Place of Birth: Ghent, Belgium  
 Civil status: legally cohabiting with Debora De Backer, father of Amalia Pieters (05/04/2008) and Thomas Pieters (07/02/2010)  
 Address: Renaat De Rudderstraat 39, 9940 Evergem  
 Telephone/GSM: 09/229 39 02, 0486 47 99 81  
 E-mail: Tim.Pieters@dmbv.VIB-UGent.be, tim\_pieters@telenet.be

### Education

---

1998 – 2001: Bachelor in Biochemistry, biotechnology (distinction), Hogeschool Ghent  
 2001 – 2003: Industrial engineer in de Biochemistry (distinction), Hogeschool Ghent  
 2003 – 2004: Master after Master in Molecular Biotechnology (distinction), Ghent University  
 2004 – 2010: Ph.D. in Biotechnology under promotorship of Prof. Dr. Frans Van Roy and Dr. Jolanda van Hengel.  
 Molecular Cell Biology Unit  
 Departement for Molecular Biomedical Research (DMBR) – VIB  
 Faculty of Science, Ghent University

### Scientific awards

---

The bachelor thesis “Constructie van plasmiden voor heterologe expressie van gekloneerde humane antilichamen” was awarded with the price Vera Dua, Vlaams minister van Leefmilieu en Landbouw.

The master thesis “Optimalisatie multiplex microsatellietanalyse in de NF1-regio” was awarded with the price Sigma-Aldrich.

### Foreign experience

---

In November 2007, I followed a one-month training in the prestigious laboratory of Prof. Dr. Rolf Kemler from the Max-Planck institute for Immunobiology in Freiburg (Germany). I was trained by Dr. Marc Stemmler and during this intensive training I mastered several techniques: Time Lapse monitoring of *in vitro* development of preimplantation embryos, immunostaining of preimplantation embryos, embryonic stem (ES) cell derivation, and generating and analysis of teratomas.

## Research support

---

- Instituut voor de Aanmoediging van Innovatie door Wetenschap en Technologie in Vlaanderen (IWT)
- Queen Elisabeth Medical Foundation (G.S.K.E.)
- Geconcerteerde Onderzoeksacties of Ghent University.

## Publications

---

- **p120ctn in normal development and disease.** Pieters T., van Hengel J. and Van Roy F. *Frontiers in Bioscience* (invited review: special issue on “E-cadherin function in development and cancer”)
- **p120 catenin: function follows isoform.** Pieters T., Van Roy F. and van Hengel J. *Frontiers in Bioscience* (invited review: special issue on “Cell Cell Adhesion and Communications in Development and Tumorigenesis”)
- **p120ctn isoform c knockout and knockin mice rescue E-cadherin loss and embryonic lethality in p120ctn-deficient embryos.** Pieters T., D'hooge P., Hulpiau P., Stemmler M., Reynolds A., Van Roy F. and van Hengel J. *Manuscript in preparation*
- **Efficient and user-friendly pluripotin-based derivation of mouse embryonic stem cells.** Pieters T., Hochepped T., Haigh J., Van Roy F. and van Hengel J. *Manuscript in preparation*
- **Time lapse monitoring of mouse preimplantation development *in vitro*.** Pieters T., Stemmler M., Hochepped T., Van Roy F. and van Hengel J. *Manuscript in preparation*
- **Knockout and Knockin of exon C of p120ctn in brain.** Pieters T., Lambrechts A., Van der Linden A., Van Roy F. and van Hengel J. *Manuscript in preparation*
- **Ocular anterior segment dysgenesis following deletion of p120ctn in neural crest stem cells.** Tian H., Sanders E., Reynolds A., Pieters T., van Roy F., and van Hengel J. Submitted to *Journal of Cell Science*

## Scientific courses

---

- Effective Writing for Life Sciences Research Course by Jane Fraser: 3-4 oktober 2007
- Basic Course in Laboratory Animal Science partim 1: General topics (2005-2006), Ghent, Belgium
- Basic Course in Laboratory Animal Science partim 2: Specific topics (2005-2006), Ghent, Belgium

## Scientific activities

---

- Assistance in practicum: “Dissection of the mouse”. 2005-2006; 2006-2007; 2007-2008 en 2008-2009.
- Assistance in practicum: “Histology: from tissue to section”. 2005-2006; 2006-2007; 2007-2008 en 2008-2009.
- Guidance of Eveline Fack (Master Biochemistry): 2006-2007
- Guidance of Laura Standaert (1<sup>e</sup> Master Biochemistry en Biotechnology): 2007-2008
- Guidance of Rindert Missiaen (Bachelor Agro- en Biotechnology): 2008-2009

## Scientific conferences

---

- IUAP cancer meeting, Belgium - Gent, December 16<sup>th</sup>, 2004
- VIB seminar, Belgium - Blankenberge, March 3<sup>rd</sup>-4<sup>th</sup>, 2005
- BSCDB meeting on cell migration and immunity, Belgium - Brussel, May, 27<sup>th</sup>-28<sup>th</sup>, 2005
- BACR meeting: viruses as an important cause of human cancer, January 28<sup>th</sup>, 2006
- IUAP cancer meeting, Belgium - Brussel, February 9<sup>th</sup>-10<sup>th</sup>, 2006
- VIB seminarie, Belgium- Blankenberge, March 9<sup>th</sup>-10<sup>th</sup>, 2006
  - Oral Presentation:** Think Twice before you splice: constitutive p120ctn exon C expression/deletion effects normal mouse embryogenesis.  
Tim Pieters, Petra D’Hooge, Frans Van Roy en Jolanda van Hengel
- BSCDB meeting, Belgium - Leuven, May, 4<sup>th</sup>-6<sup>th</sup>, 2006
- Horizons in Molecular Biology, **Germany** - Goettingen, September 14<sup>th</sup>-16<sup>th</sup>, 2006
- BSCDB meeting: cytoskeleton and Cellular Imaging, Belgium - Gent, October 14<sup>th</sup>, 2006
- IUAP cancer meeting, Belgium - Luik, October 20<sup>th</sup>, 2006
  - Member of the organizing committee and chair of the morning session**
- BACR meeting: Use of transgenic mice in cancer research, Belgium - Gent, January 20<sup>th</sup>, 2007
- VIB seminarie, Belgium - Blankenberge, March 1<sup>st</sup>-2<sup>nd</sup>, 2007
- Gordon Research Conference on Cell Contact & Adhesion, **Italy** - Lucca May 27<sup>th</sup> till June 1<sup>st</sup>, 2007. **Oral presentarion:** A transgenic approach to dissecting the functions of p120ctn isoforms in vivo: focus on p120ctn isoform C.  
Tim Pieters, Petra D’Hooge, Frans Van Roy en Jolanda van Hengel
- BSCDB meeting: Oxygen and Reactive Oxygen Species in Biology, Belgium – Louvain-la-Neuve, October 13<sup>th</sup>, 2007
- BACR meeting: The tumor environment, Belgium - Gent, February 16, 2008

*"Our real teacher, has been and still is the embryo-who is, incidentally, the only teacher who is always right"*

Viktor Hamburger